



New insights into signaling mechanisms controlling the function and fate of hepatic stellate cells

Dissertation

This dissertation is submitted
for the degree of the Doctor of Philosophy
to the Faculty of Mathematics and Natural Sciences
at the Heinrich-Heine-University Düsseldorf

Presented by

Saeideh Nakhaeirad

from Mashhad, Iran

Düsseldorf, November 2015



Neue Erkenntnisse über die Signalmechanismen in der Kontrolle der Funktion und des Schicksals hepatischer Sternzellen

Inaugural-Dissertation

zur Erlangung des Doktorgrades
der Mathematisch-Naturwissenschaftlichen Fakultät
der Heinrich-Heine-Universität Düsseldorf

vorgelegt von

Saeideh Nakhaeirad

aus Mashhad, Iran

Düsseldorf, November 2015

Aus dem Institut für Biochemie und Molekularbiologie II
der Heinrich-Heine-Universität Düsseldorf

Gedruckt mit der Genehmigung der
Mathematisch-Naturwissenschaftlichen Fakultät der
Heinrich-Heine-Universität Düsseldorf

Referent: Prof. Dr. Reza Ahmadian
Korreferent: Prof. Dr. Vlada Urlacher
Tag der mündlichen Prüfung: 25 May 2016

Table of contents

Summary	I
Zusammenfassung.....	II
Table of Figures	III
Abbreviation.....	IV
Chapter I.....	1
General introduction	1
Anatomical units and resident cells of the liver	2
Microanatomy of the liver.....	2
Hallmarks and roles of hepatic stellate cells	3
Quiescent HSC (qHSC) in the normal liver.....	3
Activated HSC (aHSC) after liver injury.....	6
Postulated signaling mechanisms in hepatic stellate cells.....	7
RAS superfamily at a glance	8
RAS family GTPases	10
Effectors and signaling of RAS proteins.....	13
RHO family GTPases	19
Signaling cross-talk between RHO and RAS GTPases.....	20
Aims and objectives.....	23
Chapter II.....	24
The function of embryonic stem cell-expressed RAS (ERAS), a unique RAS family member, correlates with its additional motifs and its structural properties	24
Chapter III.....	38
Embryonic stem cell-expressed ERAS controls quiescence of hepatic stellate cells.....	38
Chapter IV.....	39
Classical RHO proteins: biochemistry of molecular switch function and regulation	58
Chapter V.....	73
Functional cross-talk between RAS and RAS pathways: a RAS-specific GTPase activating protein (p120RASGAP) competitively inhibits the RHOGAP activity of deleted in liver cancer (DLC) tumor suppressor by masking the catalytic arginine finger.....	73
Chapter VI.....	85
IQGAP1 interaction with RHO family proteins revisited: kinetic and equilibrium evidence for two distinct binding sites	85
Chapter VII.....	117
Juvenile myelomonocytic leukemia displays mutations in components of the RAS pathway and the PRC2 network.....	117
Chapter VIII.....	142
General discussion.....	142
Biochemical characteristic of embryonic stem cell-expressed RAS (ERAS)	144
Signaling network and proposed function of endogenous ERAS in HSC.....	146
Functional cross-talk between RAS and RHO pathways	150
p120GAP links RAS and RHO pathways <i>via</i> p190GAP and DLC1	151
Scaffolding protein IQGAP modulates RHO and RAS signaling	152
The coordination of RAS (NRAS) and RHO (RAC2) mutations in tumor progression	154
Concluding remarks.....	155
References.....	157
Acknowledgments.....	178
Curriculum Vitae.....	180
Eidesstattliche Erklärung zur Dissertation	183

Summary

Hepatic stellate cells (HSCs) are non-parenchymal liver resident cells in the space of Disse, which are central to metabolism and storage of retinoids in the body and are involved in liver development, immunoregulation, homeostasis, regeneration, and fibrosis. In healthy liver, HSCs are in a state referred as quiescent. After liver injury, HSCs develop into activated HSCs, which are then able to proliferate, migrate, contract, and differentiate to other liver cell types and, in this way, contribute to liver regeneration. However, during sustained liver injury HSCs promote liver fibrosis *via* excessive extracellular matrix production. The key signaling networks, which maintain quiescent of HSCs or orchestrate their plasticity toward liver regeneration or fibrosis need further investigation. The RAS family is central in a network controlling intracellular signaling pathways, which adopt the cellular responses upon integration of external stimuli from the neighboring cells and the microenvironment. The functions and activity of RAS dependent signaling pathways in the fate of HSCs are poorly understood. This doctoral thesis provides new insights into the expression pattern, isoform specificity, activity and networking of RAS family members and their signaling components in both quiescent and activated HSCs. The obtained data revealed a differential expression pattern for RAS isoforms, where embryonic stem cell-expressed RAS (ERAS) is specifically expressed in quiescent HSCs and becomes drastically down-regulated after HSC activation. In contrast to ERAS, other members of the RAS family, *e.g.*, MRAS, RRAS, RALA, and RAP2A were rather up-regulated upon HSC activation. Comprehensive biochemical studies identified ERAS as a unique member of the RAS family with remarkable sequence deviations, additional motifs, and an extended N-terminal region. The latter appears to be important for the signaling activity of ERAS. Most remarkably, ERAS revealed a different mode of effector interaction as compared to classical HRAS signaling, thereby, correlating with deviations in the effector-binding site of ERAS. Hence, ERAS signals maintain the HSC quiescent by the inhibition of both proliferation and apoptosis *via* various pathways, such as JAK-STAT3, AKT-mTORC1-FOXO1, mTORC2-AKT, and RASSF5-HIPPO. In contrast, activated HSCs exhibited YAP-CTGF/NOTCH2 and RAS-RAF-MEK-ERK activity, which are involved in HSC proliferation and development.

Zusammenfassung

Hepatische Sternzellen (HSCs) sind nicht-parenchymale, im Dissé'schen Raum der Leber ansässige Zellen, welche für den Metabolismus und die Speicherung von Retinoiden im Körper von zentraler Bedeutung sind. HSCs sind wesentlich an der Entwicklung, Immunregulation, Homöostase, Regeneration, sowie an der Fibrose der Leber beteiligt. In gesundem Lebergewebe befinden die HSCs sich in einem ruhenden Zustand. Nach einer Leberschädigung werden sie zu aktivierten HSCs (aHSCs) umprogrammiert und gewinnen dadurch die Fähigkeit zur Proliferation, Migration, Kontraktion, sowie Differenzierung in andere hepatische Zelltypen. Somit tragen HSCs wesentlich zur Regeneration der Leber bei. Bei einer anhaltenden Leberschädigung begünstigen HSCs jedoch durch eine übermäßige Produktion an extrazellulärer Matrix die Entstehung einer Fibrose. Die zugrundeliegenden (patho)biochemischen Signalkaskaden, welche für die Aufrechterhaltung ruhender HSCs und deren Aktivierung im Rahmen regenerativer und fibrotischer Prozesse in der Leber ausschlaggebend sind, waren zu Beginn dieser Arbeit weitestgehend unklar. Die RAS-Proteinfamilie spielt eine zentrale Rolle für die Kontrolle intrazellulärer Signalwege, welche zelluläre Reaktionen entsprechend äußerer Reize benachbarter Zellen und der Mikroumgebung vermitteln. Die Analysen der Funktionen und die Aktivität RAS-abhängiger Signalwege in ruhenden vs. aktivierten HSCs war das Hauptziel dieser Doktorarbeit, die neue Einblicke in die Expressionsänderung, Isoform-Spezifität, Aktivität und die Signalnetzwerke von Mitgliedern der RAS Proteinfamilie und deren Komponente, sowohl in qHSCs, als auch in aHSCs, charakterisiert. Hierbei konnte gezeigt werden dass die bisher nur wenig charakterisierte RAS Isoform ERAS (*embryonic stem cell-expressed RAS*) spezifisch in qHSCs exprimiert wird und nach deren Aktivierung im Gegensatz zu allen anderen RAS-Isoformen drastisch runterreguliert wird. MRAS, RRAS, RALA und RAP2A wurden dagegen nach HSC-Aktivierung hochreguliert. In umfangreichen biochemischen Analysen wurde ERAS als einzigartiges Mitglied der RAS Familie identifiziert, gekennzeichnet durch deutliche Sequenzunterschiede, zusätzliche Motive, sowie einen verlängerten N-Terminus. Letzterer scheint eine Rolle in der ERAS vermittelten Signaltransduktion einzunehmen. Interessanterweise zeigen ERAS und HRAS eine größtenteils nicht überlappende Interaktion mit Effektoren. Dieser Unterschied korreliert mit Abweichungen in den Effektorbindungsstellen von ERAS. ERAS-Signale erhalten demzufolge die Quieszenz ruhender HSC durch die Inhibition von sowohl Proliferation als auch Apoptose via verschiedener Signalwege, wie JAK-STAT3, AKT-mTORC1-FOXO1, mTORC2-AKT, und RASSF5-HIPPO. Im Gegensatz dazu zeigen die aktivierten HSCs YAP-CTGF/NOTCH2- und RAS-RAF-MEK-ERK-Aktivität, die an der Proliferation und Entwicklung von HSCs beteiligt sind.

Table of Figures

Figure 1. Microanatomy of the liver and liver resident cells	4
Figure 2. Schematic view of the RAS-GTP/GDP cycle and downstream signaling pathways of RAS proteins	8
Figure 3. RAS superfamily, family members and subgroups.....	9
Figure 4. Overall sequence comparison of ERAS protein with classical RAS proteins..	10
Figure 5. Schematic view of signaling pathway of the mammalian target of rapamycin (mTOR) complexes.....	18
Figure 6. Predicted structure of full-length ERAS and exhibits of the three-dimensional places of studied ERAS mutants	144
Figure 7. Schematic view of the proposed model of HSC signaling networking and gene expressional changes	149
Figure 8. p120 interacts through SH3 domain with DLC1 and regulates RAS and RHO signaling..	151

Abbreviation

aa	amino acid
aHSC	activated HSC
ARP2/3	actin related protein 2/3
BMP-2	bone morphogenetic protein-2
CXCR4	chemokine (C-X-C motif) receptor 4
DEPTOR	DEP domain-containing mTOR-interacting protein
DLC1	deleted in liver cancer 1
ECM	extracellular matrix
ERAS	embryonic stem cell-expressed RAS
ERK	extracellular regulated kinase
FTase	farnesyltransferase
FGF	fibroblast growth factor
FOXO1	forkhead transcription factor 1
GAP	GTPase-activating protein
GDP	guanosine diphosphate
GEF	guanine nucleotide exchange factor
GFAP	glial fibrillary acidic protein
GGTase I	geranylgeranyltransferase type I
GSK3 β	glycogen synthase kinase 3 beta
GTP	guanosine triphosphate
GTPases	guanosine triphosphatase
HA	hyaluronan
HCC	hepatocellular carcinoma
HGF	hepatocyte growth factor
HRAS	harvey rat sarcoma
HSC	hepatic stellate cell
HVR	hypervariable region
IGF	insulin-like growth factor
IQGAP	IQ motif-containing GTPase-activating protein
IRSp53	insulin receptor substrate p53
JMML	juvenile myelomonocytic leukemia
KRAS	kirsten rat sarcoma
mDia	mammalian diaphanous
MEK	MAP/ERK kinase
MLST8	mammalian lethal with SEC13 protein 8
MMP	matrix-metalloproteinase
MRAS	muscle rat sarcoma
MSC	mesenchymal stem cell
mSIN1	mammalian stress-activated MAP kinase-interacting protein 1
MST	mammalian sterile 20-like kinase
mTORC	mammalian target of rapamycin
NF1	neurofibromatosis type 1
NRAS	neuroblastoma rat sarcoma
NORE1	novel RAS effector 1
OCT4	octamer-binding transcription factor 4

PAK	p21-activated kinase
PDGF	platelet-derived growth factor
PDK1	3-phosphoinositide-dependent protein kinase 1
PH	pleckstrin homology
PHx	partial hepatectomy
PIP3	phosphoinositide 3,4,5-trisphosphate
PI3K	phosphoinositide 3-kinase
PKR	protein kinase C-related kinase
PLC	phospholipase C
PP1	protein phosphatase 1
PPAR γ	peroxisome proliferator-activated receptor γ
PRAS40	40 kDa pro-rich Akt substrate
PROTOR	protein observed with RICTOR
PTM	post-translational modification
qHSC	quiescent HSC
RA	RAS association
RAC	RAS-related C3 botulinum toxin substrate
RAF	rapidly accelerated fibrosarcoma
RAL	RAS like
RALBP1	RALA binding protein 1
RALGDS	guanine nucleotide dissociation stimulator
RAP2A	RAS related protein 2A
RAPTOR	regulatory-associated protein of mTOR
RAS	rat sarcoma
RAS D	RAS, dexamethasone-induced
RASSF	RAS-association domain family
RBD	RAS binding domain
RGL	RALGDS like
RHO	RAS homolog
RICTOR	rapamycin-insensitive companion of mTOR
RLIP76	76 KDa RAL-interacting protein
RHEB	RAS homolog enriched in brain
ROCK	RHO-associated coiled-coil kinase
RRAS	related RAS
SAM	sterile α motif
SARAH	salvador-RASSF-HIPPO
SATB1	AT-rich binding protein 1
SDF α	stromal cell-derived factor α
SH2	src homology 2
SH3	src homology 3
SMA	smooth muscle actin
SREBP	sterol regulatory element-binding protein
SPRY1	sprouty homolog 1
SRA1	specifically RAC1-associated protein-1
START	steroidogenic acute regulatory related lipid transfer
STAT3	signal transducer and activator of transcription 3
TGF β	transforming growth factor beta

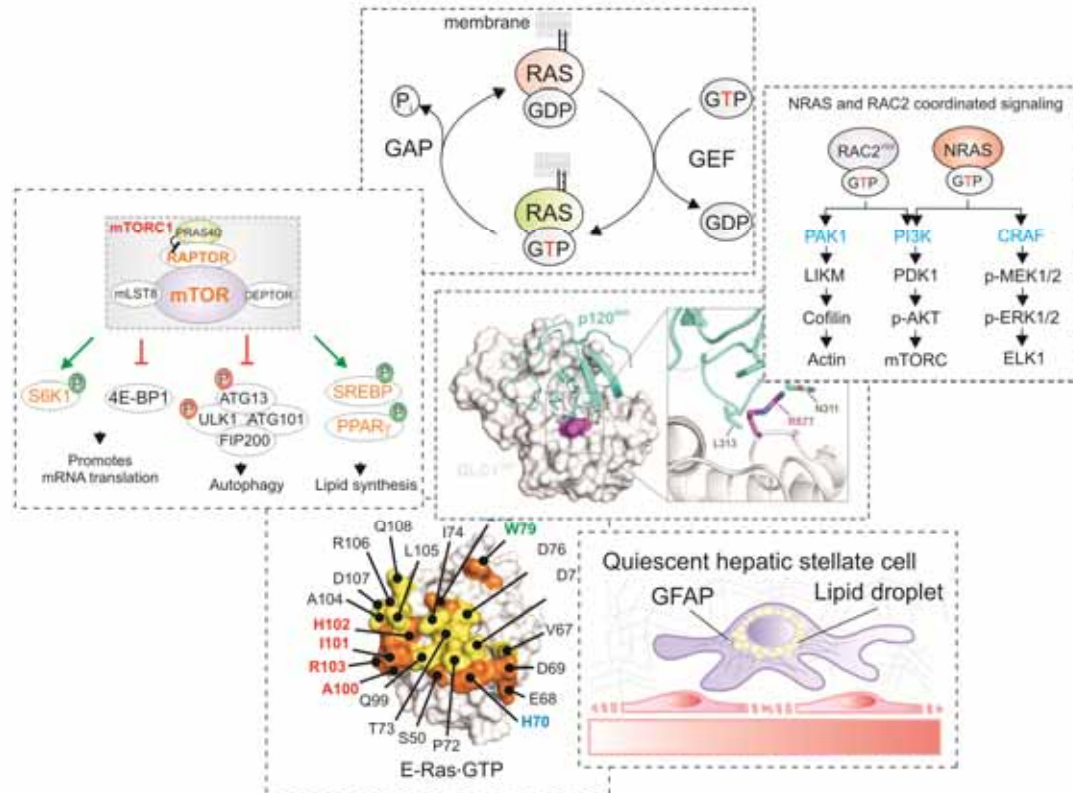
TIMP tissue inhibitors of metalloproteinase
TSC tuberous sclerosis
ULK1 Unc-51 like autophagy activating kinase 1
WASP wiskott–aldrich syndrome protein
WAVE WASP-family verprolin-homologous protein
WNT wingless-type MMTV
YAP yes-associated protein
ZONAB ZO-1 associated nucleic acid-binding protein

Amino Acids abbreviation

Name	Letter codes	Name	Letter codes	Name	Letter codes	Name	Letter codes
alanine	Ala (A)	glutamic acid	Glu (E)	leucine	Leu (L)	serine	Ser (S)
arginine	Arg (R)	glutamine	Gln (Q)	lysine	Lys (K)	threonine	Thr (T)
asparagine	Asn (N)	glycine	Gly (G)	methionine	Met (M)	tryptophan	Trp (W)
aspartic acid	Asp (D)	histidine	His (H)	phenylalanine	Phe (F)	tyrosine	Tyr (Y)
cysteine	Cys (C)	isoleucine	Ile (I)	proline	Pro (P)	valine	Val (V)

Chapter I

General introduction



Anatomical units and resident cells of the liver

Liver is located in the upper-right quadrant of the abdominal cavity below the diaphragm. It acts as a unique organ in the body with wide range of physiological functions and plays a central role in the metabolic homeostasis, glycogen storage, bile secretion, detoxification, serum protein production, *e.g.*, albumin and acute-phase proteins (Lefkowitz, 2011). The liver represents a largest organ in the body and weights around 1200-1500 g in adults and its size and weight is correlated with age and gender (Chouker *et al.*, 2004). Liver receives the blood from two sources: First, the portal vein carries nutrient rich and oxygen poor blood 70% (40% oxygen) from spleen, pancreas and intestine. Second, hepatic artery supplies 30% oxygen rich (60% oxygen) and nutrient poor blood from the celiac trunk (Burt and Day, 2003).

Microanatomy of the liver

Functional units

Based on anatomical aspects on pig dissections, Kiernan in 1833 described anatomically units of the liver as hexagonal structures named classic lobules (Fig. 1A) (Kiernan, 1833). Each lobule, periphery recognizes with around six portal triads containing terminal branches of portal vein, hepatic artery and bile duct (Fig. 1A). At the central of liver lobules placed the center vein that collects the blood from the whole lobule and drains to hepatic vein. In addition, Rappaport introduced alternative functional liver units, liver acinus, which are important for liver physiology and pathology. It lies between two classical lobules in diamond shape and involves two portal triads and two central veins in periphery (Fig. 1A). At the level of acinus, hepatocytes are grouped into three zones based on their distance from oxygen-rich portal triads and are numbered to direction of blood flow from 1 to 3 (Fig. 1A) (Rappaport *et al.*, 1954).

Microscopy structure of liver lobules composed of four major parts; I) Parenchyma, a line of organized hepatocytes; II) Connective tissues, *i.e.* vessels, ducts and nerve system. III) Hepatic capillaries which are known as sinusoids, located between planes of parenchymal cells and lined with endothelial cells, where the supplied blood from peripheral branches of hepatic artery and portal vein are combined and drained towards central vein. IV) Space of Dissé (perisinusoidal space), a narrow area between basal surface of hepatocytes and endothelial cells (Fig. 1B) (Lachman and Pawlina, 2010).

Liver specific resident cells and their functions

Hepatocytes comprise 80 % of liver cell population and are the most prominent cells of the liver according to their functions. Hepatocytes are structurally and functionally heterogenic cells depending on their position. The major functions of periportal hepatocytes (zone 1, Fig. 1A) consisting: gluconeogenesis, β -Oxidation of fatty acids, amino acid catabolism, bile secretion and, cholesterol, glycogen and urea synthesis. Whereas periventricular hepatocytes are involved on glycolysis, lipogenesis, ammonia removal, detoxifications,

ketogenesis, glycogen and bile acid synthesis (Häussinger *et al.*, 1985; Lamers *et al.*, 1989; Gumucio, 1989; Jungermann, 1988). Hepatocytes are polarized cells; the basal surface faces the sinusoidal space that covered with microvilli and apical surface form the canaliculus (Fig. 1B) (Gissen and Arias, 2015).

Cholangiocytes are epithelial cells, which line the bile duct. Bile flows from the canaliculi into the bile ducts (named bile ductules) and cholangiocytes modify and secrete bile derived (Fig. 1B, green arrow) (Kanno *et al.*, 2000).

Kupffer cells are liver resident macrophages that are associated with endothelial cells in the lumen side of sinusoid. They contribute for removal of bacteria, viruses, parasites, dead cells and tumor cells from the liver. Moreover, they are an important source of cytokines secretion (Dixon *et al.*, 2013).

Endothelial cells are elongated fenestrae cells, line sinusoidal space. They act as sieve and allow transport of macromolecules between blood sinusoids and plasma within Disse space with the size of up to 0.2 μm through their pores. In addition, they possess high capacity for receptor-mediated endocytosis. Together, with these two features, they provide the hepatocytes their substrates and *via* selective endocytosis protect hepatocytes from several harmful components (Smedsrod *et al.*, 1990; Braet *et al.*, 2009).

Hepatic stellate cells (HSCs; also called Ito cells, lipocytes, fat storing cells, or perisinusoidal cells) contribute to 5-8% of total liver-resident cells and are located between the basolateral surface of hepatocytes and sinusoidal endothelial cells in the space of Disse in the liver (Fig. 1B) (Kordes and Häussinger, 2013a).

The focus of present study is to provide a better understanding about the function and regulation of HSCs within the liver and after liver injury, therefore in following parts HSCs will be viewed in more detail.

Hallmarks and roles of hepatic stellate cells

Quiescent HSC (qHSC) in the normal liver

Characteristics

HSCs reside in the Disse space of liver in close proximity to other liver cells, i. e., hepatocytes, sinusoidal endothelial cells and Kupffer cells (Fig. 1B). In a healthy liver, stellate cells remain in quiescent state and are characterized by high content of vitamin A storage (mainly retinyl palmitate) as cytoplasmic lipid vesicles and expression of neural and mesodermal markers, i.e., glial fibrillary acidic protein (GFAP) and desmin (Wake, 1971; Yokoi *et al.*, 1984; Gard *et al.*, 1985) (see Fig. 1B and C). Under excitation by UV light, lipid-containing vesicles reflect the blue-green light due to their autofluorescence property (Blaner *et al.*, 2009; Sauvant *et al.*, 2011).

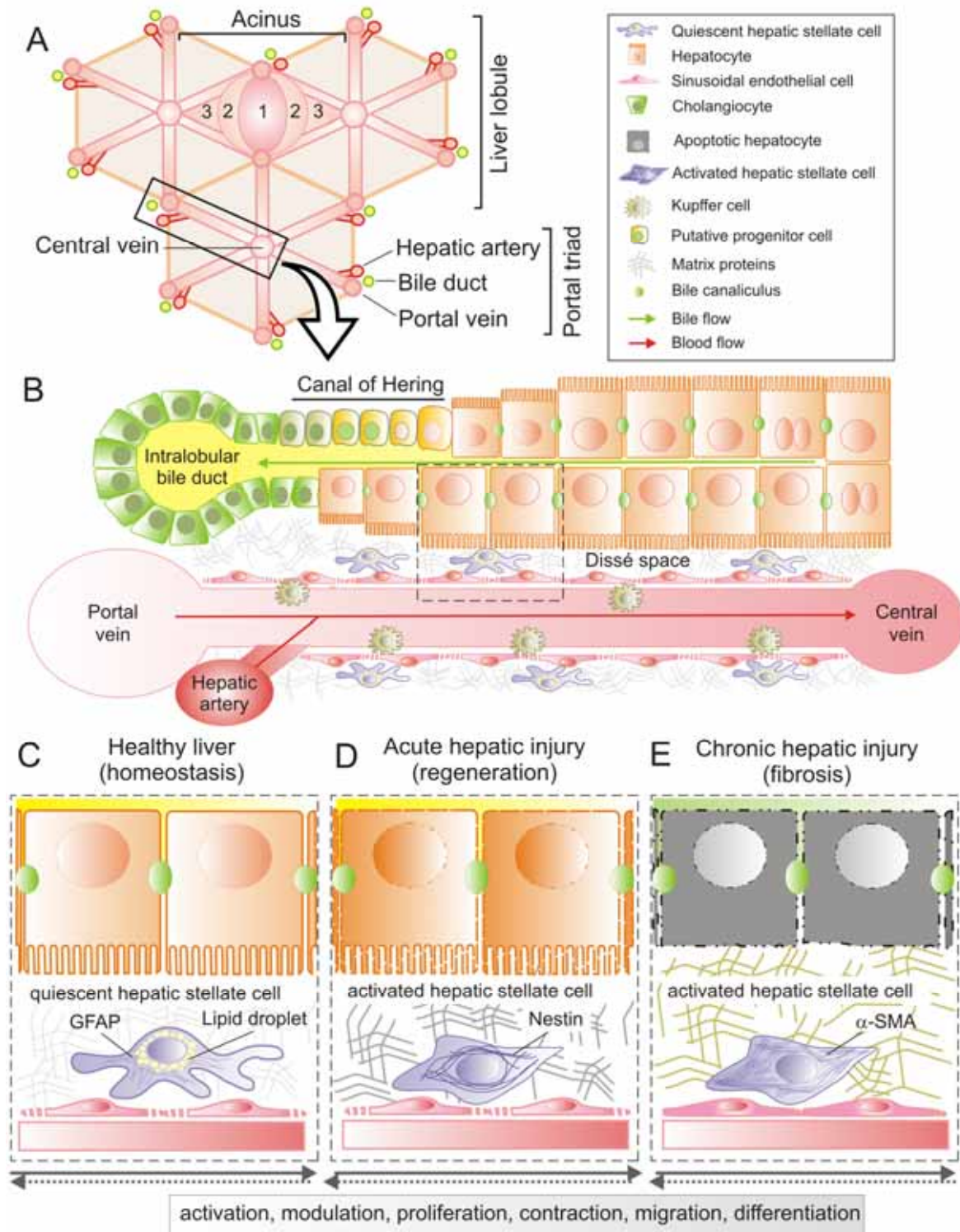


Figure 1. Microanatomy of the liver and liver resident cells. (A) Illustration of liver three lobules and acinus, zone 1 to 3. (B) Schematic view of sinusoidal space, liver resident cells, Dissé space, canal of Hering and blood vessels [adopted from (Kordes and Häussinger, 2013a)]. (C) Quiescent HSC. (D) Activated HSC in regeneration. (E) Activated HSC in fibrosis.

Functions

Development and organogenesis—HSCs originate from the mesodermal cells of septum transversum (Asahina *et al.*, 2011) and during embryogenesis, they contribute to liver development and organogenesis through: I) Progenitor proliferation, HSCs have profound impact on proliferation of hepatoblasts (epithelial progenitors of hepatocytes and cholangiocytes) by releasing the mitogen factors such as fibroblast growth factor 10 (FGF10) (Berg *et al.*, 2007), hepatocyte growth factor (HGF) (Schirmacher *et al.*, 1992; Delgado *et al.*, 2009) and WNT (Matsumoto *et al.*, 2008). II) Cell fate decision and differentiation, HSCs through extracellular matrix (ECM) protein production and NOTCH signaling control the hepatoblasts differentiation towards, either hepatocytes or cholangiocytes, respectively (Nagai *et al.*, 2002; Sawitza *et al.*, 2009; Yanai *et al.*, 2008; Zong *et al.*, 2009). III) Chemotaxis and homing, HSCs by providing the stromal cell-derived factor α (SDF1 α or CXCL12) chemokine, recruit hematopoietic stem cells and endothelial cells that express its receptor CXCR4 into the fetal liver (Wright *et al.*, 2002; Kubota *et al.*, 2007). IV) Hematopoiesis, recently it is demonstrated that HSCs similar to bone marrow mesenchymal stem cells (MSCs), have a positive influence on hematopoiesis by supporting hematopoietic stem cells and are introduced as liver-resident MSCs (Castilho-Fernandes *et al.*, 2011; Kordes *et al.*, 2013; Kordes *et al.*, 2014).

In normal liver—qHSCs are viewed for their contribution in two main processes; I) Retinoid storage and mobilization in the liver (Wake, 1971). The majority of the retinoids in the body are stored in the lipid droplets of the qHSCs. Retinoids (retinyl ester, retinol, retinal and retinoic acid), are engaged in large spectrum of the physiological processes, e.g. development, organogenesis, differentiation, vision, reproduction and immunity (Duester, 2008; Blaner *et al.*, 2009; Clagett-Dame and Knutson, 2011; Zhou *et al.*, 2012; Markgraf *et al.*, 2014). The active metabolite of retinol is retinoic acid and through binding to the nuclear receptors modulates the expression of variety of the genes, including the genes which are controlling the cell growth, differentiation and cellular metabolism (Di Masi *et al.*, 2015; Zhang *et al.*, 2015). II) Maintenance and homeostasis of stem cell niche in the liver. Stem cell microenvironment or niche provides the soluble factors and cell-cell contacts, which are critical factors for stem cells maintenance and self-renewal. qHSCs reside in the Dissé space that represents the stem cell niche within the liver. HSCs are the main source of HGF secretion that is essential for hepatocytes homeostasis (Ramadori *et al.*, 1992; Schirmacher *et al.*, 1992). Moreover, they are involved in signaling pathways such as WNT and NOTCH, which required for maintenance of stem cell niche (Kordes *et al.*, 2008a; Sawitza *et al.*, 2009; Kordes and Häussinger, 2013a). The most exciting prospects of HSCs are that in addition to their supportive roles in stem cell niche, they also possess characteristics of stem cells, like the expression of OCT4 and CD133 genes, and react as a multipotent cells with potency to differentiate into other cell lineages, such as

hepatocytes, endothelial cells, adipocytes and osteocytes (Kordes *et al.*, 2007; Kordes *et al.*, 2013; Kordes *et al.*, 2014; Sawitza *et al.*, 2015).

Activated HSC (aHSC) after liver injury

Transition to myofibroblast-like cells—Following chronic liver injury, apoptotic/necrotic hepatocytes release factors which activate HSCs and trigger their transdifferentiation into contractile, proliferative and migrating cells, so-called activated HSCs. During activation, aHSCs release their vitamin A, up-regulate various genes, including α -smooth muscle actin (α -SMA) and collagen type I, and down-regulate GFAP (Figs. 1D and E). In addition to *in vivo* activation of HSCs during the chronic liver injury, by culturing the freshly isolated HSCs on the plastic dishes, they undergo spontaneous activation and provide an *in vitro* model to study the activated HSCs which are from different aspects very close to the *in vivo* models (De Minicis *et al.*, 2007; Mannaerts *et al.*, 2015).

Physiologically, HSCs represent well-known extracellular matrix (ECM) producing cells. ECM production is important for maintenance of the tissue structure and function (Jones *et al.*, 1993; Wang *et al.*, 2004). In acute liver infection, HSCs protect hepatocytes against toxin products of ectopic pathogens by releasing type I collagen and contributing to scar tissue formation (Friedman, 2008; Bourbonnais *et al.*, 2012). However, apart from the protective function of scar tissue, in chronic liver injuries, dysregulation of fibrosis can occur and excessive scar formation interferes with normal liver function. In some pathophysiological conditions, last long activation of HSCs causes the accumulation of ECM in the liver and initiate the liver diseases like, fibrosis, cirrhosis and hepatocellular carcinoma (HCC) (Dechene *et al.*, 2010; Pellicoro *et al.*, 2014).

Matrix remodeling and controlling ECM composition—Matrix remodeling occurs *via* a balance between matrix-metalloproteinases (MMPs or matrixins) and their inhibitors, tissue inhibitors of metalloproteinases (TIMPs) and this process is important for normal function of organs. MMPs hydrolyze the ECM components and are regulated at transcriptional levels and locally *via* their specific inhibitors, TIMPs. They are zinc-calcium dependent proteinases (Werb, 1997; Parks, 1999; Sternlicht and Werb, 2001) and based on their substrate categorized in five groups; I) Collagenases, MMP-1, MMP-8, MMP-13, and MMP-18 that cleave collagens I, II, and III. II) Gelatinases, MMP-2 and MMP-9. III) Stromelysins, MMP-3, -10 and -11. IV) Matrilysins, MMP-7 and MMP-26. V) Membrane-type, MMP-14, -15, -16, -17, -24, -25 (Visse, 2003). Activated HSCs play profound roles in matrix remodeling by up-regulation and secretion of MMP-2 (Arthur *et al.*, 1992), MMP-9 (Han *et al.*, 2007), MMP-13 (Schaefer *et al.*, 2003) and stromelysin (Vyas *et al.*, 1995; Benyon and Arthur, 2001; Friedman, 2008) (Fig. 1E).

Liver regeneration after partial hepatectomy—Liver is a unique solid organ in the body with high capacity of regeneration. After surgical removal of two-thirds of the liver (termed partial hepatectomy or PHx), the remaining parts of the liver grow and enlarge until the liver mass reach to its normal size, this phenomenon is called liver regeneration (Taub, 2004; Michalopoulos, 2010). This is mainly proposed as a result of hepatocytes reentry to the cell cycle (from G0 to G1) and their proliferation (Miyaoka *et al.*, 2012). Notably, there are growing

numbers of evidences indicating the pivotal contribution of other liver cell types especially HSCs in supporting hepatocytes upon liver regeneration, by providing the high levels of growth factors (HGF), cytokines, chemokines, NOTCH signaling activity and modulation the ECM composition (Gefferers *et al.*, 2007; Roskams, 2008; Sawitza *et al.*, 2009; Friedman, 2008; Yin *et al.*, 2013b).

Stem cell-mediated liver regeneration—Under some pathological conditions, when the hepatocytes proliferation compromised, liver regeneration mediated through the progenitor cells activation, proliferation and differentiation. The liver progenitor/stem cells emerge when the hepatocytes proliferation is impaired and there are two candidate cell lineages, which are introduced as liver stem cells; I) Oval cells in the rodents appear around the canal of Hering (Fig. 1B). These cells exhibit the immature oval-shaped cells with bipotent capacity to differentiate into hepatocytes and cholangiocytes (Miyajima *et al.*, 2014). II) HSCs are the second candidate for liver stem cells and Dissé space serves as a stem cell niche by providing the soluble factors and appropriates microenvironment for cell-cell communication (Sawitza *et al.*, 2009; Kordes and Häussinger, 2013a; Kordes *et al.*, 2014). Similar to oval cells, they are multipotent cells and emit the stem cells properties (Yang *et al.*, 2008). Noteworthy, recent study demonstrated the transdifferentiation of transplanted HSCs into the progenitor cell population of the host animal during liver regeneration and their contribution to the hepatocytes and bile duct formation (Kordes *et al.*, 2014) (Fig. 1D).

In the previous part, we had a short introduction about HSCs and a view of their functions, in both quiescent and activated states. The most exciting aspects of HSCs are their bilateral roles during physiological and pathophysiological situations as positive or negative players. Therefore, there is a pivotal need to further understand the molecular mechanisms that govern the fate and contribution of HSCs in different cellular circumstances. In the next section, we will get more detailed information about the candidate pathways that may be the driven force on HSC fate decisions.

Postulated signaling mechanisms in hepatic stellate cells

To date, several studies reported the candidate pathways that regulate the plasticity of HSCs during different circumstances including liver development, hemostasis, repair and fibrosis; such as RAS-MAPK, PI3K-AKT, JAK-STAT3, HIPPO-YAP, NOTCH, WNT, Hedgehog, and importance of growth factors, like platelet-derived growth factor (PDGF), transforming growth factor beta (TGF β) and insulin-like growth factor (IGF) (Reimann *et al.*, 1997; Carloni *et al.*, 2002; Kordes *et al.*, 2008a; Lakner, 2010; Xie *et al.*, 2013; de Souza *et al.*, 2015; Mannaerts *et al.*, 2015). Among these pathways, RAS signaling is one of the earliest, which was identified to plays a role in HSC activation (Parola *et al.*, 1998). However, how the cross-talking between different RAS dependent signaling pathways modulates the HSC fate decisions, remains to be manifested. In this section, we will have an introduction to RAS superfamily of monomeric GTPases; the cellular outcomes, subgrouping, sequence highlights, lipid modification, and regulation. Then, we will take the signaling networks of two major families of RAS and RHO into consideration.

RAS superfamily at a glance

Cellular functions—Small GTPases of the RAS superfamily normally act as molecular switches within the cell, cycling between a GTP-bound (active) and a GDP-bound (inactive) states (Fig. 2) (Wittinghofer and Vetter, 2011). According to the sequence and function similarly, they fall into seven major subfamilies: RAS, RHO, RAB, RAN, RAD, RAG and ARF (Fig. 3). In 1979, the RAS protein, prototype of RAS superfamily, was first described as a phospho-protein (p) 21 kDa and later RAS term was used as a prototype of a superfamily (Fig. 3) (Shih *et al.*, 1979). These molecules trigger intracellular responses by sensing the extracellular signals through their interacting receptors or intermediate proteins and passing the signal to downstream targets (Fig. 2). Therefore, they play a key role in various cellular processes, including gene expression, metabolism, cell cycle progression, proliferation, survival, differentiation, vesicular transport, cytoskeleton organization, migration, cell motility, endocytosis, contraction and nuclear transport (Coleman *et al.*, 2004; Wennerberg, 2005; Sorkin and von Zastrow, 2009; Amin *et al.*, 2013). In pathological situations, the somatic or germline mutations in genes related to members of the RAS superfamily or their regulators are commonly associated with cancer progression or developmental disorders (Ahmadian *et al.*, 2002; Gremer *et al.*, 2011; Karnoub and Weinberg, 2008; Pylayeva-Gupta *et al.*, 2011; Tidyman and Rauen, 2009; Flex *et al.*, 2014; Cirstea *et al.*, 2013).

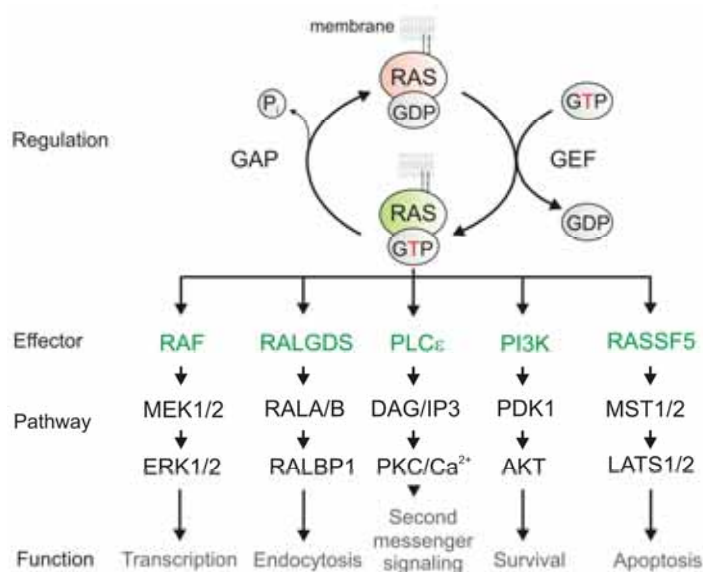


Figure 2. Schematic view of the RAS-GDP/GTP cycle and downstream signaling pathways of RAS proteins. As it is written at the top left, RAS proteins are cycling between GDP/GTP bound forms by the actions of two main regulatory proteins, GEF, and GAP. They can only exert their cellular functions when they are anchored to the membrane *via* posttranslational lipid modifications (see text for more information). Effector proteins downstream of RAS-GTP are depicted with green letters and the cellular targets of effectors in black. Through the interaction with these effectors and switching on the downstream pathways, RAS proteins emit their cellular functions, bottom in gray. DAG, diacylglycerol; ERK, extracellular regulated kinase; GAP, GTPase-activating protein; GEF, guanine nucleotide exchange factor; MEK, MAP/ERK kinase; MST, mammalian sterile 20-like kinase; PDK1, 3-phosphoinositide-dependent protein kinase; PI3K, phosphoinositide 3-kinase; PIP3, phosphoinositide 3,4,5-trisphosphate;

PKC, protein kinase C; PLC, phospholipase C; RALBP1, RALA binding protein 1; RALGDS, guanine nucleotide dissociation stimulator; RAS, rat sarcoma; RASSF5, Ras-association domain family.

Sequence highlights of RAS superfamily—RAS proteins share a highly conserved GTP-binding (G) domain with five essential motifs, termed G1-G5 (Fig. 4) (Bourne *et al.*, 1990; Bourne *et al.*, 1991). G1 or P-loop ($^{10}\text{GxxxxGKS/T}^{17}$; HRAS numbering) binds the beta and gamma phosphates of GTP (Saraste *et al.*, 1990). Substitution of glycine 12 to any other amino acids (except for proline) is most frequently found in human cancers. These mutations render RAS protein GAP-insensitive and consequently hyperactive (Bos, 1989; Tidyman and Rauen, 2009). G2 and G3, also are referred as switch I and switch II, respectively, are dynamic regions that sense the nucleotide state and provide the regulator and effector binding sites (Vetter, 2001; Herrmann, 2003). G4 and G5 are important for determining the guanine base-binding specificity of G domain (Schmidt *et al.*, 1996; Wittinghofer and Vetter, 2011) (Fig. 4).

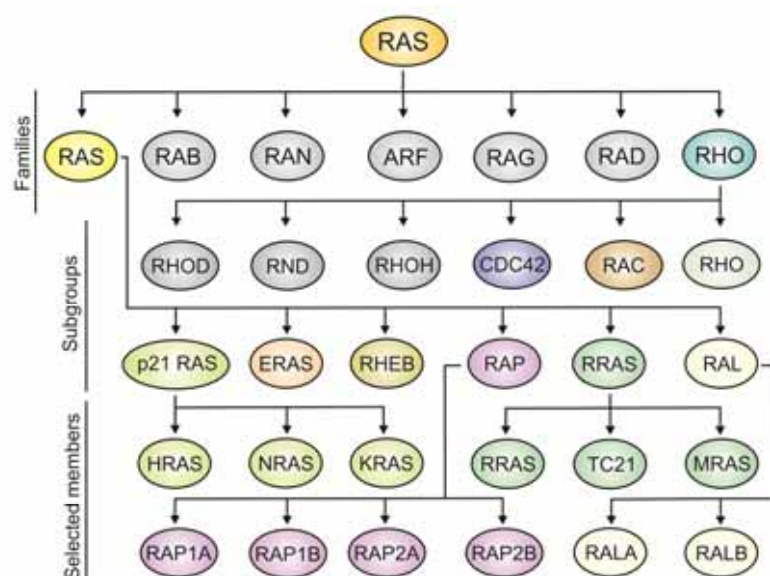


Figure 3. RAS superfamily, family members and subgroups [adopted from (Kennedy *et al.*, 2005)]. RAS superfamily consist of seven family (first row), RAS, RAB, RAN, ARF, RAG, RAD and RHO. Each family is subdivided in different subgroups, here we only depicted RAS and RHO dependent subgroups; RAS subgroups, p21 RAS, ERAS, RHEB, RAP, RRAS and RAL. RHO subgroups, RHO, RAC, CDC42, RHOH, RND and RHOD. Two last rows highlight the members of each RAS subgroups in the same colors as used for the subgroups (see the text for further information).

Lipid modifications and membrane targeting— Association of RAS proteins with cellular membranes are mediated through posttranslational (PTM) modification in their very C-terminal end, termed hypervariable region (HVR) (Figs. 2 and 4). The plasma membrane localization of RAS proteins is essential for their functionality where they physically can interact with their regulators and effector proteins (Willumsen *et al.*, 1984; Ahearn *et al.*, 2011; Schmick *et al.*, 2014). They undergo two lipid modifications; I) Prenylation, the RAS and RHO family members, mainly terminated with CAAX sequence (C is cysteine, A is any aliphatic amino acid, and X is any amino acid) (Seabra *et al.*, 1991) (Fig. 4). CAAX motif serves as

substrate for two prenyl transferases, depending on the X amino acid; If CAAX terminates with Leu at the X position, which is more prominent in RHO family, polyisoprene lipid (20 carbon length) will be bond irreversibly to the Cys residues of CAAX motif through geranylgeranyl transferase type I (GGTase I) enzyme. On the other hand, if X residue is not Leu (in almost all RASs) another lipid anchor with 15-carbon farnesyl will be added to the Cys by farnesyl transferase (FTase) activity (Reid *et al.*, 2004). Although the prenylation modification is needed for plasma membrane localization but it is not sufficient, and second signal is required for plasma membrane targeting; II) Palmitoylation modification occurs at the one or two Cys residues upstream of CAAX motif in HVR. The fatty acid chain (mainly 14-carbon myristoyl or 16-carbon palmitoyl) attachment occurs through the function of palmitoyl acyl transferase (PAT) enzyme (Buss and Sefton, 1986; Hancock *et al.*, 1989; Resh, 1999).

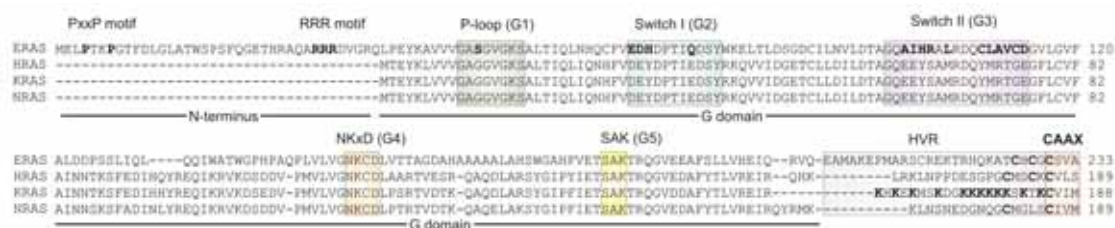


Figure 4. Overall sequence comparison of ERAS protein with classical RAS proteins. ERAS contains an extended N-terminus (aa 1-38), missing in H, K, and NRAS, with a putative SH3-binding motif (PxxP). G1 to G5 boxes indicate the presence of five essential GDP/GTP binding (G) motifs. The P-loop (G1) of ERAS contains a serine instead of a glycine (codon 12, HRAS numbering), a frequently mutated site within RAS genes in human cancer (Fasano *et al.*, 1984). Several residues in switch I (G2) and switch II (G2) regions that are responsible for effector recognition are different between ERAS and HRAS (bold letters). ERAS contains, like HRAS, a CAAX motif and two cysteines at the C-terminal hypervariable region (HVR), which are the sites for PTMs by farnesylation and palmitoylation, respectively.

Biochemical aspects and regulation—RAS proteins are inefficient GTP-hydrolyzing enzymes. Such an intrinsic GTPase reaction requires stimulation through GTPase-activating proteins (GAPs) by orders of magnitude (Scheffzek *et al.*, 1997; Ahmadian *et al.*, 1997a; Ahmadian *et al.*, 1997b) (Fig. 2). On the other hand, GDP dissociation is also a very slow reaction that needs acceleration by guanine nucleotide exchange factors (GEFs) (Lenzen *et al.*, 1998; Buday and Downward, 2008). As mentioned before, RHO protein function requires permanent posttranslational modification by isoprenyl groups. Therefore, RHO proteins underlie a third control mechanism that is achieved by the function of guanine nucleotide dissociation inhibitors (GDIs), which binds selectively to prenylated RHO proteins and control their cycle between cytosol and membrane (Ismail *et al.*, 2011; Zhang *et al.*, 2014b) (chapter IV).

RAS family GTPases

Family members—The RAS sarcoma (RAS) proteins can be activated through the action of GEF proteins and activated RASs (GTP-loaded) act as nodes in modulating intracellular signaling pathways (Fig. 2). They control the wide range of cellular functions by integrating

with distinct downstream effector proteins. Rojas and colleagues, reported 39 members of human RAS family (<http://www.cbbio.es/GTPases/>), including HRAS, KRAS, NRAS, RAP1A/B, RAP2A/B/C, RALA/B, RRAS subgroup (RRAS, TC21 and MRAS), RHEB, DIRAS (RIG), RASD (AGS1/DEXRAS), RASL10, ERAS, NKIRAS, and RIT (Rojas and Valencia, 2014) (Fig. 3).

Functions—Best investigated RAS proteins are HRAS, NRAS and KRAS4B, share overlapping functions, including cell proliferation, differentiation and apoptosis (Castellano and Santos, 2011; Ichise *et al.*, 2010; Omerovic *et al.*, 2007; Potenza *et al.*, 2005). However, different RAS isoforms exhibit a particular pattern of expression, different regulators and specific microdomains or subcellular localization, indicating their functional specificity as well as redundant roles (Leon *et al.*, 1987; Johnson *et al.*, 1997; Potenza *et al.*, 2005; Omerovic *et al.*, 2007; Nakamura *et al.*, 2008; Ichise *et al.*, 2010; Castellano and Santos, 2011; Lau and Haigis, 2009). The individual roles of other members of the RAS family, such as RRAS, TC21, MRAS, RAP2A, RASD, or the embryonic stem cell-expressed RAS (ERAS) have not been fully described. In this part, we will have a brief description of these RAS family members, ERAS, RRAS, MRAS and RAP2A.

ERAS novel members of RAS family

ERAS expression ranging from embryonic stem cells to tumors—The ERAS expression has been reported to date in embryonic stem cells and some tumor cell lines but not in the normal cells of the body. For the first time, Yamanaka and colleagues introduced ERAS in 2003 as a novel member of RAS family, specifically expressed in undifferentiated mouse embryonic stem cells to be critical for maintenance of growth and tumor-like properties in these cells (Takahashi *et al.*, 2003). Later, the ERAS expression was detected in different types of colorectal carcinoma cells (HCT116, DLD1, LS174T and HT29), pancreatic carcinomas (RWP-1 and MIAPaCa-2), breast carcinoma (AMB-231) (Yasuda *et al.*, 2007) and gastric cancer (e.g., GCIY, NUGC-4 and MKN-45) cell lines (Kubota *et al.*, 2010). Kaizaki and colleagues reported the ERAS expression in 45% of gastric cancer tissues and found correlation between ERAS-negative patients recognized with poorer prognosis (Kaizaki *et al.*, 2009). In addition, ERAS expression was also found in various neuroblastoma cell lines that has been suggested to promote transforming activity and resistance to chemotherapy (Aoyama *et al.*, 2010).

Hallmarks of ERAS. ERAS harbors, despite a conserved G domain with all essential motifs for a high-affinity binding of GTP, significant amino acid deviation as compared to other RAS proteins (Fig. 4); I) Its phosphate binding loop containing a serine (S50) instead of a glycine that is critical for the GTP hydrolysis reaction (Scheffzek *et al.*, 1997) and responsible for ERAS makes it GAP insensitivity (Nakhaei-Rad *et al.*, 2015). Substitution of G12 for any other amino acids in RAS isoforms is frequently associated with tumor formation (Tidyman and Rauen, 2009; Bos, 1989); II) ERAS contains different amino acids in the effector binding sites in comparison to other members of the RAS family; III) ERAS has a unique extended, evolutionally conserved N-terminus (Nakhaei-Rad *et al.*, 2015) (chapter II).

Sequence deviations in effector binding regions of ERAS—HRAS, NRAS and KRAS4B share an identical effector binding regions suggesting that they may share the same downstream effectors. In contrast, ERAS revealed significant differences in the effector binding regions. This implicates that it may utilize other effectors as compared to known HRAS effectors and may consequently have different cellular functions. However, the downstream effectors selective for ERAS are not fully identified yet. A known HRAS effector is phosphoinositide 3-kinase (PI3K) that has also been reported to be activated by ERAS (Fig. 2) (Takahashi *et al.*, 2003; Takahashi *et al.*, 2005; Yu *et al.*, 2014) (chapter II and III).

N-terminal extension—ERAS is distinguished from the classical RAS isoforms due to its unique extended N-terminus. This may provide a putative interaction site for a new group of proteins, which may determine its subcellular localization. For instance, it contains a PxxP motif that may serve as a putative binding motif for interaction with SH3-containing proteins (Fig. 4) (Nakhaei-Rad *et al.*, 2015) (chapter II).

RRAS subfamily of RAS proteins

RRAS shares particular cellular functions with other RASs, such as cell proliferation and transformation (Shang *et al.*, 2011; Yu and Feig, 2002; Flex *et al.*, 2014). However, *RRAS* has been implicated in specific biological processes, i.e., integrin-dependent cell adhesion, cell spreading, migration and membrane ruffling (Kinbara *et al.*, 2003; Ada-Nguema *et al.*, 2006; Goldfinger, 2006; Holly *et al.*, 2005). In comparison with HRAS, *RRAS* can interact with a set of HRAS effectors like, PI3K α/γ , CRAF, RASSF5 and PLC ϵ (Marte *et al.*, 1997; Rey *et al.*, 1994; Vavvas *et al.*, 1998; Ada-Nguema *et al.*, 2006), however, it has its own specific effector, RLIP76 (RALBP1) that has mediated cell-adhesion dependent RAC activation (Goldfinger, 2006). Interestingly, in endothelial cells the *RRAS*-RIN2-RAB5 axis stimulates endocytosis of β_1 integrin in a RAC1-dependent manner (Sandri *et al.*, 2012). Moreover, sequence analysis revealed similar to ERAS, *RRAS* harbors extended N-terminus (26 amino acid length), which modulates *RRAS* specific functions but revealed no impact in cellular localization (Holly *et al.*, 2005). Therefore, *RRAS* carries out its specific function in the cells through its unique N-terminus and individual effector protein.

Muscle RAS oncogene homolog (MRAS) is a *RRAS*-related protein that involved in different cellular processes such as cell growth and differentiation (Kimmelman *et al.*, 1997; Watanabe-Takano *et al.*, 2010). Bone morphogenetic protein-2 (BMP-2) treatment on skeletal muscle myoblasts during their transdifferentiation towards osteoblasts, results in an increased expression of *MRAS* at mRNA and protein levels as well as its activation (Watanabe-Takano *et al.*, 2010). Among the different members of RAS family, only *MRAS* can interact with SHOC2 in ternary complex with protein phosphatase 1 (PP1), which dephosphorylates autoinhibited CRAF and activate the CRAF-MEK-ERK axis (Rodriguez-Viciano *et al.*, 2006). Similar to *RRAS*, *MRAS* can stimulate the cell migration when it is overexpressed (Young *et al.*, 2013).

RAP subfamily of RAS proteins

In mammalian RAP subfamily is composed of five isoforms, RAP1 (A, B) and RAP2 (A, B and C) with 60% sequence homology. The switch I/II regions, where interact with effector proteins, have amino acid deviations between isoform RAP1 and RAP2 which specify their signaling towards different pathways (Gloerich and Bos, 2011). They are involved in different cellular processes and play pivotal roles in cell motility, endothelial barrier functions, polarity and cell adhesion (Torti and Lapetina, 1994; Paganini *et al.*, 2006; Frische and Zwartkruis, 2010; Pannekoek *et al.*, 2013). RAP2A, is reported to be involved in the polarity of intestine cells. Apical localization of PDZ-GEF activates RAP2A and GTP-bound RAP2A interacts with its effector, TNIK, and switches on the TNIK-MST4-Ezrin axis that consequently results in actin remodeling (Gloerich *et al.*, 2012). Recently, it has been shown RAP2A as a novel target gene of p53 and as a regulator of cancer cell migration (Wu *et al.*, 2015). Moreover, expression of RAP2A in cancer cells results in secretion of two matrix metalloproteinases (MMP2 and 9) and AKT phosphorylation at Ser473 that promotes tumor invasion (Wu *et al.*, 2015).

Effectors and signaling of RAS proteins

The RAS effectors carry either RAS binding (RBD) or RAS association (RA) domain and they are interacting with GTP-bound forms of RAS proteins in switch I and switch II regions. Through the interaction with effector proteins, RAS proteins are able to exert their biological functions, and depending on which target effectors get activated the cellular outcomes various (Fig. 2) (Wittinghofer and Vetter, 2011; Karnoub and Weinberg, 2008). Herein, we will have an overview about a set of well-annotated RAS effectors and their signaling cascades; RAF kinase, RALGDS, PLC ϵ , RASSFs and PI3K.

Mitogen –activated protein kinase signaling

RAF kinase (MAPKKK)—RAF family members are serine/threonine protein kinase with three RAF isoforms in mammalian, CRAF (RAF1), ARAF and BRAF. All carry an N-terminal RBD and C-terminal serine/threonine kinase domain. It is proposed that binding of RAS-GTP to N-terminal RBD of RAF kinase, relieves the auto-inhibitory effects of their N-terminus and brings the RAF on the plasma membrane, however, still the underlying mechanism that RAS can activate RAF is not fully investigated (Lavoie and Therrien, 2015). Three RAF isoforms act as an RAS effector, are direct activator of MEK1/2 and consequently ERK1/2. However, BRAF was introduced as the best activator of MEK1/2 and its mutations are association with several human cancers (Karasarides *et al.*, 2004; Cantwell-Dorris *et al.*, 2011; Barras, 2015). On the other hand, ARAF mutation is not reported in cancer and it is proposed that ARAF is not strongly activated *via* RAS (Rodriguez-Viciano *et al.*, 2004; Matallanas *et al.*, 2011). RAF-MEK1/2-ERK1/2 axis contributes in different cellular processes such as cell proliferation, differentiation and apoptosis (Leicht *et al.*, 2007). Knockout studies have revealed all RAF isoforms are required for normal embryogenesis (Pritchard *et al.*, 1996; Wojnowski *et al.*, 1997; Wojnowski *et al.*, 1998).

MAP/ERK kinase (MAPKK)—MEK1 and MEK2 are serine/threonine/tyrosine kinases that phosphorylate position T202/Y204 ERK1 and T185/Y187 ERK2. RAF kinases phosphorylate S218/S222 and S222/S226 MEK1/MEK2, respectively (Hayes and Der, 2014). Beside, RAF kinase, two other serine/threonine kinases, COT (Tp12) and MOS also serve as upstream activators of MEKs (Hagemann *et al.*, 1999; Johannessen *et al.*, 2010).

ERK kinase (MAPK)—ERK1/2 are the end kinases downstream of cascade flow which are triggered from RAS-GTP bound and are substrate of MEK1/2. There are growing number of evidences, indicating the distinct biological functions of ERK1 and ERK2 (Yoon and Seger, 2006; Shin *et al.*, 2010; Shin *et al.*, 2015; Woodson and Kedes, 2012; Krens *et al.*, 2008). Unlike, RAF kinase and MEK which have a highly imitated number of substrates, collectively, ERK1/2 possess around 200 cytoplasmic or nuclear targets (Yoon and Seger, 2006).

RAL guanine nucleotide dissociation stimulator

RAS proteins interact with a wide range of proteins, and beside activation of their specific signaling cascades, are able to regulate the parallel pathways as well. A cross-talking between RAS family members can occur by proteins which carry both RBD/RA domain and GEF catalytic domain (CDC25 homology domain), therefore first as RAS effector bind to RAS and then serve as GEF to activated another RAS family members (Quilliam *et al.*, 2002; Ferro and Trabalzini, 2010). For instance, RALGDS family consists of RALGDS, RGL (RALGDS like), RGL2 (RIF) and RGL3, they harbor RA domain that interact with GTP-bound RAS (e.g., HRAS, KRAS, RAP1, RRAS, MRAS and RIT) and after activation serve as a GEF to activate RAL subfamily of small-GTPases (Spaargaren and Bischoff, 1994; Wolthuis *et al.*, 1996; Peterson *et al.*, 1996; Shao and Andres, 2000; Nakhaei-Rad *et al.*, 2015). It is reported that RAS interaction with RALGDS does not influence its GEF activity and translocates it close to membrane where can bind to its substrate, RAL (Wolthuis *et al.*, 1997; Matsubara *et al.*, 1999). Activated RAL (GTP-loaded) emits its cellular functions through interaction with its specific effectors; RALA binding protein 1 (RALBP1/RLIP76), ZO-1 associated nucleic acid-binding protein (ZONAB), exocyst complex subunits (SEC5/EXO84) and phospholipase D1 (Bodemann and White, 2014). For instance, RALBP1 plays roles in cellular processes like, mitochondrial fission, clatherin-mediated endocytosis, and cell cycle progression (Jullien-Flores *et al.*, 2000; Kashatus *et al.*, 2011; Tazat *et al.*, 2013).

Phospholipase C enzymes

PLC enzymes, are composed of six families, PLC β , γ , δ , ϵ , ζ and η (Katan, 2005). These enzymes hydrolyze the phosphatidylinositol 4,5-bisphosphate (PIP₂) and generate two second messengers that stimulate different intracellular responses: inositol 1,4,5-trisphosphate (IP₃) and diacylglycerol (DAG) (Bunney and Katan, 2011). Among PLC families, PLC ϵ is unique in regulation and function because of its prominent sequence fingerprints; I) N-terminal CDC25 domain, which serves as a GEF for RAP1 (Bunney and Katan, 2006); II) Two C-terminal RA domains (RA1/RA2) that only RA2 interacts with small-GTPase of RAS family. Therefore, PLC ϵ

acts as both effector and regulator of RAS family, similar to RALGDS (Kelley *et al.*, 2004; Bunney *et al.*, 2006); III) It has an insertion of 65 aa within Y part of its catalytic domain, where RHO proteins can bind and regulate PLC ϵ activity (Wing *et al.*, 2003).

RAS-association domain family

RAS-association domain family (RASSF) proteins compose ten members: RASSF1A/B, 2, 3, 4, 5A/B/C (NORE1), 6A/B, 7, 8, 9 and 10 which share RA domain, however, two additional domains, are not universal; ¹C1 domain (RASSF1 and 5A/B) and SARAH domain (Salvador-RASSF-HIPPO) (RASSF1-6). Two well-characterized isoforms of RASSF1/5A proteins are recognized as unique RAS effectors which in contrast to other RAS effectors, are tumor suppressor and emerge an pro-apoptotic effects and their loss of function mutations are associated with tumors (Vavvas *et al.*, 1998; van der Weyden and Adams, 2007). MST (Drosophila orthologues of HIPPO) is a STE-20 family protein kinase, which interacts, and forms a heterodimer with RASSF1/5A and WW45 (salvador) through their SARAH domain (Scheel and Hofmann, 2003). This complex phosphorylates and activates LATS1/2, which in turn promotes phosphorylation and sequestration and proteasomal degradation of YAP in cytoplasm (Ramos and Camargo, 2012a; Oka *et al.*, 2008; Zhao *et al.*, 2007; Pfeifer *et al.*, 2010; Hwang *et al.*, 2014; Rawat and Chernoff, 2015). YAP is a transcription co-activator that promotes transcription of the genes, like *CTGF* and *NOTCH2*, which are involved in cell development and differentiation (Camargo *et al.*, 2007; Avruch *et al.*, 2010; Lu *et al.*, 2010; Yimlamai *et al.*, 2014). It has been shown that HIPPO-YAP pathway plays distinct roles in differentiated parenchymal cells and liver progenitor cells, respectively. Where MST1/2 activity plays a role in maintenance of differentiated state of parenchymal cells and YAP activity dedifferentiates the cells and induces cell proliferation (Yimlamai *et al.*, 2014). A switch between activities of two RAS effectors with opposite functions, CRAF and RASSF, which stimulate cell proliferation and apoptosis, can determine the biological outcomes of RAS signaling in different circumstances (Romano *et al.*, 2014).

Phosphatidylinositol 3-kinase signaling

PI3K isoforms—PI3Ks are the intracellular lipid kinases that phosphorylate phosphatidylinositol and phosphoinositides. Based on sequence homology and lipid substrates they fall into three groups: class I, II and III. Upstream regulators of PI3K, mainly consist, receptor tyrosine kinases, RAS proteins and G protein-coupled receptors (Vanhaesebroeck *et al.*, 2010). In mammalian, class I PI3K contains four isoforms that are heterodimer proteins compose of two subunits: catalytic and regulatory subunit. According to the regulatory subunit, class I PI3K further subdivided in two subgroups; class IA p110 α , p110 β and p110 δ accompany with p85-like regulatory subunit (p85 α/β , p50 α and p55 α/γ). Class IB has single member p110 γ and makes a heterodimer with p101 and p84 regulatory subunits (Vanhaesebroeck *et al.*, 2010; Vadas *et al.*, 2011; Jean and Kiger, 2014). p110 α and β are

¹ putative diacylglycerol binding site

reported to be ubiquitously expressed but the presence of p110 γ and δ is restricted to specific cell types or tissues, mainly hematopoietic cells (Vanhaesebroeck *et al.*, 2005; Kok *et al.*, 2009; Fritsch *et al.*, 2013; Fritsch and Downward, 2013). Class I PI3K phosphorylates 3-hydroxyle of the phosphoinositide (4,5) bisphosphate (PIP₂) and generates the second messenger of phosphoinositide (3,4,5) trisphosphate (PIP₃) that recruits the wide range of protein effectors through their pleckstrin homology (PH) domain to the membrane. Target proteins, could be kinases (e.g. AKT and PDK1), adaptor proteins, GEFs or GAPs that regulate different cellular processes (Vanhaesebroeck *et al.*, 2001).

AKT serine/threonine kinase—AKT or protein kinase B (PKB) belongs to AGC subfamily of protein kinases. AKT is one of the key proteins downstream of PI3K-PIP₃ and involves in wide range of the cellular processes, such as cell proliferation, metabolism, growth, autophagy inhibition, and survival (Pearce *et al.*, 2010; Hers *et al.*, 2011). AKT functions depend on its phosphorylation at two critical positions, T308 and S473 (Andjelkovic *et al.*, 1997). Upon extracellular stimuli and the tyrosine receptor activation, class I PI3K generates the PIP₃ that engages both PDK1 and AKT through PH domain to the plasma membrane. PDK1 phosphorylates the AKT at position T308 (here after p-AKT308) that is located on the catalytic domain of AKT (Alessi *et al.*, 1997). This phosphorylation triggers the inhibitory phosphorylation of tuberous sclerosis 1/2 (TSC1/2) that is a well-known GAP for RHEB protein of RAS family. Phosphorylation of TSC1/2 suppresses its inhibitory effect on mammalian target of rapamycin (mTOR) complex 1 (Fig. 5) (Inoki *et al.*, 2002; Inoki *et al.*, 2003). Second key phosphorylation site positions on the hydrophobic motifs of AKT S473 (here after p-AKT⁴⁷³) and occurs through the second mTOR complex (mTORC2) (see below for further information).

Organization of mammalian target of rapamycin (mTOR) complex 1 and 2—mTOR kinase is the catalytic domain of two multiprotein complexes; mTORC1 and mTORC2 (Zoncu *et al.*, 2010). These complexes are discriminated mainly based on the specific accessory proteins, in the case of mTORC1 it is called regulatory-associated protein of mTOR (RAPTOR) (Hara *et al.*, 2002) and for mTORC2 it is called rapamycin-insensitive companion of mTOR (RICTOR) (Sarbasov *et al.*, 2004) (Fig 5). In addition, they harbor unique regulatory subunits, 40 kDa Pro-rich AKT substrate (PRAS40; mTORC1), mammalian stress-activated MAP kinase-interacting protein 1 (mSIN1/MAPKAP1; mTORC2) and protein observed with RICTOR (PROTOR; mTORC2) (Sancak *et al.*, 2007; Pearce *et al.*, 2007; Frias *et al.*, 2006; Yang *et al.*, 2006). However, mTORC complexes share some negative and positive regulatory proteins, DEP domain-containing mTOR-interacting protein (DEPTOR) and mammalian lethal with SEC13 protein 8 (mLST8), respectively (Peterson *et al.*, 2009; Loewith *et al.*, 2002).

Upstream regulators and substrates of the mTOR complexes—Signal integration towards mTORC1 occurs through TSC1/2 and at the lysosome level *via* RAG GTPases (Huang and Manning, 2008; Sancak *et al.*, 2008). TSC1/2 is regulated negatively by AKT (phosphorylated at position T308) and ERK1/2 (Alessi *et al.*, 1997; Ma *et al.*, 2005), whereas GSK3 β , Hypoxia and AMPK are the positive regulators (Castilho *et al.*, 2009; Inoki *et al.*, 2006; DeYoung *et al.*, 2008). AKT activity (p-T308) results in inhibitory phosphorylation of TSC1/2 which is the RHEB-

GAP (Tee *et al.*, 2003) (Fig. 5). In physiological conditions, RHEB and RAG GTPases reside on the lysosome/endosome surface. Upon the growth factor stimuli, RHEB switches to active form (GTP-loaded) and interacts with mTORC1 which activates catalytic function of mTOR and its substrate interactions through RAPTOR (Inoki *et al.*, 2003; Avruch *et al.*, 2009; Zoncu *et al.*, 2010). One essential requirement of RHEB-mTORC1 interaction is the endomembrane translocation of the mTORC1. Amino acid stimulation of RAG GTPases results in endomembrane localization of mTORC1 (Sancak *et al.*, 2008). Therefore, both growth factors and amino acids inputs are needed for mTORC1 activity (Zoncu *et al.*, 2010). mTORC1 phosphorylates wide range of substrates and regulates the ribosome biogenesis, mRNA translation, lipid synthesis and autophagy (Fig. 5) (Kim and Chen, 2004; Porstmann *et al.*, 2008; Yu *et al.*, 2010; Iadevaia *et al.*, 2012; Gentilella *et al.*, 2015). S6 kinase 1 (S6K1) is the most prominent kinase downstream of mTORC1 and phosphorylates mTOR itself at position S2448, ribosomal protein S6, eukaryotic elongation factor 2 kinase (eEF2) kinase and eIF4B (Hara *et al.*, 1997; Wang *et al.*, 2001; Ma *et al.*, 2008; Ma and Blenis, 2009). The upstream regulators of the mTORC2 are poorly understood and growth factor signaling and its association with ribosome are indicated to control mTORC2 signaling activity (Zinzalla *et al.*, 2011). Recently, a possible cross-talk between mTORC1 and mTORC2 is reported that S6K phosphorylates a regulatory subunit of mTORC2 is called mSIN1 at two positions which is critical for the integrity and substrate recruitment (e.g. AKT) of the mTORC2 (Fig. 5) (Liu *et al.*, 2013b; Xie and Proud, 2013; Liu *et al.*, 2014b). Furthermore, upon stimulation mTORC1 exerts a negative feedback regulatory through phosphorylation of the insulin receptor substrate-1 (IRS-1) and adaptor protein Grb10 which suppress the growth factor induced signaling (Um *et al.*, 2004; Hsu *et al.*, 2011). mTORC2 phosphorylates AGC kinases, AKT (p-AKT473), serum and glucocorticoid-regulated kinase (SGK) and protein kinase C (PKC) (Sarbasov, 2005; Garcia-Martinez and Alessi, 2008; Ikenoue *et al.*, 2008; Su and Jacinto, 2011). AKT phosphorylation at the hydrophobic motifs (S473) results in full activation of AKT for special substrates, such as FOXO1 and 3. Inhibitory phosphorylation of FOXO1/3 by AKT sequesters it in the cytoplasm and impairs its translocation to the nucleus where it binds to gene promoters and induces apoptosis, therefore favors the cell survival (Wang *et al.*, 2014). Collectively, mTORC2 regulates cell cycle progression, survival, anabolism and actin cytoskeleton organization (Jacinto *et al.*, 2004).

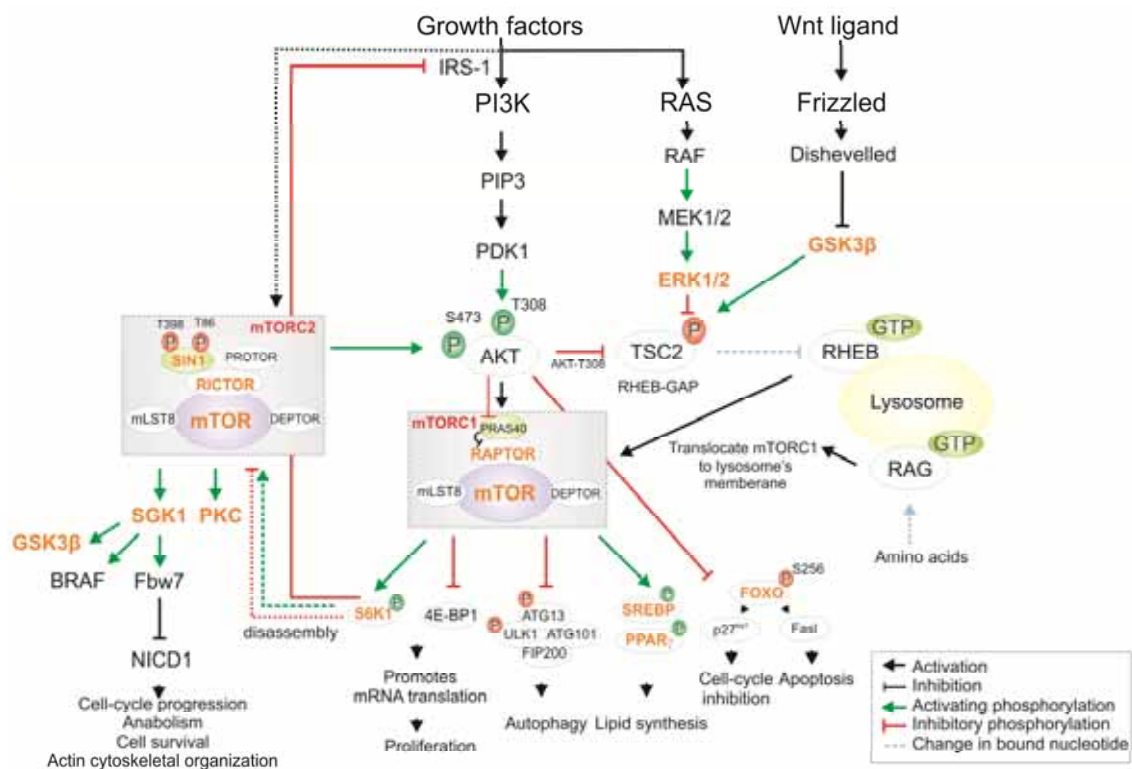


Figure 5. Schematic view of signaling pathway of the mammalian target of rapamycin (mTOR) complexes. Complexes composition, stimulation, regulation, substrates and cellular outcomes are illustrated. DEPTOR, DEP domain-containing mTOR-interacting protein; ERK, extracellular regulated kinase; Fbw7, F-box and WD repeat domain containing 7; FIP200, FAK family kinase-interacting protein of 200 kDa; 4E-BP1, eukaryotic translation initiation factor 4E binding protein 1; FOXO1, forkhead transcription factor; IRS1, insulin receptor substrate 1; GAP, GTPase activating protein; GSK3 β , glycogen synthase kinase 3 beta; MEK, MAP/ERK kinase; mLST8, mammalian lethal with SEC13 protein 8; mSIN1, mammalian stress-activated MAP kinase-interacting protein 1; mTORC, mammalian target of rapamycin; NICD1, Notch intracellular domain; PDK1, 3-phosphoinositide-dependent protein kinase; PI3K, phosphoinositide 3-kinase; PKC, protein kinase C; PPAR γ , peroxisome proliferator-activated receptor γ ; PRAS40, 40 kDa Pro-rich AKT substrate; PROTOR, protein observed with RICTOR; RAPTOR, regulatory-associated protein of mTOR; RAS, rat sarcoma; RHEB, RAS homologue enriched in brain; RICTOR, mTORC2 rapamycin-insensitive companion of mTOR; SGK, serum and glucocorticoid-regulated kinase; SREBP, sterol regulatory element-binding proteins; TSC, tuberous sclerosis; ULK, Unc-51 like autophagy activating kinase 1.

In the previous section, we had an overall view about the members, functions, target proteins and signaling activities of the RAS family of the small GTPases. In following section, we will consider second largest family of small GTPases is named RHO (RAS homologous) and the cross-talking between RAS and RHO proteins to orchestrate different cellular responses.

RHO family GTPases

RHO Family members, functions and regulation— RHO family GTPases have key functions in cytoskeletal organization, migration, adhesion, survival and cell cycle progression (Heasman and Ridley, 2008b). To date, 20 members of the RHO family have been reported, which further are subdivided into six subfamilies based on their sequence homology: I) RHO (RHOA, RHOB, RHOC); II) RAC (RAC1, RAC1b, RAC2, RAC3, RHOG); III) CDC42 (CDC42, G25K, TC10, TCL, RHOU/Wrch1, RHOV/Chp); IV) RHOD (RHOD, Rif); V) RND (RND1, RND, RND3); VI) RHOH/TTF (Fig. 3). The GDP/GTP exchange and the GTP hydrolysis of typical RHO proteins (Jaiswal *et al.*, 2013b), are regulated by RHOGEF and RHO GAP proteins, respectively. However, in comparison with RAS family, RHO proteins underlie a third control mechanism, which is achieved by the function of guanine nucleotide dissociation inhibitors (GDIs) and bind selectively to prenylated RHO proteins and control their cycle between cytosol and membrane (see chapter IV). Activation of RHO proteins results in their association with effector molecules that subsequently activate a wide variety of downstream signaling cascades (Bishop and Hall 2000; Burridge and Wennerberg 2004).

RHO subfamily

In mammalian, there are three RHO isoforms, RHOA, RHOB and RHOC with well-known function in stress fiber formation (Wheeler and Ridley, 2004). RHOA plays roles in cell migration, cytokinesis and cell cycle progression (Vega and Ridley, 2008). On the other hand, RHOB introduced as a tumor suppressor, which its down-regulation was reported in a set of tumors (Huang and Prendergast, 2006). RHOB regulates the trafficking of the cellular receptors that limits the growth factors signaling (Huang *et al.*, 2007), and by internalization of E-cadherin, and integrin, modulates the cell-cell adhesion and migration speed (Wheeler and Ridley, 2007; Vega *et al.*, 2015). RHOC isoform was reported to promote tumor metastasis and invasion (Pille *et al.*, 2005). Similar to other GTPases, RHO subfamily emerges its cellular functions by binding to a set of scaffolding: Rhotekin, Rhophilin, mammalian diaphanous (mDia) and PLC or kinase effector proteins: RHO-associated coiled-coil kinases I/II (ROCKI/II), protein kinase C-related kinase (PKR) and Citron (Reid *et al.*, 1996; Thumkeo *et al.*, 2013; Amin *et al.*, 2013).

CDC42 GTPase

CDC42 functions implicate in cellular control of cytoskeleton dynamic, cellular polarity, migration, adhesion, intracellular trafficking and proliferation (Aznar and Lacal, 2001; Cerione, 2004). CDC42 is famous for its contribution in formation of cell protrusions is called filopodia. Filopodia is the finger-shape structure that consists of parallel bundles of actin filaments and acts as antenna to sense the cellular microenvironment and plays important roles in cell migration and neuronal outgrowth (Gupton and Gertler, 2007; Mattila and Lappalainen, 2008). Activated CDC42 targets a set of effectors: p21-activated kinase (PAK), insulin receptor substrate p53 (IRSp53), mammalian diaphanous (mDia), Wiskott-Aldrich syndrome protein (WASP) (Hemsath *et al.*, 2005) and IQ motif-containing GTPase-activating protein (IQGAP)

(Cerione, 2004; Sinha and Yang, 2008). CDC42 interaction with WASP and IRSp53 activates the actin related protein 2/3 (ARP2/3) that mediates the filopodia formation (Hufner *et al.*, 2002; Lim *et al.*, 2008). mDia was known as a third effector of CDC42 which contributes in filopodia formation (Peng *et al.*, 2003). Upon CDC42 binding to PAK1 and LIM kinase (LIMK) phosphorylation, LIMK phosphorylates and inhibits actin depolymerization through cofilin (Edwards *et al.*, 1999).

RAC subfamily

Based on the sequence homology, RAC subgroup of RHO GTPases consists of five members: RAC1, RAC1b, RAC2, RAC3, RHOG. RAC proteins involve on lamellipodium formation and membrane ruffling, which are required for the maintenance of cell morphology and migration (Kurokawa *et al.*, 2004). RAC isoforms exhibit the individual pattern of gene expression and they have non-overlapping functions (Didsbury *et al.*, 1989; Shirsat *et al.*, 1990; Bolis *et al.*, 2003). RAC1b is alternative splice variant of RAC1 with 19 amino acid insertion near the switch II region that renders RAC1b in active GTP-bound form with impaired GTP hydrolysis (Fiegen *et al.*, 2004). RAC shares some effectors with CDC42 like, mDia2 and PAK, however has its specific effectors, such as WASP-family verprolin-homologous protein (WAVE), specifically RAC1-associated protein-1 (SRA1) and p67PHOX (Kobayashi *et al.*, 1998; Koronakis *et al.*, 2011; Diebold *et al.*, 2004). Upon RAC1 activation and binding to WAVE, mDia and PAK, actin polymerization and turn over will be regulated by RAC1 and results in lamellipodia formation (Jaffe and Hall, 2005; Takenawa and Suetsugu, 2007).

Signaling cross-talk between RHO and RAS GTPases

GTPase-activating proteins (GAPs) link the RAS and RHO signaling—The GAP proteins were identified to interconnect the RAS and RHO signaling, which is known to be required for cell transformation by oncogenic RAS and, cell cycle progression and proliferation by RHO proteins (Khosravi-Far *et al.*, 1998; Coleman *et al.*, 2004). Emerging evidence suggests that the GAPs, in particular p120RASGAP and the RHO-specific p190ARHOGAP, p200RHOGAP and deleted in liver cancer 1 (DLC1), act as a linker to coordinate the RAS and RHO signaling pathways (Shang *et al.*, 2007; Yang *et al.*, 2009; Asnaghi *et al.*, 2010). Frequent loss of DLC1 gene expression was first described in liver (Yuan *et al.*, 1998). DLC1RHOGAP function is required for the maintenance of cell morphology and the coordination of cell migration (Kim *et al.*, 2008). p120 contains multiple domains with different functions (Pamonsinlapatham *et al.*, 2009). While the C-terminus of p120 with the catalytic GAP activity is responsible for RAS inactivation (Ahmadian *et al.*, 1997a), its N-terminal Src homology 2 and 3 (SH2 and SH3) domains have been suggested to possess effector function (Chan and Chen, 2012). p120 functionally modulates RHO signaling by directly binding to two RHO-specific GAPs, p190 and DLC1 (Yang *et al.*, 2009; Asnaghi *et al.*, 2010). The association of p120 with the tyrosine phosphorylated p190 *via* its SH2 domain promotes RHO inactivation (Hu and Settleman, 1997; Herbrand and Ahmadian, 2006). Thus, p120 positively regulates the RHOGAP function of p190. Another mechanism, which connects the RAS and RHO pathways and regulates the actin

cytoskeleton, is dependent on p120 SH3 domain function and controls RHO activation (Leblanc *et al.*, 1998). This mechanism was later revealed to involve DLC1 but not p190. The p120 SH3 domain (called p120SH3) binds to the RHO GAP domain of DLC1 (called DLC1GAP) and inhibits the DLC1-dependent RHO inactivation (Yang *et al.*, 2009). Therefore, p120 acts as a negative regulator not only for RAS but also for the GAP activity of DLC1 (chapter V).

Scaffolding proteins cross-link the RAS/RHO signaling components—Scaffolding proteins are multidomain proteins, which are able to interact with plethora of substrates and control the spatial and temporal assembling of signaling partners. Thereby, through the tethering mechanism, they organize the discrete components of signaling pathways in place and time, (e.g., activators, enzymes and effectors) to increase their interaction efficiency (Scott and Pawson, 2009; Good *et al.*, 2011). IQGAP proteins emerge diverse cellular functions such as cell migration, adhesion, cytoskeletal dynamic and cytokinesis (Noritake *et al.*, 2005; White *et al.*, 2012). By acting as scaffold proteins, IQGAPs organize the signaling partner into close proximity to enable their interaction/activation and in some cases act as a bridge to connect distinct signaling pathways (Brown and Sacks, 2006). IQGAP family composes of three isoforms, IQGAP1, 2 and 3, which are differentially expressed in distinct tissues. In addition to share a set of binding partners, each isoform possesses its specific binding partners and therefore contributes to different cellular processes (Weissbach *et al.*, 1994; Brill *et al.*, 1996; Wang *et al.*, 2007). For instance, IQGAP1 was recognized as an oncogene where IQGAP2 is a tumor suppressor (White *et al.*, 2009b; White *et al.*, 2010b). IQGAP1 can interact with different signaling components of MAPK pathway, RTKs, KRAS, BRAF/CRAF, MEK1/2 and ERK1/2, and directs the information flow from the EGF to ERK1/2 phosphorylation (Roy *et al.*, 2004; Roy *et al.*, 2005; Ren *et al.*, 2007). In addition to scaffold the RAS signaling components, IQGAP1 was identified to interact with RHO family GTPase, RAC1 and CDC42, and promotes the cell migration (Mataraza *et al.*, 2003a). Upon hyaluronan (HA) stimulation of CD44 receptor, IQGAP1 anchors the CDC42 and ERK2 to CD44 and F-actin that results in phosphorylation of ERK2. Therefore, it bridges the MAPK pathways to cytoskeleton organization machinery (Bourguignon *et al.*, 2005) (chapter VI).

Disease models indicate the coordination of RAS and RHO mutations in tumor progression—As we discussed earlier there are different levels of RAS and RHO cross-talking: at the levels of GAP or scaffolding proteins. However, there are emerging lanes of evidences that indicate the coexistence of RAS and RHO mutations in tumors. Mano and colleagues, reported that the oncogenic mutation of RAC1^{N92I} beside the NRAS^{Q61K} mutation drives the growth of human sarcoma cell line, HT1080 (Kawazu *et al.*, 2013). Juvenile myelomonocytic leukemia (JMML) is a rare and early childhood severe myeloproliferative neoplasm that is resulted from infiltration of overproduced myelomonocytic cells to organs, such as liver, spleen and intestine. Pathological studies revealed that the JMML is initiated by germline or somatic RAS-activating mutations (Chang *et al.*, 2014). JMML is considered a unique example of RAS-driven oncogenesis since it is thought to be initiated by mutations, usually described as mutually exclusive, in RAS genes (NRAS, KRAS) or RAS-pathway regulators (PTPN11, NF1 or

CBL) (Niemeyer, 2014). Genetic profiling of the JMML patient with *NRAS* mutation depicted the second mutation which belongs to RHO GTPase (*RAC2*) (Caye *et al.*, 2015). However, the mechanisms that *RAC2* mutation coordinates with *NRAS* transformation need further investigation (chapter VII).

Aims and objectives

Hepatic stellate cells (HSCs) play pivotal roles in liver development, immunoregulation, homeostasis, regeneration, and pathology. In addition, they emit a remarkable plasticity in their phenotype, expression profile and function. HSCs are able to develop to cells that contribute in liver regeneration or in pathological situations promote scar formation and liver fibrosis (see Figs. 1C, D and E). However, little is known about the intracellular signaling networks, which orchestrate HSCs plasticity and their bilateral functions as positive and negative regulators of liver damage responses. Therefore, it is noteworthy to reconsider the impact of different signaling pathways on HSC fate decision and obtained information will lead future studies to find pharmacological drugs that target HSC activation and shift them to participate in liver regeneration. In this study, we set out to cover the activities and functions of RAS dependent signaling pathways in both quiescent HSC (qHSC) and activated HSC (aHSC) and generate a new model that will help to a better understanding of signaling networks of HSC (Fig. 8). This will provide hope for the patients with liver problems to restore their liver regeneration responses.

At the first, we tried to get an overview about which RAS isoforms are mostly influenced by the HSC activation processes. Therefore, by the aim of isoform specific qPCR primers, we sought for the expressional changes of different RAS family members and their signaling compartments during the HSC activation. We found a novel member of RAS family, *ERAS*, specifically expressed in qHSC not aHSC where other RAS isoforms did not show significant changes or get up-regulated. The molecular properties, regulation and function of this new RAS member is poorly understood. Therefore, we comprehensively investigated biochemical and structural characteristics of exogenous ERAS to get an overview of the physiological functions of ERAS (see chapter II).

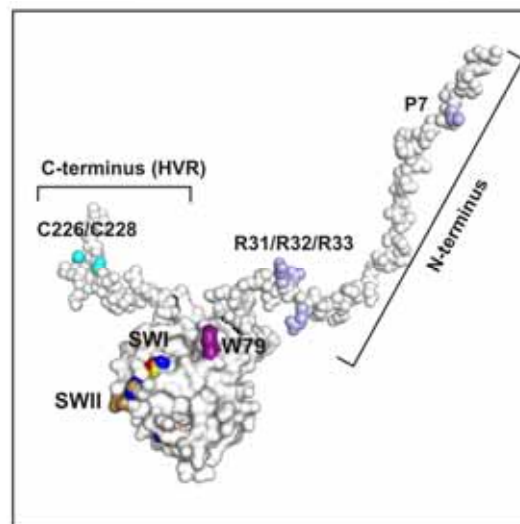
Second, we aimed to detect and analyze ERAS protein in HSC. Therefore, we generated an anti-rat ERAS antibody that specifically recognized ERAS not other RAS proteins. With this study, we reported for the first time, the endogenous expression of ERAS in non-malignant and normal cells of the body. Therefore, it was noteworthy to reinvestigate our obtained data from overexpressed ERAS in endogenous system and find out the signaling networking of ERAS in qHSC as well as monitor signaling activity of RAS proteins in aHSC (chapter III).

Activated HSCs are enabling to contract and migrate as a consequent of RHO signaling activity. We extended and shared our knowledge about molecular properties and regulation of RHO GTPases as a book chapter (chapter IV). Next, we aimed to find a possible cross-talk between RHO and RAS GTPases in two distinct levels; I) GTPase activation proteins of p120, p190 and DLC1 (deleted in liver cancer1) (chapter V). II) Scaffolding proteins such as IQGAP isoforms (chapter VI). Through conducting these studies to cell based analysis in HSCs, we revealed interesting aspect of scaffolding and cross-linking between RAS and RHO proteins. At the end, we tried to find a link between RHO and RAS mutations in disease progression with the aid of whole genomic sequencing of the juvenile myelomonocytic leukemia (JMML) patients (chapter VII).

Chapter II

The function of embryonic stem cell-expressed RAS (ERAS), a unique RAS family member, correlates with its additional motifs and its structural properties

Graphical Abstract



Published in:

The journal of biological chemistry

Impact factor:

4.56 (2014)

Own Proportion to this work:

85%

Site direct mutagenesis

Cloning

Transfection

Confocal microscopy

Pull-down assay

Immunoblotting

Preparing of the manuscript

The Function of Embryonic Stem Cell-expressed RAS (E-RAS), a Unique RAS Family Member, Correlates with Its Additional Motifs and Its Structural Properties^{*[5]}

Received for publication, January 28, 2015, and in revised form, April 21, 2015. Published, JBC Papers in Press, May 4, 2015, DOI 10.1074/jbc.M115.640607

Saeideh Nakhaei-Rad[‡], Hossein Nakhaeizadeh[‡], Claus Kordes[§], Ion C. Cirstea^{†*}, Malte Schmick^{||}, Radovan Dvorsky[‡], Philippe I. H. Bastiaens^{||}, Dieter Häussinger[§], and Mohammad Reza Ahmadian^{†1}

From the [‡]Institute of Biochemistry and Molecular Biology II and [§]Clinic of Gastroenterology, Hepatology, and Infectious Diseases, Medical Faculty of the Heinrich-Heine University, 40255 Düsseldorf, the [†]Leibniz Institute for Age Research-Fritz Lipmann Institute, 07745 Jena, and the ^{||}Department of Systemic Cell Biology, Max Planck Institute of Molecular Physiology, 44227 Dortmund, Germany

Background: E-RAS contains additional motifs and regions with unknown functions.

Results: Biochemical analysis reveals that effector selection of E-RAS significantly differs from H-RAS.

Conclusion: E-RAS selectivity and consequently cellular outcomes depend on its unique switch and interswitch regions.

Significance: E-RAS possesses specific sequence fingerprints and therefore no overlapping function with H-RAS.

E-RAS is a member of the RAS family specifically expressed in embryonic stem cells, gastric tumors, and hepatic stellate cells. Unlike classical RAS isoforms (H-, N-, and K-RAS4B), E-RAS has, in addition to striking and remarkable sequence deviations, an extended 38-amino acid-long unique N-terminal region with still unknown functions. We investigated the molecular mechanism of E-RAS regulation and function with respect to its sequence and structural features. We found that N-terminal extension of E-RAS is important for E-RAS signaling activity. E-RAS protein most remarkably revealed a different mode of effector interaction as compared with H-RAS, which correlates with deviations in the effector-binding site of E-RAS. Of all these residues, tryptophan 79 (arginine 41 in H-RAS), in the interswitch region, modulates the effector selectivity of RAS proteins from H-RAS to E-RAS features.

Small GTPases of the RAS family act as molecular switches within the cell, cycling between a GTP-bound (active) and a GDP-bound (inactive) state (1, 2). These molecules trigger intracellular responses by sensing the extracellular signals through their interacting receptors or intermediate proteins and passing the signal to downstream targets. Therefore, they play a key role in various cellular processes, including gene expression, metabolism, cell cycle progression, proliferation, survival, and differentiation. Somatic or germ line mutations in genes related to members of the RAS family or their regulators

are commonly associated with cancer progression or developmental disorders (3–9).

The best investigated RAS proteins are H-, N-, and K-RAS4B, which share overlapping functions, including cell proliferation, differentiation, and apoptosis (10–13). However, different RAS isoforms exhibit a particular pattern of expression, different regulators, and specific microdomains or subcellular localization, indicating their functional specificity as well as redundant roles (10–17). The individual roles of other members of the RAS family, such as R-RAS, TC21, M-RAS, AGS-1, or the embryonic stem cell-expressed RAS (E-RAS), have not been fully described. E-RAS was identified in 2003 as a new member of the RAS family, which is specifically expressed in undifferentiated mouse embryonic stem cells (18). In addition to stem cells, E-RAS has been detected in the several adult cynomolgus tissues (19) and in gastric cancer and neuroblastoma cell lines (20, 21).

Plasma membrane localization of the classical RAS isoforms (H-, N-, and K-RAS4B) has been shown to be critical for their functionality (22–24). The membrane association is achieved by post-translational modifications (PTMs)² at the C terminus of RAS proteins. H-RAS and N-RAS undergo two types of PTMs, farnesylation at a cysteine residue in CAAX (where C is cysteine, A is any aliphatic amino acid, and X is any amino acid) motifs and palmitoylation of one or two cysteine residues in the hypervariable region (HVR) (23, 25–27). K-RAS4B lacks the cysteine residues in its HVR; instead it has a basic sequence of six lysines that maintains its strong association with the plasma membrane (24, 28, 29).

RAS proteins are inefficient GTP-hydrolyzing enzymes. Such an intrinsic GTPase reaction requires stimulation through GTPase-activating proteins (GAPs) by orders of magnitude (30–32). However, GDP dissociation is also a very slow

* This work was supported in part by the German Research Foundation through Collaborative Research Center 974 (Grant SFB 974), Communication and Systems Relevance during Liver Injury and Regeneration. The authors declare that they have no conflicts of interest with the contents of this article.

[5] This article contains supplemental Fig. S1.

¹ To whom correspondence should be addressed: Institut für Biochemie und Molekularbiologie II, Medizinische Fakultät der Heinrich-Heine-Universität, Universitätsstr. 1, Gebäude 22.03.03, 40255 Düsseldorf, Germany. Tel.: 49-211-81-12384; Fax: 49-211-81-12726; E-mail: reza.ahmadian@uni-duesseldorf.de.

² The abbreviations used are: PTM, post-translational modification; RBD, RAS-binding domain; aa, amino acid; GEF, guanine nucleotide exchange factor; PLC, phospholipase C; PDB, Protein Data Bank; MDCK, Madin-Darby canine kidney cell; HVR, hypervariable region; PIP₃, phosphoinositide 3,4,5-trisphosphate; RA, RAS association; GAP, GTPase-activating protein; EYFP, enhanced YFP.

Functional Properties of E-RAS

reaction that needs acceleration by guanine nucleotide exchange factors (GEFs) (33, 34). RAS proteins share a highly conserved GTP-binding (G) domain with five essential motifs, termed G1 to G5 (supplemental Fig. S1) (35, 36). G1 or the P-loop ($^{10}\text{GXXXGK(S/T)}^{17}$; H-RAS numbering) binds the β - and γ -phosphates of GTP (37). Substitution of glycine 12 to any other amino acid (except for proline) is most frequently found in human cancers. These mutations render RAS protein GAP-insensitive and consequently hyperactive (7, 38). G2 and G3, also referred to as switch I and switch II, respectively, are dynamic regions that sense the nucleotide state and provide the regulator and effector-binding sites (1, 39). G4 and G5 are important for determining the guanine base-binding specificity of the G domain (40, 41). Sequence analysis revealed that E-RAS contains a G domain with five fingerprint sequence motifs almost identical to classical RAS proteins indicating that it is a functional GTP-binding protein (supplemental Fig. S1). However, E-RAS contains a serine instead of glycine 12 (H-RAS numbering), making it GAP-insensitive (18).

H-, N-, and K-RAS4B share an identical effector binding regions (switch I and II; supplemental Fig. S1), suggesting that they may share the same downstream effectors. In contrast, E-RAS revealed significant differences in the effector binding regions (supplemental Fig. S1). This implicates that it may utilize other effectors as compared with known H-RAS effectors and may consequently have different cellular functions. However, the downstream effectors selective for E-RAS are not fully identified yet. A known H-RAS effector is phosphoinositide 3-kinase (PI3K) that has also been reported to be activated by E-RAS (18, 27, 42).

In addition to effector binding regions, E-RAS is distinguished from the classical RAS isoforms due to its unique extended N terminus (Fig. 1A and supplemental Fig. S1). This may provide a putative interaction site for a new group of proteins, which may determine its subcellular localization. For instance, it contains a PXXP motif that may serve as a putative binding motif for interaction with Src homology 3-containing proteins. In this study, we comprehensively investigated human E-RAS and its variants regarding their cellular localization and functional and structural properties in direct comparison with H-RAS wild-type and its G12V hyperactive variant. We found that N-terminal extension of E-RAS is important for E-RAS signaling activity. E-RAS protein most remarkably revealed different effector selectivity as compared with H-RAS, which is influenced by deviations in the effector-binding site of E-RAS. Data presented in this study implicate that in addition to switch regions, the interswitch region of E-RAS also contributes to high affinity binding to PI3K α and low affinity to other RAS effectors, including RASSF5/Nore1, RAF1, Ral guanine nucleotide dissociation stimulator (RalGDS), and phospholipase C ϵ (PLC ϵ).

Materials and Methods

Constructs—Human E-RAS cDNA was obtained from pCMV6-AC-hsE-RAS (Origene). Human H-RAS was obtained from pTACH-RAS (43). H-RAS^{Val-12}, E-RAS^{Ser-226/Ser-228}, E-RAS^{Ser-7}, and E-RAS^{Ala-31/Ala-32/Ala-33} were generated by PCR-based site-directed mutagenesis as described (32). The E-RAS with the N-terminal deletion, lacking the first 38 amino

acids (aa) (E-RAS ^{Δ N}), was designed using primers to amplify E-RAS cDNA starting from aa 39 and ending with aa 233 (supplemental Fig. S1). The same primers were used to generate E-RAS ^{Δ N/Ser-226/Ser-228} (palmitoylation-dead variant of E-RAS lacking the N terminus) using E-RAS^{Ser-226/Ser-228} as template. To generate E-RAS constructs with mutations in their effector binding regions, we used E-RAS^{WT} cDNA as template. First, E-RAS^{SwI} (H70Y/Q75E; Tyr-32 and Glu-37 in H-RAS), E-RAS^{Arg-79} (W79R; Arg-41 in H-RAS), and E-RAS^{SwII} (A100E/I101E/H102Y/R103S; Glu-62, Glu-63, Tyr-64, and Ser-65 in H-RAS) were generated. These constructs were used to generate E-RAS^{SwI/Arg-79}, E-RAS^{SwI/SwII}, E-RAS^{Arg-79/SwII}, and E-RAS^{SwI/Arg-79/SwII}, respectively. All cDNAs were amplified via PCR and subcloned via BamHI/XhoI in pcDNA 3.1 vector with an N-terminal FLAG tag or EcoRI/BamHI in pEYFP-C1.

Cell Culture and Transfection—MDCK II and COS-7 cells were cultured in Dulbecco's modified Eagle's medium (DMEM) supplemented with 10% fetal calf serum (FCS) and 50 units of penicillin/streptomycin (Gibco® Life Technologies, Inc.). Transfection was performed by using TurboFect transfection reagent, according to manufacturer's protocol (Life Technologies, Inc.).

Immunostaining—Cells were fixed with 4% paraformaldehyde for 20 min at room temperature. After washing with PBS, the cells were permeabilized with 0.25% Triton X-100/PBS for 5 min and washed again. For blocking, the cells were treated 1 h with PBS containing 0.25% Triton X-100 and 3% bovine serum albumin (BSA, Merck) at room temperature, then incubated with primary antibodies for 1 h, then washed three times, followed by incubation with secondary antibodies for 2 h at room temperature. The coverslips were mounted using ProLong® Gold antifade reagent contained DAPI dye (Life Technologies, Inc.). Primary antibodies were rabbit anti-FLAG (1:700, catalog no. F7425 Sigma) and mouse anti-Na⁺/K⁺-ATPase (1:100, catalog no. A275 Sigma), and secondary antibodies Alexa 488-conjugated goat anti-rabbit IgG (1:500, catalog no. A11008, Life Technologies, Inc.) and Alexa 546-conjugated goat anti-mouse IgG (1:500, catalog no. A11003, Life Technologies, Inc.). The images were taken by using an LSM 510-Meta microscope (Zeiss) at excitation wavelengths of 364, 488, and 546 nm.

Live Cell Imaging—MDCK II cells were seeded on Permanox 8-well chambered slides (Lab-Tek, Nunc). LSM 510-Meta microscope (Zeiss) was equipped with $\times 63$ immersion objective, and fluorescent fusion proteins were excited using lasers with 504 nm (YFP) wavelength. An environmental chamber holds the temperature at 37 °C, and the cells were maintained in imaging medium.

Pulldown Assay and Immunoblotting—The RAS-binding domain (RBD) of RAF1 (aa 51–131), the RAS association (RA) domain of RalGDS (aa 777–872), the RA domain of PLC ϵ (aa 2130–2240), the RBD of p110 α (aa 127–314), the catalytic subunit of PI3K α , and the RA domain of RASSF5 (aa 200–358) were inserted in pGEX-4T vector and expressed in *Escherichia coli* to obtain GST-fused proteins. Bacterial lysates were used to pull down GTP-bound RAS proteins from total cell lysates. GST pull down and immunoblotting using rabbit anti-FLAG (1:5000, catalog no. F7425 Sigma) and rat anti- α -tubulin (1:2000, SM 568, Acris) were carried out as described previously (44). In

Functional Properties of E-RAS

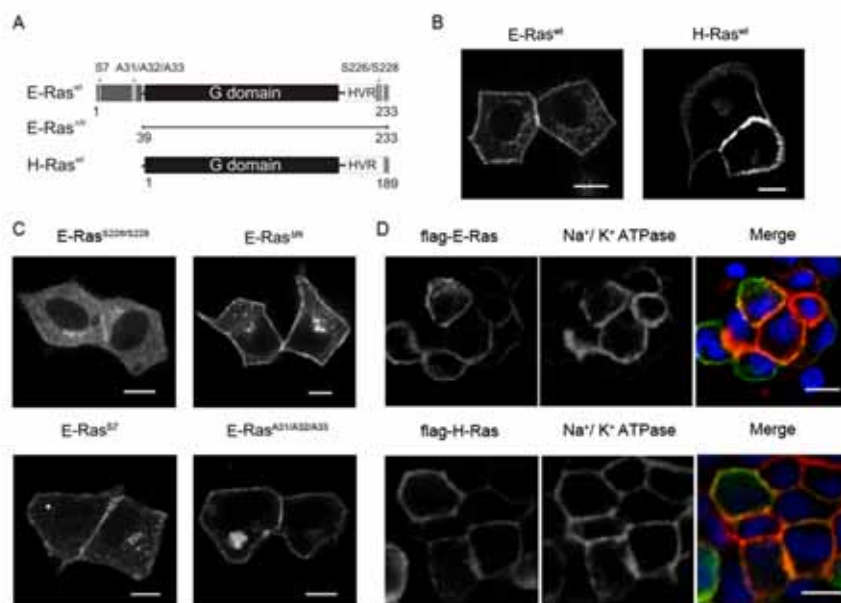


FIGURE 1. Human E-RAS is largely associated with plasma membrane and some regions of E-RAS modulating its cellular localization. A, different E-RAS variants used in this study, including N-terminal truncated E-RAS^{ΔN} (aa 39–233), palmitoylation-deficient E-RAS^{Ser-226/Ser-228} (aa 1–233), N-terminal putative PXXP motif mutant E-RAS^{Ser-7} (aa 1–233), and an N-terminal triple arginine motif variant E-RAS^{Ala-31/Ala-32/Ala-33} (aa 1–233). B and C, confocal live images of transiently transfected MDCK II cells with EYFP-tagged E-RAS^{WT}, H-RAS^{WT}, E-RAS^{Ser-226/Ser-228}, E-RAS^{ΔN}, E-RAS^{Ser-7}, and E-RAS^{Ala-31/Ala-32/Ala-33}. D, confocal imaging was performed using transiently transfected MDCK II cells with E-RAS and H-RAS. FLAG-tagged E-RAS co-localized with Na⁺/K⁺-ATPase to the plasma membrane, very similar to H-RAS, which was used as a control. Scale bar, 10 μm.

parallel, the cell lysates were used to visualize phospho-MEK1/2, phospho-ERK1/2, and phospho-AKT protein states, respectively, using antibodies against MEK1/2 (Cell SignalingTM), ERK1/2 (Cell SignalingTM), AKT (Cell SignalingTM), phospho-MEK1/2 (Ser-217/S221, Cell SignalingTM), phospho-ERK1/2 (Thr-202/Thr-204, Cell SignalingTM), and phospho-AKT (Ser-473 and Thr-308, Cell Signaling) in immunoblotting. All antibodies were diluted in 5% nonfat milk (Carl Roth GmbH).

Structural Methods—The structures of H-RAS were used in our study because no E-RAS structure was available to date. The G domains of H-RAS and E-RAS share 48% identity and were originally described to be structurally very similar, if not identical (18). The interactions with potential binding partners were analyzed on the basis of the structures of H-RAS in complexes with p120RASGAP (PDB code 1WQ1) (30), the RASGEF SOS1 (PDB codes 1NVV (45) and 4NYI), and the downstream effectors RAF1-RBD (PDB codes 1C1Y and 3KUD) (46, 47), PI3Kγ (PDB code 1HE8) (48), BYR2-RBD (PDB code 1K8R) (49), RalGDS (PDB code 1LFD) (50), PLC1 (PDB code 2C5L) (51), Grb14 (PDB code 4K81) (52), and RASSF5 (PDB code 3DDCS) (53).

Results

N-Terminus Is an Important Factor for E-RAS Function—The cellular localizations of FLAG-tagged and EYFP-tagged wild-type E-RAS (E-RAS^{WT}) were investigated in direct comparison with H-RAS^{WT} in MDCK II cells. Confocal imaging revealed that E-RAS, very similar to H-RAS, is mainly associated with the plasma membrane (Fig. 1B) as it is co-localized with the basolateral membrane marker of sodium/potassium-ATPase (Fig. 1D). This

result clearly suggests that E-RAS undergoes post-translational modifications, e.g. farnesylation and palmitoylation, at the very C-terminal cysteines (supplemental Fig. S1). Accordingly, a palmitoylation-deficient E-RAS^{Ser-226/Ser-228} variant clearly exhibited a cytoplasmic accumulation, which supports the notion that E-RAS also underlies a palmitoylation/depalmitoylation mechanism as was shown previously for H-RAS (Fig. 1C) (25).

Another question addressed in this study was the role of the 38-amino acid unique N-terminal extension in E-RAS, which does not exist in other RAS proteins (Supplemental Fig. S1). This extension contains motifs, which may act either as a PXXP motif-binding site for specific Src homology 3-containing proteins or as an electrostatic interaction site (RRR motif) with a negatively charged region of proteins or with a lipid membrane. Thus, one function of the N-terminal extension and its motifs could be providing an additional signal for subcellular localization of E-RAS. Hence, we generated the N-terminal truncated E-RAS^{ΔN} (aa 39–233), putative PXXP motif variant E-RAS^{Ser-7} (aa 1–233), and a triple arginine motif variant E-RAS^{Ala-31/Ala-32/Ala-33} (aa 1–233) (Fig. 1A), and we investigated their localization in transiently transfected MDCK II cells. Confocal imaging of the EYFP-fused E-RAS variants revealed that the N terminus of E-RAS has a slight effect on the E-RAS localization as we observed for the truncated N-terminal variant E-RAS^{ΔN}, putative PXXP motif variant E-RAS^{Ser-7}, and E-RAS^{Ala-31/Ala-32/Ala-33}-less plasma membrane localization (Fig. 1C) but not significant differences.

Effector Selection of E-RAS Significantly Differs from H-RAS—Before investigating the specific function of E-RAS in cells, it was important to gain insights into the E-RAS effector selectiv-

Functional Properties of E-RAS

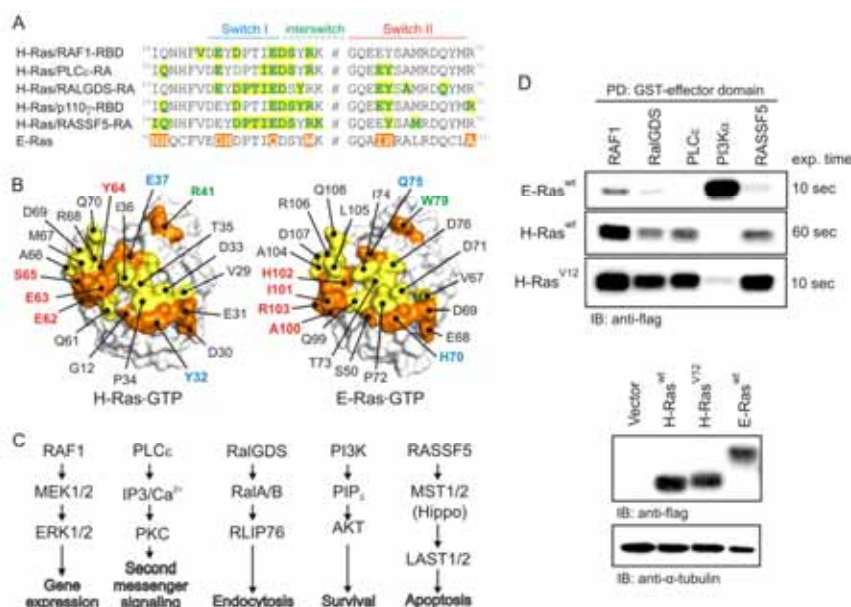


FIGURE 2. Different effector selection of E-RAS and H-RAS. A, effector-binding residues of H-RAS, obtained from various crystal structures, are highlighted with blue letters and yellow background, RAF1 (PDB code 1C1Y), PLC ϵ (PDB code 2CSL), RalGDS (PDB code 1LFD), PI3K γ (PDB code 1HE8), and RASSF5 (PDB code 3DDC). B, effector binding regions (in yellow and orange) of H-RAS and E-RAS were structurally analyzed on the basis of the H-RAS structure in complexes with p120RASGAP (PDB code 1WQ1). The orange amino acids indicate the sequence deviation between H-RAS and E-RAS. C, schematic view of RAS effector pathways and their cellular functions. D, E-RAS and H-RAS pull-down (PD) with various RAS effectors using COS-7 cell lysates transiently transfected with FLAG-tagged E-RAS^{WT}, H-RAS^{WT}, and H-RAS^{Val-12} using GST-fused effector proteins, such as RAF1-RBD, RalGDS-RA, PLC ϵ -RA, PI3K α -RBD, and RASSF5-RA. RAS proteins were analyzed by immunoblot using an anti-FLAG antibody. Immunoblots (IB) of total cell lysates were used as a control to detect FLAG-RAS. Exp. time stands for exposure time. RAF, rapidly accelerated fibrosarcoma; MEK, mitogen-activated protein kinase/ERK kinase; ERK, extracellular signal-regulated kinase; PLC ϵ , phospholipase C ϵ ; PKC, protein kinase C; RalGDS, Ral GDP dissociation stimulator; RLIP76, Ral-interacting protein 76 kDa; PI3K, phosphoinositide 3-kinase; PIP₃, phosphoinositide 3,4,5-trisphosphate; MST1/2, mammalian Ste20-like kinases 1.

ity. Effector interactions with H-RAS have been investigated both biochemically and structurally in great detail. Various amino acids of H-RAS undergo selective contacts with the effectors, including RAF1, RalGDS, RASSF5, and PLC ϵ (Fig. 2A, blue residues with yellow background). These residues, mainly switch I, interswitch, and partially in the switch II region, are conserved among common RAS proteins but vary in E-RAS proteins (supplemental Fig. S1). This suggests that classical RAS family members, except the E-RAS, are in principle able to recognize and activate various effectors. Importantly, these effector-binding residues are highly variable between H-RAS and E-RAS (supplemental Fig. S1; Fig. 2A). Structural analysis of the effector binding regions of E-RAS was performed according to H-RAS complexes with p120RASGAP (PDB code 1WQ1). In comparison with H-RAS, the exposed residues along the effector-binding surface of E-RAS revealed significant sequence deviations (Fig. 2B). This strongly indicates a differential effector selectivity of the RAS proteins.

The members of the RAS family are known to interact with a wide range of effectors (5, 54–61) and therefore stimulate various cellular responses. Regarding their physical interaction with E-RAS and H-RAS proteins, five RAS effectors (RAF1, RalGDS, PLC ϵ , PI3K α , and RASSF5), with defined cellular functions (Fig. 2C), were investigated in this study. In pull-down experiments, GST-fused RAS-binding domain of RAF1 (RAF1-RBD), the RAS association domain of RalGDS (RalGDS-RA), PLC ϵ -RA, PI3K α -RBD, and RASSF5-RA were used as baits to

pull-down FLAG-tagged E-RAS^{WT}, H-RAS^{WT}, and H-RAS^{Val-12} overexpressed in COS-7 cells. We found that H-RAS^{WT} and H-RAS^{Val-12} strongly bind RAF1 and weakly bind to PI3K α . Importantly, E-RAS^{WT} clearly showed an opposite pattern of these interactions, where it binds very tightly to PI3K α and very weakly to RAF1, RalGDS, PLC ϵ , and RASSF5 (Fig. 2D). These data confirm that the amino acid deviations in effector-binding sites (Fig. 2, A and B) make E-RAS a unique member of the RAS family and a potent activator of the PI3K-PIP₃-signaling pathways.

Effector Selection by E-RAS Is Largely Determined by Tryptophan 79—To identify the residues determining the specificity for effector binding and activation, we next analyzed the impact of deviating residues in E-RAS on its interaction with different effectors by replacing the E-RAS residues in switch I (His-70 and Gln-75, collectively named here SwI), interswitch (Arg-79), and switch II (Ala-100, Ile-101, His-102, and Arg-103, collectively named here SwII) for the equivalent residues in H-RAS (supplemental Fig. S1). The corresponding variants, E-RAS^{SwI}, E-RAS^{Arg-79}, E-RAS^{SwII}, E-RAS^{SwI/Arg-79}, E-RAS^{Arg-79/SwII}, RAS^{SwI/SwII}, and E-RAS^{SwI/Arg-79/SwII} (Fig. 3A), were analyzed for their interaction abilities with different effectors using E-RAS^{WT} and the constitutive active variant of H-RAS^{wt}, H-RAS^{Val-12}, as controls. These constructs were transiently transfected in COS-7 cells, and the GTP-bound forms of these RAS variants were pulled down using GST-fused effector proteins under the same conditions as described above. Data

Functional Properties of E-RAS

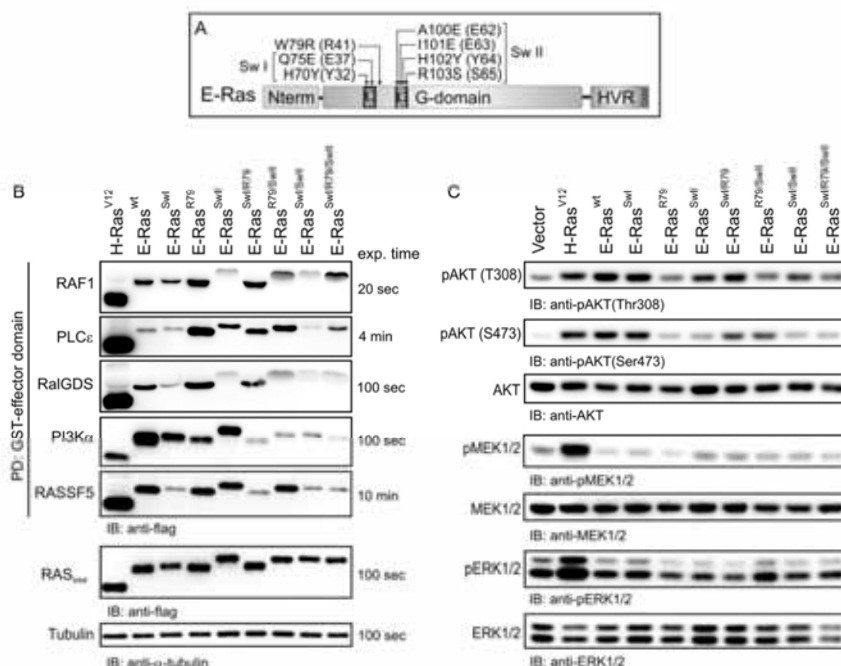


FIGURE 3. Specificity-determining residues in E-RAS-effector interaction. *A*, display of different effector binding mutations in E-RAS: E-RAS^{SwI}, H70Y/Q75E (Tyr-32 and Gln-37 in H-RAS); E-RAS^{Arg-79}, W79R (Arg-41 in H-RAS); E-RAS^{SwII}, A100E/I101E/H102Y/R103S (Glu-62, Glu-63, Tyr-64, and Ser-65 in H-RAS); E-RAS^{SwI/Arg-79}, H70Y/Q75E/W79R; E-RAS^{Arg-79/SwII}, W79R/A100E/I101E/H102Y/R103S; RAS^{SwI/SwII}, H70Y/Q75E/A100E/I101E/H102Y/R103S, and E-RAS^{SwI/Arg-79/SwII}, H70Y/Q75E/W79R/A100E/I101E/H102Y/R103S. For details about the amino acid sequences, see supplemental Fig. S1. *B*, pull-down assay of FLAG-fused E-RAS variants carried out with RBD or RA domain of GST-fused effector proteins, including RAF1-RBD, RalGDS-RA, PLC ϵ -RA, PI3K α -RBD, and RASSF5-RA. The results were analyzed by immunoblot using an anti-FLAG antibody. *Exp. time* stands for exposure time. *C*, total cell lysates were used to monitor the level of phosphorylated AKT (pAKT^{T308} and pAKT^{S473}), MEK1/2 (pMEK1/2), and ERK1/2 (pERK1/2) proteins.

obtained revealed that substitution of Trp-79 for arginine in E-RAS (E-RAS^{Arg-79}) rescued the low affinity of E-RAS for PLC ϵ , RAF1, and RalGDS, and no effect was observed on RASSF5 binding (Fig. 3*B*). In contrast, W79R-containing variants (E-RAS^{Arg-79}, E-RAS^{SwI/Arg-79}, E-RAS^{Arg-79/SwII}, and E-RAS^{SwI/Arg-79/SwII}), when compared with E-RAS^{WT}, exhibited a significant reduction of binding affinity for PI3K α , which is comparable with the levels with H-RAS^{Val-12}. Collectively, all mutations in three regions, especially W79R, affected E-RAS interaction for PI3K α (Fig. 3*B*). Mutations in the switch I region (E-RAS^{SwI}, E-RAS^{SwI/Arg-79}, RAS^{SwI/SwII}, and E-RAS^{SwI/Arg-79/SwII}) exclusively compromised E-RAS interaction with RASSF5. However, switch II variants (E-RAS^{SwII}, E-RAS^{Arg-79/SwII}, and RAS^{SwI/SwII}) more strongly diminished affinity for RalGDS and RAF1 (Fig. 3*B*).

These results raised the following question. How does the Trp-79 interaction with effectors affect the binding affinity of E-RAS for these proteins? To address this question, we inspected available H-RAS structures in complexes with investigated effector proteins and created corresponding structural models of E-RAS with particular focus on Trp-79 in E-RAS (Arg-41 in H-RAS). Data obtained pointed to an unexpected and potentially significant role of Glu-3 (Glu-41 in E-RAS) in effector selection by RAS proteins (Fig. 4; supplemental Fig. S1). Arg-41 is stabilized by intramolecular interactions with Glu-3 (Glu-41 in E-RAS) and side-chain contacts directly at Lys-65 of RAF1 among the analyzed H-RAS effector complexes but not

PI3K. Tryptophan replacing Arg-41 in E-RAS would, because of its hydrophobic nature, be expelled from Glu-41, Glu-54, and Asn-92. This generates new conformation in the effector region of E-RAS and accounts for a shift in effector selectivity. The highest probability for such adopting provides an empty space around the Arg-41 in the case of the PI3K complex thus yielding higher affinity of PI3K to E-RAS^{WT}. Trp-79 interacts best in a hydrophobic environment with PI3K as compared with RAF1. Reciprocal scenario applies in the case of RAF1 and PLC ϵ causing lower affinity of these effectors to E-RAS^{WT}. One example is the repulsion of Lys-65 of RAF1 by the W79R mutation that might be responsible for a weak reconstitution of E-RAS^{Arg-79} binding to RAF1.

We next examined the consequences of the affected effector interaction of the E-RAS variants regarding activation of the corresponding downstream cascades (see Fig. 3*C*). Interestingly, impaired PI3K α binding of E-RAS variants, particularly W79R and SwII, also strongly influenced downstream signals of PI3K monitored by pAKT levels but not that of RAF1 analyzed by pMEK/pERK levels (Fig. 3*C*). Remarkably, AKT phosphorylation at both sites, Thr-308 (PDK1) and Ser-473 (mTORC2), were impaired (see below). The E-RAS^{Arg-79} variant lost its ability to signal via the PI3K/AKT cascade almost completely, indicating a key role of tryptophan 79 in E-RAS and E-RAS-like proteins in effector association and activation. An interesting observation is that a gain of RAF1 binding to E-RAS variants, especially SwI and W79R, did not result in RAF1 activation and

Functional Properties of E-RAS

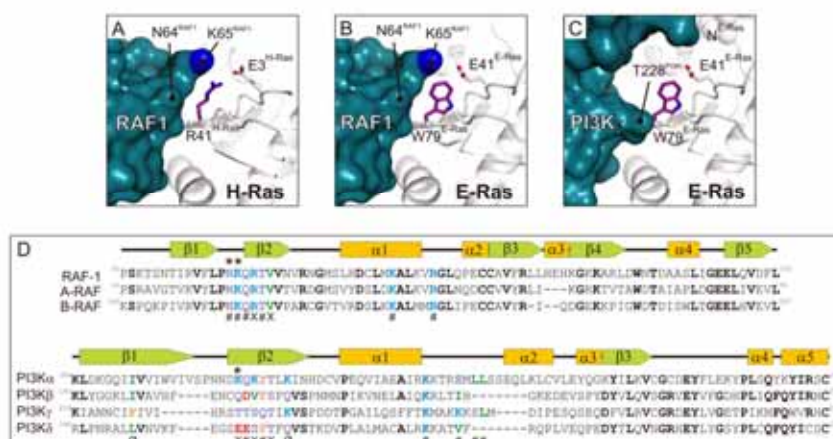


FIGURE 4. Glutamate 41 function and its role in effector selection is discharged in E-RAS. **A**, In H-RAS-GTP, Arg-41 (Trp-79 in E-RAS) is intramolecularly stabilized by Glu-3 (Glu-41 in E-RAS), attracted by backbone oxygen of Asn-64, and repulsed by Lys-65 in RAF1. **B**, In E-RAS, Trp-79 is expelled from Glu-41 and cannot adopt favorable conformation because of the close presence of Asn-64 and Lys-65 of RAF1. The conformation of arginine at the place of Trp-79 in E-RAS^{Arg-79} would be restored due to its interaction with Glu-41 similarly to H-RAS, thus increasing the binding affinity of RAF1. **C**, PI3K does not contact E-RAS tightly in the vicinity of Trp-79 leaving enough space for proper reorientation of tryptophan side chain expelled from Glu-41 and not disfavoring the affinity of their complex. Moreover, orientation of Thr-228 enables tight hydrophobic contact with Trp-79. In E-RAS^{Arg-79}, arginine attracted by Glu-41 would not contribute to the interaction with PI3K weakening its affinity to E-RAS^{Arg-79}. **D**, selectivity-determining amino acids in RAS effectors. Multiple amino acid sequence alignments of the RBD of human RAF isoforms and the catalytic subunits of human PI3K isoforms are illustrated with major focus on the some RAS-binding residues. The corresponding sequences are RAF-1 (P04049; aa 51–131), A-RAF (P10398; aa 14–91), B-RAF (P15056; aa 105–227), PI3K α (P42336; aa 184–276), PI3K β (P42338; aa 191–272), PI3K γ (P48736; aa 214–296), and PI3K δ (O00329; aa 184–226). X highlights residues interacting in β - β manner with switch I. # highlights additional residues interacting with switch I. \emptyset shows residues interacting with Tyr-64 in switch II. * shows residues close to Arg-41 in H-RAS or Trp-79 in E-RAS.

in turn phosphorylation of MEK1/2 and ERK1/2 (Fig. 3, *B* and *C*).

Distinct Downstream Signaling Pathways of E-RAS via PI3K—The data presented above shed light on the specificity determining residues for direct E-RAS-effector interaction and the consequent activation of downstream pathways. The next question we addressed was to understand the role of additional motifs within the N-terminal extension and HVR of E-RAS (see Fig. 1*A*) as potential molecular and cellular determinants required for signal transduction through PI3K-AKT-mTORC and RAF1-MEK1/2-ERK1/2. Therefore, we first investigated the ability of E-RAS variants to directly interact with PI3K α and RAF1. In this experiment, FLAG-tagged E-RAS variants, H-RAS^{WT} and H-RAS^{Val-12}, transiently transfected in COS-7 cells, were pulled down with GST-fused PI3K α -RBD and RAF1-RBD from the cell lysates (Fig. 5*A*). Similar to E-RAS^{WT}, the interactions of E-RAS variants were much stronger with PI3K α -RBD as compared with RAF1-RBD, although hyperactive H-RAS^{Val-12} mainly bound to RAF1-RBD. Moreover, this assay was used to visualize the amounts of the GTP-bound state of the E-RAS variants. Fig. 5*A* shows that all E-RAS variants exist in the active, GTP-bound forms.

To provide further insights to the downstream signaling activity of the above-mentioned E-RAS variants, we investigated the phosphorylation status of AKT (Thr-308 and Ser-473), MEK1/2 (Ser-217/Ser-221), and ERK1/2 (Thr-202/Thr-204), which are representative cellular targets of PI3K and RAF1 (Fig. 5*B*). Although the pulldown showed almost no significant difference between E-RAS variants in binding to RAS effectors, we found E-RAS^{ΔN}, E-RAS^{Ser-226/Ser-228}, and E-RAS^{ΔN/Ser-226/Ser-228} were strongly impaired in the activation of the PI3K-AKT-mTORC axis and clearly exhibited lower

phosphorylation levels for AKT, especially at Thr-308. All E-RAS variants, including E-RAS^{ΔN}, were inefficient in stimulation of MEK1/2 and ERK1/2 phosphorylation in comparison with H-RAS^{WT} and H-RAS^{Val-12} that actively contributed to activation of the RAF1-MEK1/2-ERK1/2 axis.

Next, we aimed to determine the cellular co-localization of E-RAS with PI3K α and RAF1. Transiently transfected MDCK II cells with FLAG-tagged E-RAS and H-RAS were incubated with recombinant GST-fused RBDs of PI3K α and RAF1 and stained with antibodies against GST and FLAG, respectively. We observed that PI3K α but not RAF1 localized with E-RAS mainly at the plasma membrane (Fig. 6*A*). In contrast, RAF1, and to a lower extent also PI3K α , co-localized with H-RAS at the plasma membrane (Fig. 6*B*). These data suggest that both the N-terminal extension of E-RAS and its palmitoylation are essential and critical for the cellular activation of the PI3K-AKT-mTORC cascade, although the formation of the GTP-bound state and the interaction with PI3K were not affected.

Discussion

In this study, we have investigated cellular localization and the signaling activity of human E-RAS regarding its physical interaction with RAS effectors and the roles of both its unique features, the N terminus and PTM by palmitoylation in direct comparison with human H-RAS. The structure-function relationship of the effector interaction sites of E-RAS resulted in the identification of tryptophan 79 as a specificity-determining amino acid of E-RAS, which is critical for its strong association with PI3K. In the cell, this interaction additionally requires the presence of both a functional N-terminal extension and palmitoylation at cysteines 226 and 228 that collectively lead to the precise activation of the PI3K-AKT-mTORC pathway.

Functional Properties of E-RAS

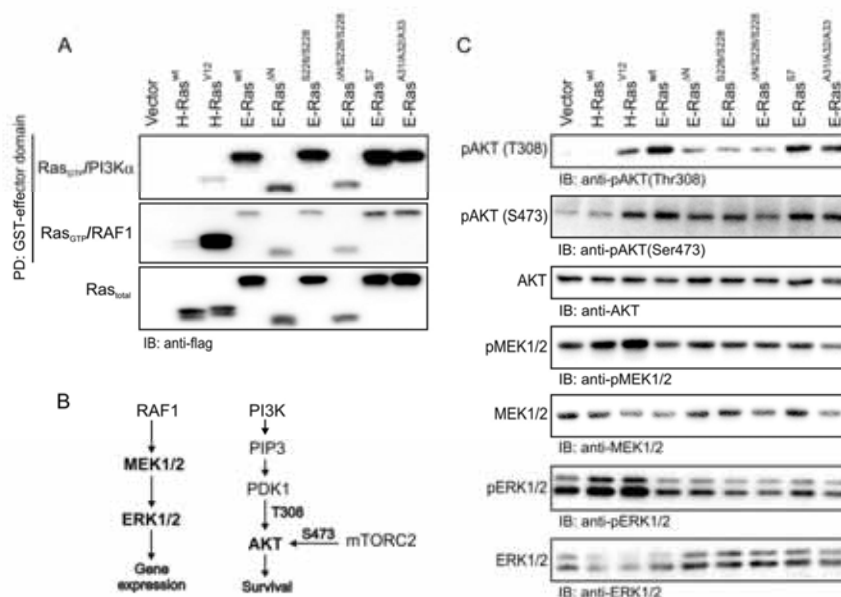


FIGURE 5. E-RAS signaling activities in COS-7 cells. Pull-down (PD) experiments and immunoblot (IB) analysis of total cell lysates were derived from transfected COS-7 cells with FLAG-tagged E-RAS variants H-RAS^{WT} and H-RAS^{V61L}. **A**, pull-down analysis revealed that E-RAS variants like E-RAS^{WT} most strongly bind to GST-fused PI3K α -RBD than RAF1-RBD, whereas hyperactive H-RAS^{V61L} mainly bound to GST-fused RAF1-RBD. In addition, PI3K α -RBD PD showed that all E-RAS variants are in the GTP-bound state and consequently in their activated forms. Total amounts of the RAS proteins were detected as a control using anti-FLAG antibody. **B**, schematic view of MAPK and PI3K-AKT cascades. **C**, total cell lysates were analyzed for the phosphorylation level of AKT (pAKT308 and pAKT473), MEK1/2 (pMEK1/2) and ERK1/2 (pERK1/2). Total amounts of AKT, MEK1/2, and ERK1/2 were applied as loading controls.

Palmitoylation Modification and E-RAS Trafficking—To transduce signals, RAS proteins should be associated with the lipid membranes. They are compartmentalized by PTMs at their C terminus, with the CAAX motif at the farnesylation site, and additional upstream cysteine residues at the palmitoylation site(s) in the case of H- and N-RAS (supplemental Fig. S1) (23–25, 29). We found that like the mouse E-RAS (42), substitution of two cysteine residues Cys-226/Cys-228 in HVR of human E-RAS with serines clearly impaired the plasma membrane localization of protein. This is a strong indication that human E-RAS undergoes palmitoylation at these sites, as described for the first time for H-RAS (62). Yamanaka and co-workers (42) reported that these cysteine residues are important for endomembrane localization of mouse E-RAS and only signals if HVR of H-RAS can rescue endomembrane localization of E-RAS^{Ser-226/Ser-228}. Our confocal microscopy data revealed that in contrast to plasma membrane localization of E-RAS^{WT}, palmitoylation-deficient E-RAS^{Ser-226/Ser-228} is mainly localized, with a clear pattern, in cytoplasm and also in endomembranes. Our data clearly support proposed reports demonstrating that H-RAS and N-RAS cycle between Golgi and the plasma membrane via reversible and dynamic palmitoylation-depalmitoylation reactions (25, 63, 64).

N-terminal Extension and C-terminal Insertion of E-RAS—A sequence comparison between E-RAS and other RAS isoforms highlighted additional regions and motifs, such as the unique N terminus of E-RAS that is not present in other RAS-like proteins. We propose that the N-terminal extension of E-RAS might modulate its localization through interaction with potential adaptor/scaffold proteins via putative PXXP and RRR motifs. With our co-localization studies, we did not observe

significant differences in localization of the N-terminal mutants of E-RAS. However, considering our results, we cannot exclude the role of the E-RAS N terminus as a putative protein interaction site, because E-RAS is not expressed endogenously in the MDCK II cells, and therefore its binding partner may not be available in this cell line. To confirm our hypothesis, we need to study a different cell line, like embryonic stem cells (42), gastric tumors (65), neuroblastoma cells (20), and also hepatic stellate cells,³ where E-RAS is endogenously expressed (unpublished data).

Imaging methods used in this study did not allow visualizing microdomain localization of E-RAS variants. The plasma membrane is not a homogeneous lipid bilayer and includes a set of microdomains, such as lipid raft and caveolae (66, 67). The HVR at the C-terminal end of RAS proteins is critical for lateral sorting and is divided into two separate domains, membrane-targeting domain and linker domain (68). Membrane targeting domain contains a CAAX box and one or two upstream cysteines that are palmitoylation sites. Palmitoylated proteins can be targeted to lipid rafts. Because H-, N-, and K-RAS are dipalmitoylated, monopalmitoylated, and nonpalmitoylated, respectively, they exhibit different lateral segregation across the plasma membrane microdomains (69). GDP-bound H-RAS is associated with the lipid raft, but when it is activated and GTP-loaded, it moves laterally to nonlipid raft regions (68, 70, 71). E-RAS, like H-RAS, is dipalmitoylated suggesting that it may favor the lipid rafts. On the contrary, E-RAS is mainly GTP-

³ S. Nakhaei-Rad, C. Kordes, H. Nakhaeizadeh, R. Dvorsky, I. C. Cirstea, I. Sawitza, S. Götze, R. P. Piekorz, B. Görg, D. Haussinger, and M. R. Ahmadian, unpublished data.

Functional Properties of E-RAS

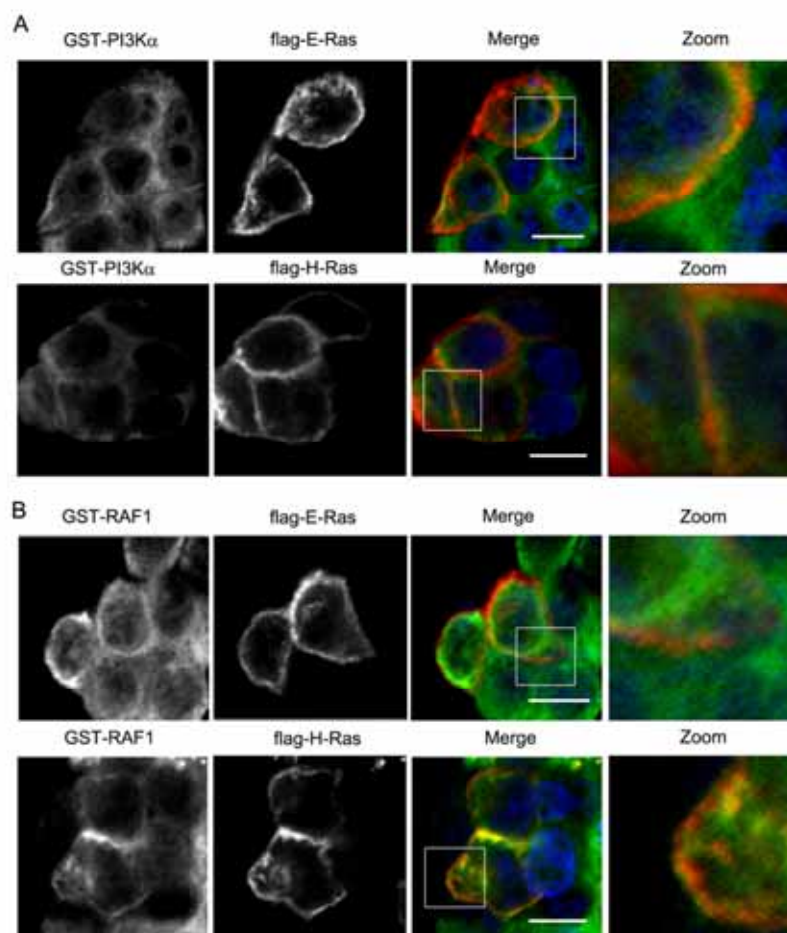


FIGURE 6. **Co-localization of E-RAS with PI3K α .** Transfected MDCKII cells with FLAG-tagged E-RAS were incubated with bacterial lysates, containing GST-RBDs of PI3K α and RAF1 proteins and stained with antibodies raised against GST and FLAG to investigate their co-localization with GTP-bound H-RAS and E-RAS proteins. E-RAS co-localized with PI3K α . Scale bar, 10 μ m.

loaded, which makes it difficult to compare it with wild-type H-RAS. It is reported that the active GTP-loaded H-RAS^{Val-12} variant occupies the nonlipid rafts so the constitutively active E-RAS may also be clustered in this region. The second domain in HVR, termed linker domain, releases GTP-loaded H-RAS from the lipid rafts. Linker domain can be divided in N- and C-terminal regions in a way that the C-terminal region is a spacer, which seems not to be important (68). Human E-RAS has an insertion in this C-terminal spacer (aa 173–179, H-RAS numbering) that may also affect microdomain migration of E-RAS. Taken together, we propose that three factors most likely modulate the microdomain targeting of E-RAS, such as an extended N terminus, a C-terminal insertion, and the GTP-loaded state due to a prominent deviation at position Ser-50 (Gly-12 in H-RAS).

Our cell-based studies revealed that the N-terminal extension of E-RAS is critical for PI3K-AKT-mTORC activation, and N-terminal truncated E-RAS variants (E-RAS^{ΔN} and E-RAS^{ΔN/Ser-226/Ser-228}) remarkably had a lower signaling activity. One explanation may be the role of the unique N ter-

minus in the lateral segregation of E-RAS across the membrane that consequently specifies association with and activation of its effectors in a manner reminiscent to microdomain localization of H-RAS that regulates its interaction with effector proteins of RAF1 and PI3K (68). In addition, E-RAS was found in membrane ruffles (data not shown), which may be induced by Rac1 activated by the E-RAS-PI3K-PIP₃-RacGEF axis (72–74). Such a scenario has been reported for the R-RAS N-terminal 26-amino acid extension, which has been proposed to positively regulate Rac activation and cell spreading (75).

Constitutively Active Form—GAPs accelerate the GTP hydrolysis reaction of RAS proteins by orders of magnitude by supplying a highly conserved, catalytic arginine finger (31, 32). H-RAS glycine 12 mutations to any other amino acid interfere with insertion of arginine finger in the GTPase active site and therefore make the enzyme GAP-insensitive (30). Interestingly, E-RAS has a deviation in the corresponding position and carries a serine instead of a glycine indicating that E-RAS is hyperactive and GAP-insensitive. Our stopped-flow data revealed that p120RASGAP was not able to accelerate the GTP hydrolysis

Functional Properties of E-RAS

reaction of E-RAS, although it can act on H-RAS and convert it to the GDP-bound inactive form (data not shown). We have shown that all E-RAS variants exist mostly in GTP-bound forms as shown by a pull-down experiment with PI3K and RAF1. This and the fact that E-RAS is GAP-insensitive suggest that E-RAS may underlie a different and yet undefined control mechanism that negatively regulates E-RAS activity and thus its signal transduction.

It seems that expression of E-RAS is highly regulated at the transcriptional levels and rather limited to special cell types, such as embryonic stem cells (42), gastric tumors (65), neuroblastoma cells (20), and also hepatic stellate cells.⁵ Moreover, the unique N terminus of E-RAS may provide specialized protein-protein interaction sites resulting in E-RAS sequestration, degradation, or membrane microdomain localization as shown for R-RAS (75, 76). E-RAS could interact with specific scaffolding proteins that bring it close to its effectors and regulate its activities. It is tempting to speculate that E-RAS may underlie a similar mechanism via serine/threonine phosphorylation and 14-3-3 binding as described for Rnd3 (75, 76), a constitutively active member of the Rho protein family (77). However, there is as yet no evidence for an E-RAS phosphorylation particularly at its N terminus that contains 4 threonines and 2 serines (supplemental Fig. S1).

Effector Binding Regions—RAS proteins transduce extracellular signals to a variety of intracellular signaling pathways through the interaction with a wide spectrum of effector proteins. Upon GDP to GTP exchange, RAS proteins undergo conformational changes in two critical regions, switch I and switch II. Notably, the GTP-bound form of RAS interacts with their target effectors through switch regions and thereby activates various pathways (5). A detailed study of structure-sequence relationships revealed a distinctive effector binding region for E-RAS in comparison with RAS isoforms (H-, N-, and K-RAS). Subsequent interaction analysis with five different RAS effectors revealed that effector binding profile of E-RAS significantly differs from H-RAS. E-RAS^{WT} tightly bound to PI3K α and revealed very low affinity for other RAS effectors. In contrast, H-RAS showed an opposite pattern with the highest affinity for RAF1. These data were confirmed by investigating the respective downstream signaling cascades (PI3K-AKT-mTORC and RAF1-MEK1/2-ERK1/2) at the level of phosphorylated AKT, MEK1/2, and ERK1/2. Our results are consistent with a previous study of Yamanaka and co-workers (18), who applied another PI3K isoform (PI3K δ) and observed differences between H-RAS and E-RAS. It seems probable that E-RAS and H-RAS possess a different affinity for distinct PI3K isoforms, α , β , γ , and δ , and this may account for their specific biological outputs (78). Consistently, the catalytic subunit of the PI3K γ isoform, PI3K γ , interacts with switch I of H-RAS in anti-parallel β -sheet fashion (48), also approaching RAS-conserved Asp-33 by two lysines. Residues in H-RAS contacting β -strand of PI3K γ and preceding amino acids differ significantly among the PI3K isoforms regarding the primary structures (Fig. 4D). Although PI3K γ has four hydroxyl-containing amino acid side chains at this place, PI3K β possesses one and PI3K δ isoform two negatively charged residues whereby both have in addition two amino acid insertions. In contrast, the PI3K α isoform has

insertion of six residues, and the hydroxyl-containing amino acids are replaced by one asparagine and two lysines (Fig. 4D). We hypothesize that these differences in PI3K isoforms are of particular importance due to the stabilization of intermolecular β -sheet interaction and especially because the contact site of the crucial Trp-79 in E-RAS (Arg-41 in H-RAS) is highly variable (Lys, Gln, Thr, and Glu; see Fig. 4D).

Substitutions for E-RAS residues in the switch I and II and interswitch regions with corresponding residues in H-RAS provided several interesting aspects and new insights (Fig. 3). One is a shift in effector selection. Strikingly, and in contrast to other investigated effectors, RAF1-RBD undergoes contacts with the switch I and the interswitch regions (Fig. 2A) (46, 47). However, E-RAS^{SwI}, which has an almost identical switch I when compared with H-RAS, showed a reduced binding to RAF1 that was clearly elevated when this was combined with the interswitch mutation W79R (E-RAS^{SwI/Arg-79}) (Fig. 3B). Consistently, the major difference was observed with E-RAS^{Arg-79}, where a tryptophan was replaced by an arginine (Arg-41 in H-RAS). This variant led to increase in RAF1 binding and partly rescued the low affinity of the wild type and the switch variants (E-RAS^{SwI/Arg-79} and E-RAS^{SwI/Arg-79/SwII}). According to the crystal structure (46), Arg-41 in H-RAS (Trp-79 in E-RAS) interestingly forms a hydrogen bond with the backbone oxygen of Asn-64 in RAF1-RBD that very likely enabled E-RAS^{Arg-79} to make additional electrostatic contacts with RAF1 (Fig. 4, A and B). In addition, E-RAS shares a glutamate (Glu-41) with H-RAS (Glu-3) (supplemental Fig. S1). Glu-3 interacts in intermolecular fashion with Arg-41 and stabilizes the H-RAS-RAF1 complex formation (Fig. 4A). Accordingly, mutation of W79R in E-RAS reconstitutes such intermolecular interaction between Glu-41 and Arg-79, thus increasing significantly the interaction between E-RAS^{Arg-79} and RAF1 (Fig. 3B). Another important contribution to effector binding concerning Trp-79 originates very likely in its expulsion from the above-mentioned Glu-41 and the ability of bound effector protein to accommodate altered conformation of Trp-79. As mentioned before, Arg-41 of H-RAS is contacted by RAF1 in its complex structure. The space where the tryptophan can be accommodated and hydrophobically interact with the effector is thus limited resulting in diminished affinity of these effectors to E-RAS^{WT}. Moreover, switch II quadruple mutation of E-RAS (E-RAS^{SwII}; see Fig. 3A) showed the largest impairment in RAF1 binding. This was not expected especially because the structural data, reported previously (46, 47), have shown that RAF1-RBD does not physically contact the switch II of RAS. Again, E-RAS^{Arg-79/SwII} partially restored the loss of RAF1 binding but most remarkably not the E-RAS^{SwI/SwII} variant that actually is almost identical to H-RAS regarding the amino acid sequence of its switch I and II regions (see Fig. 3A). Even though E-RAS^{Arg-79} binds more tightly to RAF1, it still does not activate the MAPK pathway like E-RAS^{WT}. Note that there was no increase in MEK and ERK phosphorylation, and we detected even the opposite, namely a significant decrease in pMEK1/2 and pERK1/2 as compared with the vector control (Fig. 3C; see E-RAS^{WT} and E-RAS^{Arg-79} lanes). An explanation for the absence of E-RAS^{Arg-79} signaling toward the MAPK pathway is that most probably the additional component, including scaffold proteins such as SHOC2 (79–

Functional Properties of E-RAS

81), may not exist in the E-RAS^{Arg-79}·RAF1 complex. This provides the assumption that E-RAS localizes to a different membrane region then, for example, the H-RAS, RAF1, and the components of the MAPK pathway.

PLC ϵ contains two RAS association domains, RA1 and RA2. RA2 forms a complex with H-RAS in a GTP-dependent manner by contacting nine different residues of the switch I and II regions, and also Gln-25 and Arg-41 (51), from which four (Glu-37, Arg-41, Glu-63, and Tyr-63) deviate in E-RAS (Fig. 3A). This explains why we observed an extremely weak E-RAS-PLC ϵ interaction as compared with H-RAS^{Val-12}. Most interestingly, the W79R mutation of E-RAS resulted in a strong gain of binding activity (Fig. 3B; see E-RAS^{WT} and E-RAS^{Arg-79} lanes). Notably, this effect was not so strong in the case of the switch II mutation (E-RAS^{SwII}), and the switch I mutation (E-RAS^{SwI}) did not show any change in the E-RAS association with PLC ϵ . A combination of the mutations (E-RAS^{SwI/SwII}) was hardly detectable and the combinations with W79R (E-RAS^{Arg-79/SwI}, E-RAS^{Arg-79/SwII}, and E-RAS^{SwI/Arg-79/SwII}) rather counteracted the gain of binding activity of RAS^{Arg-79}. On a molecular level, Trp-79 in wild-type E-RAS can be hydrophobically attracted to Pro-2149 of PLC ϵ but not intramolecularly to Glu-41 (data not shown), and the space for its conformational relaxation is limited similarly to RAF1 as mentioned above. We propose that W79R mutation generates stronger intramolecular contact between Glu-41 and Arg-79 and consequently stabilizes the protein complex with PLC ϵ . Katan and co-workers (51) have discussed that the H-RAS residues Tyr-64, Ile-36, and Met-67 (His-102, Ile-74, and Leu-105 in E-RAS) in combination with Phe-2138 and Val-2152 from PLC ϵ -RA2, provide a hydrophobic clusters. Introduction of another hydrophobic residue in E-RAS as demonstrated with a single point mutation at Trp-79 (E-RAS^{Arg-79}) has obviously created an additional and distinct binding site for RAS association domains, such as RA2 of PLC ϵ and most likely also RA of RalGDS. The latter, a GEF for Ral, links two RAS family members, RAS and Ral (82). Although the crystal structure of H-RAS/RalGDS-RA has not reported an involvement of Arg-41 (50), our structural analysis predicted a close hydrophobic contact of Arg-41 with Met-819 of RalGDS (3.2 Å). Notably, data obtained from the interaction of RalGDS and RAF1 with E-RAS variants appear similar as compared with that for PLC ϵ .

PI3K is a well known effector of classical RAS proteins and promotes cellular survival (78). In comparison with H-RAS, E-RAS interacts more strongly with PI3K α -RBD and activates the PI3K-AKT-mTORC cascade. Mutagenesis at switch and interswitch regions (E-RAS^{SwI}, E-RAS^{Arg-79}, and E-RAS^{SwII}), attenuated binding of E-RAS to PI3K α -RBD, demonstrating the role of critical E-RAS residues at effector binding regions. These data are consistent with a previous study that has shown that PI3K γ -RBD contacts both switch I and switch II regions of H-RAS (48). Interestingly, W79R mutation of E-RAS (Arg-41 H-RAS), which has increased binding to RAF1, PLC ϵ , and RalGDS, dramatically reduced the binding to PI3K α . The affinity of this E-RAS mutant (E-RAS^{Arg-79}) for PI3K α -RBD appears similar to that of H-RAS^{Val-12} (Fig. 3B; see H-RAS^{Val-12} and E-RAS^{Arg-79} lanes). We think that the strong interaction between E-RAS and PI3K stems from the ability of structure to

accommodate altered conformation of Trp-79 and from its hydrophobic contact to PI3K (Fig. 4C). In contrast, W79R mutation in E-RAS enables Glu-41 to attract Arg-79 and to interfere with this hydrophobic interaction, resulting in a significant reduction of the binding affinity between PI3K and E-RAS (Fig. 4C). In the same line of evidence, we also observed E-RAS^{Arg-79} deficient at the activation of RAS-PI3K-AKT-mTORC2 pathway (9) as monitored with Ser-473 phosphorylation of AKT (see result Fig. 3C). Thus, Trp-79 in E-RAS represents a specificity-determining residue for the proper binding to and activation of PI3K.

RASSF members are known as a RAS effector with tumor suppressor functions. RASSF5 have two splice variants NORE1A and RAPL, which share same RBD (53). We applied the RASSF5-RA domain to analyze the interaction of E-RAS variants with this RAS effector. As shown for RAF1 and RalGDS, switch I H70Y/Q75E mutation of E-RAS (E-RAS^{SwI}) also attenuated the binding to RASSF5, and this was the case for all E-RAS variants harboring switch I mutations (E-RAS^{SwI/Arg-79}, E-RAS^{SwI/SwII}, and E-RAS^{SwI/Arg-79/SwII}). Switch II and W79R mutations did not affect the binding affinity for RASSF5, emphasizing the importance of the more conserved switch I region in the complex formation of the RAS proteins with RASSF5 (53). It remains to be investigated whether E-RAS is an activator of RASSF5 and thus a regulator of the Hippo pathway.

In summary, we conclude that switch regions of E-RAS act as core effector binding regions that form an E-RAS-specific interaction interface for its effectors, such as PI3K. The PI3K isoform specificity in E-RAS-expressing cells remains to be investigated. Trp-79 of E-RAS appears to determine the effector selectivity. E-RAS binding to other RAS effectors, such as RASSF5, RalGDS, and RAF1, is weak but may still be of physiological relevance. Improvement of the interaction with RAF1 by mutagenesis, for example, rather exhibited an inhibitory impact on the MAPK pathway. It remains unclear whether protein phosphatases specific for MAPKs were activated. The N terminus of E-RAS is unique and may play a critical role in the interaction with its accessory proteins for positioning E-RAS to subcellular microdomains of the plasma membrane.

Acknowledgments—We are grateful to Ehsan Amin, Hedyeh Amintoosi, Silke Götze, Lothar Gremer, Ilse Meyer, Kazem Nouri, Björn Papke, Roland P. Piekorz, Georg Rosenberger, Claudia Rupperecht, Iris Sawitza, Jürgen Scheller, Madhurendra Singh, Nachiket Vartak, and Si-Cai Zhang for their helpful advice, stimulating discussions, and for sharing reagents.

Note Added in Proof—Supplemental Fig. 1 comparing mammalian E-RAS and classical RAS sequences was inadvertently omitted from the version of this article that was published May 4, 2015 as a Paper in Press. Supplemental Fig. 1 is now available on line.

References

- Vetter, I. R. (2001) The guanine nucleotide-binding switch in three dimensions. *Science* **294**, 1299–1304
- Boguski, M. S., and McCormick, F. (1993) Proteins regulating Ras and its relatives. *Nature* **366**, 643–654
- Ahmadian, M. R., Wittinghofer, A., and Schmidt, G. (2002) The actin filament architecture: tightly regulated by the cells, manipulated by patho-

Functional Properties of E-RAS

- gens. International Titisee Conference on the actin cytoskeleton: from signalling to bacterial pathogenesis. *EMBO Rep.* **3**, 214–218
4. Gremer, L., Merbitz-Zahradnik, T., Dvorsky, R., Cirstea, I. C., Kratz, C. P., Zenker, M., Wittinghofer, A., and Ahmadian, M. R. (2011) Germ line KRAS mutations cause aberrant biochemical and physical properties leading to developmental disorders. *Hum. Mutat.* **32**, 33–43
 5. Karnoub, A. E., and Weinberg, R. A. (2008) Ras oncogenes: split personalities. *Nat. Rev. Mol. Cell Biol.* **9**, 517–531
 6. Pylayeva-Gupta, Y., Grabocka, E., and Bar-Sagi, D. (2011) RAS oncogenes: weaving a tumorigenic web. *Nat. Rev. Cancer* **11**, 761–774
 7. Tidyman, W. E., and Rauen, K. A. (2009) The RASopathies: developmental syndromes of Ras/MAPK pathway dysregulation. *Curr. Opin. Genet. Dev.* **19**, 230–236
 8. Flex, E., Jaiswal, M., Pantaleoni, F., Martinelli, S., Strullu, M., Fansa, E. K., Caye, A., De Luca, A., Lepri, F., Dvorsky, R., Pannone, L., Paolacci, S., Zhang, S. C., Fodale, V., Bocchinfuso, G., et al. (2014) Activating mutations in RRAS underlie a phenotype within the RASopathy spectrum and contribute to leukaemogenesis. *Hum. Mol. Genet.* **23**, 4315–4327
 9. Cirstea, I. C., Gremer, L., Dvorsky, R., Zhang, S. C., Piekorz, R. P., Zenker, M., and Ahmadian, M. R. (2013) Diverging gain-of-function mechanisms of two novel KRAS mutations associated with Noonan and cardio-facio-cutaneous syndromes. *Hum. Mol. Genet.* **22**, 262–270
 10. Castellano, E., and Santos, E. (2011) Functional specificity of Ras isoforms: so similar but so different. *Genes Cancer* **2**, 216–231
 11. Ichise, T., Yoshida, N., and Ichise, H. (2010) H-, N- and Kras cooperatively regulate lymphatic vessel growth by modulating VEGFR3 expression in lymphatic endothelial cells in mice. *Development* **137**, 1003–1013
 12. Omerovic, J., Laude, A. J., and Prior, I. A. (2007) Ras proteins: paradigms for compartmentalised and isoform-specific signalling. *Cell. Mol. Life Sci.* **64**, 2575–2589
 13. Potenza, N., Vecchione, C., Notte, A., De Rienzo, A., Rosica, A., Bauer, L., Affuso, A., De Felice, M., Russo, T., Poulet, R., Cifelli, G., De Vita, G., Lembo, G., and Di Lauro, R. (2005) Replacement of K-Ras with H-Ras supports normal embryonic development despite inducing cardiovascular pathology in adult mice. *EMBO Rep.* **6**, 432–437
 14. Leon, J., Guerrero, I., and Pellicer, A. (1987) Differential expression of the ras gene family in mice. *Mol. Cell. Biol.* **7**, 1535–1540
 15. Johnson, L., Greenbaum, D., Cichowski, K., Mercer, K., Murphy, E., Schmitt, E., Bronson, R. T., Umanoff, H., Edelman, W., Kucherlapati, R., and Jacks, T. (1997) K-ras is an essential gene in the mouse with partial functional overlap with N-ras. *Genes Dev.* **11**, 2468–2481
 16. Nakamura, K., Ichise, H., Nakao, K., Hatta, T., Otani, H., Sakagami, H., Kondo, H., and Katsuki, M. (2008) Partial functional overlap of the three ras genes in mouse embryonic development. *Oncogene* **27**, 2961–2968
 17. Lau, K. S., and Haigis, K. M. (2009) Nonredundancy within the RAS oncogene family: insights into mutational disparities in cancer. *Mol. Cells* **28**, 315–320
 18. Takahashi, K., Mitsui, K., and Yamanaka, S. (2003) Role of ERas in promoting tumour-like properties in mouse embryonic stem cells. *Nature* **423**, 541–545
 19. Tanaka, Y., Ikeda, T., Kishi, Y., Masuda, S., Shibata, H., Takeuchi, K., Komura, M., Iwanaka, T., Muramatsu, S., Kondo, Y., Takahashi, K., Yamanaka, S., and Hanazono, Y. (2009) ERas is expressed in primate embryonic stem cells but not related to tumorigenesis. *Cell Transplant.* **18**, 381–389
 20. Aoyama, M., Kataoka, H., Kubota, E., Tada, T., and Asai, K. (2010) Resistance to chemotherapeutic agents and promotion of transforming activity mediated by embryonic stem cell-expressed Ras (ERas) signal in neuroblastoma cells. *Int. J. Oncol.* **37**, 1011–1016
 21. Kubota, E., Kataoka, H., Aoyama, M., Mizoshita, T., Mori, Y., Shimura, T., Tanaka, M., Sasaki, M., Takahashi, S., Asai, K., and Joh, T. (2010) Role of ES cell-expressed Ras (ERas) in tumorigenicity of gastric cancer. *Am. J. Pathol.* **177**, 955–963
 22. Willumsen, B. M., Christensen, A., Hubbert, N. L., Papageorge, A. G., and Lowy, D. R. (1984) The p21 ras C-terminus is required for transformation and membrane association. *Nature* **310**, 583–586
 23. Ahearn, I. M., Haigis, K., Bar-Sagi, D., and Phillips, M. R. (2012) Regulating the regulator: post-translational modification of RAS. *Nat. Rev. Mol. Cell Biol.* **13**, 39–51
 24. Schmick, M., Vartak, N., Papke, B., Kovacevic, M., Truxius, D. C., Rossmannek, L., and Bastiaens, P. I. (2014) KRas localizes to the plasma membrane by spatial cycles of solubilization, trapping and vesicular transport. *Cell* **157**, 459–471
 25. Rocks, O., Peyker, A., Kahms, M., Vermeer, P. J., Koerner, C., Lumbierres, M., Kuhlmann, J., Waldmann, H., Wittinghofer, A., and Bastiaens, P. I. (2005) An acylation cycle regulates localization and activity of palmitoylated Ras isoforms. *Science* **307**, 1746–1752
 26. Takahashi, K., Murakami, M., and Yamanaka, S. (2005) Role of the phosphoinositide 3-kinase pathway in mouse embryonic stem (ES) cells. *Biochem. Soc. Trans.* **33**, 1522–1525
 27. Yu, Y., Liang, D., Tian, Q., Chen, X., Jiang, B., Chou, B.-K., Hu, P., Cheng, L., Gao, P., Li, J., and Wang, G. (2014) Stimulation of somatic cell reprogramming by ERas-Akt-FoxO1 signaling axis. *Stem Cells* **32**, 349–363
 28. Lerner, E. C., Qian, Y., Blaskovich, M. A., Fossum, R. D., Vogt, A., Sun, J., Cox, A. D., Der, C. J., Hamilton, A. D., and Sefti, S. M. (1995) Ras CAAAX peptide-mimetic FTI-277 selectively blocks oncogenic Ras signaling by inducing cytoplasmic accumulation of inactive Ras-Raf complexes. *J. Biol. Chem.* **270**, 26802–26806
 29. Apolloni, A., Prior, I. A., Lindsay, M., Parton, R. G., and Hancock, J. F. (2000) H-ras but not K-ras traffics to the plasma membrane through the exocytic pathway. *Mol. Cell. Biol.* **20**, 2475–2487
 30. Scheffzek, K., Ahmadian, M. R., Kabsch, W., Wiesmüller, L., Lautwein, A., Schmitz, F., and Wittinghofer, A. (1997) The Ras-RasGAP complex: structural basis for GTPase activation and its loss in oncogenic Ras mutants. *Science* **277**, 333–338
 31. Ahmadian, M. R., Hoffmann, U., Goody, R. S., and Wittinghofer, A. (1997) Individual rate constants for the interaction of Ras proteins with GTPase-activating proteins determined by fluorescence spectroscopy. *Biochemistry* **36**, 4535–4541
 32. Ahmadian, M. R., Stege, P., Scheffzek, K., and Wittinghofer, A. (1997) Confirmation of the arginine-finger hypothesis for the GAP-stimulated GTP-hydrolysis reaction of Ras. *Nat. Struct. Biol.* **4**, 686–689
 33. Lenzen, C., Cool, R. H., Prinz, H., Kuhlmann, J., and Wittinghofer, A. (1998) Kinetic analysis by fluorescence of the interaction between Ras and the catalytic domain of the guanine nucleotide exchange factor Cdc25Mm. *Biochemistry* **37**, 7420–7430
 34. Buday, L., and Downward, J. (2008) Many faces of Ras activation. *Biochim. Biophys. Acta* **1786**, 178–187
 35. Bourne, H. R., Sanders, D. A., and McCormick, F. (1990) The GTPase superfamily: a conserved switch for diverse cell functions. *Nature* **348**, 125–132
 36. Bourne, H. R., Sanders, D. A., and McCormick, F. (1991) The GTPase superfamily: conserved structure and molecular mechanism. *Nature* **349**, 117–127
 37. Saraste, M., Sibbald, P. R., and Wittinghofer, A. (1990) The P-loop—a common motif in ATP- and GTP-binding proteins. *Trends Biochem. Sci.* **15**, 430–434
 38. Bos, J. L. (1989) ras oncogenes in human cancer: a review. *Cancer Res.* **49**, 4682–4689
 39. Herrmann, C. (2003) Ras-effector interactions: after one decade. *Curr. Opin. Struct. Biol.* **13**, 122–129
 40. Schmidt, G., Lenzen, C., Simon, I., Deuter, R., Cool, R. H., Goody, R. S., and Wittinghofer, A. (1996) Biochemical and biological consequences of changing the specificity of p21ras from guanosine to xanthosine nucleotides. *Oncogene* **12**, 87–96
 41. Wittinghofer, A., and Vetter, I. R. (2011) Structure-function relationships of the G domain, a canonical switch motif. *Annu. Rev. Biochem.* **80**, 943–971
 42. Takahashi, K., Nakagawa, M., Young, S. G., and Yamanaka, S. (2005) Differential membrane localization of ERas and Rheb, two Ras-related proteins involved in the phosphatidylinositol 3-kinase/mTOR pathway. *J. Biol. Chem.* **280**, 32768–32774
 43. Tucker, J., Sczakiel, G., Feuerstein, J., John, J., Goody, R. S., and Wittinghofer, A. (1986) Expression of p21 proteins in *Escherichia coli* and stereochemistry of the nucleotide-binding site. *EMBO J.* **5**, 1351–1358
 44. Cirstea, I. C., Kutsche, K., Dvorsky, R., Gremer, L., Carta, C., Horn, D.,

Functional Properties of E-RAS

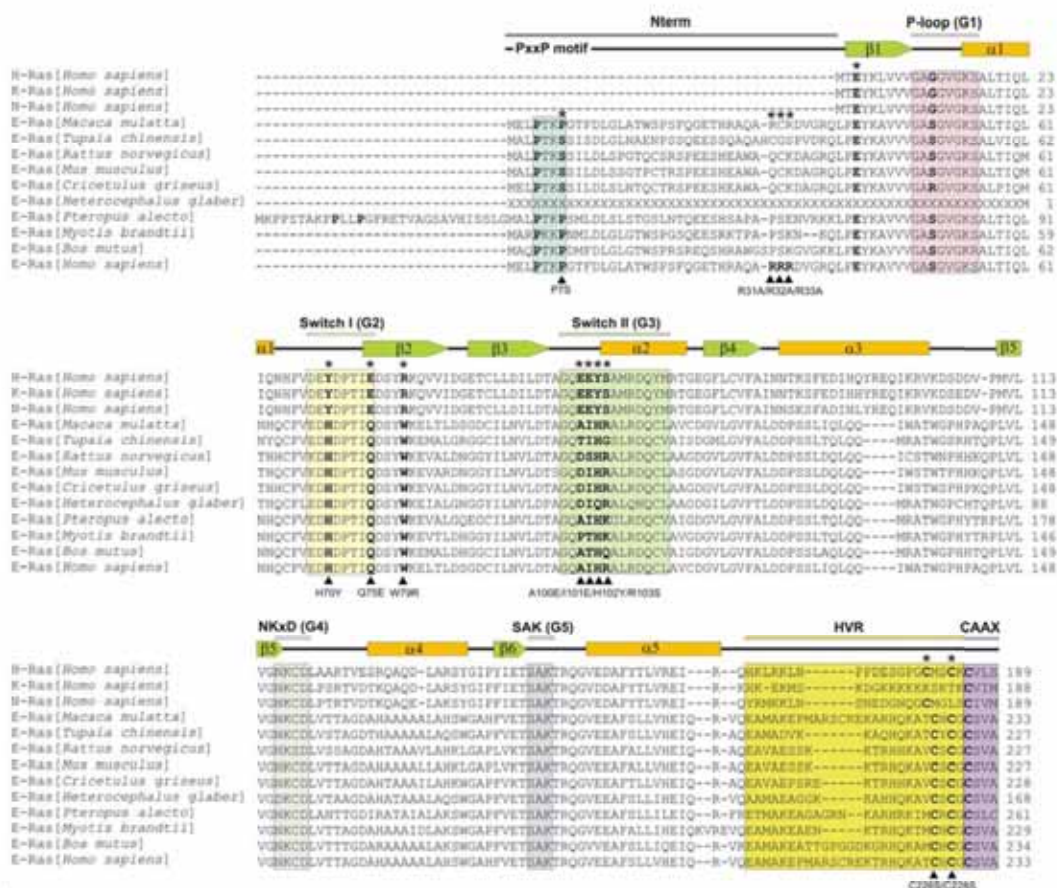
- Roberts, A. E., Lepri, F., Merbitz-Zahradnik, T., König, R., Kratz, C. P., Pantaleoni, F., Dentici, M. L., Joshi, V. A., Kuchelapati, R. S., *et al.* (2010) A restricted spectrum of NRAS mutations causes Noonan syndrome. *Nat. Genet.* **42**, 27–29
45. Margarit, S. M., Sondermann, H., Hall, B. E., Nagar, B., Hoelz, A., Pirruccello, M., Bar-Sagi, D., and Kuriyan, J. (2003) Structural evidence for feedback activation by Ras. GTP of the Ras-specific nucleotide exchange factor SOS. *Cell* **112**, 685–695
46. Nassar, N., Horn, G., Herrmann, C., Block, C., Janknecht, R., and Wittinghofer, A. (1996) Ras/Rap effector specificity determined by charge reversal. *Nat. Struct. Biol.* **3**, 723–729
47. Filchtinski, D., Sharabi, O., Ruppel, A., Vetter, I. R., Herrmann, C., and Shifman, J. M. (2010) What makes Ras an efficient molecular switch: a computational, biophysical, and structural study of Ras-GDP interactions with mutants of Raf. *J. Mol. Biol.* **399**, 422–435
48. Pacold, M. E., Suire, S., Perisic, O., Lara-Gonzalez, S., Davis, C. T., Walker, E. H., Hawkins, P. T., Stephens, L., Eccleston, J. F., and Williams, R. L. (2000) Crystal structure and functional analysis of Ras binding to its effector phosphoinositide 3-kinase γ . *Cell* **103**, 931–943
49. Scheffzek, K., Grünewald, P., Wohlgemuth, S., Kabsch, W., Tu, H., Wigler, M., Wittinghofer, A., and Herrmann, C. (2001) The Ras-Byr2RBD complex: structural basis for Ras effector recognition in yeast. *Structure* **9**, 1043–1050
50. Huang, L., Hofer, F., Martin, G. S., and Kim, S. H. (1998) Structural basis for the interaction of Ras with RalGDS. *Nat. Struct. Biol.* **5**, 422–426
51. Bunney, T. D., Harris, R., Gandarillas, N. L., Josephs, M. B., Roe, S. M., Sorli, S. C., Paterson, H. F., Rodrigues-Lima, F., Esposito, D., Ponting, C. P., Gierschik, P., Pearl, L. H., Driscoll, P. C., and Katan, M. (2006) Structural and mechanistic insights into ras association domains of phospholipase C ϵ . *Mol. Cell* **21**, 495–507
52. Qamra, R., and Hubbard, S. R. (2013) Structural basis for the interaction of the adaptor protein grb14 with activated ras. *PLoS One* **8**, e72473
53. Stieglitz, B., Bee, C., Schwarz, D., Yildiz, O., Moshnikova, A., Khokhlatchev, A., and Herrmann, C. (2008) Novel type of Ras effector interaction established between tumour suppressor NORE1A and Ras switch II. *EMBO J.* **27**, 1995–2005
54. Vavvas, D., Li, X., Avruch, J., and Zhang, X. F. (1998) Identification of Nore1 as a potential Ras effector. *J. Biol. Chem.* **273**, 5439–5442
55. González-García, A., Pritchard, C. A., Paterson, H. F., Mavria, G., Stamp, G., and Marshall, C. J. (2005) RalGDS is required for tumor formation in a model of skin carcinogenesis. *Cancer Cell* **7**, 219–226
56. Castellano, E., and Downward, J. (2011) RAS interaction with PI3K: more than just another effector pathway. *Genes Cancer* **2**, 261–274
57. Bunney, T. D., and Katan, M. (2006) Phospholipase C ϵ : linking second messengers and small GTPases. *Trends Cell Biol.* **16**, 640–648
58. Yan, J., Roy, S., Apolloni, A., Lane, A., and Hancock, J. F. (1998) Ras isoforms vary in their ability to activate Raf-1 and phosphoinositide 3-kinase. *J. Biol. Chem.* **273**, 24052–24056
59. Song, C., Hu, C. D., Masago, M., Kariyai, K., Yamawaki-Kataoka, Y., Shibatohe, M., Wu, D., Satoh, T., and Kataoka, T. (2001) Regulation of a novel human phospholipase C, PLC, through membrane targeting by Ras. *J. Biol. Chem.* **276**, 2752–2757
60. Kuriyama, M., Harada, N., Kuroda, S., Yamamoto, T., Nakafuku, M., Iwamatsu, A., Yamamoto, D., Prasad, R., Croce, C., Canaani, E., and Kaibuchi, K. (1996) Identification of AF-6 and canoe as putative targets for Ras. *J. Biol. Chem.* **271**, 607–610
61. Lambert, J. M., Lambert, Q. T., Reuther, G. W., Malliri, A., Siderovski, D. P., Sondke, J., Collard, J. G., and Der, C. J. (2002) Tiam1 mediates Ras activation of Rac by a PI(3)K-independent mechanism. *Nat. Cell Biol.* **4**, 621–625
62. Hancock, J. F., Magee, A. I., Childs, J. E., and Marshall, C. J. (1989) All ras proteins are polyisoprenylated but only some are palmitoylated. *Cell* **57**, 1167–1177
63. Matallanas, D., Sanz-Moreno, V., Arozarena, I., Calvo, F., Agudo-Ibáñez, L., Santos, E., Berciano, M. T., and Crespo, P. (2006) Distinct utilization of effectors and biological outcomes resulting from site-specific Ras activation: Ras functions in lipid rafts and Golgi complex are dispensable for proliferation and transformation. *Mol. Cell Biol.* **26**, 100–116
64. Goodwin, J. S., Drake, K. R., Rogers, C., Wright, L., Lippincott-Schwartz, J., Philips, M. R., and Kenworthy, A. K. (2005) Depalmitoylated Ras traffics to and from the Golgi complex via a nonvesicular pathway. *J. Cell Biol.* **170**, 261–272
65. Kaizaki, R., Yashiro, M., Shinto, O., Yasuda, K., Matsuzaki, T., Sawada, T., and Hirakawa, K. (2009) Expression of ERas oncogene in gastric carcinoma. *Anticancer Res.* **29**, 2189–2193
66. Simons, K., and Toomre, D. (2000) Lipid rafts and signal transduction. *Nat. Rev. Mol. Cell Biol.* **1**, 31–39
67. Iwabuchi, K., Handa, K., and Hakomori, S. (1998) Separation of “glycosphingolipid signaling domain” from caveolin-containing membrane fraction in mouse melanoma B16 cells and its role in cell adhesion coupled with signaling. *J. Biol. Chem.* **273**, 33766–33773
68. Jaumot, M., Yan, J., Clyde-Smith, J., Sluimer, J., and Hancock, J. F. (2002) The linker domain of the Ha-Ras hypervariable region regulates interactions with exchange factors, Raf-1 and phosphoinositide 3-kinase. *J. Biol. Chem.* **277**, 272–278
69. Prior, I. A., Muncke, C., Parton, R. G., and Hancock, J. F. (2003) Direct visualization of Ras proteins in spatially distinct cell surface microdomains. *J. Cell Biol.* **160**, 165–170
70. Prior, I. A., and Hancock, J. F. (2001) Compartmentalization of Ras proteins. *J. Cell Sci.* **114**, 1603–1608
71. Rotblat, B., Prior, I. A., Muncke, C., Parton, R. G., Kloog, Y., Henis, Y. I., and Hancock, J. F. (2004) Three separable domains regulate GTP-dependent association of H-ras with the plasma membrane. *Mol. Cell Biol.* **24**, 6799–6810
72. Innocenti, M., Frittoli, E., Ponzanelli, I., Falck, J. R., Brachmann, S. M., Di Fiore, P. P., and Scita, G. (2003) Phosphoinositide 3-kinase activates Rac by entering in a complex with Eps8, Abi1, and Sos-1. *J. Cell Biol.* **160**, 17–23
73. Inabe, K., Ishiai, M., Scharenberg, A. M., Freshney, N., Downward, J., and Kurosaki, T. (2002) Vav3 modulates B cell receptor responses by regulating phosphoinositide 3-kinase activation. *J. Exp. Med.* **195**, 189–200
74. Dillon, L. M., Bean, J. R., Yang, W., Shee, K., Symonds, L. K., Balko, J. M., McDonald, W. H., Liu, S., Gonzalez-Angulo, A. M., Mills, G. B., Arteaga, C. L., and Miller, T. W. (2014) P-REX1 creates a positive feedback loop to activate growth factor receptor, PI3K/AKT and MEK/ERK signaling in breast cancer. *Oncogene* **6**, 328
75. Holly, S. P., Larson, M. K., and Parise, L. V. (2005) The unique N-terminus of R-ras is required for Rac activation and precise regulation of cell migration. *Mol. Biol. Cell* **16**, 2458–2469
76. Riou, P., Kjaer, S., Garg, R., Purkiss, A., George, R., Cain, R. J., Bineva, G., Reymond, N., McColl, B., Thompson, A. J., O'Reilly, N., McDonald, N. Q., Parker, P. J., and Ridley, A. J. (2013) 14-3-3 proteins interact with a hybrid prenyl-phosphorylation motif to inhibit G proteins. *Cell* **153**, 640–653
77. Jaiswal, M., Dvorsky, R., and Ahmadian, M. R. (2013) Deciphering the molecular and functional basis of Dbl family proteins: a novel systematic approach toward classification of selective activation of the Rho family proteins. *J. Biol. Chem.* **288**, 4486–4500
78. Vanhaesebroeck, B., Guillermet-Guibert, J., Graupera, M., and Bilanges, B. (2010) The emerging mechanisms of isoform-specific PI3K signalling. *Nat. Rev. Mol. Cell Biol.* **11**, 329–341
79. Matsunaga-Udagawa, R., Fujita, Y., Yoshiki, S., Terai, K., Kamioka, Y., Kiyokawa, E., Yugi, K., Aoki, K., and Matsuda, M. (2010) The scaffold protein Shoc2/SUR-8 accelerates the interaction of Ras and Raf. *J. Biol. Chem.* **285**, 7818–7826
80. Cordeddu, V., Di Schiavi, E., Pennacchio, L. A., Ma'ayan, A., Sarkozy, A., Fodale, V., Cecchetti, S., Cardinale, A., Martin, J., Schackwitz, W., Lipzen, A., Zampino, G., Mazzanti, L., Digilio, M. C., Martinelli, S., *et al.* (2009) Mutation of SHOC2 promotes aberrant protein N-myristoylation and causes Noonan-like syndrome with loose anagen hair. *Nat. Genet.* **41**, 1022–1026
81. Rodriguez-Viciana, P., Osés-Prieto, J., Burlingame, A., Fried, M., and McCormick, F. (2006) A phosphatase holoenzyme comprised of Shoc2/Sur8 and the catalytic subunit of PP1 functions as an M-Ras effector to modulate Raf activity. *Mol. Cell* **22**, 217–230
82. Ferro, E., and Trabalzini, L. (2010) RalGDS family members couple Ras to Ral signalling and that's not all. *Cell. Signal.* **22**, 1804–1810

Supplementary Data

The function of embryonic stem cell-expressed Ras (E-Ras), a unique Ras family member, correlates with its additional motifs and its structural properties

Saeideh Nakhaei-Rad¹, Hossein Nakhaeizadeh¹, Claus Kordes², Ion C. Cirstea^{1,3}, Malte Schmick⁴, Radovan Dvorsky¹, Philippe I. H. Bastiaens⁴, Dieter Häussinger², Mohammad Reza Ahmadian¹

¹Institute of Biochemistry and Molecular Biology II, Medical Faculty of the Heinrich-Heine University, Düsseldorf, Germany; ²Clinic of Gastroenterology, Hepatology and Infectious Diseases, Medical Faculty of the Heinrich-Heine University, Düsseldorf, Germany; ³Leibniz Institute for Age Research - Fritz Lipmann Institute, 07745 Jena, Germany; ⁴Department of Systemic Cell Biology, Max Planck Institute of Molecular Physiology, Dortmund, Germany.

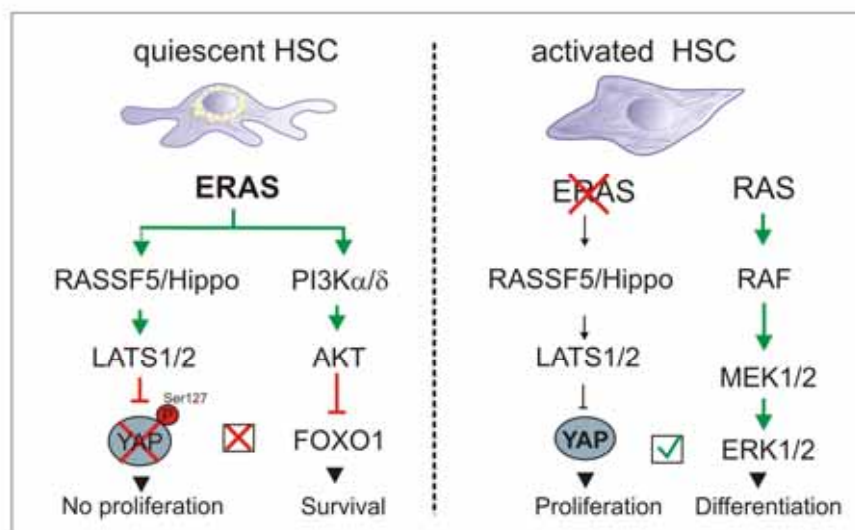


Supplementary FIGURE S1. Overall sequence comparison of mammalian E-Ras proteins with classical Ras proteins. E-Ras contains an extended N-terminus (aa 1-38), missing in H-, K-, and N-Ras, with a putative SH3-binding motif (PxxP). G1 to G5 boxes indicate the presence of five essential GDP/GTP binding (G) motifs. The P-loop (G1) of E-Ras contains a serine instead of a glycine (codon 12, H-Ras numbering), a frequently mutated site within *RAS* genes in human cancer (Fasano *et al.*, 1984). Several residues in switch I (G2) and switch II (G3) regions that are responsible for effector recognition are different between E-Ras and H-Ras (bold letters). E-Ras contains, like H-Ras, a CAAX motif and two cysteines at the C-terminal hypervariable region (HVR), which is the sites for PTMs by farnesylation and palmitoylation, respectively. The incomplete, N-terminal sequence of *Heterocephalus glaber* E-Ras is shown by X letters. The secondary structure elements, the α helices (orange) and β sheets (green), of the G domain were deduced from the H-Ras crystal structure (Pai *et al.*, 1990) (PDB code: 5p21). The mutation sites of E-Ras variants, which are used in this study, are highlighted by arrowheads below and asterisk above the sequence.

Chapter III

Embryonic stem cell-expressed ERAS controls quiescence of hepatic stellate cells

Graphical Abstract



Published in:

Impact factor:

Own Proportion to this work:

The journal of biological chemistry

4.56 (2014)

85%

Site direct mutagenesis

Cloning

Transfection

RNA isolation

Real-time PCR

Confocal microscopy

Pull-down assay

Immunoprecipitation

Immunoblotting

Preparing of the manuscript



The Role of Embryonic Stem Cell-expressed RAS (ERAS) in the Maintenance of Quiescent Hepatic Stellate Cells^{*§}

Received for publication, October 22, 2015, and in revised form, February 13, 2016. Published, JBC Papers in Press, February 16, 2016, DOI 10.1074/jbc.M115.700088

Saeideh Nakhaei-Rad[†], Hossein Nakhaeizadeh[†], Silke Götze[§], Claus Kordes[§], Iris Sawitzka[§], Michèle J Hoffmann[§], Manuel Franke[†], Wolfgang A. Schulz[§], Jürgen Scheller[†], Roland P. Piekorz[†], Dieter Häussinger[§], and Mohammad R. Ahmadian^{†1}

From the [†]Institute of Biochemistry and Molecular Biology II, Medical Faculty, the [§]Clinic of Gastroenterology, Hepatology, and Infectious Diseases, and the [‡]Department of Urology, Medical Faculty, Heinrich-Heine University, 40225 Düsseldorf, Germany

Hepatic stellate cells (HSCs) were recently identified as liver-resident mesenchymal stem cells. HSCs are activated after liver injury and involved in pivotal processes, such as liver development, immunoregulation, regeneration, and also fibrogenesis. To date, several studies have reported candidate pathways that regulate the plasticity of HSCs during physiological and pathophysiological processes. Here we analyzed the expression changes and activity of the RAS family GTPases and thereby investigated the signaling networks of quiescent HSCs *versus* activated HSCs. For the first time, we report that embryonic stem cell-expressed RAS (ERAS) is specifically expressed in quiescent HSCs and down-regulated during HSC activation via promoter DNA methylation. Notably, in quiescent HSCs, the high level of ERAS protein correlates with the activation of AKT, STAT3, mTORC2, and HIPPO signaling pathways and inactivation of FOXO1 and YAP. Our data strongly indicate that in quiescent HSCs, ERAS targets AKT via two distinct pathways driven by PI3K α/δ and mTORC2, whereas in activated HSCs, RAS signaling shifts to RAF-MEK-ERK. Thus, in contrast to the reported role of ERAS in tumor cells associated with cell proliferation, our findings indicate that ERAS is important to maintain quiescence in HSCs.

Hepatic stellate cells (HSCs²; also called Ito cells, lipocytes, fat storing cells, or perisinusoidal cells) contribute 5–8% of

total liver-resident cells and are located between sinusoidal endothelial cells and hepatocytes in the space of Dissé (1, 2). HSCs play pivotal roles in liver development, immunoregulation, regeneration, and pathology. They exhibit a remarkable plasticity in their phenotype, gene expression profile, and cellular function (3). In healthy liver, HSCs remain in a quiescent state and store vitamin A mainly as retinyl palmitate in cytoplasmic membrane-coated vesicles. Moreover, HSCs typically express neural and mesodermal markers (*i.e.* glial fibrillary acidic protein (GFAP) and desmin). They possess characteristics of stem cells, like the expression of Wnt and NOTCH, which are required for developmental fate decisions. Activated HSCs display an expression profile highly reminiscent of mesenchymal stem cells. Due to typical functions of mesenchymal stem cells, such as differentiation into adipocytes and osteocytes as well as support of hematopoietic stem cells, HSCs were identified as liver-resident mesenchymal stem cells (4).

Following liver injury, HSCs become activated and exhibit properties of myofibroblast-like cells. During activation, HSCs release vitamin A, up-regulate various genes, including α -smooth muscle actin and collagen type I, and down-regulate GFAP (2). Activated HSCs are multipotent cells, and recent studies revealed a new aspect of HSCs plasticity (*i.e.* their differentiation into liver progenitor cells during liver regeneration) (5, 6). Physiologically, HSCs represent well known extracellular matrix-producing cells. In some pathophysiological conditions, sustained activation of HSCs causes the accumulation of extracellular matrix in the liver and initiates liver diseases, such as fibrosis, cirrhosis, and hepatocellular carcinoma. Therefore, it is worthwhile to reconsider the impact of different signaling pathways on HSC fate decisions in order to be able to modulate them so that activated HSCs contribute to liver regeneration but not fibrosis. To date, several growth factors (PDGF, TGF β , and insulin-like growth factor) and signaling pathways have been described to control HSC activation through effector pathways, including Wnt, Hedgehog, NOTCH, RAS-MAPK, PI3K-AKT, JAK-STAT3, and HIPPO-YAP (7–13). However, there is a need to further identify key players that orchestrate HSC activity and to find out how they control as positive and negative regulators HSC activation in

* This work was supported by the Deutsche Forschungsgemeinschaft through Collaborative Research Center 974 (SFB 974), "Communication and System Relevance during Liver Injury and Regeneration." The authors declare that they have no conflicts of interest with the contents of this article.

§ This article contains supplemental Table S1 and Figs. S1–S4.

¹ To whom correspondence should be addressed: Institut für Biochemie und Molekularbiologie II, Medizinische Fakultät der Heinrich-Heine-Universität, Universitätsstr. 1, Gebäude 22.03, 40225 Düsseldorf, Germany. Tel.: 49-211-81-12384; Fax: 49-211-81-12726; E-mail: reza.ahmadian@uni-duesseldorf.de.

² The abbreviations used are: HSC, hepatic stellate cell; aa, amino acid(s); CTGF, connective tissue growth factor; RAS, rat sarcoma; ERAS, embryonic stem cell-expressed RAS; EYFP, enhanced YFP; FOXO1, forkhead transcription factor; GAP, GTPase-activating protein; GFAP, glial fibrillary acidic protein; HRAS, Harvey rat sarcoma; KRAS, Kirsten rat sarcoma; MMP, matrix metalloproteinase; MRAS, muscle RAS; mSIN1, mammalian stress-activated MAPK-interacting protein 1; mTORC, mammalian target of rapamycin; NRAS, neuroblastoma RAS; PDK1, 3-phosphoinositide-dependent protein kinase; PLC, phospholipase C; PPAR γ , peroxisome proliferative-activator receptor- γ ; RBD, RAS-binding domain; RA, RAS association domain; RAL, RAS-like; RALGDS, guanine nucleotide dissociation stimulator; RAP2, RAS-related protein 2; RASSF5, RAS-association domain family; RRAS, related RAS viral; SATB1, special AT-rich binding protein 1; SREBP,

sterol regulatory element-binding protein; TSC, tuberous sclerosis; YAP, Yes-associated protein; qPCR, quantitative PCR; 5-AZA, 5-aza-2'-deoxycytidine; LIF, leukemia inhibitory factor; miRNA, microRNA; d, day; p-, phosphorylated.

The Role of ERAS in Quiescent Hepatic Stellate Cells

response to liver injury. Among these pathways, RAS signaling is one of the earliest that was identified to play a role in HSC activation (14) and to act as a node of intracellular signal transduction networking. Therefore, RAS-dependent signaling pathways were the focus of the present study.

Small GTPases of the RAS family are involved in a variety of cellular processes ranging from intracellular metabolisms to proliferation, migration, and differentiation as well as embryogenesis and normal development (15–17). RAS proteins respond to extracellular signals and transform them into intracellular responses through interaction with effector proteins. The activity of RAS proteins is highly controlled through two sets of specific regulators with opposite functions, the guanine nucleotide exchange factors and the GTPase-activating proteins (GAPs), as activators and inactivators of RAS signaling, respectively (18). In the present study, we analyzed the expression profile of different *Ras* isoforms in HSCs and found embryonic stem cell-expressed RAS (*ERas*) specifically expressed in quiescent HSCs. To date, *ERAs* expression has been reported in undifferentiated embryonic stem cells and in colorectal, pancreatic, breast, gastric, and neuroblastoma cancer cell lines (19–22). Recently, we demonstrated that *ERAs* represents a unique member of the RAS family with remarkable characteristics. The most profound features of *ERAs* include its GAP insensitivity (*i.e.* constitutive activity), its unique N terminus among all RAS isoforms, its distinct effector selection properties, and the posttranslational modification site at its C terminus (23).

Here, we investigated in detail the expression, localization, and signaling network of *ERAs* in quiescent and culture-activated HSCs. During *ex vivo* culture-induced activation of HSCs, the expression of *ERAs* was significantly down-regulated at the mRNA and protein level, probably due to an increase in promoter DNA methylation. We examined possible interactions and signaling of *ERAs* via various RAS effectors in HSCs. We found that the PI3K α / δ -AKT, mTORC2-AKT, and RASSF5 (RAS association domain family)-HIPPO-YAP axis can be considered as downstream targets of *ERAs* in quiescent HSCs. In contrast, MRAS, RRAS, and RAP2A and also the RAS-RAF-MEK-ERK cascade may control proliferation and differentiation in activated HSCs.

Materials and Methods

Cell Isolation and Culture—Male Wistar rats (500–600 g) were obtained from the local animal facility of Heinrich Heine University (Düsseldorf, Germany). The livers were used for isolation of HSCs as described previously (24). Briefly, rat livers were enzymatically digested with collagenase H (Roche Applied Science) and protease E (Merck) and subjected to density gradient centrifugation to obtain primary cultures of HSCs. Purified HSCs were cultured in Dulbecco's modified Eagle's medium (DMEM) supplemented with 15% fetal calf serum and 50 units of penicillin/streptomycin (Gibco Life Technologies). Other liver cells, such as parenchymal cells, Kupffer cells, and sinusoidal liver endothelial cells were isolated and cultivated as described earlier (25). MDCKII and COS-7 cells were cultured in DMEM supplemented with 10% fetal calf serum. TurboFect transfection reagent (Life Technologies) was used to transfect

MDCKII and COS-7 cells according to the manufacturer's protocol.

DNA Methyltransferase and Histone Deacetylase Inhibitor Treatment—Primary rat HSCs at day 3 were treated with 10 μ M 5-aza-2'-deoxycytidine (5-AZA) (Decitabine, Sigma catalog no. A3656), a specific DNA methyltransferase inhibitor, for 4 successive days. In parallel, rat HSCs were treated with a 5 μ M concentration of the histone deacetylase inhibitor suberoylanilide hydroxamic acid (Vorinostat, Cayman Chemicals catalog no. 10009929) under the same conditions. The control cells were treated with DMSO only. Cells were lysed at day 8 for RNA isolation and quantitative real-time reverse transcriptase polymerase chain reaction (qPCR) analysis.

Reverse Transcriptase Polymerase Chain Reaction—Cells were disrupted by QIAzol lysis reagent (Qiagen, Germany), and total RNA was extracted via the RNeasy Plus kit (Qiagen, Germany) according to the manufacturer's protocol. The quality and quantity of isolated RNA samples were analyzed on 1% agarose gels and using a Nanodrop spectrophotometer, respectively. Possible genomic DNA contaminations were removed using the DNA-freeTM DNA removal kit (Ambion, Life Technologies). DNase-treated RNA was transcribed into complementary DNA (cDNA) using the ImProm-IITM reverse transcription system (Promega, Germany). qPCR was performed using TaqMan probes or SYBR Green reagent (Life Technologies). Probes/primers used for qPCR in the Taqman system, including Rn02098893_s1 for *ERAs* and Rn01527840_m1 for HPRT1, were purchased from Applied Biosystems (Life Technologies). Primer sequences are listed in supplemental Table S1. The $2^{-\Delta\Delta Ct}$ method was employed for estimating the relative mRNA expression levels and $2^{-\Delta\Delta Ct}$ for mRNA levels. HPRT1 was used for normalization.

Immunostaining—Immunostaining was performed as described previously (23). Briefly, cells were washed twice with ice-cold PBS containing magnesium/calcium and fixed with 4% formaldehyde (Merck) for 20 min at room temperature. To permeabilize cell membranes, cells were incubated in 0.25% Triton X-100/PBS for 5 min. Blocking was done with 3% bovine serum albumin (BSA; Merck) and 2% goat serum diluted in PBS containing 0.25% Triton X-100 for 1 h at room temperature. Incubation with primary antibodies was performed overnight at 4 °C followed by staining at room temperature for 2 h. Cells were washed three times for 10 min with PBS and incubated with secondary antibodies for 2 h at room temperature. Slides were washed three times, and the ProLong[®] Gold antifade mountant with 4',6-diamidino-2-phenylindole (DAPI) (Life Technologies) was applied to mount the coverslips. Primary antibodies included rabbit anti-FLAG (catalog no. F7425, Sigma-Aldrich), *ERAs* clone 6.5.2, and GFAP (catalog no. Z0334, Dako). Secondary antibodies included Alexa488-conjugated goat anti-rabbit IgG (catalog no. A11034), Alexa546-conjugated goat anti-mouse IgG (catalog nos. A11003 and A11008), Alexa633-conjugated goat anti-rabbit IgG (catalog no. A4671), and Alexa488-conjugated goat anti-mouse IgG (catalog no. A11029) (all from Life Technologies). Confocal images were obtained using an LSM 510-Meta microscope (Zeiss, Jena, Germany).

The Role of ERAS in Quiescent Hepatic Stellate Cells

Constructs—Rat *ERas* cDNA was amplified by PCR from a cDNA library of freshly isolated rat hepatic stellate cells and subsequently cloned into pcDNA3.1 and pEYFP-C1 vectors via the BamHI/XhoI and EcoRI/BamHI restriction sites, respectively. Mutations of G12V in *HRAS* (*HRAS^{V12}*) and C220S/C222S in *ERas* (*ERas^{S/S}*) were introduced by PCR-based site-directed mutagenesis as described earlier (26). To generate the N-terminal truncated *ERas* variants (*ERas^{ΔN}* and *ERas^{ΔN/S/S}*), *ERas^{wt}* and *ERas^{S/S}* cDNA was PCR-amplified from amino acid (aa) 39 to 227 and from aa 1 to 227, respectively. Human *HRAS*, *KRAS*, *NRAS*, *TC21*, *MRAS*, and *ERAS* as well as rat *ERas* were cloned in pGEX vectors and used for protein purification for *Escherichia coli* as described previously (27).

Pull-down Assay—FLAG-tagged rat *ERas* and human *HRAS* cDNAs were cloned into pcDNA3.1 vector and overexpressed in COS-7 cells. The RAS-binding/association domains of effector proteins, including CRAF-RBD (aa 51–131), RALGDS-RA (aa 777–872), PLC ϵ -RA (aa 2130–2240), p110 α -RBD (aa 127–314), and RASSF5-RA (aa 200–358), were constructed as GST fusions in pGEX-4T and transformed in *E. coli*. GST-fused proteins were isolated from total bacterial lysates using glutathione-Sepharose beads. GTP-bound RAS proteins were pulled down from total cell lysates and heated in Laemmli buffer for 10 min at 95 °C.

Immunoblotting—Cell lysates were made with lysis buffer (50 mM Tris-HCl, pH 7.5, 100 mM NaCl, 2 mM MgCl₂, 1% Igepal CA-630, 10% glycerol, 20 mM β -glycerolphosphate, 1 mM *ortho*-Na₃VO₄, EDTA-free protease inhibitor (Roche Applied Science)), and protein concentrations were determined with a Bradford assay (Bio-Rad). Equal amounts of cell lysates (ERAS, 120 μ g; FOXO1/p-FOXO1, 50 μ g; remaining proteins, 15 μ g), were subjected to SDS-PAGE. Following electrophoresis, the proteins were transferred to a nitrocellulose membrane by electroblotting and probed with primary antibodies overnight at 4 °C. All antibodies from Santa Cruz Biotechnology, Inc. were diluted 1:200 in 5% nonfat milk (Merck)/TBST (Tris-buffered saline, 0.05% Tween 20), and remaining antibodies were diluted 1:1000. The following antibodies were applied for immunoblotting: rabbit anti-FLAG (catalog no. F7425) and mouse γ -tubulin (catalog no. T5326) from Sigma-Aldrich; rabbit MEK1/2 (catalog no. 9126), rabbit ERK1/2 (catalog no. 9102), rabbit AKT (catalog no. 9272), rabbit phospho-MEK1/2 (Ser-217/Ser-221, catalog no. 9154), rabbit phospho-ERK1/2 (Thr-202/Thr-204, catalog no. 9106), rabbit phospho-AKT (Ser-473, catalog no. 4060; Thr-308, catalog no. 2965), rabbit p110 α (catalog no. 4249), mouse STAT3 (catalog no. 9139S), rabbit phospho-STAT3 (catalog no. 9145S), rabbit FOXO1 (catalog no. 2880), and rabbit phospho-FOXO1 (catalog no. 9461) all from Cell Signaling; and antibodies to rabbit p110 β (catalog no. sc-602), p110 γ (catalog no. sc-7177), and p110 δ (catalog no. sc-7176) from Santa Cruz Biotechnology. Mouse α -actin antibody (catalog no. MAB1510) was obtained from Millipore. Membranes were stained with horseradish peroxidase (HRP)-conjugated secondary antibodies (1:5000 dilution). Signals were visualized using ECL (enhanced chemiluminescence) reagent (GE Healthcare).

Expression and Purification of GBD-Nanotrap Beads and Co-immunoprecipitation—For immunoprecipitation studies of overexpressed EYFP-fused HRAS and ERAS in COS-7 cells, we applied a GFP-binding protein coupled to Sepharose beads. The GFP-binding protein used for Nanotrap experiments was designed as described previously (28). Briefly, the GFP-binding V_HH domain was cloned into pET23a-PelB vector adding C-terminal Myc and histidine (His₆) tags and transformed in *E. coli* BL21. An overnight 50-ml *E. coli* preculture with the antibiotic ampicillin was used to inoculate 2000 ml of medium to an A₆₀₀ of 0.8. The expression of recombinant genes was induced with 1 mM isopropyl β -D-1-thiogalactopyranoside overnight at 30 °C. Cells were harvested by centrifugation (2 h, 4 °C, 4000 rpm), and the supernatant was stored at –80 °C. For purification, the supernatant was filtered through a 0.45- μ m SFCAL NALGENE® Rapid-Flow™ Bottle Top Filter (Thermo Scientific, Waltham, MA) to remove cell debris. Flow-through was mixed 1:1 with PP buffer (500 mM NaCl, 50 mM Na₂HPO₄/NaH₂PO₄, pH 7.4) and loaded on a pre-equilibrated nickel-nitrilotriacetic acid column (GE Healthcare) and purified. His-tagged protein was eluted by PP buffer containing 500 mM imidazole. The protein was concentrated, and imidazole was removed by using Amicon® Ultra-15 10K centrifugal filter devices (Merck Millipore Ltd., Tullagreen, Ireland). To perform pull-down of proteins by the GBD-nanotrap technique, 1 mg of purified protein was covalently coupled to 2 ml of NHS-activated Sepharose 4 Fast Flow (GE Healthcare), according to the manufacturer's instructions. Thereafter, beads were washed three times in ice-cold 1 mM HCl (2 min, 5400 rpm, 4 °C), added to the purified protein, and mixed for 2 h at room temperature under constant agitation. Subsequently, free binding sites of the beads were blocked by adding blocking buffer (0.5 M ethanolamine, 0.5 M NaCl, pH 8.3) for 2 h. Finally, beads were washed twice in 0.1 M Tris-HCl (pH 8). Beads were stored in 20% ethanol. For co-immunoprecipitation, cells were lysed in immunoprecipitation buffer (20 mM Tris-HCl, pH 7.4, 150 mM NaCl, 5 mM MgCl₂, 0.5% Nonidet P-40, 10 mM β -glycerolphosphate, 0.5 mM Na₃VO₄, 10% glycerol, EDTA-free protease inhibitor). Immunoprecipitation from total cell lysates was carried out for 2 h at 4 °C with GFP-fused nanobeads. The beads were washed five times with immunoprecipitation buffer lacking Nonidet P-40, and eluted proteins were finally heated in SDS-Laemmli buffer at 95 °C and analyzed by immunoblotting.

RAS Proteins and Monoclonal Antibody against ERAS—All RAS-like proteins, including ERAS, were purified following the same protocol as described (29). The monoclonal anti-ERAS antibody was custom-generated (Biogenes, Berlin, Germany) via immunization of mice with a purified N-terminal peptide of rat ERAS and thereafter purified from the supernatant of the respective hybridoma cell line by a protein A column (GE Healthcare). The concentrated antibody solution (~3 mg/ml) was supplemented with 10% glycerol and stored at –20 °C.

Subcellular Fractionation of HSCs by Differential Centrifugation—A differential centrifugation protocol according to Taha *et al.* (30) was used in this study to fractionate HSCs.

DNA Methylation Analysis of ERAS Promoter—A genome-wide DNA methylation analysis from quiescent and early activated HSCs was used to analyze DNA methylation changes dur-

The Role of ERAS in Quiescent Hepatic Stellate Cells

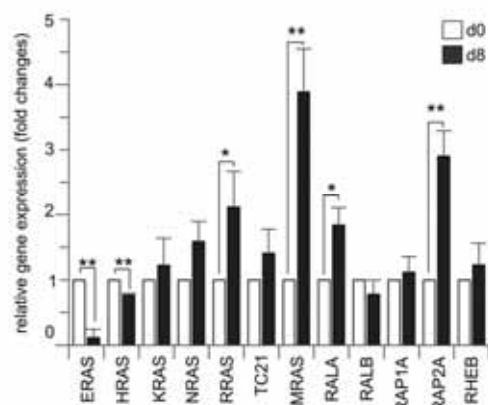


FIGURE 1. Differential transcription of genes related to the RAS family in quiescent versus activated HSCs in primary culture. qPCR analysis of RAS-related genes in freshly isolated HSCs from rat liver (d0) and after *ex vivo* cultivation for 8 days (d8) ($n = 3$, *t* test; *, $p < 0.05$; **, $p < 0.001$). Error bars, S.E.

ing HSC activation (31). The methylation data were visualized using the UCSC genome browser (University of California, Santa Cruz, CA). Verification of DNA methylation changes was performed by direct bisulfite sequencing. DNA from freshly isolated and cultured HSCs was isolated using the DNeasy blood and tissue kit (Qiagen) and subjected to bisulfite conversion by the EpiTect bisulfite kit (Qiagen). Bisulfite primers for *ERas* were designed using the MethPrimer online tool (32) covering a part of the promoter region (*ERas* 328 bp forward, 5'-GTT GGG GGT AGG GAG TAT TTT AAT-3'; *ERas* 328 bp reverse, 5'-CTC AAA ATT AAA AAA AAA AAA TAA CC-3'). Bisulfite PCR was performed using the Maxima Hot Start PCR Master Mix (Thermo Scientific) together with 20 ng of bisulfite-modified DNA and 0.6 $\mu\text{mol/liter}$ primer. After activation at 95 °C, a PCR protocol with denaturation at 95 °C, annealing at 55 °C, and elongation at 72 °C was used for 40 cycles. The PCR products were purified and sequenced at the DNA sequencing facility of Heinrich-Heine University. DNA methylation was quantified by the Mquant method as described (33). The height of the thymine peak at a CpG dinucleotide was subtracted from the average signal of 10 surrounding thymine peaks to quantify DNA methylation at this site. For the *ERas* methylation analysis, we calculated the mean DNA methylation of five CpG sites in the *ERas* promoter region.

Results

Expression of ERAS in Quiescent but Not Activated HSCs—To investigate the impact of RAS proteins on HSCs, we first investigated the expression profile of various members of the *Ras* family in quiescent versus activated rat HSCs by qPCR. Freshly isolated primary HSCs were cultivated on plastic dishes for up to 8 days, where they become activated upon *ex vivo* culture and undergo myofibroblast transition (4). HSCs were analyzed at day 8 (d8) in comparison with unseeded HSCs (d0) as representative of the activated and quiescent state, respectively. Interestingly, among the different members of the *Ras* family, *ERas* was specifically expressed in quiescent HSCs and strongly down-regulated during HSC activation (Fig. 1). In addition, we applied a probe based TaqMan real-time PCR to monitor *ERas*

expression at the different time points of HSC cultivation (d0, d1, d2, d4, and d8) and obtained comparable results (supplemental Fig. S1). In contrast, *HRas* expression decreased only slightly in HSCs (d8). In contrast, the gene expressions of *MRas*, *RRas*, *Rala*, and *Rap2A* were up-regulated in activated HSCs, whereas other genes, including *KRAS* and *NRas*, were expressed but did not significantly differ between day 0 and day 8 (Fig. 1). Collectively, these data indicate a switch from *ERas* to *MRas*, *RRas*, *Rala*, and *Rap2A* expression during HSC activation.

Generation and Validation of Specific Monoclonal Antibodies against Rat ERAS—ERAS contains an N-terminal extension upstream of its GTP-/GDP-binding (G) domain that is unique among the RAS family (23). As depicted in Fig. 2A, there is a significant difference between *Homo sapiens* (*hs*) and *Rattus norvegicus* (*rn*) ERAS proteins regarding their N terminus (Fig. 2A). Therefore, we purified the N terminus of *R. norvegicus* ERAS and generated antibodies against this unique ERAS region. Four clones of monoclonal antibodies (mAbs) were obtained and examined for anti-ERAS specificity. Immunoblot analysis of RAS proteins overexpressed in and purified from *E. coli* showed that clone mAb 6.5.2 clearly detected rat ERAS but none of the other members of the RAS family (Fig. 2B). The selectivity of mAb 6.5.2 against *H. sapiens* ERAS and *R. norvegicus* ERAS proteins was tested by using COS-7 and MDCKII cell lysates overexpressing *H. sapiens* ERAS and *R. norvegicus* ERAS as EYFP fusion proteins, respectively. As shown in Fig. 2C, mAb 6.5.2 only recognized rat ERAS (Fig. 2A). We next tested mAb 6.5.2 in confocal immunofluorescence analysis by overexpressing EYFP- and FLAG-tagged ERAS variants in MDCKII cells. As depicted in Fig. 2D, mAb 6.5.2 shows a clear specificity against full-length rat ERAS and recognized neither *H. sapiens* ERAS nor *R. norvegicus* ERAS lacking the N-terminal extension (*rnERAS* ^{Δ N}). Taken together, mAb 6.5.2 was validated as a rat-specific anti-ERAS antibody suitable for both immunoblotting and immunofluorescence analysis.

Among Various Rat Liver Cell Types, ERAS Protein Is Only Expressed in Quiescent HSCs—The mAb 6.5.2 was used to analyze the presence of ERAS protein in typical liver cell populations. Therefore, total cell lysates of freshly isolated HSCs, parenchymal cells, Kupffer cells, and sinusoidal liver endothelial cells from rat liver were used for immunoblot analysis. Interestingly, ERAS was detected as a 25 kDa band in HSCs but not in other liver cell types (Fig. 3A). Consistent with the mRNA expression data (Fig. 1), the amount of ERAS protein was drastically reduced during the activation process of HSCs, thereby correlating with the loss of GFAP (Fig. 3B), which marks quiescent HSCs. In contrast, the myofibroblast marker α -smooth muscle actin became detectable in cultured HSCs from day 4. Moreover, confocal imaging of HSCs revealed that ERAS was mainly cytosolic, which was, in contrast to GFAP, still detectable in cultivated HSCs, although at much lower amounts as compared with day 0 (Fig. 3C). Noteworthy, in subcellular fractions of HSCs (d0), ERAS was predominantly found in the light membrane fraction (Golgi apparatus, smooth endoplasmic reticulum, and various organelles) and to a minor extent in the heavy membrane fraction (plasma membrane and rough endoplasmic reticulum) and in the nucleus (Fig. 3D). Collectively,

The Role of ERAS in Quiescent Hepatic Stellate Cells

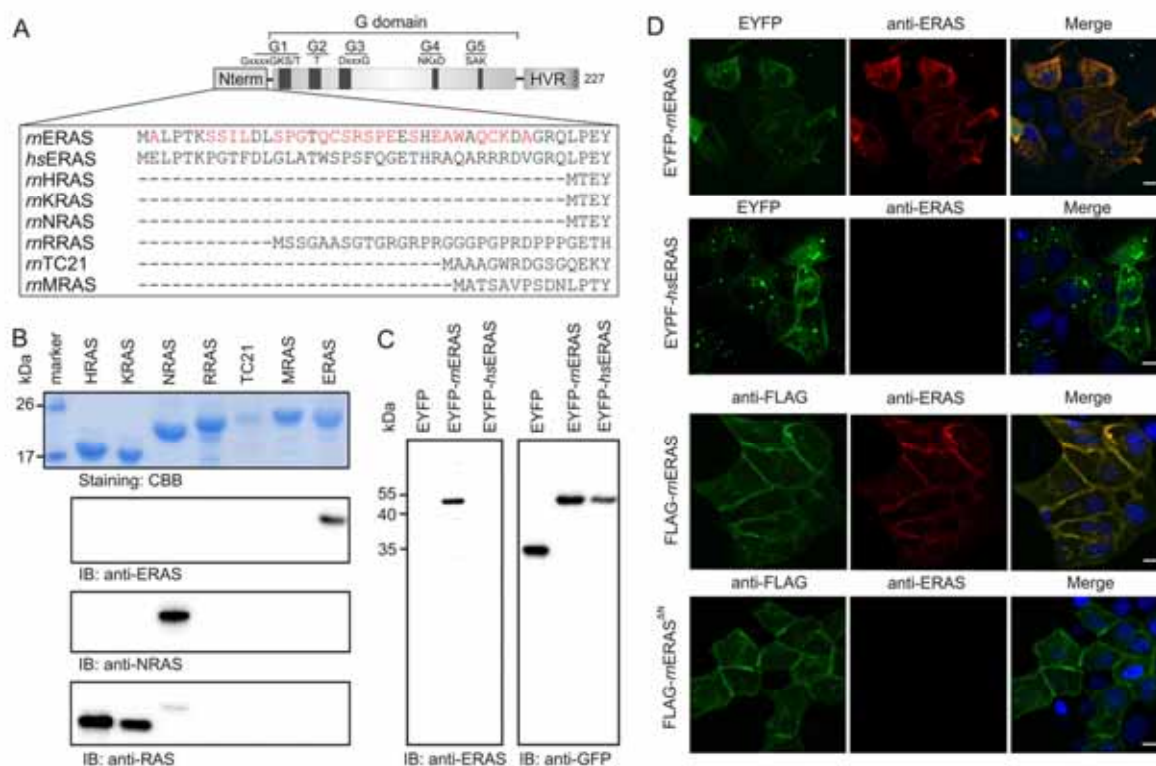


FIGURE 2. Specification and validation of a monoclonal antibody raised against the rat ERAS N terminus. *A*, a unique N-terminal extension in ERAS proteins. An amino acid sequence comparison between ERAS and other RAS proteins revealed that ERAS displays an additional region upstream of its G domain that is unique for ERAS in different organisms (23). *H. sapiens* (*hs*) and *R. norvegicus* (*m*) ERAS (NP_853510.1 and NP_001102845.1, respectively) largely differ within this region (red letters in *R. norvegicus* ERAS). *B*, the anti-ERAS monoclonal antibody, clone 6.5.2, only recognized purified ERAS protein and not other RAS family members. Immunoblotting (IB) analysis of different RAS proteins, purified from *E. coli*, showed the high specificity of clone 6.5.2 against rat ERAS and exhibited no cross-reactivity against other RAS species. Two other antibodies were used as controls, which only recognized NRAS, HRAS, and KRAS, respectively, and not ERAS. HRAS and KRAS do not contain the hypervariable region (HVR) and are therefore smaller as compared, for example, with NRAS. *C* and *D*, anti-ERAS antibody (clone 6.5.2) recognized recombinant *R. norvegicus* ERAS but not *H. sapiens* ERAS, overproduced in COS-7 cells as YFP fusion proteins by immunoblotting (*C*) and in MDCKII cells as FLAG-tagged protein by confocal imaging (*D*). The FLAG-*mERAS*^{ΔN} construct, lacking the N-terminal 38 amino acids of *R. norvegicus* ERAS, was used as a negative control. Scale bar, 10 μ m. CBB, Coomassie Brilliant Blue.

ERAS was detectable in quiescent HSCs, and its protein levels diminished remarkably during HSC activation.

Protein-Protein Interaction Profiling Identifies PI3K α as a Specific Effector of Rat ERAS—Members of the RAS family GTP-binding proteins act as molecular switches that transduce extracellular signals to intracellular responses via activation of effector proteins. To gain insights into the effector binding specificity downstream of rat ERAS, FLAG-tagged constructs of HRAS and ERAS were overexpressed in COS-7 cells, and total cell lysates were used for pull-down experiments. For pull-down analysis, five major RAS effector proteins were employed (*i.e.* CRAF-RBD, RALGDS-RA, PLC ϵ -RA, PI3K α -RBD, and RASSF5-RA) (23), which were all produced in *E. coli* as GST fusion proteins. Interestingly, we found that ERAS, in comparison with HRAS, preferentially and most strongly bound to PI3K α , whereas only a modest interaction was observed with RASSF5 and CRAF (Fig. 4A). Unlike HRAS, no ERAS association with RALGDS and PLC ϵ was detectable (Fig. 4A). Thus, ERAS and HRAS interact with and probably activate a specifically non-overlapping set of effector proteins.

Similar to HRAS and NRAS, ERAS contains conserved C-terminal motifs for posttranslational modifications, a farnesyla-

tion- and palmitoylation-like HRAS (23). ERAS has an N-terminal extension with various motifs and shows a critical amino acid deviation, a serine at position 50 instead of a glycine (Gly-12 in HRAS), which makes ERAS GAP-insensitive (23). These properties may influence physical interaction of ERAS with PI3K and its downstream signaling. Therefore, we generated and analyzed different ERAS variants, lacking either the N terminus (ERAS^{ΔN}) or conserved cysteines for palmitoylation (ERAS^{S/S}) or both (ERAS^{ΔN/S/S}) (Fig. 4B). First, we investigated binding of ERAS variants to the catalytic subunit of PI3K α . The obtained data revealed that all ERAS variants were able to associate with PI3K α -RBD (Fig. 4C, top). This suggests that the N terminus of ERAS and its C-terminal modification by palmitoylation are not essential for the association of PI3K α -RBD with the G domain of ERAS.

To examine the signaling activity of ERAS variants toward AKT via PI3K and mTORC2 pathways, we next monitored the phosphorylation states of AKT using specific anti-phospho-AKT (threonine 308 and serine 473) antibodies. It is noteworthy that ERAS strongly activated AKT and induced its phosphorylation at two distinct sites (*i.e.* at Thr-308 by PI3K-PDK1 (p-AKT^{T308}) and at Ser-473 by mTORC2 (p-AKT^{S473}; Fig. 4C,

The Role of ERAS in Quiescent Hepatic Stellate Cells

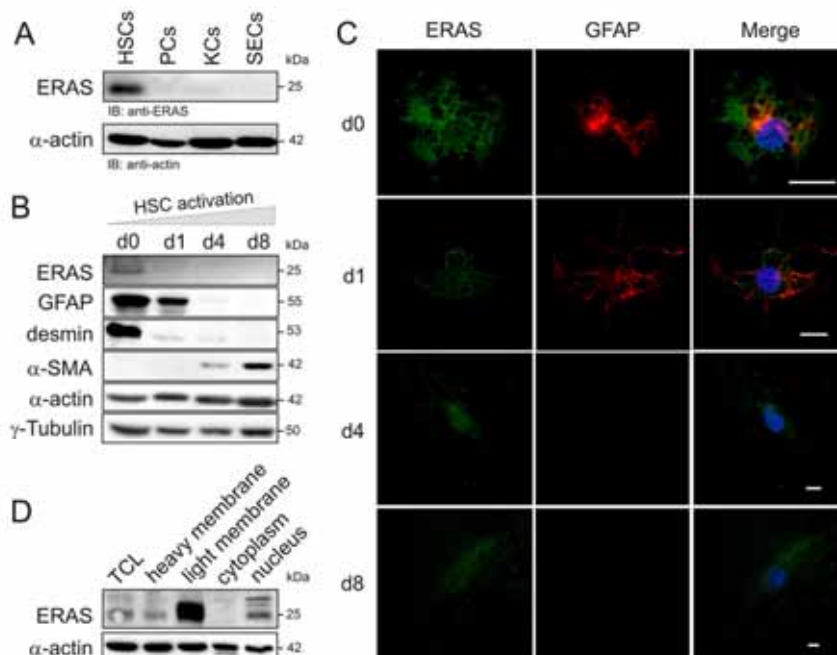


FIGURE 3. ERAS protein in HSCs. *A*, Immunoblot analysis of isolated liver cell lysates detected ERAS in HSCs but not in other liver cells. PCs, parenchymal cell; KCs, Kupffer cells; SECs, sinusoidal endothelial cells. *B*, Immunoblot analysis of ERAS from freshly isolated (*d0*) and activated HSCs maintained in monoculture up to 8 days (*d8*). GFAP and desmin were used as markers for quiescent HSCs (*d0*), and α -smooth muscle actin was used as a marker for activated HSCs (*d8*). α -actin and γ -tubulin served as loading controls. *C*, Confocal imaging of ERAS and GFAP in HSC monocultures from *d0* to *d8*. The level of ERAS and also of GFAP is significantly reduced in the course of cell culture with a trace amount of ERAS in the nucleus. Scale bar, 10 μ m. *D*, ERAS showed a diverse subcellular distribution pattern in HSCs at day 0 as revealed by subcellular fractionation analysis. HSCs were fractionated into four distinct fractions, including heavy membrane (plasma membrane and rough endoplasmic reticulum), light membrane (polysomes, Golgi apparatus, and smooth endoplasmic reticulum), cytoplasm (cytoplasm and lysosomes), and enriched nucleus.

bottom)). Interestingly, in comparison with ERAS wild type (WT), the ERAS variants, most notably the truncated N terminus (ERAS^{ΔN}), the palmitoylation-deficient variants with two cysteines 220 and 222 replaced with serines (ERAS^{S/S}), and a combination of both variants (ERAS^{ΔN/S/S}), elicited a significantly reduced AKT phosphorylation, especially of p-AKT^{S473}, which is indicative of mTORC2 activity. These data indicate that both the ERAS N terminus and its plasma membrane anchorage via palmitoylation are essential and critical for AKT activation via the PI3K and mTORC2 axis, although the formation of the GTP-bound state and the interaction with PI3K were not affected.

ERAS-PI3K α / δ -AKT and mTORC2-AKT Axis Are Highly Activated in Quiescent HSCs—Our findings suggest that the catalytic subunit of PI3K is a candidate effector downstream of ERAS. There are four isoforms of the p110 catalytic subunit of PI3K, p110 α , p110 β , p110 γ , and p110 δ , raising a question about the p110 isoform specificity in ERAS-PI3K interaction in HSCs. mRNA expression analysis data revealed that the α isoform of PI3K did not change remarkably between quiescent and activated HSCs, whereas the mRNA levels of the β and δ isoforms increased in the course of the HSC activation (Fig. 4D). At the protein level, however, α and γ isoforms were found at clearly higher levels in quiescent HSCs as compared with the β isoform (Fig. 4E). Upon HSC activation, the protein levels of β isoforms and, to a certain extent, also δ isoforms increased, whereas a decrease in α and γ isoforms was observed (Fig. 4E). Next, we

investigated the interaction of ERAS with the four PI3K isoforms in co-immunoprecipitation experiments using ERAS overexpression in COS-7 cells. Wild type and a constitutive active variant of HRAS (HRAS^{WT} and HRAS^{V12}) were used as controls. Data shown in Fig. 4F demonstrated that not only PI3K α , but also the δ isoform, co-immunoprecipitated with ERAS. Notably, PI3K δ appeared to strongly bind HRAS^{V12} (Fig. 4F). Thus, cell-based investigations confirmed the interaction between ERAS and PI3K α , which is consistent with our data obtained under cell-free conditions (Fig. 4A).

In the next step, we monitored the AKT phosphorylation states and found that quiescent HSCs at day 0 and, to a certain extent, at day 1, as compared with activated HSCs, exhibited much higher p-AKT^{S473} and p-AKT^{T308} levels, representing mTORC2 and PI3K-PDK1 activity, respectively (Fig. 4G). In addition, we also analyzed the phosphorylation states of FOXO1 and STAT3, two other signaling molecules that have been suggested to be downstream of ERAS (34). Interestingly, in ERAS-expressing quiescent HSCs, we observed high levels of STAT3 phosphorylation at Tyr-705 and of FOXO1 phosphorylation at Ser-256 (Fig. 4G). Thus, it is obvious that ERAS signaling toward PI3K-PDK1 and mTORC2 pathways activates AKT and maybe also STAT3 but inactivates FOXO1 in order to maintain HSCs in their quiescent state.

ERAS Does Not Actively Impact the MAPK Pathway—In the next step, we investigated the interaction of ERAS with CRAF-RBD and the MAPK pathway in quiescent versus activated

The Role of ERAS in Quiescent Hepatic Stellate Cells

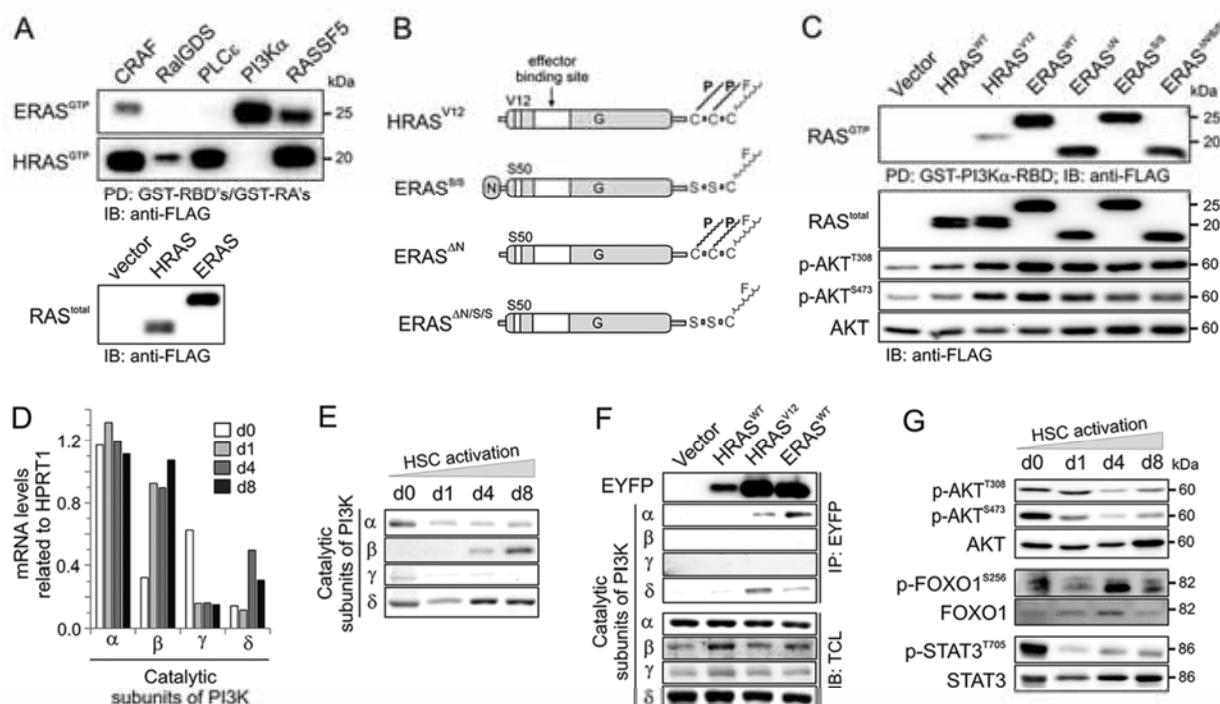


FIGURE 4. Highly active PI3K-AKT and mTORC2-AKT pathways in quiescent HSCs may be controlled by ERAS. *A*, transiently expressed FLAG-tagged rat ERAS^{WT} and human HRAS^{WT} were pulled down (PD) from COS-7 cell lysates with well known RAS effectors, including CRAF-RBD, RALGDS-RA, PLC ϵ -RA, PI3K α -RBD, and RASSF5-RA, as GST-fused proteins. Immunoblots (IB) of total cell lysates were used as a control to detect FLAG-RAS. *B*, FLAG-tagged RAS constructs used in this study, including ERAS^{WT}, ERAS^{AN} (N-terminal truncated, aa 39–227), ERAS^{S/S} (palmitoylation-deficient), and ERAS^{AN/S/S} (N-terminal truncated and palmitoylation-deficient) as well as HRAS^{WT} and HRAS^{V12} (G, G domain). *C*, PI3K α -RBD-derived pull-down (PD) of GTP-bound ERAS variants and their signaling activities were analyzed by immunoblotting of FLAG-tag and AKT phosphorylation (p-AKT) at positions Thr-308 and Ser-473. *D*, quantitative mRNA expression analysis of PI3K isoforms α , β , γ , and δ in quiescent and activated HSCs (d0–d8). *E*, immunoblot of the PI3K isoforms in quiescent and activated HSCs (d0–d8). *F*, co-immunoprecipitation analysis of the PI3K isoforms with ERAS^{WT}, HRAS^{WT}, and HRAS^{V12} overexpressed as EYFP fusion proteins in COS-7 cells. TCL, total cell lysate. *G*, immunoblot of the phosphorylated signaling proteins downstream of the PI3K-AKT and mTORC2-AKT axis in quiescent and activated HSCs (d0–d8). Total AKT, FOXO1, and STAT3 served as controls.

HSCs. Both wild-type ERAS and its palmitoylation-deficient variant (ERAS^{S/S}) strongly bound to CRAF-RBD, although with considerably lower affinity as compared with the constitutive active HRAS^{V12} variant (Fig. 5A). This binding was, however, weaker for ERAS^{AN} and ERAS^{AN/S/S}, both lacking the N-terminal extension. It is important to note that the latter variants are efficiently expressed and also exist in GTP-bound forms (Fig. 4C). The same is true for HRAS^{WT}, which was expressed to a similar level as HRAS^{V12} (Fig. 4C). However, its GTP-bound level was much lower due to its ability to hydrolyze GTP normally, therefore resulting in low amounts of HRAS^{WT} in the CRAF-RBD pull-down experiment (Fig. 5A). Most remarkably, expression of ERAS^{WT} in COS-7 cells clearly led to a strong reduction of p-MEK1/2 and p-ERK1/2 levels that were far below those obtained with vector control and the HRAS variants (Fig. 5A). Notably, similar effects were observed for all ERAS variants analyzed (ERAS^{AN}, ERAS^{S/S}, and ERAS^{AN/S/S}).

In addition, we analyzed the binding property of rat ERAS to cellular RAF isoforms (ARAF, BRAF, and CRAF) by overexpressing and immunoprecipitating EYFP-tagged ERAS from COS-7 total cell lysates. As controls, we used HRAS^{WT} and HRAS^{V12}. Fig. 5B shows that ERAS, compared with HRAS^{V12}, bound weakly only to ARAF and CRAF, which is consistent with the data obtained with CRAF-RBD in pull-down experi-

ments (Fig. 5A). Thus, we conclude that ERAS can be excluded as an activator of RAF proteins and thus of the MAPK pathway.

The MAPK Pathway Is Highly Dynamic in Activated HSCs—Our data showed that ERAS is endogenously expressed in quiescent HSCs and does not seem to be an activator of the MAPK pathway under overexpression conditions in COS-7 cells. Therefore, we analyzed the activity of the MAPK pathway in HSCs following their activation. First, we analyzed the expression of *Raf*, *MEK*, and *ERK* isoforms in quiescent versus activated HSCs by qPCR. As indicated in the legend to Fig. 5C, the overall mRNA levels were very similar except for the low expression of *BRAF* in both quiescent and activated HSCs (Fig. 5C). For further examination of the role of the MAPK pathway in HSC activation, we looked at the protein levels of phosphorylated (*i.e.* activated) versus total MEK1/2 and ERK1/2. As shown in Fig. 5D, expression of MEK1/2 increased strongly in the course of the HSC activation as compared with the relatively constant amounts of ERK1/2. The level of ERK1 (44 kDa) was much higher than ERK2 (42 kDa). In contrast, the amounts of the RAF isoforms and total RAS were highest in quiescent HSCs (day 0) and decreased during HSCs activation (Fig. 5D). Most remarkably, we observed an increase in p-MEK1/2 and p-ERK1/2, especially p-ERK2, suggesting increased activation of the MAPK pathway in activated HSCs (Fig. 5D). In contrast,

The Role of ERAS in Quiescent Hepatic Stellate Cells

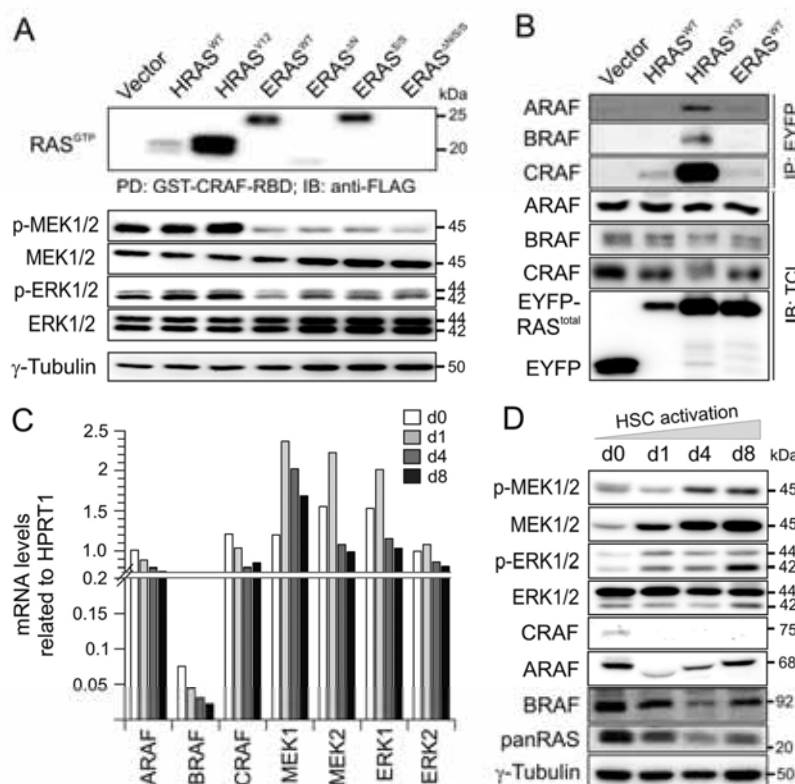


FIGURE 5. RAF-MEK-ERK signaling in activated HSCs. *A*, CRAF-RBD-derived pull-down (PD) of GTP-bound HRAS and ERAS variants and their signaling activities toward MAPK pathway were analyzed by immunoblotting (IB) of the FLAG tag and phosphorylation of MEK1/2 (p-MEK1/2) and ERK1/2 (p-ERK1/2) using total cell lysates derived from transfected COS-7 cells. γ -Tubulin was used as the loading control. *B*, co-immunoprecipitation analysis (IP) of the RAF isoforms with ERAS^{WT}, HRAS^{WT}, and HRAS^{V12} overexpressed as EYFP fusion proteins in COS-7 cells. *TCL*, total cell lysate. *C*, quantitative mRNA expression analysis of the *Raf*, *MEK*, and *ERK* isoforms in quiescent and activated HSCs (d0–d8). *D*, immunoblot analysis of the components of the MAPK pathway, including RAF isoforms, p-MEK1/2, and p-ERK1/2 in quiescent and activated HSCs (d0–d8). Total RAS was detected using a pan-RAS antibody. Total amounts of MEK1/2 and ERK1/2 as well as γ -tubulin served as loading controls.

the amounts of the RAF isoforms and total RAS were the highest in quiescent HSCs (day 0) and subsequently decreased during HSC activation (Fig. 5D). Taken together, it seems that HSCs reciprocally utilize distinct pathways downstream of ERAS to maintain their fate (*i.e.* PI3K-PDK1 and mTORC2 pathways could be activated by ERAS in quiescent HSCs, and the MAPK pathway could be activated by RAS in activated HSCs).

ERAS Contributes to Repression of YAP Activity and Thus May Counteract Activation of Quiescent HSCs—*In vitro* protein-protein interaction studies revealed that ERAS, like HRAS, directly interacts with RASSF5 (Figs. 4A and 6A). It has been reported that RASSF5 enables the HIPPO pathway (via MST2/STK3) to respond to and integrate diverse cellular signals by acting as a positive regulator of MST2/STK3 (35). A recent study revealed a role of YAP, the central effector of the HIPPO pathway during HSC activation (13); thus, we analyzed whether ERAS activates the HIPPO pathway, which may lead to phosphorylation and proteolytic degradation of YAP (supplemental Figs. S2 and S3A). We further investigated whether YAP and its target genes are expressed in activated rat HSCs. To address the first question, we used COS-7 cells, which normally contain significant amounts of YAP and its phosphorylated form

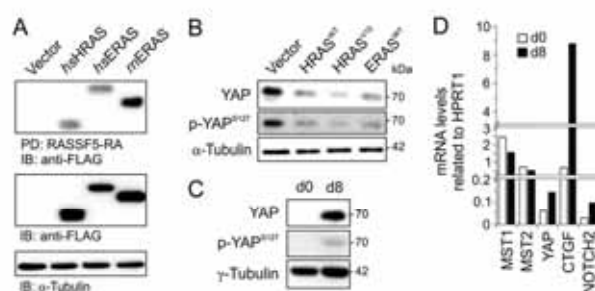


FIGURE 6. ERAS-RASSF5 interaction may repress YAP that is highly active in activated HSCs. *A*, RASSF5-RA pull-down (PD) of HRAS^{WT}, *H. sapiens* ERAS, and *R. norvegicus* ERAS overexpressed in COS-7 cells. Total amounts of FLAG-tagged RAS proteins as well as α -tubulin were detected as loading controls. *B*, immunoblotting. *C*, immunoblot of YAP and p-YAP at Ser-127 of COS-7 cell lysate overexpressing wild-type ERAS and HRAS as well as the constitutive active variant of HRAS (HRAS^{V12}). α -Tubulin was used as the loading control. *D*, immunoblot of YAP and p-YAP at Ser-127 of quiescent (d0) and activated HSCs (d8). γ -Tubulin served as a control. *E*, qPCR analysis of MST1 and -2 as well as YAP and its target genes *Ctgf* and *Notch2* in quiescent (d0) versus activated HSCs (d8).

(p-YAP^{S127}; Fig. 6B; see vector control). Interestingly, p-YAP^{S127} and YAP levels were considerably reduced when rat ERAS was overexpressed (Fig. 6B and supplemental Fig. S2),

The Role of ERAS in Quiescent Hepatic Stellate Cells

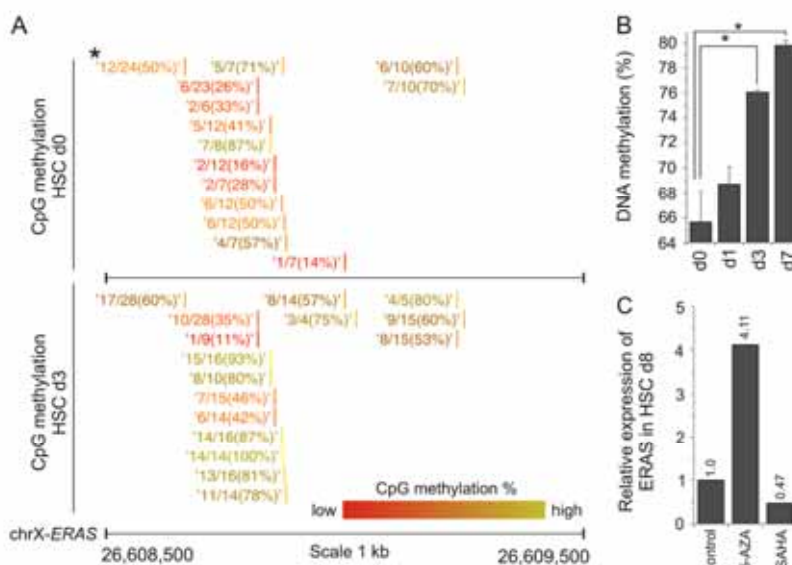


FIGURE 7. DNA methylation analyses of ERAS in quiescent and activated primary HSCs. A, results of genome-wide DNA methylation analysis of quiescent HSCs (d0) and early activated HSCs (d3) at the ERAS promoter region. DNA methylation of individual CpG dinucleotides is depicted in percent (methylated CpG/total numbers of CpG) and displayed with a color code from red (0%) to light green (100% DNA methylation). B, ERAS promoter methylation analyzed by direct bisulfite sequencing exhibited a significant increase of DNA methylation during HSCs activation ($n = 3-5$, t test; $^* p < 0.05$). C, HSC (day 3) were treated with 10 μM 5-aza-2'-deoxycytidine (5-AZA) and/or 5 μM suberoylanilide hydroxamic acid (SAHA) for 4 days, and the expression of ERAS was analyzed with qPCR at day 8. Error bars, S.E.

strongly indicating that ERAS activated the HIPPO pathway in COS-7 cells. Similar results were obtained with the HRAS variants (Fig. 6B). Importantly, we next probed YAP and p-YAP^{S127} in HSC lysates and detected them in activated HSCs (day 8) but not in quiescent HSCs (Fig. 6C). Consistently, mRNA analysis further revealed that *Mst1/2* (mammalian orthologues of *Hippo*) isoforms were expressed in both states but with more elevated levels of *Mst1* as compared with *Mst2*. *Yap* and its target genes, *Ctgf* (connective tissue growth factor) and *Notch2*, exhibited a distinct increase in their expression levels after HSC activation (Fig. 6D). Moreover, the effector binding domain (switch regions) of ERAS differs considerably from those of HRAS in critical residues, which may determine the specificity of ERAS binding to its effectors (23) (supplemental Fig. S3B). Interestingly, we found that mutation of two surface-exposed residues (H70Y/Q75E) in the effector binding region of ERAS (ERAS^{SW1}) abolishes the binding affinity for RASSF5 as compared with wild-type ERAS (supplemental Fig. S3C). These findings indicate that ERAS needs specific residues that are not conserved within HRAS to interact with RASSF5. To monitor the activity of the ERAS-RASSF5-MST1/2-LATS1/2-YAP cascade downstream of mutated ERAS, we next analyzed the levels of YAP protein in total cell lysates. Consistently, we detected larger amounts of YAP under conditions when the RASSF5 binding-deficient ERAS mutant (ERAS^{SW1}) was overexpressed (supplemental Fig. S3, D and E). These data further support the idea that ERAS is upstream of the HIPPO-YAP pathway. Collectively, activation of the HIPPO pathway appears to keep HSCs in their quiescent state, whereas YAP clearly may play a role in the activation and eventually further development of HSCs. YAP is obviously repressed in quiescent HSCs potentially mediated through ERAS-RASSF5 signaling.

Increased DNA Methylation of the ERAS Locus Is Associated with ERAS Gene Silencing in Activated HSCs—To characterize possible mechanisms responsible for the down-regulation of ERAS expression in activated HSCs, epigenetic analysis of the promoter region of the rat ERAS gene was conducted. Evaluation of a previously performed genome-wide DNA methylation analysis showed an increase of CpG methylation at the ERAS promoter of ~18% during early HSC activation (Fig. 7A). More detailed bisulfite-sequencing analysis during *in vitro* HSC activation revealed a significant increase in promoter DNA methylation, which correlates with the drastic decrease in ERAS expression in HSCs during their activation (Figs. 1 and 7B and supplemental Fig. S1). Of note, the overall degree of promoter DNA methylation increased from 65.5 to ~80% at day 7 of HSC culture. To investigate the functional impact of ERAS promoter methylation, we examined whether the DNA methyltransferase inhibitor 5-AZA could restore ERAS expression in activated HSC. Therefore, we cultivated primary rat HSC for 3 days, such that the levels of ERAS mRNA were down-regulated (supplemental Fig. S1). At day 8 of HSC activation (and 4 days of 5-AZA treatment), we analyzed ERAS expression. As indicated in Fig. 7C, 5-AZA treatment restored ERAS expression by ~4-fold in activated HSC. To test whether ERAS expression is also regulated via histone modifications, such as histone acetylation, we treated HSCs with 5 μM suberoylanilide hydroxamic acid (histone deacetylase inhibitor). As indicated in Fig. 7C, suberoylanilide hydroxamic acid treatment alone was not sufficient to rescue ERAS expression. Taken together, our data indicate that the profound decrease of ERAS expression but not NRAS and other Ras-related genes, such as RRAS and Rap2A (data not shown), during HSC activation may be caused by epigenetic gene silencing.

The Role of ERAS in Quiescent Hepatic Stellate Cells

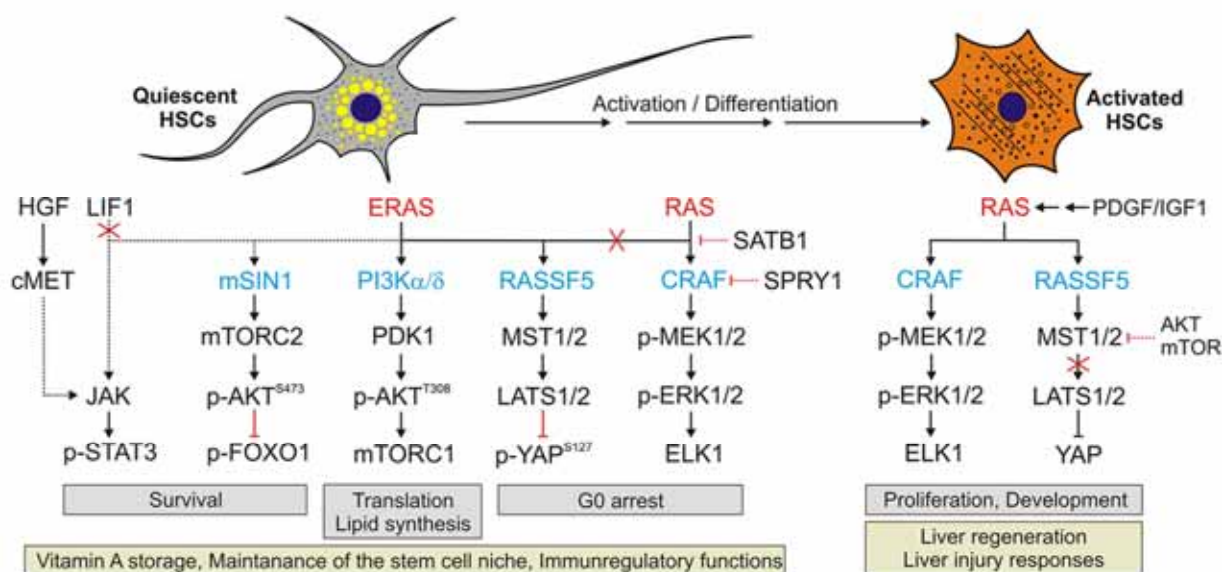


FIGURE B. Schematic view of the proposed model on reciprocal ERAS/RAS-dependent signaling pathways in quiescent versus activated HSCs (for details, see "Discussion"). ECM, extracellular matrix; IGF, insulin-like growth factor; LIF1, leukemia inhibitory factor; TSC, tuberous sclerosis.

Discussion

In this study, we found *ERAS* specifically expressed in one type of liver-resident cells, HSCs. The presence of *ERAS* mRNA was detected in quiescent HSCs but not in activated HSCs. In contrast, other RAS-related genes, such as *RRas*, *MRas*, *Rala*, and *Rap2A*, were up-regulated during HSC activation. ERAS protein was detected in quiescent HSCs but not in other liver cell types, and ERAS was considerably down-regulated during HSC activation (d4 and d8). To elucidate the functions of ERAS in quiescent HSCs, we sought ERAS-specific effectors and the corresponding downstream pathways. Interaction analyses with a set of RAS effectors showed that ERAS preferentially interacts with PI3K α and activates the PI3K-PDK1-AKT axis. The prominent AKT phosphorylation by mTORC2 in quiescent HSCs suggests that mTORC2-AKT acts as a candidate pathway mediates signaling downstream of ERAS. Interestingly, in quiescent HSCs, ERAS does not show any activity toward the MAPK cascade, which is the opposite in activated HSCs. The MST1/2-LATS1/2-YAP (HIPPO pathway) results in inactivation and proteosomal degradation of YAP if activated, for example, by RAS and RASSFs. The fact that YAP was hardly detectable in quiescent HSCs and also in COS-7 cells expressing ERAS, as well as the interaction between ERAS and RASSF5, suggests that ERAS may act as an activator of the HIPPO pathway in quiescent HSCs. Consistently, we detected both YAP protein and its up-regulated target genes in activated HSCs.

Role of the PI3K-AKT-mTORC1 Activity in Quiescent HSCs—Transient expression of ERAS in COS-7 cells and endogenous ERAS expression in quiescent HSCs strongly correlate with high levels of AKT phosphorylated at Thr-308 and Ser-473 through PDK1 and mTORC2, respectively. Protein interaction and immunoprecipitation analysis further revealed that ERAS physically interacts with PI3K α and also PI3K δ (Fig. 4, C and F).

Thus, in quiescent HSCs, we propose ERAS as a regulator of the PI3K-PDK1-AKT-mTORC1 axis. This axis is involved in various processes, including cell cycle progression, autophagy, apoptosis, lipid synthesis, and translation (36–40). The latter is controlled by mTOR-mediated activation of S6 kinase, which in turn phosphorylates different substrates, such as ribosomal protein S6, mTOR itself at Ser-2448, and mSIN1 at Thr-86, an upstream component of mTORC2 (Fig. 8) (41–43). Previous studies have shown that quiescent HSCs produce and secrete a significant amount of HGF (44, 45), which is known to regulate hepatocyte survival (46). HGF production and secretion is modulated by the mTORC1-S6 kinase pathway (47). Apart from the retinoid transport from hepatocyte to HSCs, the mTORC1 activity may influence *de novo* lipid synthesis in HSCs. mTORC1 might promote lipid synthesis in HSCs through sterol regulatory element-binding protein (SREBP) and peroxisome proliferative-activator receptor- γ (PPAR γ) (48). In this regard, it has been shown that curcumin inhibits SREBP expression in cultured HSCs by modulating the activities of PPAR γ and the specificity protein-1 (SP1), thereby repressing LDLR expression, which blocks a proposed LDL-induced HSC activation (49). Thus, the AKT-mTORC1-SREBP/PPAR γ pathway appears to play a critical role in lipid metabolism that is obviously required together with other pathways to regulate HSC fate.

Recently, Kwon *et al.* (50) have shown that in mouse embryonic stem cells overexpression of ERAS induces SP1 activation through the JNK pathways. However, it remains to be addressed whether JNK-SP1 signaling is also a downstream target of endogenous ERAS in HSC.

Activity of the mTORC2-AKT-FOXO1 Axis in Quiescent HSCs—In comparison with mTORC1, the regulation of mTORC2 is less understood (51). For example, the TSC1-TSC2 complex can physically associate with mTORC2 but not with

The Role of ERAS in Quiescent Hepatic Stellate Cells

mTORC1, which has been suggested to promote mTORC2 activity (52). Our findings indicate that ERAS may act as an activator of the mTORC2 pathway. Exogenous ERAS has been shown to promote phosphorylation of both AKT (Ser-473) and FOXO1 (Ser-256) in induced pluripotent stem cells generated from mouse embryonic fibroblasts (34). Thus, ERAS-AKT-FOXO1 signaling may be important for somatic cell reprogramming. We detected high levels of p-AKT^{S473} and p-FOXO1^{S256} in quiescent HSCs endogenously expressing ERAS (Fig. 4G). Phosphorylated FOXO1, sequestered in the cytoplasm, cannot translocate to the nucleus, where it binds to gene promoters and induces apoptosis (53). Interestingly, a possible link between ERAS and mTORC2 may be mSIN1, which appears to be an upstream component and modulator of mTORC2 activity (54). It has been reported that mSIN1 contains a RAS-binding domain with some homology to that of CRAF (55). Taken together, the ERAS-mTORC2-AKT-FOXO1 axis may ensure the survival of HSCs in the space of Dissé by interfering with programmed cell death (Fig. 8).

Role of the HGF-JAK-STAT3 Axis in Quiescent HSCs—Ectopic expression of ERAS stimulates phosphorylation of STAT3 probably downstream of leukemia inhibitory factor (LIF) (34). ERAS may compensate for lack of LIF to support the induced pluripotent stem cell generation (34). Moreover, the LIF-STAT3 axis is essential for keeping mouse stem cells undifferentiated in cultures and regulates self-renewal and pluripotency of embryonic stem cells (56). Phosphorylated STAT3 (p-STAT3) has been shown to directly interact with FOXO1/3 transcription factors and regulates their translocation into the nucleus (57). Consistently, we detected high levels of p-STAT3 and p-FOXO1 in quiescent HSCs (Fig. 4G), which may control survival, self-renewal, and multipotency of quiescent HSCs. In addition, stimulation of the HGF receptor (c-MET), which is expressed in HSCs, results in JAK activation and phosphorylation of STAT3 (1, 58). Interestingly, HGF is a target gene of IL6-STAT3 signaling (59, 60). Therefore, an autocrine HGF-JAK-STAT3 signaling may also account for STAT3 phosphorylation in quiescent HSCs (Fig. 8). However, determination of the presence and activity of a LIF-STAT3 axis in HSCs requires further investigation.

Quiescent HSCs Display a Locked RAS-MAPK Signaling Pathway—In quiescent HSCs, only basal levels of activated (phosphorylated) MEK and ERK could be observed, although all components of the RAS-RAF-MEK-ERK axis were expressed (Figs. 1 and 5 (C and D)). There are several explanations for the strongly reduced activity of RAS-MAPK signaling in quiescent HSCs (Fig. 8). (i) External stimuli, such as PDGFA and TGF β 1, are absent in healthy liver. These growth factors are strong activators of the MAPK pathway in activated HSCs (7, 8). (ii) An intracellular inhibitor, like special AT-rich binding protein 1 (SATB1), which is specifically expressed in quiescent HSCs and down-regulated during HSC activation (61), is present. Interestingly, SATB1 has been shown to be a strong inhibitor of the RAS-MAPK pathway that may block this signaling in quiescent HSCs (61). (iii) MicroRNAs (miRNAs), especially miRNA-21, may play a role in the reciprocal regulation of the RAS-MAPK pathway in quiescent *versus* activated HSCs. Up-regulated miRNA-21 in activated HSCs results in MAPK acti-

vation, which is based on depletion of SPRY1 (sprouty homolog 1), a target gene of miRNA-21 (62) and a negative regulator of the RAS-MAPK pathway (63).

Biological Functions of PI3K-AKT Pathway Regarding Different p110 Isoforms—The catalytic PI3K isoforms p110 α and - β are reported to be ubiquitously expressed, whereas the presence of p110 γ and - δ is restricted mainly to hematopoietic cell types (64–67). We identified ERAS as an activator of AKT by interacting with p110 α and moderately also with p110 δ (Fig. 4F). Our RNA and protein analyses indicated high levels of p110 α/γ in quiescent HSCs and elevated levels of p110 β/δ in activated HSCs (Fig. 4, D and E). Wetzker and colleagues (68) reported that retinoic acid treatment can stimulate expression of p110 γ , but not p110 β/δ , in U937 cells, a myelomonocytic cell line. Quiescent HSCs store high levels of retinoid acids as retinol esters in their lipid droplets, which may elicit the same function in HSCs by up-regulation of p110 γ . Khadem *et al.* (69) have shown that HSCs also express the p110 δ isoform and that p110 δ deficiency in HSCs prevents their activation and their supportive roles in T_{reg} expansion in mice infected with visceral leishmaniasis. Therefore, the high level of the p110 δ isoform in activated HSCs may correlate with its immunoregulatory functions.

Epigenetic Regulation of ERAS Expression in HSCs—Unlike other RAS proteins, ERAS is GAP-insensitive and refractory to inactivation by RASGAP proteins (21, 23). This raises the question about the potential mode(s) of ERAS regulation. Because ERAS is not ubiquitously expressed and seems to be limited to a few cell types, we proposed that ERAS is mainly regulated at the transcriptional level as described before for gastric cancers (70). Our epigenetic studies of the *ERas* promoter revealed that its DNA methylation increases (up to 18%) during HSC activation (Fig. 7, A and B). Moreover, treatment with DNA methyltransferase inhibitor induced re-expression of *ERas* in culture-activated HSCs (Fig. 7C). Consistently, *ERas* expression was also induced in certain gastric cell lines by the DNA methyltransferase inhibitor (70). Collectively, our findings clearly indicate that DNA methylation is one of the mechanisms suppressing expression of *ERas* during activation of HSCs. Conceivably, *ERas*-specific microRNAs may also control mRNA degradation and translation of *ERas* when HSC activation is induced.

Cellular Signaling Signature of Activated HSCs—*In vitro* culturing of hepatic stellate cells changes their gene expression profile and cellular properties, thereby stimulating the activation of HSCs (1, 31, 71, 72). HSCs typically lose their lipid droplets and expression of GFAP and elicit the synthesis of collagens, matrix metalloproteinases (MMP2, -9, and -13), and α -smooth muscle actin as important differentiation markers (2, 11). Collectively, during this process, HSCs alter their quiescent characteristics and develop into myofibroblast-like cells, which are recognized as proliferative, multipotent, and migratory cells (6, 73, 74). Comprehensive mRNA analysis of various RAS family members revealed that *RRas*, *MRas*, *RalA*, and *Rap2A* were up-regulated during HSC activation (Fig. 1). These genes may also play a role in the coordination of cellular processes, which are required for activation and differentiation of HSCs, such as polarity, motility, adhesion, and migration. Interestingly, *RRAS* has been implicated in integrin-dependent cell adhesion (75). Of note, in endothelial cells, the *RRAS*-*RIN2*-*RAB5* axis stimulates endo-

The Role of ERAS in Quiescent Hepatic Stellate Cells

cytosis of β_1 integrin in a RAC1-dependent manner (76). On the other hand, the muscle RAS oncogene homolog (*MRas*), an RRAS-related protein, is up-regulated during HSC activation. Among the different members of the RAS family, only *MRAS* can interact with SHOC2 in a ternary complex with protein phosphatase 1, which dephosphorylates autoinhibited CRAF and thereby activates the CRAF-MEK-ERK cascade (77). These findings and data obtained in this study suggest that *MRAS* may be responsible for the high levels of p-MEK and p-ERK in activated HSCs due to RAF kinase activation. RAP proteins, including RAP2A, are involved in different cellular processes and play pivotal roles in cell motility and cell adhesion (78, 79). Recently, it has been shown that RAP2A represents a novel target gene of p53 and a regulator of cancer cell migration (80). Moreover, expression of RAP2A in cancer cells results in secretion of two matrix metalloproteinases (MMP2 and -9) and AKT phosphorylation at Ser-473, which promotes tumor invasion (80). Notably, p53 is up-regulated in activated HSCs (81). Thus, we speculate that binding of p53 to RAP2A promoter may result in transcription of RAP2A in activated HSCs and may stimulate secretion of MMPs, which remodels the extracellular matrix and facilitates migration of HSCs in the space of Dissé.

Proliferation, Growth, and Differentiation of Activated HSCs—In comparison with quiescent HSCs, activated HSCs are proliferative cells and can pass through cellular checkpoints (82). One of the candidate pathways is the RAF-MEK-ERK cascade that can be stimulated via different growth factors. Consistent with previous studies, we detected high levels of p-MEK and p-ERK in culture-activated HSCs (7, 83). Three scenarios may explain the elevated RAF-MEK-ERK activity in activated HSCs. (i) As discussed above, *MRAS* with SHOC2 and protein phosphatase 1 is able to activate the CRAF-MEK-ERK pathway (80). Phospho-ERK translocates to the nucleus and phosphorylates different transcriptional factors, including Ets1 and c-Myc, thereby eliciting cell cycle progression and proliferation. The cytoplasmic p-ERK alternatively phosphorylates Mnk1 and p90RSK and thereby promotes protein synthesis and cell growth (84, 85). (ii) PDGF and insulin-like growth factor 1 are the most potent mitogens for activated HSCs and induce activation of MAPK pathways (7, 86). (iii) The expression of SATB1, a cellular inhibitor of the RAS-RAF-MEK-ERK pathway, significantly declines during HSC activation (61).

Putative Role of the ERAS-RASSF5-MST1/2-LATS1/2-YAP Axis in HSCs—We observed a moderate interaction between ERAS and RA of RASSF5A (Fig. 6A). Previously, we showed that the switch I region of ERAS is important for ERAS-RASSF5 interaction, and mutation in this region impairs ERAS binding to RASSF5 (23). RASSF proteins are recognized as specific RAS effectors with tumor suppressor function (87, 88). MST1/2, which are expressed in HSCs, interact with and form heterodimers with RASSF1/5A and WW45 through their SARA (SAV/RASSF/HPO) domain (89). This complex phosphorylates and activates LATS1/2, which in turn promotes phosphorylation, sequestration, and proteasomal degradation of YAP in the cytoplasm (supplemental Fig. S3A) (90, 91). YAP is a transcriptional co-activator that promotes transcription of *Ctcf* and *Notch2*, which are involved in cell development and differentiation (92–95). It has been shown that the HIPPO-YAP pathway plays a distinct role in differentiated parenchymal and

undifferentiated liver progenitor cells, respectively. Most recently, van Grunsven and colleagues (13) reported that the transcriptional co-activator of YAP controls *in vitro* and *in vivo* activation of HSCs. Consistent with this study, we observed hardly any YAP protein in quiescent HSCs in comparison with activated HSCs (Fig. 6C). Thus, our data suggest that YAP degradation through RASSF5-MST1/2-LATS1/2 may be triggered by binding and recruitment of RASSF5 to the plasma membrane via ERAS-GTP (Figs. 6B and 8).

Cell Survival and Anti-apoptotic Pathways—One of the most important features of activated HSCs is their survival and anti-apoptotic response during liver injury and regeneration (96). Here, we demonstrated elevated p-AKT levels not only in quiescent but also in activated HSCs, the latter leading to pro-survival responses, such as phosphorylation of FOXO1 (Fig. 4G). Additionally, we detected moderate levels of p-STAT3, implying that the JAK1-STAT3-SOCS3 axis may control the anti-apoptotic pathway in activated HSCs.

Last, the high levels of YAP transcriptional activity in activated HSCs, which might result from the inhibitory activities of AKT and mTOR on MST1/2 (97), may contribute to increased cell survival, proliferation, and development of activated HSCs (13) by causing antagonistic effects to the pro-apoptotic RAS-RASSF5-MST1/2-LATS1/2 pathway (Fig. 8).

Functional Similarity between Human and Rat ERAS—We observed sequence deviations between human and rat ERAS, especially at their extended N termini (Fig. 2A). Therefore, we compared the signaling activity of different human and rat ERAS variants. However, so far, we did not observe remarkable functional differences (Fig. 4 and supplemental Fig. S4). ERAS function in human diseases is poorly understood. Its expression profile ranges from embryonic stem cells to tumors (20, 21). Yamanaka and colleagues (21) have introduced ERAS as a critical factor for the maintenance of growth of embryonic stem cells. Kaizaki *et al.* (20) reported ERAS expression in 45% of gastric cancer tissues and observed a correlation between ERAS-negative patients and poorer prognosis. In addition, ERAS may promote transforming activity and chemoresistance in neuroblastoma patients (19).

In summary, expression analysis revealed a different pattern of RAS and RAS-signaling components in quiescent *versus* activated HSCs. Among different RAS family members, we identified *ERAs*, *p110 α* , and *p110 γ* to be mainly expressed in quiescent HSCs and *MRas*, *RRas*, *Rap2A*, *RalA*, *p110 β* , *p110 δ* , *Yap*, *Ctcf*, and *Notch2* expressed in activated HSCs. Our data suggest an increased activity via PI3K-AKT-mTORC1 and HIPPO signaling in quiescent HSCs. Therefore, this study adds ERAS signaling to the remarkable features of quiescent HSCs, and the cellular outcome of these signaling pathways would maintain the quiescent state of HSCs via inhibition of proliferation (HIPPO pathways, G₀ arrest) and apoptosis (PI3K-PDK1 and mTORC2) (see Fig. 8). On the other hand, activated HSCs exhibit YAP-CTGF/NOTCH2 and RAS-RAF-MEK-ERK activity, which are both involved in HSC proliferation and development (Fig. 8). Finally, we would like to point out that our study is based on the *ex vivo* activation of HSCs, which is a known model for the *in vivo* activation process (13, 72). However, there may be some aspects that could be different in the *ex vivo* model

and the *in vivo* situation. Therefore, future studies should also address the ERAS networking in an *in vivo* model of liver injury.

Author Contributions—M. R. A. conceived and coordinated the study. M. R. A. and S. N. R. designed the study and wrote the paper. S. N. R., H. N., S. G., I. S., C. K., M. J. H., and M. F. designed, performed, and analyzed the experiments. All authors reviewed the results and approved the final version of the manuscript.

Acknowledgments—We are grateful to Ehsan Amin, Doreen M. Floss, Alexander Lang, Ilse Meyer, Jens M. Moll, Boris Görg, Kazem Nouri, Claudia Rupperecht, Madhurendra Singh, and Si-Cai Zhang for helpful advice and stimulating discussion.

References

- Friedman, S. L. (2008) Hepatic stellate cells: protean, multifunctional, and enigmatic cells of the liver. *Physiol. Rev.* **88**, 125–172
- Kordes, C., and Häussinger, D. (2013) Hepatic stem cell niches. *J. Clin. Invest.* **123**, 1874–1880
- Yin, C., Evason, K. J., Asahina, K., and Stainier, D. Y. R. (2013) Hepatic stellate cells in liver development, regeneration, and cancer. *J. Clin. Invest.* **123**, 1902–1910
- Kordes, C., Sawitzka, I., Götze, S., and Häussinger, D. (2013) Hepatic stellate cells support hematopoiesis and are liver-resident mesenchymal stem cells. *Cell. Physiol. Biochem.* **31**, 290–304
- Yang, L., Jung, Y., Omenetti, A., Witek, R. P., Choi, S., Vandongen, H. M., Huang, J., Alpini, G. D., and Diehl, A. M. (2008) Fate-mapping evidence that hepatic stellate cells are epithelial progenitors in adult mouse livers. *Stem Cells* **26**, 2104–2113
- Kordes, C., Sawitzka, I., Götze, S., Herebian, D., and Häussinger, D. (2014) Hepatic stellate cells contribute to progenitor cells and liver regeneration. *J. Clin. Invest.* **124**, 5503–5515
- Reimann, T., Hempel, U., Krautwald, S., Axmann, A., Scheibe, R., Seidel, D., and Wenzel, K. W. (1997) Transforming growth factor- β 1 induces activation of Ras, Raf-1, MEK and MAPK in rat hepatic stellate cells. *FEBS Lett.* **403**, 57–60
- Carloni, V., Defranco, R. M., Caligiuri, A., Gentilini, A., Sciammetta, S. C., Baldi, E., Lottini, B., Gentilini, P., and Pinzani, M. (2002) Cell adhesion regulates platelet-derived growth factor-induced MAP kinase and PI-3 kinase activation in stellate cells. *Hepatology* **36**, 582–591
- Kordes, C., Sawitzka, I., and Häussinger, D. (2008) Canonical Wnt signaling maintains the quiescent stage of hepatic stellate cells. *Biochem. Biophys. Res. Commun.* **367**, 116–123
- Lakner, A. M., Moore, C. C., Gullledge, A. A., and Schrum, L. W. (2010) Daily genetic profiling indicates JAK/STAT signaling promotes early hepatic stellate cell transdifferentiation. *World J. Gastroenterol.* **16**, 5047–5056
- Xie, G., Karaca, G., Swiderska-Syn, M., Michelotti, G. A., Krüger, L., Chen, Y., Premont, R. T., Choi, S. S., and Diehl, A. M. (2013) Cross-talk between Notch and Hedgehog regulates hepatic stellate cell fate in mice. *Hepatology* **58**, 1801–1813
- de Souza, I. C. C., Meira Martins, L. A., de Vasconcelos, M., de Oliveira, C. M., Barbé-Tuana, F., Andrade, C. B., Pettenuzzo, L. F., Borojevic, R., Margis, R., Guaragna, R., and Guma, F. C. R. (2015) Resveratrol regulates the quiescence-like induction of activated stellate cells by modulating the PPAR γ /SIRT1 ratio. *J. Cell. Biochem.* **116**, 2304–2312
- Mannaerts, I., Leite, S. B., Verhulst, S., Claerhout, S., Eysackers, N., Thoen, L. F. R., Hoorens, A., Reynaert, H., Halder, G., and van Grunsven, L. A. (2015) The Hippo pathway effector YAP controls mouse hepatic stellate cell activation. *J. Hepatol.* **63**, 679–688
- Parola, M., Robino, G., Marra, F., Pinzani, M., Bellomo, G., Leonarduzzi, G., Chiarugi, P., Camandola, S., Poli, G., Waeg, G., Gentilini, P., and Dianzani, M. U. (1998) HNE interacts directly with JNK isoforms in human hepatic stellate cells. *J. Clin. Invest.* **102**, 1942–1950
- Nakamura, K., Ichise, H., Nakao, K., Hatta, T., Otani, H., Sakagami, H., Kondo, H., and Katsuki, M. (2008) Partial functional overlap of the three ras genes in mouse embryonic development. *Oncogene* **27**, 2961–2968
- Karnoub, A. E., and Weinberg, R. A. (2008) Ras oncogenes: split personalities. *Nat. Rev. Mol. Cell Biol.* **9**, 517–531
- Tidyman, W. E., and Rauen, K. A. (2009) The RASopathies: developmental syndromes of Ras/MAPK pathway dysregulation. *Curr. Opin. Genet. Dev.* **19**, 230–236
- Hennig, A., Markwart, R., Esparza-Franco, M. A., Ladds, G., and Rubio, I. (2015) Ras activation revisited: role of GEF and GAP systems. *Biol. Chem.* **396**, 831–848
- Aoyama, M., Kataoka, H., Kubota, E., Tada, T., and Asai, K. (2010) Resistance to chemotherapeutic agents and promotion of transforming activity mediated by embryonic stem cell-expressed Ras (ERas) signal in neuroblastoma cells. *Int. J. Oncol.* **37**, 1011–1016
- Kaizaki, R., Yashiro, M., Shinto, O., Yasuda, K., Matsuzaki, T., Sawada, T., and Hirakawa, K. (2009) Expression of ERas oncogene in gastric carcinoma. *Anticancer Res.* **29**, 2189–2193
- Takahashi, K., Mitsui, K., and Yamanaka, S. (2003) Role of ERas in promoting tumour-like properties in mouse embryonic stem cells. *Nature* **423**, 541–545
- Yasuda, K., Yashiro, M., Sawada, T., Ohira, M., and Hirakawa, K. (2007) ERas oncogene expression and epigenetic regulation by histone acetylation in human cancer cells. *Anticancer Res.* **27**, 4071–4075
- Nakhaei-Rad, S., Nakhaeizadeh, H., Kordes, C., Cirstea, I. C., Schmick, M., Dvorsky, R., Bastiaens, P. L., Häussinger, D., and Ahmadian, M. R. (2015) The function of embryonic stem cell-expressed Ras (E-Ras), a unique Ras family member, correlates with its additional motifs and its structural properties. *J. Biol. Chem.* **290**, 15892–15903
- Hendriks, H. F., Verhoofstad, W. A., Brouwer, A., de Leeuw, A. M., and Knook, D. L. (1985) Perisinusoidal fat-storing cells are the main vitamin A storage sites in rat liver. *Exp. Cell Res.* **160**, 138–149
- Kordes, C., Sawitzka, I., Müller-Marbach, A., Ale-Agha, N., Keitel, V., Klonowski-Stumpe, H., and Häussinger, D. (2007) CD133+ hepatic stellate cells are progenitor cells. *Biochem. Biophys. Res. Commun.* **352**, 410–417
- Ahmadian, M. R., Stege, P., Scheffzek, K., and Wittinghofer, A. (1997) Confirmation of the arginine-finger hypothesis for the GAP-stimulated GTP-hydrolysis reaction of Ras. *Nat. Struct. Biol.* **4**, 686–689
- Gremer, L., Merbitz-Zahradnik, T., Dvorsky, R., Cirstea, I. C., Kratz, C. P., Zenker, M., Wittinghofer, A., and Ahmadian, M. R. (2011) Germline KRAS mutations cause aberrant biochemical and physical properties leading to developmental disorders. *Hum. Mutat.* **32**, 33–43
- Rothbauer, U., Zolghadr, K., Muylderms, S., Schepers, A., Cardoso, M. C., and Leonhardt, H. (2008) A versatile nanotrapp for biochemical and functional studies with fluorescent fusion proteins. *Mol. Cell. Proteomics* **7**, 282–289
- Ahmadian, M. R., Hoffmann, U., Goody, R. S., and Wittinghofer, A. (1997) Individual rate constants for the interaction of Ras proteins with GTPase-activating proteins determined by fluorescence spectroscopy. *Biochemistry* **36**, 4535–4541
- Taha, M. S., Nouri, K., Milroy, L. G., Moll, J. M., Herrmann, C., Brunsveld, L., Piekorz, R. P., and Ahmadian, M. R. (2014) Subcellular fractionation and localization studies reveal a direct interaction of the fragile X mental retardation protein (FMRP) with nucleolin. *PLoS One* **9**, e91465
- Götze, S., Schumacher, E. C., Kordes, C., and Häussinger, D. (2015) Epigenetic changes during hepatic stellate cell activation. *PLoS One* **10**, e0128745
- Li, L. C., and Dahiya, R. (2002) MethPrimer: designing primers for methylation PCRs. *Bioinformatics* **18**, 1427–1431
- Leakey, T. L., Zielinski, J., Siegfried, R. N., Siegel, E. R., Fan, C. Y., and Cooney, C. A. (2008) A simple algorithm for quantifying DNA methylation levels on multiple independent CpG sites in bisulfite genomic sequencing electropherograms. *Nucleic Acids Res.* **36**, e64
- Yu, Y., Liang, D., Tian, Q., Chen, X., Jiang, B., Chou, B.-K., Hu, P., Cheng, L., Gao, P., Li, J., and Wang, G. (2014) Stimulation of somatic cell reprogramming by ERas-Akt-FoxO1 signaling axis. *Stem Cells* **32**, 349–363
- Ni, L., Li, S., Yu, J., Min, J., Brautigam, C. A., Tomchick, D. R., Pan, D., and Luo, X. (2013) Structural basis for autoactivation of human Mst2 kinase

The Role of ERAS in Quiescent Hepatic Stellate Cells

- and its regulation by RASSF5. *Structure* **21**, 1757–1768
36. Kim, J. B., and Spiegelman, B. M. (1996) ADD1/SREBP1 promotes adipocyte differentiation and gene expression linked to fatty acid metabolism. *Genes Dev.* **10**, 1096–1107
 37. Kim, J. B., Wright, H. M., Wright, M., and Spiegelman, B. M. (1998) ADD1/SREBP1 activates PPAR γ through the production of endogenous ligand. *Proc. Natl. Acad. Sci. U.S.A.* **95**, 4333–4337
 38. Wang, R. C., Wei, Y., An, Z., Zou, Z., Xiao, G., Bhagat, G., White, M., Reichelt, J., and Levine, B. (2012) Akt-mediated regulation of autophagy and tumorigenesis through Beclin 1 phosphorylation. *Science* **338**, 956–959
 39. Tzivion, G., Dobson, M., and Ramakrishnan, G. (2011) FoxO transcription factors: regulation by AKT and 14-3-3 proteins. *Biochim. Biophys. Acta* **1813**, 1938–1945
 40. Prasad, S. B., Yadav, S. S., Das, M., Modi, A., Kumari, S., Pandey, L. K., Singh, S., Pradhan, S., and Narayan, G. (2015) PI3K/AKT pathway-mediated regulation of p27(Kip1) is associated with cell cycle arrest and apoptosis in cervical cancer. *Cell. Oncol.* **38**, 215–225
 41. Chiang, G. G., and Abraham, R. T. (2005) Phosphorylation of mammalian target of rapamycin (mTOR) at Ser-2448 is mediated by p70S6 kinase. *J. Biol. Chem.* **280**, 25485–25490
 42. Liu, P., Guo, J., Gan, W., and Wei, W. (2014) Dual phosphorylation of Sin1 at T86 and T398 negatively regulates mTORC2 complex integrity and activity. *Protein Cell* **5**, 171–177
 43. Ma, X. M., Yoon, S. O., Richardson, C. J., Jülich, K., and Blenis, J. (2008) SKAR links pre-mRNA splicing to mTOR/S6K1-mediated enhanced translation efficiency of spliced mRNAs. *Cell* **133**, 303–313
 44. Schirmacher, P., Geerts, A., Pietrangelo, A., Dienes, H. P., and Rogler, C. E. (1992) Hepatocyte growth factor/hepatopoietin A is expressed in fat-storing cells from rat liver but not myofibroblast-like cells derived from fat-storing cells. *Hepatology* **15**, 5–11
 45. Maher, J. J. (1993) Cell-specific expression of hepatocyte growth factor in liver: up-regulation in sinusoidal endothelial cells after carbon tetrachloride. *J. Clin. Invest.* **91**, 2244–2252
 46. Wang, X., DeFrances, M. C., Dai, Y., Padiatitakis, P., Johnson, C., Bell, A., Michalopoulos, G. K., and Zarnegar, R. (2002) A mechanism of cell survival: sequestration of Fas by the HGF receptor Met. *Mol. Cell* **9**, 411–421
 47. Tomiya, T., Nishikawa, T., Inoue, Y., Ohtomo, N., Ikeda, H., Tejima, K., Watanabe, N., Tanoue, Y., Omata, M., and Fujiwara, K. (2007) Leucine stimulates HGF production by hepatic stellate cells through mTOR pathway. *Biochem. Biophys. Res. Commun.* **358**, 176–180
 48. Porstmann, T., Santos, C. R., Griffiths, B., Cully, M., Wu, M., Leevers, S., Griffiths, J. R., Chung, Y. L., and Schulze, A. (2008) SREBP activity is regulated by mTORC1 and contributes to Akt-dependent cell growth. *Cell Metab.* **8**, 224–236
 49. Kang, Q., and Chen, A. (2009) Curcumin inhibits srebp-2 expression in activated hepatic stellate cells *in vitro* by reducing the activity of specificity protein-1. *Endocrinology* **150**, 5384–5394
 50. Kwon, Y.-W., Jang, S., Paek, J.-S., Lee, J.-W., Cho, H.-J., Yang, H.-M., and Kim, H.-S. (2015) E-Ras improves the efficiency of reprogramming by facilitating cell cycle progression through JNK–Sp1 pathway. *Stem Cell Res.* **15**, 481–494
 51. Oh, W. J., and Jacinto, E. (2011) mTOR complex 2 signaling and functions. *Cell Cycle* **10**, 2305–2316
 52. Huang, J., Wu, S., Wu, C. L., and Manning, B. D. (2009) Signaling events downstream of mammalian target of rapamycin complex 2 are attenuated in cells and tumors deficient for the tuberous sclerosis complex tumor suppressors. *Cancer Res.* **69**, 6107–6114
 53. Wang, Y., Zhou, Y., and Graves, D. T. (2014) FOXO transcription factors: their clinical significance and regulation. *Biomed. Res. Int.* **2014**, 925350
 54. Huang, K., and Fingar, D. C. (2014) Growing knowledge of the mTOR signaling network. *Semin. Cell Dev. Biol.* **36**, 79–90
 55. Schroder, W. A., Buck, M., Cloonan, N., Hancock, J. F., Suhrbier, A., Sculley, T., and Bushell, G. (2007) Human Sin1 contains Ras-binding and pleckstrin homology domains and suppresses Ras signalling. *Cell. Signal.* **19**, 1279–1289
 56. Stuhlmann-Laeisz, C., Lang, S., Chalaris, A., Krzysztow, P., Enge, S., Eichler, J., Klingmüller, U., Samuel, M., Ernst, M., Rose-John, S., and Scheller, J. (2006) Forced dimerization of gp130 leads to constitutive STAT3 activation, cytokine-independent growth, and blockade of differentiation of embryonic stem cells. *Mol. Biol. Cell* **17**, 2986–2995
 57. Oh, H. M., Yu, C. R., Golestaneh, N., Amadi-Obi, A., Lee, Y. S., Eseonu, A., Mahdi, R. M., and Egwuagu, C. E. (2011) STAT3 protein promotes T-cell survival and inhibits interleukin-2 production through up-regulation of Class O Forkhead transcription factors. *J. Biol. Chem.* **286**, 30888–30897
 58. Boccaccio, C., Andò, M., Tamagnone, L., Bardelli, A., Michieli, P., Battistini, C., and Comoglio, P. M. (1998) Induction of epithelial tubules by growth factor HGF depends on the STAT pathway. *Nature* **391**, 285–288
 59. Hung, W., and Elliott, B. (2001) Co-operative effect of c-Src tyrosine kinase and Stat3 in activation of hepatocyte growth factor expression in mammary carcinoma cells. *J. Biol. Chem.* **276**, 12395–12403
 60. Nakagawa, K., Takasawa, S., Nata, K., Yamauchi, A., Itaya-Hironaka, A., Ota, H., Yoshimoto, K., Sakuramoto-Tsuchida, S., Miyaoka, T., Takeda, M., Unno, M., and Okamoto, H. (2013) Prevention of Reg I-induced beta-cell apoptosis by IL-6/dexamethasone through activation of HGF gene regulation. *Biochim. Biophys. Acta* **1833**, 2988–2995
 61. He, J., Gong, J., Ding, Q., Tan, Q., Han, P., Liu, J., Zhou, Z., Tu, W., Xia, Y., Yan, W., and Tian, D. (2015) Suppressive effect of SATB1 on hepatic stellate cell activation and liver fibrosis in rats. *FEBS Lett.* **589**, 1359–1368
 62. Coll, M., El Taghdouini, A., Perea, L., Mannaerts, I., Vila-Casadesús, M., Blaya, D., Rodrigo-Torres, D., Affò, S., Morales-Ibanez, O., Graupera, I., Lozano, J. J., Najimi, M., Sokal, E., Lambrecht, J., Ginès, P., et al. (2015) Integrative miRNA and gene expression profiling analysis of human quiescent hepatic stellate cells. *Sci. Rep.* **5**, 11549
 63. Mason, J. M., Morrison, D. J., Basson, M. A., and Licht, J. D. (2006) Sprouty proteins: multifaceted negative-feedback regulators of receptor tyrosine kinase signaling. *Trends Cell Biol.* **16**, 45–54
 64. Vanhaesebroeck, B., Ali, K., Bilancio, A., Geering, B., and Foukas, L. C. (2005) Signalling by PI3K isoforms: insights from gene-targeted mice. *Trends Biochem. Sci.* **30**, 194–204
 65. Kok, K., Geering, B., and Vanhaesebroeck, B. (2009) Regulation of phosphoinositide 3-kinase expression in health and disease. *Trends Biochem. Sci.* **34**, 115–127
 66. Fritsch, R., de Krijger, I., Fritsch, K., George, R., Reason, B., Kumar, M. S., Diefenbacher, M., Stamp, G., and Downward, J. (2013) RAS and RHO families of GTPases directly regulate distinct phosphoinositide 3-kinase isoforms. *Cell* **153**, 1050–1063
 67. Fritsch, R., and Downward, J. (2013) SnapShot: class I PI3K isoform signaling. *Cell* **154**, 940–940.e1
 68. Baier, R., Bondeva, T., Klinger, R., Bondev, A., and Wetzker, R. (1999) Retinoic acid induces selective expression of phosphoinositide 3-kinase γ in myelomonocytic U937 cells. *Cell Growth Differ.* **10**, 447–456
 69. Khadem, F., Gao, X., Mou, Z., Jia, P., Movassagh, H., Onyiah, C., Gounni, A. S., Wright, M. C., and Uzonna, J. E. (2016) Hepatic stellate cells regulate liver immunity to visceral leishmaniasis through p110delta-dependent induction and expansion of Tregs in mice. *Hepatology* **63**, 620–632
 70. Yashiro, M., Yasuda, K., Nishii, T., Kaizaki, R., Sawada, T., Ohira, M., and Hirakawa, K. (2009) Epigenetic regulation of the embryonic oncogene ERas in gastric cancer cells. *Int. J. Oncol.* **35**, 997–1003
 71. Jiang, F., Parsons, C. J., and Stefanovic, B. (2006) Gene expression profile of quiescent and activated rat hepatic stellate cells implicates Wnt signaling pathway in activation. *J. Hepatol.* **45**, 401–409
 72. De Minicis, S., Seki, E., Uchinami, H., Kluwe, J., Zhang, Y., Brenner, D. A., and Schwabe, R. F. (2007) Gene expression profiles during hepatic stellate cell activation in culture and *in vivo*. *Gastroenterology* **132**, 1937–1946
 73. Bitencourt, S., Mesquita, F., Basso, B., Schmid, J., Ferreira, G., Rizzo, L., Bauer, M., Bartrons, R., Ventura, F., Rosa, J. L., Mannaerts, I., van Grunsven, L. A., and Oliveira, J. (2014) Capsaicin modulates proliferation, migration, and activation of hepatic stellate cells. *Cell Biochem. Biophys.* **68**, 387–396
 74. Dong, S., Wu, C., Hu, J., Wang, Q., Chen, S., Zhirong, W., and Xiong, W. (2015) Wnt5a Promotes Cytokines Production and Cell Proliferation in Human Hepatic Stellate Cells Independent of Canonical Wnt Pathway. *Clin. Lab.* **61**, 537–547
 75. Kinbara, K., Goldfinger, L. E., Hansen, M., Chou, F. L., and Ginsberg, M. H.

The Role of ERAS in Quiescent Hepatic Stellate Cells

- (2003) Ras GTPases: integrins' friends or foes? *Nat. Rev. Mol. Cell Biol.* **4**, 767–776
76. Sandri, C., Caccavari, F., Valdembrì, D., Camillo, C., Veltel, S., Santambrogio, M., Lanzetti, L., Bussolino, F., Ivaska, J., and Serini, G. (2012) The R-Ras/RIN2/Rab5 complex controls endothelial cell adhesion and morphogenesis via active integrin endocytosis and Rac signaling. *Cell Res.* **22**, 1479–1501
 77. Rodriguez-Viciana, P., Osés-Prieto, J., Burlingame, A., Fried, M., and McCormick, F. (2006) A phosphatase holoenzyme comprised of Shoc2/Sur8 and the catalytic subunit of PPI functions as an M-Ras effector to modulate Raf activity. *Mol. Cell* **22**, 217–230
 78. Torti, M., and Lapetina, E. G. (1994) Structure and function of rap proteins in human platelets. *Thromb. Haemost.* **71**, 533–543
 79. Paganini, S., Guidetti, G. F., Catricalà, S., Trionfini, P., Panelli, S., Balduini, C., and Torti, M. (2006) Identification and biochemical characterization of Rap2C, a new member of the Rap family of small GTP-binding proteins. *Biochimie* **88**, 285–295
 80. Wu, J.-X., Zhang, D.-G., Zheng, J.-N., and Pei, D.-S. (2015) Rap2a is a novel target gene of p53 and regulates cancer cell migration and invasion. *Cell. Signal.* **27**, 1198–1207
 81. Saile, B., Matthes, N., El Armouche, H., Neubauer, K., and Ramadori, G. (2001) The bcl, NFκB and p53/p21/WAF1 systems are involved in spontaneous apoptosis and in the anti-apoptotic effect of TGF-β or TNF-α on activated hepatic stellate cells. *Eur. J. Cell Biol.* **80**, 554–561
 82. Soliman, E. M., Rodrigues, M. A., Gomes, D. A., Sheung, N., Yu, J., Amaya, M. J., Nathanson, M. H., and Dranoff, J. A. (2009) Intracellular calcium signals regulate growth of hepatic stellate cells via specific effects on cell cycle progression. *Cell Calcium* **45**, 284–292
 83. Gu, X., Wang, Y., Xiang, J., Chen, Z., Wang, L., Lu, L., and Qian, S. (2013) Interferon-γ triggers hepatic stellate cell-mediated immune regulation through MEK/ERK signaling pathway. *Clin. Dev. Immunol.* [10.1155/2013/389807](https://doi.org/10.1155/2013/389807)
 84. Fukunaga, R., and Hunter, T. (1997) MNK1, a new MAP kinase-activated protein kinase, isolated by a novel expression screening method for identifying protein kinase substrates. *EMBO J.* **16**, 1921–1933
 85. Pereira, A., Zhang, B., Malcolm, P., and Sundram, S. (2013) Clozapine regulation of p90RSK and c-Fos signaling via the ErbB1-ERK pathway is distinct from olanzapine and haloperidol in mouse cortex and striatum. *Prog. Neuropsychopharmacol. Biol. Psychiatry* **40**, 353–363
 86. Iwamoto, H., Nakamuta, M., Tada, S., Sugimoto, R., Enjoji, M., and Nawata, H. (2000) Platelet-derived growth factor receptor tyrosine kinase inhibitor AG1295 attenuates rat hepatic stellate cell growth. *J. Lab. Clin. Med.* **135**, 406–412
 87. Vavvas, D., Li, X., Avruch, J., and Zhang, X. F. (1998) Identification of Nore1 as a potential Ras effector. *J. Biol. Chem.* **273**, 5439–5442
 88. van der Weyden, L., and Adams, D. J. (2007) The Ras-association domain family (RASRF) members and their role in human tumorigenesis. *Biochim. Biophys. Acta* **1776**, 58–85
 89. Scheel, H., and Hofmann, K. (2003) A novel interaction motif, SARAH, connects three classes of tumor suppressor. *Curr. Biol.* **13**, R899–R900
 90. Ramos, A., and Camargo, F. D. (2012) The Hippo signaling pathway and stem cell biology. *Trends Cell Biol.* **22**, 339–346
 91. Rawat, S. J., and Chernoff, J. (2015) Regulation of mammalian Ste20 (Mst) kinases. *Trends Biochem. Sci.* **40**, 149–156
 92. Camargo, F. D., Gokhale, S., Johnnidis, J. B., Fu, D., Bell, G. W., Jaenisch, R., and Brummelkamp, T. R. (2007) YAP1 increases organ size and expands undifferentiated progenitor cells. *Curr. Biol.* **17**, 2054–2060
 93. Avruch, J., Zhou, D., Fitamant, J., and Bardeesy, N. (2011) Mst1/2 signaling to Yap: gatekeeper for liver size and tumour development. *Br. J. Cancer* **104**, 24–32
 94. Lu, L., Li, Y., Kim, S. M., Bossuyt, W., Liu, P., Qiu, Q., Wang, Y., Halder, G., Finegold, M. J., Lee, J. S., and Johnson, R. L. (2010) Hippo signaling is a potent *in vivo* growth and tumor suppressor pathway in the mammalian liver. *Proc. Natl. Acad. Sci. U.S.A.* **107**, 1437–1442
 95. Yimlamai, D., Christodoulou, C., Galli, G. G., Yanger, K., Pepe-Mooney, B., Gurung, B., Shrestha, K., Cahan, P., Stanger, B. Z., and Camargo, F. D. (2014) Hippo pathway activity influences liver cell fate. *Cell* **157**, 1324–1338
 96. Saxena, N. K., Titus, M. A., Ding, X., Floyd, J., Srinivasan, S., Sitaraman, S. V., and Anania, F. A. (2004) Leptin as a novel profibrogenic cytokine in hepatic stellate cells: mitogenesis and inhibition of apoptosis mediated by extracellular regulated kinase (Erk) and Akt phosphorylation. *FASEB J.* **18**, 1612–1614
 97. Chiang, J., and Martinez-Agosto, J. A. (2012) Effects of mTOR inhibitors on components of the Salvador-Warts-Hippo pathway. *Cells* **1**, 886–904

Supplementary Information

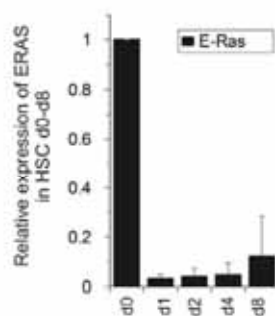
The role of embryonic stem cell-expressed RAS (ERAS) in the maintenance of quiescent hepatic stellate cells *

Saeideh Nakhaei-Rad¹, Hossein Nakhaeizadeh¹, Silke Götze², Claus Kordes², Iris Sawitza², Michèle J Hoffmann³, Manuel Franke¹, Wolfgang A. Schultz³, Jürgen Scheller¹, Roland P. Piekorz¹, Dieter Häussinger², Mohammad R. Ahmadian^{1@}

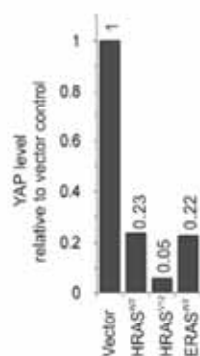
¹Institute of Biochemistry and Molecular Biology II, Medical Faculty, Heinrich-Heine University, Düsseldorf, Germany; ²Clinic of Gastroenterology, Hepatology and Infectious Diseases, Heinrich-Heine University, Düsseldorf, Germany; ³Department of Urology, Medical Faculty, Heinrich Heine University Düsseldorf, Düsseldorf, Germany

Supplementary TABLE S1. Primer sequences (5' to 3') for qPCR using the SYBR Green system obtained from PrimerBank (<http://pga.mgh.harvard.edu/primerbank>) and modified to match with rat sequences.

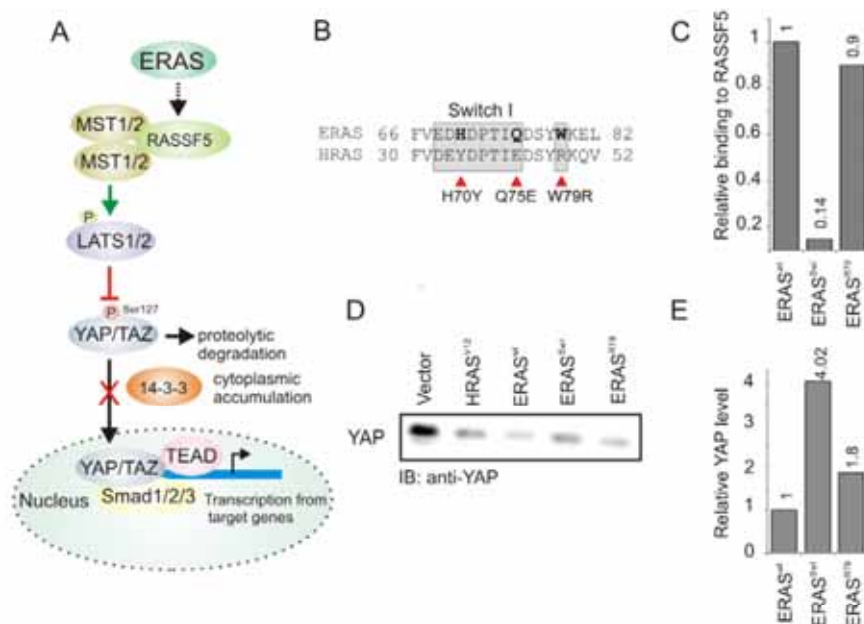
Genes	Forward primers	Reverse primers
ARAF	CCTCCTGCTAGTGGGGCT	GAGTCATAGACACTCATGCCATCC
BRAF	TTTCCTGGCTTACTGGAGAGG	GAAGTTGTGGGTTGTCAGAGG
CRAF	GATGGCAAACCTCACGGATTCTT	TGCAAGCTCATCCCATCCG
CTGF	GACCCAACCTATGATGCGAGCC	CCCATCCACAGGTCTTAGAAC
ERAS	CCTTGCCAACAAAGTCTAGCATC	GCCAGCATCTTGCATTGTGC
ERK1	ACCACATTCTAGGTATACTGGGT	AGTTTCGGGCCTTCATGTTAAT
ERK2	GGTTGTTCCCAAACGCTGACT	CAACTTCAATCCTCTTGTGAGGG
HPRT1	AAGTGTGGATACAGGCCAGA	GGCTTGTACTTGGCTTTTCC
HRAS	CGTGAGATTCGGCAGCATAAA	GACAGCACACACTTGCAGCT
KRAS	CAAGAGTGCTTGACGATACA	CCAAGAGACAGGTTTCTCCATC
MEK1	AATGGTGGAGTGGTGTCAAG	CGGATTGCGGGTTTGATCTC
MEK2	GTTACCGGCACTCACCATCAAC	CCTCCAGCCGCTTCTCTG
MRAS	TGTTCCCAAGTACAACCTTCCC	GGTTCGTAGTCAGGCACGAA
MST1	CAGTGATAGGGACACCGTTTG	GGGCTTTCCTTCAGCCATTTC
MST2	CCGGCGCCCAAGAGTAAG	GCAACAACCTTGACCAGATTCTC
NOTCH2	GAGAAGAACCGCTGTCAGAATGG	GGTCGAGTATTGGCAGTCCTC
NRAS	ACTGAGTACAACTGGTGGTGG	TCGGTAAGAATCCTCTATGGTGG
PIK3CA p110 α	CCACGACCATCTTCGGGTG	ACGGAGGCATTCTAAAGTCACT
PIK3CA p110 β	CTATGGCAGACACCCTTGACAT	CTTCCCGGGTACTTCCAACCT
PIK3CA p110 γ	CACTGGAGTCACCGGCTAC	GACACTGTGAAAACGCTCTCG
PIK3CA p110 δ	GTAACGACTTCCGCACTAAGA	GCTGACATGCAATAAGCCA
RALA	AGGAAGACTACGCTGCAATTAGA	GTAGCTGCAAAGGACTCCATC
RALB	AGCCCTGACGCTCCAGTTC	GGCTGTGTCCAGGATGTCTATCT
RAP1A	ATGCGTGAGTACAAGCTAGTG	AATCTACTTCGACTTGCTTTCTGT
RAP2A	ATGCGCGAGTACAAAGTGGT	GCGACGAGTCCACCTCGAT
RHEB	AAGTCCCGGAAGATCGCCA	GGTTGGATCGTAGGAATCAACAA
RRAS	GACCCACCATTTGAGGATTCC	CTGTGCTTAATGGCAAAACCCA
TC21	TGTGACGGACTATGATCCAACC	ACTGCTCTCATGGCTCCAA
YAP	TGAGATCCCTGATGATGTACCAT	ATGTTGTTGTCTGATCATTGTGATT



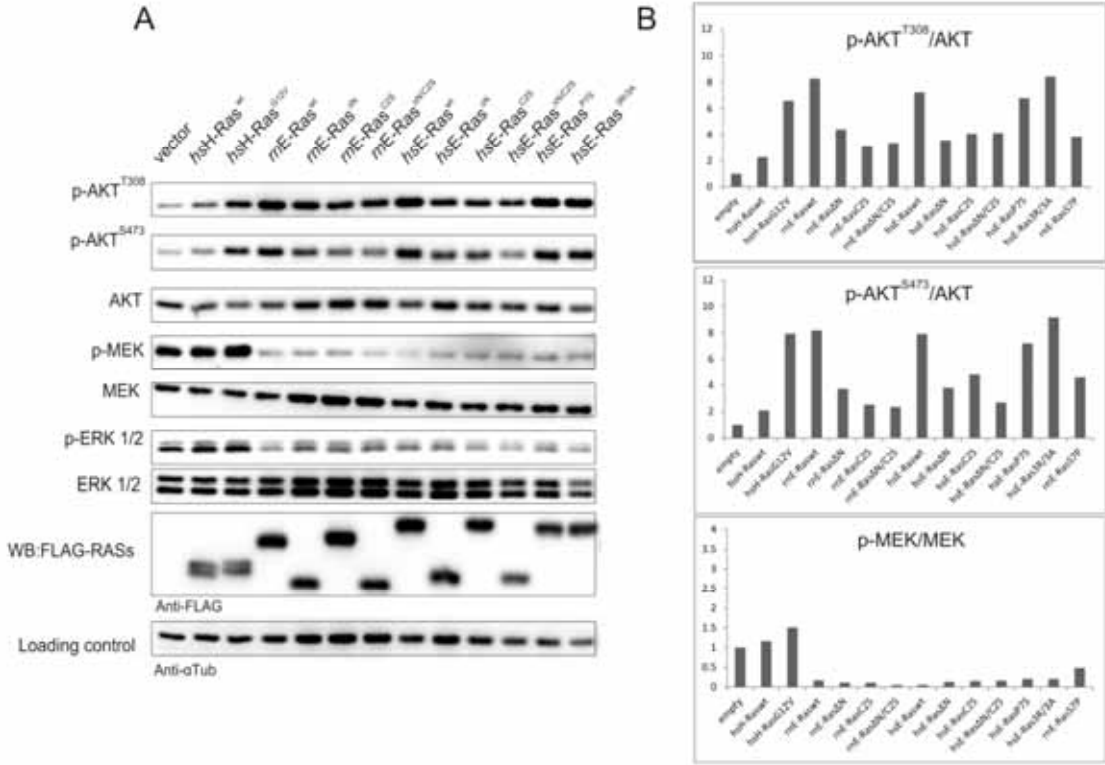
Supplementary FIGURE S1. *ERAS* re-expression in culture-activated hepatic stellate cells. *Ex-vivo* cultivation of HSCs resulted in a strong decrease in *ERAS* expression.



Supplementary FIGURE S2. *ERAS* and *HRAS* overexpression led to an overall reduction of the **YAP protein**. Densitometric quantification (ImageJ software) of YAP immunoblots (Fig. 6B) showed that *ERAS* expression resulted in a significant reduction of the YAP protein level in the same extent as observed for wild-type *HRAS*.



Supplementary FIGURE S3. ERAS-mediated activation of the HIPPO pathway may be mediated by its physical interaction with RASSF5. (A) Schematic view of the ERAS-RASSF5-MST1/2-LATS1/2-YAP pathway. (B) Sequence deviations and generated mutations (arrow heads) in the switch I and the interswitch regions of ERAS and HRAS. (C) Densitometric evaluations (ImageJ software) of the pull-down experiment of the ERAS^{wt}, ERAS^{Swi1} and ERAS^{R79} by the RAS association domain of RASSF5 (Fig. 6A) revealed that the mutations in ERAS switch I region affects its interaction with RASSF5. (D) Overexpression of the ERAS and the HRAS variants in COS-7 cells differentially affect YAP degradation. (E) Densitometric evaluations (ImageJ software) of YAP immunoblot (Fig. S3D) revealed the weaker impact of the switch I mutations on the YAP protein degradation where more YAP protein (i.e., less HIPPO activity) was observed.

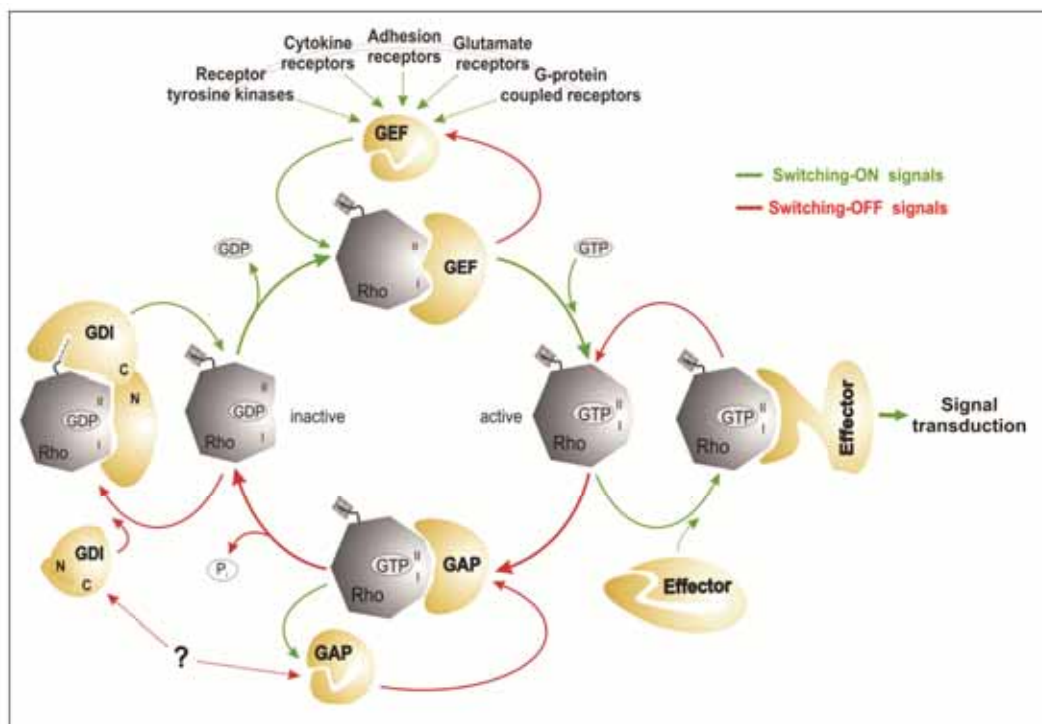


Supplementary FIGURE S4. Comparison of the signaling activity of human and rat ERAS variants. Immunoblot analysis of total cell lysates were derived from transfected COS-7 cells with FLAG-tagged human and rat ERAS variants, HRAS^{WT} and HRAS^{Val12}. Total cell lysates were analyzed for the phosphorylation level of AKT (p-AKT^{T308} and p-AKT^{S473}), MEK1/2 (p-MEK1/2) and ERK1/2 (p-ERK1/2). Total amounts of AKT, MEK1/2, and ERK1/2 were applied as loading controls. (B) Densitometry analysis (ImageJ software) revealed that N-terminal truncated and palmitoylation-dead variants of rat and human ERAS showed lower levels of p-AKT^{T308} and p-AKT^{S473}.

Chapter IV

Classical RHO proteins: biochemistry of molecular switch function and regulation

Graphical Abstract



Published in:

Springer Vienna

Impact factor:

Book chapter (not available)

Own Proportion to this work:

10%

Writing the manuscript

Chapter 14

Classical Rho Proteins: Biochemistry of Molecular Switch Function and Regulation

Si-Cai Zhang, Kazem Nouri, Ehsan Amin, Mohamed S. Taha, Hossein Nakhaeizadeh, Saeideh Nakhaei-Rad, Radovan Dvorsky, and Mohammad Reza Ahmadian

Abstract Rho family proteins are involved in an array of cellular processes by modulating cytoskeletal organization, transcription, and cell cycle progression. The signaling functions of Rho family proteins are based on the formation of distinctive protein–protein complexes with their regulators and effectors. A necessary precondition for such differential interactions is an intact molecular switch function, which is a hallmark of most members of the Rho family. Such classical Rho proteins cycle between an inactive GDP-bound state and an active GTP-bound state. They specifically interact via a consensus-binding sites called switch I and II with three structurally and functionally unrelated classes of regulatory proteins, such as guanine nucleotide dissociation inhibitors (GDIs), guanine nucleotide exchange factors (GEFs), and GTPase-activating proteins (GAPs). Extensive studies in the last 25 years have provided invaluable insights into the molecular mechanisms underlying regulation and signal transduction of the Rho family proteins. In this chapter, we will review common features of Rho protein regulations and highlight specific aspects of their structure–function relationships.

Keywords Effector • GAP • GDI • GEF • Rho GTPase • Switch region

Abbreviations

A	Aliphatic amino acid
Bcr	Breakpoint cluster region protein
C	Cysteine
CZH	CDM-zizimin homology

S.-C. Zhang • K. Nouri • E. Amin • M.S. Taha • H. Nakhaeizadeh • S. Nakhaei-Rad • R. Dvorsky • M.R. Ahmadian (✉)
 Institute of Biochemistry and Molecular Biology II, Medical Faculty, Heinrich-Heine-University, 40225 Düsseldorf, Germany
 e-mail: reza.ahmadian@uni-duesseldorf.de

Db1	Diffuse B-cell lymphoma
DH	Dbl homology domain
DHR1&2	DOCK-homology regions 1 and 2
ERM	Ezrin/radixin/moesin
GAPs	GTPase-activating proteins
GDI	Guanine nucleotide dissociation inhibitors
GDP	Guanosine diphosphate
GEFs	Guanine nucleotide exchange factors
Gln	Glutamine
Gly	Glycine
GTP	Guanosine triphosphate
p75 ^{NTR}	Neurotrophin receptor p75
PAK1	p21-activated kinase 1
PH	Pleckstrin homology domain
PKA	Protein kinase A
PKC	Protein kinase C
P-loop	Phosphate-binding loop
X	Any amino acid

14.1 General Introduction

The role of the Rho family proteins as signaling molecules in controlling a large number of fundamental cellular processes is largely dependent on a functional molecular switch between a GDP-bound, inactive state and a GTP-bound, active state (Dvorsky and Ahmadian 2004). This function underlies a so-called GTPase cycle consisting of two different, slow biochemical reactions, the GDP/GTP exchange and the GTP hydrolysis. The cellular regulation of this cycle involves guanine nucleotide exchange factors (GEFs), which accelerate the intrinsic nucleotide exchange, and GTPase-activating proteins (GAPs), which stimulate the intrinsic GTP hydrolysis activity (Cherfils and Zeghouf 2013). Rho protein function requires both posttranslational modification by isoprenyl groups and membrane association. Therefore, Rho proteins underlie a third control mechanism that directs their membrane targeting to specific subcellular sites. This mechanism is achieved by the function of guanine nucleotide dissociation inhibitors (GDIs), which bind selectively to prenylated Rho proteins and control their cycle between cytosol and membrane. Activation of Rho proteins results in their association with effector molecules that subsequently activate a wide variety of downstream signaling cascades (Bishop and Hall 2000; BurrIDGE and Wennerberg 2004), thereby regulating many important physiological and pathophysiological processes in eukaryotic cells (Etienne-Manneville and Hall 2002; Heasman and Ridley 2008) (see Chap. 16). In the following, the biochemical properties of the Rho proteins and their regulatory cycles will be described in detail. Figure 14.1 schematically summarizes the regulatory mechanism of the Rho proteins.

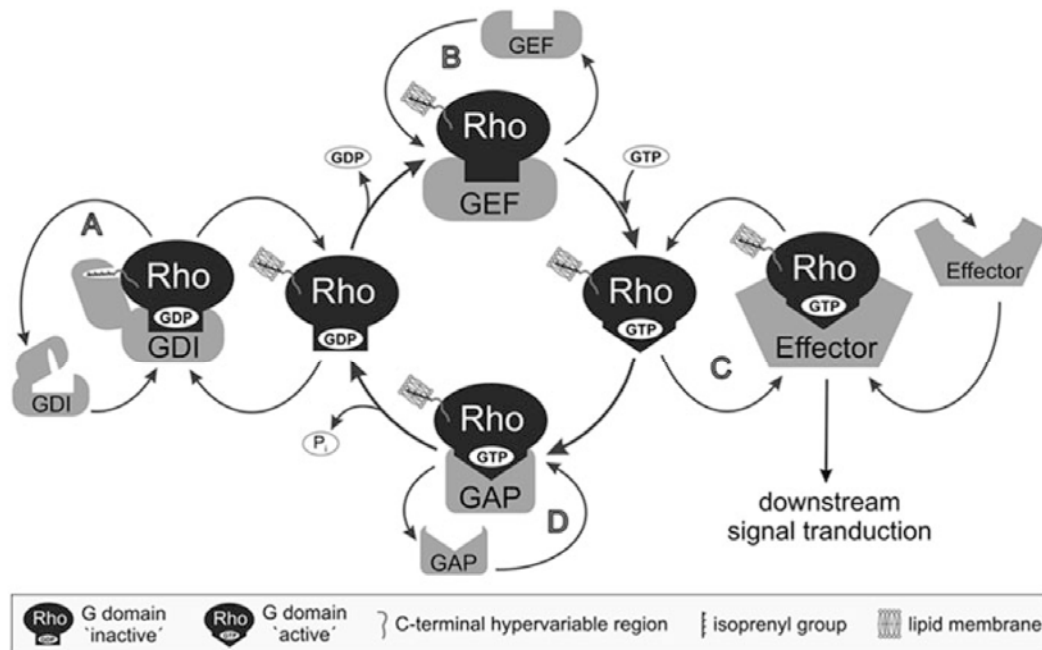


Fig. 14.1 Molecular principles of regulation and signaling of Rho Proteins. Most members of the Rho family act as molecular switches by cycling between an inactive, GDP-bound state and an active GTP-bound state. They interact specifically with four structurally and functionally unrelated classes of proteins: (a) In resting cells, guanine nucleotide dissociation inhibitors (GDIs) sequester the Rho proteins from the membrane by binding to the lipid anchor and create an inactivated cytosolic pool. (b) In stimulated cells, different classes of membrane receptors activate guanine nucleotide exchange factors (GEFs), which in turn activate their substrate Rho proteins by accelerating the slow intrinsic exchange of GDP for GTP and turn on the signal transduction. (c) The active GTP-bound Rho proteins interact with and activate their targets (the downstream effectors) to evoke a variety of intracellular responses. (d) GTPase-activating proteins (GAPs) negatively regulate the switch by stimulating the slow intrinsic GTP hydrolysis activity of the Rho proteins and turn off the signal transduction

14.2 Rho Family and the Molecular Switch Mechanism

Members of the GTP-binding proteins of the Rho family have emerged as key regulatory molecules that couple changes in the extracellular environment to intracellular signal transduction pathways. So far, 20 human members of the Rho family have been identified, which can be divided into six distinct subfamilies based on their sequence homology: (1) Rho (RhoA, RhoB, RhoC); (2) Rac (Rac1, Rac1b, Rac2, Rac3, RhoG); (3) Cdc42 (Cdc42, G25K, TC10, TCL, RhoU/Wrch1, RhoV/Chp); (4) RhoD (RhoD, Rif); (5) Rnd (Rnd1, Rnd2, Rnd3); (6) RhoH/TTF (Boureaux et al. 2007; Jaiswal et al. 2013a, b; Wennerberg and Der 2004).

Rho family proteins are approximately 21–25 kDa in size typically containing a conserved GDP/GTP-binding domain (called G domain) and a C-terminal hypervariable region ending with a consensus sequence known as CAAX (C is cysteine, A is any aliphatic amino acid, and X is any amino acid). The G domain consists of five conserved sequence motifs (G1–G5) that are involved in nucleotide binding and

hydrolysis (Wittinghofer and Vetter 2011). In the cycle between the inactive and active states at least two regions of the protein, switch I (G2) and Switch II (G3), undergo structural rearrangements and transmit the “OFF” to “ON” signal to downstream effectors (Fig. 14.1) (Dvorsky and Ahmadian 2004). Subcellular localization of Rho proteins at different cellular membranes, that is known to be critical for their biological activity, is achieved by a series of posttranslational modifications at a cysteine residue in the CAAX motif, including isoprenylation (geranylgeranyl or farnesyl), endoproteolysis, and carboxyl methylation (Roberts et al. 2008).

A characteristic region of Rho family GTPases is the insert helix (amino acids 124–136, RhoA numbering) that may play a role in effector activation and downstream process (Thapar et al. 2002). Although the function of the insert helix has not been elucidated yet, it has been reported to be involved in the Rho-dependent activation of ROCK (Zong et al. 2001), phospholipase D (Walker and Brown 2002) and mDia (Lammers et al. 2008; Rose et al. 2005), and in the Rac-dependent activation of p67phox (Joneson and Bar-Sagi 1997; Karnoub et al. 2001; Nisimoto et al. 1997) and Plexin B1 (Bouguet-Bonnet and Buck 2008).

Although the majority of the Rho family proteins are remarkably inefficient GTP hydrolyzing enzymes, in quiescent cells they rest in an inactive state because the GTP hydrolysis is in average two orders of magnitude faster than the GDP/GTP exchange (Jaiswal et al. 2013a, b). Such different intrinsic activities provide the basis for a two-state molecular switch mechanism, which highly depends on the regulatory functions of GEFs and GAPs that directly control ON and OFF states of classical type of Rho proteins (Fig. 14.1). Eleven out of twenty members of the Rho family belong to these classical molecular switches, namely RhoA, RhoB, RhoC, Rac1, Rac2, Rac3, RhoG, Cdc42, G25K, TC10, and TCL (Jaiswal et al. 2013a, b).

The atypical Rho family members, including Rnd1, Rnd2, Rnd3, Rac1b, RhoH/TTF, Wrch1, RhoD, and Rif, have been proposed to accumulate in the GTP-bound form in cells due to various biochemical properties (Jaiswal et al. 2013a, b). Rnd1, Rnd2, Rnd3, and RhoH/TTF represent a completely distinct group of proteins within the Rho family (Riou et al. 2010; Troeger et al. 2013), as they do not share several conserved and essential amino acids, including Gly-12 (Rac1 numbering) in the G1 motif (also called phosphate-binding loop or P-loop) and Gln-61 (Rac1 numbering) in the G3 motif or switch II region. The role of these residues in GTP hydrolysis is well described for Ras oncogene in human cancers (Chaps. 6 and 7). Thus, they can be considered as GTPase-deficient Rho-related GTP-binding proteins (Fiegen et al. 2002; Garavini et al. 2002; Gu et al. 2005; Li et al. 2002) (see also Chap. 15). Another example is Rac1b, which is an alternative splice variant of Rac1 and contains a 19-amino acid insertion next to the switch II region (Jordan et al. 1999). Rac1b exhibits different biochemical properties as compared to the other Rac isoforms (Fiegen et al. 2004; Haeusler et al. 2006), including an accelerated GEF-independent GDP/GTP exchange and an impaired GTP hydrolysis (Fiegen et al. 2004). RhoD and Rif are involved in the regulation of actin dynamics (Fan and Mellor 2012; Gad and Aspenstrom 2010) and exhibit a strikingly faster nucleotide exchange than GTP hydrolysis similarly to Rac1b and thus persist

mainly in the active state under resting conditions (Jaiswal et al. 2013a, b). Wrch1, a Cdc42-like protein that has been reported to be a fast cycling protein (Shutes et al. 2006), resembles in this context Rac1b, RhoD, and Rif (Jaiswal et al. 2013a, b). These atypical members of the Rho family with their distinctive biochemical features do not follow the classical switch mechanism and may thus require additional forms of regulation.

14.3 Guanine Nucleotide Dissociation Inhibitors

Multiple functions have been originally described for the Rho-specific GDIs, including the inhibition of the GDP/GTP exchange (Hiraoka et al. 1992; Ohga et al. 1989), the intrinsic and GAP-stimulated GTP hydrolysis (Chuang et al. 1993; Hancock and Hall 1993; Hart et al. 1992), and the interaction with the downstream effectors (Pick et al. 1993). However, it is generally accepted that in resting cells, RhoGDIs target the isoprenyl anchor and sequester Rho proteins from their site of action at the membrane in the cytosol (Boulter and Garcia-Mata 2010; Garcia-Mata et al. 2011).

RhoGDIs undergo a high affinity interaction with the Rho proteins using an N-terminal regulatory arm contacting the switch regions and a C-terminal domain binding the isoprenyl group (Tnimov et al. 2012). In contrast to the large number of RhoGEFs and RhoGAPs, there are only three known RhoGDIs in human (DerMardirossian and Bokoch 2005). RhoGDI-1 (also called RhoGDI α) is ubiquitously expressed (Fukumoto et al. 1990), whereas RhoGDI-2 (also called RhoGDI β , LyGDI, or D4GDI) is predominantly found in hematopoietic tissues and lymphocytes (Leonard et al. 1992; Scherle et al. 1993) and RhoGDI-3 (also called RhoGDI γ) in lung, brain, and testis (Adra et al. 1997; Zalcman et al. 1996).

Despite intensive research over the last two decades, the molecular basis by which GDI proteins associate and extract the Rho GTPases from the membrane remains to be investigated. The neurotrophin receptor p75 (p75^{NTR}) and ezrin/radixin/moesin (ERM) proteins have been proposed to displace the Rho proteins from the RhoGDI complex resulting in reassociation with the cell membrane (Takahashi et al. 1997; Yamashita and Tohyama 2003). Another regulatory mechanism is RhoGDI phosphorylation. RhoGDI has been shown to be phosphorylated by serine/threonine p21-activated kinase 1 (PAK1), protein kinase A (PKA), protein kinase C (PKC), and the tyrosine kinase Src, thereby decreasing the ability of RhoGDI to form a complex with the Rho proteins, including RhoA, Rac1, and Cdc42 (DerMardirossian et al. 2004, 2006).

14.4 Guanine Nucleotide Exchange Factors

GEFs are able to selectively bind to their respective Rho proteins and accelerate the exchange of tightly bound GDP for GTP. A common mechanism utilized by GEFs is to strongly reduce the affinity of the bound GDP, leading to its displacement and the subsequent association with GTP (Cherfils and Chardin 1999; Guo et al. 2005). This reaction involves several stages, including an intermediate state of the GEF in the complex with the nucleotide-free Rho protein. This intermediate does not accumulate in the cell and rapidly dissociates because of the high intracellular GTP concentration leading to the formation of the active Rho-GTP complex. The main reason therefore is that the binding affinity of nucleotide-free Rho protein is significantly higher for GTP than for the GEF proteins (Cherfils and Chardin 1999; Hutchinson and Eccleston 2000). Cellular activation of the Rho proteins and their cellular signaling can be selectively uncoupled from the GEFs by overexpressing dominant negative mutants of the Rho proteins (e.g., threonine 17 in Rac1 and Cdc42 or threonine 19 in RhoA to asparagine) (Heasman and Ridley 2008). Such mutations decrease the affinity of the Rho protein to nucleotide resulting in a so-called dominant negative behavior (Rossman et al. 2002). As a consequence, dominant negative mutants form a tight complex with their cognate GEFs and thus prevent them from activating the endogenous Rho proteins.

RhoGEFs of the diffuse B-cell lymphoma (Dbl) family directly activate the proteins of the Rho family (Cook et al. 2013; Jaiswal et al. 2013a, b). The prototype of this GEF family is the Dbl protein, which was isolated as an oncogenic product from diffuse B-cell lymphoma cells in an oncogene screen (Eva et al. 1988; Srivastava et al. 1986), and has been later reported to act on Cdc42 (Hart et al. 1991). The Dbl family consists of 74 members in human (Jaiswal et al. 2013a, b) with evolutionary conserved orthologs in fly (23 members), yeast (6 members), worm (18 members) (Schmidt and Hall 2002; Venter et al. 2001), and slime mold (45 members) (Vlahou and Rivero 2006). Human Dbl family proteins have recently been grouped into functionally distinct categories based on both their catalytic efficiencies and their sequence–structure relationship (Jaiswal et al. 2013a, b). The members of the Dbl family are characterized by a unique Dbl homology (DH) domain (Aittaleb et al. 2010; Erickson and Cerione 2004; Hoffman and Cerione 2002; Jaiswal et al. 2011; Viaud et al. 2012). The DH domain is a highly efficient catalytic machine (Rossman et al. 2005) that is able to accelerate the nucleotide exchange of Rho proteins up to 10^7 -fold (Jaiswal et al. 2011, 2013a, b), as efficiently as the RanGEF RCC1 (Klebe et al. 1995) and *Salmonella typhimurium* effector SopE (see below) (Bulgin et al. 2010; Rudolph et al. 1999). The DH domain is often preceded by a pleckstrin homology (PH) domain indicating an essential and conserved function. A model for PH domain-assisted nucleotide exchange has been proposed for some GEFs, such as Dbl, Dbs, and Trio (Rossman et al. 2005). Herein the PH domain serves multiple roles in signaling events anchoring GEFs to the membrane (via phosphoinositides) and directing them

towards their interacting GTPases which are already localized to the membrane (Rossman et al. 2005).

In addition to the DH-PH tandem, Dbl family proteins are highly diverse and contain additional domains with different functions, including SH2, SH3, CH, RGS, PDZ, and IQ domains for interaction with other proteins; BAR, PH FYVE, C1, and C2 domains for interaction with membrane lipids; and other functional domains like Ser/Thr kinase, RasGEF, RhoGAP, and RanGEF (Cook et al. 2013). These additional domains have been implicated in autoregulation, subcellular localization, and connection to upstream signals (Dubash et al. 2007; Rossman et al. 2005). Spatiotemporal regulation of the Dbl proteins has been implicated to specifically initiate activation of substrate Rho proteins (Jaiswal et al. 2013a, b) and to control a broad spectrum of normal and pathological cellular functions (Dubash et al. 2007; Hall and Lalli 2010; Mulinari and Hacker 2010; Mulloy et al. 2010; Schmidt and Hall 2002). Thus, it is evident that members of the Dbl protein family are attractive therapeutic targets for a variety of diseases (Bos et al. 2007; Loirand et al. 2008; Vigil et al. 2010).

Apart from conventional Dbl family RhoGEFs there are two additional proteins families, which do not share any sequence and structural similarity with each other. The dedicator of cytokinesis (DOCK) or CDM-zizimin homology (CZH) family RhoGEFs are characterized by two conserved regions, known as the DOCK-homology regions 1 and 2 (DHR1 and DHR2) domains (Meller et al. 2005; Rittinger 2009). This type of GEFs employs their DHR2 domain to activate specially Rac and Cdc42 proteins (Meller et al. 2005). Another Rho protein-specific GEF family, represented by the SopE/WxxxE-type exchange factors, is classified as type III effector proteins of bacterial pathogens (Bulgin et al. 2010). They mimic functionally, but not structurally, eukaryotic GEFs by efficiently activating Rac1 and Cdc42 and thus induce “the trigger mechanism of cell entry” (see Chap. 4) (Bulgin et al. 2010; Rudolph et al. 1999).

14.5 GTPase-Activating Proteins

Hydrolysis of the bound GTP is the timing mechanism that terminates signal transduction of the Rho family proteins and returns them to their GDP-bound inactive state (Jaiswal et al. 2012). The intrinsic GTP hydrolysis (GTPase) reaction is usually slow, but can be stimulated by several orders of magnitude through interaction with Rho-specific GAPs (Eberth et al. 2005; Fidyk and Cerione 2002; Zhang and Zheng 1998). The RhoGAP family is defined by the presence of a conserved catalytic GAP domain which is sufficient for the interaction with Rho proteins and mediating accelerated catalysis (Scheffzek and Ahmadian 2005). The GAP domain supplies a conserved arginine residue, termed “arginine finger”, into the GTP-binding site of the cognate Rho protein, in order to stabilize the transition state and catalyze the GTP hydrolysis reaction (Nassar et al. 1998; Rittinger et al. 1997). A similar mechanism is utilized by other small GTP-binding proteins

(Scheffzek and Ahmadian 2005), including Ras, Rab, and Arf, although the sequence and folding of the respective GAP families are different (Ismail et al. 2010; Pan et al. 2006; Scheffzek et al. 1997). Masking the catalytic arginine finger is an elegant mechanism for the inhibition of the GAP activity. This has been recently shown for the tumor suppressor protein DLC1, a RhoGAP, which is competitively and selectively inhibited by the SH3 domain of p120RasGAP (Jaiswal et al. 2014).

RhoGAP insensitivity can be achieved by the substitution of either the catalytic arginine of the GAP domain (Fidyk and Cerione 2002; Graham et al. 1999) or amino acids critical for the GTP hydrolysis in Rho proteins, e.g., Glycine 12 and Glutamine 61 in Rac1 and Cdc42 or Glycine 14 and Glutamine 63 in RhoA, which are known as the constitutive active mutants (Ahmadian et al. 1997; Graham et al. 1999). Most remarkably, a similar mechanistic strategy has been mimicked by bacterial GAPs (see Chap. 4), such as the *Salmonella typhimurium* virulence factor SptP, the *Pseudomonas aeruginosa* cytotoxin ExoS, and *Yersinia pestis* YopE, even though they do not share any sequence or structural similarity to eukaryotic RhoGAP domains (Evdokimov et al. 2002; Stebbins and Galan 2000; Wurtele et al. 2001).

The first RhoGAP, p50RhoGAP, was identified by biochemical analysis of human spleen cell extracts in the presence of recombinant RhoA (Garrett et al. 1989). Since then more than 80 RhoGAP containing proteins have been identified in eukaryotes, ranging from yeast to human (Lancaster et al. 1994; Moon and Zheng 2003). The RhoGAP domain (also known as Bcr-homology, BH domain) containing proteins are present throughout the genome and rarely cluster in specific chromosomal regions (Peck et al. 2002). The majority of the RhoGAP family members are frequently accompanied by several other functional domains and motifs implicated in tight regulation and membrane targeting (Eberth et al. 2009; Moon and Zheng 2003; Tcherkezian and Lamarche-Vane 2007). Numerous mechanisms have been shown to affect the specificity and the catalytic activity of the RhoGAPs, e.g., intramolecular autoinhibition (Eberth et al. 2009), posttranslational modification (Minoshima et al. 2003), and regulation by interaction with lipid membrane (Ligeti et al. 2004) and proteins (Yang et al. 2009).

14.6 Conclusions

Abnormal activation of Rho proteins has been shown to play a crucial role in cancer, infectious and cognitive disorders, and cardiovascular diseases. However, several tasks have to be yet accomplished in order to understand the complexity of Rho proteins signaling: (1) The Rho family comprises of 20 signaling proteins, of which only RhoA, Rac1, and Cdc42 have been comprehensively studied so far. The functions of the other less-characterized members of this protein family await detailed investigation. (2) Despite intensive research over the last two decades, the mechanisms by which RhoGDIs associate and extract the Rho proteins from the

membrane and the factors displacing the Rho protein from the complex with RhoGDI remain to be elucidated. (3) For the regulation of the 22 Rho proteins, a tremendous number of their regulatory proteins (>74 GEFs and >80 GAPs) exist in the human genome. How these regulators selectively recognize their Rho protein targets is not well understood and majority of GEFs and GAPs in humans so far remain uncharacterized. (4) Most of the GEFs and GAPs themselves need to be regulated and require activation through the relief of autoinhibitory elements (Chow et al. 2013; Eberth et al. 2009; Jaiswal et al. 2011; Mitin et al. 2007; Moskwa et al. 2005; Rojas et al. 2007; Yohe et al. 2008). With a few exceptions (Cherfils and Zeghouf 2013; Mayer et al. 2013), it is conceptually still unclear how such autoregulatory mechanisms are operated. A better understanding of the specificity and the mode of action of these regulatory proteins is not only fundamentally important for many aspects of biology but is also a master key for the development of drugs against a variety of diseases caused by aberrant functions of Rho proteins.

References

- Adra CN, Manor D, Ko JL et al (1997) RhoGDI γ : a GDP-dissociation inhibitor for Rho proteins with preferential expression in brain and pancreas. *Proc Natl Acad Sci USA* 94:4279–4284
- Ahmadian MR, Mittal R, Hall A et al (1997) Aluminum fluoride associates with the small guanine nucleotide binding proteins. *FEBS Lett* 408:315–318
- Aittaleb M, Boguth CA, Tesmer JJ (2010) Structure and function of heterotrimeric G protein-regulated Rho guanine nucleotide exchange factors. *Mol Pharmacol* 77:111–125
- Bishop AL, Hall A (2000) Rho GTPases and their effector proteins. *Biochem J* 348(Pt 2):241–255
- Bos JL, Rehmann H, Wittinghofer A (2007) GEFs and GAPs: critical elements in the control of small G proteins. *Cell* 129:865–877
- Bouguet-Bonnet S, Buck M (2008) Compensatory and long-range changes in picosecond-nanosecond main-chain dynamics upon complex formation: 15N relaxation analysis of the free and bound states of the ubiquitin-like domain of human plexin-B1 and the small GTPase Rac1. *J Mol Biol* 377:1474–1487
- Boulter E, Garcia-Mata R (2010) RhoGDI: a rheostat for the Rho switch. *Small GTPases* 1:65–68
- Boureaux A, Vignal E, Faure S et al (2007) Evolution of the Rho family of ras-like GTPases in eukaryotes. *Mol Biol Evol* 24:203–216
- Bulgin R, Raymond B, Garnett JA et al (2010) Bacterial guanine nucleotide exchange factors SopE-like and WxxxE effectors. *Infect Immun* 78:1417–1425
- Burridge K, Wennerberg K (2004) Rho and Rac take center stage. *Cell* 116:167–179
- Cherfils J, Chardin P (1999) GEFs: structural basis for their activation of small GTP-binding proteins. *Trends Biochem Sci* 24:306–311
- Cherfils J, Zeghouf M (2013) Regulation of small GTPases by GEFs, GAPs, and GDIs. *Physiol Rev* 93:269–309
- Chow CR, Suzuki N, Kawamura T et al (2013) Modification of p115RhoGEF Ser(330) regulates its RhoGEF activity. *Cell Signal* 25:2085–2092
- Chuang TH, Xu X, Knaus UG et al (1993) GDP dissociation inhibitor prevents intrinsic and GTPase activating protein-stimulated GTP hydrolysis by the Rac GTP-binding protein. *J Biol Chem* 268:775–778
- Cook DR, Rossman KL, Der CJ (2013) Rho guanine nucleotide exchange factors: regulators of Rho GTPase activity in development and disease. *Oncogene* 16:362

- DerMardirossian C, Bokoch GM (2005) GDIs: central regulatory molecules in Rho GTPase activation. *Trends Cell Biol* 15:356–363
- DerMardirossian C, Schnelzer A, Bokoch GM (2004) Phosphorylation of RhoGDI by Pak1 mediates, dissociation of Rac GTPase. *Mol Cell* 15:117–127
- DerMardirossian C, Rocklin G, Seo JY et al (2006) Phosphorylation of RhoGDI by Src regulates Rho GTPase binding and cytosol-membrane cycling. *Mol Biol Cell* 17:4760–4768
- Dubash AD, Wennerberg K, Garcia-Mata R et al (2007) A novel role for Lsc/p115 RhoGEF and LARG in regulating RhoA activity downstream of adhesion to fibronectin. *J Cell Sci* 120:3989–3998
- Dvorsky R, Ahmadian MR (2004) Always look on the bright site of Rho: structural implications for a conserved intermolecular interface. *EMBO Rep* 5:1130–1136
- Eberth A, Dvorsky R, Becker CF et al (2005) Monitoring the real-time kinetics of the hydrolysis reaction of guanine nucleotide-binding proteins. *Biol Chem* 386:1105–1114
- Eberth A, Lundmark R, Gremer L et al (2009) A BAR domain-mediated autoinhibitory mechanism for RhoGAPs of the GRAF family. *Biochem J* 417:371–377
- Erickson JW, Cerione RA (2004) Structural elements, mechanism, and evolutionary convergence of Rho protein-guanine nucleotide exchange factor complexes. *Biochemistry* 43:837–842
- Etienne-Manneville S, Hall A (2002) Rho GTPases in cell biology. *Nature* 420:629–635
- Eva A, Vecchio G, Rao CD et al (1988) The predicted DBL oncogene product defines a distinct class of transforming proteins. *Proc Natl Acad Sci USA* 85:2061–2065
- Evdokimov AG, Tropea JE, Routzahn KM et al (2002) Crystal structure of the Yersinia pestis GTPase activator YopE. *Protein Sci* 11:401–408
- Fan L, Mellor H (2012) The small Rho GTPase Rif and actin cytoskeletal remodelling. *Biochem Soc Trans* 40:268–272
- Fidyk NJ, Cerione RA (2002) Understanding the catalytic mechanism of GTPase-activating proteins: demonstration of the importance of switch domain stabilization in the stimulation of GTP hydrolysis. *Biochemistry* 41:15644–15653
- Fiegen D, Blumenstein L, Stege P et al (2002) Crystal structure of Rnd3/RhoE: functional implications. *FEBS Lett* 525:100–104
- Fiegen D, Haeusler LC, Blumenstein L et al (2004) Alternative splicing of Rac1 generates Rac1b, a self-activating GTPase. *J Biol Chem* 279:4743–4749
- Fukumoto Y, Kaibuchi K, Hori Y et al (1990) Molecular-cloning and characterization of a novel type of regulatory protein (Gdi) for the Rho proteins, Ras P21-Like small Gtp-binding proteins. *Oncogene* 5:1321–1328
- Gad AK, Aspenstrom P (2010) Rif proteins take to the RhoD: Rho GTPases at the crossroads of actin dynamics and membrane trafficking. *Cell Signal* 22:183–189
- Garavini H, Riento K, Phelan JP et al (2002) Crystal structure of the core domain of RhoE/Rnd3: a constitutively activated small G protein. *Biochemistry* 41:6303–6310
- Garcia-Mata R, Boulter E, BurrIDGE K (2011) The ‘invisible hand’: regulation of RHO GTPases by RHOGDIs. *Nat Rev Mol Cell Biol* 12:493–504
- Garrett MD, Self AJ, van Oers C et al (1989) Identification of distinct cytoplasmic targets for ras/R-ras and rho regulatory proteins. *J Biol Chem* 264:10–13
- Graham DL, Eccleston JF, Lowe PN (1999) The conserved arginine in rho-GTPase-activating protein is essential for efficient catalysis but not for complex formation with Rho.GDP and aluminum fluoride. *Biochemistry* 38:985–991
- Gu Y, Zheng Y, Williams DA (2005) RhoH GTPase: a key regulator of hematopoietic cell proliferation and apoptosis? *Cell Cycle* 4:201–202
- Guo Z, Ahmadian MR, Goody RS (2005) Guanine nucleotide exchange factors operate by a simple allosteric competitive mechanism. *Biochemistry* 44:15423–15429
- Haeusler LC, Hemsath L, Fiegen D et al (2006) Purification and biochemical properties of Rac1, 2, 3 and the splice variant Rac1b. *Methods Enzymol* 406:1–11
- Hall A, Lalli G (2010) Rho and Ras GTPases in axon growth, guidance, and branching. *Cold Spring Harb Perspect Biol* 2:a001818

- Hancock JF, Hall A (1993) A novel role for RhoGDI as an inhibitor of GAP proteins. *EMBO J* 12:1915–1921
- Hart MJ, Eva A, Evans T et al (1991) Catalysis of guanine nucleotide exchange on the CDC42Hs protein by the *dbl* oncogene product. *Nature* 354:311–314
- Hart MJ, Maru Y, Leonard D et al (1992) A GDP dissociation inhibitor that serves as a GTPase inhibitor for the Ras-like protein CDC42Hs. *Science* 258:812–815
- Heasman SJ, Ridley AJ (2008) Mammalian Rho GTPases: new insights into their functions from in vivo studies. *Nat Rev Mol Cell Biol* 9:690–701
- Hiraoka K, Kaibuchi K, Ando S et al (1992) Both stimulatory and inhibitory GDP/GTP exchange proteins, smg GDS and rho GDI, are active on multiple small GTP-binding proteins. *Biochem Biophys Res Commun* 182:921–930
- Hoffman GR, Cerione RA (2002) Signaling to the Rho GTPases: networking with the DH domain. *FEBS Lett* 513:85–91
- Hutchinson JP, Eccleston JF (2000) Mechanism of nucleotide release from Rho by the GDP dissociation stimulator protein. *Biochemistry* 39:11348–11359
- Ismail SA, Vetter IR, Sot B et al (2010) The structure of an Arf-ArfGAP complex reveals a Ca²⁺ regulatory mechanism. *Cell* 141:812–821
- Jaiswal M, Gremer L, Dvorsky R et al (2011) Mechanistic insights into specificity, activity, and regulatory elements of the regulator of G-protein signaling (RGS)-containing Rho-specific guanine nucleotide exchange factors (GEFs) p115, PDZ-RhoGEF (PRG), and leukemia-associated RhoGEF (LARG). *J Biol Chem* 286:18202–18212
- Jaiswal M, Dubey BN, Koessmeier KT et al (2012) Biochemical assays to characterize Rho GTPases. *Methods Mol Biol* 827:37–58
- Jaiswal M, Dvorsky R, Ahmadian MR (2013a) Deciphering the molecular and functional basis of Dbl family proteins: a novel systematic approach toward classification of selective activation of the Rho family proteins. *J Biol Chem* 288:4486–4500
- Jaiswal M, Fansa EK, Dvorsky R et al (2013b) New insight into the molecular switch mechanism of human Rho family proteins: shifting a paradigm. *Biol Chem* 394:89–95
- Jaiswal M, Dvorsky R, Amin E et al (2014) Functional crosstalk between Ras and Rho pathways: p120RasGAP competitively inhibits the RhoGAP activity of Deleted in Liver Cancer (DLC) tumor suppressors by masking its catalytic arginine finger. *J Biol Chem* 289:6839–6849
- Joneson T, Bar-Sagi D (1997) Ras effectors and their role in mitogenesis and oncogenesis. *J Mol Med (Berl)* 75:587–593
- Jordan P, Brazao R, Boavida MG et al (1999) Cloning of a novel human Rac1b splice variant with increased expression in colorectal tumors. *Oncogene* 18:6835–6839
- Karnoub AE, Der CJ, Campbell SL (2001) The insert region of Rac1 is essential for membrane ruffling but not cellular transformation. *Mol Cell Biol* 21:2847–2857
- Klebe C, Prinz H, Wittinghofer A et al (1995) The kinetic mechanism of Ran–nucleotide exchange catalyzed by RCC1. *Biochemistry* 34:12543–12552
- Lammers M, Meyer S, Kuhlmann D et al (2008) Specificity of interactions between mDia isoforms and Rho proteins. *J Biol Chem* 283:35236–35246
- Lancaster CA, Taylor-Harris PM, Self AJ et al (1994) Characterization of rhoGAP. A GTPase-activating protein for rho-related small GTPases. *J Biol Chem* 269:1137–1142
- Leonard D, Hart MJ, Platko JV et al (1992) The identification and characterization of a GDP-dissociation inhibitor (GDI) for the CDC42Hs protein. *J Biol Chem* 267:22860–22868
- Li X, Bu X, Lu B et al (2002) The hematopoiesis-specific GTP-binding protein RhoH is GTPase deficient and modulates activities of other Rho GTPases by an inhibitory function. *Mol Cell Biol* 22:1158–1171
- Ligeti E, Dagher MC, Hernandez SE et al (2004) Phospholipids can switch the GTPase substrate preference of a GTPase-activating protein. *J Biol Chem* 279:5055–5058
- Loirand G, Scalbert E, Bril A et al (2008) Rho exchange factors in the cardiovascular system. *Curr Opin Pharmacol* 8:174–180

- Mayer S, Kumar R, Jaiswal M et al (2013) Collybistin activation by GTP-TC10 enhances postsynaptic gephyrin clustering and hippocampal GABAergic neurotransmission. *Proc Natl Acad Sci USA* 110:20795–20800
- Meller N, Merlot S, Guda C (2005) CZH proteins: a new family of Rho-GEFs. *J Cell Sci* 118:4937–4946
- Minoshima Y, Kawashima T, Hirose K et al (2003) Phosphorylation by aurora B converts MgcRacGAP to a RhoGAP during cytokinesis. *Dev Cell* 4:549–560
- Mitin N, Betts L, Yohe ME et al (2007) Release of autoinhibition of ASEF by APC leads to CDC42 activation and tumor suppression. *Nat Struct Mol Biol* 14:814–823
- Moon SY, Zheng Y (2003) Rho GTPase-activating proteins in cell regulation. *Trends Cell Biol* 13:13–22
- Moskwa P, Pacllet MH, Dagher MC et al (2005) Autoinhibition of p50 Rho GTPase-activating protein (GAP) is released by prenylated small GTPases. *J Biol Chem* 280:6716–6720
- Mulinari S, Hacker U (2010) Rho-guanine nucleotide exchange factors during development: Force is nothing without control. *Small GTPases* 1:28–43
- Mulloy JC, Cancelas JA, Filippi MD et al (2010) Rho GTPases in hematopoiesis and hemopathies. *Blood* 115:936–947
- Nassar N, Hoffman GR, Manor D et al (1998) Structures of Cdc42 bound to the active and catalytically compromised forms of Cdc42GAP. *Nat Struct Biol* 5:1047–1052
- Nisimoto Y, Freeman JL, Motalebi SA et al (1997) Rac binding to p67(phox). Structural basis for interactions of the Rac1 effector region and insert region with components of the respiratory burst oxidase. *J Biol Chem* 272:18834–18841
- Ohga N, Kikuchi A, Ueda T et al (1989) Rabbit intestine contains a protein that inhibits the dissociation of GDP from and the subsequent binding of GTP to rhoB p20, a ras p21-like GTP-binding protein. *Biochem Biophys Res Commun* 163:1523–1533
- Pan X, Eathiraj S, Munson M et al (2006) TBC-domain GAPs for Rab GTPases accelerate GTP hydrolysis by a dual-finger mechanism. *Nature* 442:303–306
- Peck J, Douglas Gt WCH et al (2002) Human RhoGAP domain-containing proteins: structure, function and evolutionary relationships. *FEBS Lett* 528:27–34
- Pick E, Gorzalczany Y, Engel S (1993) Role of the rac1 p21-GDP-dissociation inhibitor for rho heterodimer in the activation of the superoxide-forming NADPH oxidase of macrophages. *Eur J Biochem* 217:441–455
- Riou P, Villalonga P, Ridley AJ (2010) Rnd proteins: multifunctional regulators of the cytoskeleton and cell cycle progression. *Bioessays* 32:986–992
- Rittinger K (2009) Snapshots form a big picture of guanine nucleotide exchange. *Sci Signal* 2:pe63
- Rittinger K, Walker PA, Eccleston JF et al (1997) Structure at 1.65 Å of RhoA and its GTPase-activating protein in complex with a transition-state analogue. *Nature* 389:758–762
- Roberts PJ, Mitin N, Keller PJ et al (2008) Rho Family GTPase modification and dependence on CAAX motif-signaled posttranslational modification. *J Biol Chem* 283:25150–25163
- Rojas RJ, Yohe ME, Gershburg S et al (2007) Galphaq directly activates p63RhoGEF and Trio via a conserved extension of the Dbl homology-associated pleckstrin homology domain. *J Biol Chem* 282:29201–29210
- Rose R, Weyand M, Lammers M et al (2005) Structural and mechanistic insights into the interaction between Rho and mammalian Dia. *Nature* 435:513–518
- Rossmann KL, Worthylake DK, Snyder JT et al (2002) Functional analysis of cdc42 residues required for Guanine nucleotide exchange. *J Biol Chem* 277:50893–50898
- Rossmann KL, Der CJ, Sondek J (2005) GEF means go: turning on RHO GTPases with guanine nucleotide-exchange factors. *Nat Rev Mol Cell Biol* 6:167–180
- Rudolph MG, Weise C, Miold S et al (1999) Biochemical analysis of SopE from *Salmonella typhimurium*, a highly efficient guanosine nucleotide exchange factor for RhoGTPases. *J Biol Chem* 274:30501–30509
- Scheffzek K, Ahmadian MR (2005) GTPase activating proteins: structural and functional insights 18 years after discovery. *Cell Mol Life Sci* 62:3014–3038

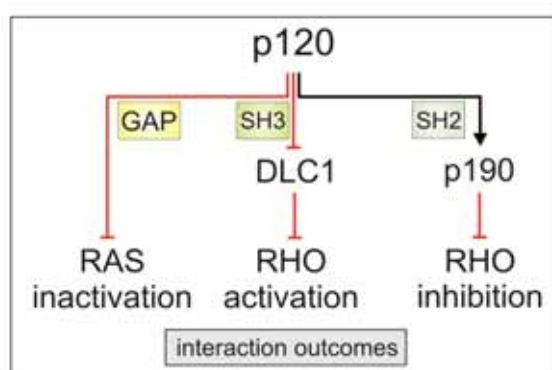
- Scheffzek K, Ahmadian MR, Kabsch W et al (1997) The Ras-RasGAP complex: structural basis for GTPase activation and its loss in oncogenic Ras mutants. *Science* 277:333–338
- Scherle P, Behrens T, Staudt LM (1993) Ly-GDI, a GDP-dissociation inhibitor of the RhoA GTP-binding protein, is expressed preferentially in lymphocytes. *Proc Natl Acad Sci USA* 90:7568–7572
- Schmidt A, Hall A (2002) Guanine nucleotide exchange factors for Rho GTPases: turning on the switch. *Genes Dev* 16:1587–1609
- Shutes A, Berzat AC, Chenette EJ et al (2006) Biochemical analyses of the Wrch atypical Rho family GTPases. *Methods Enzymol* 406:11–26
- Srivastava SK, Wheelock RH, Aaronson SA et al (1986) Identification of the protein encoded by the human diffuse B-cell lymphoma (dbl) oncogene. *Proc Natl Acad Sci USA* 83:8868–8872
- Stebbins CE, Galan JE (2000) Modulation of host signaling by a bacterial mimic: structure of the Salmonella effector SptP bound to Rac1. *Mol Cell* 6:1449–1460
- Takahashi K, Sasaki T, Mammoto A et al (1997) Direct interaction of the Rho GDP dissociation inhibitor with ezrin/radixin/moesin initiates the activation of the Rho small G protein. *J Biol Chem* 272:23371–23375
- Tcherkezian J, Lamarche-Vane N (2007) Current knowledge of the large RhoGAP family of proteins. *Biol Cell* 99:67–86
- Thapar R, Karnoub AE, Campbell SL (2002) Structural and biophysical insights into the role of the insert region in Rac1 function. *Biochemistry* 41:3875–3883
- Tnimov Z, Guo Z, Gambin Y et al (2012) Quantitative analysis of prenylated RhoA interaction with its chaperone, RhoGDI. *J Biol Chem* 287:26549–26562
- Troeger A, Chae HD, Senturk M et al (2013) A unique carboxyl-terminal insert domain in the hematopoietic-specific, GTPase-deficient Rho GTPase RhoH regulates post-translational processing. *J Biol Chem* 288:36451–36462
- Venter JC, Adams MD, Myers EW et al (2001) The sequence of the human genome. *Science* 291:1304–1351
- Viaud J, Gaits-Iacovoni F, Payrastre B (2012) Regulation of the DH-PH tandem of guanine nucleotide exchange factor for Rho GTPases by phosphoinositides. *Adv Biol Regul* 52:303–314
- Vigil D, Cherfils J, Rossman KL et al (2010) Ras superfamily GEFs and GAPs: validated and tractable targets for cancer therapy? *Nat Rev Cancer* 10:842–857
- Vlahou G, Rivero F (2006) Rho GTPase signaling in Dictyostelium discoideum: insights from the genome. *Eur J Cell Biol* 85:947–959
- Walker SJ, Brown HA (2002) Specificity of Rho insert-mediated activation of phospholipase D1. *J Biol Chem* 277:26260–26267
- Wennerberg K, Der CJ (2004) Rho-family GTPases: it's not only Rac and Rho (and I like it). *J Cell Sci* 117:1301–1312
- Wittinghofer A, Vetter IR (2011) Structure-function relationships of the G domain, a canonical switch motif. *Annu Rev Biochem* 80:943–971
- Wurtele M, Wolf E, Pederson KJ et al (2001) How the Pseudomonas aeruginosa ExoS toxin downregulates Rac. *Nat Struct Biol* 8:23–26
- Yamashita T, Tohyama M (2003) The p75 receptor acts as a displacement factor that releases Rho from Rho-GDI. *Nat Neurosci* 6:461–467
- Yang XY, Guan M, Vigil D et al (2009) p120Ras-GAP binds the DLC1 Rho-GAP tumor suppressor protein and inhibits its RhoA GTPase and growth-suppressing activities. *Oncogene* 28:1401–1409
- Yohe ME, Rossman K, Sondek J (2008) Role of the C-terminal SH3 domain and N-terminal tyrosine phosphorylation in regulation of Tim and related Dbl-family proteins. *Biochemistry* 47:6827–6839
- Zalcman G, Closson V, Camonis J et al (1996) RhoGDI-3 is a new GDP dissociation inhibitor (GDI). Identification of a non-cytosolic GDI protein interacting with the small GTP-binding proteins RhoB and RhoG. *J Biol Chem* 271:30366–30374

- Zhang B, Zheng Y (1998) Regulation of RhoA GTP hydrolysis by the GTPase-activating proteins p190, p50RhoGAP, Bcr, and 3BP-1. *Biochemistry* 37:5249–5257
- Zong H, Kaibuchi K, Quilliam LA (2001) The insert region of RhoA is essential for Rho kinase activation and cellular transformation. *Mol Cell Biol* 21:5287–5298

Chapter V

Functional cross-talk between RAS and RAS pathways: a RAS-specific GTPase activating protein (p120RASGAP) competitively inhibits the RHOGAP activity of deleted in liver cancer (DLC) tumor suppressor by masking the catalytic arginine finger

Graphical Abstract



Published in:

The journal of biological chemistry

Impact factor:

4.56 (2014)

Own Proportion to this work:

15%

RNA isolation and qPCR

Immunoblotting of p120 and p190 in liver cells

Writing the manuscript

Functional Cross-talk between Ras and Rho Pathways

*A Ras-SPECIFIC GTPase-ACTIVATING PROTEIN (p120RasGAP) COMPETITIVELY INHIBITS THE RhoGAP ACTIVITY OF DELETED IN LIVER CANCER (DLC) TUMOR SUPPRESSOR BY MASKING THE CATALYTIC ARGININE FINGER**

Received for publication, October 16, 2013, and in revised form, December 18, 2013. Published, JBC Papers in Press, January 17, 2014, DOI 10.1074/jbc.M113.527655

Mamta Jaiswal^{†1}, Radovan Dvorsky[‡], Ehsan Amin[‡], Sarah L. Risse[‡], Eyad K. Fansa[‡], Si-Cai Zhang[‡], Mohamed S. Taha[‡], Aziz R. Gauhar^{‡,2}, Saeideh Nakhaei-Rad[‡], Claus Kordes[§], Katja T. Koessmeier[‡], Ion C. Cirstea^{‡,¶}, Monilola A. Olayioye^{||3}, Dieter Häussinger[§], and Mohammad R. Ahmadian^{†,4}

From the [†]Institute of Biochemistry and Molecular Biology II and [§]Clinic for Gastroenterology, Hepatology and Infectiology, Medical Faculty, Heinrich Heine University, 40225 Düsseldorf, [¶]Leibniz Institute for Age Research, 07745 Jena, and ^{||}Institute of Cell Biology and Immunology, University of Stuttgart, 70569 Stuttgart, Germany

Background: The regulatory mechanism of the DLC1 tumor suppressor protein is unclear.

Results: Structure-function analysis revealed determinants for the selectivity, activity, and inhibition of DLC1 RhoGAP function.

Conclusion: p120RasGAP competitively and selectively inhibits DLC1 by targeting its catalytic arginine finger.

Significance: This mechanistic study emphasizes the importance of the functional inter-relationships of GTPase-activating proteins mediating cross-talk between the Ras and Rho pathways.

The three deleted in liver cancer genes (DLC1–3) encode Rho-specific GTPase-activating proteins (RhoGAPs). Their expression is frequently silenced in a variety of cancers. The RhoGAP activity, which is required for full DLC-dependent tumor suppressor activity, can be inhibited by the Src homology 3 (SH3) domain of a Ras-specific GAP (p120RasGAP). Here, we comprehensively investigated the molecular mechanism underlying cross-talk between two distinct regulators of small GTP-binding proteins using structural and biochemical methods. We demonstrate that only the SH3 domain of p120 selectively inhibits the RhoGAP activity of all three DLC isoforms as compared with a large set of other representative SH3 or RhoGAP proteins. Structural and mutational analyses provide new insights into a putative interaction mode of the p120 SH3 domain with the DLC1 RhoGAP domain that is atypical and does not follow the classical PXXP-directed interaction. Hence, p120 associates with the DLC1 RhoGAP domain by targeting the catalytic argi-

nine finger and thus by competitively and very potently inhibiting RhoGAP activity. The novel findings of this study shed light on the molecular mechanisms underlying the DLC inhibitory effects of p120 and suggest a functional cross-talk between Ras and Rho proteins at the level of regulatory proteins.

The Ras and Rho families of small GTP-binding proteins are key transducers of a variety of cellular processes ranging from reorganization of the cytoskeleton to transcriptional regulation and control of cell growth and survival (1). Loss of the control mechanisms and aberrant activation of Ras and Rho proteins are one of the most common molecular alterations found in cancer cells promoting tumor growth and metastasis (2–5). Ras signaling stimulates diverse pathways and signals toward Rho proteins, which are known to be required for cell transformation by oncogenic Ras (6–8). Emerging evidence suggests that the GTPase-activating proteins (GAPs),⁵ in particular p120RasGAP (also known as RAS p21 protein activator 1 or RASA1; here called p120) and the Rho-specific p190ARhoGAP (also known as ARHGAP35; here called p190), p200RhoGAP (also known as ARHGAP32, p250GAP, GC-GAP, Rics, or Grit) and deleted in liver cancer 1 (DLC1; also known as ARHGAP7, p122RhoGAP, or STARD12), act as a linker between Ras and Rho signaling pathways (9–11). GAPs are multifaceted and multifunctional molecules (12, 13) and are the principal inactivators of Ras and Rho signaling. They utilize a catalytic “arginine finger” to stimulate the inefficient intrinsic GTP hydrolysis reaction of these small GTP-binding proteins by several orders of magnitude (14).

* This work was supported in part by the German Research Foundation (Deutsche Forschungsgemeinschaft (DFG)) through the Collaborative Research Center 974 (SFB 974) “Communication and Systems Relevance during Liver Injury and Regeneration,” the International Research Training Group 1902 (IRGT1902), and Project Grant AH 92/5-1; the National Genome Research Network Plus program of the German Ministry of Science and Education (Bundesministerium für Bildung und Forschung Grant 01GS08100); and the International North Rhine-Westphalia Research School BioStruct granted by the Ministry of Innovation, Science and Research of the State North Rhine-Westphalia, the Heinrich Heine University of Düsseldorf, and the Entrepreneur Foundation at the Heinrich Heine University of Düsseldorf.

¹ Present address: Structural Biology Group, Max Planck Inst. for Molecular Physiology, Otto-Hahn-Strasse 11, 44227 Dortmund, Germany.

² Present address: Inst. of Physical Biology, Heinrich Heine University, 40255 Düsseldorf, Germany.

³ Supported by the DFG Heisenberg program.

⁴ To whom correspondence should be addressed: Inst. für Biochemie und Molekularbiologie II, Medizinische Fakultät der Heinrich-Heine-Universität, Universitätsstrasse 1, Gebäude 22.03, 40255 Düsseldorf, Germany. Tel.: 49-211-811-2384; Fax: 49-211-811-2726; E-mail: reza.ahmadian@uni-duesseldorf.de.

⁵ The abbreviations used are: GAP, GTPase-activating protein; DLC, deleted in liver cancer; SH, Src homology; SAM, sterile α motif; START, steroidogenic acute regulatory related lipid transfer; aa, amino acids; tamra, tetramethylrhodamine; aSEC, analytical size exclusion chromatography; ITC, isothermal titration calorimetry.

p120RasGAP Competitively Inhibits DLC RhoGAP

Frequent loss of *DLC1* gene expression was first described in liver cancer (15) and later in breast, colon, gastric, prostate, cervical, esophageal, and other cancers (16–18). DLC1 RhoGAP function is required for the maintenance of cell morphology and the coordination of cell migration (11, 19–21). DLC1 and its isoforms DLC2 (also known as ARHGAP37 or STARD13) and DLC3 (also known as ARHGAP38 or STARD8) consist of an N-terminal sterile α motif (SAM) domain, a central phosphorylation region followed by the catalytic RhoGAP domain, and a C-terminal steroidogenic acute regulatory related lipid transfer (START) domain (see Fig. 1A) (22, 23). The SAM and GAP domains are linked by a serine-containing region, which contains a recognition motif for the phosphoserine/phosphothreonine-binding 14-3-3 adaptor proteins (22). DLC1 has been reported to interact with tensin, talin, focal adhesion kinase, and α -catenin (22, 24–29) and with lipids (30). However, the precise mechanism of DLC1 regulation remains unclear.

An emerging theme is that RhoGAPs, such as the OPHN1 and GRAF1 (31, 32) and p50RhoGAP (33–36), require activation through the relief of autoinhibitory elements. These elements are collectively membrane-binding modules, including BAR (Bin/Amphiphysin/Rvs), PH (pleckstrin homology), C1, and Sec14 domains (31–33, 36). The SAM domain of DLC1 has been suggested to act as an autoinhibitory domain of DLC1 RhoGAP activity *in vitro* and *in vivo*. SAM domain-deleted DLC1 displayed enhanced catalytic activity for RhoA (20). However, it is still unclear how such an autoregulatory mechanism of DLC1 may operate.

p120 contains multiple domains with different functions (see Fig. 1B) (37). Whereas the C terminus of p120 with the catalytic GAP activity is responsible for Ras inactivation (38–40), its N-terminal Src homology 2 and 3 (SH2 and SH3) domains have been suggested to possess an effector function (41–44). p120 functionally modulates Rho signaling by direct binding to two Rho-specific GAPs, p190 and DLC1 (9, 11, 45). The association of p120 with the tyrosine phosphorylated p190 via its SH2 domain promotes Rho inactivation (45–47). Thus, p120 positively regulates the RhoGAP function of p190. Another mechanism, which connects the Ras and Rho pathways and regulates the actin cytoskeleton, is dependent on the p120 SH3 domain and controls Rho activation (41). This mechanism was later revealed to involve DLC1 but not p190 (11). Here, the p120 SH3 domain (called p120^{SH3}) binds to the RhoGAP domain of DLC1 (called DLC1^{GAP}) and inhibits the DLC1-dependent Rho inactivation (11). Hereby, p120 acts as a negative regulator not only for Ras but also for the GAP activity of DLC1. However, the molecular mechanisms underlying these cross-talk phenomena have not yet been elucidated.

In this study, we have explored the regulatory mechanism of DLC1 at the molecular level, in particular its *trans*-inhibition by p120^{SH3}. We have characterized the selectivity of the interaction between the DLC1^{GAP} and p120^{SH3} using a large number of purified SH3 and RhoGAP proteins and identified structural and functional determinants for the DLC1-p120 interaction. This study provides deep insights into the underlying regulatory cross-talk between the Rho and Ras family of small GTP-binding proteins.

EXPERIMENTAL PROCEDURES

Constructs—Human Abr^{GAP} (aa 559–822), DLC1^{fl} (aa 1–1091), DLC1^{GAP} (aa 609–878), DLC1^{SAM} (aa 1–96), DLC1^{START} (aa 880–1079), DLC2^{GAP} (aa 644–916), DLC3^{GAP} (aa 620–890), GRAF1^{GAP} (aa 383–583), MgcRac^{GAP} (aa 343–620), Nadrin^{GAP} (aa 245–499), OPHN1^{GAP} (aa 375–583), p50^{GAP} (aa 198–439), p190^{GAP} (aa 1250–1513), N-terminal truncated p120^{An128} (aa 129–1047); SH2-SH3-SH2-encoding p120^{SH2-3-2} (aa 129–447), p120^{SH3} (aa 275–350), Src^{SH3} (aa 77–140), and human RhoA (aa 1–181), Cdc42 (aa 1–178), and Rac1 (aa 1–184) were amplified by standard PCR and cloned in pGEX-4T1 and pGEX-4T1-NTEV, respectively. Constructs of SH3 domain of Crk1^{SH3} (aa 131–191), Grb2^{SH3-1} (aa 1–55), Grb2^{SH3-2} (aa 159–217), Nck1^{SH3-1} (aa 5–60), Nck1^{SH3-2} (aa 109–163), and Nck1^{SH3-3} (aa 173–262) were created as described previously (48).

Site-directed Mutagenesis—Point mutations N311R; L313A; W319G; and N311R,L313A,W319G in p120^{SH3} and R677A in DLC1^{GAP} were generated using the QuikChangeTM site-directed mutagenesis kit (Stratagene) and confirmed by DNA sequencing.

Proteins—*Escherichia coli* BL21(DE3) pLysS, BL21(DE3) CodonPlus-RIL, and Rosetta(DE3) strains containing the respective plasmids (see constructs) were grown to an A_{600} of 0.7 (37 °C at 140 rpm) and induced with 0.1 mM isopropyl β -D-thiogalactopyranoside overnight at 25 °C as described before (49, 50). All proteins were isolated in a first step as glutathione S-transferase (GST) fusion proteins by affinity chromatography on a GSH-agarose column and in a second step by size exclusion chromatography (Superdex S75 or S200) after proteolytic cleavage of GST. GTP-binding proteins without nucleotide (nucleotide-free form) or with tetramethylrhodamine-conjugated GTP (tamraGTP) were prepared as described before (49, 50). Concentrations of proteins were determined by Bradford assay or absorbance at 280 nm using the extinction coefficient deduced from the protein sequence. Purified proteins were snap frozen in liquid nitrogen and stored at –80 °C.

Analytical Size Exclusion Chromatography (aSEC)—aSEC for the detection of complex formation was performed for DLC1^{GAP} and p120^{SH3} on a Superdex 75 column (10/300) using buffer containing 30 mM HEPES, pH 7.6, 5 mM MgCl₂, 150 mM NaCl, and 3 mM DTT. 10 μ M DLC1^{GAP} was incubated with 15 μ M p120^{SH3} for 5 min at 4 °C in the same buffer in a total volume of 150 μ l. Before loading to an aSEC column, samples were spun at 13,000 rpm at 4 °C to remove any particulate impurities. The flow rate was maintained at 0.5 ml/min, and 500- μ l fractions were collected. Peak fractions were visualized by 15% SDS-PAGE and subsequent Coomassie Blue staining.

Kinetics Measurements—All fluorescence measurements were performed at 25 °C in a buffer containing 30 mM Tris-HCl, pH 7.5, 10 mM K₂HPO₄/KH₂PO₄, pH 7.4, 10 mM MgCl₂, and 3 mM DTT. The tamraGTP hydrolysis of Rho proteins (0.2 μ M) was measured in the absence and presence of different amounts of respective GAP proteins as described previously (49, 52). Fast kinetics (<1000 s) were performed with a Hi-Tech Scientific SF-61 stopped-flow instrument with a mercury xenon light source and TgK Scientific Kinetic Studio software (version

p120RasGAP Competitively Inhibits DLC RhoGAP

219). An excitation wavelength of 545 nm was used for tamra. Emission was detected through a cutoff filter of 570 nm. Slow kinetics (>1000 s) were measured on a PerkinElmer Life Sciences spectrofluorometer (LS50B) using an excitation wavelength of 545 nm and an emission wavelength of 583 nm. Data were evaluated by single exponential fitting with the GraFit program to obtain the observed rate constant (k_{obs}) for the respective reaction as described before (49, 52).

Isothermal Titration Calorimetry (ITC) Measurements—The interaction of DLC1^{GAP} and p120^{SH3} and analysis of DLC1^{GAP} variant and different p120^{SH3} variants were studied by ITC (MicroCalTM VP-ITC microcalorimeter) as described (48). All measurements were carried out in 30 mM Tris-HCl, pH 7.5, 150 mM NaCl, 5 mM MgCl₂, and 1 mM tris(2-carboxyethyl)phosphine hydrochloride. The data were analyzed using Origin 7.0 software provided by the manufacturer.

Structural Analysis—To obtain insight into the residues responsible for the binding of the SH3 domain of p120 and RhoGAP domain of DLC1, docking of their corresponding structures (Protein Data Bank code 2J05 (53) and Protein Data Bank code 3KUQ, respectively), was performed with the program PatchDock (54). From the 20 best scored models, we selected the lowest energy model, which also has the Arg finger Arg-677 at the interface, and used it for further refinement with the program CHARMM (55). As the arginine finger is assumed to be crucial for the formation of the complex, we thoroughly explored its conformation in the course of refinement. Torsion angles of its side chain were additionally set up according to the Dynamomics rotamer library (56), and the energy of each complex was minimized by 2000 steps using the adapted basis Newton-Raphson method.

RESULTS

Low GAP Activities of the DLC Isoforms—Real time kinetic measurements of the RhoGAP activities of the DLC isoforms toward Cdc42, Rac1, and RhoA were performed using purified RhoGAP domains of the DLC proteins (Fig. 1) and fluorescent tamraGTP. This GTP analog is sensitive toward conformational changes induced by GTP hydrolysis (52). As shown in Fig. 2A, the very slow intrinsic tamraGTP hydrolysis of Cdc42 (*inset*) was markedly increased in the presence of the RhoGAP domain of DLC1 (DLC1^{GAP}). Similar experiments were performed under the same conditions with Rac1 and RhoA (Fig. 2B). Observed rate constants (k_{obs}) of respective DLC1^{GAP} activities are presented in comparison with intrinsic hydrolysis rates as *bars* in Fig. 2B. DLC1^{GAP} exhibited the highest activity for RhoA (1,650-fold) and Cdc42 (332-fold) and the lowest activity for Rac1 (75-fold). We next focused on the differences among the DLC isoforms and measured the activities of DLC2 and DLC3 for Cdc42 (Fig. 2C). Obtained data show that DLC2 and DLC3 exhibit 78- and 11-fold lower GAP activities, respectively, as compared with that of DLC1. Our results indicate that the DLC family members are inefficient GAPs, at least *in vitro*, with catalytic activities that are several orders of magnitude lower than the activities of the RhoGAPs p50 and p190 (Fig. 2C) or other highly efficient RhoGAPs, such as GRAF1 or OPHN1 (32).

A comparison of the obtained data on the DLC isoforms with those of other RhoGAP family members raised the question of whether the extremely low GAP activities of DLC proteins stem from effects on either binding affinity (K_d) or catalytic activity (k_{cat}). Therefore, we measured the kinetics of tamraGTP hydrolysis of Cdc42 at increasing concentrations of DLC1^{GAP} and GRAF1^{GAP}. The rate constants (k_{obs}) of the fitted single exponential decays increased in a hyperbolic manner as a function of GAP concentrations as described previously (52, 57). We used Cdc42 in most experiments because of a large change in fluorescence upon tamraGTP hydrolysis as compared with Rac1 and RhoA. Fitting a hyperbolic curve to the points according to Equation 1 led to the corresponding kinetic parameters K_d and k_{cat} (Fig. 2D).

$$k_{\text{obs}} = \frac{k_{\text{cat}}}{1 + \frac{K_d}{[\text{DLC1}]}} \quad (\text{Eq. 1})$$

Unlike the relatively similar K_d values, there was a large difference in the k_{cat} values for the GTP hydrolysis reaction: 6.26 s⁻¹ for DLC1^{GAP} compared with 289 s⁻¹ for the highly efficient GRAF1^{GAP}. These data clearly indicate that the very low GAP activity of the DLC proteins relies more on the catalytic activity than on the binding affinity to Cdc42.

Insights into cis-Regulatory Modules of DLC1 Function—To examine the influence of other domains of DLC1 (Fig. 1A) on its GAP activity, we further measured tamraGTP hydrolysis of Cdc42 stimulated by full-length DLC1 (DLC1^{fl}). As shown in Fig. 3A, DLC1^{fl} exhibited a strongly reduced GAP activity as compared with the isolated DLC1^{GAP}. The k_{obs} values obtained from single turnover kinetic data were 0.02 and 0.47 s⁻¹, respectively, and reveal that the DLC1^{fl} activity was 23.5-fold lower than that of DLC1^{GAP} (Fig. 3B). This result strongly supports the previous notion that other regions of DLC1, such as the SAM domain (20), may undergo an intramolecular interaction with the GAP domain and thus contribute to its autoinhibition in a *cis*-inhibitory manner.

To analyze whether the autoinhibitory effect is caused by N- and C-terminal SAM and/or START domains of DLC1 (Fig. 1A), we purified these domains and measured their effects on the DLC1^{GAP} activity *in vitro*. Using high concentrations of SAM, START, or both (up to a 100-fold molar excess above the GAP domain), we did not observe any significant inhibition of the DLC1^{GAP} activity using tamraGTP hydrolysis of Cdc42 (Fig. 3C). The fact that the isolated SAM and START domains did not reveal any GAP-inhibitory activity strongly suggests that the autoinhibitory mechanism of DLC1 may require additional regions of the full-length protein. One possibility is the serine-rich 14-3-3 binding region between the SAM and the GAP domains (Fig. 1A).

p120 SH3 as a Potent trans-Inhibitory Factor of the DLC1^{GAP} Activity—The SH3 domain of p120 has been reported as a novel binding partner of DLC1 with GAP-inhibitory and growth suppression activity (11). To monitor this effect in real time, DLC1^{GAP} activity was measured in the absence and presence of purified p120^{SH3} under the same conditions as in the experiments described above (Fig. 2). As shown in Fig. 4A, DLC1^{GAP}-

p120RasGAP Competitively Inhibits DLC RhoGAP

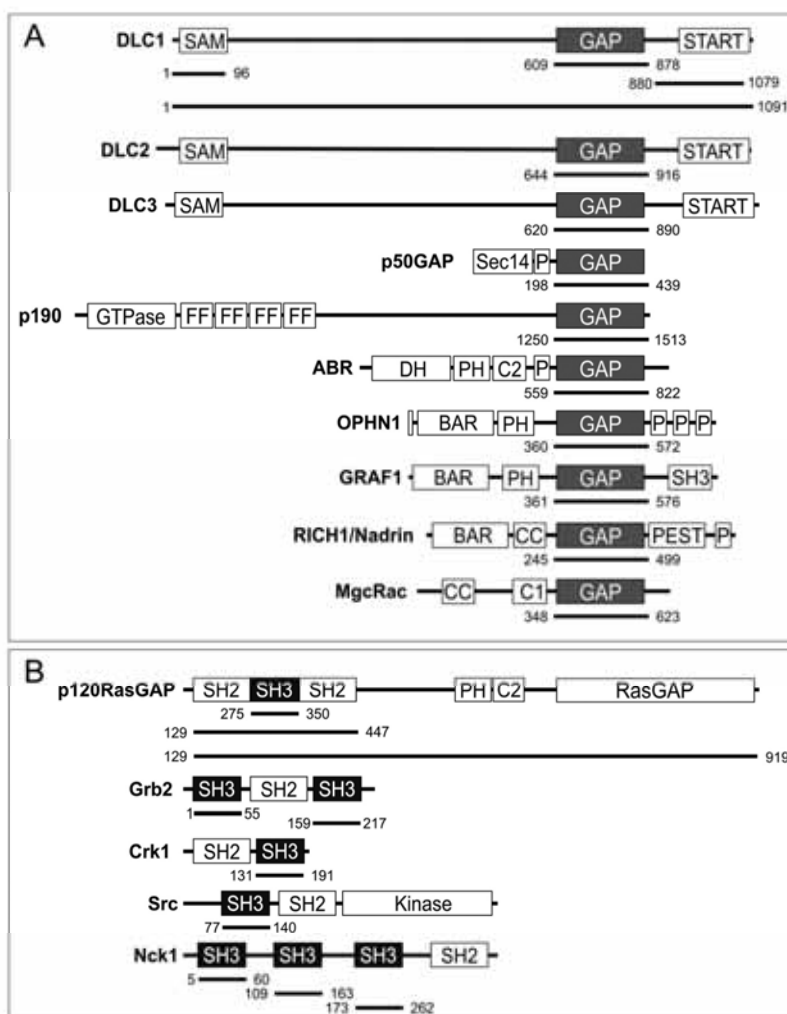


FIGURE 1. Schematic representation of domain organization and designed fragments of GAP (A) and SH3 domain-containing proteins (B) used in this study. The numbers indicate the N and C termini of the amino acids of the respective fragments. BAR, Bin/Amphiphysin/Rvs; C1, cysteine-rich region; CC, coiled coil; DH, Dbl homology domain; FF, double phenylalanine; P, proline-rich; PH, pleckstrin homology; PSET, proline, serine, glutamic acid, and threonine; RGS, regulator of G-protein signaling; Sec14, secretion and cell surface growth 14.

stimulated tamraGTP hydrolysis of Cdc42 was drastically reduced using a 10-fold excess of p120^{SH3} over the DLC1^{GAP} concentration. The respective k_{obs} value of 0.63 for DLC1^{GAP} activity was reduced by 83-fold in the presence of p120^{SH3} to 0.0076 s⁻¹ (Fig. 4B), which is close to the intrinsic tamraGTP hydrolysis of Cdc42 (0.02 s⁻¹). These measurements were also performed for RhoA and Rac1 using the same conditions as for Cdc42 (Fig. 4B). Similarly, 247- and 15.5-fold reductions of the DLC1^{GAP} activity for RhoA and Rac1, respectively, were determined in the presence of a 10-fold molar excess of p120^{SH3}. An explanation for this large variation may be the significant differences in DLC1^{GAP} binding affinity for the three members of the Rho family.

In the next step, we analyzed the inhibitory effect of p120^{SH3} on the GAP activity of DLC2 and DLC3 toward Cdc42. Fig. 4C shows that the catalytic GAP activity of purified DLC2^{GAP} and DLC3^{GAP} was also inhibited in the presence of p120^{SH3} but not

as drastically as in the case of DLC1^{GAP}. The next question we addressed was whether the SH3 domain is freely accessible to exert its inhibitory effect or whether other domains of p120 also play a role in the inhibition of DLC GAP activity (Fig. 1). Therefore, we purified the SH2-SH3-SH2-encompassing p120^{SH2-3-2} and N-terminal truncated p120^{An128} proteins and analyzed their DLC1^{GAP} inhibitory effects in direct comparison with isolated p120^{SH3}. Larger p120 fragments inhibited the DLC1^{GAP} activity but to a 19- and 10-fold lower extent than p120^{SH3} (Fig. 4D).

Taken together, our *in vitro* data demonstrate that (i) p120^{SH3} acts as a potent *trans*-inhibitory factor of the GAP activity of the DLC isoforms and (ii) the SH3 domain of p120 is not completely unmasked (freely accessible) in the presence of other p120 completed, especially the adjacent SH2 domains. Whether the N-terminal 128 amino acids play a role in this regard remains unclear. Full-length p120 could not be purified due to its instability.

p120RasGAP Competitively Inhibits DLC RhoGAP

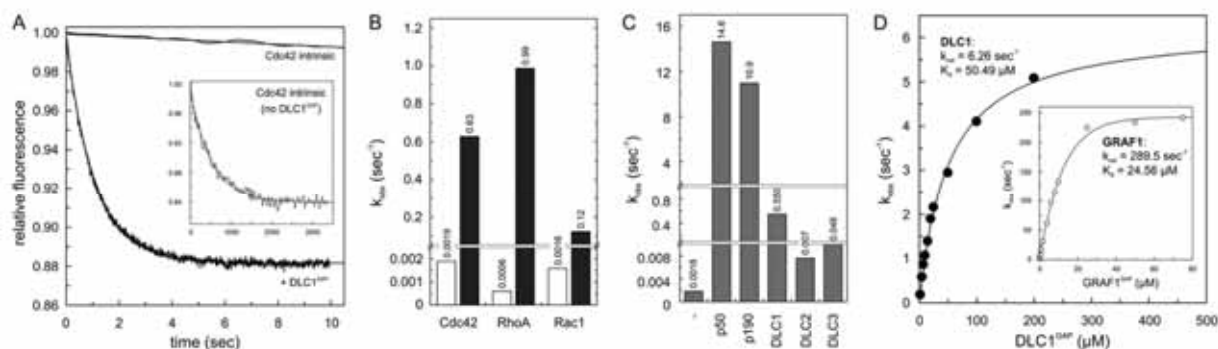


FIGURE 2. Inefficient GAP activities of the DLC isoforms. A, Cdc42-tamraGTP (0.2 μM) was rapidly mixed with 5 μM DLC1^{GAP} to monitor the GAP-stimulated tamraGTP hydrolysis reaction of Cdc42 in real time. Note the very slow intrinsic GTPase reaction of Cdc42 (inset) that was measured in the absence of GAP. Rate constants (k_{obs}) were obtained by single exponential fitting of the data. B, the k_{obs} values of GTP hydrolysis of Rho proteins (0.2 μM) measured in the presence of DLC1^{GAP} (5 μM) are represented as a column chart. Calculated-fold activation values were obtained by dividing the k_{obs} values of GAP-stimulated reactions by the k_{obs} values of the intrinsic reactions of respective GTPases. For convenience, the k_{obs} values are given above the bar charts. C, measured GAP activities of DLC1, DLC2, and DLC3 (5 μM , respectively) toward Cdc42 (0.2 μM) were very low as compared with p150 and p190. D, the GTP hydrolysis of Cdc42 (0.2 μM) was measured in the presence of increasing concentrations of the respective GAP domains of DLC1 and GRAF1 (inset). The dependence of the k_{obs} values of the GAP-stimulated GTP hydrolysis plotted on the concentrations of DLC1^{GAP} and GRAF1 was fitted by a hyperbolic curve to obtain the kinetic parameters (k_{cat} and K_d).

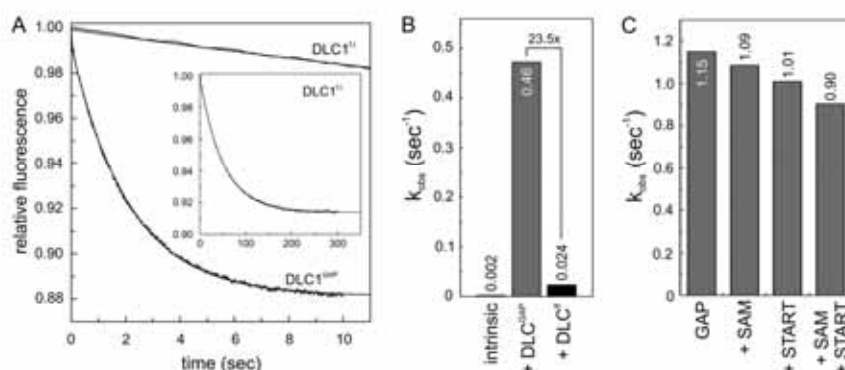


FIGURE 3. cis-Acting regulation of DLC1^{GAP} activity. A, kinetics of the tamraGTP hydrolysis reaction of Cdc42 (0.2 μM) stimulated by DLC1^{GAP} (5 μM) was much slower (inset) than that stimulated by DLC^{GAP} (5 μM). B, the k_{obs} values, illustrated as a bar chart, showed that the GAP activity of DLC1^{GAP} is reduced by 23.5-fold as compared with that of the DLC1^{GAP} but not completely inhibited as compared with the intrinsic GTPase reaction. For convenience, the k_{obs} values are given above the bar charts. C, the activity of DLC1^{GAP} (10 μM) on tamraGTP hydrolysis of Cdc42 (0.2 μM) was not significantly changed in the presence of a 100-fold excess of SAM, START, or both domains (1 mM, respectively).

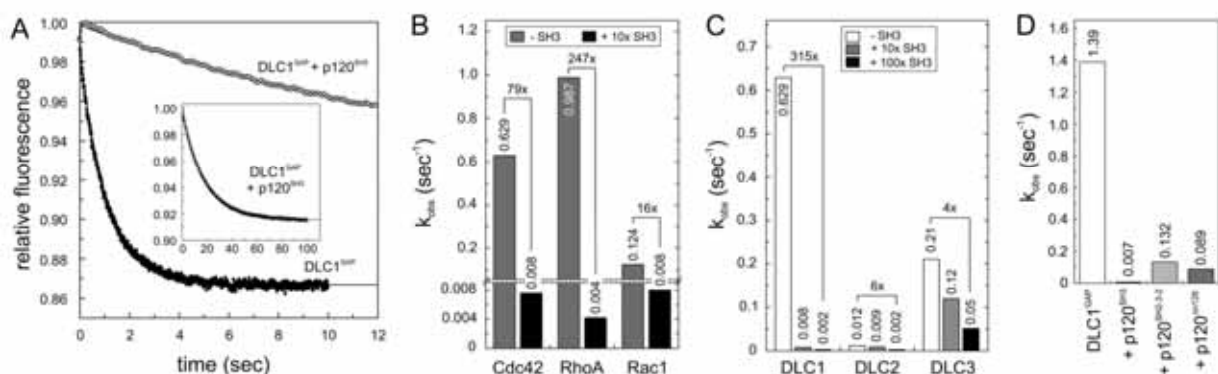


FIGURE 4. p120^{SH3} as a potent inhibitor of the DLC GAP function. A, kinetics of the tamraGTP hydrolysis reaction of Cdc42 (0.2 μM) stimulated by DLC1^{GAP} (5 μM) was reduced in the presence of a 10-fold excess of p120^{SH3} (50 μM). The complete reaction is shown in the inset. B, DLC1^{GAP} activities toward Cdc42, RhoA, and Rac1, measured under the same conditions as in A, are strongly inhibited by p120^{SH3}. For convenience, the k_{obs} values are given above the bar charts. C, DLC3^{GAP} (5 μM) was not inhibited by p120^{SH3} (50 and 500 μM) as efficiently as DLC1^{GAP} and DLC2^{GAP} (5 μM , respectively). D, p120^{SH3-3-2} and p120^{SH3-128} (40 μM) inhibited the activity of DLC^{GAP} (10 μM) but not as efficiently as p120^{SH3} (40 μM).

Highly Selective Interaction between p120^{SH3} and DLC1^{GAP}—The next issue we addressed was the selectivity of the p120^{SH3} toward DLC1^{GAP}. Therefore, we purified seven additional

RhoGAP and SH3 domains of other proteins (Fig. 1). We measured the effect of p120^{SH3} on the GAP activity of Abr, GRAF1, MgcRacGAP, Nadrin, OPHN1, p50, and p190 on the one hand

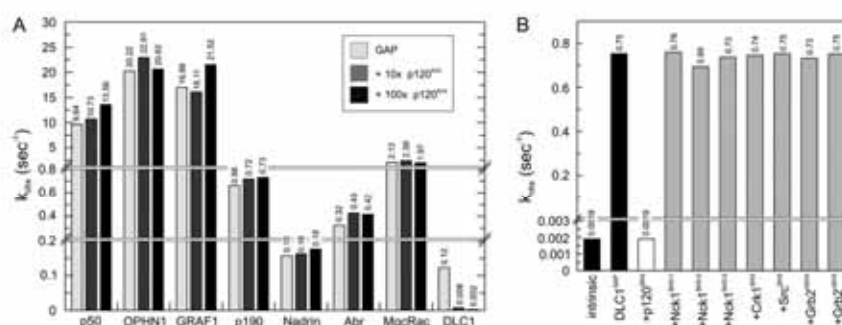
p120^{Ras}GAP Competitively Inhibits DLC RhoGAP

FIGURE 5. Highly selective interaction between p120^{SH3} and DLC1^{GAP}. A, p120^{SH3}-inhibiting effect on seven additional RhoGAPs (2 μ M, respectively) was measured using the tamraGTP hydrolysis reaction of Cdc42 (0.2 μ M) and p120^{SH3} (20 and 200 μ M, respectively). p120^{SH3} inhibited only DLC1^{GAP} but not the other RhoGAPs. For convenience, the k_{obs} values are given above the bar charts. B, the effect of seven additional SH3 proteins (100 μ M, respectively) on inhibiting DLC1^{GAP} (10 μ M) was measured. Only p120^{SH3} inhibited DLC1^{GAP} but not the other SH3 domains.

and the effects of the SH3 domains of Crk1, c-Src, Grb2 (N- and C-terminal SH3 domains), and Nck1 (all three SH3 domains) on the DLC1^{GAP} activity on the other hand. As summarized in Fig. 5, neither did p120^{SH3} inhibit the activity of other GAPs of the Rho family (Fig. 5A) nor was the DLC1^{GAP} activity affected by the presence of other SH3 domains (Fig. 5B). These data clearly demonstrate that the p120^{SH3}-mediated *trans*-inhibition of DLC isoforms is highly selective.

Potent DLC1 Inhibition Due to High Affinity p120^{SH3}-DLC1^{GAP} Complex Formation—In the next step, we characterized in more detail the interaction between p120^{SH3} and DLC1^{GAP} as well as the inhibition of the DLC1^{GAP} activity induced by p120^{SH3} using different qualitative and quantitative biophysical and biochemical methods. aSEC is an accurate and simple method to visualize high affinity protein-protein interactions. p120^{SH3} (9 kDa) and DLC1^{GAP} (31 kDa) alone and a mixture of both proteins were loaded on a Superdex 75 (10/300) column, and eluted peak fractions were analyzed by SDS-PAGE. Data summarized in Fig. 6A clearly illustrate that a mixture of p120^{SH3} and DLC1^{GAP} shift the elution profile of the respective protein domains to an elution volume of 10.5 ml, indicating the formation of a complex between both proteins. We next determined the inhibitory potency of p120^{SH3} by measuring DLC1^{GAP} activity at increasing concentrations of p120^{SH3}. An inhibitory constant (K_i) of 0.61 μ M was calculated by fitting the Morrison equation for a tight binding inhibitor (58) to individual k_{obs} values plotted against different p120^{SH3} concentrations (Fig. 6B). Furthermore, we measured the dissociation constant of the p120^{SH3}-DLC1^{GAP} interaction using ITC. The results shown in Fig. 6C allowed the determination of a stoichiometry of 1:1 and a dissociation constant (K_d) of 0.6 μ M for the binding of p120^{SH3} to DLC1^{GAP} (Fig. 6C); this value nicely resembles the K_i value obtained from inhibition kinetics (Fig. 6B). This binding affinity is remarkably high and unexpected considering the low micromolar range affinities of SH3 domains for their PXXP-containing proteins (59). Taken together, these data strongly suggest that the mode of the p120^{SH3}-DLC1^{GAP} interaction most likely differs from the conventional SH3 interaction with PXXP loop motifs as recently published (48).

Structural Insight into a Putative Binding Mode between p120^{SH3} and DLC1^{GAP}—The high nanomolar affinity of p120^{SH3} for DLC1^{GAP} and the absence of a PXXP motif in DLC1^{GAP} strongly support the notion that the p120^{SH3}-DLC1^{GAP} interaction is mediated via a novel binding mechanism. To gain insight into the structural basis of this interaction, we first performed protein-protein docking of available crystal structures of p120^{SH3} (Protein Data Bank code 2J05) (53) and DLC1^{GAP} (Protein Data Bank code 3KUQ) using the Patch-Dock program (54). The model of the complex ranked as the first among 20 resulting models fulfilled the criteria for a close proximity of p120^{SH3} to the catalytic arginine finger (Arg-677) of the DLC1^{GAP} domain and was thus selected for refinement by molecular modeling methods. Inspecting the refined model, we identified three potential DLC1^{GAP} binding residues of p120^{SH3} (Asn-311, Leu-313, and Trp-319) that were closest to the catalytic Arg-677 of DLC1^{GAP} (Fig. 7A). We proposed that mutation of these residues may impair binding of the SH3 domain, which otherwise masks the arginine finger of DLC1^{GAP}. Catalytic arginine is known to stabilize the transition intermediate state of the hydrolysis reaction in the active center of Rho proteins (Fig. 7B) (14, 60). This assumption also suggests that p120 competitively inhibits DLC1 GAP function.

To validate our assumption, we performed mutational analysis of the above mentioned key residues at the p120^{SH3}-DLC1^{GAP} interface: N311R, L313A, and W319G in p120^{SH3} (single, double, and triple single point mutations) and R677A in DLC1^{GAP}. Expectedly, DLC1^{GAP} with the catalytic arginine finger substituted to alanine was deficient in stimulating tamraGTP hydrolysis of Cdc42 (data not shown) and most remarkably in associating with p120^{SH3} (Fig. 8, A and B). The latter was examined using two independent methods, ITC and aSEC. Reciprocally, p120^{SH3(N311R,L313A,W319G)} was almost disabled in inhibiting DLC1^{GAP} activity (Fig. 8E), most probably due to its inability to bind to DLC1^{GAP} (Fig. 8, C and D). The analysis of the single point mutations revealed that W319G substitution had a minor effect on the association with (data not shown) and on the inhibition of DLC^{GAP} (Fig. 8E). p120^{SH3(N311R,L313A)} on the other hand significantly abolished both the inhibitory effect of p120^{SH3} (Fig. 8E) and the complex formation with DLC1^{GAP} (data not shown) as compared with wild-type p120^{SH3}. Taken together,

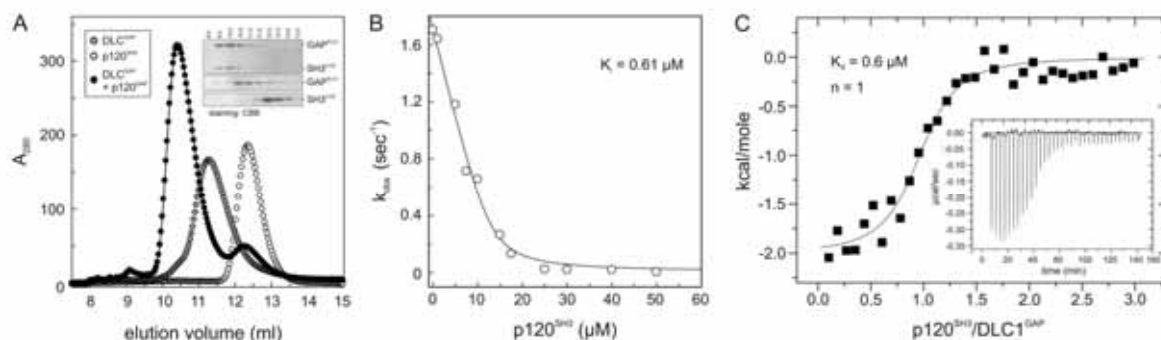
p120^{RasGAP} Competitively Inhibits DLC RhoGAP

FIGURE 6. **High affinity interaction between p120^{SH3} and DLC1^{GAP}.** A, co-elution of a mixture of DLC1^{GAP} (10 μM) and p120^{SH3} (15 μM) (open circles) from a Superdex 75 (10/300) as shown by SDS-PAGE (15%) and Coomassie Brilliant Blue (CBB) staining (inset) indicates their complex formation. B, the activity of DLC1^{GAP} (20 μM) toward Cdc42 (0.2 μM) was measured at increasing concentrations of p120^{SH3}, and the obtained k_{obs} values were plotted against increasing concentrations of the inhibitor p120^{SH3}. The K_d value was obtained by non-linear regression based on the Morrison equation for tight binding inhibitors (58). C, ITC analysis was performed by titrating DLC1^{GAP} (20 μM) with p120^{SH3} (400 μM). K_d is the dissociation constant, and n is the stoichiometry.

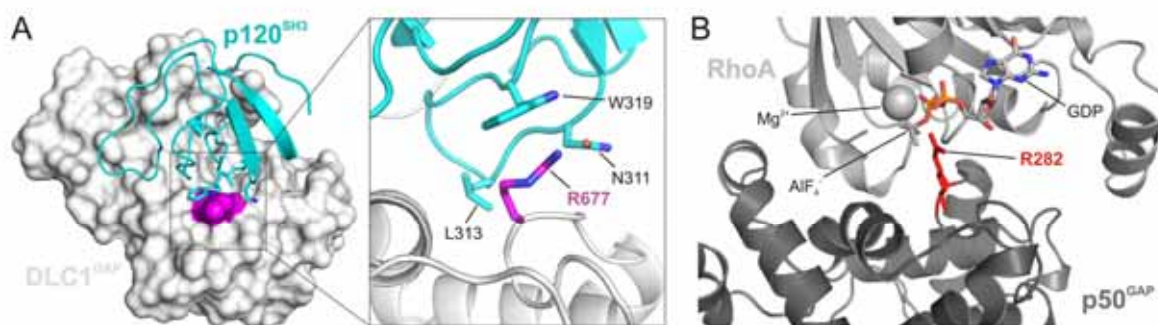


FIGURE 7. **Structural insight into a putative binding mode between p120^{SH3} and DLC1^{GAP}.** A, molecular docking analyses were performed between the available crystal structures of p120^{SH3} (Protein Data Bank code 2J05) (53) and DLC1^{GAP} (Protein Data Bank code 3KUQ) using the program PatchDock (54). In the best ranked and refined model, p120^{SH3} was located in close proximity of the catalytic arginine finger (Arg-677; magenta) of DLC1^{GAP}. In this model, p120^{SH3} supplied three amino acids (Asn-311, Leu-313, and Trp-319) to directly contact the catalytic core of DLC1^{GAP}, especially Arg-677, and mask its accessibility to the Rho proteins. B, p50GAP provides an arginine finger (Arg-282; red) in the active site of RhoA to stabilize the transition state of the GTP hydrolysis reaction (Protein Data Bank code 1TX4) (60). GDP-AIF₃ mimics the transition state of the GTP hydrolysis reaction.

our mutational and biochemical analyses support the *in silico* structural model (Fig. 7A) and provide new insight into how p120^{SH3} may bind and inhibit the catalytic activity of DLC1^{GAP}.

DISCUSSION

In this study, we have elucidated the molecular mechanism of how the RasGAP p120 selectively acts as a negative regulator of the RhoGAP activity of DLC1. We have shown that p120^{SH3}, by utilizing a novel binding mode, selectively undergoes a high affinity interaction with the RhoGAP domain of DLC1 and effectively inhibits its GAP activity by targeting its catalytic arginine finger. Interestingly, p120^{SH3} acts on the DLC isoforms but not on seven other representative members of the RhoGAP family. Our data together support the notion of a functional cross-talk between Ras and Rho proteins at the level of regulatory proteins (11, 45).

In contrast to the molecular mechanism of Rho protein inactivation by GAPs, which is well established (14, 61), it is still unclear how GAPs themselves are regulated. Different mechanisms are implicated in the regulation of GAPs, such as regulation by protein phosphorylation, proteolytic degradation, intramolecular autoinhibition, and changes in subcellular localization or protein complex formation (62, 63). "Intramolecular inhibition" (also called "autoinhibition," "cis-inhibition," "autoinhibitory

loop," "autoregulation," and "bistable switch") of biological molecules is a fundamental control mechanism in nature and is an emerging theme in the regulation of different kinds of proteins, including the regulators of small GTP-binding proteins themselves. Besides the guanine nucleotide exchange factors (64–69), GAPs also have been reported to require activation through the relief of autoinhibitory elements (20, 31–33, 35, 36). Kim *et al.* (20) have shown that DLC1^{fl} has a reduced GAP activity and have proposed that the N-terminal SAM domain may be a *cis*-inhibitory element contributing to DLC1 autoinhibition. Our real time kinetic experiments, however, have shown that neither isolated SAM or START alone nor both domains in combination are directly responsible for the observed DLC1^{fl} autoinhibition in a cell-free system (Fig. 3). Taken together, it rather seems plausible that other regions, probably together with SAM and START domains, are involved in the autoinhibition of DLC1. In addition, it is important to note that release of the autoinhibitory loop of DLC1 is most likely subjected to posttranslational modifications (21, 70) and interactions with other proteins (16, 28, 34) along with changes in subcellular localization (30), collectively contribute to the regulation of DLC1 GAP activity in intact cells. In this context, PKD-mediated phosphorylation (70) and 14-3-3 binding and

p120RasGAP Competitively Inhibits DLC RhoGAP

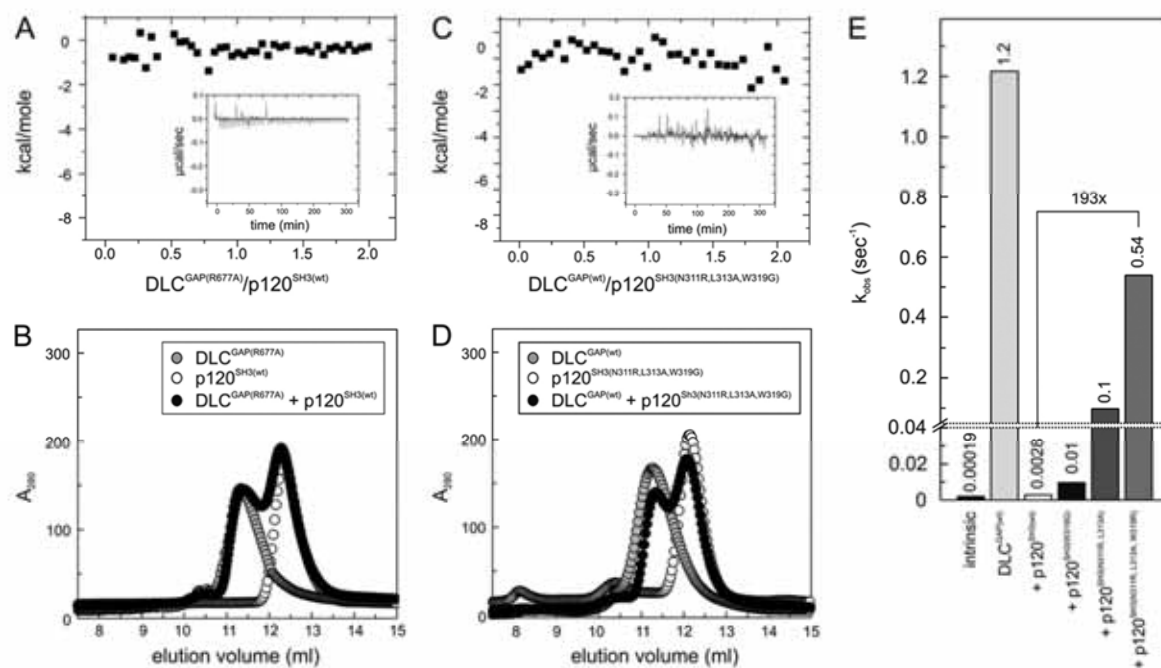


FIGURE 8. Loss of p120-DLC1 interaction by mutational analysis. No interaction was observed between DLC1^{GAP(R677A)} and p120^{SH3(WT)} (A and B) and DLC1^{GAP(WT)} and p120^{SH3(N311R,L313A,W319G)} (C and D). Loss of interaction and of inhibition was measured by ITC (A and C) and aSEC (B and D) as compared with the p120^{SH3(WT)}-DLC1^{GAP(WT)} interaction shown in Fig. 6. E, the activity of DLC1^{GAP} (25 μ M) in stimulating tamraGTP hydrolysis of Cdc42 (0.2 μ M) was measured in the presence of p120^{SH3} variants (125 μ M), respectively. For convenience, the k_{obs} values are given above the bar charts.

cytosolic sequestration (22) are good examples for the regulation of DLC1 function.

Functional characterization and structural elucidation of the *trans*-inhibitory mechanism of DLC1 mediated by the Ras-specific GAP p120 protein (11) was the central theme of this study. Our data clearly revealed that the GAP activity of not only DLC1 but also that of DLC2 and DLC3 was almost completely abolished in the presence of the SH3 domain of p120 (Fig. 4). We showed that larger fragments of p120, such as p120^{SH2-3-2} and the almost full-length p120 ^{Δ n128}, inhibit the DLC GAP function but strikingly not to the same extent as seen for the isolated SH3 domain (Fig. 4D). These data indicate that only a freely accessible and exposed SH3 domain of p120, most probably following an upstream signal and in a defined subcellular environment (11, 37), is able to potently inhibit DLC proteins. One of the p120 binding partners is p190, which has been proposed to induce a conformational change in p120 by binding to its SH2 domains and exposing the adjacent SH3 domain for additional protein interactions with additional proteins (47), one of which is most likely DLC1.

Several studies have shown that DLC1 is able to inactivate Cdc42 and the Rho isoforms (RhoA, RhoB, and RhoC) but not Rac1 *in vitro* (20, 71–73). DLC1^{GAP} activity toward other members of the Rho family has not yet been published. Our preliminary data showed that the DLC proteins are active *in vitro* on almost all members of the Rho family that are able to hydrolyze GTP.⁶

⁶ M. Jaiswal, E. Amin, and R. Dvorsky, unpublished data.

Chan *et al.* (74) have shown an increased level of RhoA-GTP in DLC2-null mice but not in samples from control mice. Consistently, the overexpression of DLC isoforms has been shown to lead to inactivation of RhoA and to the reduction of actin stress fiber formation (75, 76), suggesting that DLC proteins are Rho-selective GAPs and the role of the DLC *trans*-inhibitory protein p120 is to retain Rho proteins in their active GTP-bound states. Contrary to DLC proteins, p120 binding is part of the p190 activation process that controls inactivation of Rho-type proteins (45, 47, 77). A prerequisite for this interaction is phosphorylation of p190 at tyrosine 1105, which is a target of the p120 SH2 domains (77). In this regard, p120 oppositely controls the activities of two different Rho/Rho effector systems; one is left activated, and the other is switched off.

SH3 domain-containing cellular signaling proteins mediate interactions via specific proline-containing peptides. The SH3 domain of p120 has been discussed recently to interact with other proteins in a PXXP motif-independent manner (48). *In silico* analysis revealed that the GAP domain of DLC1 does not possess a proline-rich region and therefore, unlike classical PXXP motif-recognizing SH3 domains, the interaction mode of the p120 SH3 domain is atypical and utilizes different amino acids to bind and mask the catalytic arginine finger of the GAP domain of DLC1. The Ser/Thr kinases Aurora A and Aurora B are other examples in addition to DLC1 for negative modulation of biological processes by p120 (78). The SH3 domain of p120 binds to the catalytic domain of Aurora kinases that inhibits their kinase activity. These interactions also do not involve a

p120RasGAP Competitively Inhibits DLC RhoGAP

proline-rich consensus sequence. Two accessible hydrophobic regions of p120 SH3 have been suggested to function as binding sites for protein interaction (79). Our study supports this notion as we have shown that mutation of three amino acids close to one of these proposed binding sites indeed diminished the DLC1^{GAP} binding and inhibiting ability of p120 SH3.

We demonstrated that the interaction between p120^{SH3} and DLC1^{GAP} displays at least three remarkable characteristics, namely high affinity, high selectivity, and a non-canonical binding mode. The high affinity interaction of 0.6 μM is striking because the binding constants of SH3 domains for proline-rich motifs in their target proteins are mostly in the micromolar range (48, 59). The very few examples of high affinity binding of SH3 domains are those between Mona/Gads and SLP-76 (80), C3G and c-Crk (51), and Grb2 and Wrch1 (48).

CONCLUSION

Mechanistic and structural insights into selectivity, activity, and regulation of DLC1 presented in this study shed light on the role of the multifunctional, regulatory signaling molecule p120RasGAP. It is evident that p120 acts in addition to its RasGAP domain, which is required to switch off Ras signal transduction, as an "effector" conversely controlling, via its SH2 domains and a non-canonical SH3 domain, the RhoGAP activities of the DLC and p190 proteins and hence Rho signal transduction. Interestingly, p120 interacts, in addition to DLC1 and p190, with a third RhoGAP, called p200RhoGAP. In contrast to p190 and DLC1, which are downstream of p120, p200RhoGAP has been proposed to bind to the p120 SH3 domain via its very C-terminal proline-rich region and to sequester its RasGAP function from inactivating Ras (10). These examples nicely illustrate the interdependence of the Ras and Rho signaling pathways and underline the multifunctional and multifaceted nature of regulatory proteins beyond their critical GAP functions.

Acknowledgments—We thank Linda van Aelst, Katrin Rittinger, Olivier Dorseui, Gerard Gacon, Alan Hall, Tony Pawson, and Jeffrey Sletteman for sharing reagents with us that proved indispensable for the work.

REFERENCES

- Aznar, S., and Lacal, J. C. (2001) Searching new targets for anticancer drug design: the families of Ras and Rho GTPases and their effectors. *Prog. Nucleic Acid Res. Mol. Biol.* **67**, 193–234
- Fritz, G., Just, I., and Kaina, B. (1999) Rho GTPases are over-expressed in human tumors. *Int. J. Cancer* **81**, 682–687
- Pruitt, K., and Der, C. J. (2001) Ras and Rho regulation of the cell cycle and oncogenesis. *Cancer Lett.* **171**, 1–10
- Zondag, G. C., Evers, E. E., ten Klooster, J. P., Janssen, L., van der Kammen, R. A., and Collard, J. G. (2000) Oncogenic Ras downregulates Rac activity, which leads to increased Rho activity and epithelial-mesenchymal transition. *J. Cell Biol.* **149**, 775–782
- Sahai, E., and Marshall, C. J. (2002) RHO-GTPases and cancer. *Nat. Rev. Cancer* **2**, 133–142
- Khosravi-Far, R., Campbell, S., Rossman, K. L., and Der, C. J. (1998) Increasing complexity of Ras signal transduction: involvement of Rho family proteins. *Adv. Cancer Res.* **72**, 57–107
- Coleman, M. L., Marshall, C. J., and Olson, M. F. (2004) RAS and RHO GTPases in G1-phase cell-cycle regulation. *Nat. Rev. Mol. Cell Biol.* **5**, 355–366
- Karnoub, A. E., and Weinberg, R. A. (2008) Ras oncogenes: split personalities. *Nat. Rev. Mol. Cell Biol.* **9**, 517–531
- Asnaghi, L., Vass, W. C., Quadri, R., Day, P. M., Qian, X., Braverman, R., Papageorge, A. G., and Lowy, D. R. (2010) E-cadherin negatively regulates neoplastic growth in non-small cell lung cancer: role of Rho GTPases. *Oncogene* **29**, 2760–2771
- Shang, X., Moon, S. Y., and Zheng, Y. (2007) p200 RhoGAP promotes cell proliferation by mediating cross-talk between Ras and Rho signaling pathways. *J. Biol. Chem.* **282**, 8801–8811
- Yang, X. Y., Guan, M., Vigil, D., Der, C. J., Lowy, D. R., and Popescu, N. C. (2009) p120Ras-GAP binds the DLC1 Rho-GAP tumor suppressor protein and inhibits its RhoA GTPase and growth-suppressing activities. *Oncogene* **28**, 1401–1409
- Scheffzek, K., and Ahmadian, M. R. (2005) GTPase activating proteins: structural and functional insights 18 years after discovery. *Cell. Mol. Life Sci.* **62**, 3014–3038
- Ligeti, E., Welti, S., and Scheffzek, K. (2012) Inhibition and termination of physiological responses by GTPase activating proteins. *Physiol. Rev.* **92**, 237–272
- Scheffzek, K., Ahmadian, M. R., and Wittinghofer, A. (1998) GTPase-activating proteins: helping hands to complement an active site. *Trends Biochem. Sci.* **23**, 257–262
- Yuan, B. Z., Miller, M. J., Keck, C. L., Zimonjic, D. B., Thorgerisson, S. S., and Popescu, N. C. (1998) Cloning, characterization, and chromosomal localization of a gene frequently deleted in human liver cancer (DLC-1) homologous to rat RhoGAP. *Cancer Res.* **58**, 2196–2199
- Durkin, M. E., Yuan, B. Z., Zhou, X., Zimonjic, D. B., Lowy, D. R., Thorgerisson, S. S., and Popescu, N. C. (2007) DLC-1: a Rho GTPase-activating protein and tumour suppressor. *J. Cell. Mol. Med.* **11**, 1185–1207
- Liao, Y. C., and Lo, S. H. (2008) Deleted in liver cancer-1 (DLC-1): a tumor suppressor not just for liver. *Int. J. Biochem. Cell Biol.* **40**, 843–847
- Zimonjic, D. B., and Popescu, N. C. (2012) Role of DLC1 tumor suppressor gene and MYC oncogene in pathogenesis of human hepatocellular carcinoma: potential prospects for combined targeted therapeutics (review). *Int. J. Oncol.* **41**, 393–406
- Holeiter, G., Heering, J., Erlmann, P., Schmid, S., Jähne, R., and Olayioye, M. A. (2008) Deleted in liver cancer 1 controls cell migration through a Dia1-dependent signaling pathway. *Cancer Res.* **68**, 8743–8751
- Kim, T. Y., Healy, K. D., Der, C. J., Sciak, N., Bang, Y. J., and Juliano, R. L. (2008) Effects of structure of Rho GTPase-activating protein DLC-1 on cell morphology and migration. *J. Biol. Chem.* **283**, 32762–32770
- Kim, T. Y., Vigil, D., Der, C. J., and Juliano, R. L. (2009) Role of DLC-1, a tumor suppressor protein with RhoGAP activity, in regulation of the cytoskeleton and cell motility. *Cancer Metastasis Rev.* **28**, 77–83
- Scholz, R. P., Regner, J., Theil, A., Erlmann, P., Holeiter, G., Jähne, R., Schmid, S., Hausser, A., and Olayioye, M. A. (2009) DLC1 interacts with 14-3-3 proteins to inhibit RhoGAP activity and block nucleocytoplasmic shuttling. *J. Cell Sci.* **122**, 92–102
- Lukasik, D., Wilczek, E., Wasutynski, A., and Gornicka, B. (2011) Deleted in liver cancer protein family in human malignancies (review). *Oncol. Lett.* **2**, 763–768
- Yam, J. W., Ko, F. C., Chan, C. Y., Jin, D. Y., and Ng, I. O. (2006) Interaction of deleted in liver cancer 1 with tensin2 in caveolae and implications in tumor suppression. *Cancer Res.* **66**, 8367–8372
- Liao, Y. C., Si, L., deVere White, R. W., and Lo, S. H. (2007) The phosphotyrosine-independent interaction of DLC-1 and the SH2 domain of cten regulates focal adhesion localization and growth suppression activity of DLC-1. *J. Cell Biol.* **176**, 43–49
- Qian, X., Li, G., Asmussen, H. K., Asnaghi, L., Vass, W. C., Braverman, R., Yamada, K. M., Popescu, N. C., Papageorge, A. G., and Lowy, D. R. (2007) Oncogenic inhibition by a deleted in liver cancer gene requires cooperation between tensin binding and Rho-specific GTPase-activating protein activities. *Proc. Natl. Acad. Sci. U.S.A.* **104**, 9012–9017
- Chan, L. K., Ko, F. C., Ng, I. O., and Yam, J. W. (2009) Deleted in liver cancer 1 (DLC1) utilizes a novel binding site for Tensin2 PTB domain interaction and is required for tumor-suppressive function. *PLoS One* **4**, e5572

p120RasGAP Competitively Inhibits DLC RhoGAP

28. Tripathi, V., Popescu, N. C., and Zimonjic, D. B. (2013) DLC1 induces expression of E-cadherin in prostate cancer cells through Rho pathway and suppresses invasion. *Oncogene* **4**, 1–10
29. Li, G., Du, X., Vass, W. C., Papageorge, A. G., Lowy, D. R., and Qian, X. (2011) Full activity of the deleted in liver cancer 1 (DLC1) tumor suppressor depends on an LD-like motif that binds talin and focal adhesion kinase (FAK). *Proc. Natl. Acad. Sci. U.S.A.* **108**, 17129–17134
30. Erlmann, P., Schmid, S., Horenkamp, F. A., Geyer, M., Pomorski, T. G., and Olayioye, M. A. (2009) DLC1 activation requires lipid interaction through a polybasic region preceding the RhoGAP domain. *Mol. Biol. Cell* **20**, 4400–4411
31. Fauchereau, F., Herbrand, U., Chafey, P., Eberth, A., Koulakoff, A., Vinet, M. C., Ahmadian, M. R., Chelly, J., and Billuart, P. (2003) The RhoGAP activity of OPHN1, a new F-actin-binding protein, is negatively controlled by its amino-terminal domain. *Mol. Cell. Neurosci.* **23**, 574–586
32. Eberth, A., and Ahmadian, M. R. (2009) *In vitro* GEF and GAP assays. *Curr. Protoc. Cell Biol.* **Chapter 14**, Unit 14.19
33. Colón-González, F., Leskow, F. C., and Kazanietz, M. G. (2008) Identification of an autoinhibitory mechanism that restricts C1 domain-mediated activation of the Rac-GAP α 2-chimaerin. *J. Biol. Chem.* **283**, 35247–35257
34. Jian, X., Brown, P., Schuck, P., Gruschus, J. M., Balbo, A., Hinshaw, J. E., and Randazzo, P. A. (2009) Autoinhibition of Arf GTPase-activating protein activity by the BAR domain in ASAP1. *J. Biol. Chem.* **284**, 1652–1663
35. Zhou, Y. T., Chew, L. L., Lin, S. C., and Low, B. C. (2010) The BNIP-2 and Cdc42GAP homology (BCH) domain of p50RhoGAP/Cdc42GAP sequesters RhoA from inactivation by the adjacent GTPase-activating protein domain. *Mol. Biol. Cell* **21**, 3232–3246
36. Moskwa, P., Paclét, M. H., Dagher, M. C., and Ligeti, E. (2005) Autoinhibition of p50 Rho GTPase-activating protein (GAP) is released by prenylated small GTPases. *J. Biol. Chem.* **280**, 6716–6720
37. Pamonsinlatham, P., Hadj-Slimane, R., Lepelletier, Y., Allain, B., Toccafondi, M., Garbay, C., and Raynaud, F. (2009) p120-Ras GTPase activating protein (RasGAP): a multi-interacting protein in downstream signaling. *Biochimie* **91**, 320–328
38. Ahmadian, M. R., Hoffmann, U., Goody, R. S., and Wittinghofer, A. (1997) Individual rate constants for the interaction of Ras proteins with GTPase-activating proteins determined by fluorescence spectroscopy. *Biochemistry* **36**, 4535–4541
39. Ahmadian, M. R., Stege, P., Scheffzek, K., and Wittinghofer, A. (1997) Confirmation of the arginine-finger hypothesis for the GAP-stimulated GTP-hydrolysis reaction of Ras. *Nat. Struct. Biol.* **4**, 686–689
40. Scheffzek, K., Ahmadian, M. R., Kabsch, W., Wiesmüller, L., Lautwein, A., Schmitz, F., and Wittinghofer, A. (1997) The Ras-RasGAP complex: structural basis for GTPase activation and its loss in oncogenic Ras mutants. *Science* **277**, 333–338
41. Leblanc, V., Tocque, B., and Delumeau, I. (1998) Ras-GAP controls Rho-mediated cytoskeletal reorganization through its SH3 domain. *Mol. Cell. Biol.* **18**, 5567–5578
42. Chan, P. C., and Chen, H. C. (2012) p120RasGAP-mediated activation of c-Src is critical for oncogenic Ras to induce tumor invasion. *Cancer Res.* **72**, 2405–2415
43. Clark, G. J., and Der, C. J. (1995) Aberrant function of the Ras signal transduction pathway in human breast cancer. *Breast Cancer Res. Treat.* **35**, 133–144
44. Clark, G. J., Westwick, J. K., and Der, C. J. (1997) p120 GAP modulates Ras activation of Jun kinases and transformation. *J. Biol. Chem.* **272**, 1677–1681
45. Herbrand, U., and Ahmadian, M. R. (2006) p190-RhoGAP as an integral component of the Tiam1/Rac1-induced downregulation of Rho. *Biol. Chem.* **387**, 311–317
46. Wang, Z., Tung, P. S., and Moran, M. F. (1996) Association of p120 ras GAP with endocytic components and colocalization with epidermal growth factor (EGF) receptor in response to EGF stimulation. *Cell Growth Differ.* **7**, 123–133
47. Hu, K. Q., and Settleman, J. (1997) Tandem SH2 binding sites mediate the RasGAP-RhoGAP interaction: a conformational mechanism for SH3 domain regulation. *EMBO J.* **16**, 473–483
48. Risse, S. L., Vaz, B., Burton, M. F., Aspenström, P., Piekorz, R. P., Brunsvel, L., and Ahmadian, M. R. (2013) SH3-mediated targeting of Wrch1/RhoU by multiple adaptor proteins. *Biol. Chem.* **394**, 421–432
49. Jaiswal, M., Dubey, B. N., Koessmeier, K. T., Gremer, L., and Ahmadian, M. R. (2012) Biochemical assays to characterize Rho GTPases. *Methods Mol. Biol.* **827**, 37–58
50. Eberth, A., Lundmark, R., Gremer, L., Dvorsky, R., Koessmeier, K. T., McMahon, H. T., and Ahmadian, M. R. (2009) A BAR domain-mediated autoinhibitory mechanism for RhoGAPs of the GRAF family. *Biochem. J.* **417**, 371–377
51. Wu, X., Knudsen, B., Feller, S. M., Zheng, J., Sali, A., Cowburn, D., Hanafusa, H., and Kuriyan, J. (1995) Structural basis for the specific interaction of lysine-containing proline-rich peptides with the N-terminal SH3 domain of c-Crk. *Structure* **3**, 215–226
52. Eberth, A., Dvorsky, R., Becker, C. F., Beste, A., Goody, R. S., and Ahmadian, M. R. (2005) Monitoring the real-time kinetics of the hydrolysis reaction of guanine nucleotide-binding proteins. *Biol. Chem.* **386**, 1105–1114
53. Ross, B., Kristensen, O., Favre, D., Walicki, J., Kastrop, J. S., Widmann, C., and Gajhede, M. (2007) High resolution crystal structures of the p120 RasGAP SH3 domain. *Biochem. Biophys. Res. Commun.* **353**, 463–468
54. Schneidman-Duhovny, D., Inbar, Y., Nussinov, R., and Wolfson, H. J. (2005) PatchDock and SymmDock: servers for rigid and symmetric docking. *Nucleic Acids Res.* **33**, W363–W367
55. Brooks, B. R., Brooks, C. L., 3rd, Mackerell, A. D., Jr., Nilsson, L., Petrella, R. J., Roux, B., Won, Y., Archontis, G., Bartels, C., Boresch, S., Cafisch, A., Caves, L., Cui, Q., Dinner, A. R., Feig, M., Fischer, S., Gao, J., Hodoseck, M., Im, W., Kuczera, K., Lazaridis, T., Ma, J., Ovchinnikov, V., Paci, E., Pastor, R. W., Post, C. B., Pu, J. Z., Schaefer, M., Tidor, B., Venable, R. M., Woodcock, H. L., Wu, X., Yang, W., York, D. M., and Karplus, M. (2009) CHARMM: the biomolecular simulation program. *J. Comput. Chem.* **30**, 1545–1614
56. Scouras, A. D., and Daggett, V. (2011) The DYNAMO rotamer library: amino acid side chain conformations and dynamics from comprehensive molecular dynamics simulations in water. *Protein Sci.* **20**, 341–352
57. Eccleston, J. F., Moore, K. J., Morgan, L., Skinner, R. H., and Lowe, P. N. (1993) Kinetics of interaction between normal and proline 12 Ras and the GTPase-activating proteins, p120-GAP and neurofibromin. The significance of the intrinsic GTPase rate in determining the transforming ability of ras. *J. Biol. Chem.* **268**, 27012–27019
58. Morrison, J. F. (1969) Kinetics of the reversible inhibition of enzyme-catalysed reactions by tight-binding inhibitors. *Biochim. Biophys. Acta* **185**, 269–286
59. Kärkkäinen, S., Hiipakka, M., Wang, J. H., Kleino, I., Vähä-Jaakkola, M., Renkema, G. H., Liss, M., Wagner, R., and Saksela, K. (2006) Identification of preferred protein interactions by phage-display of the human Src homology-3 proteome. *EMBO Rep.* **7**, 186–191
60. Rittinger, K., Walker, P. A., Eccleston, J. F., Smerdon, S. J., and Gamblin, S. J. (1997) Structure at 1.65 Å of RhoA and its GTPase-activating protein in complex with a transition-state analogue. *Nature* **389**, 758–762
61. Dvorsky, R., and Ahmadian, M. R. (2004) Always look on the bright site of Rho: structural implications for a conserved intermolecular interface. *EMBO Rep.* **5**, 1130–1136
62. Moon, S. Y., and Zheng, Y. (2003) Rho GTPase-activating proteins in cell regulation. *Trends Cell Biol.* **13**, 13–22
63. Tcherkezian, J., and Lamarche-Vane, N. (2007) Current knowledge of the large RhoGAP family of proteins. *Biol. Cell* **99**, 67–86
64. Rossman, K. L., Der, C. J., and Sondek, J. (2005) GEF means go: turning on RHO GTPases with guanine nucleotide-exchange factors. *Nat. Rev. Mol. Cell Biol.* **6**, 167–180
65. Aittaleb, M., Boguth, C. A., and Tesmer, J. J. (2010) Structure and function of heterotrimeric G protein-regulated Rho guanine nucleotide exchange factors. *Mol. Pharmacol.* **77**, 111–125
66. DiNitto, J. P., Lee, M. T., Malaby, A. W., and Lambright, D. G. (2010) Specificity and membrane partitioning of Grsp1 signaling complexes with Grp1 family Arf exchange factors. *Biochemistry* **49**, 6083–6092
67. Gureasko, J., Kuchment, O., Makino, D. L., Sondermann, H., Bar-Sagi, D., and Kuriyan, J. (2010) Role of the histone domain in the autoinhibition and activation of the Ras activator Son of Sevenless. *Proc. Natl. Acad. Sci.*

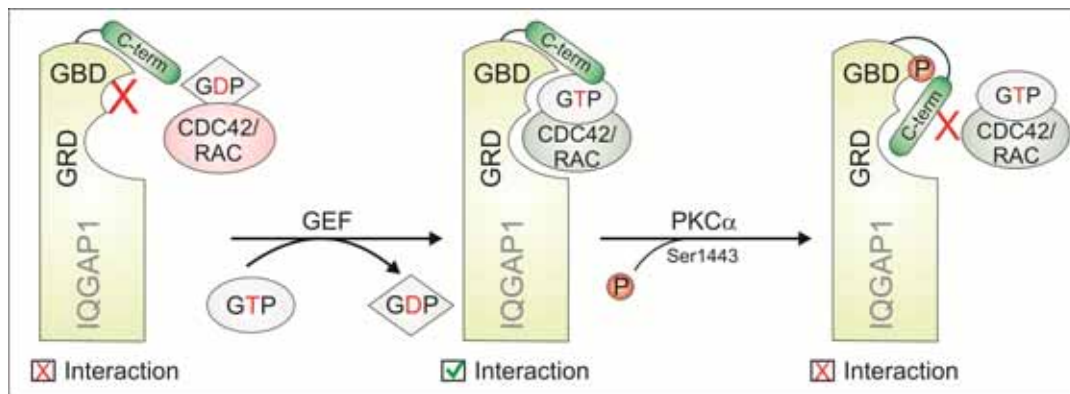
p120RasGAP Competitively Inhibits DLC RhoGAP

- U.S.A.* **107**, 3430–3435
68. Jaiswal, M., Gremer, L., Dvorsky, R., Haeusler, L. C., Cirstea, I. C., Uhlenbrock, K., and Ahmadian, M. R. (2011) Mechanistic insights into specificity, activity, and regulatory elements of the regulator of G-protein signaling (RGS)-containing Rho-specific guanine nucleotide exchange factors (GEFs) p115, PDZ-RhoGEF (PRG), and leukemia-associated RhoGEF (LARG). *J. Biol. Chem.* **286**, 18202–18212
 69. Mitin, N., Betts, L., Yohe, M. E., Der, C. J., Sondek, J., and Rossman, K. L. (2007) Release of autoinhibition of ASEF by APC leads to CDC42 activation and tumor suppression. *Nat. Struct. Mol. Biol.* **14**, 814–823
 70. Scholz, R. P., Gustafsson, J. O., Hoffmann, P., Jaiswal, M., Ahmadian, M. R., Eisler, S. A., Erlmann, P., Schmid, S., Hausser, A., and Olayioye, M. A. (2011) The tumor suppressor protein DLC1 is regulated by PKD-mediated GAP domain phosphorylation. *Exp. Cell Res.* **317**, 496–503
 71. Ching, Y. P., Wong, C. M., Chan, S. F., Leung, T. H., Ng, D. C., Jin, D. Y., and Ng, I. O. (2003) Deleted in liver cancer (DLC) 2 encodes a RhoGAP protein with growth suppressor function and is underexpressed in hepatocellular carcinoma. *J. Biol. Chem.* **278**, 10824–10830
 72. Wong, C. M., Lee, J. M., Ching, Y. P., Jin, D. Y., and Ng, I. O. (2003) Genetic and epigenetic alterations of DLC-1 gene in hepatocellular carcinoma. *Cancer Res.* **63**, 7646–7651
 73. Healy, K. D., Hodgson, L., Kim, T. Y., Shutes, A., Maddileti, S., Juliano, R. L., Hahn, K. M., Harden, T. K., Bang, Y. J., and Der, C. J. (2008) DLC-1 suppresses non-small cell lung cancer growth and invasion by RhoGAP-dependent and independent mechanisms. *Mol. Carcinog.* **47**, 326–337
 74. Chan, F. K., Chung, S. S., Ng, I. O., and Chung, S. K. (2012) The RhoA GTPase-activating protein DLC2 modulates RhoA activity and hyperalgesia to noxious thermal and inflammatory stimuli. *Neurosignals* **20**, 112–126
 75. Leung, T. H., Ching, Y. P., Yam, J. W., Wong, C. M., Yau, T. O., Jin, D. Y., and Ng, I. O. (2005) Deleted in liver cancer 2 (DLC2) suppresses cell transformation by means of inhibition of RhoA activity. *Proc. Natl. Acad. Sci. U.S.A.* **102**, 15207–15212
 76. Kawai, K., Kiyota, M., Seike, J., Deki, Y., and Yagisawa, H. (2007) START-GAP3/DLC3 is a GAP for RhoA and Cdc42 and is localized in focal adhesions regulating cell morphology. *Biochem. Biophys. Res. Commun.* **364**, 783–789
 77. Roof, R. W., Haskell, M. D., Dukes, B. D., Sherman, N., Kinter, M., and Parsons, S. J. (1998) Phosphotyrosine (p-Tyr)-dependent and -independent mechanisms of p190 RhoGAP-p120 RasGAP interaction: Tyr 1105 of p190, a substrate for c-Src, is the sole p-Tyr mediator of complex formation. *Mol. Cell. Biol.* **18**, 7052–7063
 78. Gigoux, V., L'Hoste, S., Raynaud, F., Camonis, J., and Garbay, C. (2002) Identification of Aurora kinases as RasGAP Src homology 3 domain-binding proteins. *J. Biol. Chem.* **277**, 23742–23746
 79. Yang, Y. S., Garbay, C., Duchesne, M., Cornille, F., Jullian, N., Fromage, N., Tocque, B., and Roques, B. P. (1994) Solution structure of GAP SH3 domain by ¹H NMR and spatial arrangement of essential Ras signaling-involved sequence. *EMBO J.* **13**, 1270–1279
 80. Harkiolaki, M., Lewitzky, M., Gilbert, R. J., Jones, E. Y., Bourette, R. P., Mouchiroud, G., Sondermann, H., Moarefi, I., and Feller, S. M. (2003) Structural basis for SH3 domain-mediated high-affinity binding between Mona/Gads and SLP-76. *EMBO J.* **22**, 2571–2582

Chapter VI

IQGAP1 interaction with RHO family proteins revisited: kinetic and equilibrium evidence for two distinct binding sites

Graphical Abstract



Published in:

Manuscript in preparation

Impact factor:

-

Own Proportion to this work:

15%

Analysis of IQGAPs/RAC1 and CDC42 in HSCs
with qPCR and Western blotting
Writing the manuscript

IQGAP1 interaction with RHO family proteins revisited: kinetic and equilibrium evidence for two distinct binding sites*

Kazem Nouri¹, Eyad K. Fansa^{1§}, Ehsan Amin¹, Saeideh Nakhaei-Rad¹, Radovan Dvorsky¹, Lothar Gremer², David J. Timson³, Lutz Schmitt⁴, Dieter Häussinger⁵, and Mohammad R. Ahmadian^{1@}

¹Institute of Biochemistry and Molecular Biology II, Medical faculty of the Heinrich-Heine University, 40225 Düsseldorf, Germany

²Institute of Physical Biology, Heinrich-Heine University, Düsseldorf, Germany

³School of Pharmacy and Biomolecular Sciences, University of Brighton, Huxley Building, Lewes Road, Brighton BN2 4GJ, United Kingdom

⁴Institute of Biochemistry, Heinrich-Heine University, Düsseldorf, Germany

⁵Clinic of Gastroenterology, Hepatology and Infectious Diseases, Medical Faculty of the Heinrich-Heine University, Düsseldorf, Germany

*Running title: New IQGAP binding mode for the RAC-/CDC42-like proteins

[§]Current Address: Structural Biology Group, Max Planck Institute, Dortmund, Germany

[@]To whom correspondence should be addressed: Prof. Dr. Mohammad Reza Ahmadian, Institut für Biochemie und Molekularbiologie II, Medizinische Fakultät der Heinrich-Heine-Universität, Universitätsstr. 1, Gebäude 22.03, 40255 Düsseldorf, Germany, Tel.: #49-211-811 2384, #Fax: 49-211-811 2726, e-mail: reza.ahmadian@uni-duesseldorf.de

Abbreviations: aa, amino acids; A (ala), alanine; CBB, coomassie brilliant blue; CDC42, cell division control protein 42 homolog; CHD, calponine homology domain; D (asp), aspartic acid; E (glu), glutamic acid; FL, full-length; GAP, GTPase-activating protein; GBD, GTPase-binding domain; GDP, guanosine diphosphate; GEF, guanine-nucleotide-exchange factor; GRD, GAP-related domain; GTP, guanosine triphosphate; GTPases, guanosine triphosphatases; H (his), histidine; HCC, hepatocellular carcinoma; HSC, hepatic stellate cell; IQ, protein sequences containing Iso/Leu and Gln residues; IQGAPs, IQ-domain GTPase-activating proteins; kDa, kilo dalton; PAK, p21-activated kinase; PKC, protein kinase C; RAC, RAS-related C3 botulinum toxin substrate; RHO, RAS homolog; S (ser), serine; W (trp), tryptophan; WASP, wiskott-aldrich-syndrome protein; WT, wild type; WW, tryptophan-containing protein domain

ABSTRACT

The scaffolding IQ motif-containing GTPase activating protein 1 (IQGAP1) plays a central role in the physical assembly of relevant signaling networks that are responsible for various cellular processes, including cell adhesion, polarity and transmigration. Amongst various proteins, RAC1 and CDC42, have been also proposed to interact with the GAP-related domain (GRD) of IQGAP1, however, the exact nature of this interaction process has remained obscure. Here, we demonstrate that (i) IQGAP1 associates with six different RAC- and CDC42-related proteins but not with other members of the RHO family, including the RHO-and RND-proteins, and (ii) unlike published models, IQGAP1 interaction with RAC- and CDC42-related proteins underlies a two-step binding mechanism, first a low-affinity, largely nucleotide-independent binding of GRD outside the switch regions, and second a high-affinity, GTP-dependent binding of the RHO GTPase binding domain (GBD) to the switch region. These data were confirmed by phosphomimetic mutations of S1443 in GBD, which resulted in complete abolishment of the IQGAP1 interaction with RAC1 and CDC42, clearly indicating that S1443 phosphorylation by protein kinase C is critical for these interactions. Taken together, these results provide the field with new insights into interaction characteristics of IQGAP1 and highlight the complementary importance of kinetic and equilibrium analyses. Therefore, herein, we challenge the paradigm that the ability of IQGAP1 to interact with RAC/CDC42 proteins is based on a two-step binding process which is a prerequisite for IQGAP1 activation and a critical mechanism in temporal regulation and integration of IQGAP1-mediated cellular responses.

Key words: CDC42, GBD, GRD, stopped-flow, fluorescence, polarization, anisotropy, interaction, IQGAPs, RAC1, RHOA, RHO family

INTRODUCTION

The RHO family proteins are known to play an important role in diverse cellular processes and progression of different diseases, such as cardiovascular diseases, developmental and neurological disorders, tumor invasion and metastasis as well as regulating liver regeneration (Yuan *et al.*, 2009; Fukata *et al.*, 2003; Hall, 2012). RHO proteins share two common functional characteristics, membrane anchorage and an on/off switch cycle (Dvorsky and Ahmadian, 2004). Subcellular localization of RHO proteins to different cellular membranes is known to be critical for their biological activity. This is achieved by a hyper variable region (HVR) (Lam and Hordijk, 2013) and a lipid anchor in their C-terminal tail at a distinct cysteine residue in the CAAX motif (C is cysteine, A is any aliphatic amino acid, and X is any amino acid) (Wennerberg and Der, 2004). RHO protein function is dependent on the guanine nucleotide-binding (G) domain that contains the principle binding center for GDP and GTP and presents depending on its nucleotide-bound state various contact sites for regulators and effectors (Dvorsky and Ahmadian, 2004). Thus, membrane-associated RHO proteins act, with some exceptions (Jaiswal *et al.*, 2013b), as molecular switches by cycling between an inactive GDP-bound state and an active GTP-bound state. This cycle underlies two critical intrinsic functions, the GDP-GTP exchange and GTP hydrolysis (Jaiswal *et al.*, 2013b) and is controlled at least three classes of regulatory proteins (Dvorsky and Ahmadian, 2004): (i) Guanine nucleotide exchange factors (GEFs) catalyze the exchange of GDP to GTP and activate the RHO protein (Jaiswal *et al.*, 2013a; Rossman *et al.*, 2005); (ii) GTPase activating proteins (GAPs) stimulate the GTP hydrolysis and convey the RHO protein in its inactive conformation (Tcherkezian and Lamarche-Vane, 2007; Jaiswal *et al.*, 2014); (iii) Guanine nucleotide dissociation inhibitors (GDIs) bind to prenylated RHO proteins and extract them from the membranes into the cytoplasm (DerMardirossian and Bokoch, 2005; Garcia-Mata *et al.*, 2011; Tnimov *et al.*, 2012; Zhang *et al.*, 2014a). The formation of the active GTP-bound state of RHO proteins is accompanied by a conformational change in two regions, known as switch I and II (Dvorsky and Ahmadian, 2004), which provide a platform for the selective interaction with structurally and functionally diverse effectors, *e.g.* p21-activated kinase 1 (PAK1) (Lei *et al.*, 2000), p67^{phox} a member of the NSDPH oxidase (Lapouge *et al.*, 2000), semaphorin receptor Plexin B1 (Fansa *et al.*, 2013; Hota and Buck, 2012) as well as the IQ motif-containing GTPase activating proteins (IQGAPs) (Watanabe *et al.*, 2015; Hedman *et al.*, 2015).

In mammals, three isoforms of IQGAPs are expressed: IQGAP1, IQGAP2 and IQGAP3. These homologues have similar domain compositions but different subcellular localization, tissue expression and functions (White *et al.*, 2009a; Watanabe *et al.*, 2015). This class of proteins activates a wide variety of downstream signaling cascades (Bishop and Hall, 2000; White *et al.*, 2012; White *et al.*, 2009a; Abel *et al.*, 2015), thereby regulating many important physiological and pathophysiological processes in eukaryotic cells (Heasman and Ridley, 2008a; Watanabe *et al.*, 2015; Smith *et al.*, 2015b). Among IQGAP isoforms, IQGAP1 is ubiquitously expressed and is the most investigated member of IQGAP family, and our understanding mainly relies on the evidences from IQGAP1. IQGAP1 is involved in wide spectrum of cellular processes, such as adhesion, cell polarity and directional migration (White *et al.*, 2012) and also cancer progression (White *et al.*, 2009a; Johnson *et al.*, 2009) *via* binding to RHO protein. The domain organization of IQGAP1 is highly conserved in IQGAP family consisting of an N-terminal calponin homology domain (CHD), a coiled-coil repeat region (CC), a tryptophan-containing proline-rich motif-

binding region (WW), four isoleucine/glutamine-containing motifs (IQ), a RASGAP-related domain (GRD), an originally called RASGAP C-terminal domain (RGTC) (White *et al.*, 2012), which we called a GTPase-binding domain (GBD) in this study, and a C-terminal domain (C).

IQGAP2 and IQGAP3 are also able to bind RHO proteins (McCallum *et al.*, 1996; Brill *et al.*, 1996; Wang *et al.*, 2007; Nojima *et al.*, 2008). IQGAP2 has 62% sequence identity to IQGAP1 and is expressed predominantly in the liver, but can be detected in stomach, prostate, thyroid, testis, kidney, platelets and salivary glands (Watanabe *et al.*, 2015; Brill *et al.*, 1996; Wang *et al.*, 2007; Schmidt *et al.*, 2003; Cupit *et al.*, 2004). IQGAP3 is enriched in brain, testis, lung, small intestine, and colon (Mateer *et al.*, 2003; Wang *et al.*, 2007; Brandt and Grosse, 2007; Smith *et al.*, 2015a; Schmidt *et al.*, 2003; Nojima *et al.*, 2008). Recent differential gene expression analysis revealed a reciprocal expression of IQGAPs in Hepatocellular carcinoma (HCC) and subsequently opposing functions (White *et al.*, 2010a). Given that IQGAP proteins share a domain structure and have sequence homology, such a paradoxical phenomenon may be due to their protein binding partners, subcellular localization and diverse tissue expression.

Furthermore, in hepatic stellate cells (HSCs) has been shown that *Iqgap1* deficiency promotes myofibroblast activation, tumor implantation, and metastatic growth in mice *via* upregulation of paracrine signaling molecules (Liu *et al.*, 2013a). In spite of having RASGAP homology domain, none of these three isoforms have GTPase-activating protein (GAP) activity. GAPs increase the intrinsic activity of RHO proteins and inactivate them. By contrast, IQGAP proteins exhibit an inhibitory effect on the intrinsic GTPase activity of the RHO family members CDC42 and RAC1, thereby stabilize them in their active GTP-bound form (Hart *et al.*, 1996; Ho *et al.*, 1999; Brill *et al.*, 1996). Apart from RAC1 and CDC42, a multitude of IQGAP interacting partners have been reported to date (White *et al.*, 2012; Malarkannan *et al.*, 2012; Liu *et al.*, 2014a; Pathmanathan *et al.*, 2011; Abel *et al.*, 2015; Smith *et al.*, 2015b; Watanabe *et al.*, 2015). From IQGAP family, IQGAP1 has been implicated as a drug target although the molecular mechanism of the IQGAP1 functions is unclear. A prerequisite to achieve these functions is the dissection of its distinct domains and the analysis of their interactions with desired protein partners.

Work from several laboratories has shown that the C-terminal half of IQGAP1 (amino acids 863-1657), encompassing GRD (amino acids 1025-1238) and RGTC (called GBD in this study; amino acids 1451-1583), binds physically to active, GTP-bound forms of CDC42 and RAC1 (McCallum *et al.*, 1996; Zhang *et al.*, 1998; Elliott *et al.*, 2012; Owen *et al.*, 2008). IQGAP1 GRD, which is structurally a homologous but functionally an inactive RASGAP (Kurella *et al.*, 2009), also undergoes interaction with RAC1 and CDC42, although with a lower affinity than the larger protein fragment, containing GRD and RGTC (Owen *et al.*, 2008; Kurella *et al.*, 2009). These works together with homology modeling, based on the RHOGAP in complex with RHOA (Rittinger *et al.*, 1997) and CDC42 (Nassar *et al.*, 1998), and RASGAP in complex with HRAS (Scheffzek *et al.*, 1997), provided a structural model of IQGAP1 GRD that contacts the switch regions of the GTP-bound CDC42 (Mataraza *et al.*, 2003b; Owen *et al.*, 2008; Kurella *et al.*, 2009). In contrast, another study has shown phosphomimetic variants of IQGAP1 at position S1441 and S1443 were significantly impaired in interacting with active CDC42 (Elliott *et al.*, 2012). This strongly indicates that regions downstream of GRD, may also be critical in the interaction with RAC1 and CDC42. In an attempt to resolve this controversy, we set out to investigate comprehensively the structure-function relationship of IQGAP1 interaction with the RHO proteins. Detailed characterization of

the IQGAP1 interaction with the RHO family members, using time-resolved fluorescence spectroscopy, provided unprecedented insights into the structure, function, and mechanistic properties of IQGAP1, especially regarding its interaction with RAC- and CDC42-like proteins. Obtained data showed that GRD-C associated with the RAC- and CDC42-like proteins (RAC1, RAC2, RAC3, RHOG, CDC42, and TC10), but not with RHOA, RHOB, RHOC, RHOD, TCL, RND and RIF. Furthermore, GRD1 and GRD2 do not associate with RAC1 under this experimental condition. We next investigated the effect of the last 99 amino acids of IQGAP1 on RAC1 and CDC42 binding and our results clearly suggest that the very C-terminal region of IQGAP1 may negatively regulate GBD-RAC1/CDC42 interaction. Moreover, we found that point mutations of the PKC α phosphorylation sites (S1441 and S1443) differently affect GRD-GBD association with RAC1/CDC42-mantGppNHp. Additionally, equilibrium measurement using fluorescence polarization experiments showed that IQGAP1GRD2 also interacts with RAC1 and CDC42 but with a much lower affinity and in a largely nucleotide-independent manner as compared with IQGAP1GRD-C. Results described here clearly suggest that IQGAP1 binds RAC1- and CDC42-like proteins at least at two sites by utilizing the GBD domain rather than the GRD domain to contact the switch regions.

MATERIALS AND METHODS

Constructs. Different variants of pGEX vectors (pGEX2T, pGEX4T-1, pGEX3) encoding an N-terminal glutathione S-transferase (GST) fusion protein were used for the overexpression of various human IQGAP1 (Acc. no. P46940) variants (aa 863-1345, 962-1345, and 863-1657, 877-1558, 877-1558 S1443E and S1443A), human Plexin-B1 (Acc. no. O43157) (aa 1724-1903), human p67^{phox} (Acc. no. P19878) (aa 1-203), human PAK1 (Acc. No. Q13153) (aa 57-141), murine TIAM1 DH-PH (Acc. no. Q60610) (aa 1033–1404), human TrioN DH-PH (Acc. no. O75962) (aa 1226–1535), and human RHOGDI α (Acc. no. P52565) as well as human RHO-related genes, i.e. RAC1 (Acc. no. P63000) (aa 1-179), RAC2 (Acc. no. P15153) (aa 1-192), RAC3 (Acc. no. P60763) (aa 1-192), RHOG (Acc. no. P84095) (aa 1-178), RHOA (Acc. no. P61586) (aa 1-181), RHOB (Acc. no. P62745) (aa 1-181), RHOC (Acc. no. P08134) (aa 1-181), CDC42 (Acc. no. P60953) (aa 1-178), TC10 (Acc. no. P17081) (aa 2-193), TCL (Acc. no. Q9H4E5) (aa 2 – 197), RND1 (Acc. no. Q92730) (aa 1-232), RND2 (Acc. no. P52198) (aa 26-184), RND3 (Acc. no. P61587) (aa, 1-244), RIF (Acc. no. Q9HBH0) (aa 1-195), and mouse RHOD (Acc. no. P97348) (aa 2-193). pET46 EkLIC vector (Merck, Nottingham, United Kingdom) was used for the overexpression of IQGAP1 877-1558 S1441E, S1143D, S1441A/S1443A, and S1441E/S1443D mutants as a his tag protein. The Kazusa cDNA clone KIAA0051 (Suyama *et al.*, 1999) was used as a template for making mutants.

Proteins. All proteins were purified according to the protocols described (Fiegen *et al.*, 2002; Hemsath and Ahmadian, 2005; Jaiswal *et al.*, 2013b). Nucleotide-free RHO proteins were prepared using alkaline phosphatase (Roche) and phosphodiesterase (Sigma Aldrich) at 4°C as described (Jaiswal *et al.*, 2012). Fluorescent methylanthraniloyl (mant) was used to generate mantGDP and mantGppNHp bound RHO proteins, where GppNHp is non hydrolyzable analog of GTP. Quality and concentrations of labeled proteins were determined as described (Jaiswal *et al.*, 2012).

Fluorescence measurements. Kinetics measurements were monitored by stopped-flow apparatus (Hi-Tech Scientific SF-61 with a mercury xenon light source and TgK Scientific Kinetic Studio software), and performed as described (Hemsath and Ahmadian, 2005). The observed rate constants were fitted single exponentially using the GraFit program (Erithacus software).

Fluorescence polarization. Experiments were performed in a Fluoromax 4 fluorimeter in polarization mode as described (Nouri *et al.*, 2015). The dissociation constant (K_d) were calculated by fitting the concentration dependent binding curve using a quadratic ligand binding equation.

Cell isolation and culture. Livers from male Wistar rats (local animal facility of the Heinrich Heine University) were enzymatically digested with collagenase H (Roche, Germany) and protease E (Merck, Germany). Primary hepatic stellate cell (HSC) isolation was followed by density gradient centrifugation. HSCs were feeded with Dulbecco's Modified Eagle Medium (DMEM) supplemented with 15% fetal calf serum and 50 units of penicillin/streptomycin (Gibco® Life Technologies).

Reverse transcriptase polymerase chain reaction. To isolated RNA, cells were lysed by QIAzol lysis reagent (QIAGEN, Germany) and proceed with RNeasy plus kit (Qiagen, Germany). To eliminate any possible genomic DNA contaminations, isolated RNAs were subjected to DNase with the DNA-free™ DNA Removal Kit (Ambion, Life Technologies, Germany). Transcription of the RNA to first strand complementary DNA (cDNA) was followed by using the ImProm-II™ reverse transcription system (Promega, Germany). Quantitative polymerase chain reaction (qPCR) was performed using the SYBR Green reagent (Life Technologies, Germany). Primers are listed in Table S1. $2^{-\Delta Ct}$ method was used to calculate the mRNA levels according to relative endogenous levels of the HPRT1.

Immunoblotting. Cell membranes and nuclei were disturbed with lysis buffer (50 mM Tris-HCl pH 7.5, 100 mM NaCl, 2 mM MgCl₂, 1% Igepal CA-630, 10% glycerol, 20 mM beta-glycerolphosphate, 1 mM Ortho-Na₃VO₄, 1 EDTA-free inhibitor tablet). To normalize the amount of the total proteins, the Bradford assay applied to measure the protein concentration (Bio-Rad). Primary antibodies to mouse γ -tubulin (# T5326) Sigma-Aldrich; mouse RAC1 (05-389) millipore; rabbit CDC42 (2462) cell signaling; mouse IQGAP1 (ab56529) and rabbit IQGAP2 (ab181127) abcam were diluted in 5% non-fat milk (Merck, Germany)/TBST (Tris-buffered saline, 0.05% Tween 20), and incubated overnight in 4°C. After washing steps, membranes were incubated with horseradish peroxidase-coupled secondary antibodies for 1 h and signals were visualized by the ECL detection system (GE Healthcare) and images were collected using the ChemoCam Imager ECL (INTAS science imaging, Germany).

RESULTS

IQGAP1^{GRD-C} selectively associates with various RAC- and CDC42-like proteins

Kinetics of IQGAP1^{GRD-C} (IQGAP1⁸⁶³⁻¹⁶⁵⁷; **Fig. 1**) association with different RHO proteins was monitored using stopped-flow fluorescence spectroscopic methods established previously (Hemsath *et al.*, 2005). MantGppNHp (**Fig. 2A**) is a fluorescent, non-hydrolysable GTP analog and stopped-flow fluorescence is a direct way to monitor the association between two proteins in

real-time (Jaiswal *et al.*, 2012). Rapid mixing of GRD-C with active, mantGppNHp bound RAC1 and CDC42 resulted in change in fluorescence (**Figs. 2B and 2F green trace**), which represents the RAC1/CDC42-IQGAP1 association reaction. Under the same conditions, most remarkably, we did not observe any fluorescence change when mixing RAC1/CDC42-mantGppNHp with GRD itself (IQGAP1⁹⁶²⁻¹³⁴⁵) (**Figs. 2B and 2F red trace**). This was unexpected because GRD has been generally accepted as the RAC1- and CDC42-binding domain of IQGAP1 to date (Owen *et al.*, 2008; Kurella *et al.*, 2009; Elliott *et al.*, 2012; Hart *et al.*, 1996; Ho *et al.*, 1999; Kuroda *et al.*, 1998; Mataraza *et al.*, 2003b). Under the same conditions we measured kinetics for other members of the RHO family and evaluated the data by single exponential fitting to obtain the respective observed rate constants (k_{obs}). Data presented in **figure 2B-G** show that GRD-C associated with various RAC- and CDC42-like proteins (RAC1, RAC2, RAC3, RHOG, CDC42 and TC10), but not with RHOA, RHOB, RHOC, RHOD, TCL and RIF. Mixing of mantGppNHp-bound form of the latter did not result in a fluorescence change (**Fig. 2H**). Due to instability, fluorescently labeled RND proteins could not be prepared. Therefore, their association with GRD-C was measured indirectly by premixing excess amounts of GTP-bound RND proteins with GRD-C before measuring its association with RAC1-mantGppNHp. RND1, RND2 and RND3 did not interfere with the RAC1-IQGAP1 interaction (**Fig. 2I**), indicating that IQGAP1 does also not associate with RND proteins under these conditions, while **Figure 2J** shows association competition of mantGppNHp-RAC1 with IQGAP1^{GRD-C} in the presence of excess amount of CDC42, or *vice versa*.

RAC2 showed highest affinity for IQGAP1^{GRD-C}

In some studies was previously shown that the binding affinity of CDC42 for IQGAP1 was considerably higher than that of RAC1 for IQGAP1 (see **Table 1**) (Zhang *et al.*, 1998; McCallum *et al.*, 1996; Zhang *et al.*, 1997). Later Owen *et al.* reported that, IQGAP1 has similar affinities for both RAC1 and CDC42 (see **Table 1**) (Owen *et al.*, 2008). Here individual kinetic parameters were determined for the interaction of IQGAP1^{GRD-C} with RAC- and CDC42-like proteins under conditions described previously (Hemsath and Ahmadian, 2005). An incremental increase in fluorescence was observed when increasing the concentrations of GRD-C were rapidly mixed with RAC1-mantGppNHp (**Fig. 3A**). Increase in fluorescence was also observed for other RAC- and CDC42-like proteins except for CDC42 that the mode of interaction was different and we observed decrease in fluorescence (**Fig. S3**). Association kinetics was then performed for all other RAC- and CDC42-like proteins. k_{obs} values obtained by a single exponential fitting were evaluated in a linear fashion as a function of the GRD-C concentration (**Fig. 3B**), which yielded the respective association rate constants (k_{on}). The dissociation of GRD-C from its complex with RAC1-mantGppNHp was measured in a displacement experiment when excess amounts of RAC1-GppNHp were rapidly mixed with the complex. This led expectedly to fast decrease (for CDC42; increase) in fluorescence (**Figs. S2 and S4**), which was also observed for other RAC- and CDC42-like proteins (data not shown). Exponential fitting of the curves yielded the dissociation rate constants (k_{off}). The dissociation constants (K_d) (**Fig. 3D**, Green bars), which is the binding affinity and defined as the strength of IQGAP-RHO protein interactions was ultimately calculated from the ratio of the k_{off} values (**Fig. 3D**, Orange bars) divided by the k_{on} values (**Fig. 3D**, Blue bars). Accordingly, RAC2 turned out to possess the highest affinity for GRD-C that was between 16- and 75-fold higher than that of the other RHO proteins (**Fig. 4D**, Green bars). All individual data are summarized in **Table 1**.

GBD but not GRD appears to be critical for the IQGAP1 interaction with RAC1 and CDC42

To further prove the critical role of the more C-terminal domains of IQGAP1 beyond GRD we generated various deletion and point mutations of IQGAP1 (**Fig. 1**). **Figures 4A, S1, and S3** clearly show that GRD1 and GRD2 do not associate with RAC1 and CDC42 under this experimental condition. We next measured the effect of the last 99 amino acids of IQGAP1 on RAC1 and CDC42 binding and found that GRD-GBD (IQGAP1⁸⁷⁷⁻¹⁵⁵⁸), which lacks this region associated 3-fold faster with RAC1 as compared to GRD-C. Moreover, we found that point mutations of the PKC α phosphorylation sites (S1441 and S1443; **Fig. 1**) differently affect GRD-GBD association with RAC1-mantGppNHp. In contrast to GRD-GBD^{SE} (Ser1441 substituted by Glu), GRD-GBD^{SD} (Ser1443 substituted by Asp), and the double mutations GRD-GBD SE/SD (phosphomimetic substitutions) and GRD-GBD SA/SA (neutral substitutions to Ala) completely abolished GRD-GBD association with RAC1 and CDC42 (**Fig. 4A**).

As it is shown in **Figures 4B and 4C**, association kinetics were performed for the interaction of GRD-C, GRD-GBD, and GRD-GBD^{SE} with RAC1 and CDC42. k_{obs} values gained by a single exponential fitting were evaluated in a linear fashion as a function of the GRD-C, GRD-GBD, and GRD-GBD^{SE} concentrations, which yielded the respective association rate constants (k_{on}). The k_{on} for all three variants was almost similar and the same pattern was observed for RAC1 and CDC42 (**Figs. 4B and 4C**). The dissociation of all three proteins from their complex with RAC1-/CDC42-mantGppNHp was measured in a displacement experiment in the presence of excess amounts of RAC1- and CDC42-GppNHp mixed with the complex (**Figs. S2 and S4**). Exponential fitting of the curves yielded the dissociation rate constants (k_{off}) (**Figs. 4B and 4C**). The binding affinity (K_d) as the strength of IQGAP1-RAC1/CDC42 interactions was calculated from the ratio of the k_{off} values divided by the k_{on} values. Our results showed 2 folds lower K_d of GRD-GBD^{SE} compared to GRD-GBD in the case of RAC1, and K_d for CDC42 was not significantly changed (**Figs. 4B and C**, Green bars).

IQGAP1 possesses at least two RAC/CDC42-binding domains

To further shed light on the potent interaction of GRD-C versus GRD alone we used a different method, fluorescence polarization, that measures the binding affinity of two proteins and provide an equilibrium dissociation constant (K_d) of their interaction. As shown in figures 5A-5C, both IQGAP1 variants, GRD-C and GRD do in fact interact with mantGppNHp-bound RAC1 and CDC42 but as expected not with RHOA using fluorescence polarization (equilibrium mode). Evaluated K_d values obtained from the measurements showed that GRD-C is a high affinity binder as compared to GRD with 10-15-fold lower affinity for mantGppNHp-bound RAC1 and CDC42 (Fig. 5C; Table 1). This was not observed using Stopped-flow fluorescence, measuring the kinetics of the association in real-time, as is shown in figures 2 and 4A. Furthermore, for GRD-GBD and GRD-GBD^{SE} with mantGppNHp-bound RAC1 comparable affinity to GRD-C was observed but GRD-GBD^{SD} showed 5-8 folds lower affinity (Figs. 5E and 5F; Table 1). The explanation for our observations regarding binding of RAC1 to GRD is simple; in direct mode only a change in fluorescence can be observed when the associating protein (IQGAP1) binds to close vicinity of the fluorophore (mant group of the bound GppNHp) on the surface of RAC1 and CDC42 (Fig. 2). This surface covers the switch regions that changes their conformation upon a GDP/GTP exchange (Dvorsky and Ahmadian, 2004). This is of fundamental importance because binding

effectors (such as IQGAP1) to the switch regions determines the specificity of the signal transduction (Dvorsky and Ahmadian, 2004; Hemsath *et al.*, 2005). To prove this idea we repeated the measurements by using inactive RHO proteins bound to mantGDP. Both GRD-C and GRD were able to interact with CDC42-mantGDP although with very low affinities (Fig. 5G-H). This strongly suggests that IQGAP1 consists of two distinct binding domains, with GBD binding to the switch regions and with GRD that binds to other regions of CDC42 beyond the switch regions in a largely nucleotide-independent manner.

Differential expression analysis of IQGAPs in hepatic stellate cells

Each IQGAP isoform possess its specific binding partners and therefore contribute to different cellular processes. For instance, IQGAP1 is known as an oncogene where IQGAP2 is a tumor suppressor (White *et al.*, 2009a; White *et al.*, 2010a). IQGAP2 is shown to express predominantly in liver. We asked the questions, is there any isoform preference for IQGAPs in the specific liver cell types called hepatic stellate cells and how they could scaffold the RHO proteins in these cells? Hepatic stellate cells (HSCs) reside in the Disse space of the liver and during chronic liver injuries become activated and contribute in either liver repair or fibrosis (Kordes and Häussinger, 2013b; Yin *et al.*, 2013a). It is reported that the IQGAP1 play a role in HSC activation by binding to TGF- β receptor II and suppress HSC activation (Liu *et al.*, 2013a). To investigate the biological function of IQGAP isoforms and their responsive target proteins (RAC and CDC42), freshly isolated HSCs were cultivated for 8 days that induce spontaneous activation of these cells. Quantitative RNA analysis revealed that IQGAP1 and 3 were upregulated during the activation process of HSCs where the IQGAP2 was downregulated. RAC2 exhibits the drastic increased in HSC d8, however, other RAC isoforms (RAC1 and 3) did not altered. To further investigate the correlation between the IQGAP1 regulation of RAC1 and CDC42 mechanisms in HSCs, the protein levels of IQGAP1, 2, RAC1, and CDC42 were detected. Consistent with qPCR data, obtained data showed IQGAP1 increase at proteins levels, where IQGAP2 is downregulated. The RAC1 and CDC42 exist at higher levels in activated HSCs (Fig. 6).

DISCUSSION

The interaction with the active, GTP-bound form of RAC1 and CDC42 identified IQGAP1 as a putative downstream effector (Mataraza *et al.*, 2003b; Hart *et al.*, 1996; Kuroda *et al.*, 1999; Izumi *et al.*, 2004; Watanabe *et al.*, 2004; Kholmanskikh *et al.*, 2006; Brown *et al.*, 2007; Sakurai-Yageta *et al.*, 2008; McCallum *et al.*, 1996; Zhang *et al.*, 1998; Owen *et al.*, 2008; Elliott *et al.*, 2012; Kurella *et al.*, 2009; Noritake *et al.*, 2005). Subsequent studies have shown that the interaction between IQGAP1 and the RHO proteins has significance on variety of biological functions. Accumulating evidence supports diverse roles for IQGAP-RHO protein interaction in vertebrates. However, the nature of such a protein-protein recognition process has remained obscure. While modulation of the cytoskeletal architecture was initially thought to be the primary function of the interaction of IQGAP1 with RHO proteins, it is now clear that they have some critical physiological roles beyond the cytoskeleton. CDC42 promotes the interaction of PTPI with IQGAP1 to stimulate actin remodeling and, eventually, neurite outgrowth (Li *et al.*, 2005), and also complex of active CDC42, Lis1, and CLIP-170 with IQGAP1 seems to be crucial for

cerebellar neuronal motility (Kholmanskikh *et al.*, 2006). Another example is in the pancreatic β -cells. Analysis of the insulin secretory pathway has shown that IQGAP1 scaffolds CDC42, RAB27A, and coronin-3 and this complex controls endocytosis of insulin secretory membranes (Kimura *et al.*, 2013).

Of the RHO family proteins, RAC1, RHOA, and CDC42 have been most extensively studied and characterized (Etienne-Manneville and Hall, 2002). In this study, a comprehensive interaction study of RHO proteins and C-terminal domain of IQGAP1⁸⁶³⁻¹⁶⁵⁷ (here called GRD-C) was conducted. Kinetics of GRD-C association with different RHO proteins was monitored using stopped-flow fluorescence spectroscopic methods (**Fig. 2**). The results clearly indicate that IQGAP1 binds among RHO proteins selectively to RAC- and CDC42-like proteins in the active form and that GRD-C most obviously recognizes and binds to the switch regions but however not, as previously proposed by several groups (Mataraza *et al.*, 2003b; Owen *et al.*, 2008; Kurella *et al.*, 2009), the GRD alone. In contrast to our data, Casteel *et al.* have shown that GRD-C interacts with the active, G14V variant of RHOA and RHOC but not with that of RHOB, which were overexpressed in, and immunoprecipitated from human embryonic kidney 293T cell lysates (Casteel *et al.*, 2012). In addition, recent immunoprecipitation studies have shown that IQGAP1 binds to both RHOA and p190A-RHOGAP to inactivate RHOA, and to modulate contractility of airway smooth muscle cells (Bhattacharya *et al.*, 2014). Wu *et al.* have also found RHOC and IQGAP1 in immunoprecipitates. This study has shown that an isoform-specific interaction of RHO proteins with IQGAP1 regulates cancer cell proliferation, and has been proposed that IQGAP1 is a downstream effector of RHOC in the regulation of gastric cancer cell migration (Wu *et al.*, 2012; Clark *et al.*, 2000). In contrast, our study showed no physical interaction between GRD-C and the RHO isoforms, including RHOA or RHOC, under cell-free conditions using purified proteins. In this context, we think that observed interactions of GRD-C with RHOA and RHOC most likely are indirect, mediated by other proteins co-immunoprecipitated from cells expressing tagged RHO protein. We also exclude an interaction with other regions of RHOA outside switch regions evident from our fluorescence polarization data (**Figs. 5A-5C**).

Another striking observation was an increase in fluorescence upon association of GRD-C with RAC1, RAC2, RAC3, RHOG, and TC10 but a decrease in fluorescence with CDC42 (**Figs. 2, S1 and S3**). In contrast, we have monitored in an earlier study a fluorescence decrease for the association of the CDC42/RAC-interacting binding (CRIB) motif of the Wiskott-Aldrich syndrome protein (WASP) with the CDC42, RAC1 and TC10, respectively (Hemsath *et al.*, 2005). This observation indicates that (i) the binding mode of CDC42 interaction with IQGAP1 is different from that of TC10 and the RAC-like proteins, and (ii) the binding mode of IQGAP1 interaction with these RHO proteins differs from that of WASP. Owen *et al.* have studied GRD-C interaction with a large panel of RAC1 and CDC42 variants and have suggested, despite their 71% identity, RAC1 and CDC42 appear to have only partially overlapping binding sites on IQGAP1, and each uses different determinants to achieve high affinity binding (Owen *et al.*, 2008). However, our competition experiment has shown in **figure 2J** clearly indicated that GRD-C competitively associates with an overlapping binding region of RAC1 and CDC42.

The determination of individual kinetics parameters for the interaction of GRD-C with RAC- and CDC42-like proteins indicates that GRD-C may utilize a homologous set of associating residues of various CDC42-/RAC-like proteins, in spite of differences in the reaction rates (**Fig.**

3D; Table 1). The fact that six members of the RHO family and probably also WRCH1 and Chp/WRCH2 (not analyzed in this study), associate with IQGAP1 raises the question of how an interaction specificity is achieved in cells. RHOG is due to its high sequence similarity with the RAC proteins classified as a RAC-related protein, although it shares with RAC1 overlapping signal transduction pathways (Prieto-Sanchez and Bustelo, 2003). TC10 and RHOG interaction with IQGAP1 and IQGAP2, respectively, has been previously reported (Wennerberg *et al.*, 2002; Neudauer *et al.*, 1998). RHOG has been reported that do not bind to effectors such as PAK1, PAK5, PAK6, PAR6, IRSp53, WASP, or POSH, but on the other hand it binds in an activated GTP bound form to the RAC/CDC42-specific effectors MLK3, PLD1, and IQGAP2 which in turn, stimulates some downstream signaling targets of activated RAC1 and CDC42 such as JNK and Akt (Wennerberg *et al.*, 2002). Although the consequence of TC10-IQGAP1 interaction is not defined, it seems to play a role in exocytosis and cell polarity. EXO70, a component of the exocyst complex, has been shown to bind to the N-terminal IQGAP1, most likely to the WW motif (Prieto-Sanchez and Bustelo, 2003) but probably not to the IQ region because Exo70 was not found as binding partner of this region (Hedman *et al.*, 2015). In mammals, RALA, a member of the RAS family, and TC10 have been shown to bind the exocyst (Inoue *et al.*, 2003). TC10-EXO70 interaction is implicated in the tethering of GLUT4 vesicles to the plasma membrane in response to insulin (Inoue *et al.*, 2003; Inoue *et al.*, 2006; Chiang *et al.*, 2006), and in promoting neurite outgrowth (Pommereit and Wouters, 2007; Dupraz *et al.*, 2009; Fujita *et al.*, 2013). IQGAP proteins has been shown to be involved in both processes (Ory and Gasman, 2011; Wang *et al.*, 2007; Hedman *et al.*, 2015). Data presented in this study, revealed that TC10 has the fastest dissociation rate from GRD-C (**Fig. 3D**), suggesting that the IQGAP-TC10 complex requires stabilization by additional binding proteins, for example EXO70. Investigating the protein interaction network of the IQGAPs, modulating their function in space and time, remains an open and very interesting issue for future studies.

The highest affinity of RAC2 for GRD-C can most likely be attributed to distinct amino acid sequence deviations. The high affinity of RAC2 for IQGAP1 cannot be explained by comparing potential residues that may undergo direct interacting contacts in spite of high amino acid sequence identity of RAC isoforms. An aspect to be considered is the overall dynamics of the protein parts originated from few different amino acids all over the molecule. The lower flexibility of the switch I region of RAC2 in comparison to RAC1 and RAC3 may explain the functional differences of these proteins as it has been previously proposed to contribute to a higher TIAM1 activity on RAC2 compared to RAC1 and RAC3 (Haeusler *et al.*, 2003).

Previous studies by other groups have shown that shorter IQGAP1 fragments, encompassing the GRD domain, are responsible for the RAC1 and CDC42 interactions. For the first time, *Zhang and coworkers* have shown that activated form of CDC42 is able to bound IQGAP1 GRD-C (aa 864-1657) (Zhang *et al.*, 1997). One year later the same group reported that not only CDC42 but also RAC1, although with lower affinity, could interact to GRD-C (Zhang *et al.*, 1998). Afterwards, *Nomanbhoy and Cerione*, have shown that GRD-C interacts tightly to CDC42-mantGTP using fluorescence assay (Nomanbhoy and Cerione, 1999). *Owen et al.* have also reported that a GRD protein (aa 950-1407) was able to tightly bind CDC42(Q61L) with a K_d value of 140 nM but failed to bind RAC1(Q61L) using scintillation proximity assay (Owen *et al.*, 2008). In this study, GRD-C (aa 864-1657) has shown a much higher affinity for the Q61L mutant of not only CDC42 but also

RAC1, and yet the GRD was proposed to be the binding domain of IQGAP1 that associates with the switch regions of CDC42. Correspondingly, Kurella *et al.* have reported that GRD2 (aa 62-1345) binds CDC42 in a GTP-dependent manner with an affinity of 1300 nM using isothermal titration calorimetry (Kurella *et al.*, 2009). These biochemical data (summarized in **Table 1**) along with homology modeling, based on the RAS-RASGAP structure (Scheffzek *et al.*, 1997), provided up to date a structural model of IQGAP1 GRD contacting the switch regions of the CDC42 which is generally accepted (Kurella *et al.*, 2009; Owen *et al.*, 2008; Elliott *et al.*, 2012; Hart *et al.*, 1996; Ho *et al.*, 1999; Kuroda *et al.*, 1998; Mataraza *et al.*, 2003b). Contrary to the existing model, we observed a low-affinity, largely nucleotide-independent binding of GRD that associates with RAC- and CDC42-like proteins outside the switch regions. This was evidenced by kinetic measurements of GRD-GBD and GRD-C association, but not GDR, with RAC1 and CDC42 proteins (**Figs. 2 and 4**; no changes in fluorescence were observed with GRD). Conducted equilibrium measurements using fluorescence polarization not only substantiated the essential role of IQGAP1 GBD in a GTP-dependent interaction with RAC1 and CDC42 in support with our kinetic analysis but also provided striking insights into the main feature of IQGAP1 GRD. Our quantitative analysis under equilibrium conditions clearly revealed that GRD indeed undergoes a low-affinity, largely nucleotide-independent interaction with CDC42 and also RAC1 but in contrast to GBD its binding site resides outside the critical switch regions (**Fig. 5**). The significance of GBD (previously called RGTC) as a GTP-dependent interacting domain for RAC- and CDC42-like proteins was proved using single point mutants of GRD-GBD (e.g. Ser1443 substituted by Asp and Ala but not Ser1441 to Glu and Ala, two PKC α phosphorylation sites), which led to the abolishment of a GTP-dependent interaction of GRD-GBD while nucleotide-independent association through the GRD was unchanged. Grohmanova and coworkers previously have shown *via* GST pull down experiments and using MCF10A cell lysate, that in the presence of phosphatase inhibitor there is a significant reduction in the interaction between IQGAP1 and CDC42-GTP bound in contrast to CDC42 nucleotide depleted which bound to phosphorylated IQGAP1 much stronger (Grohmanova *et al.*, 2004). In addition, our data have clearly demonstrated that the region upstream of GRD2 (aa 863-961) is dispensable for the RAC1 and CDC42 interaction. Another interesting issue was the inhibitory effect of the very C-terminal 99 amino acids (C domain) on the GBD determined through a 3-fold faster association of GRD-GBD (lacking the C domain) with RAC1 and CDC42 as compared to GRD-C. This is consistent with observations regarding the interaction of GRD and GBD-C domains with each other, favoring GTP-dependent binding to CDC42 (Grohmanova *et al.*, 2004; Le Clainche *et al.*, 2007).

Upon HSCs activation, quiescent HSCs develop into the cells that are able to contract and migrate. It is reported that IQGAP1 plays a role in HSC activation by binding to TGF- β receptor II and suppress HSC activation (Liu *et al.*, 2013a). These observations raised the questions, which IQGAP isoforms are present in HSCs and is there any evidence that IQGAPs actively scaffolds RHO proteins in HSCs? To address these questions, first we investigated the expression pattern of IQGAP1, 2, 3, RAC1, 2, 3, and CDC42 in quiescent vs. activated HSCs. Our quantitative RNA analysis revealed that *IQGAP1* and *3* isoforms get upregulated during the activation process of HSCs while *IQGAP2* is down-regulated. At protein levels, we were able to detect IQGAP2 isoform only in quiescent HSCs while IQGAP1 was presented in both states of HSCs, and became upregulated during HSC activation. These results are in consistent with what Schmidt and

colleagues, have reported regarding the reciprocal expression of IQGAP1 and 2 in human hepatocellular carcinomas, where IQGAP1 increased and IQGAP2 decreased (White *et al.*, 2010b). In quiescent HSCs, we speculate that IQGAP2 exerts its specific functions by scaffolding the distinct signaling components in different protein complexes than IQGAP1. Canonical Wnt signaling is very dynamic in quiescent HSCs and it is shown in other cells that IQGAP2 can interact with Dishevelled/ β -catenin, therefore in qHSCs IQGAP2 may modulate Wnt- β -catenin signaling and stimulate GFAP synthesis and cell-cycle arrest (Kordes *et al.*, 2008b; Schmidt *et al.*, 2008). Another possibility would be, IQGAP2 competes with other scaffolding proteins to recruits RHO proteins and may interfere with RHO-dependent cell migration. The functions and specific binding partners of IQGAP2 in qHSCs remain to be investigated. aHSCs display the elevated levels of PDGF signaling and focal adhesion kinase (FAK), acts downstream of PDGF (Carlioni *et al.*, 2000). PDGF induces the IQGAP1-dependent complex formation of focal adhesion proteins (paxillin and vinculin) and PDGF receptor β (Kohno *et al.*, 2013). IQGAP1 also binds to FAK (Cheung *et al.*, 2013), therefore, PDGF-IQGAP1 may regulate the focal adhesion assembly in aHSCs that is important for cell motility and migration.

Elevated levels of the RAC1 and CDC42 correlate with high amount of IQGAP1 in activated HSCs; we detected higher levels of RAC1, RAC2 and CDC42 in aHSCs than qHSCs. On the other hand, our biochemical studies demonstrated that RAC1 and CDC42 interact in GTP-bound forms with IQGAP1. Therefore, we suggest that IQGAP1 scaffolds RAC1 and CDC42 to regulate cell-adhesion and migration in these cells. However, the role of IQGAP1 in aHSCs needs to be investigated.

Taken together, our kinetic and equilibrium measurements clearly challenge the paradigm that the ability of IQGAP1 to interact with RAC/CDC42 proteins is mainly attributed to its GRD. On the contrary, we propose that the C-terminal half of IQGAP1 utilize at least three functionally distinct units, including GRD, GBD and C, to achieve the interaction with RAC1- and CDC42-like proteins. Keeping this in mind, the switch regions of the RHO family proteins have been previously proposed as the first binding site for the downstream effectors and if this first contact is achieved then additional contacts outside the switch regions will be required to guarantee effector activation (Dvorsky and Ahmadian, 2004). Remarkably, IQGAP1 seems to employ a different strategy to interact with RAC1 and CDC42 proteins as schematically illustrated in **Figure 7**: (i) GRD undergoes a low-affinity, GDP-/GTP-independent complex with RAC1 and CDC42 proteins outside their switch regions in a way that is independent of the upstream signals, providing it is structurally accessible and available for interactions; (ii) GBD only binds to the RAC1 and CDC42 proteins if they are active and exist in the GTP-bound forms; (iii) the C-terminal region of IQGAP1 may potentiate the IQGAP1 interaction with RAC1 and CDC42 proteins by probably extending the resident time of the respective proteins complexes. Such a sequential association with the RAC1 and CDC42 proteins most likely leads to activation of IQGAP1, can be envisaged as conformational changes allowing further IQGAP1 interaction with its downstream targets depending on both the cell types and the upstream signals. We further propose that this is a conserved control mechanism also for IQGAP2 and probably also IQGAP3 due to high sequence homology.

CONFLICT OF INTEREST

The authors declare no conflict of interest.

ACKNOWLEDGEMENTS

This work was supported in part by the German Research Foundation (Deutsche Forschungsgemeinschaft or DFG) through both the Collaborative Research Center 974 (SFB 974) “Communication and Systems Relevance during Liver Injury and Regeneration” and the International Research Training Group 1902 (IRTG 1902) “Intra- and interorgan communication of the cardiovascular system”, and by the International Graduate School of Protein Science and Technology (iGRASP), and the Research committee of the Medical Faculty of the Heinrich-Heine University Düsseldorf (Grant Number 9772617).

REFERENCES

1. Yuan H, Zhang H, Wu X, Zhang Z, Du D, et al. (2009) Hepatocyte-specific deletion of Cdc42 results in delayed liver regeneration after partial hepatectomy in mice. *Hepatology* 49: 240-249.
2. Fukata M, Nakagawa M, Kaibuchi K (2003) Roles of Rho-family GTPases in cell polarisation and directional migration. *Curr Opin Cell Biol* 15: 590-597.
3. Hall A (2012) Rho family GTPases. *Biochem Soc Trans* 40: 1378-1382.
4. Dvorsky R, Ahmadian MR (2004) Always look on the bright side of Rho: structural implications for a conserved intermolecular interface. *EMBO Rep* 5: 1130-1136.
5. Lam BD, Hordijk PL (2013) The Rac1 hypervariable region in targeting and signaling: a tail of many stories. *Small GTPases* 4: 78-89.
6. Wennerberg K, Der CJ (2004) Rho-family GTPases: it's not only Rac and Rho (and I like it). *J Cell Sci* 117: 1301-1312.
7. Jaiswal M, Fansa EK, Dvorsky R, Ahmadian MR (2013) New insight into the molecular switch mechanism of human Rho family proteins: shifting a paradigm. *Biol Chem* 394: 89-95.
8. Jaiswal M, Dvorsky R, Ahmadian MR (2013) Deciphering the molecular and functional basis of Dbl family proteins: a novel systematic approach toward classification of selective activation of the Rho family proteins. *J Biol Chem* 288: 4486-4500.
9. Rossman KL, Der CJ, Sondek J (2005) GEF means go: turning on RHO GTPases with guanine nucleotide-exchange factors. *Nature reviews Molecular cell biology* 6: 167-180.
10. Tcherkezian J, Lamarche-Vane N (2007) Current knowledge of the large RhoGAP family of proteins. *Biology of the Cell* 99: 67-86.
11. Jaiswal M, Dvorsky R, Amin E, Risse SL, Fansa EK, et al. (2014) Functional cross-talk between ras and rho pathways: a Ras-specific GTPase-activating protein (p120RasGAP) competitively inhibits the RhoGAP activity of deleted in liver cancer (DLC) tumor suppressor by masking the catalytic arginine finger. *J Biol Chem* 289: 6839-6849.
12. DerMardirossian C, Bokoch GM (2005) GDIs: central regulatory molecules in Rho GTPase activation. *Trends Cell Biol* 15: 356-363.
13. Garcia-Mata R, Boulter E, Burridge K (2011) The 'invisible hand': regulation of RHO GTPases by RHOGDIs. *Nature reviews Molecular cell biology* 12: 493-504.
14. Tnimov Z, Guo Z, Gambin Y, Nguyen UT, Wu YW, et al. (2012) Quantitative analysis of prenylated RhoA interaction with its chaperone, RhoGDI. *J Biol Chem* 287: 26549-26562.
15. Zhang SC, Gremer L, Heise H, Janning P, Shymanets A, et al. (2014) Liposome Reconstitution and Modulation of Recombinant Prenylated Human Rac1 by GEFs, GDI1 and Pak1. *PLoS ONE* 9: e102425.
16. Lei M, Lu W, Meng W, Parrini MC, Eck MJ, et al. (2000) Structure of PAK1 in an autoinhibited conformation reveals a multistage activation switch. *Cell* 102: 387-397.
17. Lapouge K, Smith SJ, Walker PA, Gamblin SJ, Smerdon SJ, et al. (2000) Structure of the TPR domain of p67phox in complex with Rac.GTP. *Mol Cell* 6: 899-907.
18. Fansa EK, Dvorsky R, Zhang SC, Fiegen D, Ahmadian MR (2013) Interaction characteristics of Plexin-B1 with Rho family proteins. *Biochem Biophys Res Commun* 434: 785-790.
19. Hota PK, Buck M (2012) Plexin structures are coming: opportunities for multilevel investigations of semaphorin guidance receptors, their cell signaling mechanisms, and functions. *Cell Mol Life Sci* 69: 3765-3805.
20. Watanabe T, Wang S, Kaibuchi K (2015) IQGAPs as Key Regulators of Actin-cytoskeleton Dynamics. *Cell Struct Funct* 40: 69-77.
21. Hedman AC, Smith JM, Sacks DB (2015) The biology of IQGAP proteins: beyond the cytoskeleton. *EMBO reports* 16: 427-446.
22. White CD, Brown MD, Sacks DB (2009) IQGAPs in cancer: a family of scaffold proteins underlying tumorigenesis. *FEBS Lett* 583: 1817-1824.
23. Bishop AL, Hall A (2000) Rho GTPases and their effector proteins. *Biochem J* 348 Pt 2: 241-255.
24. White CD, Erdemir HH, Sacks DB (2012) IQGAP1 and its binding proteins control diverse biological functions. *Cell Signal* 24: 826-834.
25. Abel AM, Schuldt KM, Rajasekaran K, Hwang D, Riese MJ, et al. (2015) IQGAP1: insights into the function of a molecular puppeteer. *Mol Immunol* 65: 336-349.

26. Heasman SJ, Ridley AJ (2008) Mammalian Rho GTPases: new insights into their functions from in vivo studies. *Nature reviews Molecular cell biology* 9: 690-701.
27. Smith JM, Hedman AC, Sacks DB (2015) IQGAPs choreograph cellular signaling from the membrane to the nucleus. *Trends Cell Biol* 25: 171-184.
28. Johnson M, Sharma M, Henderson BR (2009) IQGAP1 regulation and roles in cancer. *Cell Signal* 21: 1471-1478.
29. McCallum SJ, Wu WJ, Cerione RA (1996) Identification of a putative effector for Cdc42Hs with high sequence similarity to the RasGAP-related protein IQGAP1 and a Cdc42Hs binding partner with similarity to IQGAP2. *J Biol Chem* 271: 21732-21737.
30. Brill S, Li S, Lyman CW, Church DM, Wasmuth JJ, et al. (1996) The Ras GTPase-activating-protein-related human protein IQGAP2 harbors a potential actin binding domain and interacts with calmodulin and Rho family GTPases. *Mol Cell Biol* 16: 4869-4878.
31. Wang S, Watanabe T, Noritake J, Fukata M, Yoshimura T, et al. (2007) IQGAP3, a novel effector of Rac1 and Cdc42, regulates neurite outgrowth. *J Cell Sci* 120: 567-577.
32. Nojima H, Adachi M, Matsui T, Okawa K, Tsukita S (2008) IQGAP3 regulates cell proliferation through the Ras/ERK signalling cascade. *Nat Cell Biol* 10: 971-978.
33. Schmidt VA, Scudder L, Devoe CE, Bernards A, Cupit LD, et al. (2003) IQGAP2 functions as a GTP-dependent effector protein in thrombin-induced platelet cytoskeletal reorganization. *Blood* 101: 3021-3028.
34. Cupit LD, Schmidt VA, Miller F, Bahou WF (2004) Distinct PAR/IQGAP expression patterns during murine development: implications for thrombin-associated cytoskeletal reorganization. *Mamm Genome* 15: 618-629.
35. Mateer SC, Wang N, Bloom GS (2003) IQGAPs: integrators of the cytoskeleton, cell adhesion machinery, and signaling networks. *Cell Motil Cytoskeleton* 55: 147-155.
36. Brandt DT, Grosse R (2007) Get to grips: steering local actin dynamics with IQGAPs. *EMBO Rep* 8: 1019-1023.
37. Smith JM, Hedman AC, Sacks DB (2015) IQGAPs choreograph cellular signaling from the membrane to the nucleus. *Trends Cell Biol*.
38. White CD, Khurana H, Gnatenko DV, Li Z, Odze RD, et al. (2010) IQGAP1 and IQGAP2 are reciprocally altered in hepatocellular carcinoma. *BMC Gastroenterol* 10: 125.
39. Liu C, Billadeau DD, Abdelhakim H, Leof E, Kaibuchi K, et al. (2013) IQGAP1 suppresses TbetaRII-mediated myofibroblastic activation and metastatic growth in liver. *J Clin Invest* 123: 1138-1156.
40. Hart MJ, Callow MG, Souza B, Polakis P (1996) IQGAP1, a calmodulin-binding protein with a rasGAP-related domain, is a potential effector for cdc42Hs. *Embo J* 15: 2997-3005.
41. Ho YD, Joyal JL, Li Z, Sacks DB (1999) IQGAP1 integrates Ca²⁺/calmodulin and Cdc42 signaling. *J Biol Chem* 274: 464-470.
42. Malarkannan S, Awasthi A, Rajasekaran K, Kumar P, Schuldt KM, et al. (2012) IQGAP1: a regulator of intracellular spacetime relativity. *J Immunol* 188: 2057-2063.
43. Liu J, Guidry JJ, Worthylake DK (2014) Conserved sequence repeats of IQGAP1 mediate binding to Ezrin. *J Proteome Res* 13: 1156-1166.
44. Pathmanathan S, Hamilton E, Atcheson E, Timson DJ (2011) The interaction of IQGAPs with calmodulin-like proteins. *Biochem Soc Trans* 39: 694-699.
45. Zhang B, Chernoff J, Zheng Y (1998) Interaction of Rac1 with GTPase-activating proteins and putative effectors. A comparison with Cdc42 and RhoA. *J Biol Chem* 273: 8776-8782.
46. Elliott SF, Allen G, Timson DJ (2012) Biochemical analysis of the interactions of IQGAP1 C-terminal domain with CDC42. *World J Biol Chem* 3: 53-60.
47. Owen D, Campbell LJ, Littlefield K, Evetts KA, Li Z, et al. (2008) The IQGAP1-Rac1 and IQGAP1-Cdc42 interactions: interfaces differ between the complexes. *J Biol Chem* 283: 1692-1704.
48. Kurella VB, Richard JM, Parke CL, Lecour LF, Jr., Bellamy HD, et al. (2009) Crystal structure of the GTPase-activating protein-related domain from IQGAP1. *J Biol Chem* 284: 14857-14865.
49. Rittinger K, Walker PA, Eccleston JF, Nurmahomed K, Owen D, et al. (1997) Crystal structure of a small G protein in complex with the GTPase-activating protein rhoGAP. *Nature* 388: 693-697.
50. Nassar N, Hoffman GR, Manor D, Clardy JC, Cerione RA (1998) Structures of Cdc42 bound to the active and catalytically compromised forms of Cdc42GAP. *Nat Struct Biol* 5: 1047-1052.

51. Scheffzek K, Ahmadian MR, Kabsch W, Wiesmuller L, Lautwein A, et al. (1997) The Ras-RasGAP complex: structural basis for GTPase activation and its loss in oncogenic Ras mutants. *Science* 277: 333-338.
52. Mataraza JM, Briggs MW, Li Z, Frank R, Sacks DB (2003) Identification and characterization of the Cdc42-binding site of IQGAP1. *Biochem Biophys Res Commun* 305: 315-321.
53. Suyama M, Nagase T, Ohara O (1999) HUGE: a database for human large proteins identified by Kazusa cDNA sequencing project. *Nucleic Acids Res* 27: 338-339.
54. Fiegen D, Blumenstein L, Stege P, Vetter IR, Ahmadian MR (2002) Crystal structure of Rnd3/RhoE: functional implications. *FEBS letters* 525: 100-104.
55. Hemsath L, Ahmadian MR (2005) Fluorescence approaches for monitoring interactions of Rho GTPases with nucleotides, regulators, and effectors. *Methods* 37: 173-182.
56. Jaiswal M, Dubey BN, Koessmeier KT, Gremer L, Ahmadian MR (2012) Biochemical assays to characterize Rho GTPases. *Methods in molecular biology* 827: 37-58.
57. Nouri K, J. MM, Milroy LG, Hain A, Dvorsky R, et al. (2015) Biophysical Characterization of Nucleophosmin Interactions with Human Immunodeficiency Virus Rev and Herpes Simplex Virus US11. *PLoS ONE*.
58. Hemsath L, Dvorsky R, Fiegen D, Carlier MF, Ahmadian MR (2005) An electrostatic steering mechanism of Cdc42 recognition by Wiskott-Aldrich syndrome proteins. *Mol Cell* 20: 313-324.
59. Kuroda S, Fukata M, Nakagawa M, Fujii K, Nakamura T, et al. (1998) Role of IQGAP1, a target of the small GTPases Cdc42 and Rac1, in regulation of E-cadherin-mediated cell-cell adhesion. *Science* 281: 832-835.
60. Zhang B, Wang ZX, Zheng Y (1997) Characterization of the interactions between the small GTPase Cdc42 and its GTPase-activating proteins and putative effectors. Comparison of kinetic properties of Cdc42 binding to the Cdc42-interactive domains. *J Biol Chem* 272: 21999-22007.
61. Kordes C, Häussinger D (2013) Hepatic stem cell niches. *Journal of Clinical Investigation* 123: 1874-1880.
62. Yin C, Evason KJ, Asahina K, Stainier DYS (2013) Hepatic stellate cells in liver development, regeneration, and cancer. *Journal of Clinical Investigation* 123: 1902-1910.
63. Kuroda S, Fukata M, Nakagawa M, Kaibuchi K (1999) Cdc42, Rac1, and their effector IQGAP1 as molecular switches for cadherin-mediated cell-cell adhesion. *Biochem Biophys Res Commun* 262: 1-6.
64. Izumi G, Sakisaka T, Baba T, Tanaka S, Morimoto K, et al. (2004) Endocytosis of E-cadherin regulated by Rac and Cdc42 small G proteins through IQGAP1 and actin filaments. *J Cell Biol* 166: 237-248.
65. Watanabe T, Wang S, Noritake J, Sato K, Fukata M, et al. (2004) Interaction with IQGAP1 links APC to Rac1, Cdc42, and actin filaments during cell polarization and migration. *Dev Cell* 7: 871-883.
66. Kholmanskikh SS, Koeller HB, Wynshaw-Boris A, Gomez T, Letourneau PC, et al. (2006) Calcium-dependent interaction of Lis1 with IQGAP1 and Cdc42 promotes neuronal motility. *Nat Neurosci* 9: 50-57.
67. Brown MD, Bry L, Li Z, Sacks DB (2007) IQGAP1 regulates Salmonella invasion through interactions with actin, Rac1, and Cdc42. *J Biol Chem* 282: 30265-30272.
68. Sakurai-Yageta M, Recchi C, Le Dez G, Sibarita JB, Daviet L, et al. (2008) The interaction of IQGAP1 with the exocyst complex is required for tumor cell invasion downstream of Cdc42 and RhoA. *J Cell Biol* 181: 985-998.
69. Noritake J, Watanabe T, Sato K, Wang S, Kaibuchi K (2005) IQGAP1: a key regulator of adhesion and migration. *J Cell Sci* 118: 2085-2092.
70. Li Z, McNulty DE, Marler KJ, Lim L, Hall C, et al. (2005) IQGAP1 promotes neurite outgrowth in a phosphorylation-dependent manner. *J Biol Chem* 280: 13871-13878.
71. Kimura T, Yamaoka M, Taniguchi S, Okamoto M, Takei M, et al. (2013) Activated Cdc42-bound IQGAP1 determines the cellular endocytic site. *Mol Cell Biol* 33: 4834-4843.
72. Etienne-Manneville S, Hall A (2002) Rho GTPases in cell biology. *Nature* 420: 629-635.
73. Casteel DE, Turner S, Schwappacher R, Rangaswami H, Su-Yuo J, et al. (2012) Rho isoform-specific interaction with IQGAP1 promotes breast cancer cell proliferation and migration. *The Journal of biological chemistry* 287: 38367-38378.
74. Bhattacharya M, Sundaram A, Kudo M, Farmer J, Ganesan P, et al. (2014) IQGAP1-dependent scaffold suppresses RhoA and inhibits airway smooth muscle contraction. *J Clin Invest* 124: 4895-4898.

75. Wu Y, Tao Y, Chen Y, Xu W (2012) RhoC regulates the proliferation of gastric cancer cells through interaction with IQGAP1. *PLoS ONE* 7: 7.
76. Clark EA, Golub TR, Lander ES, Hynes RO (2000) Genomic analysis of metastasis reveals an essential role for RhoC. *Nature* 406: 532-535.
77. Prieto-Sanchez RM, Bustelo XR (2003) Structural basis for the signaling specificity of RhoG and Rac1 GTPases. *J Biol Chem* 278: 37916-37925.
78. Wennerberg K, Ellerbroek SM, Liu RY, Karnoub AE, Burridge K, et al. (2002) RhoG signals in parallel with Rac1 and Cdc42. *J Biol Chem* 277: 47810-47817.
79. Neudauer CL, Joberty G, Tatsis N, Macara IG (1998) Distinct cellular effects and interactions of the Rho-family GTPase TC10. *Curr Biol* 8: 1151-1160.
80. Inoue M, Chang L, Hwang J, Chiang SH, Saltiel AR (2003) The exocyst complex is required for targeting of Glut4 to the plasma membrane by insulin. *Nature* 422: 629-633.
81. Inoue M, Chiang SH, Chang L, Chen XW, Saltiel AR (2006) Compartmentalization of the exocyst complex in lipid rafts controls Glut4 vesicle tethering. *Mol Biol Cell* 17: 2303-2311.
82. Chiang SH, Chang L, Saltiel AR (2006) TC10 and insulin-stimulated glucose transport. *Methods Enzymol* 406: 701-714.
83. Pommereit D, Wouters FS (2007) An NGF-induced Exo70-TC10 complex locally antagonises Cdc42-mediated activation of N-WASP to modulate neurite outgrowth. *J Cell Sci* 120: 2694-2705.
84. Dupraz S, Grassi D, Bernis ME, Sosa L, Bisbal M, et al. (2009) The TC10-Exo70 complex is essential for membrane expansion and axonal specification in developing neurons. *J Neurosci* 29: 13292-13301.
85. Fujita A, Koinuma S, Yasuda S, Nagai H, Kamiguchi H, et al. (2013) GTP hydrolysis of TC10 promotes neurite outgrowth through exocytic fusion of Rab11- and L1-containing vesicles by releasing exocyst component Exo70. *PLoS ONE* 8.
86. Ory S, Gasman S (2011) Rho GTPases and exocytosis: what are the molecular links? *Semin Cell Dev Biol* 22: 27-32.
87. Haeusler LC, Blumenstein L, Stege P, Dvorsky R, Ahmadian MR (2003) Comparative functional analysis of the Rac GTPases. *FEBS letters* 555: 556-560.
88. Nomanbhoy T, Cerione RA (1999) Fluorescence assays of Cdc42 interactions with target/effector proteins. *Biochemistry* 38: 15878-15884.
89. Grohmanova K, Schlaepfer D, Hess D, Gutierrez P, Beck M, et al. (2004) Phosphorylation of IQGAP1 modulates its binding to Cdc42, revealing a new type of rho-GTPase regulator. *J Biol Chem* 279: 48495-48504.
90. Le Clainche C, Schlaepfer D, Ferrari A, Klingauf M, Grohmanova K, et al. (2007) IQGAP1 stimulates actin assembly through the N-WASP-Arp2/3 pathway. *J Biol Chem* 282: 426-435.
91. White CD, Khurana H, Gnatenko DV, Li Z, Odze RD, et al. (2010) IQGAP1 and IQGAP2 are Reciprocally Altered in Hepatocellular Carcinoma. *BMC Gastroenterology* 10: 125.
92. Kordes C, Sawitza I, Häussinger D (2008) Canonical Wnt signaling maintains the quiescent stage of hepatic stellate cells. *Biochemical and Biophysical Research Communications* 367: 116-123.
93. Schmidt VA, Chiariello CS, Capilla E, Miller F, Bahou WF (2008) Development of hepatocellular carcinoma in *Iqgap2*-deficient mice is IQGAP1 dependent. *Mol Cell Biol* 28: 1489-1502.
94. Carloni V, Pinzani M, Giusti S, Romanelli RG, Parola M, et al. (2000) Tyrosine phosphorylation of focal adhesion kinase by PDGF is dependent on ras in human hepatic stellate cells. *Hepatology* 31: 131-140.
95. Kohno T, Urao N, Ashino T, Sudhakar V, Inomata H, et al. (2013) IQGAP1 links PDGF receptor-beta signal to focal adhesions involved in vascular smooth muscle cell migration: role in neointimal formation after vascular injury. *Am J Physiol Cell Physiol* 305: C591-600.
96. Cheung KL, Lee JH, Shu L, Kim JH, Sacks DB, et al. (2013) The Ras GTPase-activating-like protein IQGAP1 mediates Nrf2 protein activation via the mitogen-activated protein kinase/extracellular signal-regulated kinase (ERK) kinase (MEK)-ERK pathway. *J Biol Chem* 288: 22378-22386.

The RHO family proteins are known to play an important role in diverse cellular processes and

Table 1. Data summary for the interaction of RHO proteins with IQGAP variants

Proteins ^a	K _d (nM) ^{b1}	Method ^c	Reference
IQGAP1 ⁸⁶³⁻¹³⁴⁵ /RAC1-mantGppNHp	no binding	FM	this study
IQGAP1 ⁸⁶³⁻¹³⁴⁵ /CDC42-mantGppNHp	no binding	FM	this study
IQGAP1 ⁹⁶²⁻¹³⁴⁵ /RAC1-mantGppNHp	no binding	FM	this study
IQGAP1 ⁹⁶²⁻¹³⁴⁵ /CDC42-mantGppNHp	no binding	FM	this study
IQGAP1 ⁸⁶³⁻¹⁶⁵⁷ /RAC1-mantGppNHp	1,420	FM	this study
IQGAP1 ⁸⁶³⁻¹⁶⁵⁷ /CDC42-mantGppNHp	2,000	FM	this study
IQGAP1 ⁸⁶³⁻¹⁶⁵⁷ /RAC2-mantGppNHp	27	FM	this study
IQGAP1 ⁸⁶³⁻¹⁶⁵⁷ /RAC3-mantGppNHp	450	FM	this study
IQGAP1 ⁸⁶³⁻¹⁶⁵⁷ /RHOA-mantGppNHp	490	FM	this study
IQGAP1 ⁸⁶³⁻¹⁶⁵⁷ /TC10-mantGppNHp	1,530	FM	this study
IQGAP1 ⁸⁷⁷⁻¹⁵⁵⁸ /RAC1-mantGppNHp	4,110	FM	this study
IQGAP1 ⁸⁷⁷⁻¹⁵⁵⁸ /CDC42-mantGppNHp	4,200	FM	this study
IQGAP1 ^{877-1558(S1441E)} /RAC1-mantGppNHp	9,960	FM	this study
IQGAP1 ^{877-1558(S1441E)} /CDC42-mantGppNHp	6,060	FM	this study
IQGAP1 ^{877-1558(S1443D)} /RAC1-mantGppNHp	no binding	FM	this study
IQGAP1 ^{877-1558(S1443D)} /CDC42-mantGppNHp	no binding	FM	this study
IQGAP1 ^{877-1558(SS/AA)} /RAC1-mantGppNHp	no binding	FM	this study
IQGAP1 ^{877-1558(SS/AA)} /CDC42-mantGppNHp	no binding	FM	this study
IQGAP1 ^{877-1558(SS/ED)} /RAC1-mantGppNHp	no binding	FM	this study
IQGAP1 ^{877-1558(SS/ED)} /CDC42-mantGppNHp	no binding	FM	this study
IQGAP1 ⁸⁷⁷⁻¹⁵⁵⁸ /CDC42-GTP	1,300	SPR	(Elliott <i>et al.</i> , 2012)
IQGAP1 ^{877-1558(S1441E)} /CDC42-GTP	220,000	SPR	(Elliott <i>et al.</i> , 2012)
Proteins ^a	eK _d (nM) ^{b2}	Method ^c	Reference
IQGAP ⁹⁶²⁻¹³⁴⁵ /RAC1-mantGppNHp	8,145	FP	this study
IQGAP ⁹⁶²⁻¹³⁴⁵ /CDC42-mantGDP	184,700	FP	this study
IQGAP ⁸⁶³⁻¹⁶⁵⁷ /RAC1-mantGppNHp	5,530	FP	this study
IQGAP ⁸⁶³⁻¹⁶⁵⁷ /CDC42-mantGDP	95,100	FP	this study
IQGAP ⁹⁶²⁻¹³⁴⁵ /CDC42-mantGppNHp	30,200	FP	this study
IQGAP ⁸⁶³⁻¹⁶⁵⁷ /CDC42-mantGppNHp	3,400	FP	this study
IQGAP ⁹⁶²⁻¹³⁴⁵ /RHOA-mantGppNHp	no binding	FP	this study
IQGAP ⁸⁶³⁻¹⁶⁵⁷ /RHOA-mantGppNHp	no binding	FP	this study
IQGAP1 ⁸⁷⁷⁻¹⁵⁵⁸ /RAC1-mantGppNHp	4,570	FP	this study
IQGAP1 ^{877-1558(S1441E)} /RAC1-mantGppNHp	6,680	FP	this study
IQGAP1 ^{877-1558(S1443D)} /RAC1-mantGppNHp	288,300	FP	this study
IQGAP1 ⁸⁶⁴⁻¹⁶⁵⁷ /CDC42-mantdGTP	28	FA	(Nomanbhoy and Cerione, 1999)
IQGAP1 ⁸⁶⁴⁻¹⁶⁵⁷ /RAC1 ^{Q61L} -[³ H]GTP	18	SPA	(Owen <i>et al.</i> , 2008)
IQGAP1 ⁹⁵⁰⁻¹⁴⁰⁷ /RAC1 ^{Q61L} -[³ H]GTP	no binding	SPA	(Owen <i>et al.</i> , 2008)
IQGAP1 ⁸⁶⁴⁻¹⁶⁵⁷ /CDC42 ^{Q61L} -[³ H]GTP	24	SPA	(Owen <i>et al.</i> , 2008)
IQGAP1 ⁹⁵⁰⁻¹⁴⁰⁷ /CDC42 ^{Q61L} -[³ H]GTP	140	SPA	(Owen <i>et al.</i> , 2008)
IQGAP1 ⁹⁶²⁻¹³⁴⁵ /CDC42-GTP	1,300	ITC	(Kurella <i>et al.</i> , 2009)
IQGAP1 ⁹⁶²⁻¹³⁴⁵ /CDC42-GDP	no binding	ITC	(Kurella <i>et al.</i> , 2009)

Proteins ^a	K_i (nM) ^{b3}	Method ^c	Reference 2009)
IQGAP1 ⁸⁶⁴⁻¹⁶⁵⁷ /CDC42-GTP	82	PRA	(Zhang <i>et al.</i> , 1997)
IQGAP1 ⁸⁶⁴⁻¹⁶⁵⁷ /CDC42-GTP	390	PRA	(Zhang <i>et al.</i> , 1998)
IQGAP1 ⁸⁶⁴⁻¹⁶⁵⁷ /RAC1-GTP	2,130	PRA	(Zhang <i>et al.</i> , 1998)

^aIQGAP1 proteins; ^bthe binding affinity of the IQGAP proteins for various RHO proteins has been analyze in different ways: ^{b1}under kinetic condition that provides the individual association and dissociation rate constant (k_{on} and k_{off}) and determines the dissociation constants (K_d) or ^{b2}under equilibrium conditions by determining the equilibrium dissociation constants (eK_d) or ^{b3}under competitive reaction conditions, for example inhibition the intrinsic GTP-hydrolysis reaction the RHO proteins that determines the equilibrium inhibition constant (K_i); ^c FM, fluorescence measurement by stopped flow, FA, fluorescence assay; FP, fluorescence polarization; ITC, isothermal titration calorimetry; PRA, Phosphate-release assay; SPA, scintillation proximity assay; SPR, surface plasmon resonance.

FIGURE LEGENDS

Figure 1. Schematic representation of domain organization and various constructs and proteins of IQGAP1. (A) Domain organization (color coded) along with the PKC α phosphorylation sites and constructs relevant to this project. (B) Coomassie brilliant blue (CBB) stained SDS-PAGE of purified IQGAP1 used in this study.

Figure 2. GRD-C selectively associates with various RAC- and CDC42-like proteins. (A) Chemical structure of mantGppNHp, a fluorescently labelled, non-hydrolyzable GTP analog. (B-H) Association of GRD-C (2 μ M) with mantGppNHp-bound RHO proteins (0.2 μ M). B and F also show the association of RAC1 and CDC42 with GRD-C (green), but not with GRD (red). (I) Association of mantGppNHp-RAC1 (0.2 μ M) with IQGAP1^{GRD-C} (2 μ M) in the presence of excess amount of RND1, RND2 or RND3 (10 μ M). (J) Association of RAC1-mantGppNHp (0.2 μ M) with IQGAP1GRD-C (2 μ M) in the presence of excess amount of CDC42-GppNHp (10 μ M), and *vice versa*.

Figure 3. Kinetic measurements of GRD-C with RAC- and CDC42-like proteins. (A) Association of RAC1-mantGppNHp (0.2 μ M) with increasing GRD-C concentrations (0.25-8 μ M). (B) Association rates (k_{on}) of GRD-C binding RHO proteins. (C) Dissociation of GRD-C (2 μ M) from RAC1-mantGppNHp (0.2 μ M) in the presence of unlabeled RAC1-GppNHp (10 μ M). (D) Association rates (k_{on}), dissociation rates (k_{off}) and dissociation constants (k_d) of GRD-C binding RHO proteins.

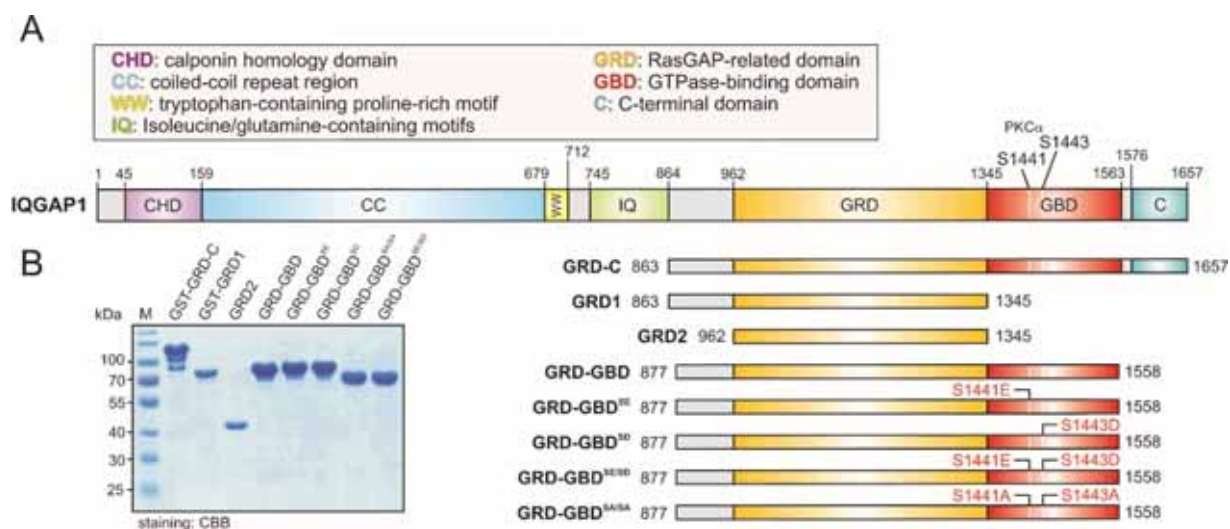
Figure 4. Interaction of different C-terminal variants and phosphomimicking mutants of IQGAP1 with RAC1 and CDC42. (A) Association of different IQGAP1 variants with RAC1/CDC42-mantGppNHp (0.2 μ M) was measured and the observed rate constants (k_{obs}) were plotted against the investigated IQGAP1 C-terminal domains. In contrast to GRD-C, GDR-GBD and GRD-GBR^{SD} of IQGAP1, which efficiently interact with RAC1 and CDC42, GRD1, GRD2, and GDR-GBD variants (SD, SE/SD and SA/SA) were disabled to associate RAC1 and CDC42. (B, C) Kinetic measurements were performed to obtain the k_{on} and the k_{off} values, and to calculate the K_d values for the interaction of GRD-C, GRD-GBD, and GRD-GBD^{SE} with RAC1 (B) and CDC42 (C). Obtained data show the comparable results for RAC1 and CDC42.

Figure 5. GRD binds RAC-/CDC42 like proteins but outside the switch regions. (A-C) Fluorescence polarization experiments were conducted to measure the interaction of mantGppNHp-bound RAC1, CDC42 and RHOA (1 μ M, respectively) with increasing concentrations of GRD-C (0-20 μ M) (A), and GRD (0-120 μ M) (B). (C) Evaluated data and obtained dissociation constant (K_d) shown in the bars illustrates a significant difference in the binding affinities of these two IQGAP1 proteins. (D) Binding of mantGppNHp-bound RAC1 protein (1 μ M) with increasing concentrations (0-45 μ M) of GRD-GBD, GRD-GBD^{SE} and GRD-GBD^{SD}. (E) Calculated dissociation constants (k_d) shown in the bars reveal a significant decrease in the affinities of GRD-GBD^{SD} compared to GRD-GBD and GRD-GBD^{SE}. (F-G) Fluorescence polarization experiments were conducted under the same conditions as in A and B, the only different was that inactive mantGDP-bound CDC42 was used. Calculated K_d values were 95 μ M for GRD-C and 184 μ M for GRD, respectively.

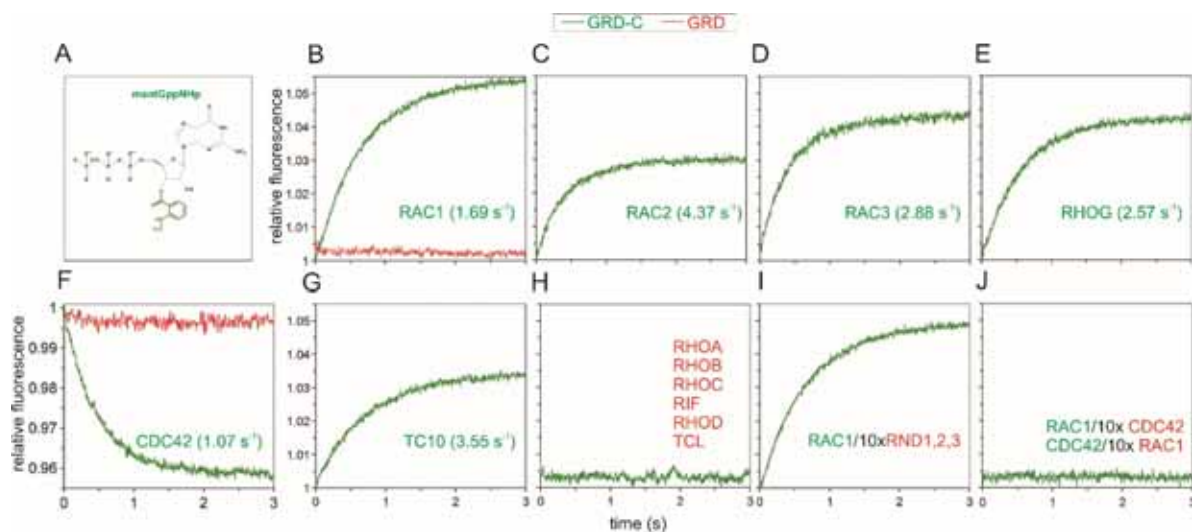
Figure 6. Reciprocal expression of IQGAP isoforms and RHO proteins in hepatic stellate cells. (A) qPCR analysis of IQGAP1, 2, 3, RAC1, 2, 3, and CDC42 in freshly isolated (quiescent, d0) and activated HSCs (day 8) revealed that IQGAP1, 3 and RAC2 preferentially expressed in aHSCs where IQGAP2 is downregulated. (B) Western blot analysis of RAC1, CDC42, IQGAP1 and 2 were performed at different time points after HSC isolation (d0, d1, d4 and d8). On contrary to IQGAP2 which was expressed more in qHSCs and lesser in aHSCs, IQGAP1, RAC1, and CDC42 had higher levels of expression in aHSCs. γ -tubulin was applied as a internal control for western blotting.

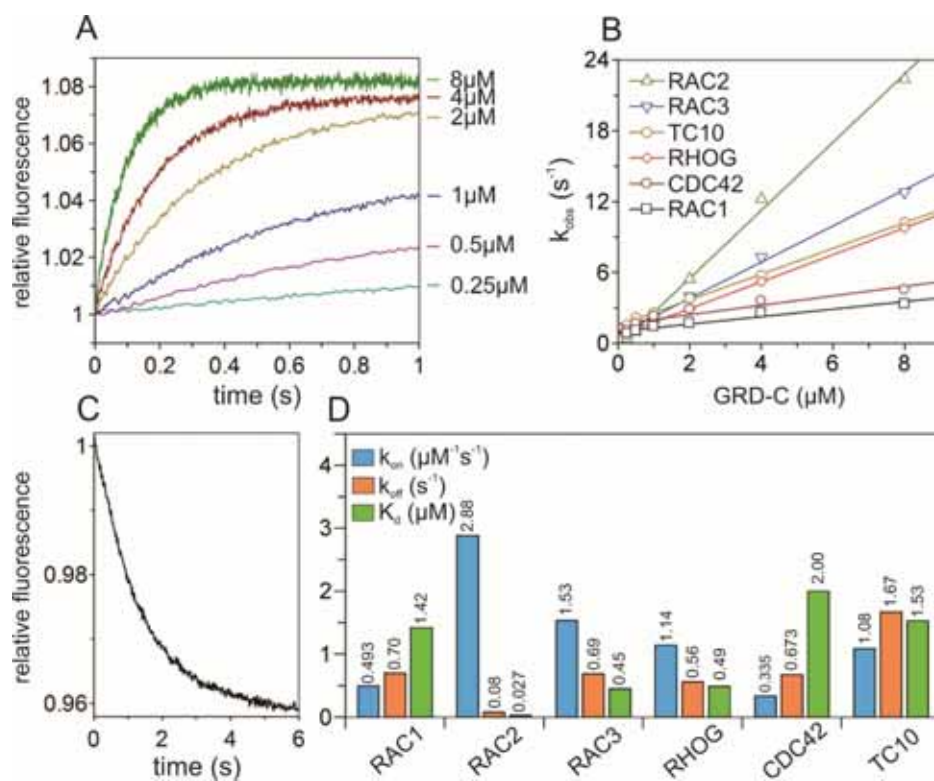
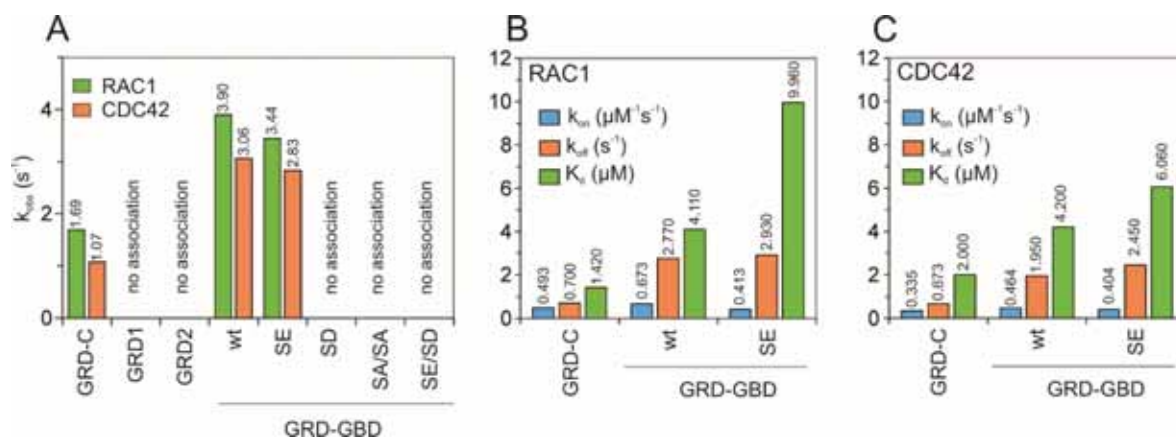
Figure 7. A proposed multi-stage mechanistic model of IQGAP interaction with IQGAP1. Low-affinity, GDP-/GTP-independent interaction of GRD with RAC1 and CDC42 proteins outside their switch regions occurs in a way that is independent of the upstream signals, providing it is structurally accessible and available for interactions. GBD only binds to the RAC1 and CDC42 proteins after GEFs catalyze the exchange of GDP to GTP, and they exist in an active GTP-bound forms. The C-terminal domain of IQGAP1 may potentiate the IQGAP1 interaction with RAC1 and CDC42 proteins by probably extending the resident time of the respective proteins complexes.

Nouri *et al.*, Figure 1

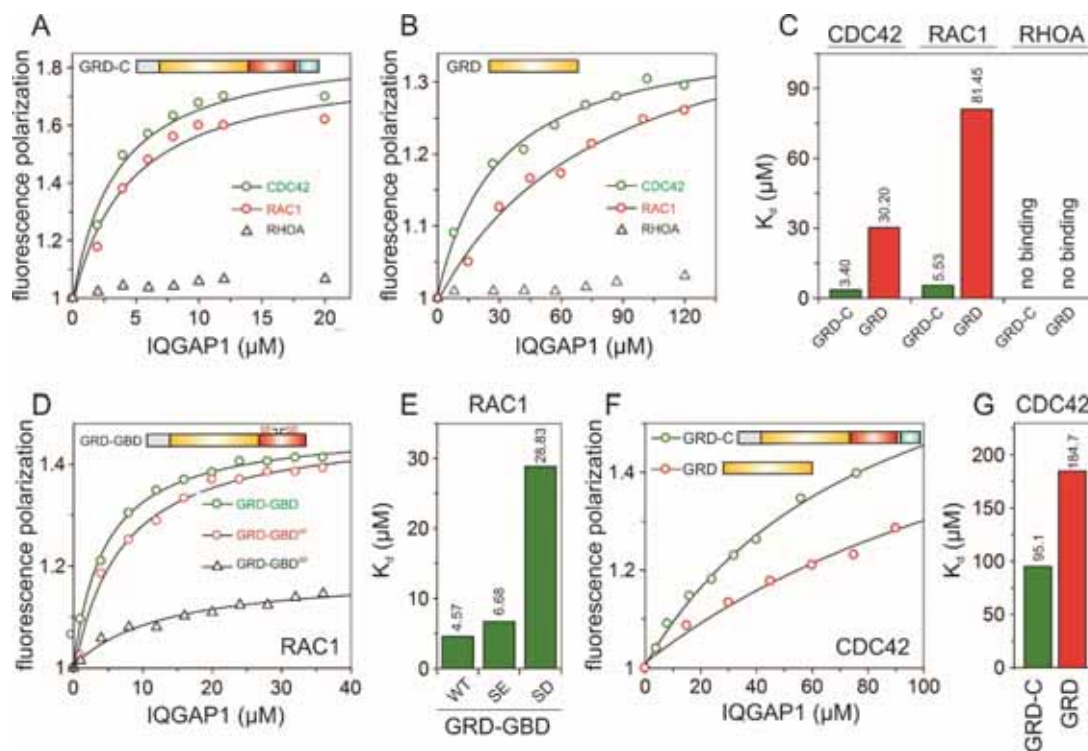


Nouri *et al.*, Figure 2

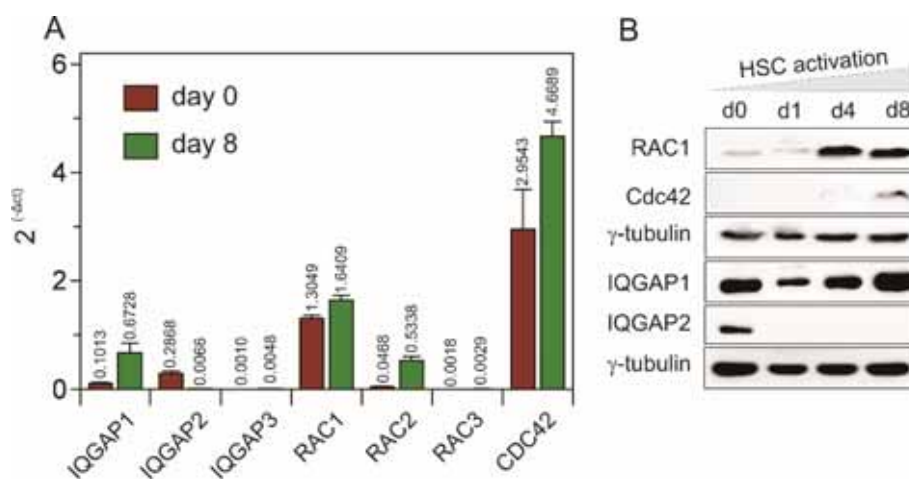


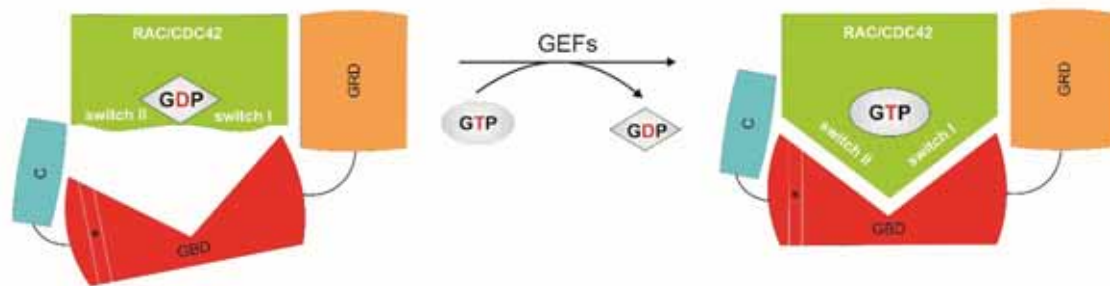
Nouri *et al.*, Figure 3Nouri *et al.*, Figure 4

Nouri *et al.*, Figure 5



Nouri *et al.*, Figure 6



Nouri *et al.*, Figure 7

SUPPORTING INFORMATION

IQGAP1 interaction with RHO family proteins revisited: kinetic and equilibrium evidence for two distinct binding sites*

Kazem Nouri¹, Eyad K. Fansa^{1§}, Ehsan Amin¹, Saeideh Nakhaei-Rad¹, Radovan Dvorsky¹, Lothar Gremer², David J. Timson³, Lutz Schmitt⁴, Dieter Häussinger⁵, and Mohammad R. Ahmadian^{1@}

¹Institute of Biochemistry and Molecular Biology II, Medical faculty of the Heinrich-Heine University, 40225 Düsseldorf, Germany

²Institute of Physical Biology, Heinrich-Heine University, Düsseldorf, Germany

³School of Pharmacy and Biomolecular Sciences, University of Brighton, Huxley Building, Lewes Road, Brighton BN2 4GJ, United Kingdom

⁴Institute of Biochemistry, Heinrich-Heine University, Düsseldorf, Germany

⁵Clinic of Gastroenterology, Hepatology and Infectious Diseases, Medical Faculty of the Heinrich-Heine University, Düsseldorf, Germany

Table S1: Primer sequences were obtained from Primer Bank (<http://pga.mgh.harvard.edu/primerbank>) with small modifications match with rat sequences.

Target	Primer	Source
IQGAP1	FW: 5'-GAGAAGACCGTTTTGGAGCTAAT -'3 RV: 5'-GGGTGAGGCTATGCTCAGG -'3	NM_001 1 08489.1
IQGAP2	FW: 5'-GCTGTCAAACTTCAGCAGAC-'3 RV: 5'- AGGTTGTCTACACAGGTCTTGA-'3	XM_008760685.1
IQGAP3	FW: 5'-AACTTCTGGCTTTCTGCGGTA -'3 RV: 5'-AATGCAGTAGATCACCCGAGG-'3	NM_001 1 91 709.1
RAC1	FW: 5'- ACGGAGCCGTTGGTAAAACC-'3 RV: 5'- AGACGGTGGGGATGTACTCTC-'3	NM_1 34366.1
RAC2	FW: 5'- GACAGTAAACCTGTGAACCTGG-'3 RV: 5'- CTGACTAGCGAGAAGCAGATG-'3	XM_006242028.1
RAC3	FW: 5'- TATCCCCACAGTTTTCGACAAC-'3 RV: 5'-GAGAGTGGCCGAAGCCTAT -'3	XM_006247966.1
CDC42	FW: 5'-GAAAATGTGAAAGAAAAGTGGGTG-'3 RV: 5'-TCTGGAGTAATAGGCTTCTGTTTG-'3	XM_006239270.1
HPRT1	FW: 5'-AAG TGT TGG ATA CAG GCC AGA-'3 RV: 5'-GGC TTT GTA CTT GGC TTT TCC-'3	self-designed

Nouri et al. Figure S1

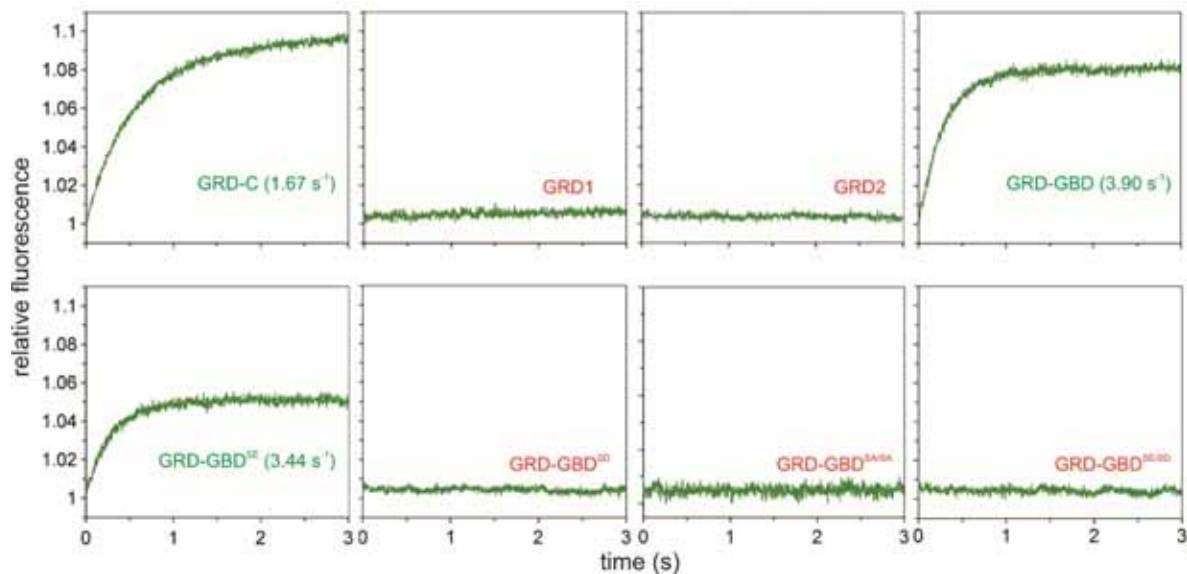


Figure S1. IQGAP1^{GBD} is crucial for the interaction with RAC1. Association of RAC1 mantGppNHp labeled (0.2 μM) and various IQGAP1 variants (2 μM) were measured. In contrast to GRD-C, GRD-GBD, and GRD-GBD^{SE} variants of IQGAP1, GRD1, GRD2, and GRD-GBD variants (SD, SE/SD, and SA/SA) failed to associate with RAC1. Calculated k_{obs} values for associating IQGAP1 fragments with RAC1 are shown in parenthesis.

Nouri et al. Figure S2

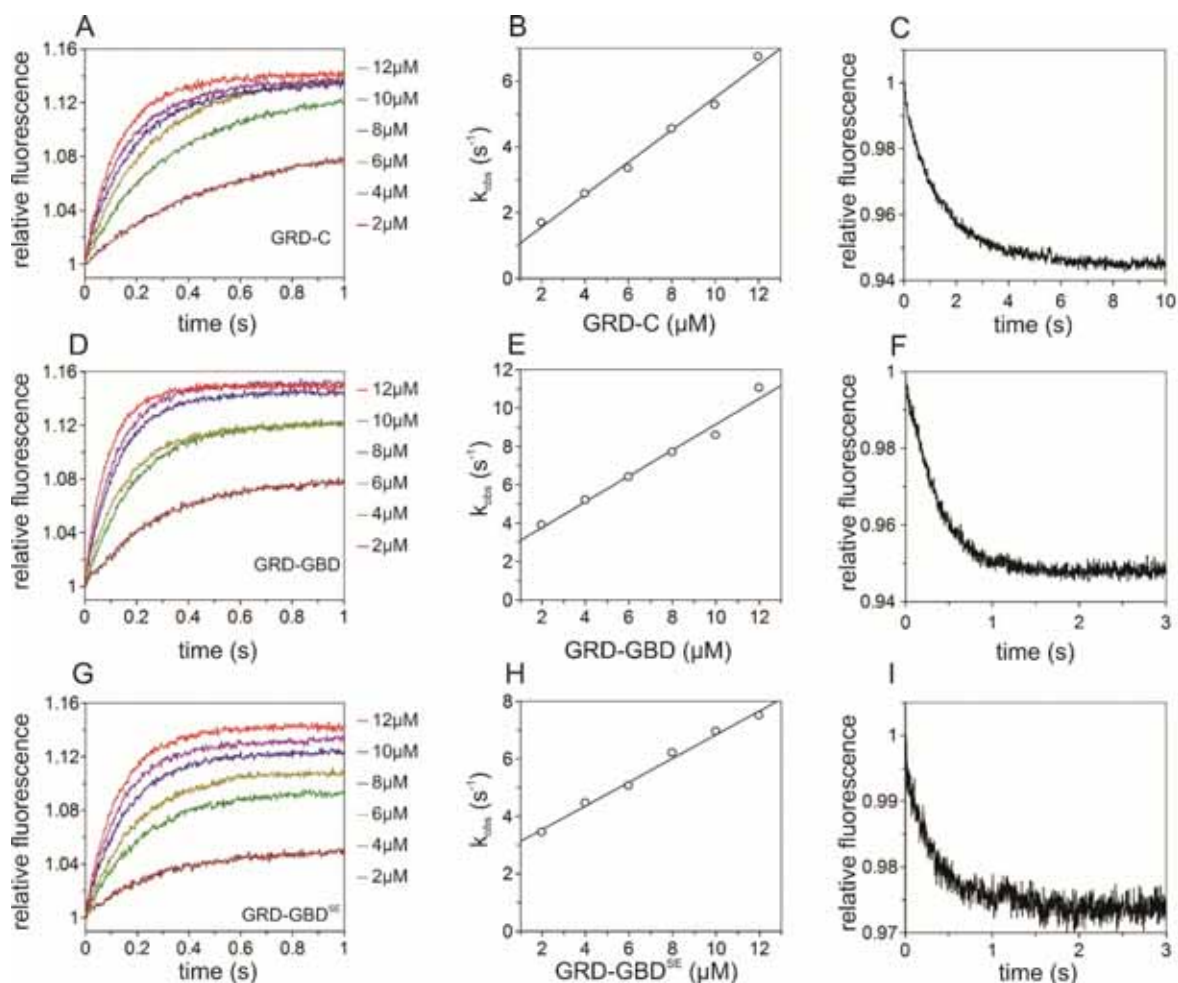


Figure S2. Kinetic measurements of GRD-C, GRD-GBD, and GRD-GBD^{SE} association with RAC1. Association of mantGppNHp-RAC1 (0.2 μM) with increasing concentrations (2-12 μM) of IQGAP1, association rates (k_{on}), and dissociation of IQGAP1 (2 μM) from RAC1-mantGppNHp (0.2 μM) in the presence of unlabeled RAC1-GppNHp (10 μM) are shown for **(A-C)** GRD-C, **(D-F)** GRD-GBD, and **(G-I)** GRD-GBD^{SE}, respectively. Quantitative data are presented in figure 4B

Nouri et al. Figure S3

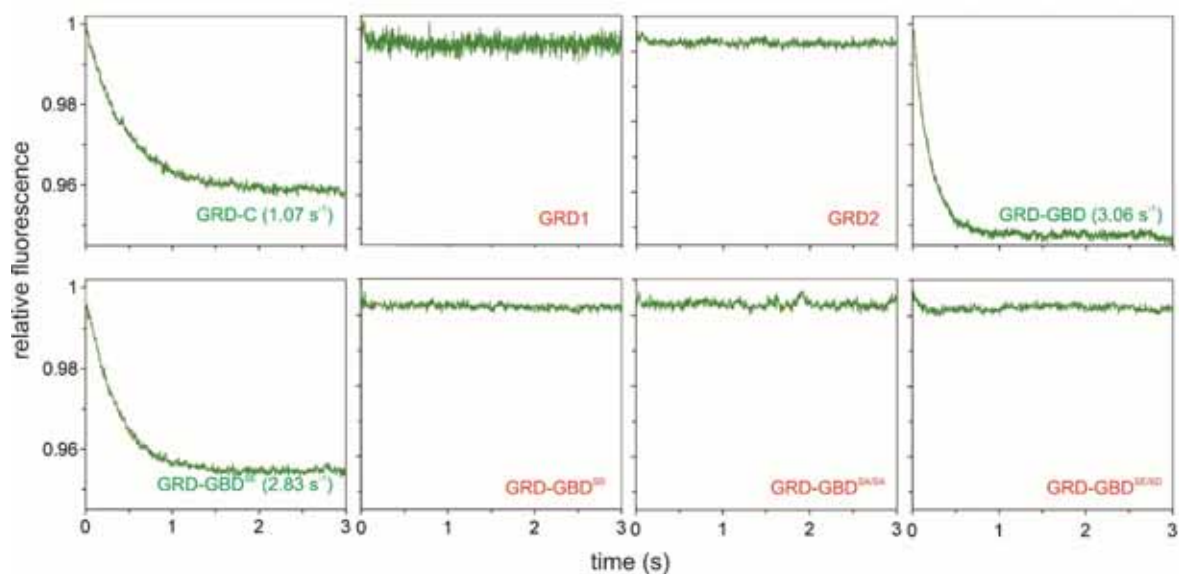


Figure S3. IQGAP1^{GBD} is essential for the CDC42 interaction. Association of different IQGAP1 variants (2 μM) with CDC42-mantGppNHp (0.2 μM) was measured under the same conditions as in **S1**. CDC42 associates with GRD-C, GDR-GBD, and GRD-GBR^{SE}, but not with GRD1, GRD2, and GDR-GBD variants (SD, SE/SD and SA/SA). k_{obs} values are presented in parenthesis in front of each associating fragment.

Nouri et al. Figure S4

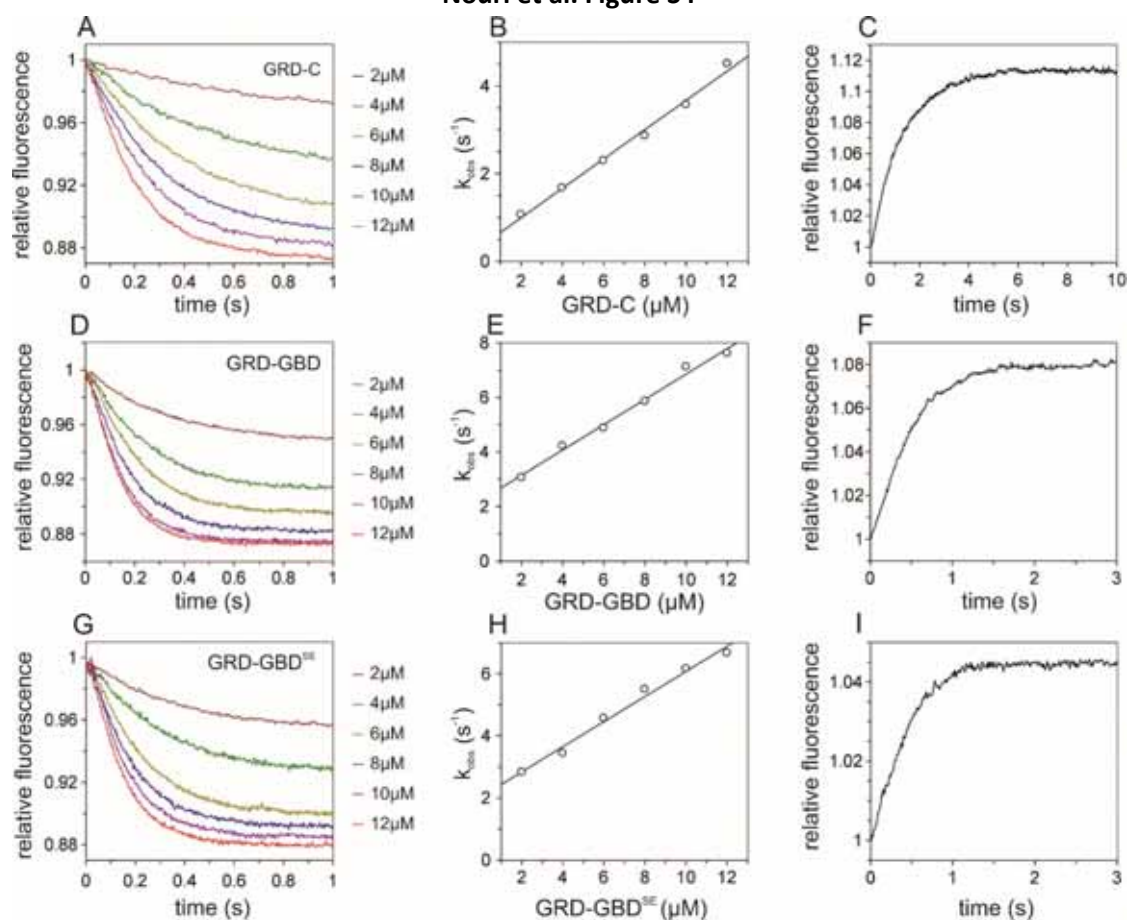
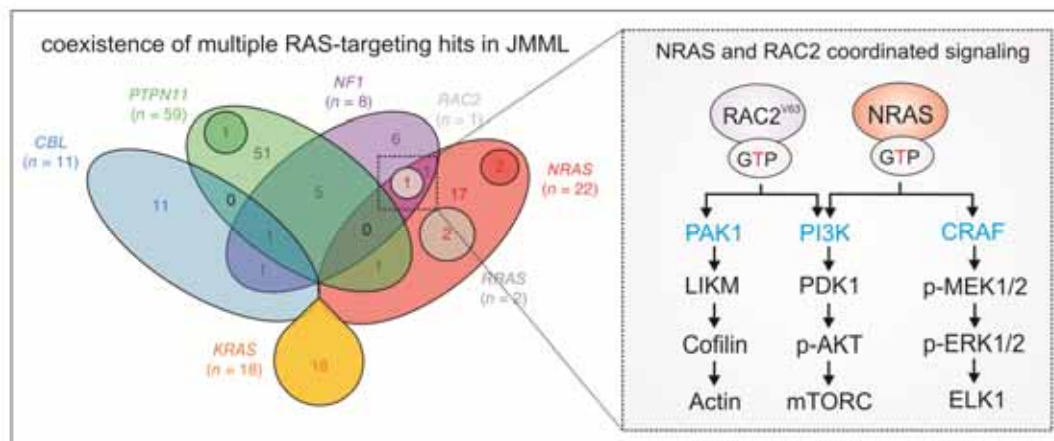


Figure S4. Kinetic measurements of GRD-C, GRD-GBD, and GRD-GBD^{SE} association with CDC42. Kinetic measurements were performed under the same conditions as in S2. Association of mantGppNHp-CDC42 (0.2 μM) with increasing concentrations (2-12 μM) of IQGAP1 proteins, association rates (k_{on}), and dissociation of IQGAP1 (2 μM) from CDC42-mantGppNHp (0.2 μM) in the presence of unlabeled CDC42-GppNHp (10 μM) are shown for GRD-C (A-C), GRD-GBD (D-F), and GRD-GBD^{SE} (G-I), respectively. Corresponding quantitative data are presented in figure 4C.

Chapter VII

Juvenile myelomonocytic leukemia displays mutations in components of the RAS pathway and the PRC2 network

Graphical Abstract



Published in:

Nature Genetics

Impact factor:

29.35 (2014)

Own Proportion to this work:

20%

Site direct mutagenesis

Cloning

Transfection

Analysis of interaction between RAC2 mutants and RAC effector with pull-down assay

Monitoring the signaling activity of RAC2 mutants towards AKT/mTORC and MAP kinase pathways with immunoblotting

Writing the manuscript

Juvenile myelomonocytic leukemia displays mutations in components of the RAS pathway and the PRC2 network

Aurélie Caye¹⁻³, Marion Strullu^{1,3}, Fabien Guidez¹, Bruno Cassinat^{1,4}, Steven Gazal^{5,6}, Odile Fenneteau⁷, Elodie Lainey^{1,2,7}, Kazem Nouri⁸, Saeideh Nakhaei-Rad⁸, Radovan Dvorsky⁸, Julie Lachenaud^{1,3}, Sabrina Pereira³, Jocelyne Vivent^{1,3}, Emmanuelle Verger^{1,4}, Dominique Vidaud^{9,10}, Claire Galambrun¹¹, Capucine Picard¹²⁻¹⁴, Arnaud Petit¹⁵, Audrey Contet¹⁶, Marilyne Poirée¹⁷, Nicolas Sirvent¹⁸, Françoise Méchinaud¹⁹, Dalila Adjaoud²⁰, Catherine Paillard²¹, Brigitte Nelken²², Yves Reguerre²³, Yves Bertrand²⁴, Dieter Häussinger²⁵, Jean-Hugues Dalle^{2,26}, Mohammad Reza Ahmadian⁸, André Baruchel^{2,26}, Christine Chomienne^{1,2,4} & Hélène Cavé¹⁻³

Juvenile myelomonocytic leukemia (JMML) is a rare and severe myelodysplastic and myeloproliferative neoplasm of early childhood initiated by germline or somatic RAS-activating mutations¹⁻³. Genetic profiling and whole-exome sequencing of a large JMML cohort (118 and 30 cases, respectively) uncovered additional genetic abnormalities in 56 cases (47%). Somatic events were rare (0.38 events/Mb/case) and restricted to sporadic (49/78; 63%) or neurofibromatosis type 1 (NF1)-associated (8/8; 100%) JMML cases. Multiple concomitant genetic hits targeting the RAS pathway were identified in 13 of 78 cases (17%), disproving the concept of mutually exclusive RAS pathway mutations and defining new pathways activated in JMML involving phosphoinositide 3-kinase (PI3K) and the mTORC2 complex through *RAC2* mutation. Furthermore, this study highlights PRC2 loss (26/78; 33% of sporadic JMML cases) that switches the methylation/acetylation status of lysine 27 of histone H3 in JMML cases with altered RAS and PRC2 pathways. Finally, the association between JMML outcome and mutational profile suggests a dose-dependent effect for RAS pathway activation, distinguishing very aggressive JMML rapidly progressing to acute myeloid leukemia.

JMML is considered a unique example of RAS-driven oncogenesis because it is thought to be initiated by mutations, usually described as mutually exclusive, in RAS genes (*NRAS* or *KRAS*) or RAS pathway regulators (*PTPN11*, *NF1* or *CBL*)¹. JMML can be sporadic or develop in patients displaying syndromic diseases with constitutional RAS overactivation such as Noonan syndrome, NF1 and CBL syndrome, which are caused by heterozygous germline mutations in *PTPN11*, *NF1* and *CBL*, respectively⁴.

We first explored the somatic mutation landscape of 30 patients with syndromic ($n = 8$) or sporadic ($n = 22$) JMML by combining genome-wide DNA array analysis, whole-exome sequencing and targeted sequencing in paired germline and tumoral samples

(Supplementary Table 1). In total, 85 somatically acquired genetic alterations were found in 25 of 30 (83%) patients in this subcohort (Supplementary Fig. 1 and Supplementary Tables 2 and 3). The low rate of somatic events (0.38 events/Mb/case versus 0.61 events/Mb/case on average in childhood cancer)⁵ confirms the paucity of oncogenic events required for JMML oncogenesis⁶.

Genes containing somatic variations detected by whole-exome sequencing or previously reported to be mutated in JMML (Supplementary Table 4) were then sequenced in the full cohort of 118 JMML cases (Supplementary Figs. 2 and 3). In total, 122 secondary clonal abnormalities in addition to initiating RAS pathway mutations were uncovered in 58 of the 118 (49%) patients (Fig. 1 and Supplementary Tables 2, 5 and 6). Interestingly, almost no additional mutations were detected in patients with CBL syndrome or Noonan syndrome. In line with phenotype-genotype correlations⁷⁻⁹, this observation supports an endogenous role for germline *PTPN11* and *CBL* mutations in the occurrence of myeloproliferative neoplasms and suggests that parameters other than additional somatic gene mutations, such as, for instance, a mutated hematopoietic microenvironment, might be involved in supporting leukemogenesis.

In contrast, at least one additional somatic hit was found in eight of eight (100%) NF1-associated JMML cases and 49 of 78 (63%) sporadic JMML cases. The percentage of sporadic JMML cases with secondary genetic alterations was similar in all subgroups, but the pattern of mutations varied substantially depending on the initiating lesion. JMML cases with an initiating *KRAS* lesion (*KRAS*-JMML) mostly displayed chromosomal abnormalities, including del7 or del7q in 56% of cases, unlike other genetic subgroups that mostly had point mutations (Supplementary Fig. 4 and Supplementary Table 5). Further studies are required to understand why RAS-driven oncogenesis proceeds through the acquisition of various patterns of secondary mutation that depend on the initiating lesion.

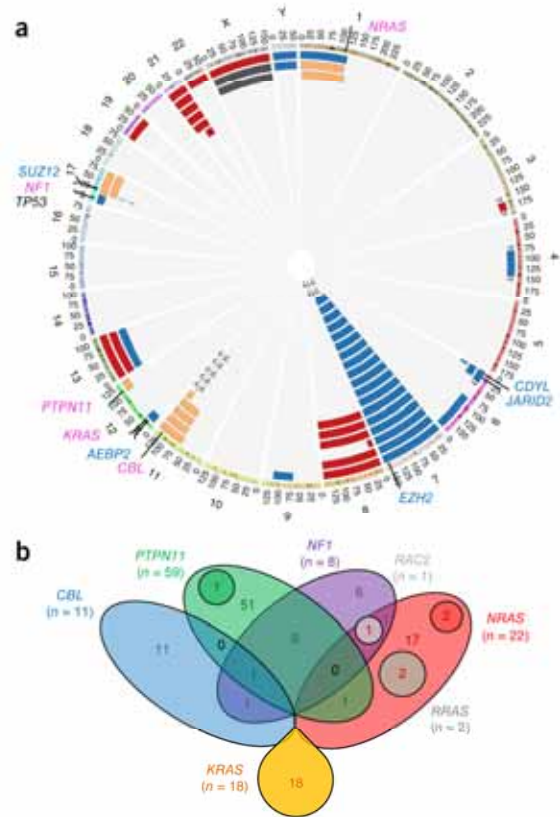
The secondary somatic mutations targeted genes known to be involved in myeloproliferative neoplasms, albeit with a much lower

A full list of author affiliations appears at the end of the paper.

Received 13 March; accepted 16 September; published online 12 October 2015; doi:10.1038/ng.3420

LETTERS

Figure 1 Combinations of multiple hits targeting the RAS pathway and PRC2 network. **(a)** Circos plot representing CNVs in 118 JMML cases. Copy number profiles are shown in red (somatic gain) or blue (somatic loss), aUPD regions are shown in orange and germline aneuploidies are shown in black. A question mark indicates undetermined boundaries. Relevant genes in the RAS pathway and PRC2 network are indicated in pink and blue, respectively. All aUPD events ($n = 16$) resulted in the duplication of oncogenic RAS-related variants. An aUPD region encompassed the second allele of *NF1* ($n = 3$) and *CBL* ($n = 10$) in patients with germline mutations of these genes or somatically acquired oncogenic *PTPN11* ($n = 1$) or *NRAS* ($n = 2$) mutations in sporadic JMML cases. Deletions targeted various PRC2 components. *EZH2* was haploinsufficient in patients with del7 or del7q, *AEBP2* was deleted in one patient with del12p. A 6p deletion encompassed *CDYL* (6p25.1) in three patients, with co-deletion of *JARID2* (6p22.3) in two of them. **(b)** Venn diagram showing the coexistence of multiple RAS-targeting hits in JMML. Both germline and somatically acquired mutations of canonical RAS pathway genes and orthologs are represented. Each colored segment corresponds to a different gene. In three cases (two NRAS-JMML and one PTPN11-JMML), represented by darker circles embedded in the segment of the altered gene, RAS double mutation corresponded to LOH of the oncogenic mutation. RRAS mutations are represented by a gray circle embedded in the NRAS segment, as the two RRAS mutations were found in patients with concomitant NRAS mutation.



prevalence than in adult diseases^{6,10} (Fig. 2). *SETBP1* was mutated in ten of the 118 (9%) cases, and the spliceosome gene *ZRSR2* was mutated in three cases. In contrast with a previous report, *JAK3* mutations were found in only four JMML cases⁶. The acquisition of *SETBP1*, *ASXL1*, *JAK3* and other somatic alterations, including monosomy 7, consistently appeared secondary to the RAS pathway mutation, usually following a linear pattern, except in two patients (Fig. 3). An active role for the variants in leukemogenesis is supported by the high proportion predicted to be deleterious (Supplementary Fig. 5) and, most notably, by their striking enrichment in RAS pathway and Polycomb repressive complex 2 (PRC2) network components (Fig. 1 and Supplementary Table 6).

Surprisingly, a second hit targeting the RAS pathway was observed in 13 of 78 (17%) sporadic JMML cases and two of eight (25%) *NF1*-associated JMML cases (Fig. 1b and Supplementary Table 5), hereafter termed 'RAS double mutants'. Duplication of the oncogenic mutation due to acquired uniparental disomy (aUPD) was observed in three patients. Various combinations of mutations activating the canonical RAS pathway were also found, with the most frequent being *NF1* haploinsufficiency in six sporadic JMML cases with an initiating lesion in *PTPN11* (*PTPN11*-JMML) (Supplementary Fig. 6).

Mutations in RAS regulators were also found. *PDE8A*, mutated in one *PTPN11*-JMML case, protects *RAF1* from inhibitory phosphorylation by protein kinase A (PKA), enhancing its activity¹¹. Two JMML cases with initiating lesions in *NRAS* (*NRAS*-JMML) had mutations in *RRAS*, an inducer of RAS-mitogen-activated protein kinase (MAPK) activation¹² and upstream regulator of RAC in hematopoietic stem cells¹³, and another had a mutation in the RHO GTPase *RAC2*. The coexistence of RAC and RAS-MAPK mutations in some tumors and cooperation between oncogenic *NRAS* and RAC has previously been demonstrated¹⁴. Investigations into the functional and structural properties of the Asp63Val *RAC2* mutant, which predominantly occurred in its active, GTP-loaded form, as compared to wild-type *RAC2* and the constitutively active Gly12Val *RAC2* variant demonstrated a drastic gain-of-function effect (Fig. 4). Interestingly, an analysis of signaling downstream of RAS showed that Asp63Val *RAC2* activated the PI3K-PDK1-AKT and mTORC2 pathways but did not have a significant effect on the RAF-MEK-ERK pathway (Fig. 4 and Supplementary Fig. 7). This finding is consistent with several

lines of evidence indicating a strong impact of the PI3K-PDK-AKT pathway on JMML¹⁵, and activating the catalytic p110 δ subunit of PI3K has recently been shown to promote the effects of Shp2 on granulocyte-macrophage colony-stimulating factor (GM-CSF) hypersensitivity¹⁶. Plexins catalyze *RRAS* inactivation via their GTPase-activating protein (GAP) domain¹⁷, and *PLXNB2* was mutated in one *PTPN11*-JMML case. Finally, *ABII*, belonging to a multimolecular complex required for SOS-mediated RAC activation^{18,19}, was mutated in one case. Together, these findings suggest that the *RRAS*-RAC pathway represents a meaningful mutated subnetwork in JMML.

Although no *KRAS*-JMML case was a RAS double mutant at diagnosis, loss of heterozygosity (LOH) for oncogenic *KRAS* during disease progression in one patient suggests that this could occur (Supplementary Fig. 8).

Sequencing of isolated myeloid colonies demonstrated the coexistence of multiple RAS hits in the same myeloid progenitors in three JMML cases tested (Supplementary Table 7). With the exception of *NF1* mutations, which were subclonal in four of six cases, consistent with their late acquisition (Supplementary Fig. 6), RAS mutations could not be temporally hierarchized at diagnosis, despite extensive colony screening. This suggests a role for mutational combinations in the early stages of the disease and a strong selective benefit for double mutants. Surprisingly, however, in one patient with both an *NRAS* and *RRAS* mutation at diagnosis, the *NRAS* mutation was lost after intensive chemotherapy whereas the *RRAS* mutation was still detected. This finding strongly suggests that *RRAS* mutations may initiate JMML (Fig. 3), a hypothesis consistent with the recent report of a myeloid

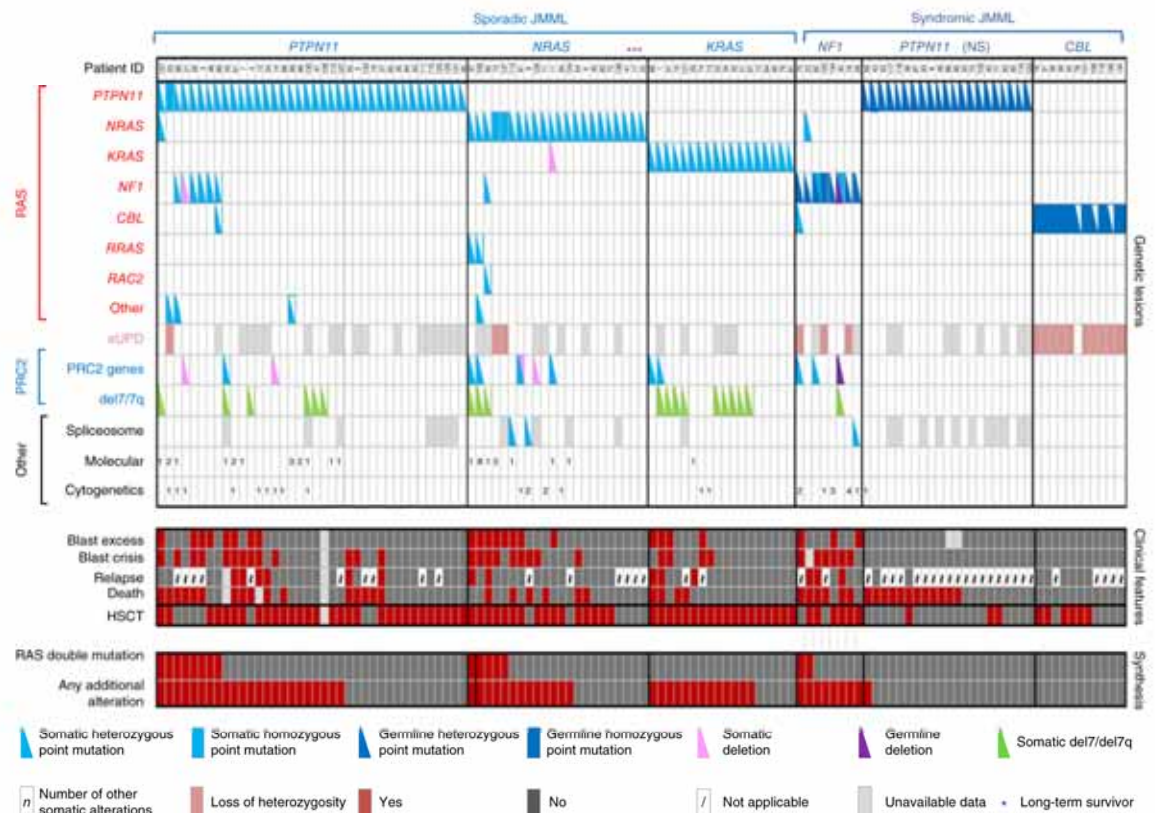


Figure 2 Alteration profiles in individual JMML cases. Germline and somatically acquired alterations with recurring hits in the RAS pathway and PRC2 network are shown for 118 patients with JMML who underwent detailed genetic analysis. Blast excess was defined as a blast count $\geq 10\%$ but $< 20\%$ of nucleated cells in the bone marrow at diagnosis. Blast crisis was defined as a blast count $\geq 20\%$ of nucleated cells in the bone marrow. NS, Noonan syndrome.

hemopathy in a patient harboring a germline *RRAS* mutation¹². Our findings challenge the dogma of the mutual exclusivity of RAS pathway mutations, supporting a dose-dependent effect for oncogenic RAS. The cooperative effects of RAS-activating events that were previously viewed as functionally equivalent have been evidenced in several mouse models^{20–22}. *Nf1* and *Kras* double-mutant mice have been shown to develop myeloid malignancies with reduced latency and increased severity in comparison to mice with only one of the two defects. More recently, the role of oncogene dosage has been demonstrated in the context of *Nras*-driven myeloid transformation^{21,22}. Our findings based on patient samples provide evidence that these models are fully relevant to human disease.

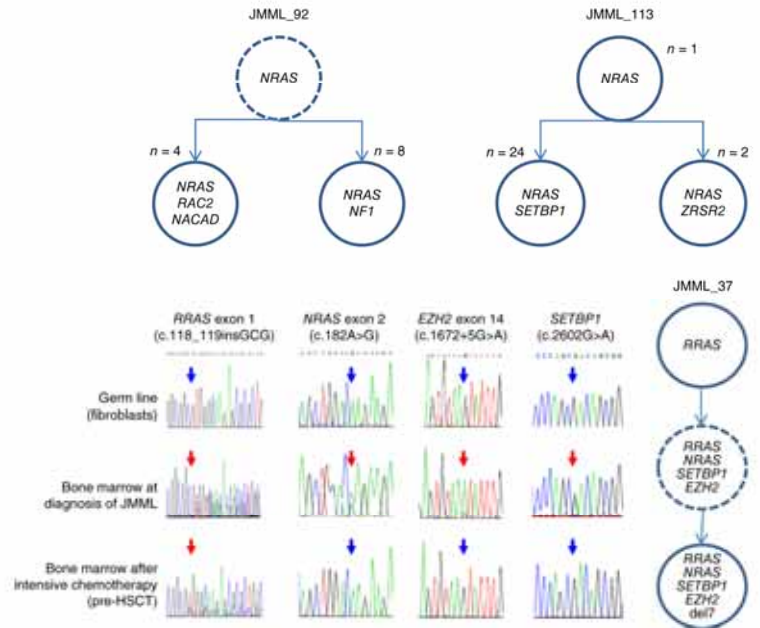
Another major group of genes targeted in JMML belonged to the PRC2 complex, involved in the transcriptional repression of target genes via methylation at lysine 27 of histone H3 (H3K27me3). In our cohort, copy number variations (CNVs) frequently resulted in haploinsufficiency for PRC2 core subunits (*SUZ12* or *EZH2*) or PRC2-associated factors necessary for optimal PRC2 activity (*AEBP2*, *CDYL* or *JARID2*) (Fig. 1a). In two patients, an *EZH2* point mutation became hemizygous by loss of the copy of chromosome 7 bearing the wild-type *EZH2* allele. *EZH2* haploinsufficiency induced by del7 or del7q reduces H3K27me3 levels at specific loci²³. *JARID2* is involved in the recruitment of the PRC2 complex to its target genes in hematopoietic stem cells^{24,25}, and *A2BP2* is an evolutionarily conserved PRC2 cofactor²⁶.

Hemizygous *JARID2* and *AEBP2* deletions have been described in the clonal evolution of myeloproliferative neoplasms²⁷. *CDYL*, for which three of our patients were haploinsufficient, encodes a transcriptional corepressor that recruits PRC2 to the chromatin substrate²⁸ but has not been demonstrated to undergo alteration in myeloid malignancies before now. Finally, inactivating mutations in the Polycomb-associated gene *ASXL1* were observed in eight of 118 (7%) JMML cases, all sporadic. *ASXL1* silencing reduces H3K27me3 levels through the inhibition of PRC2 recruitment to specific oncogenic target loci and collaborates with *NRAS* mutation encoding p.Gly12Asp *in vivo* to promote myeloid leukemogenesis^{29,30}. Thus, non-mutually exclusive genetic alterations impairing PRC2 function occurred in 26 of 78 (33%) sporadic JMML cases and five of eight (63%) *NF1*-associated JMML cases. Interestingly, hemizygous spliceosomal mutations similar to those found in three of our patients have recently been shown to induce nonsense-mediated decay of *EZH2*, reducing its expression to levels observed with hemizygous deletion^{23,31} and possibly further increasing the rate of PRC2 alterations in JMML.

Our findings extend a previous observation that components of epigenetic regulation are mutated at high frequencies in a subset of pediatric cancers³². Moreover, recent data show that haploinsufficiencies for multiple genes that regulate PRC2 function can cooperate in myeloid transformation^{23,33} and result in an antagonistic methylation-to-acetylation switch at H3K27, with the transcriptional activation of

LETTERS

Figure 3 Clonal evolution of JMML. Clonal architecture was investigated by sequencing isolated colonies (colony forming unit monocyte (CFU-M) or colony forming unit granulocyte-monocyte (CFU-GM)) obtained by culturing patient-derived myeloid progenitors *in vitro* and calculating the variant allele frequency (VAF) of each variant by next-generation sequencing (Supplementary Table 6). The clonal architecture of three NRAS-JMML cases, including the two cases displaying a nonlinear clonal architecture (JMML_92 and JMML_113), is represented. Each circle represents a clone. Dashed lines indicate clones whose presence was not directly assessed but was deduced from experimental data. At diagnosis, JMML_113 showed heterozygous mutations in *NRAS* and *SETBP1* and a subclonal frameshift mutation in *ZRSR2*. Sequencing of isolated myeloid colonies showed that both *SETBP1* and *ZRSR2* mutations were secondary and occurred in distinct *NRAS*-mutated clones. At diagnosis, JMML_92 had mutations in *NRAS* (VAF = 0.49), *RAC2* (VAF = 0.27), *NACAD* (VAF = 0.32) and *NF1* (VAF = 0.04). Colonies obtained at relapse confirmed that the *RAC2* and *NACAD* mutations were secondary to the *NRAS* mutation and showed that the *RAC2*-mutated clone was progressively outcompeted by another clone presenting biallelic *NF1* mutations. In JMML_37, the *NRAS* mutation was lost in a follow-up sample collected after intensive chemotherapy for blast crisis, whereas a subclonal *RRAS* mutation was still detected. This suggests that the *RRAS* and not the *NRAS* mutation initiated the JMML. The allelic imbalance of the *EZH2* mutation indicates that it preceded the loss of chromosome 7.



PRC2 target genes³⁴. Concordantly, using antibodies to H3K27me3 and H3K27ac, we found that primary JMML samples with decreased PRC2 activity due to *ASXL1* mutation or monosomy 7 showed a global

decrease in H3K27 trimethylation with a concomitant increase in acetylation (Fig. 5). The identification of recurrently affected biological pathways is a strong and powerful indication that mutations

Figure 4 The p.Asp63Val substitution in *RAC2* results in a gain-of-function effect associated with an increase in effector binding and a massive decrease in GAP function, leading to AKT activation via two distinct pathways. (a,b) Analysis of active, GTP-bound *RAC2* protein using a pull-down assay with glutathione S-transferase (GST) fused to the PAK1 GTPase-binding domain (GBD) and densitometric quantification of three separate blots (b) showed, in contrast to wild-type (WT) *RAC2*, strong accumulation of active Asp63Val *RAC2* comparable to that seen with constitutively active Gly12Val *RAC2*. PD, pull-down; IB, immunoblot. (c,d) Immunoblot analysis of the phosphorylation levels of MEK1 and MEK2 (pMEK1/2), ERK1 and ERK2 (pERK1/2) and AKT (pAKT) (c) and densitometric quantification of three separate blots (d) showed clear activation of AKT but not MEK1/2 or ERK1/2, correlating with levels of the GTP-bound form of Asp63Val *RAC2* in regulating signaling cascades (PI3K-PDK1 and mTORC2) responsible for AKT activation (Supplementary Fig. 6). AKT, MEK1/2, ERK1/2 and α -actin were used as loading controls. (e-g) Biochemical analysis of Asp63Val *RAC2* *in vitro*. Wild-type *RAC2* and the Asp63Val mutant were analyzed for catalyzed nucleotide exchange by the RAC guanine nucleotide exchange factor (GEF) TIAM1 (e), interaction with the effector PAK1 (f) and stimulated GTP hydrolysis by the RACGAP p50^{GAP} (g) using purified proteins and fluorescently labeled nucleotides. k_{obs} is the observed rate constant, and K_d is the dissociation constant. (h) In the *RAC2* structure, Asp63 is located at the edge of the TIAM1- and PAK1-binding sites and rather central to the GAP-binding site, clarifying the reason for the robust decrease in GAP-accelerated GTP hydrolysis observed with alteration of this site.

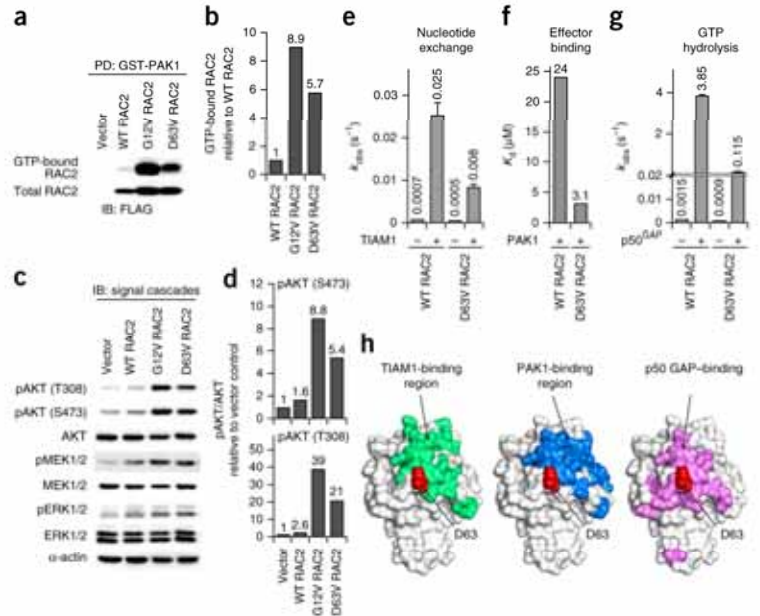
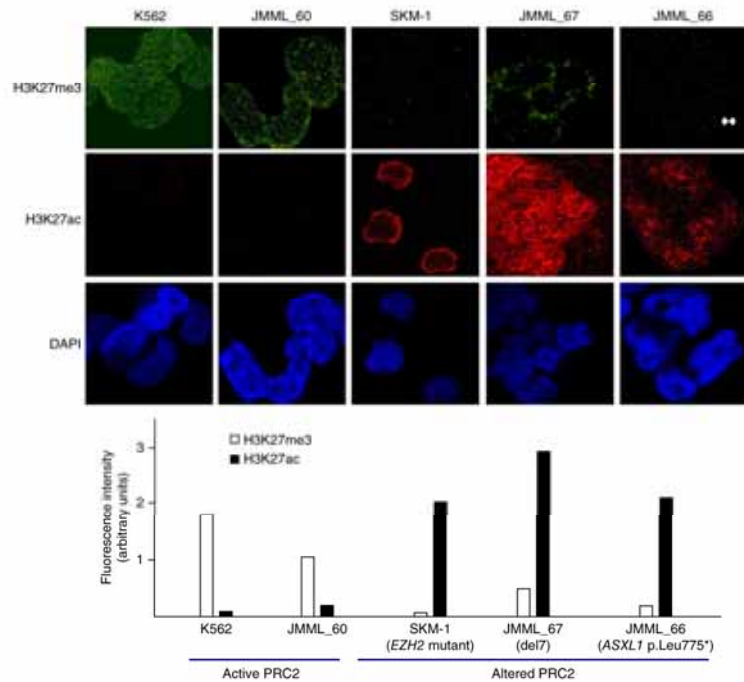


Figure 5 Reduced PRC2 dosage and histone H3 modifications. H3K27me3 and H3K27ac levels were detected by immunofluorescence in K562 cells (positive control for PRC2 activity), bone marrow mononuclear cells from patient JMML_60 without known PRC2 alterations, SKM-1 cells with a homozygous *EZH2* mutation, bone marrow mononuclear cells from patient JMML_67 with a PRC2 alteration (monosomy 7) and bone marrow mononuclear cells from patient JMML_66 with a PRC2 alteration (*ASXL1* mutation encoding p.Leu775*). Scale bar, 2 μ m. Immunofluorescence for H3K27me3 (white bars) and H3K27ac (black bars) was quantified in the cell lines and cells derived from patients with JMML with respect to PRC2 complex status. Mutations reducing PRC2 dosage resulted in reduced H3K27me3 levels and a concomitant increase in H3K27ac levels.



targeting these pathways drive the oncogenic process in JMML³⁵. The clonal architecture studies we performed by sequencing isolated colonies obtained by the *in vitro* culture of progenitors derived from patients with JMML consistently showed that RAS activation was the initiating oncogenic event, with PRC2 impairment being a secondary event. Our results suggest that neither PRC2 impairment nor any other genetic lesion can drive JMML in the absence of preexisting RAS pathway deregulation. Most interestingly, a cooperative effect from RAS activation and PRC2 impairment has recently been reported in NF1-associated cancers^{36–38}, where PRC2 component haploinsufficiency exerts a disproportionately suppressive effect on methylation at H3K27, augmenting acetylation and further elevating the transcription of RAS-regulated genes³⁸. Our data suggest that this molecular mechanism is also relevant in JMML.

Other additional mutations had unknown functions and/or affected single individuals. However, considering both our selective mutation filters, which included germline DNA screening, and the

extremely low frequency of clonal mosaicism in peripheral blood from normal children^{39–42}, most somatic variants detected in our patients are also likely to drive clonal selection.

Most JMML cases are severe, with the only curative treatment being hematopoietic stem cell transplantation (HSCT)^{2,3,43}. However, clinical evolution is heterogeneous, with transformation to acute myeloid leukemia (AML) in one of three cases and frequent relapses after HSCT, whereas some rare 'long-term survivors' experience spontaneous remission and survive without treatment^{3,44,45}. The management of patients with JMML urgently requires parameters to help in patient risk stratification. Unfortunately, the initiating RAS pathway lesion incompletely predicts outcome (Supplementary Fig. 9). We thus asked whether the newly identified alterations could improve the prediction of JMML outcome. Secondary alterations accumulated in a limited number of patients (Fig. 2 and Supplementary Table 5) and were associated with a poorer outcome, with a 3-year overall survival of 61% as compared with 85% in other patients ($P = 0.028$) (Fig. 6). Yet, it was possible to see that RAS double-mutant JMML had the most severe presentation, with an increase in the number of blasts in the bone marrow ($\geq 10\%$) in nine of 13 (69%) double-mutant cases versus

npg

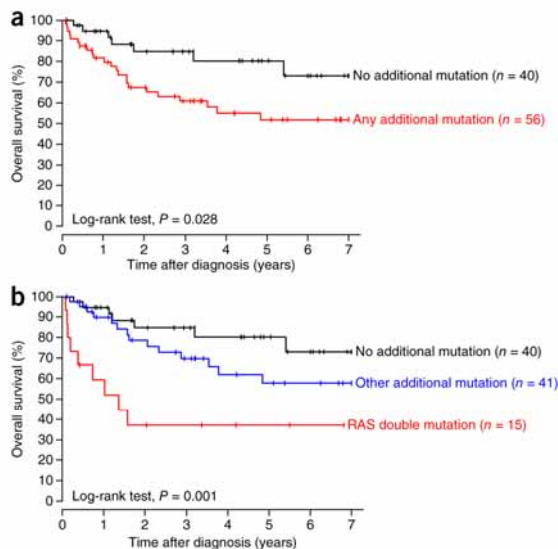


Figure 6 Overall survival of patients with sporadic JMML according to the presence and type of additional somatic mutations. Kaplan-Meier representations of overall survival are shown for 96 patients with JMML having clinical follow-up information available. Patients with Noonan syndrome were excluded from the analysis because non-hematological comorbidities may have jeopardized their survival⁷. As in Supplementary Table 5, additional somatic alterations were defined as somatically acquired mutations other than the somatic RAS pathway mutations assumed to be either the initiating event or part of the classical mechanism of leukemogenesis, such as hits targeting the wild-type *NF1* or *CBL* allele in germline-mutated patients^{8,9,48}. (a,b) The presence of any additional somatic alterations (a) together with RAS double mutations (b) allowed us to distinguish patients with a significantly poorer outcome.

LETTERS

11 of 64 (17%) other cases ($P < 0.001$) and rapid evolution to AML with myelodysplasia-related changes (AML-MRC), in line with previous single-case reports^{12,46,47} (Fig. 6). The outcome of RAS double-mutant cases was thus significantly poorer than that of other JMML cases, with a 3-year overall survival rate of 37% versus rates of 85% and 70% in patients with no or one other secondary alteration, respectively ($P = 0.001$) (Fig. 6). In NRAS-JMML cases, which display the greatest clinical diversity⁴⁴, three long-term survivors were observed; none of these patients had secondary abnormalities. In contrast, ten of 11 (91%) patients with aggressive disease, as assessed by blast excess at diagnosis or blast crisis before HSCT, had additional abnormalities, including double mutation of RAS pathway components in five cases. These findings suggest that oncogenic NRAS proteins require additional transforming hits to give rise to aggressive JMML and provide a useful prognostic tool to differentiate patients with NRAS-associated JMML who require HSCT from those who could benefit from a 'wait-and-see' approach.

In conclusion, our study shows for the first time, to our knowledge, that concomitant mutations in JMML target a small number of interacting networks, with a striking enrichment in components of the RAS and PRC2 networks. These findings extend and reinforce the notion that JMML is a RASopathy while showing that RAS activation is the major but not the only player in JMML. Such new information on the pathogenesis of JMML should provide functional guidance, prognostic markers and patient selection criteria for new therapeutic options in this very severe childhood leukemia.

URLs. UCSC Genome Browser, <http://www.genome.ucsc.edu/>; dbSNP137, <http://www.ncbi.nlm.nih.gov/projects/SNP/>; HapMap, <http://hapmap.ncbi.nlm.nih.gov/>; 1000 Genomes Project, <http://www.1000genomes.org/>; Catalogue of Somatic Mutations in Cancer (COSMIC), <http://cancer.sanger.ac.uk/cancergenome/projects/cosmic/>; SIFT, <http://sift.jcvi.org/>; PolyPhen-2, <http://genetics.bwh.harvard.edu/pph2/>; MutationTaster, <http://www.mutationtaster.org/>; Leiden Open Variation Database (LOVD), <http://www.lovd.nl/3.0/>; R survival library, <http://CRAN.R-project.org/package=survival>; ArrayExpress database, <http://www.ebi.ac.uk/arrayexpress/>; European Genome-phenome Archive (EGA) database, <https://www.ebi.ac.uk/ega/>.

METHODS

Methods and any associated references are available in the online version of the paper.

Accession codes. SNP array data have been deposited in the ArrayExpress database under accessions E-MTAB-3399 and E-MTAB-3729. Targeted sequencing data have been deposited in the European Genome-phenome Archive (EGA), which is hosted by the European Bioinformatics Institute (EBI), under accession EGAS00001001324.

Note: Any Supplementary Information and Source Data files are available in the online version of the paper.

ACKNOWLEDGMENTS

We thank N. Roodur, M. Keita (Unité de Génétique Moléculaire, Hôpital Robert Debré) and L. Coste-Sarguet (INSERM UMR 1131) for expert technical assistance. We thank E. Martin, J.-P. Sarava and M. Letexier (Integrigen) for advice and assistance in whole-exome sequencing analysis. SNP array analyses were performed by the Plateforme de Génomique Constitutionnelle–Nord (PGC-Nord) (J. Soulier, S. Quentin and S. Drunat). We thank the technical team, and more particularly P. Aubin, from the Service de Biologie Cellulaire, Hôpital Saint Louis, for excellent technical help in the management of myeloid progenitor assays. We also thank S. Rasika for careful editing of the manuscript.

This work was supported by the Ligue contre le Cancer (LCC)–Ile-de-France, by the Société Française de Lutte contre les Cancers et Leucémies de l'Enfant (SFCE), the Association pour la Recherche et pour les Etudes dans les Maladies Infantiles Graves (AREMIG, Nancy) and the German Research Foundation (Deutsche Forschungsgemeinschaft, DFG) through the Collaborative Research Center 974 (SFB 974) Communication and Systems Relevance during Liver Injury and Regeneration and the International Graduate School of Protein Science and Technology (iGRASP).

AUTHOR CONTRIBUTIONS

A. Caye collected subject samples, participated in the study design, performed laboratory assays, analyzed data and wrote the manuscript. M.S. and J.L. performed analyses and collected clinical data. F.G. performed epigenetic studies, and B.C. and E.V. performed colony assays. S.G. performed biostatistical analyses. O.F. and E.L. performed the cytological review. K.N., S.N.-R., R.D., D.H. and M.R.A. performed the functional and biochemical RAC2 studies. J.V. collected clinical data. S.P. performed laboratory assays. D.V. performed NF1 diagnosis. J.-H.D., A.B., C. Pailard, C. Picard, C.G., A.P., Y.R., E.M., B.N., Y.B., M.P., D.A., N.S. and A. Contet contributed subject samples and clinical data. M.S., A.B., C.C., B.C. and M.R.A. reviewed the manuscript. H.C. collected subject samples, designed and coordinated the study, analyzed data and wrote the manuscript.

COMPETING FINANCIAL INTERESTS

The authors declare no competing financial interests.

Reprints and permissions information is available online at <http://www.nature.com/reprints/index.html>.

- Chang, T.Y., Dvorak, C.C. & Loh, M.L. Bedside to bench in juvenile myelomonocytic leukemia: insights into leukemogenesis from a rare pediatric leukemia. *Blood* **124**, 2487–2497 (2014).
- Niemeyer, C.M. *et al.* Chronic myelomonocytic leukemia in childhood: a retrospective analysis of 110 cases. European Working Group on Myelodysplastic Syndromes in Childhood (EWOG-MDS). *Blood* **89**, 3534–3543 (1997).
- Locatelli, F. & Niemeyer, C.M. How I treat juvenile myelomonocytic leukemia. *Blood* **125**, 1083–1090 (2015).
- Niemeyer, C.M. RAS diseases in children. *Haematologica* **99**, 1653–1662 (2014).
- Shlien, A. *et al.* Combined hereditary and somatic mutations of replication error repair genes result in rapid onset of ultra-hypermutated cancers. *Nat. Genet.* **47**, 257–262 (2015).
- Sakaguchi, H. *et al.* Exome sequencing identifies secondary mutations of *SETBP1* and *JAK3* in juvenile myelomonocytic leukemia. *Nat. Genet.* **45**, 937–941 (2013).
- Strullu, M. *et al.* Juvenile myelomonocytic leukaemia and Noonan syndrome. *J. Med. Genet.* **51**, 689–697 (2014).
- Niemeyer, C.M. *et al.* Germline *CBL* mutations cause developmental abnormalities and predispose to juvenile myelomonocytic leukemia. *Nat. Genet.* **42**, 794–800 (2010).
- Pérez, B. *et al.* Germline mutations of the *CBL* gene define a new genetic syndrome with predisposition to juvenile myelomonocytic leukaemia. *J. Med. Genet.* **47**, 686–691 (2010).
- Makishima, H. *et al.* Somatic *SETBP1* mutations in myeloid malignancies. *Nat. Genet.* **45**, 942–946 (2013).
- Brown, K.M. *et al.* Phosphodiesterase-8A binds to and regulates Raf-1 kinase. *Proc. Natl. Acad. Sci. USA* **110**, E1533–E1542 (2013).
- Flex, E. *et al.* Activating mutations in *RRAS* underlie a phenotype within the RASopathy spectrum and contribute to leukaemogenesis. *Hum. Mol. Genet.* **23**, 4315–4327 (2014).
- Shang, X. *et al.* R-Ras and Rac GTPase cross-talk regulates hematopoietic progenitor cell migration, homing, and mobilization. *J. Biol. Chem.* **286**, 24068–24078 (2011).
- Kawazu, M. *et al.* Transforming mutations of RAC guanosine triphosphatases in human cancers. *Proc. Natl. Acad. Sci. USA* **110**, 3029–3034 (2013).
- Emanuel, P.D. Hallway gossip between Ras and PI3K pathways. *Blood* **123**, 2751–2753 (2014).
- Goodwin, C.B. *et al.* PI3K p110 δ uniquely promotes gain-of-function Shp2-induced GM-CSF hypersensitivity in a model of JMML. *Blood* **123**, 2838–2842 (2014).
- Worfeld, T. *et al.* Genetic dissection of plexin signaling *in vivo*. *Proc. Natl. Acad. Sci. USA* **111**, 2194–2199 (2014).
- Innocenti, M. *et al.* Phosphoinositide 3-kinase activates Rac by entering in a complex with Eps8, Ahi1, and Sos-1. *J. Cell Biol.* **160**, 17–23 (2003).
- Offenhäuser, N. *et al.* The eps8 family of proteins links growth factor stimulation to actin reorganization generating functional redundancy in the Ras/Rac pathway. *Mol. Biol. Cell* **15**, 91–98 (2004).
- Cutts, B.A. *et al.* *Nf1* deficiency cooperates with oncogenic K-RAS to induce acute myeloid leukemia in mice. *Blood* **114**, 3629–3632 (2009).

21. Xu, J. *et al.* Dominant role of oncogene dosage and absence of tumor suppressor activity in *Nras*-driven hematopoietic transformation. *Cancer Discov.* **3**, 993–1001 (2013).
22. Wang, J. *et al.* Endogenous oncogenic *Nras* mutation initiates hematopoietic malignancies in a dose- and cell type-dependent manner. *Blood* **118**, 368–379 (2011).
23. Khan, S.N. *et al.* Multiple mechanisms deregulate EZH2 and histone H3 lysine 27 epigenetic changes in myeloid malignancies. *Leukemia* **27**, 1301–1309 (2013).
24. Son, J., Shen, S.S., Margueron, R. & Reinberg, D. Nucleosome-binding activities within JARID2 and EZH1 regulate the function of PRC2 on chromatin. *Genes Dev.* **27**, 2663–2677 (2013).
25. Kinkel, S.A. *et al.* Jarid2 regulates hematopoietic stem cell function by acting with Polycomb repressive complex 2. *Blood* **125**, 1890–1900 (2015).
26. Ciferri, C. *et al.* Molecular architecture of human Polycomb repressive complex 2. *eLife* **1**, e00005 (2012).
27. Puda, A. *et al.* Frequent deletions of *JARID2* in leukemic transformation of chronic myeloid malignancies. *Am. J. Hematol.* **87**, 245–250 (2012).
28. Zhang, Y. *et al.* Corepressor protein CDYL functions as a molecular bridge between Polycomb repressor complex 2 and repressive chromatin mark trimethylated histone lysine 27. *J. Biol. Chem.* **286**, 42414–42425 (2011).
29. Abdel-Wahab, O. *et al.* *ASXL1* mutations promote myeloid transformation through loss of PRC2-mediated gene repression. *Cancer Cell* **22**, 180–193 (2012).
30. Abdel-Wahab, O. & Levine, R.L. Mutations in epigenetic modifiers in the pathogenesis and therapy of acute myeloid leukemia. *Blood* **121**, 3563–3572 (2013).
31. Kim, E. *et al.* *SRSF2* mutations contribute to myelodysplasia by mutant-specific effects on exon recognition. *Cancer Cell* **27**, 617–630 (2015).
32. Huether, R. *et al.* The landscape of somatic mutations in epigenetic regulators across 1,000 paediatric cancer genomes. *Nat. Commun.* **5**, 3630 (2014).
33. Yang, F. PRC2 dysfunction through multiple mechanisms in myeloid malignancies. *Epigenomics* **5**, 481 (2013).
34. Pasini, D. *et al.* Characterization of an antagonistic switch between histone H3 lysine 27 methylation and acetylation in the transcriptional regulation of Polycomb group target genes. *Nucleic Acids Res.* **38**, 4958–4969 (2010).
35. Leiserson, M.D. *et al.* Pan-cancer network analysis identifies combinations of rare somatic mutations across pathways and protein complexes. *Nat. Genet.* **47**, 106–114 (2015).
36. Lee, W. *et al.* PRC2 is recurrently inactivated through EED or SUZ12 loss in malignant peripheral nerve sheath tumors. *Nat. Genet.* **46**, 1227–1232 (2014).
37. Zhang, M. *et al.* Somatic mutations of *SUZ12* in malignant peripheral nerve sheath tumors. *Nat. Genet.* **46**, 1170–1172 (2014).
38. De Raedt, T. *et al.* PRC2 loss amplifies Ras-driven transcription and confers sensitivity to BRD4-based therapies. *Nature* **514**, 247–251 (2014).
39. Jaiswal, S. *et al.* Age-related clonal hematopoiesis associated with adverse outcomes. *N. Engl. J. Med.* **371**, 2488–2498 (2014).
40. Genovese, G. *et al.* Clonal hematopoiesis and blood-cancer risk inferred from blood DNA sequence. *N. Engl. J. Med.* **371**, 2477–2487 (2014).
41. Jacobs, K.B. *et al.* Detectable clonal mosaicism and its relationship to aging and cancer. *Nat. Genet.* **44**, 651–658 (2012).
42. Laurie, C.C. *et al.* Detectable clonal mosaicism from birth to old age and its relationship to cancer. *Nat. Genet.* **44**, 642–650 (2012).
43. Locatelli, F. *et al.* Hematopoietic stem cell transplantation (HSCT) in children with juvenile myelomonocytic leukemia (JMML): results of the EWOG-MDS/EBMT trial. *Blood* **105**, 410–419 (2005).
44. Takagi, M. *et al.* Autoimmunity and persistent RAS-mutated clones long after the spontaneous regression of JMML. *Leukemia* **27**, 1926–1928 (2013).
45. Matsuda, K. *et al.* Spontaneous improvement of hematologic abnormalities in patients having juvenile myelomonocytic leukemia with specific RAS mutations. *Blood* **109**, 5477–5480 (2007).
46. Matsuda, K. *et al.* Acquisition of loss of the wild-type *NRAS* locus with aggressive disease progression in a patient with juvenile myelomonocytic leukemia and a heterozygous *NRAS* mutation. *Haematologica* **92**, 1576–1578 (2007).
47. Kato, M. *et al.* Aggressive transformation of juvenile myelomonocytic leukemia associated with duplication of oncogenic *KRAS* due to acquired uniparental disomy. *J. Pediatr.* **162**, 1285–1288 (2013).
48. Kalra, R., Paderanga, D.C., Olson, K. & Shannon, K.M. Genetic analysis is consistent with the hypothesis that NF1 limits myeloid cell growth through p21ras. *Blood* **84**, 3435–3439 (1994).

¹INSERM UMR 1131, Institut Universitaire d'Hématologie, Paris, France. ²Université Paris Diderot, Paris Sorbonne Cité, Paris, France. ³Assistance Publique des Hôpitaux de Paris (AP-HP), Hôpital Robert Debré, Département de Génétique, Paris, France. ⁴Assistance Publique des Hôpitaux de Paris (AP-HP), Hôpital Saint Louis, Service de Biologie Cellulaire, Paris, France. ⁵Assistance Publique des Hôpitaux de Paris (AP-HP), Plateforme de Génétique Constitutionnelle-Nord (PfGC-Nord), Paris, France. ⁶INSERM UMR 1137, Infection Antimicrobienne Modelling and Evolution (IAME) Laboratory, Paris, France. ⁷Assistance Publique des Hôpitaux de Paris (AP-HP), Hôpital Robert Debré, Service d'Hématologie Biologique, Paris, France. ⁸Institute of Biochemistry and Molecular Biology II, Medical Faculty of the Heinrich Heine University, Düsseldorf, Germany. ⁹Equipe d'Accueil 7331, Université Paris Descartes, Sorbonne Paris Cité, Faculté de Pharmacie de Paris, Paris, France. ¹⁰Assistance Publique des Hôpitaux de Paris (AP-HP), Hôpital Cochin, Service de Biochimie Génétique, Paris, France. ¹¹Assistance Publique des Hôpitaux de Marseille (AP-HM), Hôpital de la Timone, Service d'Hématologie Pédiatrique, Marseille, France. ¹²Assistance Publique des Hôpitaux de Paris (AP-HP), Hôpital Necker-Enfants Malades Paris, Centre d'Etudes des Déficits Immunitaires, Immuno-Hematology Unit, Paris, France. ¹³Université Paris Descartes, Paris Sorbonne Cité, Paris, France. ¹⁴INSERM UMR 1163, Institut Imagine, Laboratory of Human Genetics of Infectious Diseases, Paris, France. ¹⁵Assistance Publique des Hôpitaux de Paris (AP-HP), Hôpital Armand Trousseau, Service d'Hématologie Oncologie Pédiatrique, Paris, France. ¹⁶Hôpital d'Enfants de Brabois, Service d'Onco-Hématologie Pédiatrique, Vandoeuvre lès Nancy, France. ¹⁷Hôpital l'Archet, Service d'Onco-Hématologie Pédiatrique, Nice, France. ¹⁸Centre Hospitalier Universitaire (CHU) de Montpellier, Service d'Onco-Hématologie Pédiatrique, Montpellier, France. ¹⁹CHU de Nantes, Service d'Onco-Hématologie Pédiatrique, Nantes, France. ²⁰CHU de Grenoble, Service d'Onco-Hématologie Pédiatrique, Grenoble, France. ²¹Hôpital de Haute-pierre, Service de Pédiatrie, Strasbourg, France. ²²CHU de Lille, Unité d'Hématologie Pédiatrique, Lille, France. ²³Centre Hospitalier Félix Guyon, Saint-Denis, La Réunion, France. ²⁴Institut d'Hémo-Oncologie Pédiatrique (IHOP), Département d'Immunologie et Hématologie Pédiatrique, Lyon, France. ²⁵Clinic of Gastroenterology, Hepatology and Infectious Diseases, Medical Faculty of the Heinrich Heine University, Düsseldorf, Germany. ²⁶Assistance Publique des Hôpitaux de Paris (AP-HP), Hôpital Robert Debré, Service d'Hématologie Pédiatrique, Paris, France. Correspondence should be addressed to H.C. (helene.cave@rdp.aphp.fr).

ONLINE METHODS

Patients. The study included 118 patients with JMML consecutively referred to our laboratory between 1995 and 2014, for whom a RAS-activating mutation was identified as part of the routine diagnostic workup (**Supplementary Note**).

All patients fulfilled the consensus JMML criteria reported recently by Chan *et al.*⁴⁹. Centralized cytomorphological review was performed on bone marrow and blood samples. Measurement of fetal hemoglobin (HbF) dosage and karyotyping were systematically performed using standard procedures.

Diagnosis with JMML was based on clinical and hematological findings, cytomorphological examination of blood and bone marrow smears, *in vitro* growth of myeloid progenitors and mutation screening of DNA obtained from the leukemia sample.

A somatically acquired RAS-activating mutation was identified at diagnosis in 78 of 118 (66%) patients in the following genes: *PTPN11* ($n = 38$), *KRAS* ($n = 18$) and *NRAS* ($n = 22$). JMML cases were classified according to these initial lesions as *PTPN11*-JMML, *KRAS*-JMML and *NRAS*-JMML, respectively. In 40 of 118 (34%) cases, JMML was syndromic with a germline *PTPN11* mutation consistent with Noonan syndrome features ($n = 22$), a germline *CBL* mutation consistent with CBL syndrome ($n = 11$) or molecularly confirmed *NF1* ($n = 8$) (**Supplementary Fig. 3** and **Supplementary Table 5**). The sex ratio (males/females) was 2.1. The median age at diagnosis was 18 months. Seventy-eight of 118 (66%) patients received bone marrow transplantation. Blast excess was defined as a blast count $\geq 10\%$ but $< 20\%$ in the bone marrow at diagnosis. Blast crisis was defined as a blast count $\geq 20\%$ in the bone marrow. Two patients with sporadic JMML were lost to follow-up.

Samples. Peripheral blood and/or bone marrow aspirates were collected on EDTA at diagnosis. Non-hematopoietic tissues (fibroblasts, nails or hair follicles) were also collected. Genomic DNA was extracted using a Qiagen Mini or Midi kit.

To use minimal amounts of native DNA, all diagnostic DNA samples underwent whole-genome amplification using the RepliG Midi kit (Qiagen) according to the manufacturer's instructions.

Diagnostic workup. Mutational screening using bidirectional Sanger sequencing of exons and their flanking intron-exon boundaries was performed on genomic DNA as part of the classic diagnostic workup for JMML and included analysis of *NRAS* exons 2 and 3 (NM_002524.4), *KRAS* exons 2 and 3 (NM_033360.3), *PTPN11* exons 3 and 13 (NM_002834.3) and *CBL* exons 8 and 9 (NM_005188.3). Genes recently shown to be involved in JMML (*ASXL1* exon 14 (NM_015338.5) and the *SETBP1* sequence in exon 6 encoding the SKI-homologous region (NM_015559.2)) were also systematically screened by Sanger sequencing as previously described⁵⁰. The germline origin of mutations was tested using constitutional DNA. Microsatellite analysis of the 17p region encompassing *NF1* was performed as previously described⁵⁰. Primer sequences are given in **Supplementary Table 8**.

Genome-wide DNA array analysis. Genomic DNA from 78 leukemia samples was analyzed by SNP array technologies using the Genome-Wide GeneChip Human SNP Array 6.0 (Affymetrix) ($n = 63$) and/or by high-density array comparative genomic hybridization (CGH) technologies using the 4 \times 180M Microarray SurePrint G3 Catalog (Agilent Technologies) ($n = 16$), according to the manufacturers' recommendations. Analyses were performed using CytoGenomics (Agilent Technologies) for array CGH data and Genomic Suite 6.5 software (Partek) and the hidden Markov model and segmentation algorithms for the analysis of both CNVs and LOH. The final abnormalities retained were validated by visual analysis, considering the sizes and \log_2 (ratios) of the abnormalities with respect to the individual background noise of each array at each particular chromosomal location. Polymorphic CNVs were excluded using the Database of Genomic Variants track in the UCSC Genome Browser in Cartagenia Bench Lab CNV software. Human genome assembly GRCh37/hg19 was used as a reference. Final validated data are provided in **Supplementary Table 3**.

Whole-exome sequencing. Targeted enrichment and massively parallel sequencing were performed on paired genomic DNA samples from leukocytes and fibroblasts. Exome capture was carried out using SureSelect Human All

Exon v4+UTRs (Agilent Technologies), and sequencing was performed with a HiSeq 2000 instrument (Illumina). Image analysis and base calling were performed using the Real-Time Analysis (RTA) pipeline, v. 1.14 (Illumina). Alignment of paired-end reads to the reference human genome (UCSC GRCh37/hg19), variant calling and generation of quality scores for variants were carried out using the CASAVA v.1.8 pipeline (Illumina).

Variant annotation, SNP filtering and patient-matched germline variant filtering were achieved using an in-house pipeline by IntegraGen. Gene and transcript names, strand and position (intron, 5' UTR, 3' UTR, etc.) were reported for each variant. Nucleotide, codon and amino acid changes as well as functional class (synonymous, missense, nonsense, splice site, etc.) were reported for coding variants. Annotation content was compiled from several sources: 1000 Genomes Project, dbSNP rsID and frequencies from the IntegraGen Exome Database, which comprises 200 reference exomes. Finally, germline and tumoral genotypes were compared to determine the somatic nature of each variant. Only positions that were present in both files and met the minimum coverage requirement ($\geq 6\times$) were compared. The significance of the allele frequency difference (as a *P* value) was calculated by Fisher's exact test for each variant, taking into account the counts of the mutated allele in both samples. A somatic score was calculated for each variant (from 1 to 30, with 30 indicating the highest confidence). The somatic variant caller handled indels similarly, determining the number of alignments covering a given position that included a particular indel (variant count) versus the overall coverage at that position. Yield per exome ranged between 3.64 and 7.17 Mb (mean of 4.78 Mb). Mean coverage per sample is given in **Supplementary Figure 10**.

Known polymorphisms reported at a frequency $> 0.1\%$ in at least one of the above-mentioned databases, low-coverage variants (< 10 reads in germline and/or tumoral samples) and low-quality variants (Q variant score from IntegraGen ≤ 30) were systematically excluded. Only variants with a probable impact at the protein level (nonsynonymous exonic variants and abnormalities located at intron-exon junctions) were considered for further analysis. All putative somatic events (absent in the germline sample but acquired in tumoral DNA or heterozygous in the germline sample but homozygous in the tumoral sample) were verified by conventional Sanger sequencing and searched for in constitutional DNA, when available.

The previous involvement of confirmed somatic variants in cancer was verified by consulting the Catalogue of Somatic Mutations in Cancer (COSMIC). Prediction of the effects of amino acid substitutions on the function and structure of proteins was achieved using dedicated prediction software: Scale-Invariant Feature Transform (SIFT), MutationTaster and PolyPhen-2. Final validated data are provided in **Supplementary Table 2**.

High-throughput targeted sequencing. High-throughput targeted sequencing by multiplex PCR was performed on whole genome-amplified tumoral DNA diluted 1:5. The coding regions of 38 genes were targeted. The complete list of targeted genes and their corresponding sequencing performance are available in **Supplementary Figure 11** and **Supplementary Table 4**. Primer pairs were designed with the IntegraGen internal pipeline (**Supplementary Table 8**). DNA samples were amplified on an Access Array system (Fluidigm) and subjected to six additional PCR cycles to add specific barcodes and P5 and P7 adaptors. An equimolar pool of all PCR products was sequenced on the MiSeq instrument (Illumina), with MiSeq Reagent Kit V2 cycles and paired-end 2 \times 150 bases. Image analysis and base calling, alignment of reads to the reference human genome, variant calling, variant annotation and subsequent mutational analysis were performed as for whole-exome sequencing. All identified variants were verified in native tumoral DNA and searched for by Sanger sequencing in constitutional DNA, when available.

Sanger sequencing. PCR was performed using the GoTaq DNA Polymerase kit (Promega) or the FastStart Taq DNA Polymerase kit (Roche) according to the manufacturer's instructions. Primer sequences for Sanger sequencing performed in the whole JMML cohort are provided in **Supplementary Table 8**. Primer sequences used for control variants found by whole-exome sequencing and high-throughput targeted sequencing are available on request. PCR products were purified using the Illustra ExoStar 1-Step kit (GE Healthcare, Life Sciences), and direct sequencing was performed using the BigDye Terminator Ready Reaction Cycle Sequencing kit (Applied Biosystems). Reaction products

were run on an automated capillary sequencer (ABI 3130 Genetic Analyzer, Applied Biosystems). Sequences were aligned using Seqscape analysis software (Applied Biosystems) or visualized on Chromas software (Technelysium) and were compared with the reference sequences for genomic DNA.

Myeloid progenitor cell growth and genetic testing. *In vitro* growth assays of myeloid progenitors were performed by plating bone marrow and/or peripheral blood mononucleated cells in semisolid methylcellulose with or without leukocyte-conditioned medium (cytokine medium, LCM, Stemcell Technologies), as previously described⁵⁰. Colonies (aggregates containing >50 cells) were scored on days 11 and 14 after plating.

Targeted sequencing of isolated colonies. Colonies obtained from the *in vitro* growth of myeloid progenitors were picked and resuspended in 100 μ l of sterile water. Isolated colonies were lysed with proteinase K (10 μ g) in 50 μ l of lysis buffer (50 mM KCl, 10 mM Tris-HCl, pH 8, 2.5 mM MgCl₂, 0.45% NP-40 and 0.45% Tween-20). Sanger direct sequencing was performed as described above. Genetic screening was restricted to colonies obtained from JMML cases displaying at least two somatically acquired genetic lesions ($n = 6$, with 8–93 colonies successfully screened per patient).

RAC2 constructs. Different variants of the pGEX vector (pGEX2T and pGEX4T-1) encoding N-terminal GST were used for the overexpression of wild-type RAC2, Asp63Val RAC2, the GBD of PAK1 (amino acids 57–141), the catalytic domains of TIAM1 (DH-PH; amino acids 1033–1404) and p50^{GAP} (a GAP; amino acids 198–439). To generate RAC2 constructs with mutation, wild-type RAC2 in pGEX4T-1 and pcDNA3.1 vectors was used as the template and the mutation encoding p.Asp63Val was generated by PCR-based site-directed mutagenesis as described⁵¹.

Proteins. All proteins were purified as GST fusion proteins from *Escherichia coli* as previously described^{52–56}. The GST tag was cleaved off with purified tobacco etch virus (Tev) protease and removed by reverse glutathione affinity purification in the case of the RAC2 proteins. Nucleotide-free RAC2 proteins were prepared using alkaline phosphatase (Roche) and phosphodiesterase (Sigma-Aldrich) at 4 °C, as described⁵⁴. Fluorescent methylantraniloyl (mant) and tetramethylrhodamine (tamra) were used to generate fluorescent mantGDP-, mantGppNHp- and tamraGTP-bound RAC2 proteins.

Fluorescence polarization. Experiments were performed in a Fluoromax 4 fluorometer in polarization mode as previously described⁵⁷. Briefly, an increasing amount of GST-PAK GBD was titrated into mantGppNHp-bound wild-type and Asp63Val RAC2 (1 μ M) in a buffer containing 30 mM Tris-HCl, pH 7.5, 150 mM NaCl, 5 mM MgCl₂ and 1 mM Tris-(2-carboxyethyl) phosphine (TCEP) in a total volume of 200 μ l at 25 °C. The dissociation constant (K_d) was calculated by fitting the concentration-dependent binding curve using a quadratic ligand-binding equation.

Fluorescence measurements. Kinetic measurements of intrinsic and GEF-catalyzed nucleotide exchange and of intrinsic and GAP-stimulated GTP hydrolysis for wild-type and Asp63Val RAC2 were monitored by stopped-flow apparatus (Hi-Tech Scientific SF-61 with a mercury xenon light source and TgK Scientific Kinetic Studio software) and performed as described^{52–54}. The observed rate constants (K_{obs}) were fitted single exponentially using the GraFit program (Erithacus software)⁵².

Pulldown assays and immunoblotting. Sequences encoding human wild-type, Gly12Val and Asp63Val RAC2, Gly12Val NRAS, Gly12Val HRAS and Gly12Val KRAS were cloned into pcDNA3.1, and constructs were overexpressed in COS-7 cells (ACC-60, Deutsche Sammlung von Mikroorganismen und Zellkulturen (DSMZ); cells were tested for mycoplasma by the DSMZ and used freshly) for 48 h. Cells were lysed with fish buffer (50 mM Tris-HCl, pH 7.5, 100 mM NaCl, 2 mM MgCl₂, 1% Igepal CA-630, 10% glycerol, 20 mM β -glycerophosphate, 1 mM sodium orthovanadate and one EDTA-free inhibitor tablet). GST-fused PAK1 GBD (amino acids 57–141) was expressed in *E. coli* for 4 h at 37 °C, and total bacterial proteins were released by sonication.

The bacterial lysates were incubated with glutathione-conjugated beads for 30 min, and beads were washed three times with fish buffer. The total cell lysates from COS-7 cells were divided into two parts. One part was added to the GST-PAK1 GBD/glutathione-conjugated bead complex for 30 min, and beads were washed three times with fish buffer. The second part was used to check the activity of the PI3K-AKT-mTORC and RAF-MEK1/2-ERK1/2 cascades in transfected cells by immunoblotting. Immunoblotting was carried out using rabbit antibody to FLAG (F7425, Sigma-Aldrich), mouse antibody to α -actin (MAB1510), and rabbit antibodies to MEK1/2 (9126), phosphorylated MEK1/2 (Ser217/Ser221, 9154), ERK1/2 (9102), phosphorylated ERK1/2 (Thr202/Thr204, 9106), AKT (9272) and phosphorylated AKT (Ser473, 4060 and Thr308, 2965) from Cell Signaling Technology as described⁵⁸.

Structural analysis. Interaction interfaces for RAC GTPases were analyzed on base RAC1 structures for RAC1 in complex with TIAM1 (ref. 59; Protein Data Bank (PDB) 1FOE) and with PAK1 (ref. 60). As there is no complex structure for any RAC GTPase interacting with a GAP, the corresponding interaction interface was deduced from the structure of Cdc42 in complex with Cdc42GAP⁶¹. Interacting residues were considered to be amino acids from GTPases that had at least one atom within 4.0 Å of the interacting protein. Individual as well as overlapping interaction surfaces were finally projected onto the molecular surface of RAC1 in the active, GTP-bound state using the program PyMOL (PyMOL Molecular Graphics System, version 1.7.4, Schrödinger).

Immunofluorescence and confocal microscopy. Cells were cytospun onto polylysine-coated slides, fixed in 4% paraformaldehyde for 15 min at room temperature and permeabilized with 0.3% Triton in PBS for 15 min at room temperature, washed twice for 5 min each wash in PBS and incubated in blocking buffer (1% BSA in PBS) for 1 h at room temperature. Cells were then incubated with mouse monoclonal antibody to histone H3 (H3K27me3, Abcam, 6002; following the manufacturer's instructions) for 1 h at room temperature, followed by three 5-min washes in PBS. Secondary Alexa Fluor 488-conjugated goat anti-mouse IgG (Life Technologies, A11001) was then applied for 1 h. The second incubation was identical to the first one, using as primary antibody rabbit polyclonal antibody to histone H3 (H3K27ac, Abcam, Ab4729) and as secondary antibody Alexa Fluor 594-conjugated goat anti-rabbit IgG (Life Technologies, A11012). Cells were subsequently washed three times for 5 min each wash in PBS and were then mounted in SlowFade Gold Antifade Reagent with DAPI (Life Technologies, S36939), coverslips were sealed with nail varnish and slides were visualized using the Zeiss LSM 510 confocal system. The SKM-1 and K562 myeloid cell lines were purchased from DSMZ and the American Type Culture Collection (ATCC), respectively. The presence of an *EZH2* mutation encoding p.Tyr646Cys (COSMIC, 37032) was checked, with the mutation found to be homozygous, by Sanger sequencing (data not shown).

Statistical methods. Statistical analyses were performed with R version 3.1.2. Fisher's exact test was used to determine whether different groups of cases were significantly different with respect to the number of individuals with somatic alterations. Overall survival was calculated from the date of diagnosis to the date of death. Distribution of overall survival in the different groups of cases was estimated by the Kaplan-Meier technique implemented in the survival library of R. Tabular data for survival curves are given in **Supplementary Table 9**.

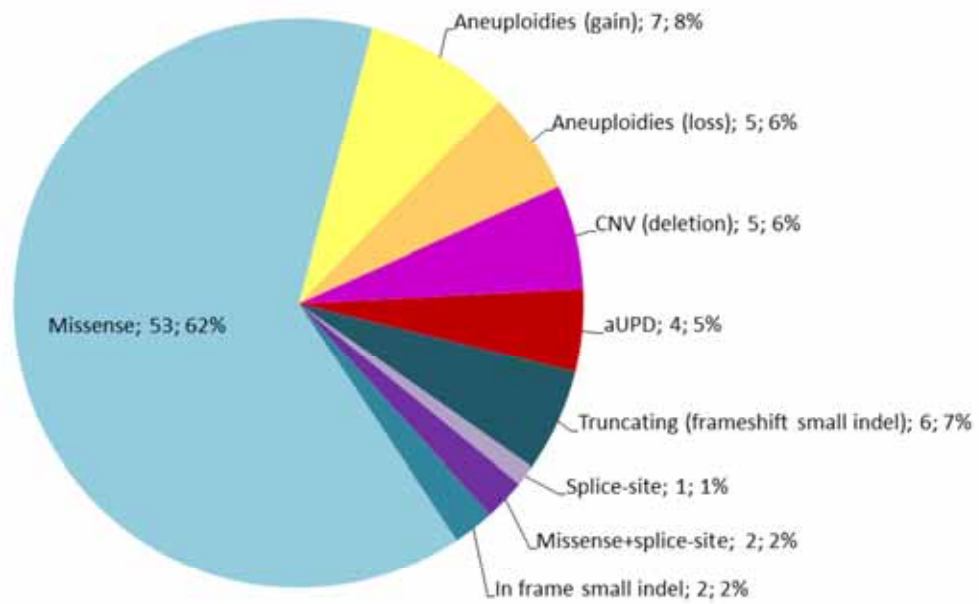
The differences between the Kaplan-Meier curves for different groups of cases were tested using the two-tailed Mantel-Haenszel log-rank test.

49. Chan, R.J., Cooper, T., Kratz, C.P., Weiss, B. & Loh, M.L. Juvenile myelomonocytic leukemia: a report from the 2nd International JMML Symposium. *Leuk. Res.* **33**, 355–362 (2009).

50. Pérez, B. *et al.* Genetic typing of *CBL*, *ASXL1*, *RUNX1*, *TET2* and *JAK2* in juvenile myelomonocytic leukaemia reveals a genetic profile distinct from chronic myelomonocytic leukaemia. *Br. J. Haematol.* **151**, 460–468 (2010).

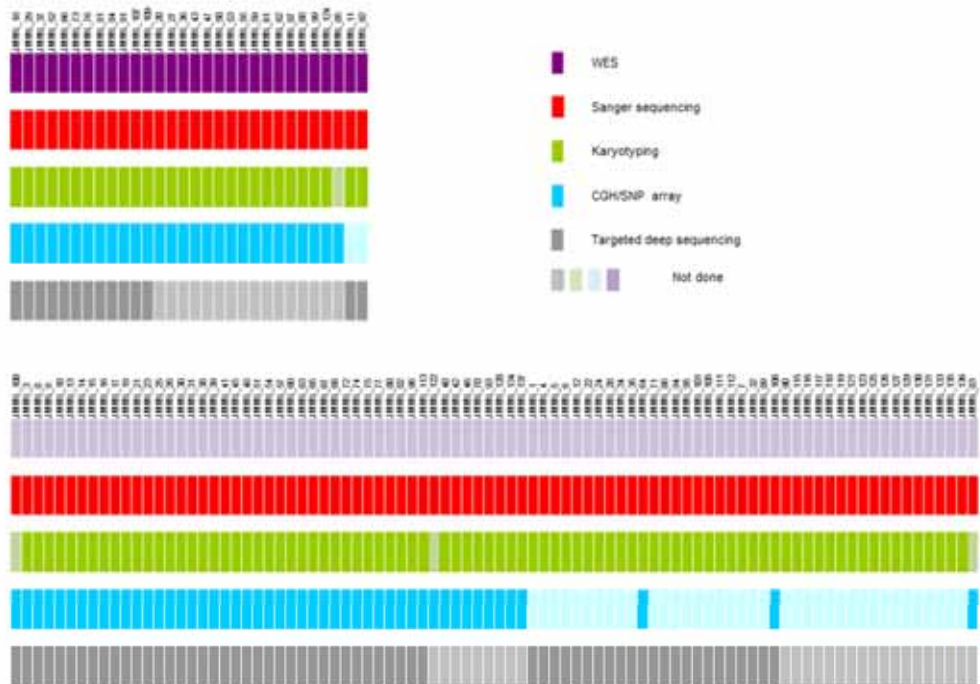
51. Ahmadian, M.R., Stege, P., Scheffzek, K. & Wittinghofer, A. Confirmation of the arginine-finger hypothesis for the GAP-stimulated GTP-hydrolysis reaction of Ras. *Nat. Struct. Biol.* **4**, 686–689 (1997).

52. Hemsath, L. & Ahmadian, M.R. Fluorescence approaches for monitoring interactions of Rho GTPases with nucleotides, regulators, and effectors. *Methods* **37**, 173–182 (2005).
53. Eberth, A. & Ahmadian, M.R. *In vitro* GEF and GAP assays. *Curr. Protoc. Cell Biol.* Chapter 14, Unit 14.9 (2009).
54. Jaiswal, M., Dubey, B.N., Koessmeier, K.T., Gremer, L. & Ahmadian, M.R. Biochemical assays to characterize Rho GTPases. *Methods Mol. Biol.* **827**, 37–58 (2012).
55. Eberth, A. *et al.* A BAR domain-mediated autoinhibitory mechanism for RhoGAPs of the GRAF family. *Biochem. J.* **417**, 371–377 (2009).
56. Jaiswal, M., Dubey, B.N., Koessmeier, K.T., Gremer, L. & Ahmadian, M.R. Biochemical assays to characterize Rho GTPases. *Methods Mol. Biol.* **827**, 37–58 (2012).
57. Gremer, L. *et al.* Germline *KRAS* mutations cause aberrant biochemical and physical properties leading to developmental disorders. *Hum. Mutat.* **32**, 33–43 (2011).
58. Nakhai-Rad, S. *et al.* The function of embryonic stem cell-expressed RAS (E-RAS), a unique RAS family member, correlates with its additional motifs and its structural properties. *J. Biol. Chem.* **290**, 15892–15903 (2015).
59. Worthylake, D.K., Rossman, K.L. & Sondek, J. Crystal structure of Rac1 in complex with the guanine nucleotide exchange region of Tiam1. *Nature* **408**, 682–688 (2000).
60. Morreale, A. *et al.* Structure of Cdc42 bound to the GTPase binding domain of PAK. *Nat. Struct. Mol. Biol.* **7**, 384–388 (2000).
61. Nassar, N., Hoffman, G.R., Manor, D., Clardy, J.C. & Cerione, R.A. Structures of Cdc42 bound to the active and catalytically compromised forms of Cdc42GAP. *Nat. Struct. Biol.* **5**, 1047–1052 (1998).

**Supplementary Figure 1**

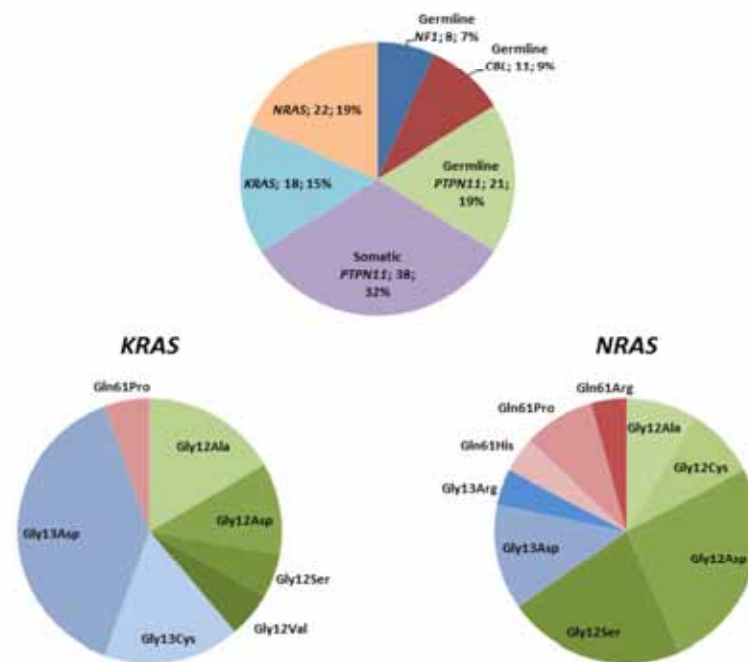
Spectrum of somatically acquired mutations identified by combining WES and genome-wide DNA array analysis in the discovery cohort of 30 JMML cases.

A total of 85 somatically acquired alterations were found, including 64 nonsynonymous point mutations or small insertion-deletions (indels) identified in the coding regions of these tumors by WES and 21 somatic cytogenetic alterations evidenced by SNP/CGH array, WES and/or metaphase cytogenetics.

**Supplementary Figure 2**

Graphical representation of the type of data obtained by sample in a cohort of 118 patients with JMML.

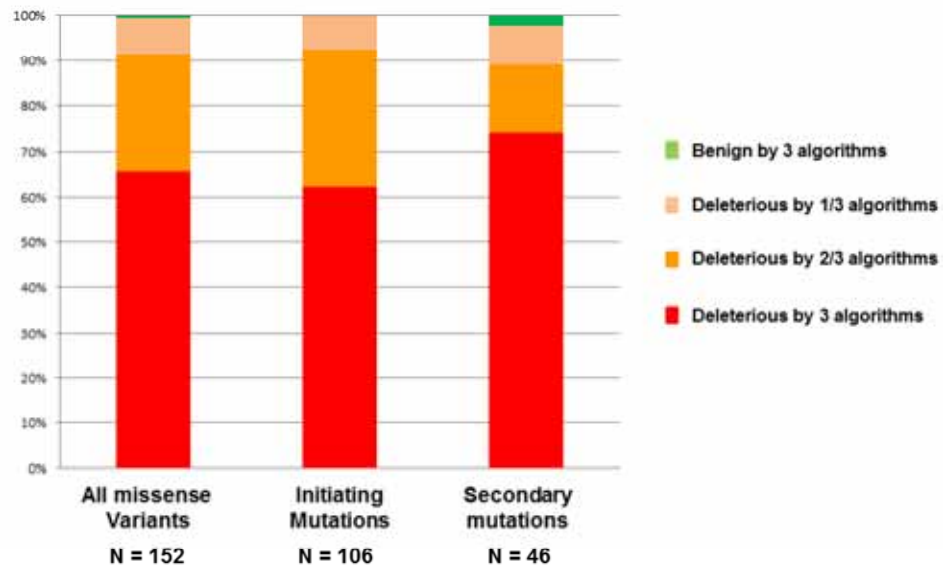
Both the discovery cohort (top; $n = 30$) and validation cohort (bottom; $n = 88$) are represented.



Supplementary Figure 3

Distribution of RAS-related mutations in a cohort of 118 patients with JMML as detected by routine workup.

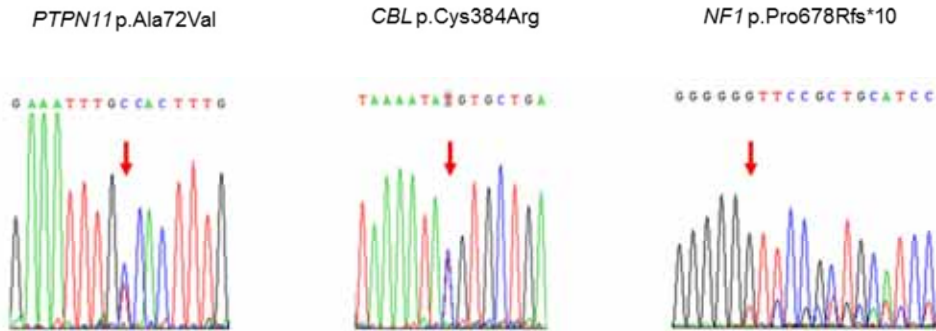
Distribution of RAS-related mutations in 118 consecutively diagnosed JMML cases as detected by routine workup and detailed spectrum of *KRAS* ($n = 18$) and *NRAS* ($n = 22$) mutations.



Supplementary Figure 5

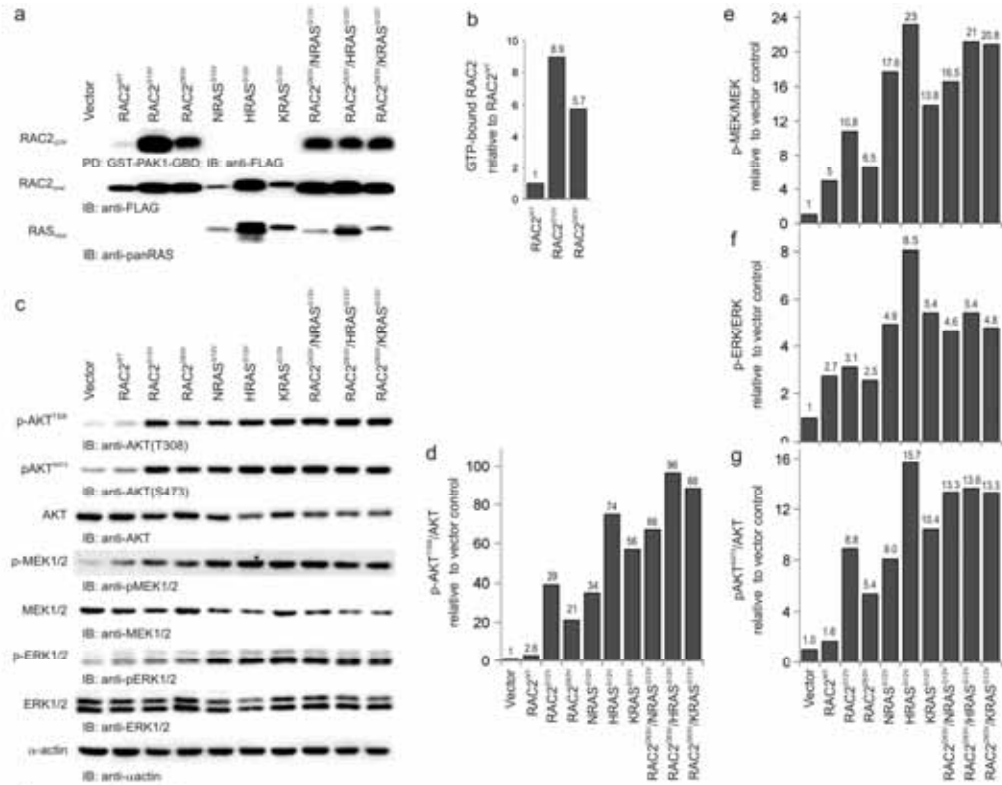
Proportion of mutations predicted to be deleterious versus non-pathogenic substitutions.

The pathogenicity of somatic nonsynonymous exonic missense variants with respect to gene function was predicted using the SIFT, PolyPhen-2 and MutationTaster algorithms (**Supplementary Table 6**). A total of 91% of all missense mutations were predicted to result in functionally relevant alterations by at least two of the three methods used for functional prediction. This percentage was similar when considering only initiating mutations, known to be deleterious in all cases (92%), as well as secondary mutations (89%).

**Supplementary Figure 6**

Sequence electrophoregram showing the presence of three concomitant mutations targeting the RAS pathway at diagnosis of JMML_89.

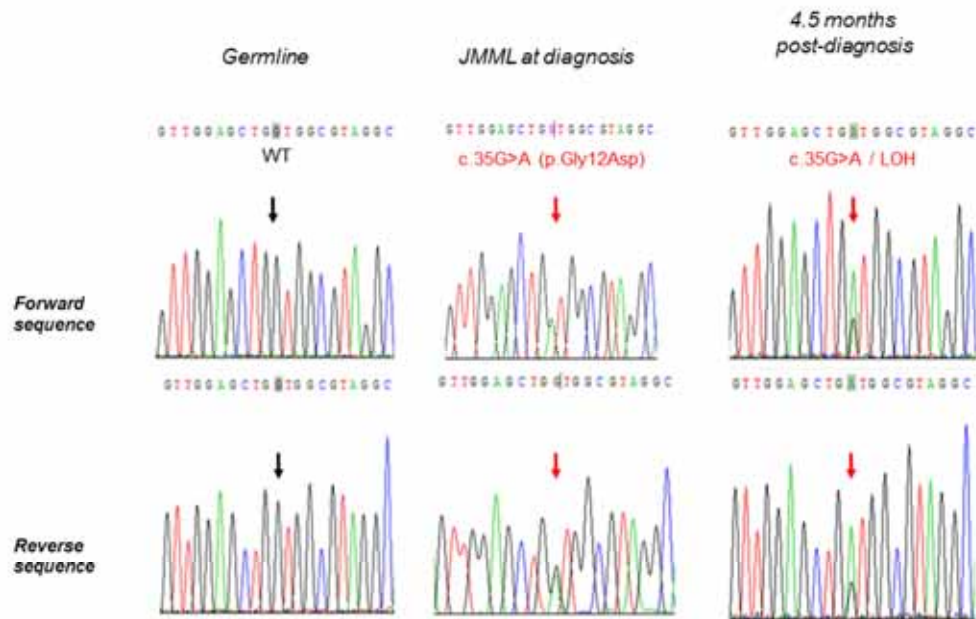
Mutated nucleotides are indicated by a red arrow. The subclonal pattern of *NF1* mutation is consistent with late acquisition. *NF1* haploinsufficiency was due to a recurrent c.2033delG mutation of a G homopolymer within the *NF1* coding region (exon 18). The frequency of this mutation appeared strikingly higher among somatic variants (5/6 cases with a secondary *NF1* mutation) than among germline variants (Leiden Open Variation Database, LOVD).



Supplementary Figure 7

Hyperactive RAC2 Asp63Val contributes to AKT activation via both the PI3K-PDK1 and mTORC2 cascades.

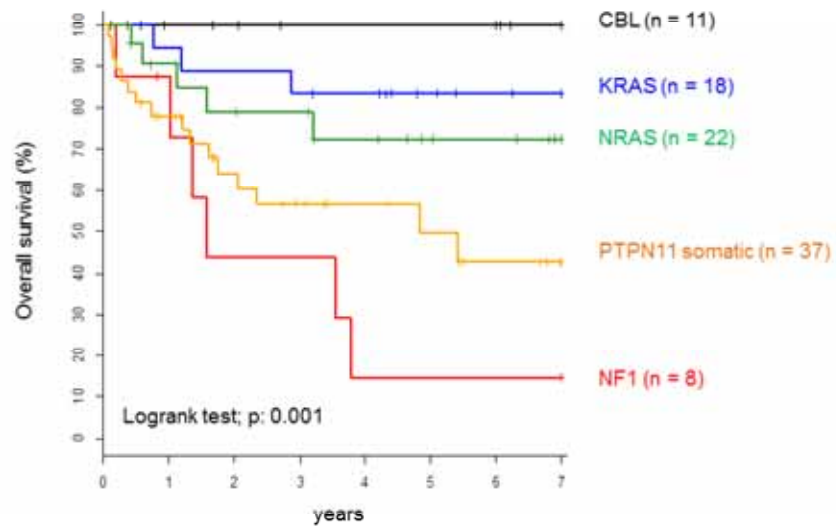
Pull-down experiments (a,b) and immunoblot (IB) analysis were conducted using total cell lysates (c–g) derived from transfected COS-7 cells with FLAG-tagged RAC2 and RAS variants. The GTPase-binding domain (GBD) of the RAC effector PAK1 was used as a GST fusion protein for the pull-down experiment. All experiments were performed three times. (a) Pull-down analysis showed that RAC2 Asp63Val largely exists in an active, GTP-bound state as compared to wild-type RAC2 (RAC2 WT), but activation is not as strong as for constitutively active RAC2 Gly12Val. Total RAC2 and RAS proteins were detected using antibody to FLAG and pan-RAS antibody to show the total amounts of the transfected FLAG-tagged RAC2 and RAS variants. (b) The RAC2 protein bands in a were densitometrically quantified (depicted as numbers and bars) as the amount of the GTP-bound RAC2 protein relative to wild-type RAC2. Coexpression of constitutively active NRAS Gly12Val, HRAS Gly12Val and KRAS Gly12Val did not change the level of GTP-bound RAC2 Asp63Val. (c) Total cell lysates were analyzed for the phosphorylation levels of AKT (pAKT 308 and pAKT 473), MEK1/2 (pMEK1/2) and ERK1/2 (pERK1/2). Total amounts of these kinases were used as loading controls. AKT is phosphorylated at Thr308 by the PI3K-PDK1 pathway, whereas the mTORC2 complex phosphorylates AKT at Ser473. (d–g) The protein bands in c were densitometrically quantified (depicted as numbers and bars), clearly showing that the presence of RAC2 Asp63Val resulted in strong AKT phosphorylation and slight MEK phosphorylation but no ERK phosphorylation. Interestingly, a comparison of RAC2 Asp63Val and RAC2 Gly12Val showed that the relative amount of phosphorylated protein was proportional to the amount of the GTP-bound protein.



Supplementary Figure 8

Sequence electrophoregram showing progressive LOH of the *KRAS* locus with an allelic imbalance in favor of the oncogenic allele in JMML_24.

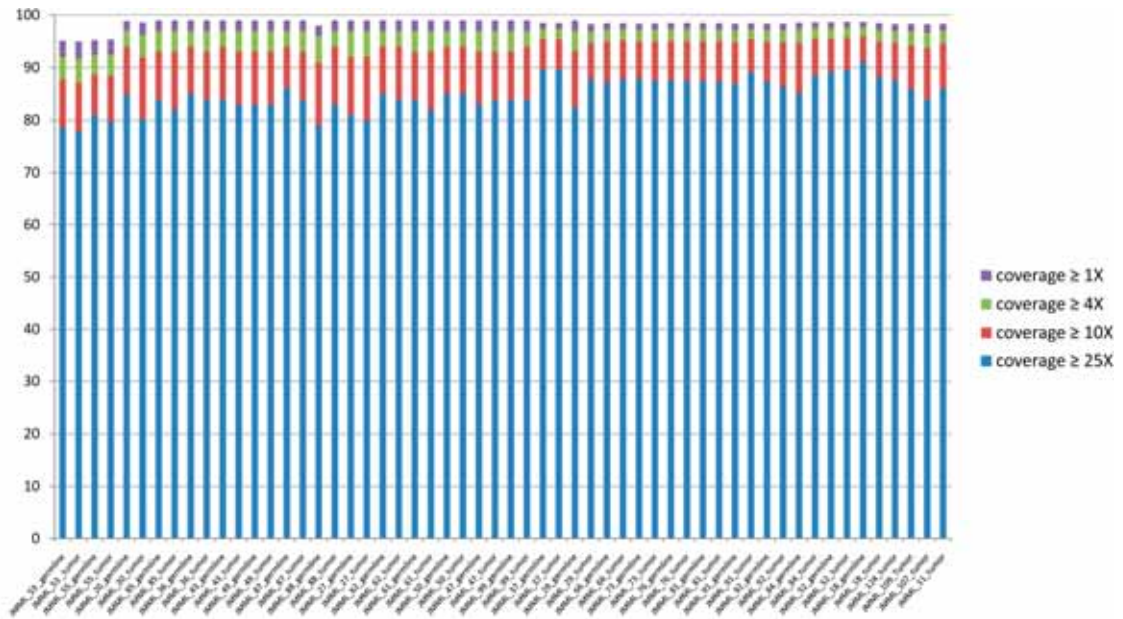
Wild-type (WT) and mutated nucleotides are indicated by black and red arrows, respectively.



Supplementary Figure 9

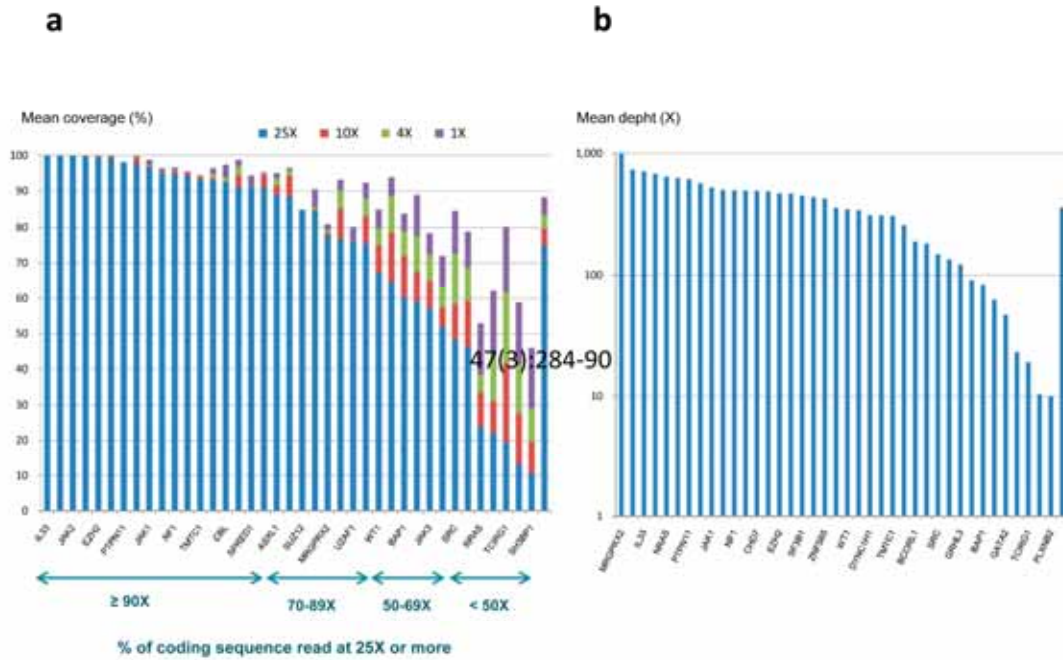
Overall survival in sporadic JMML according to initiating RAS-activating lesion.

Kaplan-Meier representation of the overall survival (%) in 96 patients with JMML evaluable for follow-up. Patients with Noonan syndrome were excluded from the analysis.



Supplementary Figure 10

Mean coverage of whole-exome sequencing in 30 paired JMML and germline DNA samples.



Supplementary Figure 11

Performances of PCR-based targeted deep sequencing in 75 JMML samples.

(a) The mean coverage of the coding regions is plotted for each gene by 25 \times descending order. (b) The mean depth of sequencing is plotted for each gene on a logarithmic scale, by descending order.

Supplementary Table 1: Characteristics of 30 patients with JMML subjected to whole exome sequencing

	Gender	Age at onset (yrs)	Underlying genetic condition	PB blasts (%)	BM blasts (%)	Karyotype	RAS pathway mutation	ASXL1	SETBP1	Leukemia sample	Germline control sample
JMML_11	M	7.2	-	0.5	7	46,XY,del(12)(p713)(11)46,XY[9]	<i>NRAS</i> (p.G13D) Somatic	p.G645Vfs*58	p.G870S	BM	Hair follicles
JMML_18	M	0.3	NF1	3	16	46,XY[33]	<i>NF1</i> (p.R1241X) Germline/somatic	-	-	BM	Fibroblasts
JMML_20	F	0.0	NS	2	8	46,XX[20]	<i>PTPN11</i> (p.G503R) Germline	-	-	PB	Fibroblasts
JMML_27	F	0.9	-	0	8	46,XY[26]	<i>PTPN11</i> (p.E76A) Somatic	-	-	BM	Fibroblasts
JMML_29	F	1.1	-	0	9	46,XX[20]	<i>KRAS</i> (p.G13C) Somatic	-	-	BM	Fibroblasts
JMML_36	M	0.7	NS	4	7	46,XY[20]	<i>PTPN11</i> (p.G503R) Germline	-	-	BM	Fibroblasts
JMML_37	F	9.8	-	4	14	45,XX-7[20]/46,XX[1]	<i>NRAS</i> (p.Q61R) Somatic	-	p.D868N	BM	Fibroblasts
JMML_43	M	0.0	NS	4	8	46,XY[22]	<i>PTPN11</i> (p.D61H) Germline	-	-	PB	Fibroblasts
JMML_47	M	0.5	-	3	5.5	45,XY,-7[19]/46,XY[1]	<i>PTPN11</i> (p.D61Y) Somatic	-	-	BM	Fibroblasts
JMML_50	F	0.7	-	1.5	5	46,XX[20]	<i>PTPN11</i> (p.D61V) Somatic	-	-	BM	Fibroblasts
JMML_52	M	2.2	-	2	0	46,XY[20]	<i>PTPN11</i> (p.E76K) Somatic	-	-	BM	Fibroblasts
JMML_53	M	2.2	-	2	6	46,XY[15]/45,X,-Y[12]	<i>PTPN11</i> (p.G503A) Somatic	-	-	BM	Fibroblasts
JMML_55	F	1.1	CBL5	0.5	8.5	46,XX[20]	<i>CBL</i> (p.Y371H) Germline/somatic	-	-	PB	Fibroblasts
JMML_59	M	0.1	NS	1	2	46,XY[20]	<i>PTPN11</i> (p.D61H) Germline	-	-	BM	Fibroblasts
JMML_61	M	2.2	-	27	32	46,XY,del9(q21q32)(10)/48,idem,+21,+22[1]/48,XY,+21,+22[3]/46,XY[16]	<i>PTPN11</i> (p.E76G) Somatic	-	p.D868N	BM	Fibroblasts
JMML_62	F	0.7	-	3	3	46,XX[30]	<i>PTPN11</i> (p.D61Y) Somatic	-	-	BM	Fibroblasts
JMML_66	F	2.1	-	2	10	46,XX[25]	<i>KRAS</i> (p.Q61P) Somatic	p.L775X	-	BM	Fibroblasts
JMML_73	M	4.2	-	2	35	46,XY[20]	<i>NRAS</i> (p.G12D) Somatic	-	-	BM	Fibroblasts
JMML_76	M	0.3	-	0	4	46,XY[20]	<i>KRAS</i> (p.G13C) Somatic	-	-	BM	Fibroblasts
JMML_81	M	0.3	-	4	5	46,XY[25]	<i>KRAS</i> (p.G13D) Somatic	-	-	BM	Fibroblasts
JMML_84	M	0.1	-	6	6	46,XY[25]	<i>PTPN11</i> (p.E76K) Somatic	-	-	PB	Normal HC
JMML_85	M	0.6	NS	0.7	2	Failure	<i>PTPN11</i> (p.A72G) Germline	-	-	BM	Fibroblasts
JMML_87	M	0.0	NS	ND	<5%	47,XXY(13)/46,XY[7]	<i>PTPN11</i> (p.A72G) Germline	-	-	PB	Fibroblasts
JMML_88	M	2.8	-	2	3.5	46,XY[20]	<i>PTPN11</i> (p.E76V) Somatic	-	-	BM	Fibroblasts
JMML_91	F	2.9	-	21	37	46,XX,del(6)(22)	<i>NRAS</i> (p.Asp54_Ala59dup) Somatic	p.E635Rfs*15	-	BM	Fibroblasts
JMML_92	F	4.5	-	1	15	46,XX,del(7)(q375q376)(3)/46,XX[17]	<i>NRAS</i> (p.G12D) Somatic	-	-	BM	Fibroblasts
JMML_99	M	2.5	-	3	5	46,XY[20]	<i>PTPN11</i> (p.D61V) Somatic	-	p.G870S	PB	Fibroblasts
JMML_107	F	3.7	-	13	30	45,XX,-7[24]	<i>PTPN11</i> (p.G60R) Somatic	-	-	BM	Fibroblasts
JMML_109	F	13.3	-	10.5	19	45,XX,-7[20]	<i>NRAS</i> (p.G12D) Somatic	p.G646Wfs*12	p.E645K p.D868N	PB	Skin Biopsy
JMML_124	M	1.5	-	1	2	46,XY[20]	<i>NRAS</i> (p.G12A) Somatic	-	p.D868N	BM	Fibroblasts

M: male; F: female; BM: bone marrow; PB: peripheral blood; yrs: years; NS: Noonan syndrome; CBL5: CBL syndrome; NF1: type 1-neurofibromatosis; HC: hematopoietic cells;

Supplementary Table 4: Gene panel for targeted sequencing and NGS performances

gene symbol	method	Target region	(bp)	Mean depth (X)	Rational for sequencing
ASXL1	NGS	whole coding region	5 067	626	Mutations reported in JMML
ASXL2	NGS	whole coding region	4 676	565	ASXL1-related
ASXL3	NGS	whole coding region	7 239	345	ASXL1-related
BAP1	NGS	whole coding region	2 887	83	ASXL1-related
BCORL1	NGS	whole coding region	5 628	190	Mutations reported in JMML
CBL	NGS	whole coding region	3 377	499	Mutations reported in JMML
CHD7	NGS	whole coding region	10 511	491	Mutated in a NS-AML with RRAS germline mutation
DYNC1H1	NGS	whole coding region	17 139	314	Mutation(s) found by WES in our cohort of JMML
EZH2	NGS	whole coding region	3 035	466	PRC2-related
GATA2	NGS	whole coding region	1 648	47	Mutated in a NS-AMLwith RRAS germline mutation
GATA3	NGS	whole coding region	1 540	183	GATA2-related
GRHL3	NGS	whole coding region	2 766	123	Mutated in a NS-AML with RRAS germline mutation
IL33	NGS	whole coding region	1 100	710	Mutation(s) found by WES in our cohort of JMML
ITPR3	NGS	whole coding region	10 394	62	Mutation(s) found by WES in our cohort of JMML
JAK1	NGS	whole coding region	4 449	524	JAK3-related
JAK2	NGS	whole coding region	4 342	677	JAK3-related
JAK3	NGS	whole coding region	4 318	91	Mutations reported in JMML
KRAS	NGS	whole coding region	892	466	Mutations reported in JMML
KRT1	NGS	whole coding region	2 304	484	Mutation(s) found by WES in our cohort of JMML
MRGPRX2	NGS	whole coding region	1 034	1 028	Mutation(s) found by WES in our cohort of JMML
NF1	NGS	whole coding region	10 524	496	Mutations reported in JMML
NRAS	NGS	whole coding region	734	642	Mutations reported in JMML
PDE8A	NGS	whole coding region	3 392	495	Mutation(s) found by WES in our cohort of JMML
PLXNB2	NGS	whole coding region	6 952	10	Mutation(s) found by WES in our cohort of JMML
PTPN11	NGS	whole coding region	2 401	612	Mutations reported in JMML
RRAS	NGS	whole coding region	903	23	RAS-related
SETBP1	NGS	whole coding region	5 226	435	Mutations reported in JMML
SF3B1	NGS	whole coding region	5 001	446	Mutations reported in JMML
SH3BP1	NGS	whole coding region	2 844	10	Mutations reported in JMML
SPRED1	NGS	whole coding region	1 622	734	related to NF1
SRC	NGS	whole coding region	1 771	149	RAS-related
SRSF2	NGS	whole coding region	748	135	Mutations reported in JMML (spliceosome)
SUZ12	NGS	whole coding region	2 182	361	PRC2 component
TCIRG1	NGS	whole coding region	3 272	19	Osteopetrosis-related
TMTC1	NGS	whole coding region	3 387	310	Mutation(s) found by WES in our cohort of JMML
U2AF1	NGS	whole coding region	1 159	259	Mutations reported in JMML (spliceosome)
WT1	NGS	whole coding region	2 015	352	Mutated in a NS-AML with RRAS germline mutation
ZNF565	NGS	whole coding region	1 664	423	Mutated in a NS-AML with RRAS germline mutation
ZRSR2	NGS	whole coding region	1 900	313	Spliceosome-related
CDYL	Sanger	NM_004824.3 (ex 7b-12)	NA	NA	Deletion found in our cohort of JMML
RRAS	Sanger	NM_006270.3 (ex 1-6)	NA	NA	RAS-related
RAC2	Sanger	NM_002872.4 (1-3)	NA	NA	RAS-related
NF1	Sanger	NM_001042492.2 (ex 18)	NA	NA	RAS-related
JAK3	Sanger	NM_000215.3 (ex 15)	NA	NA	Mutations reported in JMML
SH3BP1	Sanger	NM_018957.3 (ex 10; 11)	NA	NA	Mutations reported in JMML
GATA2	Sanger	NM_032638.4 (ex 2-6)	NA	NA	Mutations reported in JMML
SETBP1	Sanger	NM_015559.2 (ex 6 part)	NA	NA	Diagnostic workup
ASXL1	Sanger	NM_015338.5 (ex 14)	NA	NA	Diagnostic workup
PTPN11	Sanger	NM_002834.3 (ex 3;13)	NA	NA	Diagnostic workup
CBL	Sanger	NM_005188.3 (ex 7;8;9)	NA	NA	Diagnostic workup
KRAS	Sanger	NM_033360.3 (ex 2; 3)	NA	NA	Diagnostic workup
NRAS	Sanger	NM_002524.4 (ex 2; 3)	NA	NA	Diagnostic workup

bp: base pairs; NA: not applicable

Supplementary Table 5: General features of 118 JMML cases, additional somatic mutations and outcome according to genetic status. The number of additional somatic alterations was evaluated by disregarding somatic RAS-pathway mutations assumed to be either the initiating event or part of the classic mechanism of leukemogenesis, such as hits targeting the wild-type *NF1* or *CBL* allele in germline-mutated patients^{5,9,48}. Despite a trend toward more cytogenetic alterations and fewer point mutations in the KRAS-JMML group, no significant difference was found in the total number of additional somatic alterations ($p = 0.683$), cytogenetic alterations ($p = 0.103$) or point mutations ($p = 0.242$) between genetically-defined sporadic JMML groups. However, *del7/7q* was significantly more frequent in KRAS-JMML ($p = 0.004$), whereas no difference was observed for aUPD ($p = 0.433$), CNV (0.431) and other aneuploidies (0.134) between groups.^{*}

Genetic group	SOMATIC (sporadic JMML)				GERMLINE (syndromic JMML)			TOTAL
	PTPN11	NRAS	KRAS	Total	NF1	PTPN11	CBL	
Number of cases	38	22	18	78	8	21	11	118
M/F sex ratio	30/8 (3.7)	12/10 (1.2)	12/6 (2.0)	54/25 (2.2)	8/0	14/7 (2.0)	4/7 (0.6)	79/38 (2.1)
Median age at onset (yrs)	2.7 [0.1 – 8.1]	2.7 [0.2 – 13.3]	1.1 [0.3 – 3.0]	2.2 [0.1 – 13.3]	3.0 [0.3 – 15.7]	0.1 [0 – 0.8]	1.3 [0.2 – 5.1]	1.6 [0 – 13.3]
WBC counts, median [IQ], x10 ⁹ /L	24.4 [1.7 – 106.0]	26.8 [7.4 – 86.7]	20.8 [4.0 – 167.8]	24.7 [1.7 – 167.8]	29.6 [11.6 – 83.0]	37.5 [9.2 – 70.0]	26.7 [9.4 – 79.0]	28.3 [1.7 – 167.8]
Platelet counts, median [IQ], x10 ⁹ /L	33.0 [3.0 – 292.0]	129.5 [23.0 – 238.0]	59.0 [3.0 – 153.0]	54.5 [3.0 – 292.0]	146.5 [15.0 – 302.0]	68.0 [4.0 – 281.0]	130.0 [6.0 – 286.0]	60.5 [3.0 – 302.0]
Myeloid precursors in peripheral blood, no. of patients (%)	35 (92)	20 (91)	17 (94)	72 (92)	7 (88)	20 (95)	9 (82)	108 (91)
Circulating blasts ≥10%, no. of patients (%)	7 (18)	6 (27)	3 (17)	16 (21)	3 (37)	0 (0)	0 (0)	19 (16)
Myelodysplastic features, no. of patients (%)	24 (63)	11 (50)	14 (78)	49 (63)	6 (75)	11 (52)	6 (55)	72 (61)
HbF elevated for age, no. of patients (%) [*]	21/35 (60)	5/19 (26)	3/15 (20)	29/69 (42)	5/8 (62)	1/14 (18)	2/10 (20%)	37/101 (37)
Additional somatic alterations[†]								
No. of patients with ≥ 1 additional somatic alteration [Max. no. of alterations per patient]	23 (60) [5]	13 (59) [12]	13 (72) [3]	49 (63) [12]	8 (100) [4]	1 (5) [1]	0 (0) -	58 (49) [12]
No. of additional somatic alterations	45	43	16	104	19	1	0	124
No. of patients with ≥ 1 cytogenetic alteration [Max. no. of alterations per patient]	14 (37) [3]	11 (50) [2]	11 (61) [2]	36 (46) [3]	5 (63) [4]	1 (5) [1]	0 (0) [0]	42 (36) [4]
No. of cytogenetic alterations	19	14	12	45	12 [‡]	1	0 [‡]	58
Translocation, no. of patients (%)	-	-	1	1	2	-	-	3
<i>Del7/7q</i> , no. of patients (%)	6 (16)	3 (14)	10 (56)	19 (25)	1 (13)	-	-	20 (17)
Other aneuploidies, no. of patients (%)	7 (18)	2 (9)	-	9 (12)	3 (38)	1 (5)	-	12 (10)
CNV, no. of patients (%)	3 (8)	4 (18)	1 (6)	8 (10)	2 [‡] (25)	-	-	10 (8)
aUPD, no. of patients (%)	1 (3)	2 (9)	0 (0)	3 (4)	0 [‡] (0)	-	-	3 (3)
No. of patients with ≥ 1 point mutation [Max no. of alterations per patient]	14 (37) [4]	9 (41) [11]	3 (16) [2]	26 (33) [11]	4 (50) [2]	-	-	30 (25) [11]
No. of point mutations	27	29	4	60	7	-	-	67

Nature Genetics: doi:10.1038/ng.3420

Genetic group	SOMATIC (sporadic JMML)				GERMLINE (syndromic JMML)			TOTAL
	PTPN11	NRAS	KRAS	Total	NF1	PTPN11	CBL	
Additional RAS-related mutations, no. of patients (%) [Max. no. of alterations per patient]	8 (21) [2]	5 (23) [1]	0 (0)	13 (18) [2]	2 (25) [1]	-	-	15 (13) [2]
PRC2-related mutations, no. of patients (%) without <i>del7/7q</i> [Max. no. of alterations per patient]	3 (8) [2]	7 (32) [3]	2 (11) [2]	12 (15) [3]	5 (63) [1]	-	-	18 (15) [3]
PRC2-related mutations, no. of patients (%) including <i>del7/7q</i> [Max. no. of alterations per patient]	8 (21) [2]	8 (36) [3]	10 (56) [3]	26 (33) [3]	5 (63) [2]	-	-	31 (26) [3]
Outcome								
Blast crisis before HSCT, no. of patients (%)	13 (34)	9 (41)	4 (22)	26 (33)	5 (62)	1 (5)	0 (0)	32 (27)
HSCT, no. of patients (%)	29 (76)	15 (68)	18 (100)	62 (79)	6 (62)	3 (14)	6 (56)	76 (64)
Autologous reconstitution, no. of patients (% of HSCT)	1 (3)	2 (13)	3 (17)	6 (10)	0 (0)	0 (0)	3 (50)	9 (12)
Relapse / disease progression, no. of patients (% HSCT)	6 (21)	2 (13)	3 (17)	11 (18)	2 (40)	0 (0)	0 (0)	13 (17)
Death, no. of patients (%)	16 (42)	6 (27)	4 (22)	26 (33)	6 (75)	12 (57)	0 (0)	44 (37)

[IQ] : interquartile range; CNV: copy-number variations; aUPD: acquired uniparental disomy; HSCT: hematopoietic stem cell transplantation.

^{*} the number of patients who were evaluated is indicated.

[†] In patients with NF1 and CBL syndrome, events targeting the second allele of *NF1* and *CBL* were not considered as additional events since the loss of the wild-type allele is part of the classic mechanism of leukemogenesis in these settings. 10/11 patients with germline CBL mutations had an aUPD encompassing *CBL* whereas 5/8 patients with neurofibromatosis had a somatically acquired event targeting *NF1* (including 3 aUPDs).

[‡] One patient had a germline codeletion of *SUZ12*.

Nature Genetics: doi:10.1038/ng.3420

Chapter VIII

General discussion



General discussion

Hepatic stellate cells (HSCs) are central to metabolism and storage of retinoids in the body and are involved in liver development, immunoregulation, homeostasis, regeneration and fibrosis (Winau et al., 2008; Blaner et al., 2009; Yin et al., 2013; Kordes et al., 2014). In healthy liver HSCs are in a state referred as quiescent (G0). Quiescent HSCs (qHSCs) are multipotent cells that after activation could differentiate to other liver cell types (Kordes et al., 2007; Kordes et al., 2008; Sawitza et al., 2009b; Kordes et al., 2013; Sawitza et al., 2015). Throughout activation, HSCs alter their quiescent characteristics and adopt into the cells, which are recognized as proliferative, multipotent, contractile and migratory cells (Kordes et al., 2014; Bitencourt et al., 2014; Dong et al., 2015) (chapter I, hallmarks and roles of hepatic stellate cells). In some pathophysiological conditions, sustained activation of HSC causes the accumulation of extracellular matrix (ECM) in the liver and initiates the liver diseases, such as fibrosis, cirrhosis and hepatocellular carcinoma (HCC) (Yin *et al.*, 2013b). The molecular mechanisms that maintain the quiescent of HSC and trigger HSC activation and differentiation are poorly understood and needs further investigation. Therefore, it is noteworthy to search for key signaling pathways that govern HSCs fate decision and modulate them in a way that activated HSC (aHSC) contributes into liver regenerative not fibrosis. RAS molecular switches are nodes of intracellular signaling pathways. RAS superfamily is composed of different families (RAS, RHO, RAN, RAD, RAG, RAB and ARF) with specific mode of regulation, expression, effector proteins and subcellular localization, which through the activation of individual signaling pathways exert their cellular functions. RAS and RHO family GTPases are well-recognized for their involvement in the wide spectrum of cellular responses, such as cell growth, proliferation, survival, differentiation, adhesion, contraction, motility and migration (Karnoub and Weinberg, 2008; Heasman and Ridley, 2008b). These families are subdivided farther to the different subgroups and isoforms with individual functions (chapter I, RAS/RHO family GTPases sections). The focus of this study was to consider the RAS GTPases activity, networking, cross-talking and biological functions in modulating the HSC activation processes and fate cell decisions.

This doctoral thesis provided new insights into the expression pattern, isoform specificity, activity and networking of RAS family members and their signaling components in both quiescent (here after, d0) and activated (d8) HSCs. Obtained data revealed differential expression pattern for RAS isoforms, where embryonic stem cell-expressed RAS (ERAS) specifically expressed in quiescent HSCs and drastically down-regulated after activation. ERAS was identified in 2003 as a new member of the RAS family, which is specifically expressed in undifferentiated mouse embryonic stem cells (Takahashi *et al.*, 2003). In addition to stem cells, ERAS has been detected in the several adult cynomolgus tissues (Tanaka *et al.*, 2009), and in gastric cancer and neuroblastoma cell lines (Aoyama *et al.*, 2010; Kubota *et al.*, 2010). Still the individual roles of ERAS have not been fully described. This raised the question, what would be the function of ERAS in quiescent and non-proliferative cells? To address this question, first we investigated the biochemical and molecular features of ERAS with generating different ERAS mutants and analyzed the cellular outcomes in overexpressed system (chapter II). Second, we monitored the signaling networking of the endogenous ERAS/RAS in quiescent HSC vs. activated HSC (chapter

III). Third, we aimed to investigate the cross-talking between the RAS-RHO signaling in both *in vitro* and disease progression (chapter V-VII).

Biochemical characteristic of embryonic stem cell-expressed RAS (ERAS)

Comprehensive sequence and structural analysis between ERAS and other Ras isoforms, revealed ERAS harbors additional motifs, regions and sequence deviations (in critical locations of G1, G2 and G3, see figure 6) which are not present in classical members of RAS family (HRAS, NRAS and KRAS). Therefore, we generated different ERAS variants with mutations and deletion of these motifs and region and investigated their impact on ERAS specific function and localization. These ERAS variants included ERAS^{ΔN}, ERAS^{S7}, ERAs^{A31/A32/A33}, ERAS^{S226/S228}, ERAS^{SwI}, ERAS^{SwII}, ERAS^{SwI/SwII}, ERAS^{R79}, ERAS^{SwI/R79}, ERAS^{R79/SwII} and ERAS^{SwI/R79/SwII}. We depicted the place of these mutations in the predicted structure of ERAS with colors in the figure 6. Here we will discuss the new findings about each of this sequence fingerprints (chapter II) (Nakhaei-Rad *et al.*, 2015).

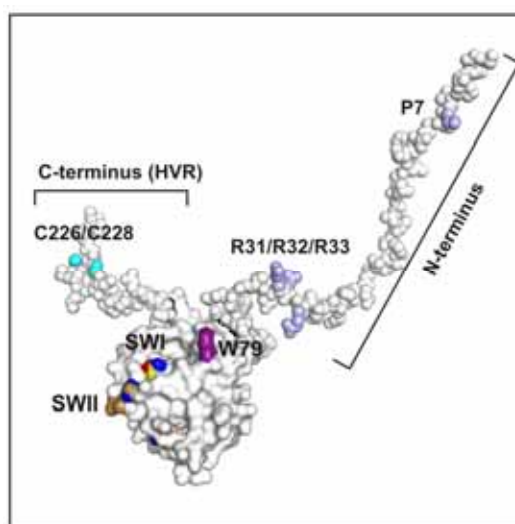


Figure 6. Predicted structure of full-length ERAS and exhibits of the three-dimensional places of studied ERAS mutants. In contrast to the G domain as well as N- and C-terminus of ERAS appear as disordered/unstructured regions. P7 and RRR motifs are shown in purple, W79 in deep purple, mutations in switch I in yellow, mutations in switch II in brown, C226/C228 at the very C-terminus in cyan. HVR, hypervariable region; SWI, switch I; SWII, switch II.

N-terminal extension of ERAS—We proposed that N-terminal extension of ERAS might modulate its localization through interaction with potential adaptor/scaffold proteins *via* putative PxxP and RRR motifs. With our co-localization studies we did not observed significant differences in localization of the N-terminus mutants of ERAS (ERAS^{ΔN}, ERAS^{S7} and ERAs^{A31/A32/A33}). However, considering our results we cannot exclude the role of ERAS N-terminus as a putative protein interaction site, since ERAS is not expressed endogenously in the MDCK II cells (used for confocal studies) and therefore its binding partner may not be available in this cell line. To confirm our hypothesis we need to study ERAS localization in the cells that endogenously express

ERAS such as hepatic stellate cells (chapter III). However, our cell-based studies revealed that the N-terminal extension of ERAS is critical for PI3K-AKT-mTORC activation and N-terminal truncated ERAS variants (ERAS^{ΔN} and ERAS^{ΔN/S226/S228}) remarkably had a lower signaling activity. One explanation maybe the role of the unique N-terminus in lateral segregation of ERAS across the membrane that consequently specifies association with and activation of its effectors in a manner reminiscent to microdomain localization of HRAS that regulates its interaction with effector proteins of CRAF and PI3K (Jaumot *et al.*, 2002). In addition, ERAS was found in membrane ruffles (data not shown) maybe induced by RAC1, which can be activated by the ERAS-PI3K-PIP3-RACGEF axis (Innocenti *et al.*, 2003; Inabe *et al.*, 2002; Dillon *et al.*, 2014). Such a scenario has been reported for the RRAS N-terminal 26 amino acid extension, which has been proposed to positively regulation RAC activation and cell spreading (Holly *et al.*, 2005). Similar to ERAS, RRAS N-terminus modulates its specific functions but revealed no impact in cellular localization (Holly *et al.*, 2005).

Palmitoylation modification and ERAS trafficking—RAS proteins are compartmentalized by PTMs at their C-terminus, with the CAAX motif as the farnesylation site and additional upstream cysteine residues as the palmitoylation site(s) in the case of H, and NRAS (Ahearn *et al.*, 2011; Apolloni *et al.*, 2000; Rocks *et al.*, 2005; Schmick *et al.*, 2014). We found substitution of two cysteine residues C226/C228 in HVR of ERAS with serines clearly impaired the plasma membrane localization of protein. In addition, our confocal microscopy data revealed that in contrast to plasma membrane localization of ERAS^{WT}, palmitoylation-deficient ERAS^{S226/S228} is mainly localized, with clear pattern, in cytoplasm and also in endomembrane. These data, support proposed reports demonstrating that HRAS and NRAS cycle between Golgi and the plasma membrane *via* reversible and dynamic palmitoylation-depalmitoylation reactions (Matallanas *et al.*, 2006; Rocks *et al.*, 2005; Goodwin *et al.*, 2005).

Effector binding regions—A detailed study of structure–sequence relationships revealed a distinctive effector binding regions for ERAS in comparison with RAS isoforms (H, N, and KRAS). Subsequent interaction analysis with five different RAS effectors revealed that effector binding profile of ERAS significantly differs from HRAS. ERAS tightly bounds to PI3K α and revealed very low affinity for other RAS effectors. In contrast, HRAS showed an opposite pattern with highest affinity for CRAF. These data were confirmed by investigating the respective downstream signaling cascades (PI3K-AKT-mTORC and CRAF-MEK1/2-ERK1/2) at the level of phosphorylated AKT, MEK1/2 and ERK1/2.

ERAS-CRAF interaction—Substitutions for corresponding residues in HRAS of deviating residues in switch I, II and interswitch regions of ERAS for corresponding residues in HRAS provided several interesting and new insights. One is a large shift in effector binding affinity of ERAS gain of CRAF binding. The major difference was observed with ERAS^{R79}, where a tryptophan was replaced by an arginine (R41 in HRAS). This variant led to a significant increase of CRAF binding and partly rescued the low affinity of the switch variants (ERAS^{SwI/R79} and ERAS^{SwI/R79/SwII}). According to the crystal structure (Nassar *et al.*, 1996), R41 (W79 in ERAS) forms hydrogen bonds with Q66 and N64 of CRAF-RBD, which enables ERAS^{R79} to make additional electrostatic contacts with CRAF and to bind tighter.

ERAS-PI3K interaction—In comparison with HRAS, ERAS interacts much strongly with PI3K α -RBD and activates PI3K-AKT-mTORC cascade. Mutagenesis at switch and interswitch regions (ERAS^{SwI}, ERAS^{R79} and ERAS^{SwII}), attenuated binding of ERAS to PI3K α -RBD, demonstrating the role of critical ERAS residues at effector binding regions. These data are consistent with previous study that has shown PI3K γ -RBD contacts both switch I and switch II regions of HRAS (Pacold *et al.*, 2000). Interestingly, W79R mutation of ERAS (R41 HRAS), which has increased binding to CRAF, PLC ϵ , and RALGDS, dramatically reduced the binding to PI3K α . The affinity of this ERAS mutant (ERAS^{R79}) for PI3K α -RBD appears similar to that of HRAS^{V12}. In the same line of evidence, we observed ERAS^{R79} also was deficient at activation of RAS-PI3K-AKT-mTORC2 pathway as monitored with S473 phosphorylation of AKT. Thus, W79 in ERAS, represents a specificity-determining residue for the proper binding to and activation of PI3K.

ERAS-RASSF5 interaction—RASSF members are known as a RAS effector with tumor suppressor functions. RASSF5, have two splice variants NORE1A and RAPL, which share same RBD (Stieglitz *et al.*, 2008). We applied RASSF5-RBD domain to analyze the interaction of ERAS variants with this RAS effector. Switch I H70Y/Q75E mutation of ERAS (ERAS^{SwI}) attenuated the binding to RASSF5 and this was the case for all ERAS variant harboring switch I mutations (ERAS^{SwI/R79}, ERAS^{SwI/SwII}, and ERAS^{SwI/R79/SwII}). Switch II and W79R mutations did not affect the binding affinity for RASSF5, emphasizing the importance of the more conserved switch I region in the complex formation of the RAS proteins with RASSF5 (Stieglitz *et al.*, 2008). It remains to be investigated whether ERAS is an activator of RASSF5 and thus a regulator of HIPPO pathway.

With the aim of this study, we shed light on the sequence fingerprint and cellular targets of ERAS and intruded ERAS as a unique member of RAS family with its own mode of regulation and function. N-terminal of ERAS is important for its cellular functions and probably not for its localization. We found that switch regions of ERAS act as core effector binding regions that form an ERAS specific interaction interface for its effectors such as PI3K α . ERAS binding to other RAS effectors, such as RASSF5, RALGDS and CRAF, is weak but may still be of physiologically relevance. W79 of ERAS appears to determine the effector selectivity.

However, this study raised several questions. What is the function of endogenous ERAS in normal cells of the body? Which isoform of PI3K is the main target of ERAS? Which signaling pathways are downstream of endogenous ERAS? We identified that one of the liver cell types, is called hepatic stellate cells, which endogenously express ERAS. To address these questions, we, therefore, investigated the ERAS regulation, downstream pathways and functions in hepatic stellate cells (chapter III).

Signaling network and proposed function of endogenous ERAS in HSC

In this study, we found embryonic stem cell-expressed RAS (*ERAS*) expressed in hepatic stellate cells (HSCs). The presence of *ERAS* mRNA was detected in quiescent HSCs but not in activated HSCs where other RAS-related genes, such as *RRAS*, *MRAS*, *RALA* and *RAP2A*, were upregulated during HSC activation. This observation raised the questions, what would be the function of ERAS in quiescent (G0) cells and why do we need a reciprocal expression of these RAS isoforms in quiescent vs. activated HSC? To address these questions, first we investigated the

presence of ERAS protein with our monoclonal antibody against rat ERAS in different liver cells and checked the activity and isoform specificity of RAS and their signaling components in quiescent and activated HSC (chapter III).

Obtained data, revealed ERAS protein in quiescent HSC but not in other liver cell types, and ERAS was considerably reduced during HSC activation (d4 and d8). To elucidate the ERAS functions in quiescent HSCs, we sought for ERAS specific effectors and the corresponding downstream pathways.

Role of the ERAS-PI3K-AKT-mTORC1 activity in quiescent HSCs—Endogenous ERAS expression in quiescent HSCs strongly correlates with high levels of AKT phosphorylated at T308 and S473 through PDK1 and mTORC2, respectively. Protein interaction and immunoprecipitation analysis further revealed that ERAS physically interacts with PI3K α/δ . Thus, we propose ERAS as a regulator of the PI3K-PDK1-AKT-mTORC1 axis in quiescent HSCs. This axis controls various processes including cell cycle progress, autophagy, apoptosis, lipid synthesis and translation (Kim and Spiegelman, 1996; Kim *et al.*, 1998; Wang *et al.*, 2012; Tzivion *et al.*, 2011; Prasad *et al.*, 2015). The latter is controlled by mTOR mediated activation of S6 kinase, which in turn phosphorylates different substrates, such as ribosomal protein S6, mTOR itself at S2448 and mSIN1 at T86, which is an upstream component of mTORC2 (Fig. 5) (Chiang and Abraham, 2005; Liu *et al.*, 2014b; Ma *et al.*, 2008). Previous studies have shown that quiescent HSCs produce and secrete a significant amount of HGF (Schirmacher *et al.*, 1992; Maher, 1993), which is modulated by the mTORC1-S6 kinase pathway (Tomiyama *et al.*, 2007) and is known to regulate hepatocyte survival (Wang *et al.*, 2002).

Activity of the mTORC2-AKT-FOXO1 axis in quiescent HSCs. In comparison with mTORC1, the regulation of mTORC2 is less understood (Oh and Jacinto, 2011). Our findings indicate that ERAS may act as an activator of the mTORC2 pathway. Retrovirally expressed ERAS has been shown to promote phosphorylation of both AKT (S473) and FOXO1 (S256) in induced pluripotent stem cells (iPSCs) generated from mouse embryonic fibroblasts (Yu *et al.*, 2014). Thus, ERAS-AKT-FOXO1 signaling has been suggested to be important for somatic cell reprogramming. We detected high levels of p-AKT^{S473} and p-FOXO1^{S256} in quiescent HSCs endogenously expressing ERAS. Phosphorylated FOXO1 is sequestered in the cytoplasm and cannot translocate to the nucleus where it binds to gene promoters and induces apoptosis (Fig. 7) (Wang *et al.*, 2014). Interestingly, a possible link between ERAS and mTORC2 may be mSIN1, which appears to be an upstream component and modulator of mTORC2 activity (Huang and Fingar, 2014). It has been reported that mSIN1 contains a RAS-binding domain with some homology to that of CRAF (Schroder *et al.*, 2007). Taken together, ERAS-mTORC2-AKT-FOXO1 axis may insure the survival of HSCs in the space of Disse by interfering with the programmed cell death (Fig. 7B).

Role of the HGF-JAK-STAT3 axis in quiescent HSCs—Ectopic expression of ERAS stimulates phosphorylation of STAT3 likely downstream of leukemia inhibitory factor (LIF) (Yu *et al.*, 2014). ERAS may compensate for lack of LIF in support of iPSC generation (Yu *et al.*, 2014). Moreover, the LIF-STAT3 axis is essential for keeping mouse stem cells undifferentiated in cultures and regulates self-renewal and pluripotency of embryonic stem cells (Stuhlmann-Laeisz *et al.*, 2006).

Consistently, we detected high levels of p-STAT3 and p-FOXO1 in quiescent HSCs, which may control survival, self-renewal, and multipotency of quiescent HSCs. In addition, stimulation of the HGF receptor (c-MET) that is expressed in HSCs results in JAK activation and phosphorylation of STAT3 (Boccaccio *et al.*, 1998; Friedman, 2008). However, the presence and activity of LIF-STAT3 axis in HSCs needs further investigations.

Quiescent HSCs display a locked RAS-MAPK signaling pathway—In quiescent HSCs only basal levels of activated (phosphorylated) MEK and ERK could be observed although all components of the RAS-RAF-MEK-ERK axis were expressed. There are several explanations for the strongly reduced activity of RAS-MAPK signaling in quiescent HSCs (Fig. 7B); I) Absence of external stimuli, such as PDGF1 and TGF β 1 in healthy liver. These growth factors are strong activators of the MAPK pathway in activated HSCs (Reimann *et al.*, 1997; Carloni *et al.*, 2002); II) Presence of an intracellular inhibitor, like special AT-rich binding protein 1 (SATB1), which is specifically expressed in quiescent HSCs and down-regulated during HSC activation (He *et al.*, 2015). Interestingly, SATB1 has been shown to be a strong inhibitor of RAS-MAPK pathway that may lock this signaling in quiescent HSCs (He *et al.*, 2015); III) MicroRNAs (miRNAs), especially miRNA-21, may play a role in the reciprocal regulation of the RAS-MAPK pathway in quiescent vs. activated HSCs. Upregulated miRNA-21 in activated HSCs results in MAPK activation, which is based on depletion of sprouty homolog 1 (SPRY1), a target gene of miRNA-21 (Coll *et al.*, 2015) and negative regulator of the RAS-MAPK pathway (Mason *et al.*, 2006).

Up-regulation of individual RAS isoforms in activated HSCs—Comprehensive mRNA analysis of various RAS family members revealed that *RRAS*, *MRAS*, *RALA* and *RAP2A* were upregulated during HSC activation. These genes may also play a role in the coordination of the cellular processes, required for activation and differentiation of HSCs, such as polarity, motility, adhesion and migration. Interestingly, *RRAS* has been implicated in integrin-dependent cell adhesion (Kinbara *et al.*, 2003). Of note, in endothelial cells the *RRAS*-*RIN2*-*RAB5* axis stimulates endocytosis of β_1 integrin in a *RAC1*-dependent manner (Sandri *et al.*, 2012). On the other hand, the muscle RAS oncogene homolog (*MRAS*), a *RRAS*-related protein, is upregulated during HSC activation. Among the different members of RAS family, only *MRAS* can interact with *SHOC2* in ternary complex with protein phosphatase 1 (*PP1*), which dephosphorylates autoinhibited *CRAF* and activates the *CRAF*-*MEK*-*ERK* axis (Rodriguez-Viciano *et al.*, 2006). These findings and data obtained in this study suggest that *MRAS* may be responsible for high level of p-MEK and p-ERK in activated HSCs due to the *RAF* kinase activation. *RAP* proteins, including *RAP2A*, are involved in different cellular processes and play pivotal roles in cell motility and cell adhesion (Torti and Lapetina, 1994; Paganini *et al.*, 2006). Recently, it has been shown *RAP2A* is a novel target gene of p53 and a regulator of cancer cell migration (Wu *et al.*, 2015). Moreover, expression of *RAP2A* in cancer cells results in secretion of two matrix metalloproteinases (*MMP2* and *9*) and *AKT* phosphorylation at Ser473, which promotes tumor invasion (Wu *et al.*, 2015). Notably, p53 is unregulated in activated HSCs (Saile *et al.*, 2001). Thus, we speculate the binding of p53 to *RAP2A* promoter may results in transcription of *RAP2A* in activated HSCs and stimulates secretion of *MMPs*, which remodels the extracellular matrix and facilitate the migration of HSCs in the space or Dissé.

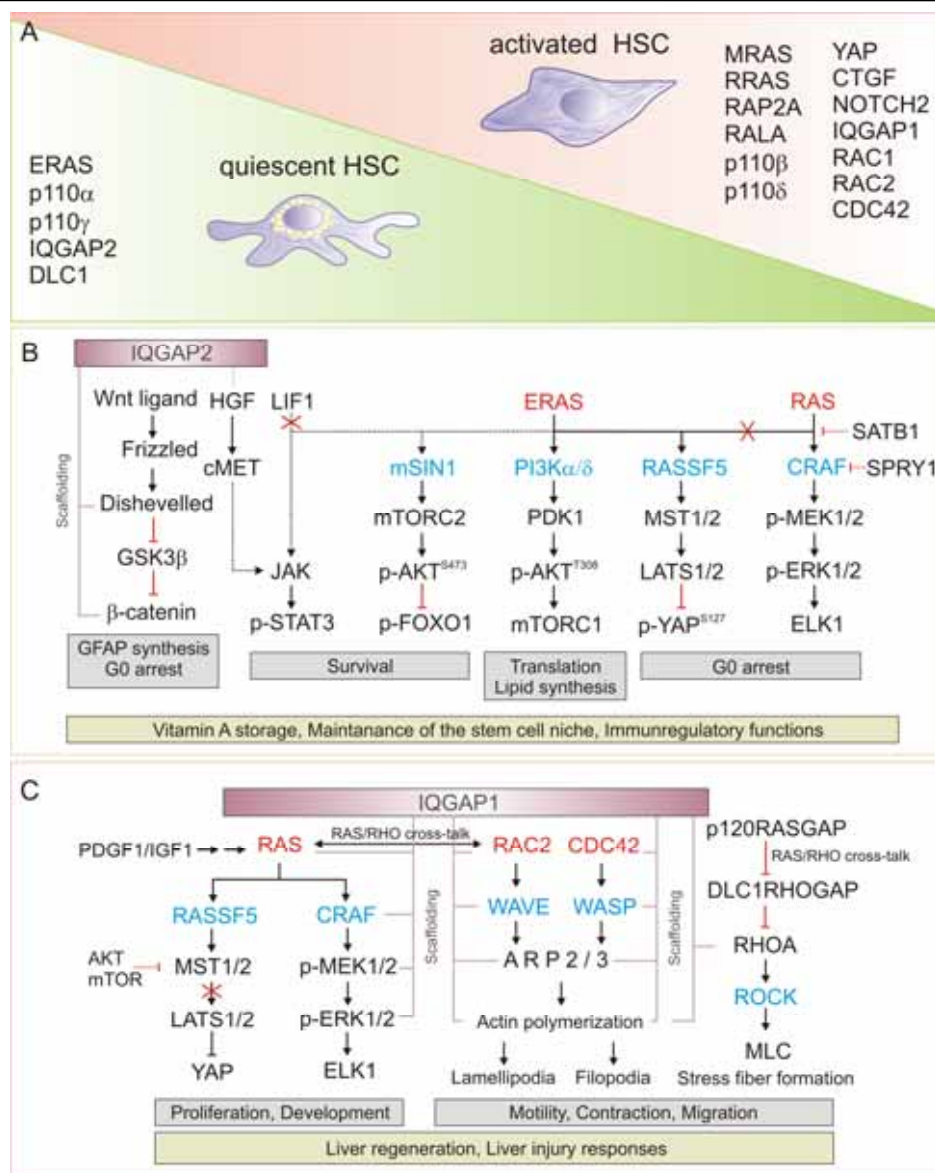


Figure 7. Schematic view of the proposed model of HSC signaling networking and gene expressional changes. (A) The expressional changes of investigated genes that are involved in RAS-dependent signaling in qHSC vs. aHSC. (B,C) A reciprocal ERAS/RAS/RHO dependent signaling pathways in qHSC (B) vs. aHSC (C). ARP2/3, actin related protein 2/3; DLC1, deleted in liver cancer; ERAS, embryonic stem cell-expressed RAS; ERK, extracellular regulated kinase; FOXO1, forkhead transcription factor; GAP, GTPase activating protein; GFAP, glial fibrillary acidic protein; GSK3 β , glycogen synthase kinase 3 beta; HGF, hepatocyte growth factor; HSC, hepatic stellate cell; IGF, insulin-like growth factor; IQGAP, IQ motif-containing GTPase-activating protein; JAK1, Janus kinase 1; LIF1, Leukemia inhibitory factor 1; MEK, MAP/ERK kinase; MMP, matrix metalloproteinases; mSIN1, mammalian stress-activated MAP kinase-interacting protein 1; MST, mammalian sterile 20-like kinase; mTORC, mammalian target of rapamycin; PDGF, platelet-derived growth factor; PDK1, 3-phosphoinositide-dependent protein kinase 1; PI3K, phosphoinositide 3-kinase; RAS, rat sarcoma; RASSF5, RAS-association domain family 5; ROCK; RHO-associated coiled-coil kinases; SATB1, special AT-rich binding protein 1; SPRY1, sprouty homolog 1; STAT3, signal transducer and activator of transcription 3; WASP, wiskott-aldrich syndrome protein; WAVE; WASP-family verprolin-homologous protein; YAP, Yes-associated protein (for details see discussion).

Proliferation and differentiation of activated HSCs—In comparison with quiescent HSCs, activated HSCs are proliferative cells and can pass through cellular checkpoints (Soliman *et al.*, 2009). One of the candidate pathways is the RAF-MEK-ERK cascade that can be stimulated *via*

different growth factors. Consistent with previous studies, we detected high levels of p-MEK and p-ERK in culture-activated HSCs (Reimann *et al.*, 1997; Gu *et al.*, 2013). Three scenarios may explain the elevated RAF-MEK-ERK activity in activated HSCs: I) As discussed above, MRAS in the complex with SHOC2 and PP1 is able to activate the CRAF-MEK-ERK pathway (Wu *et al.*, 2015). p-ERK translocates to the nucleus and phosphorylates different transcriptional factors, including Ets1 and c-Myc thereby eliciting cell cycle progression and proliferation. The cytoplasmic p-ERK alternatively phosphorylates Mnk1 and p90RSK and thereby promotes protein synthesis and cell growth (Fukunaga and Hunter, 1997; Pereira *et al.*, 2013) II) PDGF and IGF1 are the most potent mitogens for activated HSCs and induce activation of MAPK pathways (Reimann *et al.*, 1997; Iwamoto *et al.*, 2000). III) The expression of SATB1, a cellular inhibitor of the RAS-RAF-MEK-ERK pathway, significantly declines during HSC activation (He *et al.*, 2015).

YAP controls cell cycle arrest vs. proliferation of HSCs—We observed a moderate interaction between ERAS and RAS-association domain (RA) of RASSF5A. Previously, we showed that switch I of ERAS is important for ERAS-RASSF5 interaction and mutation in this region impairs ERAS binding to RASSF5 (Nakhaei-Rad *et al.*, 2015). RASSF5-MST1/2-LATS1/2 activity promotes phosphorylation, and therefore sequestration and proteasomal degradation of YAP in cytoplasm (Ramos and Camargo, 2012b; Rawat and Chernoff, 2015). YAP is a transcriptional co-activator that promotes transcription of *CTGF* and *NOTCH2*, which are involved in cell development and differentiation (Camargo *et al.*, 2007; Avruch *et al.*, 2010; Lu *et al.*, 2010; Yimlamai *et al.*, 2014). Recently, van Grunsven and colleagues reported that transcriptional co-activator of YAP controls *in vitro* and *in vivo* activation of HSCs (Mannaerts *et al.*, 2015). Consistent with this study we observed hardly any YAP protein in quiescent HSCs in comparison to activated HSCs. Thus, our data suggest that YAP degradation through RASSF5-MST1/2-LATS1/2 may be triggered by binding and recruitment of RASSF5 to the plasma membrane *via* ERAS-GTP. High levels of YAP transcriptional activity in activated HSCs, may be due to the inhibitory activities of AKT and mTOR on MST1/2 (Chiang and Martinez-Agosto, 2012) and may thus cause opposite effects of the pro-apoptotic RAS-RASSF5-MST1/2-LATS1/2 pathway (Fig. 7C), leading to increased cell survival, proliferation and development of activated HSCs (Mannaerts *et al.*, 2015).

Overexpression and endogenous studies of ERAS (chapter II and III), demonstrate that ERAS preferentially interact with PI3K α/δ and RASS5A, is able to signal through the PI3K-PDK1-AKT-mTORC and RASSF5-MST1/2-LATS1/2 axis. Therefore, this study adds ERAS signaling to the remarkable features of quiescent HSCs and the cellular outcome of these signaling pathways would maintain quiescent state of HSCs by the inhibition of proliferation (HIPPO pathways, G0 arrest) and apoptosis (PI3K-PDK1 and mTORC2) (see Fig. 7B). On the other hand, activated HSCs exhibit YAP-CTGF/NOTCH2 and RAS-RAF-MEK-ERK activity, which are involved in HSC proliferation and development (Fig. 7C). This information helps us to get one-step closer to the RAS dependent signaling pathways, which maintain quiescent and modulate activation of HSCs.

Functional cross-talk between RAS and RHO pathways

One of the important features of activated HSC is their ability to contract and migrate, which should be controlled by RHO family GTPases (chapter IV). There are growing numbers of

evidences that show RAS signaling controls RHO activity and *vice versa* (Shang *et al.*, 2007; Yang *et al.*, 2009; Asnaghi *et al.*, 2010). We asked the question, does RAS family actively influence HSC migration through RHO proteins or not? To approach this question, it is noteworthy to investigate the intracellular communication of RAS and RHO families. In following sections, we will discuss our finding that shed light on the RAS and RHO cross-talk in two levels, GAP (chapter V) and scaffolding proteins (chapter VI) and how these connection modulates disease progression (chapter VII).

p120GAP links RAS and RHO pathways *via* p190GAP and DLC1

p120 is a GTPase activating proteins (GAPs) for RAS family GTPases that contains several domains (Fig. 8). Through its C-terminal GAP domain, interacts with switch regions of RAS proteins where accelerates GTP to GDP hydrolysis (Ahmadian *et al.*, 1997a). p120 contains an N-terminal Src homology domain 2 and 3 (SH2² and SH3³) that enable its intracellular protein-protein interactions with other regulatory proteins. In addition to GAP function, p120 can be viewed as a RAS effector that binds to GTP-bound RAS and signals to other pathways (Chan and Chen, 2012). p120 controls RHO activity by interacting with RHOGAPs, p190 and deleted in liver cancer 1 (DLC1). DLC1 is frequently silenced in a variety of human cancers (Yuan *et al.*, 1998) and acts as a linker that coordinates the RAS and RHO signaling pathways (Shang *et al.*, 2007; Yang *et al.*, 2009; Asnaghi *et al.*, 2010). DLC1 RHOGAP function is required for the maintenance of cell morphology and the coordination of cell migration (Kim *et al.*, 2008). The preliminary data, revealed the elevated levels of *DLC1* mRNA in quiescent HSC *vs.* activated HSC and in qHSC we detected more *DLC1* than *p120* (data not shown). These observations raised the question, how RHO activity could be controlled *via* cross-link between p120GAP and DLC1 that may impair the RHO-dependent cell migration of qHSC. Therefore, we mechanistically and structurally analyzed the p120 interaction with DLC1 (chapter V) (Jaiswal *et al.*, 2014).

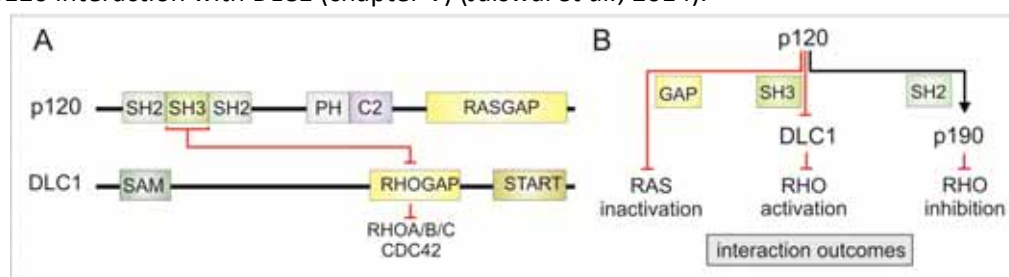


Figure 8. p120 interacts through SH3 domain with DLC1 and regulates RAS and RHO signaling. (A) Representation of p120 and DLC1 domain organization and interaction *via* SH3-GAP domain. (B) Schematic view of the p120 controlling RAS and RHO proteins. DLC1, deleted in liver cancer; PH, pleckstrin homology; SAM, sterile α motif; SH, Src homology; START, steroidogenic acute regulatory related lipid transfer.

GAPs function as a negative regulator of small GTPases, however the mechanisms which control GAP activity are poorly understood. To date, two mechanisms are proposed for DLC1GAP regulation; First, through *cis*-inhibition or autoinhibition, for instance, Kim and colleagues

² sequence-specific phosphotyrosine-binding module

³ recognition of proline-rich sequences

reported SAM domain of DLC1 acts as an autoinhibitor of this GAP (Kim *et al.*, 2008); Second, *trans*-inhibition of DLC1 through a RASGAP protein, p120 (Yang *et al.*, 2009).

p120 binds through SH3 domain to DLC1 and inhibits DLC1 in PxxP independent manner— Our *in silico* analysis revealed that the GAP domain of DLC1 does not possess a proline-rich region. Therefore, unlike classical PxxP motif-recognizing SH3 domains, the interaction mode of the p120 SH3 domain is atypical, utilizes different amino acids to bind, and masks the catalytic arginine finger of the GAP domain of DLC1. The Ser/Thr kinases Aurora A and Aurora B are other examples in addition to DLC1 for negative modulation of biological processes by p120 (Gigoux *et al.*, 2002). The SH3 domain of p120 binds to the catalytic domain of Aurora kinases that inhibits their kinase activity. These interactions also do not involve a proline-rich consensus sequence. Two accessible hydrophobic regions of p120 SH3 have been suggested to function as binding sites for protein interaction (Yang *et al.*, 1994).

Collectively, SH3 domain of p120 inhibits specifically DLC1GAP activity where p120 activated p190, through its SH2 domain (Fig. 8A and B). Our qPCR analysis showed that quiescent HSC harbors elevated levels of *DLC1* that were more than *p120* and *p190* levels. The overexpression of DLC isoforms has been shown to lead to inactivation of RHOA and to the reduction of actin stress-fiber formation (Leung *et al.*, 2005; Kawai *et al.*, 2007). On the other hand, RHOA controls the contraction and migration of activated HSC (Li *et al.*, 2012; Sohail *et al.*, 2009). Therefore, we speculated that a high level of DLC1 might inhibit the stress-fiber formation in quiescent HSC, where down-regulation of DLC1 in activated HSC results in increased RHOA activity and HSC contraction (Fig. 7C).

Scaffolding protein IQGAP modulates RHO and RAS signaling

Upon HSCs activation, quiescent HSCs develop into the cells that are able to contract and migrate. As we discussed earlier, our signaling analysis revealed the high levels of RAS-dependent signaling activity in activated HSCs (chapter III). Besides GAP proteins, scaffold proteins can cross-link RAS to RHO signaling. It is shown that IQGAPs scaffold different components of RAS-MAPK pathways as well as RHO GTPases, such as CDC42 and RAC proteins (Mataraza *et al.*, 2003a; Roy *et al.*, 2004; Roy *et al.*, 2005; Ren *et al.*, 2007); therefore, they may connect RAS signaling to RHO proteins and modulate the cell-adhesion and migration. Moreover, it is reported that the IQGAP1 plays a role in HSC activation by binding to TGF- β receptor II and suppresses HSC activation (Liu *et al.*, 2013a). These observations raised the questions; are there any evidences that IQGAPs actively scaffolds RHO proteins in HSCs? Which IQGAP isoforms are present in HSCs? Which regions of IQGAP determine the interaction specificity for RHO proteins? To address these questions, first, we generated various IQGAP1 constructs and with the aim of biochemical studies of IQGAP1 interaction with different RHO family members, we identified the C-terminal region of IQGAP1⁸⁶³⁻¹⁶⁵⁷ (here after called GRD-C) is responsible for high affinity of IQGAP1 to interact with GTP-loaded RAC and CDC42 proteins but not RHO subgroup. Second, we investigated the expression pattern of IQGAP1/2/3, RAC1/2/3 and CDC42 in quiescent vs. activated HSC.

GBD domain (1345-1563) of IQGAP1 tightly binds to RAC and CDC42 in GTP-dependent fashion—In this study, a comprehensive interaction study of RHO GTPases and C-terminal domain of IQGAP1⁸⁶³⁻¹⁶⁵⁷ (here called GRD-C) was conducted. Kinetics of GRD-C association with fourteen different RHO proteins was monitored using stopped-flow fluorescence spectroscopic methods. The results clearly indicate that IQGAP1 binds among RHO proteins selectively to RAC- and CDC42-like proteins only in the active form and that GRD-C containing IQGAP1¹³⁴⁶⁻¹⁶⁵⁷ most probably recognizes and binds to the switch regions but however not, as previously proposed by several groups (Mataraza *et al.*, 2003b; Owen *et al.*, 2008; Kurella *et al.*, 2009), the GRD-containing IQGAP⁹⁶²⁻¹³⁴⁵.

Reciprocal expression of IQGAP isoforms during activation of the hepatic stellate cells—IQGAP family composes of three isoforms, IQGAP1, 2 and 3, which are differentially expressed in distinct tissues. In addition to share a set of binding partners, each isoforms possess its specific binding partners and therefore contribute to different cellular processes (Weissbach *et al.*, 1994; Brill *et al.*, 1996; Wang *et al.*, 2007). For instance, IQGAP1 is recognized as an oncogene where IQGAP2 is a tumor suppressor (White *et al.*, 2009b; White *et al.*, 2010b). IQGAP2 is shown to be expressed predominantly in liver. We asked the question, is there any isoform preference for IQGAPs during HSC activation? Our quantitative RNA analysis revealed that *IQGAP1* and *3* isoforms, get upregulated during the activation process of HSC where the *IQGAP2* down-regulated. At protein levels, we were able to detect IQGAP2 isoform only in quiescent HSC where IQGAP1 presented in both states of HSC and became up-regulated during HSC activation. Consistently, Schmidt and colleagues, reported the reciprocal expression of IQGAP1 and 2 in human hepatocellular carcinomas where IQGAP1 increased and IQGAP2 decreased (White *et al.*, 2010b). Domain organization of IQGAP1 and 2 are similar, and both are reported to interact with GTP-loaded CDC42 and RAC1 (Smith *et al.*, 2015c). In quiescent HSC, we speculate that IQGAP2 exerts its specific functions by scaffolding the distinct signaling components in different protein complexes than IQGAP1. Canonical Wnt signaling is very dynamic in quiescent HSC and it is shown in other cells, IQGAP2 can interact with Dishevelled/ β -catenin, therefore in qHSC IQGAP2 may modulate Wnt- β -catenin signaling and stimulate GFAP synthesis and cell-cycle arrest (Kordes *et al.*, 2008a; Schmidt *et al.*, 2008). Another possibility would be, IQGAP2 competes with other scaffolding proteins to recruits RHO proteins and may interfere with RHO dependent-cell migration (Fig. 7B). The functions and specific binding partners of IQGAP2 in qHSC remain to be investigated. aHSCs display the elevated levels of PDGF signaling and focal adhesion kinase (FAK) acts downstream of PDGF (Carloni *et al.*, 2000). PDGF induces the IQGAP1-dependent complex formation of focal adhesion proteins (paxillin and vinculin) and PDGF receptor β (Kohno *et al.*, 2013). IQGAP1 also binds to FAK (Cheung *et al.*, 2013), therefore, PDGF-IQGAP1 may regulate the focal adhesion assembly in aHSCs that is important for cell motility and migration.

Elevated levels of the RAC and CDC42 correlate with high amount of IQGAP1 in activated HSC—We detected higher levels of RAC1, RAC2 and CDC42 in aHSCs than qHSC. On the other hand, our biochemical studies demonstrated that RAC1 and CDC42 interact in GTP-bound forms with IQGAP1-GBD. Therefore, we suggest that IQGAP1 scaffolds RAC1/2 and CDC42 to regulate cell-adhesion and migration in these cells. However, the role of IQGAP1 in aHSC needs to be investigated.

IQGAP1 exhibits the highest affinity for RAC2 isoform—qPCR data reveals in hepatic stellate cells, *RAC2* drastically increased in activated state. In addition, the interaction of *IQGAP1*^{GRD-C} with *RAC*- and *CDC42*-like proteins revealed the fastest association with *RAC2*, which is 2-9 fold higher than others. The highest affinity of *RAC2* for GRD-C can most likely be attributed to distinct amino acid sequence deviations. The high affinity of *RAC2* for *IQGAP1* cannot be explained by comparing potential residues that may undergo direct interacting contacts in spite of high amino acid sequence identity. Another aspect to be considered is the overall dynamics of the G domain, which has been previously proposed to contribute to a higher affinity, in the case of *RAC2* compared to *RAC1* and *RAC3* (Haeusler *et al.*, 2003). Due to the highest affinity of *IQGAP1* for *RAC2* and up-regulation of *RAC2/IQGAP1* in activated HSCs, we suggest that *IQGAP1* might associate *RAC2* with its specific protein complex to accelerate their interaction (Fig. 7C).

Cross-link between RAS-MAPK and RHO pathways—In addition to scaffold the RHO signaling components (*RAC* and *CDC42*), *IQGAP1* identified to interact with different signaling components of RAS-MAPK pathway, RTKs, *KRAS*, *BRAF/CRAF*, *MEK1/2* and *ERK1/2*, and directs the information flow from the EGF to *ERK1/2* phosphorylation (Roy *et al.*, 2004; Roy *et al.*, 2005; Ren *et al.*, 2007) (Fig. 7C). It is reported upon hyaluronan (HA) stimulation of *CD44* receptor, *IQGAP1* anchors the *CDC42* and *ERK2* to *CD44* and F-actin that results in phosphorylation of *ERK2*. Moreover, at the level of focal adhesions, it is reported that RAS proteins mediate the Tyrosine phosphorylation of *FAK* via *PDGF* receptor in activated HSC (Carloni *et al.*, 2000) that most probably this complex can form through the *IQGAP1*. Therefore, *IQGAP1* may bridge the MAPK pathways to cytoskeleton organization machinery in hepatic stellate cells. On the other hand, our genetic screening of JMML patients revealed a correlation between *RAC2* and *NRAS* double mutants in one patient which *RAC2* mutation drives the *PI3K-AKT-mTORC* pathway in parallel to *NRAS* mutation (chapter VII) (see below).

The coordination of RAS (NRAS) and RHO (RAC2) mutations in tumor progression

In pathological conditions, the aberrant activation of RAS proteins due to the somatic or germline mutations in the critical residues of RAS proteins (G12, G13 or Q61; HRAS numbering) or their regulators are very common in a wide spectrum of human cancers and genetic disorders (Ratner and Miller, 2015). Juvenile myelomonocytic leukemia (JMML) is a rare and severe myelodysplastic and myeloproliferative neoplasm of early childhood is initiated by germline or somatic RAS-activating mutations (Chang *et al.*, 2014). JMML is considered a unique example of RAS-driven oncogenesis since it is thought to be initiated by mutations, usually described as mutually exclusive, in *RAS* genes (*NRAS*, *KRAS*) or *RAS*-pathway regulators (*PTPN11*, *NF1* or *CBL*). JMML can be sporadic or develop in patients displaying syndromic diseases with constitutional RAS overactivation such as Noonan syndrome (NS), type 1-neurofibromatosis (NF1) and CBL syndrome, caused by heterozygous germline mutations in *PTPN11*, *NF1* and *CBL*, respectively (Niemeyer, 2014). In this study, multiple concomitant genetic hits targeting the RAS-pathway were identified in 13/78 cases (17%), disproving the concept of exclusive *RAS* mutations and defining novel activated JMML pathways involving *PI3K* and the *mTORC2* complex through *RAC2* mutation (chapter VII) (Caye *et al.*, 2015).

JMML pathways involving PI3K and the mTORC2 complex through RAC2 mutation— Multiple concomitant genetic hits targeting the RAS pathway in JMML patients, identified mutations in *RAS* genes. Two *NRAS*-JMML patients had mutations in *RRAS*, an inducer of RAS/MAPK activation (Flex *et al.*, 2014) and upstream regulator of RAC in hematopoietic stem cells (Shang *et al.*, 2011), and another had a mutation in the RHO GTPase *RAC2*^{V63}. The coexistence of *RAC* and *RAS/MAPK* mutations in some tumors and cooperation between oncogenic *NRAS* and *RAC* has been previously demonstrated (Kawazu *et al.*, 2013). Investigations into the functional and structural properties of *RAC2*^{V63}, which predominantly occurs in its active, GTP-loaded state as compared to wild-type *RAC2* and the constitutive variant *RAC2*^{V12}, have revealed a drastic gain-of-function effect. Interestingly, an analysis of signaling downstream to RAS has shown that *RAC2*^{V63} activates the PI3K-PDK1-AKT and the mTORC2 pathways but has no significant effect on the RAF-MEK-ERK pathway. This is consistent with several lines of evidence indicating a strong impact of the PI3K-PDK1-AKT pathway on JMML (Emanuel, 2014), and activating the catalytic p110 γ subunit of PI3K has recently been shown to promote the effects of Shp2 on GM-CSF hypersensitivity (Goodwin *et al.*, 2014).

This study sheds light on the intercommunication of *RAC2*-GTP with *NRAS*-GTP to induce the mTORC2 and PI3K pathways and provides evidence for *in vivo* RHO and RAS cross-talk in disease model. On the other hand, we detected high levels of *RAC2* in aHSC that may also signal towards the PI3K-mTORC2 and MAPK therefore promotes cell survival, proliferation, which needs further investigations (Fig. 7C).

Concluding remarks

Collectively, with aim of this doctoral thesis, we shed light on the RAS-dependent intracellular signaling pathways that drive the fate decisions of HSC and maintain the quiescence of HSC or induce HSC activation, proliferation, contraction and migration (Fig. 7). We identified *ERAS*, *p110 α* , *p110 γ* , *IQGAP2* and *DLC1* expressed mainly in qHSCs, and *MRAS*, *RRAS*, *RAP2A*, *RALA*, *p110 β* , *p110 δ* , *YAP*, *CTGF*, *NOTCH2*, *IQGAP1*, *RAC1*, *RAC2* and *CDC42* in aHSCs (Fig. 7A). Obtained data suggested elevated *ERAS*-dependent signaling pathway activity *via* PI3K-AKT-mTORC1, mSIN1-mTORC2-AKT-FOXO1, LIF-STAT3, and HIPPO signaling in qHSCs (Fig. 7B). However, we detected high levels of RAS-MAPK and YAP-NOTCH2/CTGF in aHSCs. Moreover, our cell-based studies were combined with biochemical and mechanistic studies of highlighted molecules in qHSC and aHSC that provided detailed information about the mode of regulation and networking of these molecules. Biochemical analysis demonstrated that effector selection of *ERAS* significantly differs from *HRAS* (chapter II). *ERAS* specificity and consequently cellular outcomes depend on its unique switch and interswitch regions and W79 of *ERAS* appears to determine the effector selectivity. Expressional analysis reveals a different expression pattern of RAS and RAS-signaling components in qHSCs vs. aHSCs. Among the RHO regulators, we observed more *DLC1*RHOGAP in qHSC than aHSC, which were higher than *p120RASGAP* in both state. On the other hand, our mechanistic and structural studies of *DLC1*RHOGAP and *p120RASGAP* revealed interesting aspects of RHO regulations *via* a well-known RAS regulator (chapter V). We found *p120RASGAP* competitively and selectively inhibits *DLC1* by targeting its catalytic arginine finger that is mediated through *p120* SH3 and *DLC1* RHOGAP domain interaction (Fig. 8A).

Therefore, herein, we emphasize the functional inter-relationships of GAPs that mediate a cross-talk between the RAS and RHO pathways. Beside GAPs, scaffolding proteins, such as IQGAPs, link RAS to RHO signaling. We observed reciprocal expression of IQGAP isoforms and RHO proteins in hepatic stellate cells; IQGAP1/3, RAC2 and CDC42 are upregulated during the activation process of HSCs while IQGAP2 is down-regulated. Amongst different RHO proteins, our kinetic and equilibrium measurements implicated that IQGAP1 selectively interacts in a GTP-dependent manner with RAC and CDC42 (chapter VI). We showed that these interactions are mediated through the C-terminal half of IQGAP1 composing three functionally distinct units, including GRD, GBD and C-terminus. GBD only binds to the RAC1 and CDC42 proteins if they are active and exist in the GTP-bound forms, where GRD undergoes a low-affinity, GDP-/GTP-independent complex with these proteins. Consistent with our data on GAP and IQGAP proteins, which may link signal transduction of RAS to RHO, we found a functional cross-talk between RHO and RAS mutations in disease progression with the aid of whole genomic sequencing of the juvenile myelomonocytic leukemia (JMML) patients (chapter VII). Genetic profiling and whole-exome sequencing of a large JMML cohort, showed for the first time that concomitant mutations in JMML target a small number of interacting networks, with a striking enrichment in components of the RAS and PRC2 networks. This study sheds light on the inter-communication of RAC2 with NRAS to activate the mTORC2 and PI3K pathways. Consistent with data from JMML patient, high levels of RAC2 in aHSC may also signal towards the PI3K-mTORC2 and MAPK, therefore, promotes cell survival, proliferation (Fig. 7C). Collectively, with the aim of cell biological and biochemical studies, we suggest a possible ERAS/RAS signaling networks in qHSC vs. aHSC and propose a model that links RAS and RHO signaling in order to regulate cellular processes, such as cell migration (Fig. 7). Therefore, this study adds additional clues to the remarkable signaling features of qHSC and how the cellular outcome of these signaling pathways would maintain quiescent state of qHSC by the inhibition of proliferation (HIPPO pathways, G0 arrest) and apoptosis (PI3K-PDK1 and mTORC2) (see Fig. 7B). Where, in aHSC the activity of YAP-CTGF/NOTCH2, RAS-RAF-MEK-ERK, RAC2, CDC42 and RHOA may contribute to the HSC proliferation, development and migration (Fig. 7C).

References

- Abel, A. M., Schuldt, K. M., Rajasekaran, K., Hwang, D., Riese, M. J., Rao, S., Thakar, M. S. & Malarkannan, S. (2015). IQGAP1: insights into the function of a molecular puppeteer. *Mol Immunol* 65(2): 336-349.
- Ada-Nguema, A. S., Xenias, H., Hofman, J. M., Wiggins, C. H., Sheetz, M. P. & Keely, P. J. (2006). The small GTPase R-Ras regulates organization of actin and drives membrane protrusions through the activity of PLCepsilon. *J Cell Sci* 119(Pt 7): 1307-1319.
- Ahearn, I. M., Haigis, K., Bar-Sagi, D. & Philips, M. R. (2011). Regulating the regulator: post-translational modification of RAS. *Nat Rev Mol Cell Biol* 13(1): 39-51.
- Ahmadian, M. R., Hoffmann, U., Goody, R. S. & Wittinghofer, A. (1997a). Individual rate constants for the interaction of Ras proteins with GTPase-activating proteins determined by fluorescence spectroscopy. *Biochemistry* 36(15): 4535-4541.
- Ahmadian, M. R., Stege, P., Scheffzek, K. & Wittinghofer, A. (1997b). Confirmation of the arginine-finger hypothesis for the GAP-stimulated GTP-hydrolysis reaction of Ras. *Nat Struct Biol* 4(9): 686-689.
- Ahmadian, M. R., Wittinghofer, A. & Schmidt, G. (2002). The actin filament architecture: tightly regulated by the cells, manipulated by pathogens. International Titisee Conference on the actin cytoskeleton: from signalling to bacterial pathogenesis. *EMBO Rep* 3(3): 214-218.
- Alessi, D. R., James, S. R., Downes, C. P., Holmes, A. B., Gaffney, P. R., Reese, C. B. & Cohen, P. (1997). Characterization of a 3-phosphoinositide-dependent protein kinase which phosphorylates and activates protein kinase Balpha. *Curr Biol* 7(4): 261-269.
- Amin, E., Dubey, B. N., Zhang, S. C., Gremer, L., Dvorsky, R., Moll, J. M., Taha, M. S., Nagel-Steger, L., Piekorz, R. P., Somlyo, A. V. & Ahmadian, M. R. (2013). Rho-kinase: regulation, (dys)function, and inhibition. *Biol Chem* 394(11): 1399-1410.
- Andjelkovic, M., Alessi, D. R., Meier, R., Fernandez, A., Lamb, N. J., Frech, M., Cron, P., Cohen, P., Lucocq, J. M. & Hemmings, B. A. (1997). Role of translocation in the activation and function of protein kinase B. *J Biol Chem* 272(50): 31515-31524.
- Aoyama, M., Kataoka, H., Kubota, E., Tada, T. & Asai, K. (2010). Resistance to chemotherapeutic agents and promotion of transforming activity mediated by embryonic stem cell-expressed Ras (ERas) signal in neuroblastoma cells. *Int J Oncol* 37(4): 1011-1016.
- Apolloni, A., Prior, I. A., Lindsay, M., Parton, R. G. & Hancock, J. F. (2000). H-ras but not K-ras traffics to the plasma membrane through the exocytic pathway. *Mol Cell Biol* 20(7): 2475-2487.
- Arthur, M. J., Stanley, A., Iredale, J. P., Rafferty, J. A., Hembry, R. M. & Friedman, S. L. (1992). Secretion of 72 kDa type IV collagenase/gelatinase by cultured human lipocytes. Analysis of gene expression, protein synthesis and proteinase activity. *Biochem J* 287 (Pt 3): 701-707.
- Asahina, K., Zhou, B., Pu, W. T. & Tsukamoto, H. (2011). Septum transversum-derived mesothelium gives rise to hepatic stellate cells and perivascular mesenchymal cells in developing mouse liver. *Hepatology* 53(3): 983-995.
- Asnaghi, L., Vass, W. C., Quadri, R., Day, P. M., Qian, X., Braverman, R., Papageorge, A. G. & Lowy, D. R. (2010). E-cadherin negatively regulates neoplastic growth in non-small cell lung cancer: role of Rho GTPases. *Oncogene* 29(19): 2760-2771.
- Avruch, J., Long, X., Lin, Y., Ortiz-Vega, S., Rapley, J., Papageorgiou, A., Oshiro, N. & Kikkawa, U. (2009). Activation of mTORC1 in two steps: Rheb-GTP activation of catalytic function and increased binding of substrates to raptor1. *Biochem Soc Trans* 37(1): 223-226.
- Avruch, J., Zhou, D., Fitamant, J. & Bardeesy, N. (2010). Mst1/2 signalling to Yap: gatekeeper for liver size and tumour development. *Br J Cancer* 104(1): 24-32.
- Aznar, S. & Lacal, J. C. (2001). Rho signals to cell growth and apoptosis. *Cancer Lett* 165(1): 1-10.
- Barras, D. (2015). BRAF Mutation in Colorectal Cancer: An Update. *Biomark Cancer* 7(Suppl 1): 9-12.
- Benyon, R. C. & Arthur, M. J. (2001). Extracellular matrix degradation and the role of hepatic stellate cells. *Semin Liver Dis* 21(3): 373-384.
- Berg, T., Rountree, C. B., Lee, L., Estrada, J., Sala, F. G., Choe, A., Veltmaat, J. M., De Langhe, S., Lee, R., Tsukamoto, H., Crooks, G. M., Bellusci, S. & Wang, K. S. (2007). Fibroblast growth factor 10 is critical for liver growth during embryogenesis and controls hepatoblast survival via beta-catenin activation. *Hepatology* 46(4): 1187-1197.

- Bhattacharya, M., Sundaram, A., Kudo, M., Farmer, J., Ganesan, P., Khalifeh-Soltani, A., Arjomandi, M., Atabai, K., Huang, X. & Sheppard, D. (2014). IQGAP1-dependent scaffold suppresses RhoA and inhibits airway smooth muscle contraction. *J Clin Invest* 124(11): 4895-4898.
- Bishop, A. L. & Hall, A. (2000). Rho GTPases and their effector proteins. *Biochem J* 348 Pt 2: 241-255.
- Blaner, W. S., O'Byrne, S. M., Wongsiriroj, N., Kluwe, J., D'Ambrosio, D. M., Jiang, H., Schwabe, R. F., Hillman, E. M. C., Piantedosi, R. & Libien, J. (2009). Hepatic stellate cell lipid droplets: A specialized lipid droplet for retinoid storage. *Biochim Biophys Acta* 1791(6): 467-473.
- Boccaccio, C., Ando, M., Tamagnone, L., Bardelli, A., Michieli, P., Battistini, C. & Comoglio, P. M. (1998). Induction of epithelial tubules by growth factor HGF depends on the STAT pathway. *Nature* 391(6664): 285-288.
- Bodemann, B. O. & White, M. A. (2014). The Coordinated Biology and Signaling Partners of Ral G-Proteins. In *Ras Superfamily Small G Proteins: Biology and Mechanisms 1*, 257-279 (Ed A. Wittinghofer). Springer Vienna.
- Bolis, A., Corbetta, S., Cioce, A. & de Curtis, I. (2003). Differential distribution of Rac1 and Rac3 GTPases in the developing mouse brain: implications for a role of Rac3 in Purkinje cell differentiation. *Eur J Neurosci* 18(9): 2417-2424.
- Bos, J. L. (1989). ras oncogenes in human cancer: a review. *Cancer Res* 49(17): 4682-4689.
- Bourbonnais, E., Raymond, V. A., Ethier, C., Nguyen, B. N., El-Leil, M. S., Meloche, S. & Bilodeau, M. (2012). Liver fibrosis protects mice from acute hepatocellular injury. *Gastroenterology* 142(1): 130-139 e134.
- Bourguignon, L. Y., Gilad, E., Rothman, K. & Peyrollier, K. (2005). Hyaluronan-CD44 interaction with IQGAP1 promotes Cdc42 and ERK signaling, leading to actin binding, Elk-1/estrogen receptor transcriptional activation, and ovarian cancer progression. *J Biol Chem* 280(12): 11961-11972.
- Bourne, H. R., Sanders, D. A. & McCormick, F. (1990). The GTPase superfamily: a conserved switch for diverse cell functions. *Nature* 348(6297): 125-132.
- Bourne, H. R., Sanders, D. A. & McCormick, F. (1991). The GTPase superfamily: conserved structure and molecular mechanism. *Nature* 349(6305): 117-127.
- Braet, F., Riches, J., Geerts, W., Jahn, K. A., Wisse, E. & Frederik, P. (2009). Three-dimensional organization of fenestrae labyrinths in liver sinusoidal endothelial cells. *Liver Int* 29(4): 603-613.
- Brandt, D. T. & Grosse, R. (2007). Get to grips: steering local actin dynamics with IQGAPs. *EMBO Rep* 8(11): 1019-1023.
- Brill, S., Li, S., Lyman, C. W., Church, D. M., Wasmuth, J. J., Weissbach, L., Bernards, A. & Snijders, A. J. (1996). The Ras GTPase-activating-protein-related human protein IQGAP2 harbors a potential actin binding domain and interacts with calmodulin and Rho family GTPases. *Mol Cell Biol* 16(9): 4869-4878.
- Brown, M. D., Bry, L., Li, Z. & Sacks, D. B. (2007). IQGAP1 regulates Salmonella invasion through interactions with actin, Rac1, and Cdc42. *J Biol Chem* 282(41): 30265-30272.
- Brown, M. D. & Sacks, D. B. (2006). IQGAP1 in cellular signaling: bridging the GAP. *Trends Cell Biol* 16(5): 242-249.
- Buday, L. & Downward, J. (2008). Many faces of Ras activation. *Biochim Biophys Acta* 1786(2): 178-187.
- Bunney, T. & Katan, M. (2006). Phospholipase C epsilon: linking second messengers and small GTPases. *Trends Cell Biol* 16(12): 640-648.
- Bunney, T. D., Harris, R., Gandarillas, N. L., Josephs, M. B., Roe, S. M., Sorli, S. C., Paterson, H. F., Rodrigues-Lima, F., Esposito, D., Ponting, C. P., Gierschik, P., Pearl, L. H., Driscoll, P. C. & Katan, M. (2006). Structural and Mechanistic Insights into Ras Association Domains of Phospholipase C Epsilon. *Mol Cell* 21(4): 495-507.
- Bunney, T. D. & Katan, M. (2011). PLC regulation: emerging pictures for molecular mechanisms. *Trends Biochem Sci* 36(2): 88-96.
- Burt, A. D. & Day, C. P. (2003). Pathophysiology of the liver. In *Pathology of the Liver*, 67-105 (Ed R. MacSween). New York: Churchill Livingstone.
- Buss, J. E. & Sefton, B. M. (1986). Direct identification of palmitic acid as the lipid attached to p21ras. *Mol Cell Biol* 6(1): 116-122.
- Camargo, F. D., Gokhale, S., Johnnidis, J. B., Fu, D., Bell, G. W., Jaenisch, R. & Brummelkamp, T. R. (2007). YAP1 Increases Organ Size and Expands Undifferentiated Progenitor Cells. *Curr Biol* 17(23): 2054-2060.

- Cantwell-Dorris, E. R., O'Leary, J. J. &Sheils, O. M. (2011). BRAFV600E: Implications for Carcinogenesis and Molecular Therapy. *Mol Cancer Ther* 10(3): 385-394.
- Carloni, V., Defranco, R. M., Caligiuri, A., Gentilini, A., Sciammetta, S. C., Baldi, E., Lottini, B., Gentilini, P. &Pinzani, M. (2002). Cell adhesion regulates platelet-derived growth factor-induced MAP kinase and PI-3 kinase activation in stellate cells. *Hepatology* 36(3): 582-591.
- Carloni, V., Pinzani, M., Giusti, S., Romanelli, R. G., Parola, M., Bellomo, G., Failli, P., Hamilton, A. D., Sebti, S. M., Laffi, G. &Gentilini, P. (2000). Tyrosine phosphorylation of focal adhesion kinase by PDGF is dependent on ras in human hepatic stellate cells. *Hepatology* 31(1): 131-140.
- Casteel, D. E., Turner, S., Schwappacher, R., Rangaswami, H., Su-Yuo, J., Zhuang, S., Boss, G. R. &Pilz, R. B. (2012). Rho isoform-specific interaction with IQGAP1 promotes breast cancer cell proliferation and migration. *J Biol Chem* 287(45): 38367-38378.
- Castellano, E. &Santos, E. (2011). Functional Specificity of Ras Isoforms: So Similar but So Different. *Genes Cancer* 2(3): 216-231.
- Castilho-Fernandes, A., de Almeida, D. C., Fontes, A. M., Melo, F. U., Picanco-Castro, V., Freitas, M. C., Orellana, M. D., Palma, P. V., Hackett, P. B., Friedman, S. L. &Covas, D. T. (2011). Human hepatic stellate cell line (LX-2) exhibits characteristics of bone marrow-derived mesenchymal stem cells. *Exp Mol Pathol* 91(3): 664-672.
- Castilho, R. M., Squarize, C. H., Chodosh, L. A., Williams, B. O. &Gutkind, J. S. (2009). mTOR mediates Wnt-induced epidermal stem cell exhaustion and aging. *Cell Stem Cell* 5(3): 279-289.
- Caye, A., Strullu, M., Guidez, F., Cassinat, B., Gazal, S., Fenneteau, O., Lainey, E., Nouri, K., Nakhaei-Rad, S., Dvorsky, R., Lachenaud, J., Pereira, S., Vivent, J., Verger, E., Vidaud, D., Galambrun, C., Picard, C., Petit, A., Contet, A., Poirée, M., Sirvent, N., Méchinaud, F., Adjaoud, D., Paillard, C., Nelken, B., Reguerre, Y., Bertrand, Y., Häussinger, D., Dalle, J.-H., Ahmadian, M. R., Baruchel, A., Chomienne, C. &Cavé, H. (2015). Juvenile myelomonocytic leukemia displays mutations in components of the RAS pathway and the PRC2 network. *Nat Genet*.
- Cerione, R. A. (2004). Cdc42: new roads to travel. *Trends Cell Biol* 14(3): 127-132.
- Chan, P. C. &Chen, H. C. (2012). p120RasGAP-mediated activation of c-Src is critical for oncogenic Ras to induce tumor invasion. *Cancer Res* 72(9): 2405-2415.
- Chang, T. Y., Dvorak, C. C. &Loh, M. L. (2014). Bedside to bench in juvenile myelomonocytic leukemia: insights into leukemogenesis from a rare pediatric leukemia. *Blood* 124(16): 2487-2497.
- Cheung, K. L., Lee, J. H., Shu, L., Kim, J. H., Sacks, D. B. &Kong, A. N. (2013). The Ras GTPase-activating-like protein IQGAP1 mediates Nrf2 protein activation via the mitogen-activated protein kinase/extracellular signal-regulated kinase (ERK) kinase (MEK)-ERK pathway. *Journal of Biological Chemistry* 288(31): 22378-22386.
- Chiang, G. G. &Abraham, R. T. (2005). Phosphorylation of Mammalian Target of Rapamycin (mTOR) at Ser-2448 Is Mediated by p70S6 Kinase. *Journal of Biological Chemistry* 280(27): 25485-25490.
- Chiang, J. &Martinez-Agosto, J. A. (2012). Effects of mTOR Inhibitors on Components of the Salvador-Warts-Hippo Pathway. *Cells* 1(4): 886-904.
- Chiang, S. H., Chang, L. &Saltiel, A. R. (2006). TC10 and insulin-stimulated glucose transport. *Methods Enzymol* 406: 701-714.
- Chouker, A., Martignoni, A., Dugas, M., Eisenmenger, W., Schauer, R., Kaufmann, I., Schelling, G., Lohe, F., Jauch, K. W., Peter, K. &Thiel, M. (2004). Estimation of liver size for liver transplantation: the impact of age and gender. *Liver Transpl* 10(5): 678-685.
- Cirstea, I. C., Gremer, L., Dvorsky, R., Zhang, S. C., Piekorz, R. P., Zenker, M. &Ahmadian, M. R. (2013). Diverging gain-of-function mechanisms of two novel KRAS mutations associated with Noonan and cardio-facio-cutaneous syndromes. *Hum Mol Genet* 22(2): 262-270.
- Clagett-Dame, M. &Knutson, D. (2011). Vitamin A in Reproduction and Development. *Nutrients* 3(12): 385-428.
- Clark, E. A., Golub, T. R., Lander, E. S. &Hynes, R. O. (2000). Genomic analysis of metastasis reveals an essential role for RhoC. *Nature* 406(6795): 532-535.
- Coleman, M. L., Marshall, C. J. &Olson, M. F. (2004). RAS and RHO GTPases in G1-phase cell-cycle regulation. *Nat Rev Mol Cell Biol* 5(5): 355-366.
- Coll, M., El Taghdouini, A., Perea, L., Mannerts, I., Vila-Casadesus, M., Blaya, D., Rodrigo-Torres, D., Affo, S., Morales-Ibanez, O., Graupera, I., Lozano, J. J., Najimi, M., Sokal, E., Lambrecht, J., Gines, P., van Grunsven, L. A. &Sancho-Bru, P. (2015). Integrative miRNA and Gene Expression Profiling Analysis of Human Quiescent Hepatic Stellate Cells. *Sci Rep* 5: 11549.

- Cupit, L. D., Schmidt, V. A., Miller, F. & Bahou, W. F. (2004). Distinct PAR/IQGAP expression patterns during murine development: implications for thrombin-associated cytoskeletal reorganization. *Mamm Genome* 15(8): 618-629.
- De Minicis, S., Seki, E., Uchinami, H., Kluwe, J., Zhang, Y., Brenner, D. A. & Schwabe, R. F. (2007). Gene Expression Profiles During Hepatic Stellate Cell Activation in Culture and In Vivo. *Gastroenterology* 132(5): 1937-1946.
- de Souza, I. C. C., Meira Martins, L. A., de Vasconcelos, M., de Oliveira, C. M., Barbé-Tuana, F., Andrade, C. B., Pettenuzzo, L. F., Borojevic, R., Margis, R., Guaragna, R. & Guma, F. C. R. (2015). Resveratrol Regulates the Quiescence-Like Induction of Activated Stellate Cells by Modulating the PPAR γ /SIRT1 Ratio. *J Cell Biochem*: n/a-n/a.
- Dechene, A., Sowa, J. P., Gieseler, R. K., Jochum, C., Bechmann, L. P., El Fouly, A., Schlattjan, M., Saner, F., Baba, H. A., Paul, A., Dries, V., Odenthal, M., Gerken, G., Friedman, S. L. & Canbay, A. (2010). Acute liver failure is associated with elevated liver stiffness and hepatic stellate cell activation. *Hepatology* 52(3): 1008-1016.
- Delgado, J. P., Vanneaux, V., Branger, J., Touboul, T., Sentilhes, L., Mainot, S., Lainas, P., Leclerc, P., Uzan, G., Mahieu-Caputo, D. & Weber, A. (2009). The role of HGF on invasive properties and repopulation potential of human fetal hepatic progenitor cells. *Exp Cell Res* 315(19): 3396-3405.
- DerMardirossian, C. & Bokoch, G. M. (2005). GDIs: central regulatory molecules in Rho GTPase activation. *Trends Cell Biol* 15(7): 356-363.
- DeYoung, M. P., Horak, P., Sofer, A., Sgroi, D. & Ellisen, L. W. (2008). Hypoxia regulates TSC1/2-mTOR signaling and tumor suppression through REDD1-mediated 14-3-3 shuttling. *Genes Dev* 22(2): 239-251.
- Di Masi, A., Leboffe, L., De Marinis, E., Pagano, F., Cicconi, L., Rochette-Egly, C., Lo-Coco, F., Ascenzi, P. & Nervi, C. (2015). Retinoic acid receptors: from molecular mechanisms to cancer therapy. *Mol Aspects Med* 41: 1-115.
- Didsbury, J., Weber, R. F., Bokoch, G. M., Evans, T. & Snyderman, R. (1989). rac, a novel ras-related family of proteins that are botulinum toxin substrates. *J Biol Chem* 264(28): 16378-16382.
- Diebold, B. A., Fowler, B., Lu, J., Dinauer, M. C. & Bokoch, G. M. (2004). Antagonistic cross-talk between Rac and Cdc42 GTPases regulates generation of reactive oxygen species. *J Biol Chem* 279(27): 28136-28142.
- Dillon, L. M., Bean, J. R., Yang, W., Shee, K., Symonds, L. K., Balko, J. M., McDonald, W. H., Liu, S., Gonzalez-Angulo, A. M., Mills, G. B., Arteaga, C. L. & Miller, T. W. (2014). P-REX1 creates a positive feedback loop to activate growth factor receptor, PI3K/AKT and MEK/ERK signaling in breast cancer. *Oncogene* 6(10): 328.
- Dixon, L. J., Barnes, M., Tang, H., Pritchard, M. T. & Nagy, L. E. (2013). Kupffer cells in the liver. *Compr Physiol* 3(2): 785-797.
- Duester, G. (2008). Retinoic Acid Synthesis and Signaling during Early Organogenesis. *Cell* 134(6): 921-931.
- Dupraz, S., Grassi, D., Bernis, M. E., Sosa, L., Bisbal, M., Gastaldi, L., Jausoro, I., Caceres, A., Pfenninger, K. H. & Quiroga, S. (2009). The TC10-Exo70 complex is essential for membrane expansion and axonal specification in developing neurons. *J Neurosci* 29(42): 13292-13301.
- Dvorsky, R. & Ahmadian, M. R. (2004). Always look on the bright side of Rho: structural implications for a conserved intermolecular interface. *EMBO Rep* 5(12): 1130-1136.
- Edwards, D. C., Sanders, L. C., Bokoch, G. M. & Gill, G. N. (1999). Activation of LIM-kinase by Pak1 couples Rac/Cdc42 GTPase signalling to actin cytoskeletal dynamics. *Nat Cell Biol* 1(5): 253-259.
- Elliott, S. F., Allen, G. & Timson, D. J. (2012). Biochemical analysis of the interactions of IQGAP1 C-terminal domain with CDC42. *World J Biol Chem* 3(3): 53-60.
- Emanuel, P. D. (2014). Hallway gossip between Ras and PI3K pathways. *Blood* 123(18): 2751-2753.
- Etienne-Manneville, S. & Hall, A. (2002). Rho GTPases in cell biology. *Nature* 420(6916): 629-635.
- Fansa, E. K., Dvorsky, R., Zhang, S. C., Fiegen, D. & Ahmadian, M. R. (2013). Interaction characteristics of Plexin-B1 with Rho family proteins. *Biochem Biophys Res Commun* 434(4): 785-790.
- Fasano, O., Aldrich, T., Tamanoi, F., Taparowsky, E., Furth, M. & Wigler, M. (1984). Analysis of the transforming potential of the human H-ras gene by random mutagenesis. *Proc Natl Acad Sci U S A* 81(13): 4008-4012.
- Ferro, E. & Trabalzini, L. (2010). RalGDS family members couple Ras to Ral signalling and that's not all. *Cell Signal* 22(12): 1804-1810.

- Fiegen, D., Blumenstein, L., Stege, P., Vetter, I. R. &Ahmadian, M. R. (2002). Crystal structure of Rnd3/RhoE: functional implications. *FEBS Lett* 525(1-3): 100-104.
- Fiegen, D., Haeusler, L. C., Blumenstein, L., Herbrand, U., Dvorsky, R., Vetter, I. R. &Ahmadian, M. R. (2004). Alternative splicing of Rac1 generates Rac1b, a self-activating GTPase. *J Biol Chem* 279(6): 4743-4749.
- Flex, E., Jaiswal, M., Pantaleoni, F., Martinelli, S., Strullu, M., Fansa, E. K., Caye, A., De Luca, A., Lepri, F., Dvorsky, R., Pannone, L., Paolacci, S., Zhang, S. C., Fodale, V., Bocchinfuso, G., Rossi, C., Burkitt-Wright, E. M., Farrotti, A., Stellacci, E., Cecchetti, S., Ferese, R., Bottero, L., Castro, S., Fenneteau, O., Brethon, B., Sanchez, M., Roberts, A. E., Yntema, H. G., Van Der Burgt, I., Cianci, P., Bondeson, M. L., Cristina Digilio, M., Zampino, G., Kerr, B., Aoki, Y., Loh, M. L., Palleschi, A., Di Schiavi, E., Care, A., Selicorni, A., Dallapiccola, B., Cirstea, I. C., Stella, L., Zenker, M., Gelb, B. D., Cave, H., Ahmadian, M. R. &Tartaglia, M. (2014). Activating mutations in RRAS underlie a phenotype within the RASopathy spectrum and contribute to leukaemogenesis. *Hum Mol Genet* 23(16): 4315-4327.
- Frias, M. A., Thoreen, C. C., Jaffe, J. D., Schroder, W., Sculley, T., Carr, S. A. &Sabatini, D. M. (2006). mSin1 is necessary for Akt/PKB phosphorylation, and its isoforms define three distinct mTORC2s. *Curr Biol* 16(18): 1865-1870.
- Friedman, S. L. (2008). Hepatic stellate cells: protean, multifunctional, and enigmatic cells of the liver. *Physiol Rev* 88(1): 125-172.
- Frische, E. W. &Zwartkuis, F. J. (2010). Rap1, a mercenary among the Ras-like GTPases. *Dev Biol* 340(1): 1-9.
- Fritsch, R., de Krijger, I., Fritsch, K., George, R., Reason, B., Kumar, Madhu S., Diefenbacher, M., Stamp, G. &Downward, J. (2013). RAS and RHO Families of GTPases Directly Regulate Distinct Phosphoinositide 3-Kinase Isoforms. *Cell* 153(5): 1050-1063.
- Fritsch, R. &Downward, J. (2013). SnapShot: Class I PI3K Isoform Signaling. *Cell* 154(4): 940-940.e941.
- Fujita, A., Koinuma, S., Yasuda, S., Nagai, H., Kamiguchi, H., Wada, N. &Nakamura, T. (2013). GTP hydrolysis of TC10 promotes neurite outgrowth through exocytic fusion of Rab11- and L1-containing vesicles by releasing exocyst component Exo70. *PLoS ONE* 8(11).
- Fukata, M., Nakagawa, M. &Kaibuchi, K. (2003). Roles of Rho-family GTPases in cell polarisation and directional migration. *Curr Opin Cell Biol* 15(5): 590-597.
- Fukunaga, R. &Hunter, T. (1997). MNK1, a new MAP kinase-activated protein kinase, isolated by a novel expression screening method for identifying protein kinase substrates. *EMBO J* 16(8): 1921-1933.
- Garcia-Martinez, J. M. &Alessi, D. R. (2008). mTOR complex 2 (mTORC2) controls hydrophobic motif phosphorylation and activation of serum- and glucocorticoid-induced protein kinase 1 (SGK1). *Biochem J* 416(3): 375-385.
- Garcia-Mata, R., Boulter, E. &Burridge, K. (2011). The 'invisible hand': regulation of RHO GTPases by RHOGDIs. *Nat Rev Mol Cell Biol* 12(8): 493-504.
- Gard, A. L., White, F. P. &Dutton, G. R. (1985). Extra-neural glial fibrillary acidic protein (GFAP) immunoreactivity in perisinusoidal stellate cells of rat liver. *J Neuroimmunol* 8(4-6): 359-375.
- Geffers, I., Serth, K., Chapman, G., Jaekel, R., Schuster-Gossler, K., Cordes, R., Sparrow, D. B., Kremmer, E., Dunwoodie, S. L., Klein, T. &Gossler, A. (2007). Divergent functions and distinct localization of the Notch ligands DLL1 and DLL3 in vivo. *J Cell Biol* 178(3): 465-476.
- Gentilella, A., Kozma, S. C. &Thomas, G. (2015). A liaison between mTOR signaling, ribosome biogenesis and cancer. *Biochim Biophys Acta* 1849(7): 812-820.
- Gigoux, V., L'Hoste, S., Raynaud, F., Camonis, J. &Garbay, C. (2002). Identification of Aurora kinases as RasGAP Src homology 3 domain-binding proteins. *J Biol Chem* 277(26): 23742-23746.
- Gissen, P. &Arias, I. M. (2015). Structural and functional hepatocyte polarity and liver disease. *J Hepatol* 63(4): 1023-1037.
- Gloerich, M. &Bos, J. L. (2011). Regulating Rap small G-proteins in time and space. *Trends Cell Biol* 21(10): 615-623.
- Gloerich, M., ten Klooster, J. P., Vliem, M. J., Koorman, T., Zwartkuis, F. J., Clevers, H. &Bos, J. L. (2012). Rap2A links intestinal cell polarity to brush border formation. *Nat Cell Biol* 14(8): 793-801.
- Goldfinger, L. E. (2006). RLIP76 (RalBP1) is an R-Ras effector that mediates adhesion-dependent Rac activation and cell migration. *J Cell Biol* 174(6): 877-888.
- Good, M. C., Zalatan, J. G. &Lim, W. A. (2011). Scaffold proteins: hubs for controlling the flow of cellular information. *Science* 332(6030): 680-686.

- Goodwin, C. B., Li, X. J., Mali, R. S., Chan, G., Kang, M., Liu, Z., Vanhaesebroeck, B., Neel, B. G., Loh, M. L., Lannutti, B. J., Kapur, R. & Chan, R. J. (2014). PI3K p110delta uniquely promotes gain-of-function Shp2-induced GM-CSF hypersensitivity in a model of JMML. *Blood* 123(18): 2838-2842.
- Goodwin, J. S., Drake, K. R., Rogers, C., Wright, L., Lippincott-Schwartz, J., Philips, M. R. & Kenworthy, A. K. (2005). Depalmitoylated Ras traffics to and from the Golgi complex via a nonvesicular pathway. *J Cell Biol* 170(2): 261-272.
- Gremer, L., Merbitz-Zahradnik, T., Dvorsky, R., Cirstea, I. C., Kratz, C. P., Zenker, M., Wittinghofer, A. & Ahmadian, M. R. (2011). Germline KRAS mutations cause aberrant biochemical and physical properties leading to developmental disorders. *Hum Mutat* 32(1): 33-43.
- Grohmanova, K., Schlaepfer, D., Hess, D., Gutierrez, P., Beck, M. & Kroschewski, R. (2004). Phosphorylation of IQGAP1 modulates its binding to Cdc42, revealing a new type of rho-GTPase regulator. *J Biol Chem* 279(47): 48495-48504.
- Gu, X., Wang, Y., Xiang, J., Chen, Z., Wang, L., Lu, L. & Qian, S. (2013). Interferon- γ Triggers Hepatic Stellate Cell-Mediated Immune Regulation through MEK/ERK Signaling Pathway. *Clinical and Developmental Immunology* 2013: 1-6.
- Gumucio, J. J. (1989). Hepatocyte heterogeneity: the coming of age from the description of a biological curiosity to a partial understanding of its physiological meaning and regulation. *Hepatology* 9(1): 154-160.
- Gupton, S. L. & Gertler, F. B. (2007). Filopodia: the fingers that do the walking. *Sci STKE* 2007(400): re5.
- Haeusler, L. C., Blumenstein, L., Stege, P., Dvorsky, R. & Ahmadian, M. R. (2003). Comparative functional analysis of the Rac GTPases. *FEBS letters* 555(3): 556-560.
- Hagemann, D., Troppmair, J. & Rapp, U. R. (1999). Cot protooncogene protein activates the dual specificity kinases MEK-1 and SEK-1 and induces differentiation of PC12 cells. *Oncogene* 18(7): 1391-1400.
- Hall, A. (2012). Rho family GTPases. *Biochem Soc Trans* 40(6): 1378-1382.
- Han, Y. P., Yan, C., Zhou, L., Qin, L. & Tsukamoto, H. (2007). A matrix metalloproteinase-9 activation cascade by hepatic stellate cells in trans-differentiation in the three-dimensional extracellular matrix. *J Biol Chem* 282(17): 12928-12939.
- Hancock, J. F., Magee, A. I., Childs, J. E. & Marshall, C. J. (1989). All ras proteins are polyisoprenylated but only some are palmitoylated. *Cell* 57(7): 1167-1177.
- Hara, K., Maruki, Y., Long, X., Yoshino, K., Oshiro, N., Hidayat, S., Tokunaga, C., Avruch, J. & Yonezawa, K. (2002). Raptor, a binding partner of target of rapamycin (TOR), mediates TOR action. *Cell* 110(2): 177-189.
- Hara, K., Yonezawa, K., Kozlowski, M. T., Sugimoto, T., Andrabi, K., Weng, Q. P., Kasuga, M., Nishimoto, I. & Avruch, J. (1997). Regulation of eIF-4E BP1 phosphorylation by mTOR. *J Biol Chem* 272(42): 26457-26463.
- Hart, M. J., Callow, M. G., Souza, B. & Polakis, P. (1996). IQGAP1, a calmodulin-binding protein with a rasGAP-related domain, is a potential effector for cdc42Hs. *Embo J* 15(12): 2997-3005.
- Häussinger, D., Sies, H. & Gerok, W. (1985). Functional hepatocyte heterogeneity in ammonia metabolism. The intercellular glutamine cycle. *J Hepatol* 1(1): 3-14.
- Hayes, T. K. & Der, C. J. (2014). Targeting the Raf-MEK-ERK Mitogen-Activated Protein Kinase Cascade for the Treatment of RAS Mutant Cancers. In *Ras Superfamily Small G Proteins: Biology and Mechanisms* 1, 135-156 (Ed A. Wittinghofer). Springer Vienna.
- He, J., Gong, J., Ding, Q., Tan, Q., Han, P., Liu, J., Zhou, Z., Tu, W., Xia, Y., Yan, W. & Tian, D. (2015). Suppressive effect of SATB1 on hepatic stellate cell activation and liver fibrosis in rats. *FEBS Letters* 589(12): 1359-1368.
- Heasman, S. J. & Ridley, A. J. (2008a). Mammalian Rho GTPases: new insights into their functions from in vivo studies. *Nat Rev Mol Cell Biol* 9(9): 690-701.
- Heasman, S. J. & Ridley, A. J. (2008b). Mammalian Rho GTPases: new insights into their functions from in vivo studies. *Nat Rev Mol Cell Biol* 9(9): 690-701.
- Hedman, A. C., Smith, J. M. & Sacks, D. B. (2015). The biology of IQGAP proteins: beyond the cytoskeleton. *EMBO reports* 16(4): 427-446.
- Hemsath, L. & Ahmadian, M. R. (2005). Fluorescence approaches for monitoring interactions of Rho GTPases with nucleotides, regulators, and effectors. *Methods* 37(2): 173-182.
- Hemsath, L., Dvorsky, R., Fiegen, D., Carlier, M. F. & Ahmadian, M. R. (2005). An electrostatic steering mechanism of Cdc42 recognition by Wiskott-Aldrich syndrome proteins. *Mol Cell* 20(2): 313-324.

- Herbrand, U. &Ahmadian, M. R. (2006). p190-RhoGAP as an integral component of the Tiam1/Rac1-induced downregulation of Rho. *Biol Chem* 387(3).
- Herrmann, C. (2003). Ras-effector interactions: after one decade. *Curr Opin Struct Biol* 13(1): 122-129.
- Hers, I., Vincent, E. E. &Tavaré, J. M. (2011). Akt signalling in health and disease. *Cell Signal* 23(10): 1515-1527.
- Ho, Y. D., Joyal, J. L., Li, Z. &Sacks, D. B. (1999). IQGAP1 integrates Ca²⁺/calmodulin and Cdc42 signaling. *J Biol Chem* 274(1): 464-470.
- Holly, S. P., Larson, M. K. &Parise, L. V. (2005). The unique N-terminus of R-ras is required for Rac activation and precise regulation of cell migration. *Mol Biol Cell* 16(5): 2458-2469.
- Hota, P. K. &Buck, M. (2012). Plexin structures are coming: opportunities for multilevel investigations of semaphorin guidance receptors, their cell signaling mechanisms, and functions. *Cell Mol Life Sci* 69(22): 3765-3805.
- Hsu, P. P., Kang, S. A., Rameseder, J., Zhang, Y., Ottina, K. A., Lim, D., Peterson, T. R., Choi, Y., Gray, N. S., Yaffe, M. B., Marto, J. A. &Sabatini, D. M. (2011). The mTOR-regulated phosphoproteome reveals a mechanism of mTORC1-mediated inhibition of growth factor signaling. *Science* 332(6035): 1317-1322.
- Hu, K. Q. &Settleman, J. (1997). Tandem SH2 binding sites mediate the RasGAP-RhoGAP interaction: a conformational mechanism for SH3 domain regulation. *EMBO J* 16(3): 473-483.
- Huang, J. &Manning, B. D. (2008). The TSC1-TSC2 complex: a molecular switchboard controlling cell growth. *Biochem J* 412(2): 179-190.
- Huang, K. &Fingar, D. C. (2014). Growing knowledge of the mTOR signaling network. *Semin Cell Dev Biol* 36: 79-90.
- Huang, M., Duhadaway, J. B., Prendergast, G. C. &Laury-Kleintop, L. D. (2007). RhoB regulates PDGFR-beta trafficking and signaling in vascular smooth muscle cells. *Arterioscler Thromb Vasc Biol* 27(12): 2597-2605.
- Huang, M. &Prendergast, G. C. (2006). RhoB in cancer suppression. *Histol Histopathol* 21(2): 213-218.
- Hufner, K., Schell, B., Aepfelbacher, M. &Linder, S. (2002). The acidic regions of WASp and N-WASP can synergize with CDC42Hs and Rac1 to induce filopodia and lamellipodia. *FEBS Lett* 514(2-3): 168-174.
- Hwang, E., Cheong, H.-K., Mushtaq, A. U., Kim, H.-Y., Yeo, K. J., Kim, E., Lee, W. C., Hwang, K. Y., Cheong, C. &Jeon, Y. H. (2014). Structural basis of the heterodimerization of the MST and RASSF SARAH domains in the Hippo signalling pathway. *Acta Crystallogr D Biol Crystallogr* 70(7): 1944-1953.
- Iadevaia, V., Huo, Y., Zhang, Z., Foster, L. J. &Proud, C. G. (2012). Roles of the mammalian target of rapamycin, mTOR, in controlling ribosome biogenesis and protein synthesis. *Biochem Soc Trans* 40(1): 168-172.
- Ichise, T., Yoshida, N. &Ichise, H. (2010). H-, N- and Kras cooperatively regulate lymphatic vessel growth by modulating VEGFR3 expression in lymphatic endothelial cells in mice. *Development* 137(6): 1003-1013.
- Ikenoue, T., Inoki, K., Yang, Q., Zhou, X. &Guan, K. L. (2008). Essential function of TORC2 in PKC and Akt turn motif phosphorylation, maturation and signalling. *EMBO J* 27(14): 1919-1931.
- Inabe, K., Ishiai, M., Scharenberg, A. M., Freshney, N., Downward, J. &Kurosaki, T. (2002). Vav3 modulates B cell receptor responses by regulating phosphoinositide 3-kinase activation. *J Exp Med* 195(2): 189-200.
- Innocenti, M., Frittoli, E., Ponzanelli, I., Falck, J. R., Brachmann, S. M., Di Fiore, P. P. &Scita, G. (2003). Phosphoinositide 3-kinase activates Rac by entering in a complex with Eps8, Abi1, and Sos-1. *J Cell Biol* 160(1): 17-23.
- Inoki, K., Li, Y., Xu, T. &Guan, K. L. (2003). Rheb GTPase is a direct target of TSC2 GAP activity and regulates mTOR signaling. *Genes Dev* 17(15): 1829-1834.
- Inoki, K., Li, Y., Zhu, T., Wu, J. &Guan, K. L. (2002). TSC2 is phosphorylated and inhibited by Akt and suppresses mTOR signalling. *Nat Cell Biol* 4(9): 648-657.
- Inoki, K., Ouyang, H., Zhu, T., Lindvall, C., Wang, Y., Zhang, X., Yang, Q., Bennett, C., Harada, Y., Stankunas, K., Wang, C. Y., He, X., MacDougald, O. A., You, M., Williams, B. O. &Guan, K. L. (2006). TSC2 integrates Wnt and energy signals via a coordinated phosphorylation by AMPK and GSK3 to regulate cell growth. *Cell* 126(5): 955-968.
- Inoue, M., Chang, L., Hwang, J., Chiang, S. H. &Saltiel, A. R. (2003). The exocyst complex is required for targeting of Glut4 to the plasma membrane by insulin. *Nature* 422(6932): 629-633.

- Inoue, M., Chiang, S. H., Chang, L., Chen, X. W. & Saltiel, A. R. (2006). Compartmentalization of the exocyst complex in lipid rafts controls Glut4 vesicle tethering. *Mol Biol Cell* 17(5): 2303-2311.
- Ismail, S. A., Chen, Y. X., Rusinova, A., Chandra, A., Bierbaum, M., Gremer, L., Triola, G., Waldmann, H., Bastiaens, P. I. & Wittinghofer, A. (2011). Arl2-GTP and Arl3-GTP regulate a GDI-like transport system for farnesylated cargo. *Nat Chem Biol* 7(12): 942-949.
- Iwamoto, H., Nakamuta, M., Tada, S., Sugimoto, R., Enjoji, M. & Nawata, H. (2000). Platelet-derived growth factor receptor tyrosine kinase inhibitor AG1295 attenuates rat hepatic stellate cell growth. *J Lab Clin Med* 135(5): 406-412.
- Izumi, G., Sakisaka, T., Baba, T., Tanaka, S., Morimoto, K. & Takai, Y. (2004). Endocytosis of E-cadherin regulated by Rac and Cdc42 small G proteins through IQGAP1 and actin filaments. *J Cell Biol* 166(2): 237-248.
- Jacinto, E., Loewith, R., Schmidt, A., Lin, S., Ruegg, M. A., Hall, A. & Hall, M. N. (2004). Mammalian TOR complex 2 controls the actin cytoskeleton and is rapamycin insensitive. *Nat Cell Biol* 6(11): 1122-1128.
- Jaffe, A. B. & Hall, A. (2005). Rho GTPases: biochemistry and biology. *Annu Rev Cell Dev Biol* 21: 247-269.
- Jaiswal, M., Dubey, B. N., Koessmeier, K. T., Gremer, L. & Ahmadian, M. R. (2012). Biochemical assays to characterize Rho GTPases. *Methods Mol Biol* 827: 37-58.
- Jaiswal, M., Dvorsky, R. & Ahmadian, M. R. (2013a). Deciphering the molecular and functional basis of Dbl family proteins: a novel systematic approach toward classification of selective activation of the Rho family proteins. *J Biol Chem* 288(6): 4486-4500.
- Jaiswal, M., Dvorsky, R., Amin, E., Risse, S. L., Fansa, E. K., Zhang, S. C., Taha, M. S., Gauhar, A. R., Nakhaei-Rad, S., Kordes, C., Koessmeier, K. T., Cirstea, I. C., Olayioye, M. A., Haussinger, D. & Ahmadian, M. R. (2014). Functional cross-talk between ras and rho pathways: a Ras-specific GTPase-activating protein (p120RasGAP) competitively inhibits the RhoGAP activity of deleted in liver cancer (DLC) tumor suppressor by masking the catalytic arginine finger. *J Biol Chem* 289(10): 6839-6849.
- Jaiswal, M., Fansa, E. K., Dvorsky, R. & Ahmadian, M. R. (2013b). New insight into the molecular switch mechanism of human Rho family proteins: shifting a paradigm. *Biol Chem* 394(1): 89-95.
- Jaumot, M., Yan, J., Clyde-Smith, J., Sluimer, J. & Hancock, J. F. (2002). The linker domain of the Ha-Ras hypervariable region regulates interactions with exchange factors, Raf-1 and phosphoinositide 3-kinase. *J Biol Chem* 277(1): 272-278.
- Jean, S. & Kiger, A. A. (2014). Classes of phosphoinositide 3-kinases at a glance. *J Cell Sci* 127(Pt 5): 923-928.
- Johannessen, C. M., Boehm, J. S., Kim, S. Y., Thomas, S. R., Wardwell, L., Johnson, L. A., Emery, C. M., Stransky, N., Cogdill, A. P., Barretina, J., Caponigro, G., Hieronymus, H., Murray, R. R., Salehi-Ashtiani, K., Hill, D. E., Vidal, M., Zhao, J. J., Yang, X., Alkan, O., Kim, S., Harris, J. L., Wilson, C. J., Myer, V. E., Finan, P. M., Root, D. E., Roberts, T. M., Golub, T., Flaherty, K. T., Dummer, R., Weber, B. L., Sellers, W. R., Schlegel, R., Wargo, J. A., Hahn, W. C. & Garraway, L. A. (2010). COT drives resistance to RAF inhibition through MAP kinase pathway reactivation. *Nature* 468(7326): 968-972.
- Johnson, L., Greenbaum, D., Cichowski, K., Mercer, K., Murphy, E., Schmitt, E., Bronson, R. T., Umanoff, H., Edelman, W., Kucherlapati, R. & Jacks, T. (1997). K-ras is an essential gene in the mouse with partial functional overlap with N-ras. *Genes Dev* 11(19): 2468-2481.
- Johnson, M., Sharma, M. & Henderson, B. R. (2009). IQGAP1 regulation and roles in cancer. *Cell Signal* 21(10): 1471-1478.
- Jones, P. L., Schmidhauser, C. & Bissell, M. J. (1993). Regulation of gene expression and cell function by extracellular matrix. *Crit Rev Eukaryot Gene Expr* 3(2): 137-154.
- Jullien-Flores, V., Mahe, Y., Mirey, G., Leprince, C., Meunier-Bisceuil, B., Sorkin, A. & Camonis, J. H. (2000). RLIP76, an effector of the GTPase Ral, interacts with the AP2 complex: involvement of the Ral pathway in receptor endocytosis. *J Cell Sci* 113 (Pt 16): 2837-2844.
- Jungermann, K. (1988). Metabolic zonation of liver parenchyma. *Semin Liver Dis* 8(4): 329-341.
- Kaizaki, R., Yashiro, M., Shinto, O., Yasuda, K., Matsuzaki, T., Sawada, T. & Hirakawa, K. (2009). Expression of ERas oncogene in gastric carcinoma. *Anticancer Res* 29(6): 2189-2193.
- Kanno, N., LeSage, G., Glaser, S., Alvaro, D. & Alpini, G. (2000). Functional heterogeneity of the intrahepatic biliary epithelium. *Hepatology* 31(3): 555-561.
- Karasarides, M., Chilocheas, A., Hayward, R., Niculescu-Duvaz, D., Scanlon, I., Friedlos, F., Ogilvie, L., Hedley, D., Martin, J., Marshall, C. J., Springer, C. J. & Marais, R. (2004). B-RAF is a therapeutic target in melanoma. *Oncogene* 23(37): 6292-6298.

- Karnoub, A. E. & Weinberg, R. A. (2008). Ras oncogenes: split personalities. *Nat Rev Mol Cell Biol* 9(7): 517-531.
- Kashatus, D. F., Lim, K. H., Brady, D. C., Pershing, N. L., Cox, A. D. & Counter, C. M. (2011). RALA and RALBP1 regulate mitochondrial fission at mitosis. *Nat Cell Biol* 13(9): 1108-1115.
- Katan, M. (2005). New insights into the families of PLC enzymes: looking back and going forward. *Biochem J* 391(Pt 3): e7-9.
- Kawai, K., Kiyota, M., Seike, J., Deki, Y. & Yagisawa, H. (2007). START-GAP3/DLC3 is a GAP for RhoA and Cdc42 and is localized in focal adhesions regulating cell morphology. *Biochem Biophys Res Commun* 364(4): 783-789.
- Kawazu, M., Ueno, T., Kontani, K., Ogita, Y., Ando, M., Fukumura, K., Yamato, A., Soda, M., Takeuchi, K., Miki, Y., Yamaguchi, H., Yasuda, T., Naoe, T., Yamashita, Y., Katada, T., Choi, Y. L. & Mano, H. (2013). Transforming mutations of RAC guanosine triphosphatases in human cancers. *Proc Natl Acad Sci U S A* 110(8): 3029-3034.
- Kelley, G. G., Reks, S. E. & Smrcka, A. V. (2004). Hormonal regulation of phospholipase Cepsilon through distinct and overlapping pathways involving G12 and Ras family G-proteins. *Biochem J* 378(Pt 1): 129-139.
- Kennedy, M. B., Beale, H. C., Carlisle, H. J. & Washburn, L. R. (2005). Integration of biochemical signalling in spines. *Nat Rev Neurosci* 6(6): 423-434.
- Kholmanskikh, S. S., Koeller, H. B., Wynshaw-Boris, A., Gomez, T., Letourneau, P. C. & Ross, M. E. (2006). Calcium-dependent interaction of Lis1 with IQGAP1 and Cdc42 promotes neuronal motility. *Nat Neurosci* 9(1): 50-57.
- Khosravi-Far, R., Campbell, S., Rossman, K. L. & Der, C. J. (1998). Increasing complexity of Ras signal transduction: involvement of Rho family proteins. *Adv Cancer Res* 72: 57-107.
- Kiernan, F. (1833). The anatomy and physiology of the liver *Phil. Trans. R. Soc. Lond.* 123: 711 – 770.
- Kim, J. B. & Spiegelman, B. M. (1996). ADD1/SREBP1 promotes adipocyte differentiation and gene expression linked to fatty acid metabolism. *Genes Dev* 10(9): 1096-1107.
- Kim, J. B., Wright, H. M., Wright, M. & Spiegelman, B. M. (1998). ADD1/SREBP1 activates PPARgamma through the production of endogenous ligand. *Proc Natl Acad Sci U S A* 95(8): 4333-4337.
- Kim, J. E. & Chen, J. (2004). regulation of peroxisome proliferator-activated receptor-gamma activity by mammalian target of rapamycin and amino acids in adipogenesis. *Diabetes* 53(11): 2748-2756.
- Kim, T. Y., Healy, K. D., Der, C. J., Sciaky, N., Bang, Y. J. & Juliano, R. L. (2008). Effects of structure of Rho GTPase-activating protein DLC-1 on cell morphology and migration. *J Biol Chem* 283(47): 32762-32770.
- Kimmelman, A., Tolacheva, T., Lorenzi, M. V., Osada, M. & Chan, A. M. (1997). Identification and characterization of R-ras3: a novel member of the RAS gene family with a non-ubiquitous pattern of tissue distribution. *Oncogene* 15(22): 2675-2685.
- Kimura, T., Yamaoka, M., Taniguchi, S., Okamoto, M., Takei, M., Ando, T., Iwamatsu, A., Watanabe, T., Kaibuchi, K., Ishizaki, T. & Niki, I. (2013). Activated Cdc42-bound IQGAP1 determines the cellular endocytic site. *Mol Cell Biol* 33(24): 4834-4843.
- Kinbara, K., Goldfinger, L. E., Hansen, M., Chou, F. L. & Ginsberg, M. H. (2003). Ras GTPases: integrins' friends or foes? *Nat Rev Mol Cell Biol* 4(10): 767-776.
- Kobayashi, K., Kuroda, S., Fukata, M., Nakamura, T., Nagase, T., Nomura, N., Matsuura, Y., Yoshida-Kubomura, N., Iwamatsu, A. & Kaibuchi, K. (1998). p140Sra-1 (specifically Rac1-associated protein) is a novel specific target for Rac1 small GTPase. *J Biol Chem* 273(1): 291-295.
- Kohno, T., Urao, N., Ashino, T., Sudhakar, V., Inomata, H., Yamaoka-Tojo, M., McKinney, R. D., Fukai, T. & Ushio-Fukai, M. (2013). IQGAP1 links PDGF receptor-beta signal to focal adhesions involved in vascular smooth muscle cell migration: role in neointimal formation after vascular injury. *Am J Physiol Cell Physiol* 305(6): C591-600.
- Kok, K., Geering, B. & Vanhaesebroeck, B. (2009). Regulation of phosphoinositide 3-kinase expression in health and disease. *Trends Biochem Sci* 34(3): 115-127.
- Kordes, C. & Häussinger, D. (2013a). Hepatic stem cell niches. *J Clin Invest* 123(5): 1874-1880.
- Kordes, C. & Häussinger, D. (2013b). Hepatic stem cell niches. *Journal of Clinical Investigation* 123(5): 1874-1880.
- Kordes, C., Sawitzka, I., Götze, S. & Häussinger, D. (2013). Hepatic Stellate Cells Support Hematopoiesis and are Liver-Resident Mesenchymal Stem Cells. *Cell Physiol Biochem* 31(2-3): 290-304.

- Kordes, C., Sawitzka, I., Götze, S., Herebian, D. & Häussinger, D. (2014). Hepatic stellate cells contribute to progenitor cells and liver regeneration. *J Clin Invest* 124(12): 5503-5515.
- Kordes, C., Sawitzka, I. & Häussinger, D. (2008a). Canonical Wnt signaling maintains the quiescent stage of hepatic stellate cells. *Biochem Biophys Res Commun* 367(1): 116-123.
- Kordes, C., Sawitzka, I. & Häussinger, D. (2008b). Canonical Wnt signaling maintains the quiescent stage of hepatic stellate cells. *Biochemical and Biophysical Research Communications* 367(1): 116-123.
- Kordes, C., Sawitzka, I., Müller-Marbach, A., Ale-Agha, N., Keitel, V., Klonowski-Stumpe, H. & Häussinger, D. (2007). CD133+ hepatic stellate cells are progenitor cells. *Biochem Biophys Res Commun* 352(2): 410-417.
- Koronakis, V., Hume, P. J., Humphreys, D., Liu, T., Horning, O., Jensen, O. N. & McGhie, E. J. (2011). WAVE regulatory complex activation by cooperating GTPases Arp and Rac1. *Proc Natl Acad Sci U S A* 108(35): 14449-14454.
- Krens, S. F., Corredor-Adamez, M., He, S., Snaar-Jagalska, B. E. & Spaik, H. P. (2008). ERK1 and ERK2 MAPK are key regulators of distinct gene sets in zebrafish embryogenesis. *BMC Genomics* 9: 196.
- Kubota, E., Kataoka, H., Aoyama, M., Mizoshita, T., Mori, Y., Shimura, T., Tanaka, M., Sasaki, M., Takahashi, S., Asai, K. & Joh, T. (2010). Role of ES cell-expressed Ras (ERas) in tumorigenicity of gastric cancer. *Am J Pathol* 177(2): 955-963.
- Kubota, H., Yao, H. L. & Reid, L. M. (2007). Identification and characterization of vitamin A-storing cells in fetal liver: implications for functional importance of hepatic stellate cells in liver development and hematopoiesis. *Stem Cells* 25(9): 2339-2349.
- Kurella, V. B., Richard, J. M., Parke, C. L., Lecour, L. F., Jr., Bellamy, H. D. & Worthylake, D. K. (2009). Crystal structure of the GTPase-activating protein-related domain from IQGAP1. *J Biol Chem* 284(22): 14857-14865.
- Kuroda, S., Fukata, M., Nakagawa, M., Fujii, K., Nakamura, T., Ookubo, T., Izawa, I., Nagase, T., Nomura, N., Tani, H., Shoji, I., Matsuura, Y., Yonehara, S. & Kaibuchi, K. (1998). Role of IQGAP1, a target of the small GTPases Cdc42 and Rac1, in regulation of E-cadherin-mediated cell-cell adhesion. *Science* 281(5378): 832-835.
- Kuroda, S., Fukata, M., Nakagawa, M. & Kaibuchi, K. (1999). Cdc42, Rac1, and their effector IQGAP1 as molecular switches for cadherin-mediated cell-cell adhesion. *Biochem Biophys Res Commun* 262(1): 1-6.
- Kurokawa, K., Itoh, R. E., Yoshizaki, H., Nakamura, Y. O. & Matsuda, M. (2004). Coactivation of Rac1 and Cdc42 at lamellipodia and membrane ruffles induced by epidermal growth factor. *Mol Biol Cell* 15(3): 1003-1010.
- Lachman, N. & Pawlina, W. (2010). The Liver and Biliary Apparatus: Basic Structural Anatomy and Variations. In *Practical Gastroenterology and Hepatology: Liver and Biliary Disease*, 3-16 (Eds N. J. Talley, K. D. Lindor and H. E. Vargas). Oxford: Wiley-Blackwell.
- Lakner, A. M. (2010). Daily genetic profiling indicates JAK/STAT signaling promotes early hepatic stellate cell transdifferentiation. *World J Gastroenterol* 16(40): 5047.
- Lam, B. D. & Hordijk, P. L. (2013). The Rac1 hypervariable region in targeting and signaling: a tail of many stories. *Small GTPases* 4(2): 78-89.
- Lamers, W. H., Hilberts, A., Furt, E., Smith, J., Jonges, G. N., van Noorden, C. J., Janzen, J. W., Charles, R. & Moorman, A. F. (1989). Hepatic enzymic zonation: a reevaluation of the concept of the liver acinus. *Hepatology* 10(1): 72-76.
- Lapouge, K., Smith, S. J., Walker, P. A., Gamblin, S. J., Smerdon, S. J. & Rittinger, K. (2000). Structure of the TPR domain of p67phox in complex with Rac.GTP. *Mol Cell* 6(4): 899-907.
- Lau, K. S. & Haigis, K. M. (2009). Non-redundancy within the RAS oncogene family: insights into mutational disparities in cancer. *Mol Cells* 28(4): 315-320.
- Lavoie, H. & Therrien, M. (2015). Regulation of RAF protein kinases in ERK signalling. *Nat Rev Mol Cell Biol* 16(5): 281-298.
- Le Clainche, C., Schlaepfer, D., Ferrari, A., Klingauf, M., Grohmanova, K., Veligodskiy, A., Didry, D., Le, D., Egile, C., Carlier, M. F. & Kroschewski, R. (2007). IQGAP1 stimulates actin assembly through the N-WASP-Arp2/3 pathway. *J Biol Chem* 282(1): 426-435.
- Leblanc, V., Tocque, B. & Delumeau, I. (1998). Ras-GAP controls Rho-mediated cytoskeletal reorganization through its SH3 domain. *Mol Cell Biol* 18(9): 5567-5578.
- Lefkowitz, J. H. (2011). Anatomy and Function. In *Sherlock's Diseases of the Liver and Biliary System*, 1-19 (Eds J. S. Dooley, A. S. F. Lok, A. K. Burroughs and E. J. Heathcote). Wiley-Blackwell.

- Lei, M., Lu, W., Meng, W., Parrini, M. C., Eck, M. J., Mayer, B. J. & Harrison, S. C. (2000). Structure of PAK1 in an autoinhibited conformation reveals a multistage activation switch. *Cell* 102(3): 387-397.
- Leicht, D. T., Balan, V., Kaplun, A., Singh-Gupta, V., Kaplun, L., Dobson, M. & Tzivion, G. (2007). Raf kinases: function, regulation and role in human cancer. *Biochim Biophys Acta* 1773(8): 1196-1212.
- Lenzen, C., Cool, R. H., Prinz, H., Kuhlmann, J. & Wittinghofer, A. (1998). Kinetic analysis by fluorescence of the interaction between Ras and the catalytic domain of the guanine nucleotide exchange factor Cdc25Mm. *Biochemistry* 37(20): 7420-7430.
- Leon, J., Guerrero, I. & Pellicer, A. (1987). Differential expression of the ras gene family in mice. *Mol Cell Biol* 7(4): 1535-1540.
- Leung, T. H., Ching, Y. P., Yam, J. W., Wong, C. M., Yau, T. O., Jin, D. Y. & Ng, I. O. (2005). Deleted in liver cancer 2 (DLC2) suppresses cell transformation by means of inhibition of RhoA activity. *Proc Natl Acad Sci U S A* 102(42): 15207-15212.
- Li, L., Wang, J. Y., Yang, C. Q. & Jiang, W. (2012). Effect of RhoA on transforming growth factor beta1-induced rat hepatic stellate cell migration. *Liver Int* 32(7): 1093-1102.
- Li, Z., McNulty, D. E., Marler, K. J., Lim, L., Hall, C., Annan, R. S. & Sacks, D. B. (2005). IQGAP1 promotes neurite outgrowth in a phosphorylation-dependent manner. *J Biol Chem* 280(14): 13871-13878.
- Lim, K. B., Bu, W., Goh, W. I., Koh, E., Ong, S. H., Pawson, T., Sudhakaran, T. & Ahmed, S. (2008). The Cdc42 effector IRSp53 generates filopodia by coupling membrane protrusion with actin dynamics. *J Biol Chem* 283(29): 20454-20472.
- Liu, C., Billadeau, D. D., Abdelhakim, H., Leof, E., Kaibuchi, K., Bernabeu, C., Bloom, G. S., Yang, L., Boardman, L., Shah, V. H. & Kang, N. (2013a). IQGAP1 suppresses TbetaRII-mediated myofibroblastic activation and metastatic growth in liver. *J Clin Invest* 123(3): 1138-1156.
- Liu, J., Guidry, J. J. & Worthylake, D. K. (2014a). Conserved sequence repeats of IQGAP1 mediate binding to Ezrin. *J Proteome Res* 13(2): 1156-1166.
- Liu, P., Gan, W., Inuzuka, H., Lazorchak, A. S., Gao, D., Arojo, O., Liu, D., Wan, L., Zhai, B., Yu, Y., Yuan, M., Kim, B. M., Shaik, S., Menon, S., Gygi, S. P., Lee, T. H., Asara, J. M., Manning, B. D., Blenis, J., Su, B. & Wei, W. (2013b). Sin1 phosphorylation impairs mTORC2 complex integrity and inhibits downstream Akt signalling to suppress tumorigenesis. *Nat Cell Biol* 15(11): 1340-1350.
- Liu, P., Guo, J., Gan, W. & Wei, W. (2014b). Dual phosphorylation of Sin1 at T86 and T398 negatively regulates mTORC2 complex integrity and activity. *Protein Cell* 5(3): 171-177.
- Loewith, R., Jacinto, E., Wullschleger, S., Lorberg, A., Crespo, J. L., Bonenfant, D., Oppliger, W., Jenoe, P. & Hall, M. N. (2002). Two TOR complexes, only one of which is rapamycin sensitive, have distinct roles in cell growth control. *Mol Cell* 10(3): 457-468.
- Lu, L., Li, Y., Kim, S. M., Bossuyt, W., Liu, P., Qiu, Q., Wang, Y., Halder, G., Finegold, M. J., Lee, J. S. & Johnson, R. L. (2010). Hippo signaling is a potent in vivo growth and tumor suppressor pathway in the mammalian liver. *Proc Natl Acad Sci U S A* 107(4): 1437-1442.
- Ma, L., Chen, Z., Erdjument-Bromage, H., Tempst, P. & Pandolfi, P. P. (2005). Phosphorylation and functional inactivation of TSC2 by Erk implications for tuberous sclerosis and cancer pathogenesis. *Cell* 121(2): 179-193.
- Ma, X. M. & Blenis, J. (2009). Molecular mechanisms of mTOR-mediated translational control. *Nat Rev Mol Cell Biol* 10(5): 307-318.
- Ma, X. M., Yoon, S. O., Richardson, C. J., Julich, K. & Blenis, J. (2008). SKAR links pre-mRNA splicing to mTOR/S6K1-mediated enhanced translation efficiency of spliced mRNAs. *Cell* 133(2): 303-313.
- Maher, J. J. (1993). Cell-specific expression of hepatocyte growth factor in liver. Upregulation in sinusoidal endothelial cells after carbon tetrachloride. *Journal of Clinical Investigation* 91(5): 2244-2252.
- Malarkannan, S., Awasthi, A., Rajasekaran, K., Kumar, P., Schuldt, K. M., Bartoszek, A., Manoharan, N., Goldner, N. K., Umhoefer, C. M. & Thakar, M. S. (2012). IQGAP1: a regulator of intracellular spacetime relativity. *J Immunol* 188(5): 2057-2063.
- Mannaerts, I., Leite, S. B., Verhulst, S., Claerhout, S., Eysackers, N., Thoen, L. F. R., Hoorens, A., Reynaert, H., Halder, G. & van Grunsven, L. A. (2015). The Hippo pathway effector YAP controls mouse hepatic stellate cell activation. *J Hepatol* 63(3): 679-688.
- Markgraf, Daniel F., Klemm, Robin W., Junker, M., Hannibal-Bach, Hans K., Ejsing, Christer S. & Rapoport, Tom A. (2014). An ER Protein Functionally Couples Neutral Lipid Metabolism on Lipid Droplets to Membrane Lipid Synthesis in the ER. *Cell Rep* 6(1): 44-55.

- Marte, B. M., Rodriguez-Viciano, P., Wennstrom, S., Warne, P. H. & Downward, J. (1997). R-Ras can activate the phosphoinositide 3-kinase but not the MAP kinase arm of the Ras effector pathways. *Curr Biol* 7(1): 63-70.
- Mason, J. M., Morrison, D. J., Basson, M. A. & Licht, J. D. (2006). Sprouty proteins: multifaceted negative-feedback regulators of receptor tyrosine kinase signaling. *Trends Cell Biol* 16(1): 45-54.
- Matallanas, D., Birtwistle, M., Romano, D., Zebisch, A., Rauch, J., von Kriegsheim, A. & Kolch, W. (2011). Raf family kinases: old dogs have learned new tricks. *Genes Cancer* 2(3): 232-260.
- Matallanas, D., Sanz-Moreno, V., Arozarena, I., Calvo, F., Agudo-Ibanez, L., Santos, E., Berciano, M. T. & Crespo, P. (2006). Distinct utilization of effectors and biological outcomes resulting from site-specific Ras activation: Ras functions in lipid rafts and Golgi complex are dispensable for proliferation and transformation. *Mol Cell Biol* 26(1): 100-116.
- Mataraza, J. M., Briggs, M. W., Li, Z., Entwistle, A., Ridley, A. J. & Sacks, D. B. (2003a). IQGAP1 promotes cell motility and invasion. *J Biol Chem* 278(42): 41237-41245.
- Mataraza, J. M., Briggs, M. W., Li, Z., Frank, R. & Sacks, D. B. (2003b). Identification and characterization of the Cdc42-binding site of IQGAP1. *Biochem Biophys Res Commun* 305(2): 315-321.
- Mateer, S. C., Wang, N. & Bloom, G. S. (2003). IQGAPs: integrators of the cytoskeleton, cell adhesion machinery, and signaling networks. *Cell Motil Cytoskeleton* 55(3): 147-155.
- Matsubara, K., Kishida, S., Matsuura, Y., Kitayama, H., Noda, M. & Kikuchi, A. (1999). Plasma membrane recruitment of RalGDS is critical for Ras-dependent Ral activation. *Oncogene* 18(6): 1303-1312.
- Matsumoto, K., Miki, R., Nakayama, M., Tatsumi, N. & Yokouchi, Y. (2008). Wnt9a secreted from the walls of hepatic sinusoids is essential for morphogenesis, proliferation, and glycogen accumulation of chick hepatic epithelium. *Dev Biol* 319(2): 234-247.
- Mattila, P. K. & Lappalainen, P. (2008). Filopodia: molecular architecture and cellular functions. *Nat Rev Mol Cell Biol* 9(6): 446-454.
- McCallum, S. J., Wu, W. J. & Cerione, R. A. (1996). Identification of a putative effector for Cdc42Hs with high sequence similarity to the RasGAP-related protein IQGAP1 and a Cdc42Hs binding partner with similarity to IQGAP2. *J Biol Chem* 271(36): 21732-21737.
- Michalopoulos, G. K. (2010). Liver Regeneration after Partial Hepatectomy: Critical Analysis of Mechanistic Dilemmas. *Am J Pathol* 176(1): 2-13.
- Miyajima, A., Tanaka, M. & Itoh, T. (2014). Stem/Progenitor Cells in Liver Development, Homeostasis, Regeneration, and Reprogramming. *Cell Stem Cell* 14(5): 561-574.
- Miyaoka, Y., Ebato, K., Kato, H., Arakawa, S., Shimizu, S. & Miyajima, A. (2012). Hypertrophy and unconventional cell division of hepatocytes underlie liver regeneration. *Curr Biol* 22(13): 1166-1175.
- Nagai, H., Terada, K., Watanabe, G., Ueno, Y., Aiba, N., Shibuya, T., Kawagoe, M., Kameda, T., Sato, M., Senoo, H. & Sugiyama, T. (2002). Differentiation of liver epithelial (stem-like) cells into hepatocytes induced by coculture with hepatic stellate cells. *Biochem Biophys Res Commun* 293(5): 1420-1425.
- Nakamura, K., Ichise, H., Nakao, K., Hatta, T., Otani, H., Sakagami, H., Kondo, H. & Katsuki, M. (2008). Partial functional overlap of the three ras genes in mouse embryonic development. *Oncogene* 27(21): 2961-2968.
- Nakhaei-Rad, S., Nakhaeizadeh, H., Kordes, C., Cirstea, I. C., Schmick, M., Dvorsky, R., Bastiaens, P. I., Haussinger, D. & Ahmadian, M. R. (2015). The function of embryonic stem cell-expressed Ras (E-Ras), a unique Ras family member, correlates with its additional motifs and its structural properties. *J Biol Chem*.
- Nassar, N., Hoffman, G. R., Manor, D., Clardy, J. C. & Cerione, R. A. (1998). Structures of Cdc42 bound to the active and catalytically compromised forms of Cdc42GAP. *Nat Struct Biol* 5(12): 1047-1052.
- Nassar, N., Horn, G., Herrmann, C., Block, C., Janknecht, R. & Wittinghofer, A. (1996). Ras/Rap effector specificity determined by charge reversal. *Nat Struct Biol* 3(8): 723-729.
- Neudauer, C. L., Joberty, G., Tatsis, N. & Macara, I. G. (1998). Distinct cellular effects and interactions of the Rho-family GTPase TC10. *Curr Biol* 8(21): 1151-1160.
- Niemeyer, C. M. (2014). RAS diseases in children. *Haematologica* 99(11): 1653-1662.
- Nojima, H., Adachi, M., Matsui, T., Okawa, K. & Tsukita, S. (2008). IQGAP3 regulates cell proliferation through the Ras/ERK signalling cascade. *Nat Cell Biol* 10(8): 971-978.
- Nomanbhoy, T. & Cerione, R. A. (1999). Fluorescence assays of Cdc42 interactions with target/effector proteins. *Biochemistry* 38(48): 15878-15884.

- Noritake, J., Watanabe, T., Sato, K., Wang, S. & Kaibuchi, K. (2005). IQGAP1: a key regulator of adhesion and migration. *J Cell Sci* 118(Pt 10): 2085-2092.
- Nouri, K., J. M. M., Milroy LG, Hain, A., Dvorsky, R., Amin, E., Lenders, M., Nagel-Steger, L., Howe, S., Smits, S. H. J., Hengel, H., Schmitt, L., Münk, C., Brunsveld, L. & Ahmadian, M. R. (2015). Biophysical Characterization of Nucleophosmin Interactions with Human Immunodeficiency Virus Rev and Herpes Simplex Virus US11. *PLoS ONE*.
- Oh, W. J. & Jacinto, E. (2011). mTOR complex 2 signaling and functions. *Cell Cycle* 10(14): 2305-2316.
- Oka, T., Mazack, V. & Sudol, M. (2008). Mst2 and Lats kinases regulate apoptotic function of Yes kinase-associated protein (YAP). *J Biol Chem* 283(41): 27534-27546.
- Omerovic, J., Laude, A. J. & Prior, I. A. (2007). Ras proteins: paradigms for compartmentalised and isoform-specific signalling. *Cell Mol Life Sci* 64(19-20): 2575-2589.
- Ory, S. & Gasman, S. (2011). Rho GTPases and exocytosis: what are the molecular links? *Semin Cell Dev Biol* 22(1): 27-32.
- Owen, D., Campbell, L. J., Littlefield, K., Evetts, K. A., Li, Z., Sacks, D. B., Lowe, P. N. & Mott, H. R. (2008). The IQGAP1-Rac1 and IQGAP1-Cdc42 interactions: interfaces differ between the complexes. *J Biol Chem* 283(3): 1692-1704.
- Pacold, M. E., Suire, S., Perisic, O., Lara-Gonzalez, S., Davis, C. T., Walker, E. H., Hawkins, P. T., Stephens, L., Eccleston, J. F. & Williams, R. L. (2000). Crystal structure and functional analysis of Ras binding to its effector phosphoinositide 3-kinase gamma. *Cell* 103(6): 931-943.
- Paganini, S., Guidetti, G. F., Catricala, S., Trionfini, P., Panelli, S., Balduini, C. & Torti, M. (2006). Identification and biochemical characterization of Rap2C, a new member of the Rap family of small GTP-binding proteins. *Biochimie* 88(3-4): 285-295.
- Pamonsinlapatham, P., Hadj-Slimane, R., Lepelletier, Y., Allain, B., Toccafondi, M., Garbay, C. & Raynaud, F. (2009). p120-Ras GTPase activating protein (RasGAP): a multi-interacting protein in downstream signaling. *Biochimie* 91(3): 320-328.
- Pannekoek, W. J., Linnemann, J. R., Brouwer, P. M., Bos, J. L. & Rehmann, H. (2013). Rap1 and Rap2 antagonistically control endothelial barrier resistance. *PLoS One* 8(2): e57903.
- Parks, W. C. (1999). Matrix metalloproteinases in repair. In *Wound Repair and Regeneration*, Vol. 7, 423-432.
- Parola, M., Robino, G., Marra, F., Pinzani, M., Bellomo, G., Leonarduzzi, G., Chiarugi, P., Camandola, S., Poli, G., Waeg, G., Gentilini, P. & Dianzani, M. U. (1998). HNE interacts directly with JNK isoforms in human hepatic stellate cells. *J Clin Invest* 102(11): 1942-1950.
- Pathmanathan, S., Hamilton, E., Atcheson, E. & Timson, D. J. (2011). The interaction of IQGAPs with calmodulin-like proteins. *Biochem Soc Trans* 39(2): 694-699.
- Pearce, L. R., Huang, X., Boudeau, J., Pawlowski, R., Wullschleger, S., Deak, M., Ibrahim, A. F., Gurlay, R., Magnuson, M. A. & Alessi, D. R. (2007). Identification of Protor as a novel Rictor-binding component of mTOR complex-2. *Biochem J* 405(3): 513-522.
- Pearce, L. R., Komander, D. & Alessi, D. R. (2010). The nuts and bolts of AGC protein kinases. *Nat Rev Mol Cell Biol* 11(1): 9-22.
- Pellicoro, A., Ramachandran, P., Iredale, J. P. & Fallowfield, J. A. (2014). Liver fibrosis and repair: immune regulation of wound healing in a solid organ. *Nat Rev Immunol* 14(3): 181-194.
- Peng, J., Wallar, B. J., Flanders, A., Swiatek, P. J. & Alberts, A. S. (2003). Disruption of the Diaphanous-related formin Drf1 gene encoding mDia1 reveals a role for Drf3 as an effector for Cdc42. *Curr Biol* 13(7): 534-545.
- Pereira, A., Zhang, B., Malcolm, P. & Sundram, S. (2013). Clozapine regulation of p90RSK and c-Fos signaling via the ErbB1-ERK pathway is distinct from olanzapine and haloperidol in mouse cortex and striatum. *Prog Neuropsychopharmacol Biol Psychiatry* 40: 353-363.
- Peterson, S. N., Trabalzini, L., Brtva, T. R., Fischer, T., Altschuler, D. L., Martelli, P., Lapetina, E. G., Der, C. J. & White, G. C., 2nd (1996). Identification of a novel RalGDS-related protein as a candidate effector for Ras and Rap1. *J Biol Chem* 271(47): 29903-29908.
- Peterson, T. R., Laplante, M., Thoreen, C. C., Sancak, Y., Kang, S. A., Kuehl, W. M., Gray, N. S. & Sabatini, D. M. (2009). DEPTOR is an mTOR inhibitor frequently overexpressed in multiple myeloma cells and required for their survival. *Cell* 137(5): 873-886.
- Pfeifer, G. P., Dammann, R. & Tommasi, S. (2010). RASSF proteins. *Curr Biol* 20(8): R344-R345.

- Pille, J. Y., Denoyelle, C., Varet, J., Bertrand, J. R., Soria, J., Opolon, P., Lu, H., Pritchard, L. L., Vannier, J. P., Malvy, C., Soria, C. & Li, H. (2005). Anti-RhoA and anti-RhoC siRNAs inhibit the proliferation and invasiveness of MDA-MB-231 breast cancer cells in vitro and in vivo. *Mol Ther* 11(2): 267-274.
- Pommereit, D. & Wouters, F. S. (2007). An NGF-induced Exo70-TC10 complex locally antagonises Cdc42-mediated activation of N-WASP to modulate neurite outgrowth. *J Cell Sci* 120(Pt 15): 2694-2705.
- Porstmann, T., Santos, C. R., Griffiths, B., Cully, M., Wu, M., Leever, S., Griffiths, J. R., Chung, Y. L. & Schulze, A. (2008). SREBP activity is regulated by mTORC1 and contributes to Akt-dependent cell growth. *Cell Metab* 8(3): 224-236.
- Potenza, N., Vecchione, C., Notte, A., De Rienzo, A., Rosica, A., Bauer, L., Affuso, A., De Felice, M., Russo, T., Poulet, R., Cifelli, G., De Vita, G., Lembo, G. & Di Lauro, R. (2005). Replacement of K-Ras with H-Ras supports normal embryonic development despite inducing cardiovascular pathology in adult mice. *EMBO Reports* 6(5): 432-437.
- Prasad, S. B., Yadav, S. S., Das, M., Modi, A., Kumari, S., Pandey, L. K., Singh, S., Pradhan, S. & Narayan, G. (2015). PI3K/AKT pathway-mediated regulation of p27(Kip1) is associated with cell cycle arrest and apoptosis in cervical cancer. *Cell Oncol (Dordr)* 38(3): 215-225.
- Prieto-Sanchez, R. M. & Bustelo, X. R. (2003). Structural basis for the signaling specificity of RhoG and Rac1 GTPases. *J Biol Chem* 278(39): 37916-37925.
- Pritchard, C. A., Bolin, L., Slattery, R., Murray, R. & McMahon, M. (1996). Post-natal lethality and neurological and gastrointestinal defects in mice with targeted disruption of the A-Raf protein kinase gene. *Curr Biol* 6(5): 614-617.
- Pylayeva-Gupta, Y., Grabocka, E. & Bar-Sagi, D. (2011). RAS oncogenes: weaving a tumorigenic web. *Nat Rev Cancer* 11(11): 761-774.
- Quilliam, L. A., Rebhun, J. F. & Castro, A. F. (2002). A growing family of guanine nucleotide exchange factors is responsible for activation of Ras-family GTPases. *Prog Nucleic Acid Res Mol Biol* 71: 391-444.
- Ramadori, G., Neubauer, K., Odenthal, M., Nakamura, T., Knittel, T., Schwogler, S. & Meyer zum Buschenfelde, K. H. (1992). The gene of hepatocyte growth factor is expressed in fat-storing cells of rat liver and is downregulated during cell growth and by transforming growth factor-beta. *Biochem Biophys Res Commun* 183(2): 739-742.
- Ramos, A. & Camargo, F. D. (2012a). The Hippo signaling pathway and stem cell biology. *Trends Cell Biol* 22(7): 339-346.
- Ramos, A. & Camargo, F. D. (2012b). The Hippo signaling pathway and stem cell biology. *Trends in Cell Biology* 22(7): 339-346.
- Rappaport, A. M., Borowy, Z. J., Loughheed, W. M. & Lotto, W. N. (1954). Subdivision of hexagonal liver lobules into a structural and functional unit; role in hepatic physiology and pathology. *Anat Rec* 119(1): 11-33.
- Ratner, N. & Miller, S. J. (2015). A RASopathy gene commonly mutated in cancer: the neurofibromatosis type 1 tumour suppressor. *Nature Reviews Cancer* 15(5): 290-301.
- Rawat, S. J. & Chernoff, J. (2015). Regulation of mammalian Ste20 (Mst) kinases. *Trends Biochem Sci* 40(3): 149-156.
- Reid, T., Furuyashiki, T., Ishizaki, T., Watanabe, G., Watanabe, N., Fujisawa, K., Morii, N., Madaule, P. & Narumiya, S. (1996). Rhotekin, a new putative target for Rho bearing homology to a serine/threonine kinase, PKN, and rhophilin in the rho-binding domain. *J Biol Chem* 271(23): 13556-13560.
- Reid, T. S., Terry, K. L., Casey, P. J. & Beese, L. S. (2004). Crystallographic analysis of CaaX prenyltransferases complexed with substrates defines rules of protein substrate selectivity. *J Mol Biol* 343(2): 417-433.
- Reimann, T., Hempel, U., Krautwald, S., Axmann, A., Scheibe, R., Seidel, D. & Wenzel, K. W. (1997). Transforming growth factor-beta1 induces activation of Ras, Raf-1, MEK and MAPK in rat hepatic stellate cells. *FEBS Lett* 403(1): 57-60.
- Ren, J. G., Li, Z. & Sacks, D. B. (2007). IQGAP1 modulates activation of B-Raf. *Proc Natl Acad Sci U S A* 104(25): 10465-10469.
- Resh, M. D. (1999). Fatty acylation of proteins: new insights into membrane targeting of myristoylated and palmitoylated proteins. *Biochim Biophys Acta* 1451(1): 1-16.
- Rey, I., Taylor-Harris, P., van Erp, H. & Hall, A. (1994). R-ras interacts with rasGAP, neurofibromin and c-raf but does not regulate cell growth or differentiation. *Oncogene* 9(3): 685-692.

- Rittinger, K., Walker, P. A., Eccleston, J. F., Nurmahomed, K., Owen, D., Laue, E., Gamblin, S. J. & Smerdon, S. J. (1997). Crystal structure of a small G protein in complex with the GTPase-activating protein rhoGAP. *Nature* 388(6643): 693-697.
- Rocks, O., Peyker, A., Kahms, M., Verveer, P. J., Koerner, C., Lumbierres, M., Kuhlmann, J., Waldmann, H., Wittinghofer, A. & Bastiaens, P. I. (2005). An acylation cycle regulates localization and activity of palmitoylated Ras isoforms. *Science* 307(5716): 1746-1752.
- Rodriguez-Viciano, P., Oses-Prieto, J., Burlingame, A., Fried, M. & McCormick, F. (2006). A phosphatase holoenzyme comprised of Shc2/Sur8 and the catalytic subunit of PP1 functions as an M-Ras effector to modulate Raf activity. *Mol Cell* 22(2): 217-230.
- Rodriguez-Viciano, P., Sabatier, C. & McCormick, F. (2004). Signaling specificity by Ras family GTPases is determined by the full spectrum of effectors they regulate. *Mol Cell Biol* 24(11): 4943-4954.
- Rojas, A. M. & Valencia, A. (2014). Evolution of the Ras Superfamily of GTPases. In *Ras Superfamily Small G Proteins: Biology and Mechanisms 1*, 3-23 (Ed A. Wittinghofer). Springer Vienna.
- Romano, D., Nguyen, L. K., Matallanas, D., Halasz, M., Doherty, C., Kholodenko, B. N. & Kolch, W. (2014). Protein interaction switches coordinate Raf-1 and MST2/Hippo signalling. *Nat Cell Biol* 16(7): 673-684.
- Roskams, T. (2008). Relationships among stellate cell activation, progenitor cells, and hepatic regeneration. *Clin Liver Dis* 12(4): 853-860, ix.
- Rossman, K. L., Der, C. J. & Sondek, J. (2005). GEF means go: turning on RHO GTPases with guanine nucleotide-exchange factors. *Nat Rev Mol Cell Biol* 6(2): 167-180.
- Roy, M., Li, Z. & Sacks, D. B. (2004). IQGAP1 binds ERK2 and modulates its activity. *J Biol Chem* 279(17): 17329-17337.
- Roy, M., Li, Z. & Sacks, D. B. (2005). IQGAP1 is a scaffold for mitogen-activated protein kinase signaling. *Mol Cell Biol* 25(18): 7940-7952.
- Saile, B., Matthes, N., El Armouche, H., Neubauer, K. & Ramadori, G. (2001). The bcl, NFkappaB and p53/p21WAF1 systems are involved in spontaneous apoptosis and in the anti-apoptotic effect of TGF-beta or TNF-alpha on activated hepatic stellate cells. *Eur J Cell Biol* 80(8): 554-561.
- Sakurai-Yageta, M., Recchi, C., Le Dez, G., Sibarita, J. B., Daviet, L., Camonis, J., D'Souza-Schorey, C. & Chavrier, P. (2008). The interaction of IQGAP1 with the exocyst complex is required for tumor cell invasion downstream of Cdc42 and RhoA. *J Cell Biol* 181(6): 985-998.
- Sancak, Y., Peterson, T. R., Shaul, Y. D., Lindquist, R. A., Thoreen, C. C., Bar-Peled, L. & Sabatini, D. M. (2008). The Rag GTPases bind raptor and mediate amino acid signaling to mTORC1. *Science* 320(5882): 1496-1501.
- Sancak, Y., Thoreen, C. C., Peterson, T. R., Lindquist, R. A., Kang, S. A., Spooner, E., Carr, S. A. & Sabatini, D. M. (2007). PRAS40 is an insulin-regulated inhibitor of the mTORC1 protein kinase. *Mol Cell* 25(6): 903-915.
- Sandri, C., Caccavari, F., Valdembri, D., Camillo, C., Veltel, S., Santambrogio, M., Lanzetti, L., Bussolino, F., Ivaska, J. & Serini, G. (2012). The R-Ras/RIN2/Rab5 complex controls endothelial cell adhesion and morphogenesis via active integrin endocytosis and Rac signaling. *Cell Res* 22(10): 1479-1501.
- Saraste, M., Sibbald, P. R. & Wittinghofer, A. (1990). The P-loop--a common motif in ATP- and GTP-binding proteins. *Trends Biochem Sci* 15(11): 430-434.
- Sarbassov, D. D. (2005). Phosphorylation and Regulation of Akt/PKB by the Rictor-mTOR Complex. *Science* 307(5712): 1098-1101.
- Sarbassov, D. D., Ali, S. M., Kim, D. H., Guertin, D. A., Latek, R. R., Erdjument-Bromage, H., Tempst, P. & Sabatini, D. M. (2004). Rictor, a novel binding partner of mTOR, defines a rapamycin-insensitive and raptor-independent pathway that regulates the cytoskeleton. *Curr Biol* 14(14): 1296-1302.
- Sauvant, P., Cansell, M. & Atgié, C. (2011). Vitamin A and lipid metabolism: relationship between hepatic stellate cells (HSCs) and adipocytes. *J Physiol Biochem* 67(3): 487-496.
- Sawitzka, I., Kordes, C., Gotze, S., Herebian, D. & Haussinger, D. (2015). Bile acids induce hepatic differentiation of mesenchymal stem cells. *Sci Rep* 5: 13320.
- Sawitzka, I., Kordes, C., Reister, S. & Haussinger, D. (2009). The niche of stellate cells within rat liver. *Hepatology* 50(5): 1617-1624.
- Schaefer, B., Rivas-Estilla, A. M., Meraz-Cruz, N., Reyes-Romero, M. A., Hernández-Nazara, Z. H., Domínguez-Rosales, J.-A., Schuppan, D., Greenwel, P. & Rojkind, M. (2003). Reciprocal Modulation of Matrix Metalloproteinase-13 and Type I Collagen Genes in Rat Hepatic Stellate Cells. *Am J Pathol* 162(6): 1771-1780.

- Scheel, H. & Hofmann, K. (2003). A novel interaction motif, SARAH, connects three classes of tumor suppressor. *Curr Biol* 13(23): R899-900.
- Scheffzek, K., Ahmadian, M. R., Kabsch, W., Wiesmuller, L., Lautwein, A., Schmitz, F. & Wittinghofer, A. (1997). The Ras-RasGAP complex: structural basis for GTPase activation and its loss in oncogenic Ras mutants. *Science* 277(5324): 333-338.
- Schirmacher, P., Geerts, A., Pietrangelo, A., Dienes, H. P. & Rogler, C. E. (1992). Hepatocyte growth factor/hepatopoietin A is expressed in fat-storing cells from rat liver but not myofibroblast-like cells derived from fat-storing cells. *Hepatology* 15(1): 5-11.
- Schmick, M., Vartak, N., Papke, B., Kovacevic, M., Truxius, Dina C., Rossmannek, L. & Bastiaens, Philippe I. H. (2014). KRas Localizes to the Plasma Membrane by Spatial Cycles of Solubilization, Trapping and Vesicular Transport. *Cell* 157(2): 459-471.
- Schmidt, G., Lenzen, C., Simon, I., Deuter, R., Cool, R. H., Goody, R. S. & Wittinghofer, A. (1996). Biochemical and biological consequences of changing the specificity of p21ras from guanosine to xanthosine nucleotides. *Oncogene* 12(1): 87-96.
- Schmidt, V. A., Chiariello, C. S., Capilla, E., Miller, F. & Bahou, W. F. (2008). Development of hepatocellular carcinoma in Iqgap2-deficient mice is IQGAP1 dependent. *Mol Cell Biol* 28(5): 1489-1502.
- Schmidt, V. A., Scudder, L., Devoe, C. E., Bernards, A., Cupit, L. D. & Bahou, W. F. (2003). IQGAP2 functions as a GTP-dependent effector protein in thrombin-induced platelet cytoskeletal reorganization. *Blood* 101(8): 3021-3028.
- Schroder, W. A., Buck, M., Cloonan, N., Hancock, J. F., Suhrbier, A., Sculley, T. & Bushell, G. (2007). Human Sin1 contains Ras-binding and pleckstrin homology domains and suppresses Ras signalling. *Cell Signal* 19(6): 1279-1289.
- Scott, J. D. & Pawson, T. (2009). Cell signaling in space and time: where proteins come together and when they're apart. *Science* 326(5957): 1220-1224.
- Seabra, M. C., Reiss, Y., Casey, P. J., Brown, M. S. & Goldstein, J. L. (1991). Protein farnesyltransferase and geranylgeranyltransferase share a common alpha subunit. *Cell* 65(3): 429-434.
- Shang, X., Cancelas, J. A., Li, L., Guo, F., Liu, W., Johnson, J. F., Ficker, A., Daria, D., Geiger, H., Ratner, N. & Zheng, Y. (2011). R-Ras and Rac GTPase cross-talk regulates hematopoietic progenitor cell migration, homing, and mobilization. *J Biol Chem* 286(27): 24068-24078.
- Shang, X., Moon, S. Y. & Zheng, Y. (2007). p200 RhoGAP promotes cell proliferation by mediating cross-talk between Ras and Rho signaling pathways. *J Biol Chem* 282(12): 8801-8811.
- Shao, H. & Andres, D. A. (2000). A novel RalGEF-like protein, RGL3, as a candidate effector for rit and Ras. *J Biol Chem* 275(35): 26914-26924.
- Shih, T. Y., Weeks, M. O., Young, H. A. & Scholnick, E. M. (1979). Identification of a sarcoma virus-coded phosphoprotein in nonproducer cells transformed by Kirsten or Harvey murine sarcoma virus. *Virology* 96(1): 64-79.
- Shin, S., Buel, G. R., Wolgamott, L., Plas, D. R., Asara, J. M., Blenis, J. & Yoon, S. O. (2015). ERK2 Mediates Metabolic Stress Response to Regulate Cell Fate. *Mol Cell* 59(3): 382-398.
- Shin, S., Dimitri, C. A., Yoon, S. O., Dowdle, W. & Blenis, J. (2010). ERK2 but not ERK1 induces epithelial-to-mesenchymal transformation via DEF motif-dependent signaling events. *Mol Cell* 38(1): 114-127.
- Shirsat, N. V., Pignolo, R. J., Kreider, B. L. & Rovera, G. (1990). A member of the ras gene superfamily is expressed specifically in T, B and myeloid hemopoietic cells. *Oncogene* 5(5): 769-772.
- Sinha, S. & Yang, W. (2008). Cellular signaling for activation of Rho GTPase Cdc42. *Cell Signal* 20(11): 1927-1934.
- Smedsrod, B., Pertoft, H., Gustafson, S. & Laurent, T. C. (1990). Scavenger functions of the liver endothelial cell. *Biochem J* 266(2): 313-327.
- Smith, J. M., Hedman, A. C. & Sacks, D. B. (2015a). IQGAPs choreograph cellular signaling from the membrane to the nucleus. *Trends Cell Biol*.
- Smith, J. M., Hedman, A. C. & Sacks, D. B. (2015b). IQGAPs choreograph cellular signaling from the membrane to the nucleus. *Trends Cell Biol* 25(3): 171-184.
- Smith, J. M., Hedman, A. C. & Sacks, D. B. (2015c). IQGAPs choreograph cellular signaling from the membrane to the nucleus. *Trends Cell Biol* 25(3): 171-184.
- Sohail, M. A., Hashmi, A. Z., Hakim, W., Watanabe, A., Zipprich, A., Groszmann, R. J., Dranoff, J. A., Torok, N. J. & Mehal, W. Z. (2009). Adenosine induces loss of actin stress fibers and inhibits contraction in hepatic stellate cells via Rho inhibition. *Hepatology* 49(1): 185-194.

- Soliman, E. M., Rodrigues, M. A., Gomes, D. A., Sheung, N., Yu, J., Amaya, M. J., Nathanson, M. H. & Dranoff, J. A. (2009). Intracellular calcium signals regulate growth of hepatic stellate cells via specific effects on cell cycle progression. *Cell Calcium* 45(3): 284-292.
- Sorkin, A. & von Zastrow, M. (2009). Endocytosis and signalling: intertwining molecular networks. *Nat Rev Mol Cell Biol* 10(9): 609-622.
- Spaargaren, M. & Bischoff, J. R. (1994). Identification of the guanine nucleotide dissociation stimulator for Ral as a putative effector molecule of R-ras, H-ras, K-ras, and Rap. *Proc Natl Acad Sci U S A* 91(26): 12609-12613.
- Sternlicht, M. D. & Werb, Z. (2001). How matrix metalloproteinases regulate cell behavior. *Annu Rev Cell Dev Biol* 17: 463-516.
- Stieglitz, B., Bee, C., Schwarz, D., Yildiz, O., Moshnikova, A., Khokhlatchev, A. & Herrmann, C. (2008). Novel type of Ras effector interaction established between tumour suppressor NORE1A and Ras switch II. *EMBO J* 27(14): 1995-2005.
- Stuhlmann-Laeisz, C., Lang, S., Chalaris, A., Krzysztof, P., Enge, S., Eichler, J., Klingmuller, U., Samuel, M., Ernst, M., Rose-John, S. & Scheller, J. (2006). Forced dimerization of gp130 leads to constitutive STAT3 activation, cytokine-independent growth, and blockade of differentiation of embryonic stem cells. *Mol Biol Cell* 17(7): 2986-2995.
- Su, B. & Jacinto, E. (2011). Mammalian TOR signaling to the AGC kinases. *Crit Rev Biochem Mol Biol* 46(6): 527-547.
- Suyama, M., Nagase, T. & Ohara, O. (1999). HUGE: a database for human large proteins identified by Kazusa cDNA sequencing project. *Nucleic Acids Res* 27(1): 338-339.
- Takahashi, K., Mitsui, K. & Yamanaka, S. (2003). Role of ERas in promoting tumour-like properties in mouse embryonic stem cells. *Nature* 423(6939): 541-545.
- Takahashi, K., Nakagawa, M., Young, S. G. & Yamanaka, S. (2005). Differential Membrane Localization of ERas and Rheb, Two Ras-related Proteins Involved in the Phosphatidylinositol 3-Kinase/mTOR Pathway. *J Biol Chem* 280(38): 32768-32774.
- Takenawa, T. & Suetsugu, S. (2007). The WASP-WAVE protein network: connecting the membrane to the cytoskeleton. *Nat Rev Mol Cell Biol* 8(1): 37-48.
- Tanaka, Y., Ikeda, T., Kishi, Y., Masuda, S., Shibata, H., Takeuchi, K., Komura, M., Iwanaka, T., Muramatsu, S., Kondo, Y., Takahashi, K., Yamanaka, S. & Hanazono, Y. (2009). ERas is expressed in primate embryonic stem cells but not related to tumorigenesis. *Cell Transplant* 18(4): 381-389.
- Taub, R. (2004). Liver regeneration: from myth to mechanism. *Nat Rev Mol Cell Biol* 5(10): 836-847.
- Tazat, K., Harsat, M., Goldshmid-Shagal, A., Ehrlich, M. & Henis, Y. I. (2013). Dual effects of Ral-activated pathways on p27 localization and TGF-beta signaling. *Mol Biol Cell* 24(11): 1812-1824.
- Tcherkezian, J. & Lamarche-Vane, N. (2007). Current knowledge of the large RhoGAP family of proteins. *Biology of the Cell* 99(2): 67-86.
- Tee, A. R., Manning, B. D., Roux, P. P., Cantley, L. C. & Blenis, J. (2003). Tuberous sclerosis complex gene products, Tuberin and Hamartin, control mTOR signaling by acting as a GTPase-activating protein complex toward Rheb. *Curr Biol* 13(15): 1259-1268.
- Thumkeo, D., Watanabe, S. & Narumiya, S. (2013). Physiological roles of Rho and Rho effectors in mammals. *Eur J Cell Biol* 92(10-11): 303-315.
- Tidyman, W. E. & Rauen, K. A. (2009). The RASopathies: developmental syndromes of Ras/MAPK pathway dysregulation. *Curr Opin Genet Dev* 19(3): 230-236.
- Tnimov, Z., Guo, Z., Gambin, Y., Nguyen, U. T., Wu, Y. W., Abankwa, D., Stigter, A., Collins, B. M., Waldmann, H., Goody, R. S. & Alexandrov, K. (2012). Quantitative analysis of prenylated RhoA interaction with its chaperone, RhoGDI. *J Biol Chem* 287(32): 26549-26562.
- Tomiya, T., Nishikawa, T., Inoue, Y., Ohtomo, N., Ikeda, H., Tejima, K., Watanabe, N., Tanoue, Y., Omata, M. & Fujiwara, K. (2007). Leucine stimulates HGF production by hepatic stellate cells through mTOR pathway. *Biochem Biophys Res Commun* 358(1): 176-180.
- Torti, M. & Lapetina, E. G. (1994). Structure and function of rap proteins in human platelets. *Thromb Haemost* 71(5): 533-543.
- Tzivion, G., Dobson, M. & Ramakrishnan, G. (2011). FoxO transcription factors; Regulation by AKT and 14-3-3 proteins. *Biochim Biophys Acta* 1813(11): 1938-1945.
- Um, S. H., Frigerio, F., Watanabe, M., Picard, F., Joaquin, M., Sticker, M., Fumagalli, S., Allegrini, P. R., Kozma, S. C., Auwerx, J. & Thomas, G. (2004). Absence of S6K1 protects against age- and diet-induced obesity while enhancing insulin sensitivity. *Nature* 431(7005): 200-205.

- Vadas, O., Burke, J. E., Zhang, X., Berndt, A. & Williams, R. L. (2011). Structural basis for activation and inhibition of class I phosphoinositide 3-kinases. *Sci Signal* 4(195): re2.
- van der Weyden, L. & Adams, D. J. (2007). The Ras-association domain family (RASSF) members and their role in human tumorigenesis. *Biochim Biophys Acta* 1776(1): 58-85.
- Vanhaesebroeck, B., Ali, K., Bilancio, A., Geering, B. & Foukas, L. C. (2005). Signalling by PI3K isoforms: insights from gene-targeted mice. *Trends Biochem Sci* 30(4): 194-204.
- Vanhaesebroeck, B., Leever, S. J., Ahmadi, K., Timms, J., Katso, R., Driscoll, P. C., Woscholski, R., Parker, P. J. & Waterfield, M. D. (2001). Synthesis and function of 3-phosphorylated inositol lipids. *Annu Rev Biochem* 70: 535-602.
- Vanhaesebroeck, B., Vogt, P. K. & Rommel, C. (2010). PI3K: from the bench to the clinic and back. *Curr Top Microbiol Immunol* 347: 1-19.
- Vavvas, D., Li, X., Avruch, J. & Zhang, X. F. (1998). Identification of Nore1 as a Potential Ras Effector. *J Biol Chem* 273(10): 5439-5442.
- Vega, F. M. & Ridley, A. J. (2008). Rho GTPases in cancer cell biology. *FEBS Lett* 582(14): 2093-2101.
- Vega, F. M., Thomas, M., Reymond, N. & Ridley, A. J. (2015). The Rho GTPase RhoB regulates cadherin expression and epithelial cell-cell interaction. *Cell Commun Signal* 13(1).
- Vetter, I. R. (2001). The Guanine Nucleotide-Binding Switch in Three Dimensions. *Science* 294(5545): 1299-1304.
- Visse, R. (2003). Matrix Metalloproteinases and Tissue Inhibitors of Metalloproteinases: Structure, Function, and Biochemistry. *Circ Res* 92(8): 827-839.
- Vyas, S. K., Leyland, H., Gentry, J. & Arthur, M. J. (1995). Rat hepatic lipocytes synthesize and secrete transin (stromelysin) in early primary culture. *Gastroenterology* 109(3): 889-898.
- Wake, K. (1971). "Sternzellen" in the liver: perisinusoidal cells with special reference to storage of vitamin A. *Am J Anat* 132(4): 429-462.
- Wang, D. R., Sato, M., Sato, T., Kojima, N., Higashi, N. & Senoo, H. (2004). Regulation of matrix metalloproteinase expression by extracellular matrix components in cultured hepatic stellate cells. *Comp Hepatol* 3 Suppl 1: S20.
- Wang, R. C., Wei, Y., An, Z., Zou, Z., Xiao, G., Bhagat, G., White, M., Reichelt, J. & Levine, B. (2012). Akt-mediated regulation of autophagy and tumorigenesis through Beclin 1 phosphorylation. *Science* 338(6109): 956-959.
- Wang, S., Watanabe, T., Noritake, J., Fukata, M., Yoshimura, T., Itoh, N., Harada, T., Nakagawa, M., Matsuura, Y., Arimura, N. & Kaibuchi, K. (2007). IQGAP3, a novel effector of Rac1 and Cdc42, regulates neurite outgrowth. *J Cell Sci* 120(Pt 4): 567-577.
- Wang, X., DeFrances, M. C., Dai, Y., Padiaditakis, P., Johnson, C., Bell, A., Michalopoulos, G. K. & Zarnegar, R. (2002). A mechanism of cell survival: sequestration of Fas by the HGF receptor Met. *Mol Cell* 9(2): 411-421.
- Wang, X., Li, W., Williams, M., Terada, N., Alessi, D. R. & Proud, C. G. (2001). Regulation of elongation factor 2 kinase by p90(RSK1) and p70 S6 kinase. *EMBO J* 20(16): 4370-4379.
- Wang, Y., Zhou, Y. & Graves, D. T. (2014). FOXO transcription factors: their clinical significance and regulation. *Biomed Res Int* 2014: 925350.
- Watanabe-Takano, H., Takano, K., Keduka, E. & Endo, T. (2010). M-Ras is activated by bone morphogenetic protein-2 and participates in osteoblastic determination, differentiation, and transdifferentiation. *Exp Cell Res* 316(3): 477-490.
- Watanabe, T., Wang, S. & Kaibuchi, K. (2015). IQGAPs as Key Regulators of Actin-cytoskeleton Dynamics. *Cell Struct Funct* 40(2): 69-77.
- Watanabe, T., Wang, S., Noritake, J., Sato, K., Fukata, M., Takefuji, M., Nakagawa, M., Izumi, N., Akiyama, T. & Kaibuchi, K. (2004). Interaction with IQGAP1 links APC to Rac1, Cdc42, and actin filaments during cell polarization and migration. *Dev Cell* 7(6): 871-883.
- Weissbach, L., Settleman, J., Kalady, M. F., Snijders, A. J., Murthy, A. E., Yan, Y. X. & Bernard, A. (1994). Identification of a human rasGAP-related protein containing calmodulin-binding motifs. *J Biol Chem* 269(32): 20517-20521.
- Wennerberg, K. (2005). The Ras superfamily at a glance. *J Cell Sci* 118(5): 843-846.
- Wennerberg, K. & Der, C. J. (2004). Rho-family GTPases: it's not only Rac and Rho (and I like it). *J Cell Sci* 117(Pt 8): 1301-1312.
- Wennerberg, K., Ellerbroek, S. M., Liu, R. Y., Karnoub, A. E., Burrridge, K. & Der, C. J. (2002). RhoG signals in parallel with Rac1 and Cdc42. *J Biol Chem* 277(49): 47810-47817.

- Werb, Z. (1997). ECM and cell surface proteolysis: regulating cellular ecology. *Cell* 91(4): 439-442.
- Wheeler, A. P. & Ridley, A. J. (2004). Why three Rho proteins? RhoA, RhoB, RhoC, and cell motility. *Exp Cell Res* 301(1): 43-49.
- Wheeler, A. P. & Ridley, A. J. (2007). RhoB affects macrophage adhesion, integrin expression and migration. *Exp Cell Res* 313(16): 3505-3516.
- White, C. D., Brown, M. D. & Sacks, D. B. (2009a). IQGAPs in cancer: a family of scaffold proteins underlying tumorigenesis. *FEBS Lett* 583(12): 1817-1824.
- White, C. D., Brown, M. D. & Sacks, D. B. (2009b). IQGAPs in cancer: A family of scaffold proteins underlying tumorigenesis. *FEBS Lett* 583(12): 1817-1824.
- White, C. D., Erdemir, H. H. & Sacks, D. B. (2012). IQGAP1 and its binding proteins control diverse biological functions. *Cell Signal* 24(4): 826-834.
- White, C. D., Khurana, H., Gnatenko, D. V., Li, Z., Odze, R. D., Sacks, D. B. & Schmidt, V. A. (2010a). IQGAP1 and IQGAP2 are reciprocally altered in hepatocellular carcinoma. *BMC Gastroenterol* 10: 125.
- White, C. D., Khurana, H., Gnatenko, D. V., Li, Z., Odze, R. D., Sacks, D. B. & Schmidt, V. A. (2010b). IQGAP1 and IQGAP2 are Reciprocally Altered in Hepatocellular Carcinoma. *BMC Gastroenterology* 10(1): 125.
- Willumsen, B. M., Christensen, A., Hubbert, N. L., Papageorge, A. G. & Lowy, D. R. (1984). The p21 ras C-terminus is required for transformation and membrane association. *Nature* 310(5978): 583-586.
- Wing, M. R., Snyder, J. T., Sondek, J. & Harden, T. K. (2003). Direct activation of phospholipase C-epsilon by Rho. *J Biol Chem* 278(42): 41253-41258.
- Wittinghofer, A. & Vetter, I. R. (2011). Structure-Function Relationships of the G Domain, a Canonical Switch Motif. *Annual Review of Biochemistry* 80(1): 943-971.
- Wojnowski, L., Stancato, L. F., Zimmer, A. M., Hahn, H., Beck, T. W., Larner, A. C., Rapp, U. R. & Zimmer, A. (1998). Crf-1 protein kinase is essential for mouse development. *Mech Dev* 76(1-2): 141-149.
- Wojnowski, L., Zimmer, A. M., Beck, T. W., Hahn, H., Bernal, R., Rapp, U. R. & Zimmer, A. (1997). Endothelial apoptosis in Braf-deficient mice. *Nat Genet* 16(3): 293-297.
- Wolthuis, R. M., Bauer, B., van 't Veer, L. J., de Vries-Smits, A. M., Cool, R. H., Spaargaren, M., Wittinghofer, A., Burgering, B. M. & Bos, J. L. (1996). RalGDS-like factor (Rlf) is a novel Ras and Rap 1A-associating protein. *Oncogene* 13(2): 353-362.
- Wolthuis, R. M., de Ruiter, N. D., Cool, R. H. & Bos, J. L. (1997). Stimulation of gene induction and cell growth by the Ras effector Rlf. *EMBO J* 16(22): 6748-6761.
- Woodson, E. N. & Kedes, D. H. (2012). Distinct roles for extracellular signal-regulated kinase 1 (ERK1) and ERK2 in the structure and production of a primate gammaherpesvirus. *J Virol* 86(18): 9721-9736.
- Wright, D. E., Bowman, E. P., Wagers, A. J., Butcher, E. C. & Weissman, I. L. (2002). Hematopoietic stem cells are uniquely selective in their migratory response to chemokines. *J Exp Med* 195(9): 1145-1154.
- Wu, J.-X., Zhang, D.-G., Zheng, J.-N. & Pei, D.-S. (2015). Rap2a is a novel target gene of p53 and regulates cancer cell migration and invasion. *Cell Signal* 27(6): 1198-1207.
- Wu, Y., Tao, Y., Chen, Y. & Xu, W. (2012). RhoC regulates the proliferation of gastric cancer cells through interaction with IQGAP1. *PLoS ONE* 7(11): 7.
- Xie, G., Karaca, G., Swiderska-Syn, M., Michelotti, G. A., Krüger, L., Chen, Y., Premont, R. T., Choi, S. S. & Diehl, A. M. (2013). Cross-talk between Notch and Hedgehog regulates hepatic stellate cell fate in mice. *Hepatology* 58(5): 1801-1813.
- Xie, J. & Proud, C. G. (2013). Crosstalk between mTOR complexes. *Nat Cell Biol* 15(11): 1263-1265.
- Yanai, M., Tatsumi, N., Hasunuma, N., Katsu, K., Endo, F. & Yokouchi, Y. (2008). FGF signaling segregates biliary cell-lineage from chick hepatoblasts cooperatively with BMP4 and ECM components in vitro. *Dev Dyn* 237(5): 1268-1283.
- Yang, L., Jung, Y., Omenetti, A., Witek, R. P., Choi, S., Vandongen, H. M., Huang, J., Alpini, G. D. & Diehl, A. M. (2008). Fate-mapping evidence that hepatic stellate cells are epithelial progenitors in adult mouse livers. *Stem Cells* 26(8): 2104-2113.
- Yang, Q., Inoki, K., Ikenoue, T. & Guan, K. L. (2006). Identification of Sin1 as an essential TORC2 component required for complex formation and kinase activity. *Genes Dev* 20(20): 2820-2832.
- Yang, X. Y., Guan, M., Vigil, D., Der, C. J., Lowy, D. R. & Popescu, N. C. (2009). p120Ras-GAP binds the DLC1 Rho-GAP tumor suppressor protein and inhibits its RhoA GTPase and growth-suppressing activities. *Oncogene* 28(11): 1401-1409.

- Yang, Y. S., Garbay, C., Duchesne, M., Cornille, F., Jullian, N., Fromage, N., Tocque, B. &Roques, B. P. (1994). Solution structure of GAP SH3 domain by 1H NMR and spatial arrangement of essential Ras signaling-involved sequence. *EMBO J* 13(6): 1270-1279.
- Yasuda, K., Yashiro, M., Sawada, T., Ohira, M. &Hirakawa, K. (2007). ERas oncogene expression and epigenetic regulation by histone acetylation in human cancer cells. *Anticancer Res* 27(6B): 4071-4075.
- Yimlamai, D., Christodoulou, C., Galli, Giorgio G., Yanger, K., Pepe-Mooney, B., Gurung, B., Shrestha, K., Cahan, P., Stanger, Ben Z. &Camargo, Fernando D. (2014). Hippo Pathway Activity Influences Liver Cell Fate. *Cell* 157(6): 1324-1338.
- Yin, C., Evason, K. J., Asahina, K. &Stainier, D. Y. R. (2013a). Hepatic stellate cells in liver development, regeneration, and cancer. *Journal of Clinical Investigation* 123(5): 1902-1910.
- Yin, C., Evason, K. J., Asahina, K. &Stainier, D. Y. R. (2013b). Hepatic stellate cells in liver development, regeneration, and cancer. *J Clin Invest* 123(5): 1902-1910.
- Yokoi, Y., Namihisa, T., Kuroda, H., Komatsu, I., Miyazaki, A., Watanabe, S. &Usui, K. (1984). Immunocytochemical detection of desmin in fat-storing cells (Ito cells). *Hepatology* 4(4): 709-714.
- Yoon, S. &Seeger, R. (2006). The extracellular signal-regulated kinase: multiple substrates regulate diverse cellular functions. *Growth Factors* 24(1): 21-44.
- Young, Lucy C., Hartig, N., Muñoz-Alegre, M., Osés-Prieto, Juan A., Durdu, S., Bender, S., Vijayakumar, V., Vietri Rudan, M., Gewinner, C., Henderson, S., Jathoul, Amit P., Ghatrora, R., Lythgoe, Mark F., Burlingame, Alma L. &Rodriguez-Viciano, P. (2013). An MRAS, SHOC2, and SCRIB Complex Coordinates ERK Pathway Activation with Polarity and Tumorigenic Growth. *Mol Cell* 52(5): 679-692.
- Yu, L., McPhee, C. K., Zheng, L., Mardones, G. A., Rong, Y., Peng, J., Mi, N., Zhao, Y., Liu, Z., Wan, F., Hailey, D. W., Oorschot, V., Klumperman, J., Baehrecke, E. H. &Lenardo, M. J. (2010). Termination of autophagy and reformation of lysosomes regulated by mTOR. *Nature* 465(7300): 942-946.
- Yu, Y. &Feig, L. A. (2002). Involvement of R-Ras and Ral GTPases in estrogen-independent proliferation of breast cancer cells. *Oncogene* 21(49): 7557-7568.
- Yu, Y., Liang, D., Tian, Q., Chen, X., Jiang, B., Chou, B.-K., Hu, P., Cheng, L., Gao, P., Li, J. &Wang, G. (2014). Stimulation of Somatic Cell Reprogramming by ERas-Akt-FoxO1 Signaling Axis. *Stem Cells* 32(2): 349-363.
- Yuan, B. Z., Miller, M. J., Keck, C. L., Zimonjic, D. B., Thorgeirsson, S. S. &Popescu, N. C. (1998). Cloning, characterization, and chromosomal localization of a gene frequently deleted in human liver cancer (DLC-1) homologous to rat RhoGAP. *Cancer Res* 58(10): 2196-2199.
- Yuan, H., Zhang, H., Wu, X., Zhang, Z., Du, D., Zhou, W., Zhou, S., Brakebusch, C. &Chen, Z. (2009). Hepatocyte-specific deletion of Cdc42 results in delayed liver regeneration after partial hepatectomy in mice. *Hepatology* 49(1): 240-249.
- Zhang, B., Chernoff, J. &Zheng, Y. (1998). Interaction of Rac1 with GTPase-activating proteins and putative effectors. A comparison with Cdc42 and RhoA. *J Biol Chem* 273(15): 8776-8782.
- Zhang, B., Wang, Z. X. &Zheng, Y. (1997). Characterization of the interactions between the small GTPase Cdc42 and its GTPase-activating proteins and putative effectors. Comparison of kinetic properties of Cdc42 binding to the Cdc42-interactive domains. *J Biol Chem* 272(35): 21999-22007.
- Zhang, R., Wang, Y., Li, R. &Chen, G. (2015). Transcriptional Factors Mediating Retinoic Acid Signals in the Control of Energy Metabolism. *Int J Mol Sci* 16(6): 14210-14244.
- Zhang, S. C., Gremer, L., Heise, H., Janning, P., Shymanets, A., Cirstea, I. C., Krause, E., Nurnberg, B. &Ahmadian, M. R. (2014a). Liposome Reconstitution and Modulation of Recombinant Prenylated Human Rac1 by GEFs, GDI1 and Pak1. *PLoS ONE* 9(7): e102425.
- Zhang, S. C., Nouri, K., Amin, E., Taha, M. S., Nakhaeizadeh, H., Nakhaei-Rad, S., Dvorsky, R. &Ahmadian, M. R. (2014b). Classical Rho Proteins: Biochemistry of Molecular Switch Function and Regulation. In *Ras Superfamily Small G Proteins: Biology and Mechanisms 1*, 327-340 (Ed A. Wittinghofer). Springer Vienna.
- Zhao, B., Wei, X., Li, W., Udan, R. S., Yang, Q., Kim, J., Xie, J., Ikenoue, T., Yu, J., Li, L., Zheng, P., Ye, K., Chinnaiyan, A., Halder, G., Lai, Z. C. &Guan, K. L. (2007). Inactivation of YAP oncoprotein by the Hippo pathway is involved in cell contact inhibition and tissue growth control. *Genes Dev* 21(21): 2747-2761.
- Zhou, T.-B., Drummen, G. &Qin, Y.-H. (2012). The Controversial Role of Retinoic Acid in Fibrotic Diseases: Analysis of Involved Signaling Pathways. *Int J Mol Sci* 14(1): 226-243.

- Zinzalla, V., Stracka, D., Oppliger, W. & Hall, Michael N. (2011). Activation of mTORC2 by Association with the Ribosome. *Cell* 144(5): 757-768.
- Zoncu, R., Efeyan, A. & Sabatini, D. M. (2010). mTOR: from growth signal integration to cancer, diabetes and ageing. *Nat Rev Mol Cell Biol* 12(1): 21-35.
- Zong, Y., Panikkar, A., Xu, J., Antoniou, A., Raynaud, P., Lemaigre, F. & Stanger, B. Z. (2009). Notch signaling controls liver development by regulating biliary differentiation. *Development* 136(10): 1727-1739.

Acknowledgments

First, I would like to express my deepest thanks to Prof. Dr. Reza Ahmadian who accepted me to join his scientific group and for continuous supports of my Ph.D. study, patience, motivation, and immense knowledge. Especially, I would like to thank you for allowing me to grow as a research scientist and opening new windows to my scientific life. These years provided me an opportunity to beside Cell biology, in some extends, I entered to Biochemistry and specifically Cell signaling fields, which allowed me to have a better understanding of Cell biology as well. In addition, I would like to emphasize my thanks also for your positives critics after my presentations and for the time you spent on them that let me to work in my weak points and promoted my presentations.

I would like to express my special appreciation and thanks to Prof. Dr. Vlader Urlacher who his guidance helped me in all the time of Ph.D. research. You were always patient and welcome to answer my questions and helps me to extent my knowledge.

My sincere thanks also go to Prof. Dr. Dieter Häussinger, Dr. Claus Kordes, Dr. Silke Götze, Dr. Iris Sawitza and Dr. Boris Görg, for sharing their knowledge and experiences in this study. I express my special thanks to Ms. Claudia Rupprecht for helping me with isolation of the primary liver cells.

I take this opportunity to express my sincere gratitude to all of my colleagues and coordinators in Integrated Graduate School SFB 974 (iGK). Being a part of iGK was a wonderful opportunity for me to expand my knowledge in distinct aspects of the liver regeneration and good start to learn about how different projects with variety of scientific backgrounds could be interconnected in one research program (SFB974). This provided me a unique chance to attend weekly Ph.D. seminars, skill workshops, lectures and international conferences that all together helped me to grow as a scientist in this excellent program. I would like to express my sincere thanks to coordinate of iGK, Sandra Berger, Eva-Maria Grimm-Guenter, Inga Nissen and Ute Albrecht.

My sincere thanks goes to the German Research Foundation (Deutsche Forschungsgemeinschaft or DFG) through the Collaborative Research Center 974 (SFB 974) "Communication and System Relevance during Liver Injury and Regeneration" for generous sponsoring of this thesis and without their support this study was not possible.

I would like to extend my thanks to Prof. Dr. Jürgen Scheller and Dr. Roland P. Piekorz for their motivating discussions and guiding me in the right direction during my Ph.D. study. I had a chance that beside my official supervisors I benefited from your knowledge, experiences and insightful comments.

I also appreciate Dr. Radovan Dvorsky for his generous help, patience and guiding me for structural analysis and sharing his idea and knowledge. Working with you, gave me a chance to start imagination about the protein structures and you encouraged me for being brave in this field.

I would like to express my thanks to all members of institute of biochemistry and molecular biology II, you were all beside me during my Ph.D. time and we had memorable times together. I thank my fellow labmates Dr. Si-Cai Zhang, Dr. Madhurendra Singh, Ehsan Amin, Kazem Nouri, Hossein Nakhezadeh, Dr. Mohammad Saleh Taha, Niloufar Monhasery, Alexander Lang, Manuel Franke, Dr. Doreen Floss and Dr. Jens Moll, for the stimulating discussions, supports, sharing the knowledge and for all the fun we have had in the my Ph.D. years. My special thanks goes to my friends from the institute, Simone Hambuechen, Inga Rebecca Heinen, Jana Kremer, Bach-Ngan Nguyen, Nirina Sivakumar and Timo Faustmann, I am very happy to know all of you, being with you provided me an opportunity to be more familiar with German culture and you encouraged me for learning language. In particular, I am grateful to Petra Oprea, Fereshteh Kamrani, Ilse Meyer, Nadine Horstick, Hakima Ezzahoini, and Zeynep Tokyürek.

Last but not the least; I would like to thank my lovely and unique family: with words, I cannot express my deep thanks to you! My dear parents, I am devoted to both of you. By loving me, you taught me how to like other peoples. You spent your best time of your lives for training me and with putting yourself in front of the life problems, I never felt the hard times in my life. You were my motivators from elementary school up to now (my Ph.D.) and always encouraged me. Thank you for allowing me to study abroad although being far from me was very difficult for you and you never complained about this situation because my success and my future career were more important for you. I cannot say how grateful I am from my brothers (Mohammad and Mojtaba) and my only sister (Tayebe) for supporting me spiritually throughout my studying times and my life in general. I would like to express my special thanks to Hedyeh Amintoosi (my bother wife), who helped me to correct grammar mistakes in my dissertation.

Curriculum Vitae

Personal data

Date of Birth: 30th March 1986

Place of Birth: Mashhad, Iran

Nationality: Iranian (Persian)

Academic education

Oct 2008- Sep 2011: Master studies in Cell and Molecular Biology

Ferdowsi University of Mashhad, Iran

Degree: ***Master of Science in Cell and Molecular Biology***

Oct 2004 – Sep 2008 Bachelor studies in Animal Biology

Ferdowsi University of Mashhad, Iran

Degree: ***Bachelor of Science in Animal Biology***

School education

Oct 1992 – Oct 2004: Elementary, Junior and Senior high school in Mashhad, Iran

Degree: ***Diploma of Natural Science***

Work experience

Since May 2012: Ph.D. student with Prof. Dr. Mohammad Reza Ahmadian

Institute of Biochemistry and Molecular Biology II

Heinrich Heine University, Düsseldorf, Germany

Oct 2011-Mar 2012: collaboration and managements of the technical workshops

Institute of Biotechnology

Ferdowsi University of Mashhad, Iran

Poster presentation:

Jan 2016 22-23th, 32nd GASL Annual Meeting, Expression, epigenetical regulation and signaling network of embryonic stem cell-expressed RAS in hepatic stellate cells, Düsseldorf, Germany.

Sep 24-26th 2014, First international meeting “Building the cells”, Insights into the molecular mechanism of hepatic stellate cells activation, Paris, France.

Nov 15-16th 2013, International conference of SFB 974 "Liver Damage and Regeneration", The properties and functions of embryonic stem cell-expressed Ras (ERAS) with respect to liver regeneration, Düsseldorf, Germany.

Apr 27-29th 2011, Iranian congress on “Biology and Application of Stem cells”, Improve the efficiency and safety of induced pluripotent stem cells technology, Ferdowsi University of Mashhad, Iran.

Awards and scholarships

Inlands patent (Iran) “the small molecules kit for the dedifferentiation induction”, 2014, No. 83648.

Prizes for the first grade student on M.Sc. between Cell and molecular biology students on the faculty of Science, for three years 2008-2011, Ferdowsi University of Mashhad, Iran.

Prizes for the first grade student on B.Sc. between Biology students on the faculty of Science, for three years 2005, 2006 and 2007, Ferdowsi University of Mashhad, Iran.

Jan 2001 School prize in general science exam between the high schools of the city (Mashhad)

University scholarship for doing M.Sc., Ferdowsi University of Mashhad.

University scholarship for B.Sc., Ferdowsi University of Mashhad, based on entrance examination.

Training, commitments and workshops

Dec 2012-Jan 2016: Member of the graduate school iGRAD

May 2012-Jan 2016: Member of the integrated graduate school iGK974 of the SFB974

iGRAD Workshops, Heinrich Heine University:

- Good scientific practice for doctoral researchers
- Optimizing writing strategies for publishing in English
- Get into teaching for doctoral researchers
- Leadership skills for scientists
- Scientific image processing and analysis

Stem cell biology and differentiation workshop 'induced pluripotent stem cells cultivation and cardio-myocyte differentiation' (Klinik für Herz- und Thoraxchirurgie, Universität Magdeburg, Germany in 2016, 5 days).

Data analysis with GraphPad Prism workshop (Heinrich-Heine-Universität Düsseldorf, Germany, 2016 2 days).

Gene Trapping/Knock-out workshop (Institut für Medizinische Mikrobiologie und Krankenhaushygiene Heinrich-Heine-Universität Düsseldorf, Germany, 2014 2 days).

List of publications

Nakhaei-Rad, S., Bahrami, A. R., Mirahmadi, M. &Matin, M. M. (2012). New windows to enhance direct reprogramming of somatic cells towards induced pluripotent stem cells. *Biochem Cell Biol* 90(2): 115-123.

Zhang, S. C., Nouri, K., Amin, E., Taha, M. S., Nakhaeizadeh, H., **Nakhaei-Rad, S.**, Dvorsky, R. &Ahmadian, M. R. (2014). Classical Rho Proteins: Biochemistry of Molecular Switch Function and Regulation. In *Ras Superfamily Small G Proteins: Biology and Mechanisms* 1, 327-340 (Ed A. Wittinghofer). *Springer Vienna*.

Jaiswal, M., Dvorsky, R., Amin, E., Risse, S. L., Fansa, E. K., Zhang, S. C., Taha, M. S., Gauhar, A. R., **Nakhaei-Rad, S.**, Kordes, C., Koessmeier, K. T., Cirstea, I. C., Olayioye, M. A., Haussinger, D. &Ahmadian, M. R. (2014). Functional cross-talk between ras and rho pathways: a Ras-specific GTPase-activating protein (p120RasGAP) competitively inhibits the RhoGAP activity of deleted in liver cancer (DLC) tumor suppressor by masking the catalytic arginine finger. *J Biol Chem* 289(10): 6839-6849.

Nakhaei-Rad, S., Nakhaeizadeh, H., Kordes, C., Cirstea, I. C., Schmick, M., Dvorsky, R., Bastiaens, P. I., Haussinger, D. &Ahmadian, M. R. (2015). The Function of Embryonic Stem Cell-expressed RAS (ERAS), a Unique RAS Family Member, Correlates with Its Additional Motifs and Its Structural Properties. *J Biol Chem* 290(25): 15892-15903.

Caye, A., Strullu, M., Guidez, F., Cassinat, B., Gazal, S., Fenneteau, O., Lainey, E., Nouri, K., **Nakhaei-Rad, S.**, Dvorsky, R., Lachenaud, J., Pereira, S., Vivent, J., Verger, E., Vidaud, D., Galambrun, C., Picard, C., Petit, A., Contet, A., Poirée, M., Sirvent, N., Méchinaud, F., Adjaoud, D., Paillard, C., Nelken, B., Reguerre, Y., Bertrand, Y., Häussinger, D., Dalle, J.-H., Ahmadian, M. R., Baruchel, A., Chomienne, C. &Cavé, H. (2015). Juvenile myelomonocytic

leukemia displays mutations in components of the RAS pathway and the PRC2 network. *Nat Genet* 47(11): 1334-1340.

Nakhaei-Rad, S., Nakhaeizadeh, H., Götze, S., Kordes, C., Sawitza, I., Franke, M., Scheller, J., Piekorz, R. P., Häussinger, D. & Ahmadian, M. R. (2016). Embryonic stem cell-expressed ERAS controls the quiescence of hepatic stellate cells. *J Biol Chem* 291(16):8399-413.

Mirahmadi, M*., **Nakhaei-Rad, S***., Matin, M. M., Shahriari, M., Saeinasab, M., Mahmoudi, Z., Haghghi-Talab, A., Mahdavi-Shahri, N., & Bahrami, A. R. (2016). Dedifferentiation effects of rabbit regenerating tissue on partially differentiated cells. *CELL REPROGRAM*. DOI: 10.1089/cell.2016.0008.

Eidesstattliche Erklärung zur Dissertation

Hiermit versichere ich, dass die vorliegende Dissertation von mir selbstständig und ohne unzulässige fremde Hilfe unter Beachtung der Grundsätze zur Sicherung guter wissenschaftlicher Praxis an der Heinrich-Heine-Universität Düsseldorf verfasst worden ist. Die Dissertation wurde in der vorgelegten oder in ähnlicher Form noch bei keiner anderen Institution eingereicht. Ich habe bisher keine erfolglosen Promotionsversuche unternommen.

Düsseldorf, den

Saeideh Nakhaeirad